FINAL REPORT

Groundwater Availability Model for the Seymour Aquifer

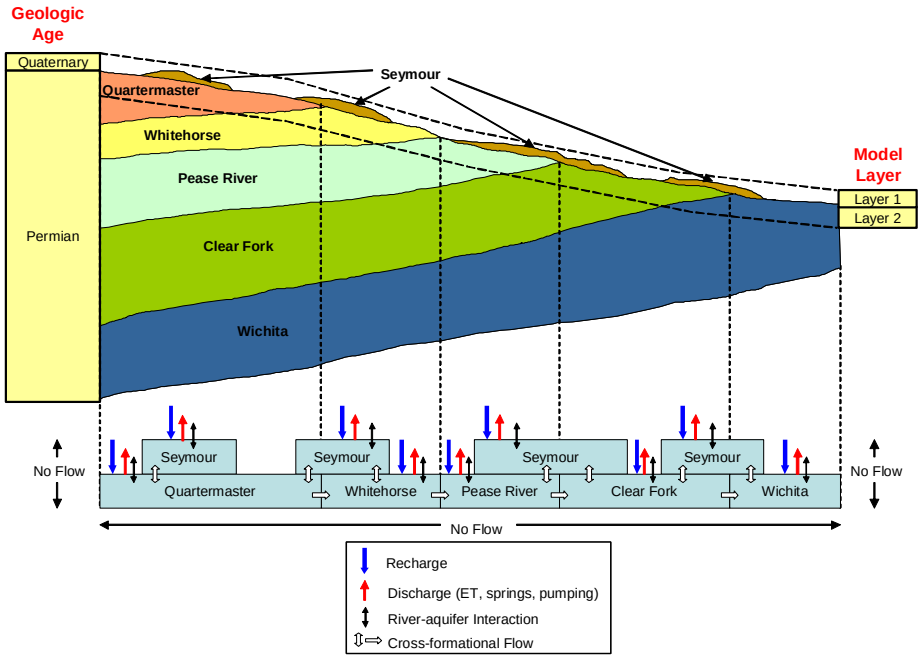

Prepared for the:

Texas Water Development Board

Prepared by:

John E. Ewing, Toya L. Jones, and John F. Pickens
9111A Research Blvd
Austin, TX 78758
512/425-2000

Andrew Chastain-Howley

Kirk E. Dean

Aubrey A. Spear

July 2004

TABLE OF CONTENTS

TABLE OF CONTENTS (continued)

TABLE OF CONTENTS (continued)

LIST OF FIGURES

LIST OF FIGURES (continued)

LIST OF FIGURES (continued)

LIST OF FIGURES (continued)

LIST OF FIGURES (continued)

LIST OF FIGURES (continued)

LIST OF FIGURES (continued)

LIST OF FIGURES (continued)

LIST OF FIGURES (continued)

LIST OF FIGURES (continued)

LIST OF TABLES

LIST OF TABLES (continued)

APPENDICES

ACRONYMS AND ABBREVIATIONS

AFY	acre-feet per year
CCUWD	Collingsworth County Underground Water District
cfs	cubic feet per second
DEM	Digital Elevation Map
DF	damping factor
DOR	drought of record
EPA	Environmental Protection Agency
ET	evapotranspiration
GAM	Groundwater Availability Model
GCD	Groundwater Conservation District
GIS	Geographic Information Systems
GLIS	Global Land Information System
GMG	Geometric Multigrid
K	hydraulic conductivity
K_h	horizontal hydraulic conductivity
K_v	vertical hydraulic conductivity
k	hydraulic permeability
LSD	land surface datum
MAE	mean absolute error
MB	megabytes
MCL	maximum contaminant level
MD	mean head difference
ME	mean error
MODFLOW	USGS Modular Three-Dimensional Finite-Difference Groundwater Flow Model
MRLC	Multi-Resolution Land Characteristics
NAWQA	National Water Quality Assessment
NRCS	Natural Resources Conservation Service
OWRB	Oklahoma Water Resources Board

ACRONYMS AND ABBREVIATIONS (continued)

PEST	Parameter Estimation
PMWIN	Processing MODFLOW for Windows
PRISM	Parameter-elevation Regressions on Independent Slopes Model
RAM	random access memory
RF1	U.S. Environmental Protection Agency River Reach File 1
RMS	root mean square
RPGCD	Rolling Plains Groundwater Conservation District
RRA	Red River Authority
RWPG	Regional Water Planning Group
S	Storativity
SAF	Stakeholder Advisory Forum
SC	specific capacity
SCS	Soil Conservation Service
SOP	Standard Operating Procedures
SPI	Standardized Precipitation Index
STATSGO	State Soil Geographic
SWAT	Soil Water Assessment Tool
T	Transmissivity
TCEQ	Texas Commission on Environmental Quality
TDS	total dissolved solids
TWDB	Texas Water Development Board
URL	Universal Resource Locator
US	United States
USDA	United States Department of Agriculture
USGS	United States Geological Survey
UWCD	Underground Water Conservation District

ABSTRACT

This report documents the development of a three-dimensional groundwater model for the Seymour aquifer in north-central Texas. The Seymour aquifer is the principal source of water in this part of Texas with irrigation being the main water use. The model was developed using MODFLOW and consists of two layers, an upper layer comprising the remnant areas (pods) of the Seymour Formation and other Quaternary-age alluvium that comprise the Seymour aquifer, and a second layer comprising the underlying Permian deposits. Characterization of the Blaine aquifer was presented in greater detail than the other Permian units because it is the most important underlying stratum for water-supply purposes. The model comprises dimensions of 180 miles east-west by 208 miles north-south, with 3,436 active cells in the Seymour layer and 20,001 active cells in the Permian layer. The model incorporates the available information on structure, hydrostratigraphy, hydraulic properties, stream flow, recharge, and pumping. The underlying data for these parameters are presented and discussed in detail.

The model was first calibrated to steady-state conditions. The time periods for steady state were selected for the individual pods of the Seymour aquifer and included various time periods in the 1960s and 1970s. The steady-state model reproduced the aquifer water levels or heads well and within the uncertainty in the head estimates. The model was also calibrated to transient aquifer conditions from January 1980 through December 1989 by incorporating monthly variations in recharge, streamflow, and pumping and fitting various hydrographs from across the region. The transient model reproduced aquifer heads well and within the uncertainty in the head estimates. The transient-calibrated model was verified by simulating aquifer conditions for the verification period from January 1990 through December 1999, reproducing observed aquifer heads within the calibration measures.

All parameters common to the steady-state and transient models are identical. The geometric mean of the horizontal hydraulic conductivity for the Seymour aquifer is 68.5 ft/day. For the calibrated steady-state and transient models, the average recharge rate over the Seymour aquifer is 2 in/yr. In the transient model, recharge accounts for approximately 94 percent of the aquifer inflow, and streams, ET, and pumping discharge approximately 35, 20, and 20 percent of the aquifer outflow, respectively. A sensitivity analysis was performed to determine which parameters had the most influence on model performance and calibration. The most sensitive

parameters for the steady-state model are recharge, stream conductance, and the horizontal hydraulic conductivity of layer 2, whereas the most sensitive parameters for the transient model are recharge and pumping.

The verified model was used to make predictions of aquifer conditions for the period 2000 to 2050 based upon projected pumping demands as developed by the Regional Water Planning Groups. The predictive modeling indicates that average water levels are not expected to change by more than several feet in the Seymour or Blaine aquifers based on future estimates of pumping and with or without a drought of record. Localized areas were predicted to have water-level declines in the Seymour aquifer up to about 30 feet.

The applicability of the model is limited to regional-scale assessments of groundwater availability (e.g., an area smaller than a county and larger than a square mile) due to the relatively large grid blocks (1 square mile) over which pumping and hydraulic property data are averaged in the model. In addition to uncertainty in pumping and hydraulic property data, the model is limited to a first-order approach of coupling surface water and groundwater and does not provide a rigorous solution to surface-water flow in the region.

The purpose of this model is to provide a tool for making predictions of groundwater availability in the Seymour aquifer through 2050 based on current projections of groundwater demands and including one period of drought-of-record conditions. This model provides a documented, publicly-available, integrated tool for the assessment of water management strategies by state planners, Regional Water Planning Groups, Groundwater Conservation Districts, Underground Water Conservation Districts, and other interested stakeholders.

1.0 INTRODUCTION

The Texas Water Development Board (TWDB) has identified the major and minor aquifers in Texas on the basis of regional extent and amount of water produced. The major and minor aquifers are shown in Figures 1.1 and 1.2, respectively. General discussion of the major and minor aquifers is given in Ashworth and Hopkins (1995).

The focus of the study contained in this report is the development of a groundwater availability model (GAM) for the Seymour aquifer, a major aquifer in Texas (see Figure 1.1). Sections 1 through 5 document development of the conceptual model for the Seymour aquifer. All aspects of the numerical model are discussed in Sections 6 through 11. Section 12 provides suggestions for future improvements to the model, and Section 13 presents conclusions.

The Seymour aquifer is present in parts of 23 north-central and panhandle counties (Ashworth and Hopkins, 1995). Groundwater use for the Seymour aquifer in Texas was reported at 120,000 acre-feet per year (AFY) in 1997, and the groundwater availability estimate under drought conditions in the year 2000 was reported at 250,000 AFY (TWDB, 2002). The majority of the water pumped from the aquifer is used for irrigation purposes (Ashworth and Hopkins, 1995) with minor pumpage for livestock, domestic, municipal, and industrial use.

The modeling approach adopted for the Seymour GAM is to represent the Seymour aquifer as a single layer and the underlying strata as a second layer having separate hydraulic characteristics. The most important underlying stratum in the region for water-supply purposes is the Blaine aquifer. The Blaine aquifer, as defined by the TWDB, is present in nine north-central and panhandle counties in Texas and is classified as a minor aquifer (see Figure 1.2). The Blaine aquifer is also present in southwestern Oklahoma. Although the Blaine Formation extends further south in Texas than does the Blaine aquifer, the limited use of its water to the south has precluded its identification as a minor aquifer in that area (Ashworth and Hopkins, 1995). Groundwater use for the Blaine aquifer in Texas was reported at 17,000 AFY in 1997, and the groundwater availability estimate under drought conditions in the year 2000 was reported at 180,000 AFY (TWDB, 2002). The majority of the water pumped from the Blaine aquifer is used for irrigation of highly salt-tolerant crops (Ashworth and Hopkins, 1995). Due to its high sulfate content, groundwater from the Blaine aquifer is not used for human consumption (Baker et al., 1963).

The Texas Water Code codified the requirement for generation of a State Water Plan that allows for the development, management, and conservation of water resources and the preparation and response to drought, while maintaining sufficient water available for the citizens of Texas (TWDB, 2002). Senate Bill 1 and subsequent legislation directed the TWDB to coordinate regional water planning with a process based upon public participation. Also, as a result of Senate Bill 1, the approach to water planning in the state of Texas has shifted from a water-demand based allocation approach to an availability-based approach.

Groundwater models provide a tool to estimate groundwater availability for various water use strategies and to determine the cumulative effects of increased water use and drought. A groundwater model is a numerical representation of the aquifer system capable of simulating historical conditions and predicting future aquifer conditions. Inherent to the groundwater model are a set of equations that are developed and applied to describe the physical processes considered to be controlling groundwater flow in the aquifer system. Groundwater models are essential to performing complex analyses and in making informed predictions and related decisions (Anderson and Woessner, 1992). As a result, development of Groundwater Availability Models (GAMs) for the major and minor Texas aquifers is integral to the state water planning process. The purpose of the GAM program is to provide a tool that can be used to develop reliable and timely information on groundwater availability for the citizens of Texas and to ensure adequate supplies or recognize inadequate supplies over a 50-year planning period.

The Seymour GAM was developed using a modeling protocol standard to the groundwater modeling industry. This protocol includes: (1) the development of a conceptual model for groundwater flow in the aquifer, (2) model design, (3) model calibration, (4) model verification, (5) sensitivity analysis, (6) model prediction, and (7) reporting. The conceptual model is a conceptual description of the physical processes that govern groundwater flow in the aquifer system. Available data and reports for the model area were reviewed in the conceptual model development stage. Model design is the process used to translate the conceptual model into a physical model, in this case a numerical model of groundwater flow. This involves organizing and distributing model parameters, developing a model grid and model boundary conditions, and determining the model integration time scale. Model calibration is the process of modifying model parameters so that observed field measurements (e.g., water levels in wells) can be reproduced. The model was calibrated to steady-state conditions in the late 1960s and

early 1970s and to transient aquifer conditions from January 1980 through December 1989. Model verification is the process of using the calibrated model to reproduce observed field measurements not used in the calibration to test the model's predictive ability. The model was verified against measured aquifer conditions from January 1990 through December 1999. Sensitivity analyses were performed on both the steady-state and transient models to offer insight on the uniqueness of the model and the impact of uncertainty in model parameter estimates. Model predictions were performed from 2000 to 2050 to estimate aquifer conditions for the next 50 years based upon projected pumping demands developed by the Regional Water Planning Groups (RWPGs).

Consistent with state water planning policy, the Seymour GAM was developed with the support of stakeholders through stakeholder forums held approximately every four months. The purpose of the GAMs is to provide a tool for RWPGs, Groundwater Conservation Districts, River Authorities, and state planners for the evaluation of groundwater availability and to support the development of water management strategies and drought planning. The Seymour GAM intersects five of the sixteen Texas RWPGs. The Seymour aquifer supplies from existing sources under drought conditions, as reported by the Planning Groups, is expected to remain at or slightly below the year 2000 estimate (150,741 AFY) which is about 26 percent higher than the reported use in 1997 of 120,000 AFY (TWDB, 2002). The Blaine aquifer supplies from existing sources under drought conditions, as reported by the Planning Groups, is expected to remain at or slightly below the year 2000 estimate (25,850 AFY) which is about 52 percent higher than the reported use in 1997 of 17,000 AFY (TWDB, 2002). The Seymour aquifer GAM provides a tool for use in assessing water planning strategies.

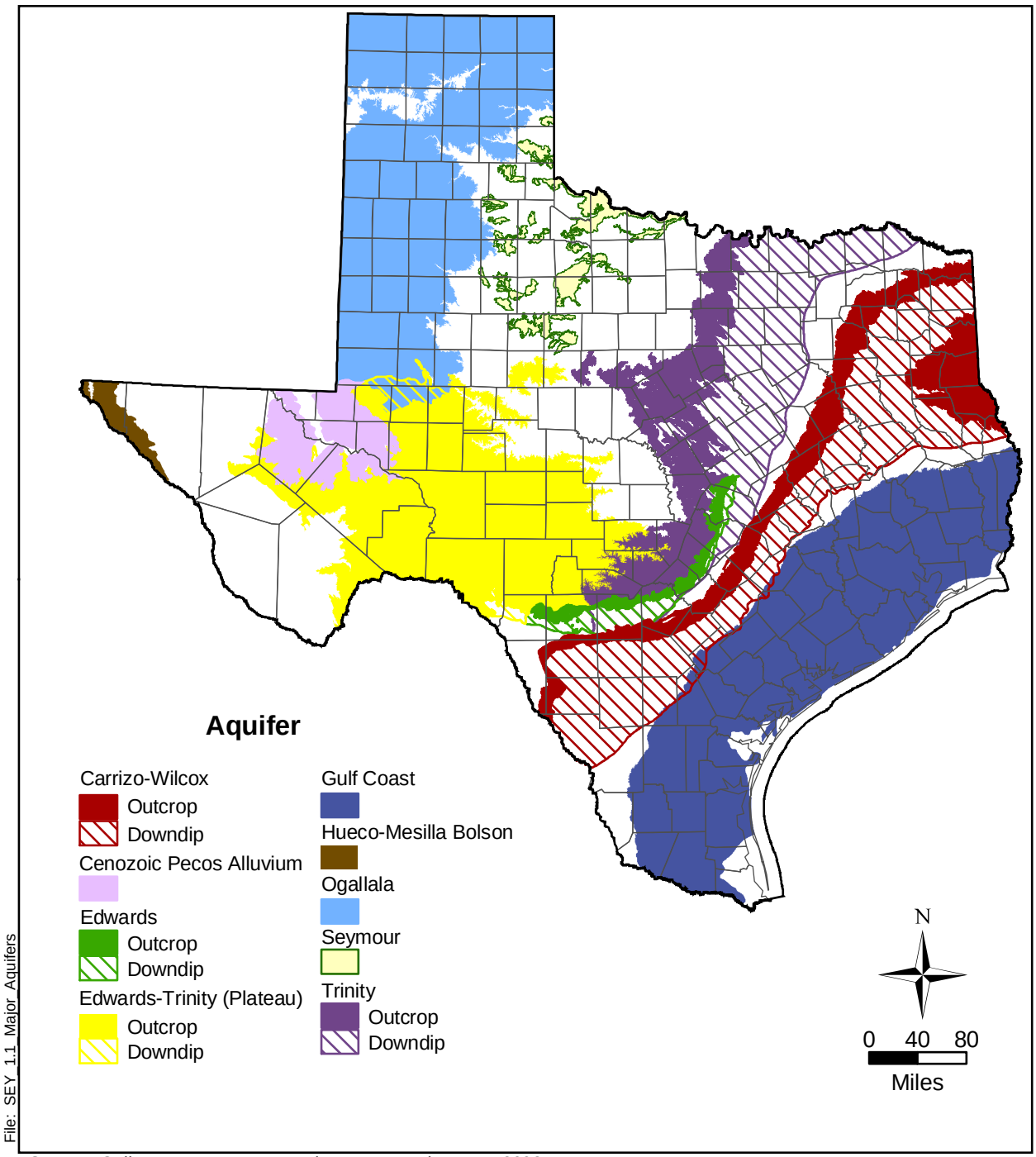

Source: Online: Texas Water Development Board, August 2003

Figure 1.1 Location of major aquifers in Texas.

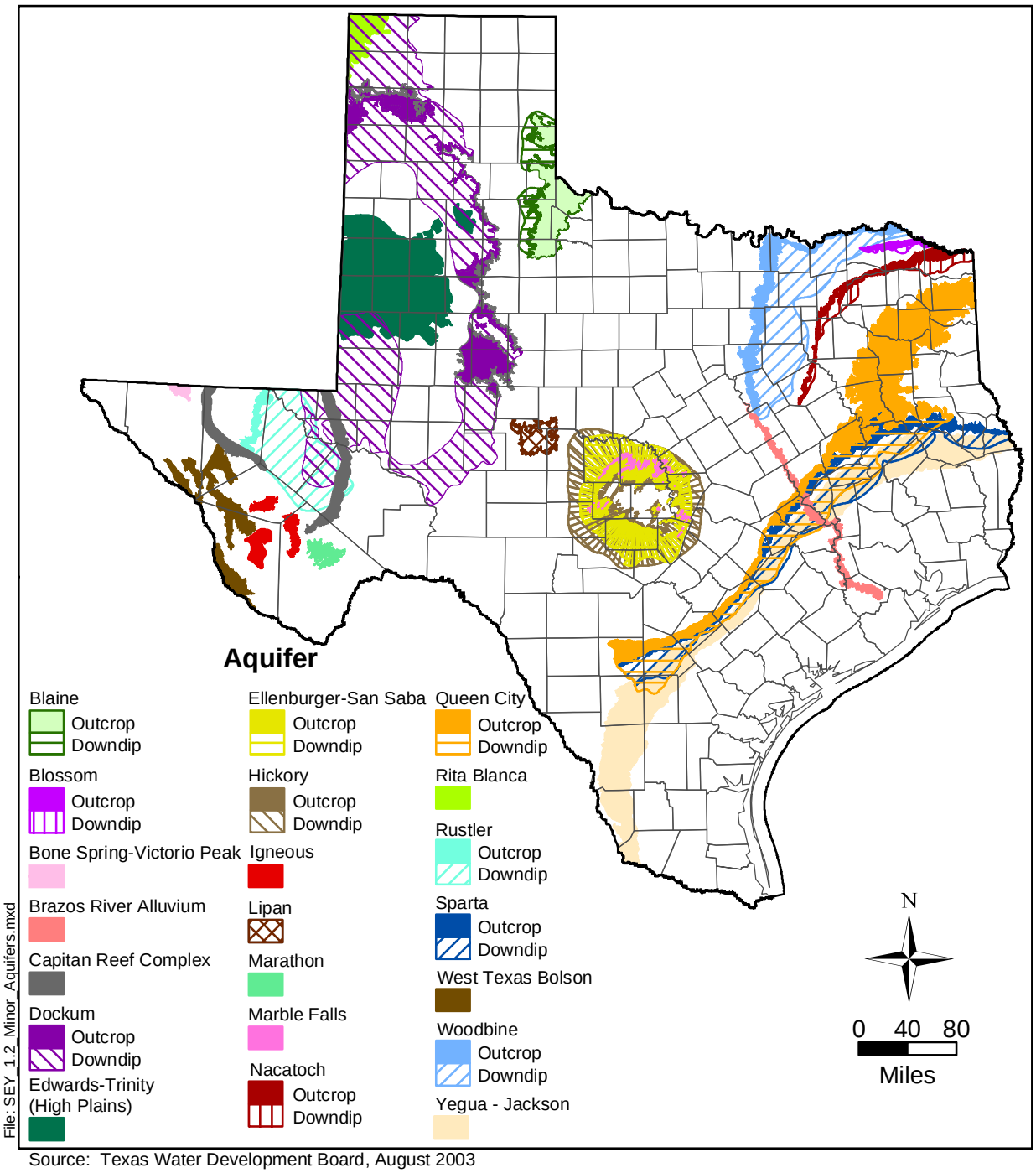

Source: Texas Water Development Board, August 2003

Figure 1.2 Location of minor aquifers in Texas.

This page intentionally left blank.

2.0 STUDY AREA

The Seymour aquifer, as defined by the TWDB, consists of isolated pods of unconsolidated alluvium deposits of Quaternary age. The aquifer, classified as a major aquifer in Texas, extends from the southern Brazos river watershed northward to the border with Oklahoma. The Seymour aquifer overlies Permian-age deposits that generally dip to the west. The most important underlying formation with respect to water supply is the Blaine Formation. The northern and north-central portions of this formation make up the Blaine aquifer, which is a minor aquifer in Texas. The Blaine aquifer consists of anhydrite, gypsum, shale, and dolomite (Baker et al., 1963). Where both aquifers are present, the Blaine aquifer directly underlies the Seymour aquifer with the exception of in Collingsworth County and northeastern Childress County where the two are separated by the Whitehorse Group. Groundwater use for the Seymour and Blaine aquifers were 120,000 and 17,000 AFY, respectively, in 1997 (TWDB, 2002).

The study area and active model boundary for the Seymour GAM are shown in Figure 2.1. The individual pods of the Seymour aquifer are shown in Figure 2.2. Not all of the pods are included in the Seymour GAM. Per the TWDB, only those pods shown shaded in Figure 2.2 are to be included in the model. All subsequent figures in this report show only the pods included in the Seymour GAM. Figure 2.3 shows the counties, roadways, cities, and towns included in the study area. All or part of 32 Texas counties and four Oklahoma counties are included in the active model area. The locations of rivers, streams, lakes, and reservoirs in the study area are shown on Figure 2.4.

Figure 2.5 shows the surface outcrop and downdip subcrop of the major and minor aquifers in the study area. Major aquifers located in the study area include the Seymour aquifer and small portions of the Ogallala and Edwards-Trinity (Plateau) aquifers. Note that the Seymour aquifer is exclusively a water-table aquifer with no subcrop. Minor aquifers located in the study area include the Blaine aquifer and small portions of the Dockum and Edwards-Trinity (High Plains) aquifers.

Groundwater model boundaries are typically defined on the basis of surface or groundwater hydrologic boundaries. The lateral boundaries of the active model area are defined to include the extent of the Seymour and Blaine aquifers. Boundaries were generally placed

along topographic highs or rivers since these features should behave as lateral no-flow boundaries for the shallow flow system. This boundary, projected to plan view, is shown in report figures as a red solid line and provides the limits of the active model area. The upper model boundary is defined as ground surface across the entire model region. The lower model boundary is defined as the base of the Blaine aquifer where it is present. Beyond the extent of the Blaine aquifer, the lower model boundary has been placed 500 feet below the topographic surface in areas where the Seymour aquifer is absent and 500 feet below the base of the Seymour in areas where it is present, with one exception. In order to avoid a sudden change in thickness along the eastern edge of the Blaine aquifer, a gradual increase in thickness was implemented across 10 miles on either side of the aquifer's eastern edge.

The active model area encompasses all or part of five RWPGs (Figure 2.6). From north to south they are (1) the Panhandle RWPG (Region A), (2) the Llano Estacado RWPG (Region O), (3) Region B RWPG, (4) the Brazos G RWPG (Region G), and (5) Region F RWPG. The active model area includes all or part of ten Groundwater Conservation Districts (GCD) and Underground Water Conservation Districts (UWCD) (Figure 2.7). Table 2.1 summarizes the GCDs and UWCDs in which the Seymour and Blaine aquifers are present. The study area intersects two river authority regions: (1) the Red River Authority of Texas, and (2) the Brazos River Authority.

Table 2.1 Groundwater and Underground Water Conservation Districts in which the Seymour and Blaine aquifers are present.

Seymour Aquifer	Blaine Aquifer
Collingsworth County UWCD	Panhandle GCD
Tri-County GCD	Collingsworth County UWCD
Rolling Plains GCD	Tri-County GCD
Salt Fork UWCD	Rolling Plains GCD
Clear Fork GCD	
Lower Seymour GCD	

The major river basins in the active model area are the Red and Brazos river basins (Figure 2.8). Climate is the major control on flow in rivers and streams. The primary climatic factors are precipitation and evapotranspiration (water not available for recharge to the aquifer due to evaporation or use by the biological processes of plants). For all but the major rivers,

flow in the rivers throughout the model area is generally episodic with extended periods of low-flow or no-flow conditions. In general, most rivers within the active model area tend to gain flow from the adjacent geology. Table 2.2 provides a listing of the river basins in the study area along with the river length in Texas, the river basin area in Texas, and the number of major reservoirs within the river basin in Texas.

Table 2.2 River basins in the Seymour GAM study area (after Wermund, 1996).

River Basin	Texas River Length (miles)	Texas River Basin Drainage Area (square miles)	Number of Major Reservoirs
Brazos	840	42,800	19
Red	680	30,823	7

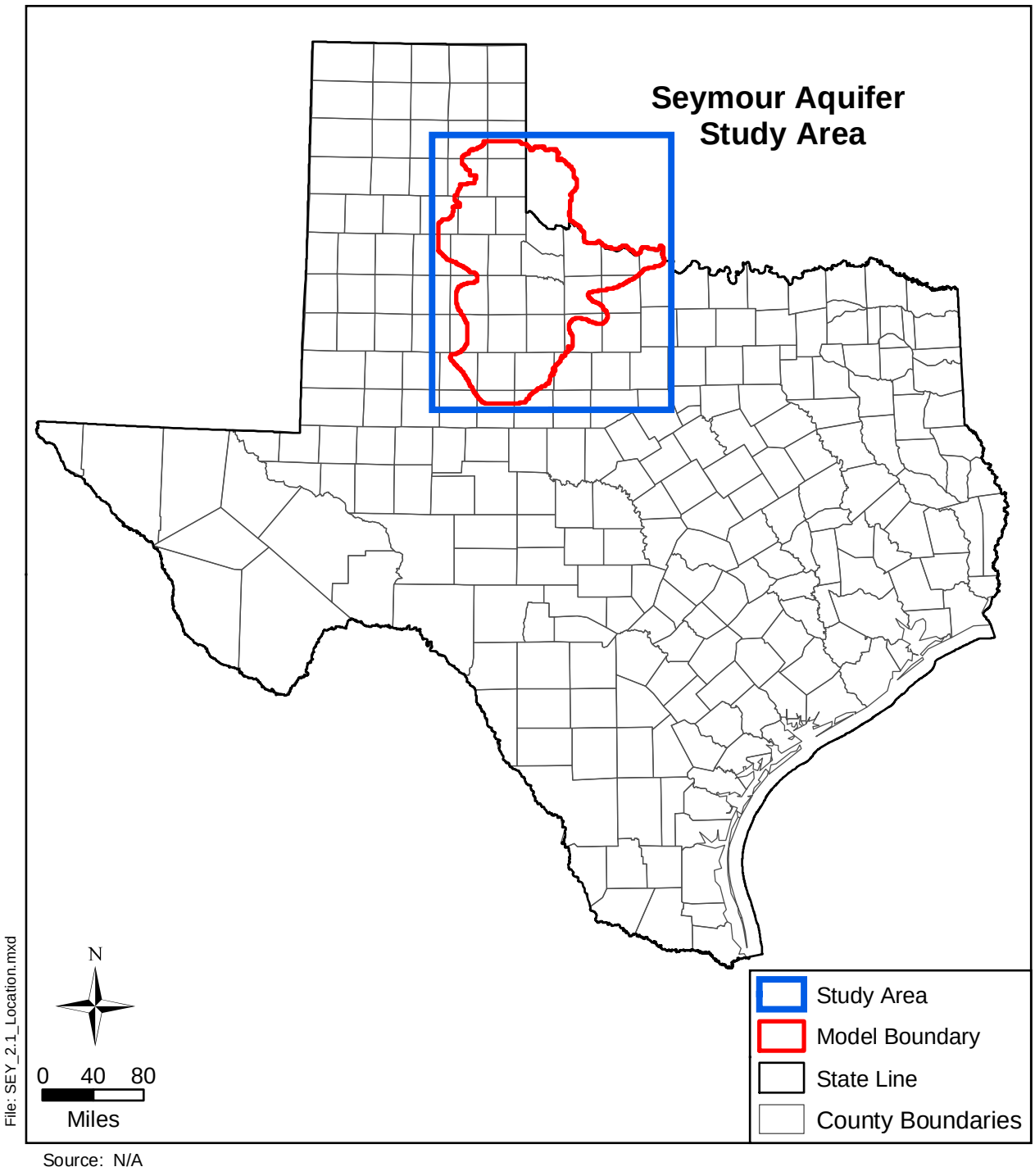

Figure 2.1 Location of Seymour GAM.

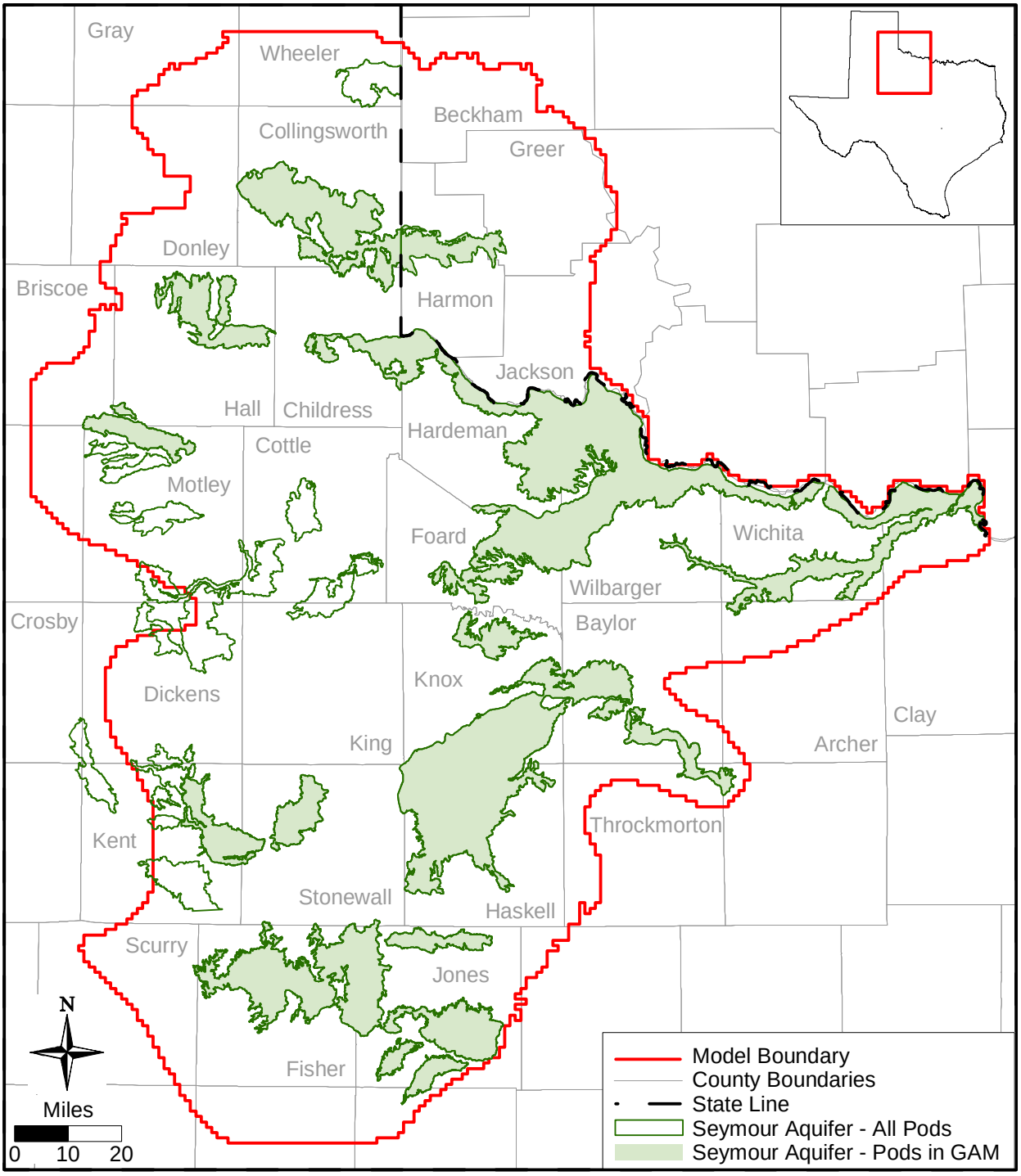

Figure 2.2 Pods of the Seymour aquifer included and not included in the GAM.

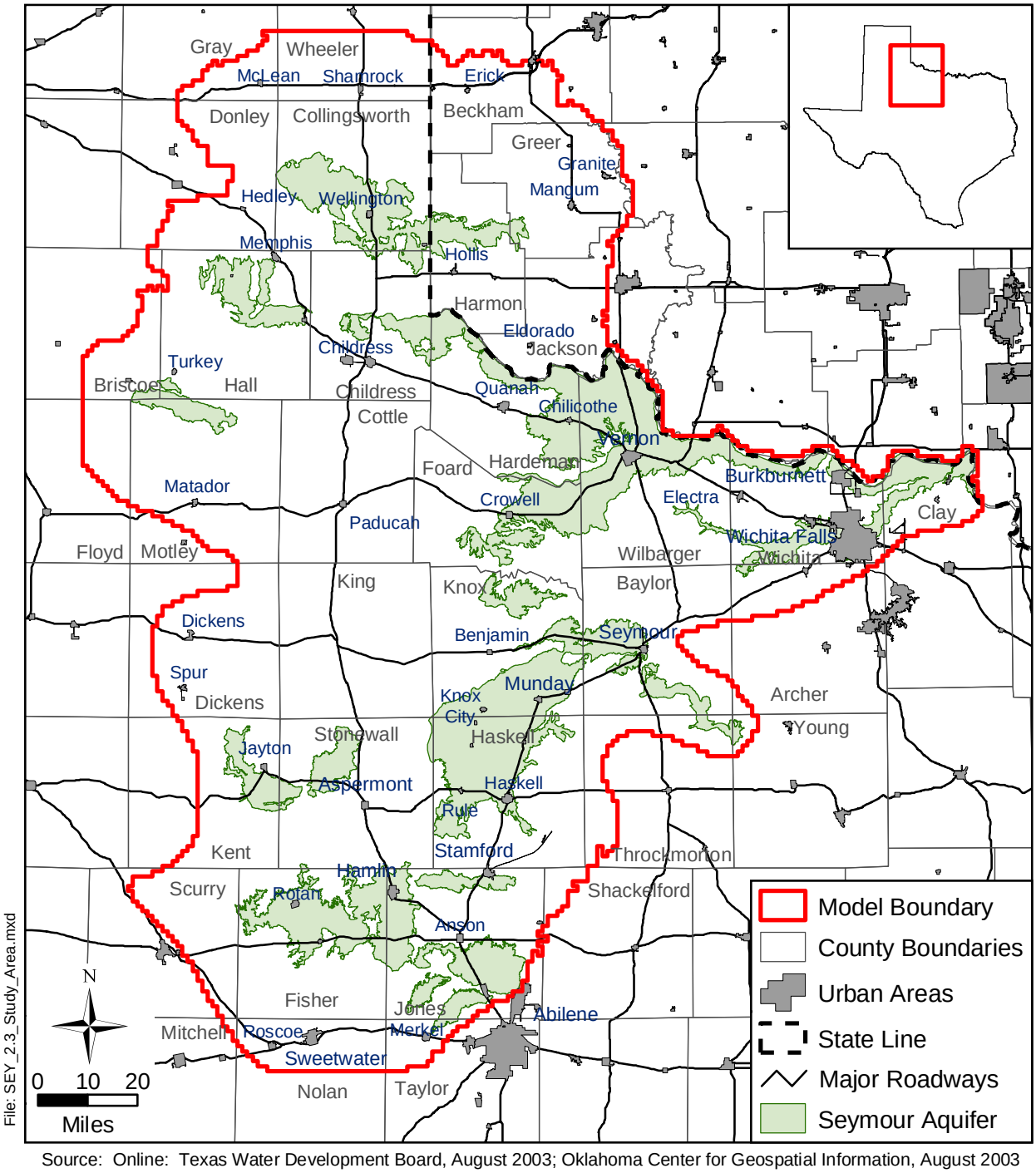

Source: Online: Texas Water Development Board, August 2003; Oklahoma Center for Geospatial Information, August 2003

Figure 2.3 Location of study area showing county boundaries, cities, and roadways.

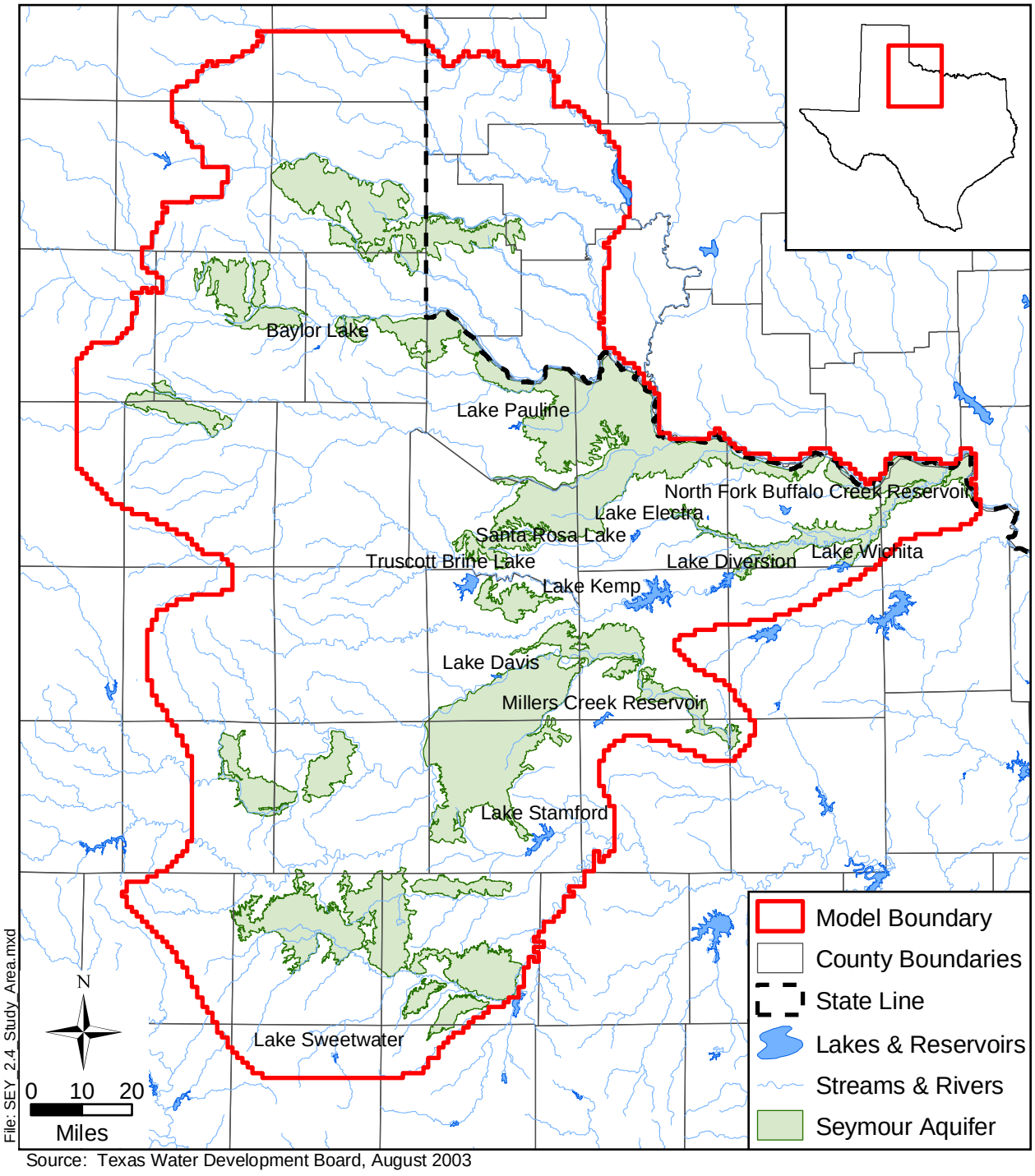

Figure 2.4 Location of study area showing lakes and rivers.

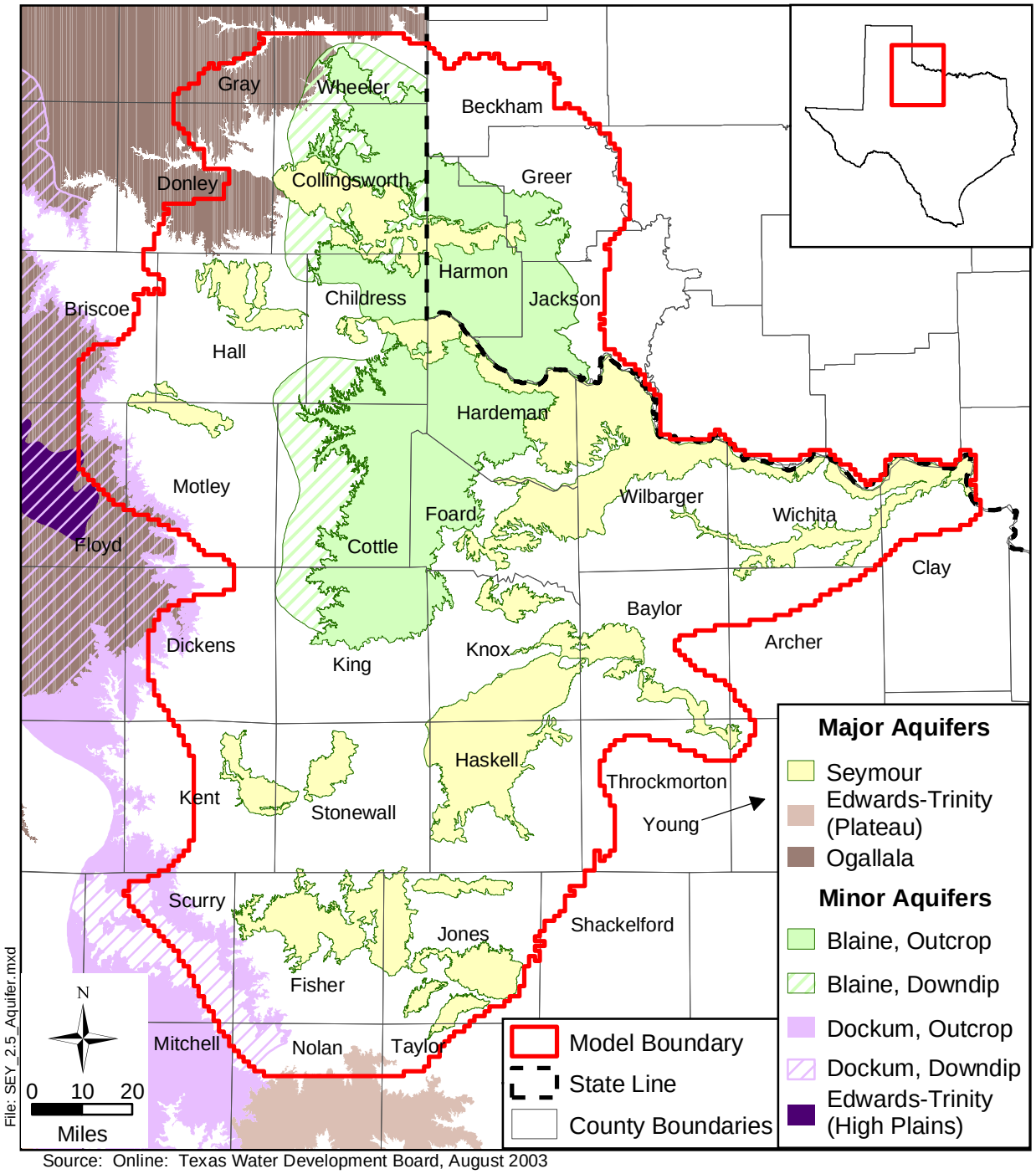

Source: Online: Texas Water Development Board, August 2003

Figure 2.5 Areal extents of the major and minor aquifers in the study area.

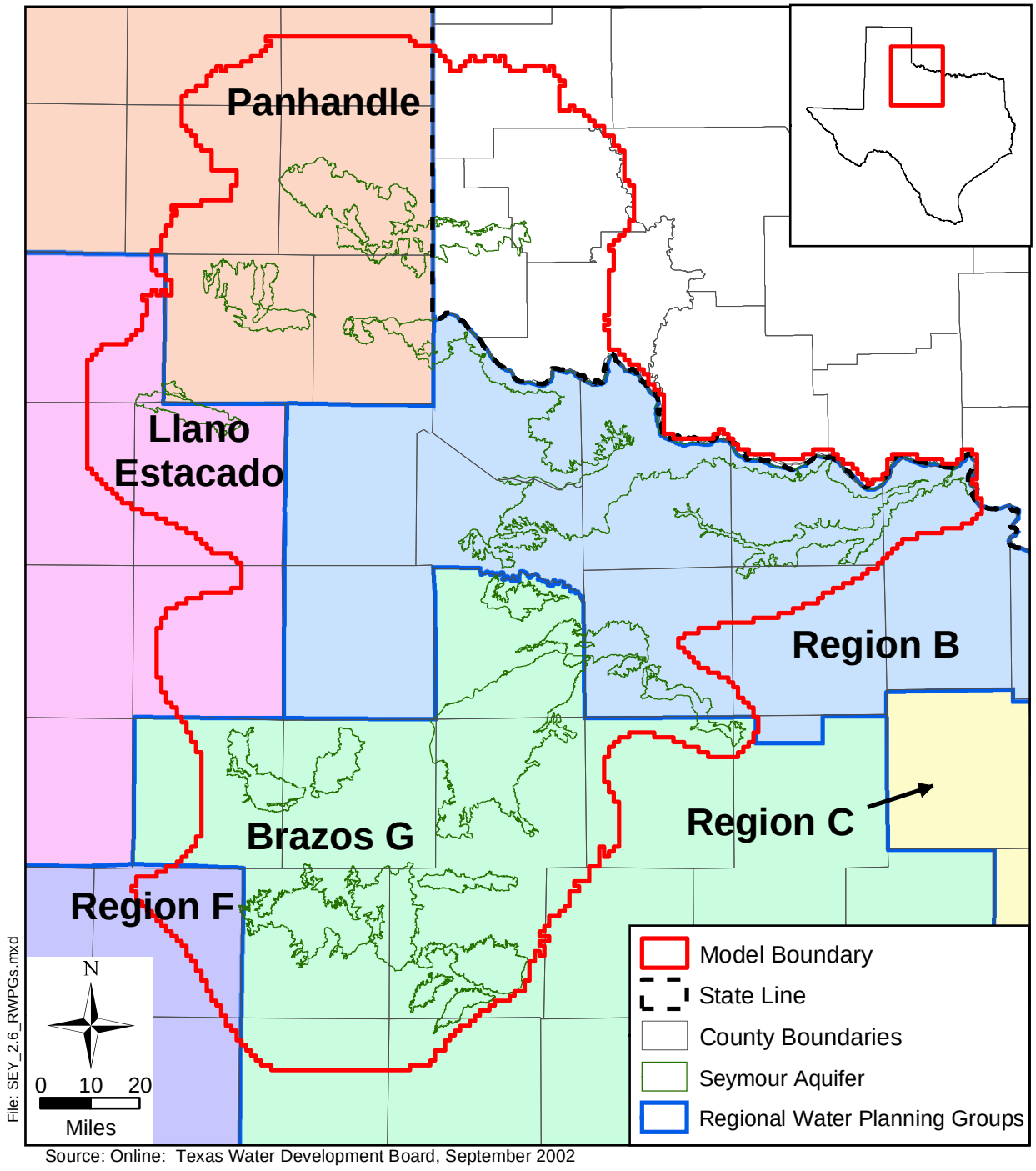

Figure 2.6 Location of Regional Water Planning Groups in the study area.

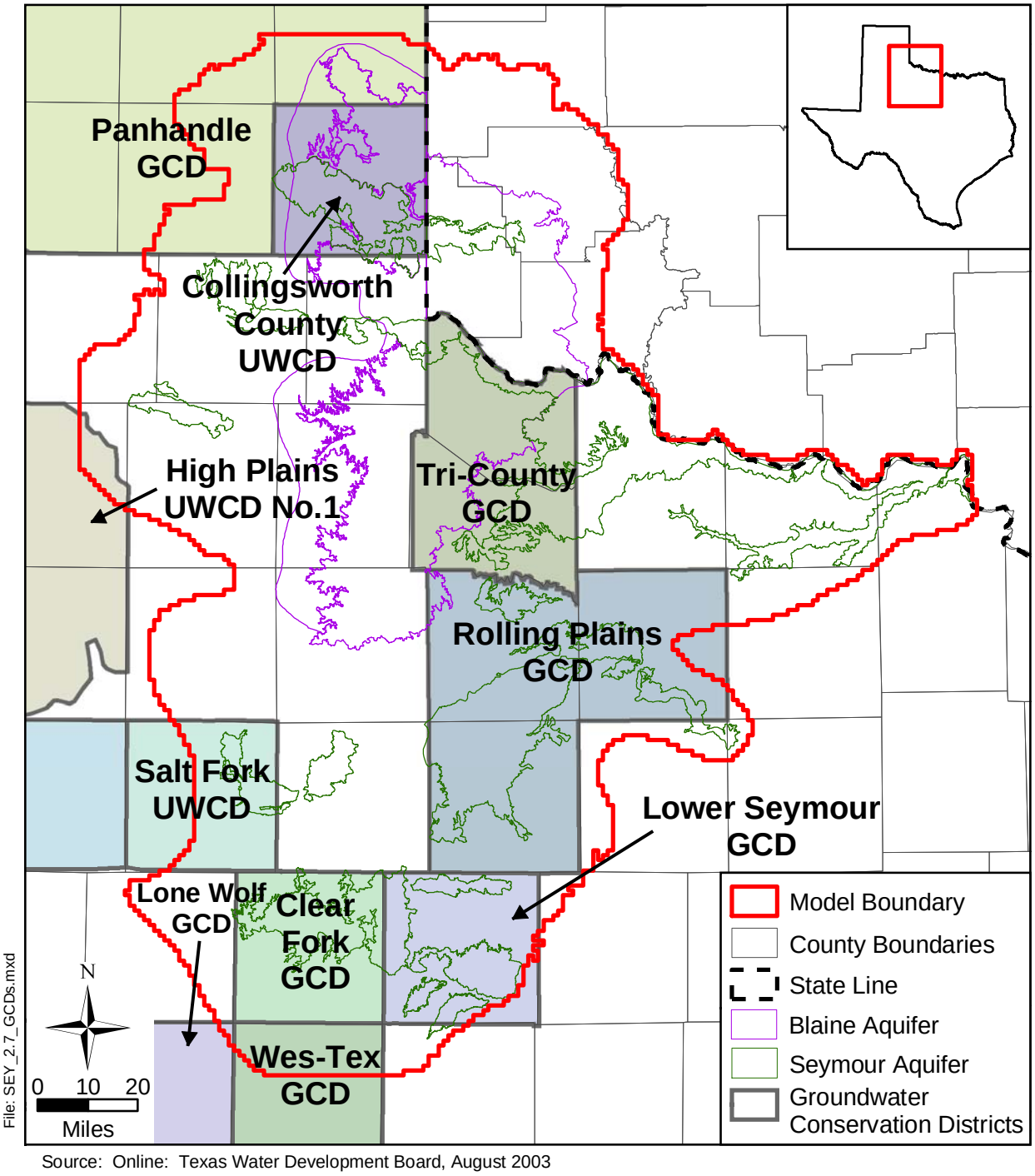

Figure 2.7 Location of Groundwater and Underground Water Conservation Districts in the study area.

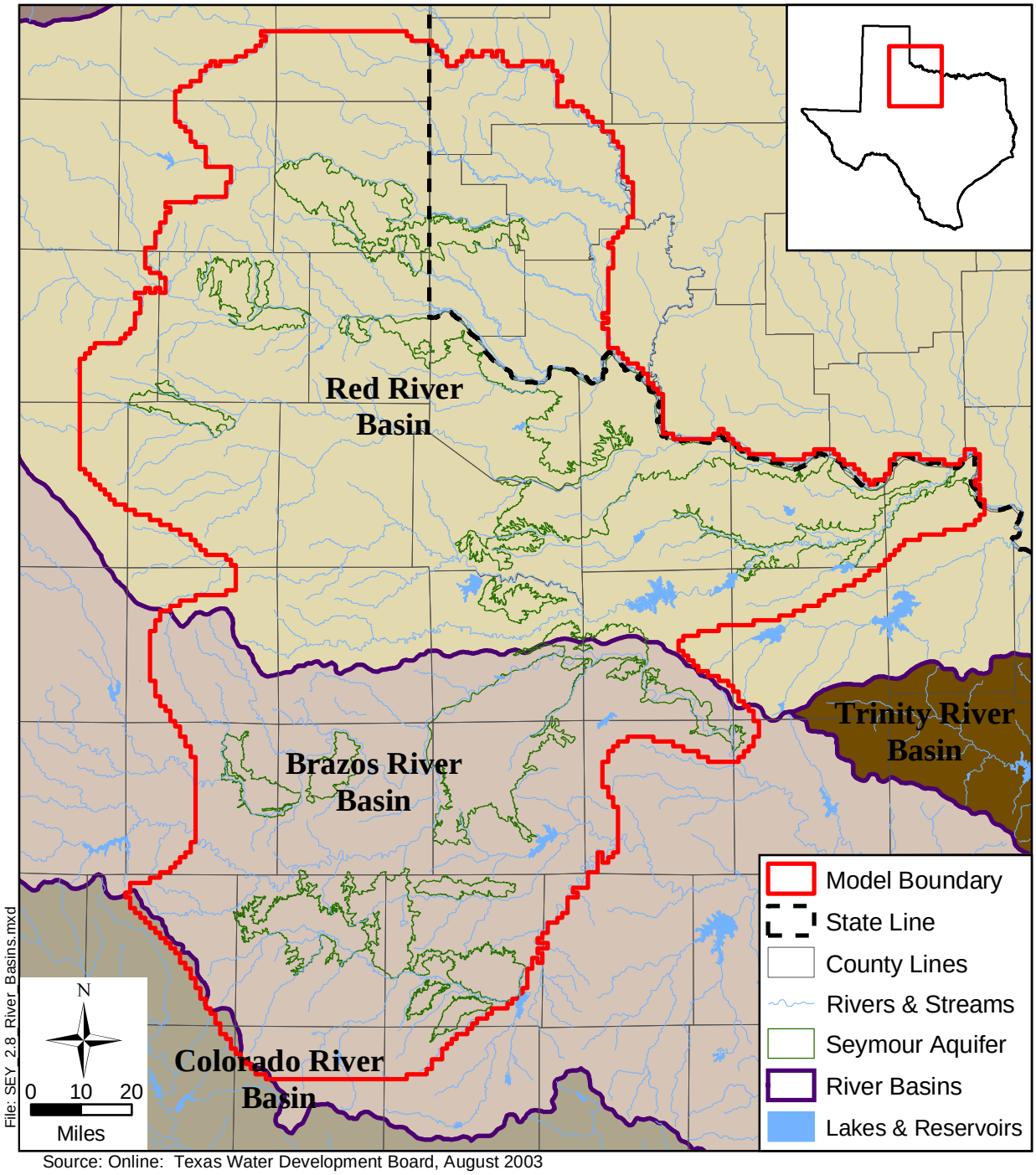

Figure 2.8 Major river basins in the study area.

2.1 Physiography and Climate

The study area is located almost completely within the North-Central Plains physiographic province (Figure 2.9). This province is distinguished by "An erosional surface that developed on upper Paleozoic formations..."[1]. The topography, which ranges in elevation from 3,000 to 900 feet above sea level from east to west, is characterized by low north-south trending ridges. The geologic structure is predominantly a westward dip with minor faults. The bedrock types for this province are limestone, sandstone, and shale.

The study area is located almost completely within the Rolling Plains ecological region, which covers an estimated 27 million acres in Texas[2]. Together with the High Plains region, the Rolling Plains represent the southern end of the Great Plains of the Central United States. The Rolling Plains ecological region is bordered to the west by the High Plains ecological region, to the east by the Oak Woods and Prairies ecological region, and by the Edwards Plateau ecological region to the south (Figure 2.10). The northern border is less definitive and continues into the Great Plains. Changes in vegetation mark the differences between the High Plains and the Rolling Plains in Texas. The study area is characterized by mesquite and oak trees with the density of trees decreasing from the southeast to the northwest. Grasses with scattered mesquite trees dominate on the prairie areas and grasses with juniper and oak trees dominate on the rough and broken ground in the study area. The active model area was considered a prairie ecosystem and was populated with bison until about 1870 when the bison were removed and most of the grassland areas with level terrain were broken out for cropland.[3]

Figure 2.11 provides a topographic map of the study area. Generally, the surface elevations decrease from west to east across the active model area. The ground-surface elevation varies from over 3,000 feet above sea level in the west on the Caprock to less than 900 feet above sea level in the east along the Red and Wichita river valleys. Several canyons of moderate depth are located in the western portion of the area. West to east trending river systems have created broadly incised river valleys that are up to 100 feet lower than the surrounding ground.

[1] http://www.lib.utexas.edu/geo/physography.html
[2] http://www.tpwd.state.tx.us/nature/ecoreg/pages/rolplain.htm
[3] http://www.tpwd.state.tx.us/expltx/eft/bison/rollingplains.htm

Erosion by these river systems has created the discrete pods of Quaternary-age alluvial deposits making up the Seymour aquifer.

The climate in the active model area is classified as Modified Marine[4]. Onshore flow of air from the Gulf of Mexico causes the marine climate. Distinctions in the climate occur based on the moisture content of the maritime air. Air from the Gulf decreases in moisture content from east to west as it travels across the state. Intrusion of continental air into the maritime air occurs seasonally and also affects the moisture content of the air. In Texas, the Modified Marine climate is classified as Subtropical, which is further divided into Humid, Subhumid, Steppe, and Arid. Over the study area, the subdivision Subhumid is applied. A Subtropical Subhumid climate is characterized by long, hot summers and moderately severe winters. In general, most rainfall occurs during the growing season from April through October. Often, rainfall is heavy over short periods of time. This leads to occasional severe flooding and significant periods of drought. The most extensive drought on record was in the early 1950s. Portions of the active model area (Baylor, Haskell, and Knox counties) have experienced drought conditions since 1998. This current drought is of similar duration as the drought in the 1950s but currently is not quite as severe. Average annual air temperature across the study area is mostly between 60 and 65°F as illustrated in Figure 2.12.

The average annual net pan evaporation rate in the active model area is high, ranging from a low of 82 inches per year in northern Wichita and Clay counties to a high of 102 inches per year in Scurry County (Figure 2.13). Precipitation data are available at approximately 90 stations within the active model area (Figure 2.14). Measurement of precipitation at most gages began in the 1930s or 1940s. In general, measurements are not continuous on a month by month or year by year basis for the gages. Historical average annual precipitation varies from a low of 19.8 inches in Hall County to a high of 28.9 inches in Wichita County. The absolute minimum and maximum annual precipitation within the active model area over the period of record varies from 6.0 inches in 1956 in Motley County to 53.6 inches in 1941 in Hardeman County, respectively. Annual precipitation recorded at six stations within the active model area is shown in Figure 2.15.

[4] http://www.met.tamu.edu/osc/TXclimat.htm

The PRISM (Parameter-elevation Regressions on Independent Slopes Model) precipitation dataset developed and presented online by the Oregon Climate Service at Oregon State University provides a good distribution of average annual precipitation across the model area based on the period from 1961 to 1990. Figure 2.16 provides a raster data post plot of the PRISM average annual precipitation across the model study area. Generally, the average annual precipitation decreases from the east to the west. The pan evaporation rate significantly exceeds the annual average rainfall, with the greatest rainfall deficit (approximately 78 inches per year) occurring in the central and western portion of the active model area.

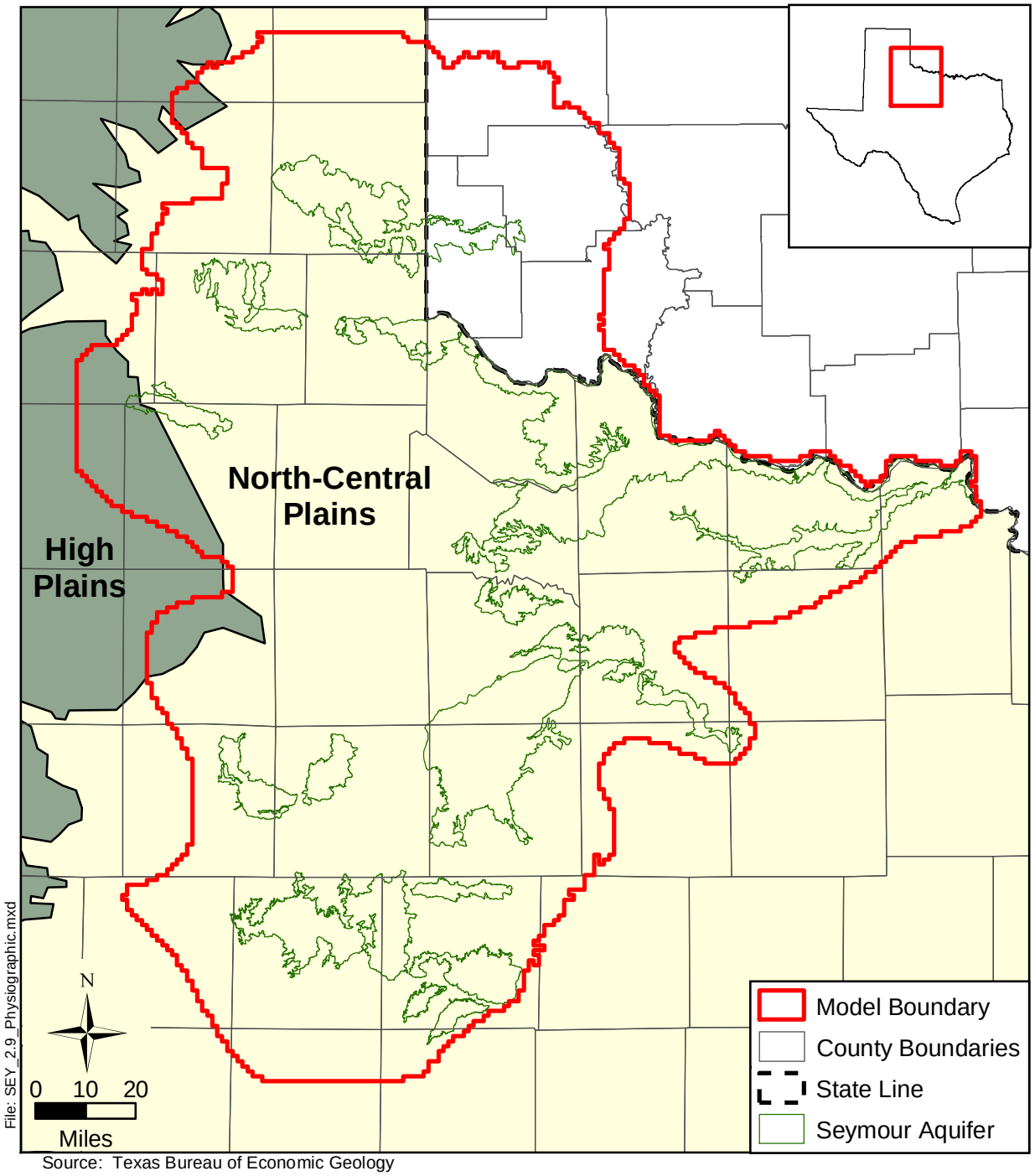

Figure 2.9 Physiographic provinces in the study area.

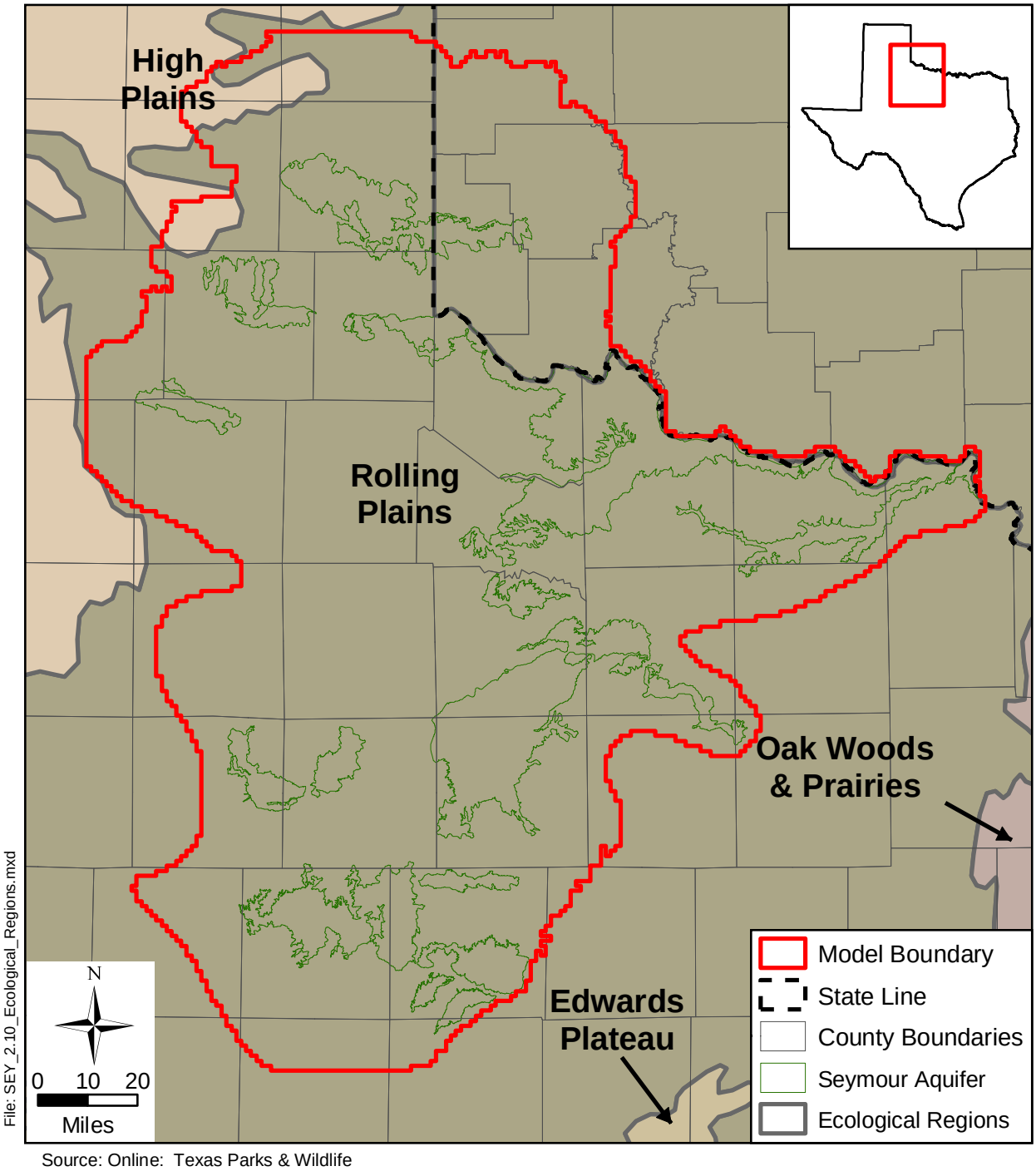

Figure 2.10 Ecological regions in the study area.

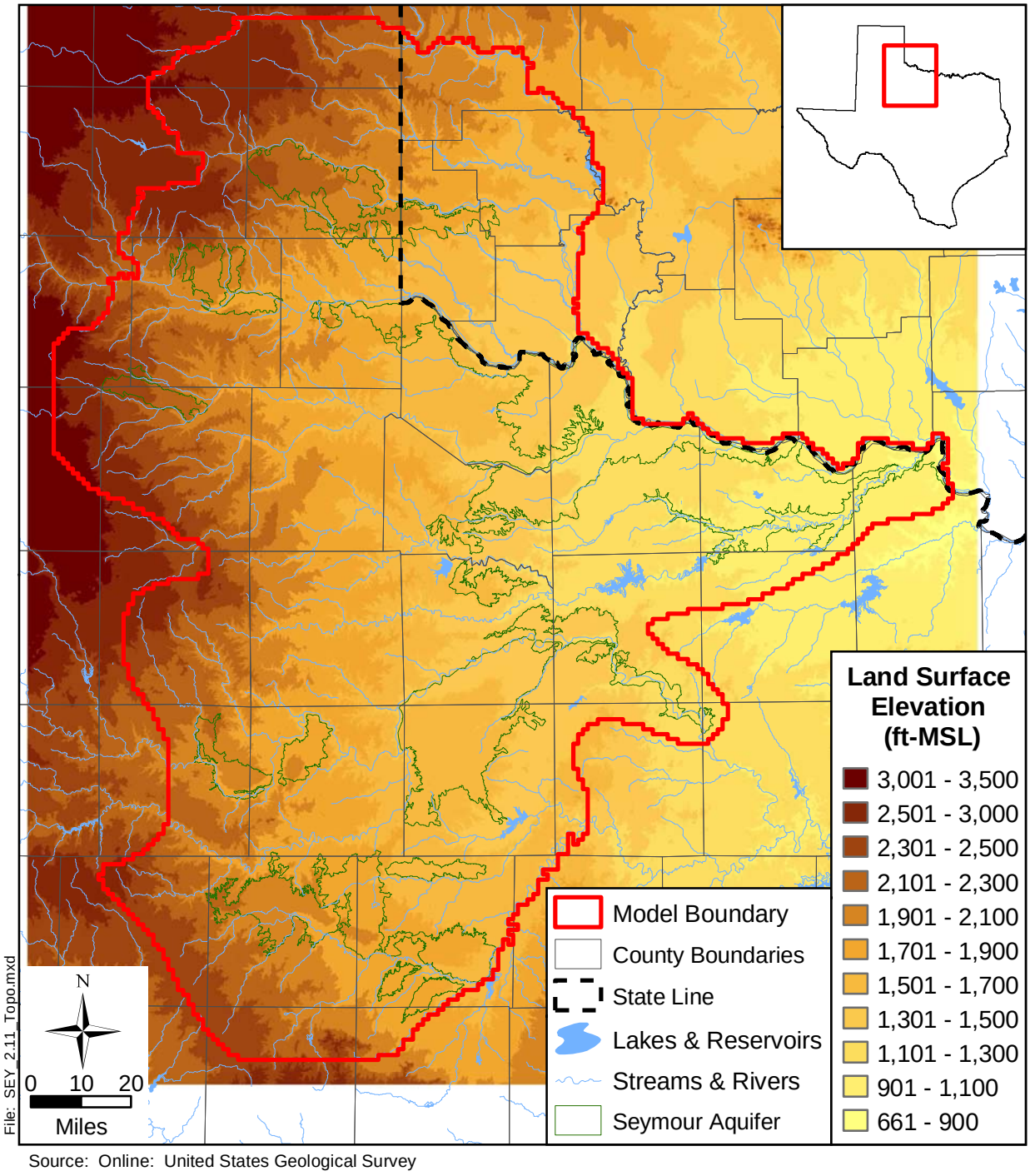

Figure 2.11 Topographic map of the study area.

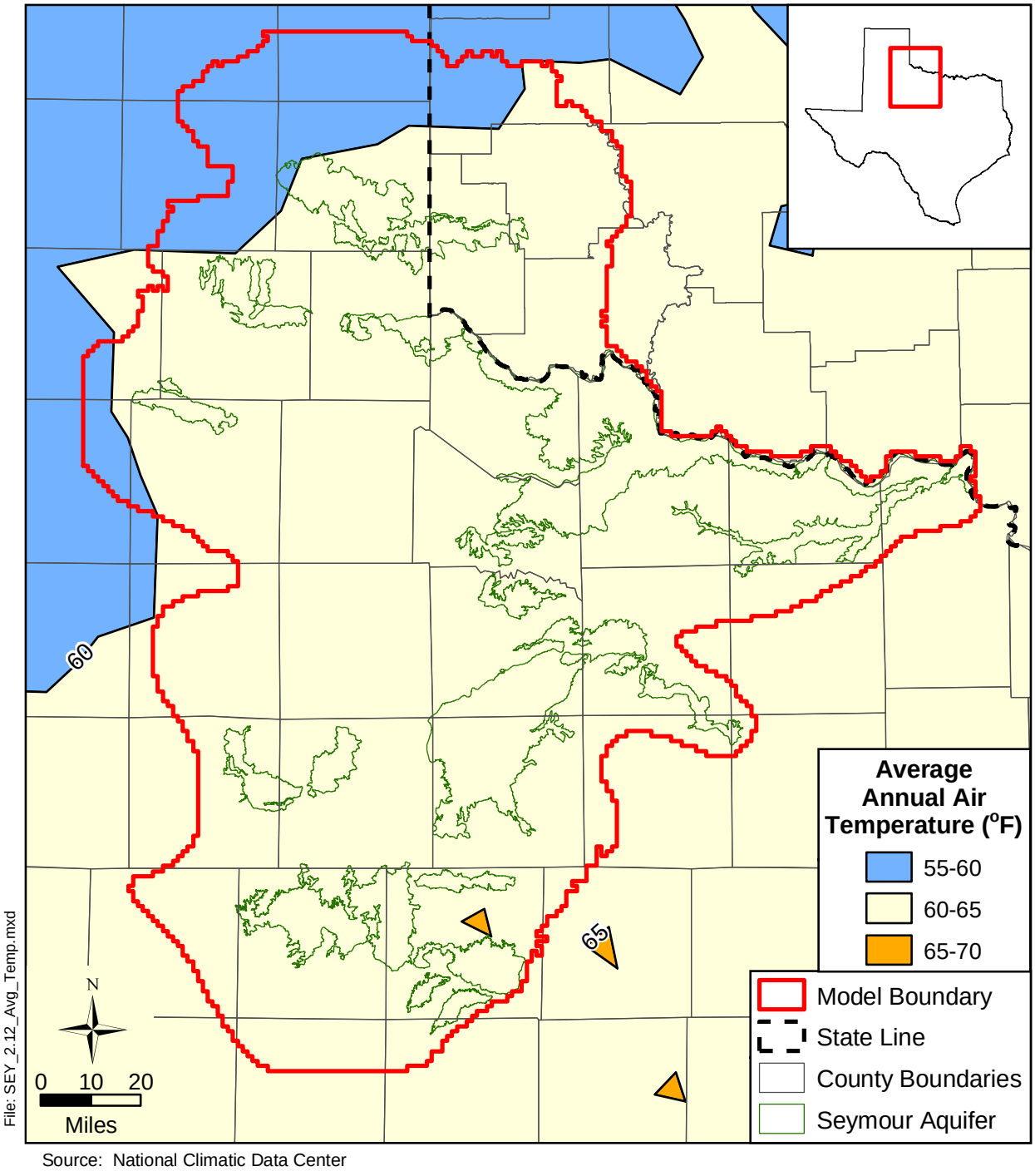

Figure 2.12 Average annual air temperature for the study area.

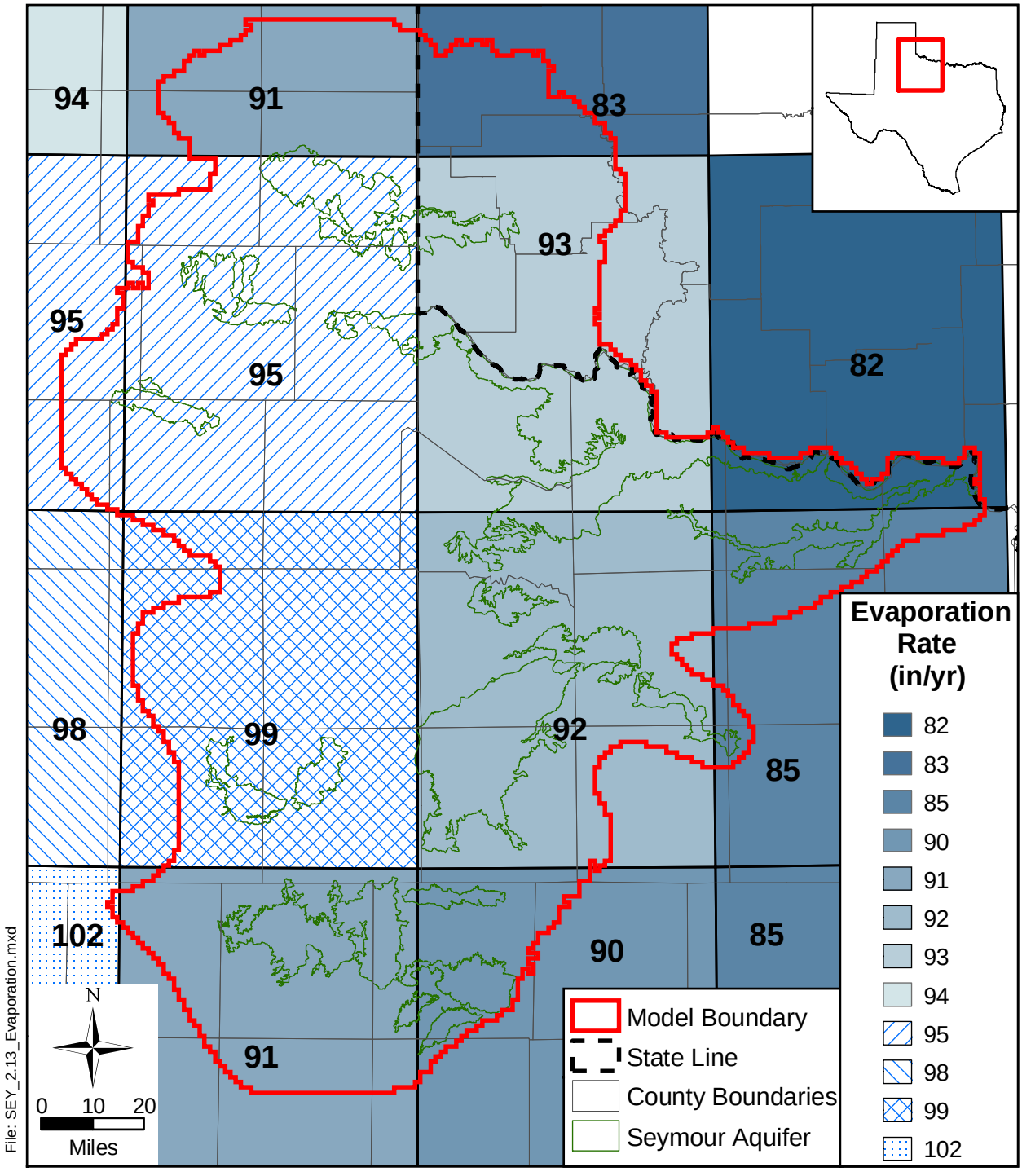

Source: Online: Texas Water Development Board, June 2003

Figure 2.13 Average annual net pan evaporation rate in inches per year over the study area.

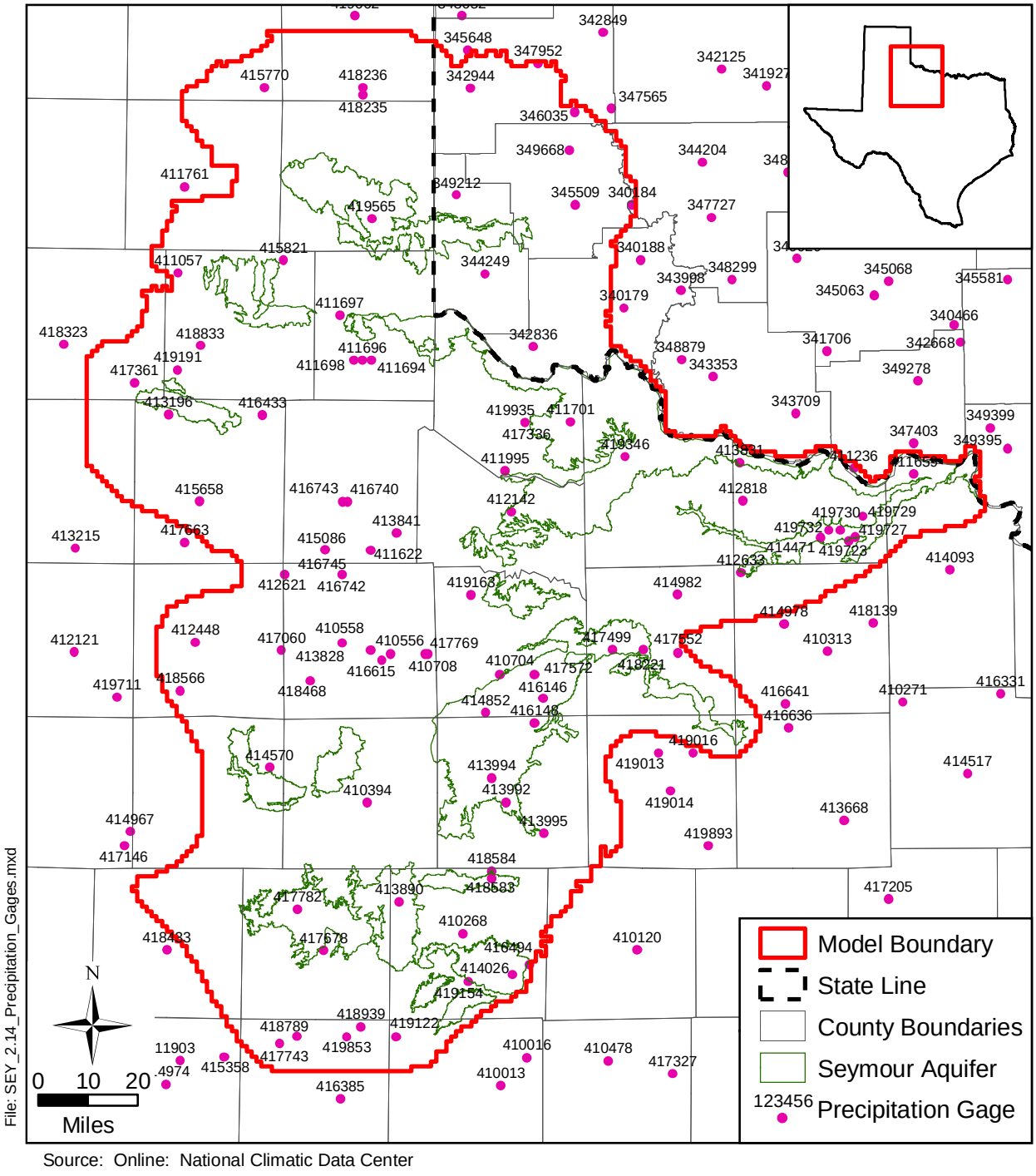

Figure 2.14 Location of precipitation gages in the study area.

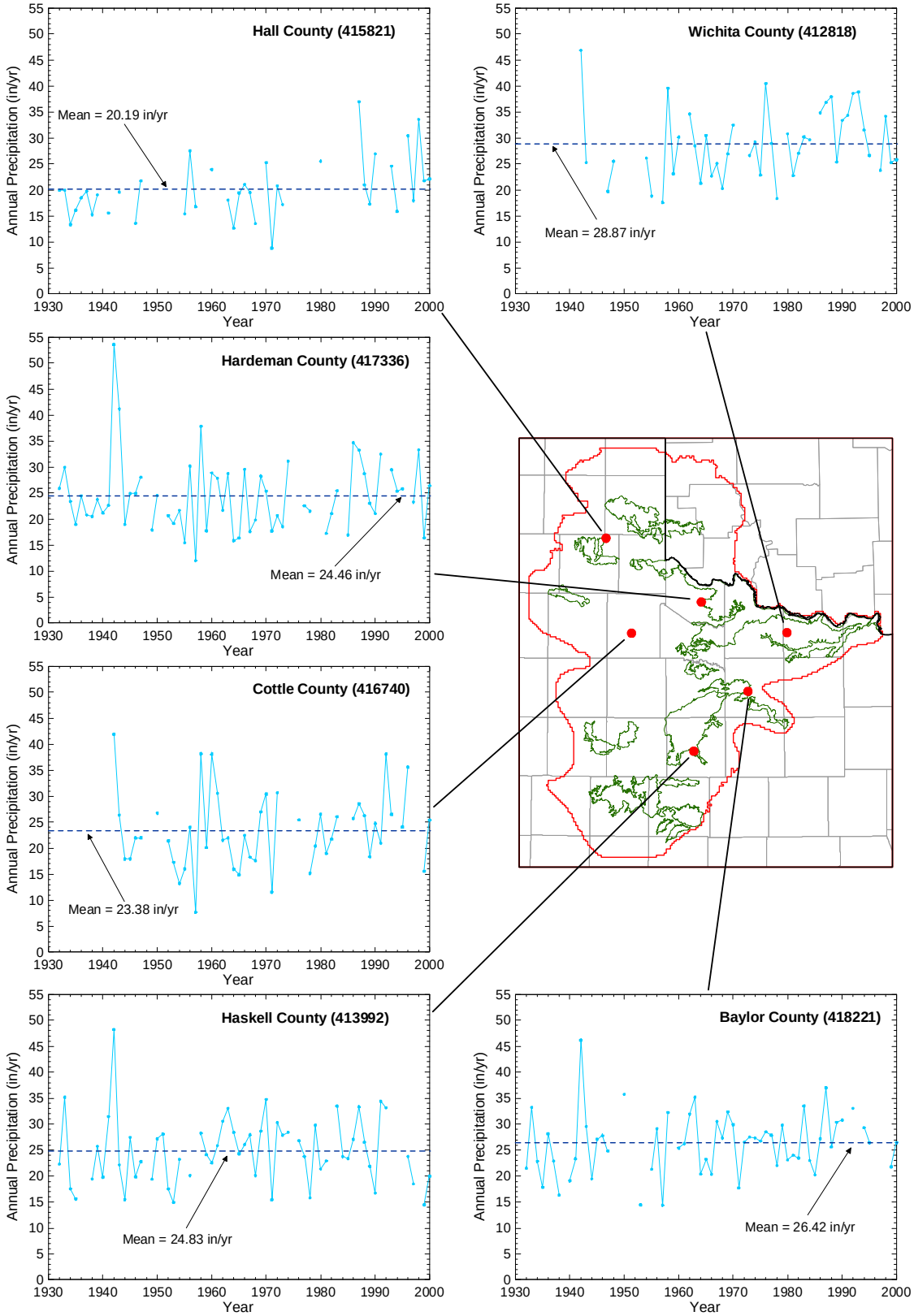

Figure 2.15 Annual precipitation time series for study area.

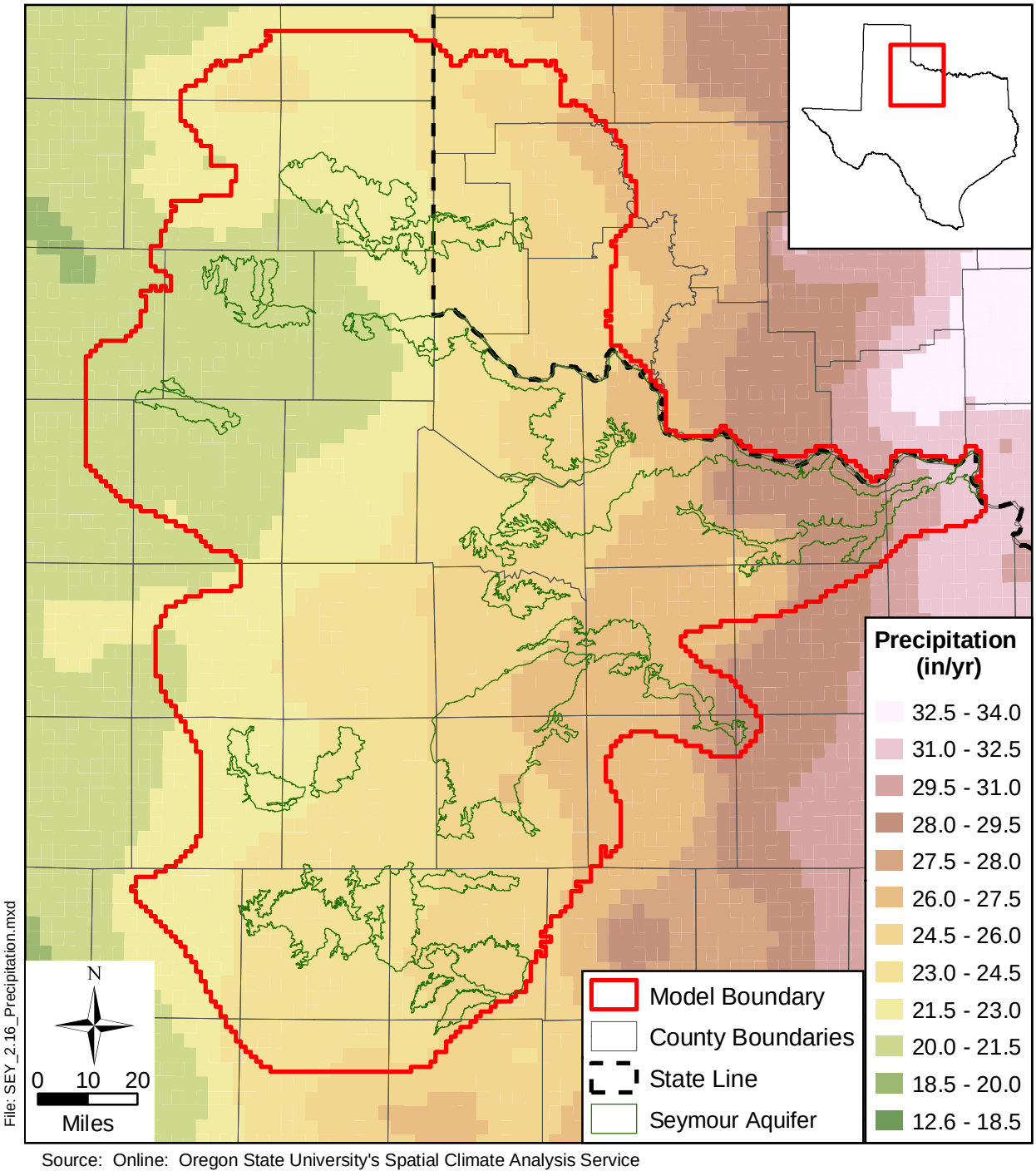

Figure 2.16 Average annual precipitation over the study area in inches per year (Source: Oregon Climate Service, Oregon State University, PRISM dataset).

2.2 Geology

The structural setting for the active model area is shown in Figure 2.17. In the subsurface, the area is characterized by the Hardeman Basin (also referred to as the Hollis Basin in the literature), the Wichita Mountains, the Red River Arch, the Baylor Syncline, and the Concho Shelf. The following discussion of these features is from Price (1979) unless otherwise indicated. The oldest feature is the Red River Arch which has existed since Cambrian time and has been buried since Pennsylvanian time. Development of the Hardeman Basin and Wichita Mountains was coincident. Further deepening of the basin occurred during the Arbuckle orogeny in Pennsylvanian time. The Baylor Syncline along with the Bend Flexure were also formed during Pennsylvanian time. The Concho Shelf "is the result of subsidence and tilting, beneath the Midland basin, of the Concho arch which was once the most dominant feature of north-central and northwest Texas." (Price, 1978). This shelf, which is actually a portion of the former Concho Arch, is of upper-Pennsylvanian, early-Permian age (Price, 1978). None of these structural deformations have affected the Seymour or Blaine aquifers.

The surface geology in the study area (Figure 2.18) consists of Permian- through Quaternary-aged deposits. The Quaternary-age deposits making up the Seymour aquifer almost exclusively overlie Permian deposits. From oldest to youngest and east to west, these Permian deposits form the Wichita Group, the Clear Fork Group, the Pease River Group (of which the Blaine Formation is a member), the Whitehorse Group, and the Quartermaster Formation. The strike of the Permian units is from north-northeast to south-southwest. A schematic of the stratigraphy in the active model area is provided in Figure 2.19. The westerly dip of the Permian strata shown on this figure is the result of westerly tilting caused by development of the Concho Arch. Stratigraphic cross sections in Figures 2.20 and 2.21 show the eastwardly dip of the ground surface and the westerly dip of the Permian formations. The cross section in Figure 2.22 shows the relationship between the alluvium deposits (Seymour aquifer), the Whitehorse Group, the Dog Creek Shale, and the Blaine Formation in Collingsworth County.

The Seymour aquifer, as defined by the TWDB, is composed of remnants of the Seymour Formation, the Lingos Formation, and younger alluvial deposits all of Quaternary age (Figure 2.23). All material forming the Seymour aquifer are unconsolidated alluvial sediments of non-marine origin deposited on the erosional surface of Permian beds. In general, sediments

of the Seymour aquifer are predominantly material eroded from the High Plains and deposited by eastward moving streams (R.W. Harden and Associates, 1978; Nordstrom, 1991; Duffin and Beynon, 1992). It is likely that the sediments originally blanketed the entire region but were subsequently eroded by recent streams, leaving only remnants of the once continuous deposits (Ogilbee and Osborne, 1962; Preston, 1978; Price, 1978). Alluvial deposits of the Seymour aquifer also include recent fluvial sedimentation from rivers and streams, terrace deposits, and eolian (windblown) sands.

Sediments of the Seymour aquifer are composed of clay, silt, sand, conglomerate, gravel, and some caliche. In general, the sediments are finer near the top and coarsen with depth. The upper portion contains beds of fine-grained sand with silt or clay and some caliche. A basal section of coarse sand and gravel beds is present in many portions of the aquifer. Individual beds within the Seymour aquifer are discontinuous and grade laterally into beds of coarser or finer grained material. The thickness of the Seymour aquifer varies from 0 to 360 feet but is usually less than 100 feet (Duffin and Beynon, 1992). This variation is due to the uneven erosional surface of the underlying Permian beds. Where the aquifer overlies a buried channel, it has a greater thickness and an increased amount of coarse material at its base. Where the aquifer is thin, it consists predominantly of finer-grained material.

The Blaine Formation of the Pease River Group was created during the Permian-age deposition of redbeds and evaporites when the southwestern United States was covered by a broad, shallow sea. The formation consists of beds of gypsum, anhydrite, halite, dolomite, sandstone, and shale. The evaporite beds originated from marine deposits from the shallow sea, and the sandstone and shale deposits originated from the deposition of stream and river sediments into the sea (Johnson, 1990). Not all bed materials are found throughout the formation. In general, the individual beds of gypsum and dolomite are laterally continuous. The different beds within the Blaine Formation were deposited in a cyclic manner (Johnson, 1990). More than seven distinct cycles have been identified within the formation. The Blaine Formation is described as having five predominant members in both Hardeman and Wheeler counties and eastern Gray County. In Hardeman County, the major members consist of three gypsum beds and two dolomite beds (Maderak, 1972). Four gypsum beds and one dolomite bed make up the five major members in Wheeler and eastern Gray counties (Maderak, 1973). Sediments of the Blaine Formation were deposited in the Hardeman Basin between the Wichita

Mountains and the Red River Arch. The Blaine Formation is overlain by the Dog Creek Shale. In some areas, distinguishing between these two units is difficult, and the two are combined. The Flowerpot Shale confines the Blaine Formation from below.

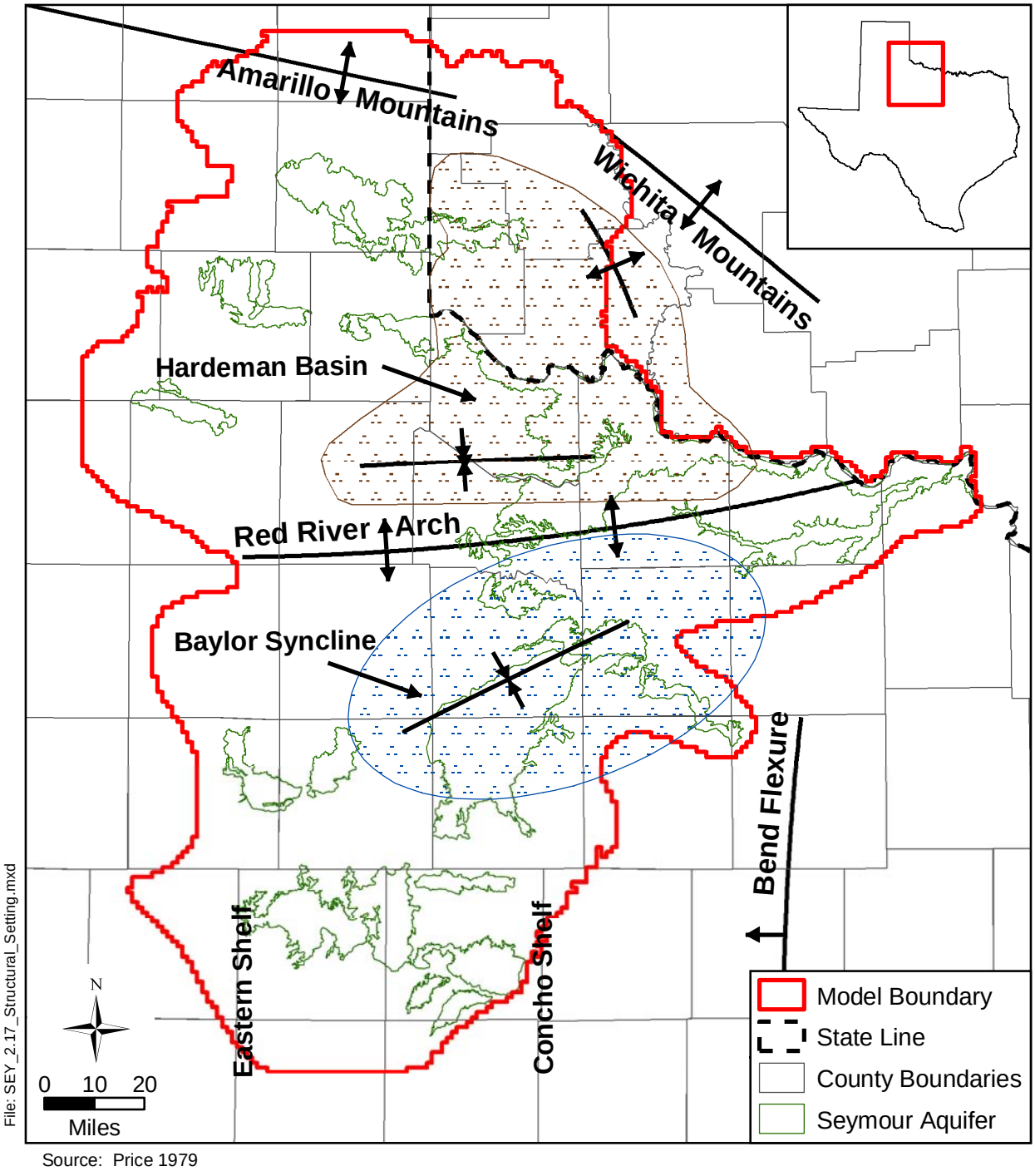

Figure 2.17 Map of major structural features in the study area (after Price, 1979).

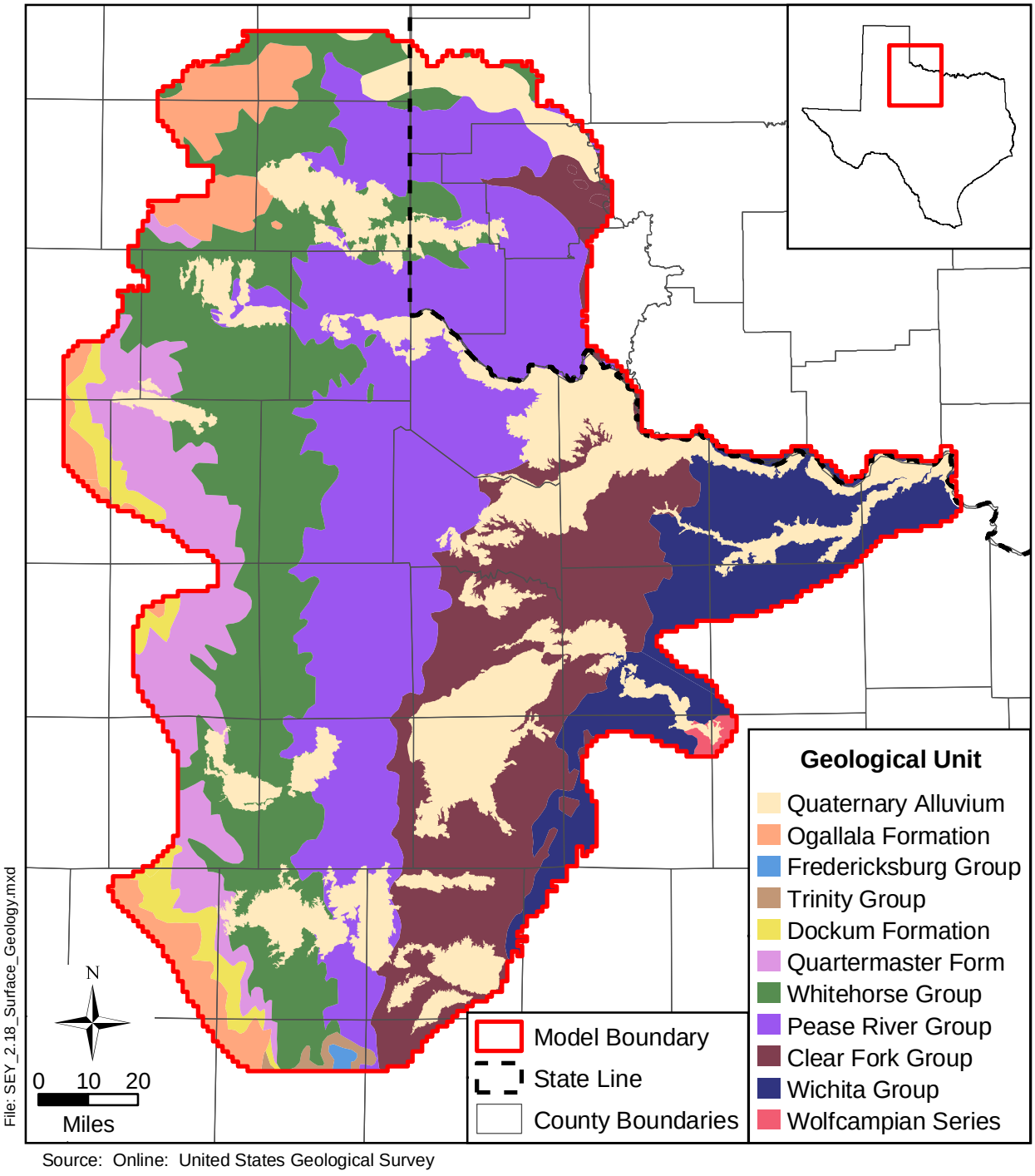

Figure 2.18 Surface geology of the study area.

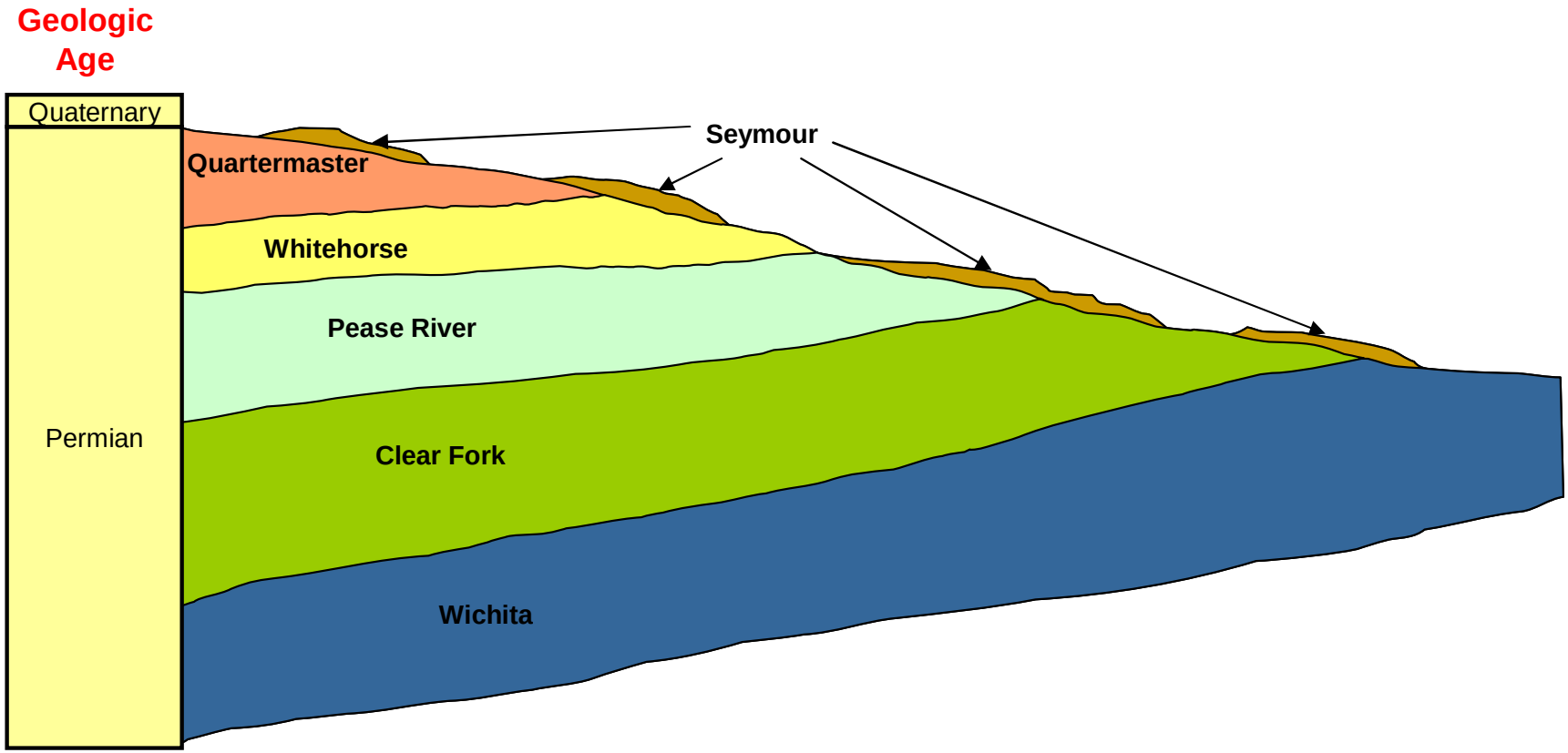

Figure 2.19 Schematic of generalized stratigraphy across the study area.

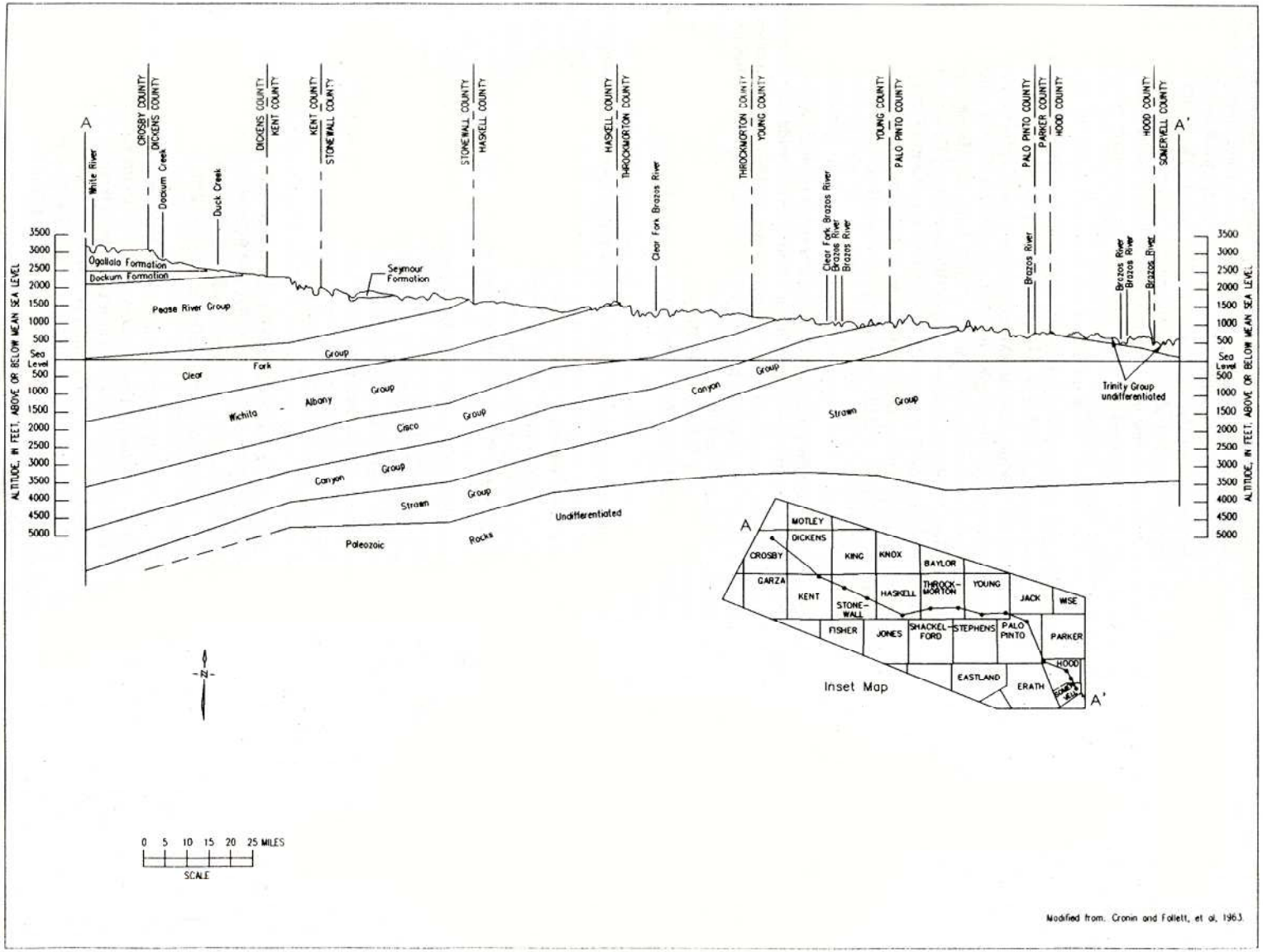

Figure 2.20 Cross section showing the major stratigraphic units across the active model area (from Duffin and Beynon, 1992).

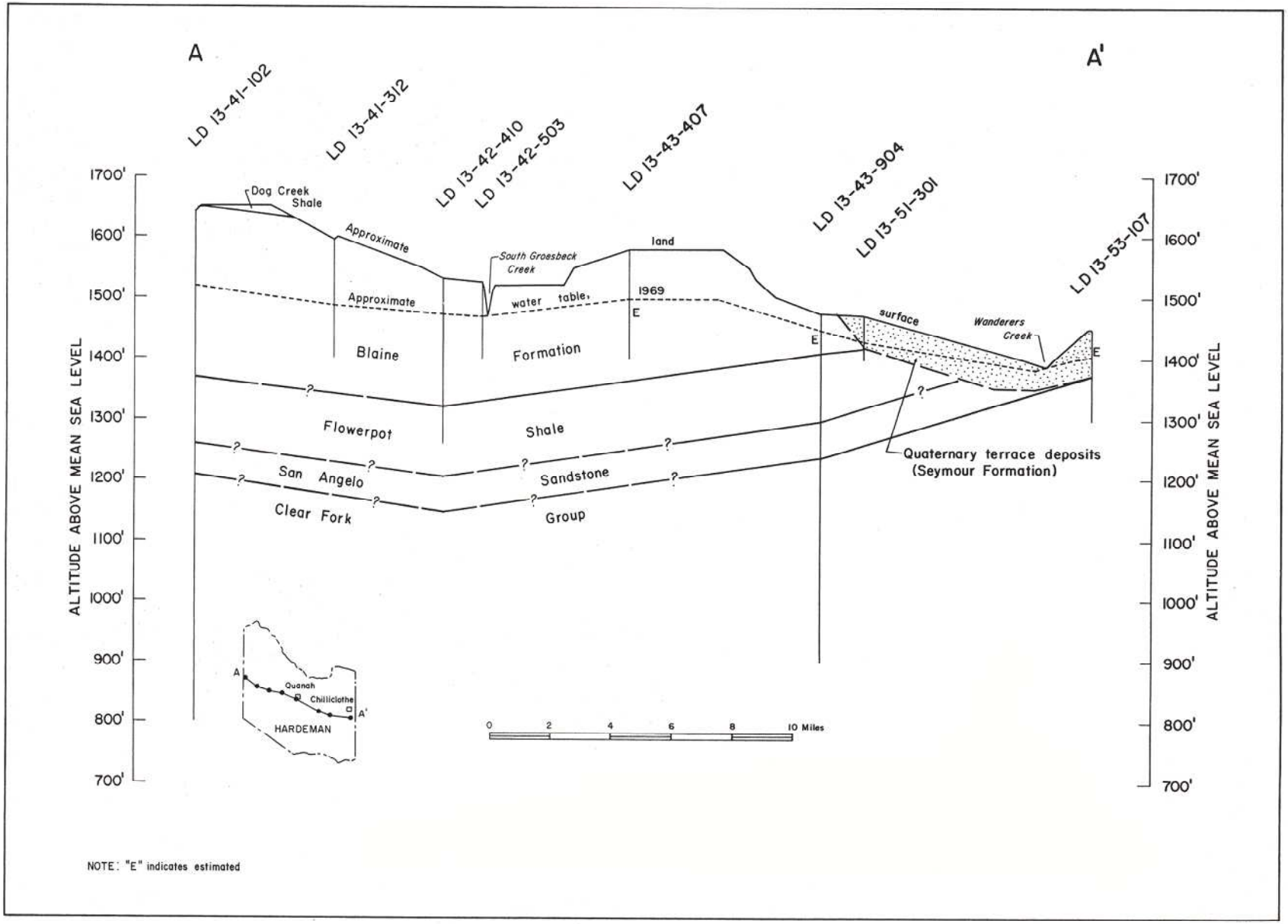

Figure 2.21 East-west structural cross section across Hardeman County (from Maderak, 1972).

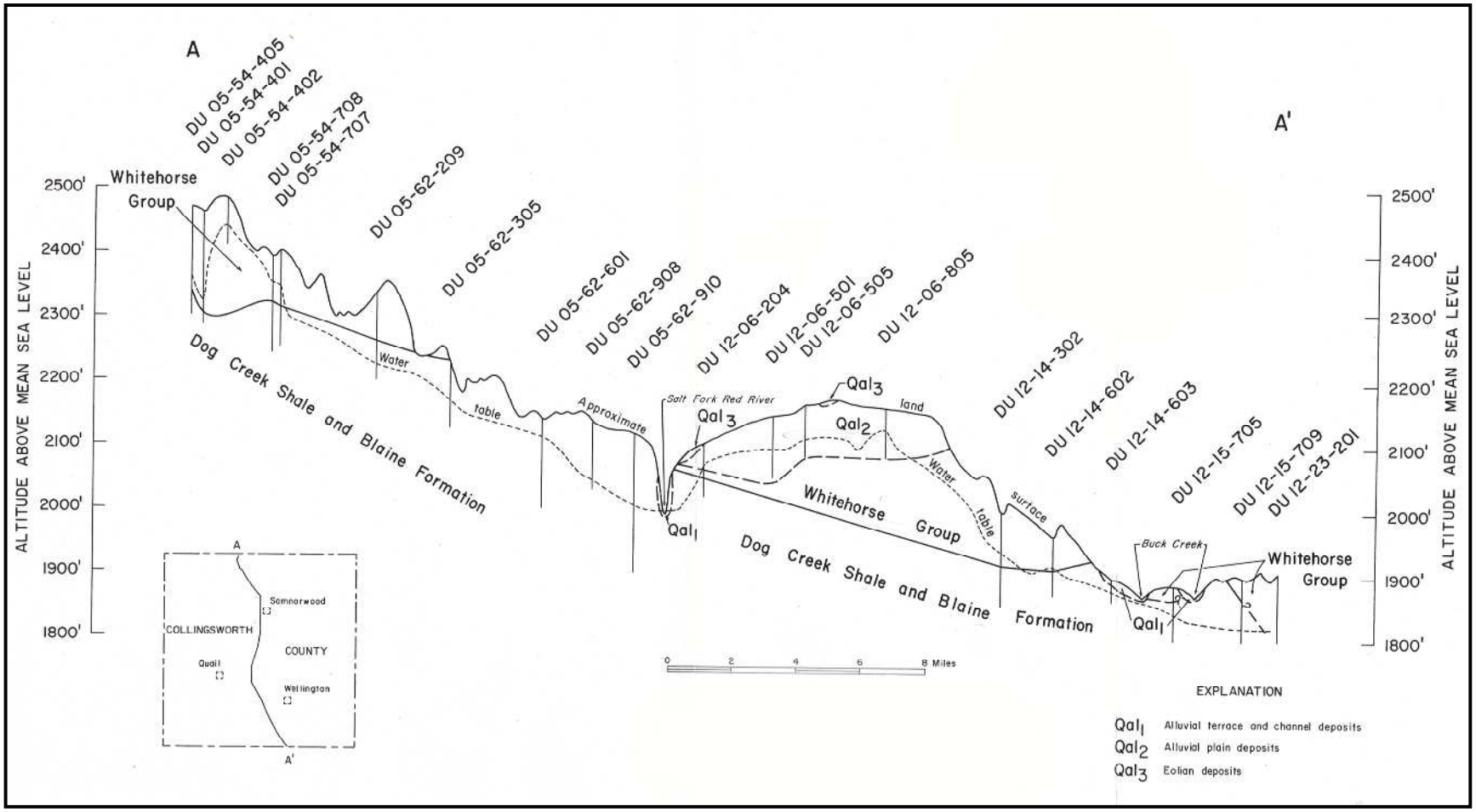

Figure 2.22 North-south structural cross section across Collingsworth County (from Smith, 1970).

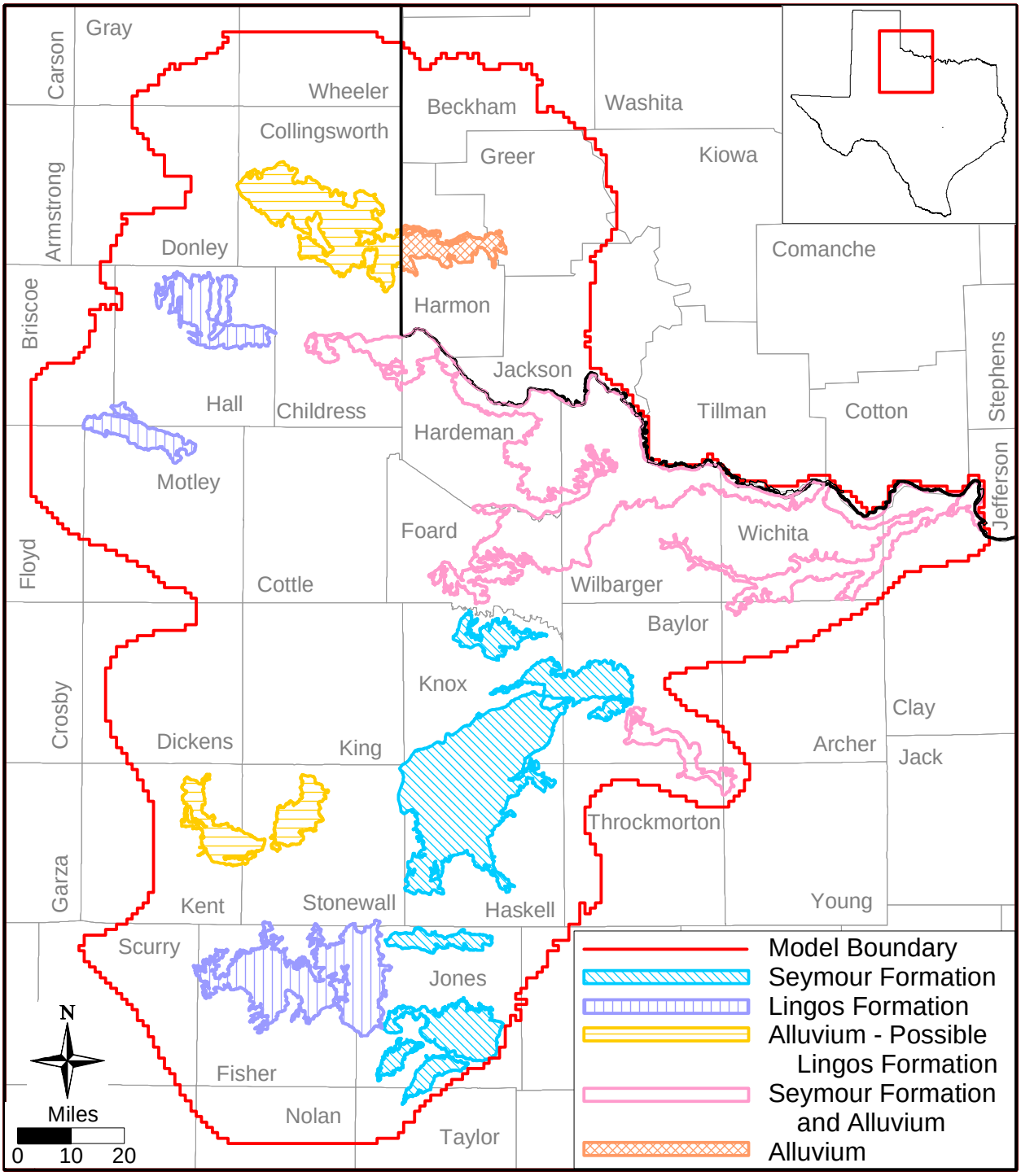

Figure 2.23 Various geologic materials forming the Seymour aquifer.

3.0 PREVIOUS INVESTIGATIONS

The Seymour aquifer has been studied by the various past and present Texas state agencies responsible for water resources (i.e., the Texas Board of Water Engineers, the Texas Water Commission, the Texas Department of Water Resources, and the Texas Water Development Board), the U.S. Geological Survey (USGS), and the Bureau of Economic Geology. Numerous documents have been published for the counties in the study area. A review of groundwater development in the Seymour and Blaine aquifers based upon the available county groundwater reports can be found in Appendix A of this report. Several investigators have studied the stratigraphy and depositional history of the sediments of Texas including those for the Seymour and Blaine aquifers. The most relevant of these within the Seymour include R.W. Harden and Associates (1978), which analyzed data from the Seymour Formation in Haskell and Knox counties, as well as a number of county reports (including reports for Baylor, Wilbarger, and Jones counties) developed in the late 1970s by the Texas Department of Water Resources. The development of the Seymour GAM has borrowed extensively from the works described above.

In addition to these stratigraphic and groundwater studies, there has been one groundwater model developed with a model domain that overlaps the Seymour GAM study area. Figure 3.1 shows the model boundaries for this previous modeling study by Runkle & McLean (1995) for the Blaine aquifer in Oklahoma. The Blaine aquifer was modeled as a single layer. The model was developed for steady-state conditions corresponding to February 1988. Simulations were performed with the finite-difference model of McDonald and Harbaugh (1988). The grid consisted of 43 x 47 1-mile by 1-mile grid blocks with 1,030 active blocks over a 2,021 square-mile area. Hydraulic conductivity was spatially zoned (71, 17, and 4.2 ft/day). The highest hydraulic conductivity value was assigned where the overlying Dog Creek Shale was thinnest. Recharge was estimated to range from 0.1 to 2.5 inches per year across the study area and average 1.5 inches per year (6.3 percent of precipitation). The highest recharge rate was applied where the overlying Dog Creek Shale was thinnest. The hydrogeologic data collected for the Blaine aquifer investigation and modeling study are reported in Runkle et al. (1997).

This model provides information which is both relevant and useful to the study of groundwater availability in the Seymour aquifer study area, although that information is specific

to the Blaine aquifer and principally in Oklahoma. This previous modeling study does not address a number of the GAM specifications or requirements defined by the TWDB. Specifically, the GAM models are expected to be calibrated to both steady-state and transient conditions.

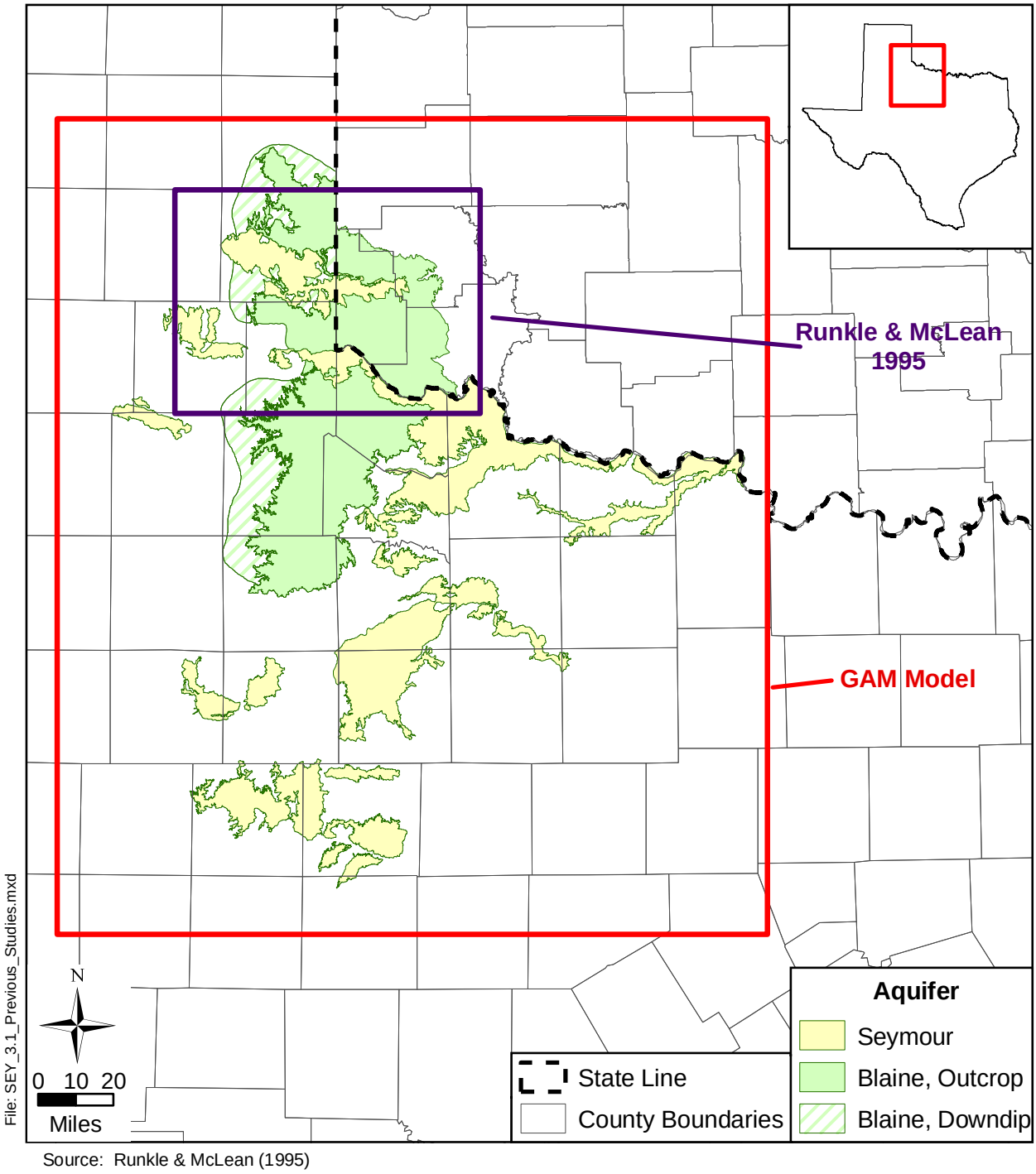

Figure 3.1 **Seymour GAM model boundary with previous modeling study boundary which included the Blaine aquifer.**

This page intentionally left blank.

4.0 HYDROGEOLOGIC SETTING

The hydrogeologic setting of the Seymour aquifer is defined by the hydrostratigraphy, hydraulic properties, structure, regional groundwater flow, surface and groundwater interaction, and recharge and discharge. The characterization of the hydrogeologic setting is based on previous geologic and hydrologic studies in the area and compilation and analyses of structure maps, hydraulic properties, water-level data, spring and stream flow data, and climatic information.

4.1 Hydrostratigraphy

The Seymour aquifer is a water-table aquifer located in the Rolling Plains of north-central Texas. The TWDB identifies the existence of the aquifer in isolated remnants of Quaternary-age deposits. The individual remnants are referred to as 'pods' in this report. A pod is meant to refer to an area of the Seymour aquifer that is physically and hydraulically isolated from other portions of the aquifer. Figure 4.1.1 shows numbers associated with each pod which will be used in the remainder of this report to facilitate the discussion. The hydrostratigraphic units for the Seymour aquifer include the Seymour Formation, Lingos Formation (as defined in Caran and Baumgardner, 1990) and alluvial deposits of Quaternary age (see Figure 2.23). All material forming the Seymour aquifer are unconsolidated alluvial sediments of non-marine origin deposited on the erosional surface of Permian beds. In general, sediments of the Seymour aquifer are predominantly material eroded from the High Plains and deposited by eastward moving streams (R.W. Harden and Associates, 1978; Nordstrom, 1991; Duffin and Beynon, 1992). It is likely that the sediments originally blanketed the entire region but were subsequently eroded by recent streams leaving only remnants of the once continuous deposits (Ogilbee and Osborne, 1962; Preston, 1978; Price, 1978).

Sediments of the Seymour aquifer are composed of clay, silt, sand, conglomerate, gravel, and some caliche. In general, the sediments are finer near the top and coarsen with depth. The upper portion contains beds of fine-grained sand with silt or clay and some caliche. A basal portion of coarse sand and gravel beds is present in many portions of the aquifer. This basal section is the predominant water-producing zone. Individual beds within the Seymour aquifer are discontinuous and grade laterally into beds of coarser or finer grained material. Sediments of

the aquifer are heterogeneous with the exception of the basal coarse material which is present inconsistently throughout the aquifer.

Permian sediments of the Wichita Group, Clear Fork Group, Pease River Group, Whitehorse Group, and Quartermaster Formation underlie the Seymour aquifer. The stratigraphic units making up the Permian sediments in the study area are summarized in Table 4.1.1. During the Permian period, the study area was covered by shallow seas characterized by continued rapid transgression and regression events. Sedimentation during these events yielded "…a thick sequence of relatively thin-bedded deposits of almost every type of depositional environment from shallow-shelf, through deltaic, fluvial, and continental..." (Preston, 1978). Ogilbee and Osborne (1962) state that the "Permian rocks are characterized by a large variety of sedimentary facies which include clastic and calcareous sediments, anhydrite, gypsum, salt, and other evaporites, and nonmarine red beds."

Table 4.1.1 Hydrostratigraphy and model layers.

System	Series	Group	Formation	Layer
Quaternary	Recent to Pleistocene		Alluvium	1
			Seymour	
Tertiary	missing			
Cretaceous				
Jurassic				
Triassic				
Permian	Ochoa		Quartermaster	2
	Guadalupe	Whitehorse		
		Pease River	Dog Creek Shale	
			Blaine Gypsum	
			Flowerpot Shale	
			San Angelo	
	Leonard	Clear Fork	Choza	
			Vale	
			Arroyo	
		Wichita (upper portion only)	Lueders	
			Clyde	

In general, the depositional environment was marine during early Permian time then changed to arid and continental in late Permian time (Ogilbee and Osborne, 1962). The following brief discussion of deposition of the Permian-age sediments is taken from Price (1978; 1979). Deposits of the Wichita Group consist of predominantly marine shales and shelf

limestones, indicating the presence of shallow seas. The seas became more restricted and the climate became more arid as indicated by the deposition of poorly developed limestones and dolomites interbedded with red beds and local anhydrite in the Clear Fork Group. The beginning of deposition of the Pease River Group is marked by an increase in nonmarine clastics. The subsequent deposition of thick evaporate beds interfingered with red beds, thin limestones, and dolomitic limestones suggests even more restriction of the seas and an even more arid climate. The clastic sediments at the base of the Pease River Group unconformably overlie the Clear Fork Group, suggesting uplift of the area between deposition of the sediments of the Clear Fork and Pease River groups. Table 4.1.2 summarizes general descriptions of the sediments found in the Permian units. The periods between the Permian and Quaternary are not recorded in the rock sequence in the study area due predominantly to continental uplift and erosion.

Table 4.1.2 General description of Permian units.

Group/Formation	General Description	Source
Quartermaster	Interbedded silt, siltstone, sand, silty to sandy shale, and sandstone with thin beds of gypsum, anhydrite, and dolomite.	Smith (1973)
Whitehorse	Interbedded sand, silty to sandy shale, sandstone, gypsum, and dolomite.	Smith (1973)
Dog Creek Shale	Shale with some thin beds of gypsum, anhydrite, and dolomite.	Maderak (1972)
Blaine Gypsum	Gypsum, anhydrite, dolomite, and limestone separated by shale beds.	Maderak (1972)
Flowerpot Shale	Shale with some thin beds of gypsum, anhydrite, and dolomite.	Maderak (1972)
San Angelo	Nonmarine series of sandstones, conglomerates, and shales.	Price (1979)
Choza	Persistent dolomite (Merkel Dolomite Member) at top of formation. Semi-persistent beds of dolomitic limestones and gypsum interbedded with shale and locally thin sandstone.	Price (1978)
Vale	Upper portion contains many thin beds of dolomite and gypsum interbedded with clay and shales; lower portion dominated by shale with thin stringers of dolomite and shaley sandstones.	Price (1978)
Arroyo	Thin bedded and poorly developed limestones, dolomites, and marls interbedded with thick shales and shaley sandstones.	Price (1978)
Lueders	Massive to thin beds of fossiliferous limestone interbedded with argillaceous limestone and shale.	Price (1978)
Clyde	Interbedded fossiliferous limestone, argillaceous limestone, and shale.	Price (1978)

The most important Permian unit in the model area for water-supply purposes is the Blaine Formation. A portion of this formation is considered a minor aquifer in Texas. The limited use of the Blaine Formation as a source for water south of central King County has precluded its identification as a minor aquifer in that area (Ashworth and Hopkins, 1995). The

Blaine Formation consists of cyclic deposits of marine and non-marine origin. The marine deposits include evaporates and limestone beds originating from the broad, shallow sea that once covered the southwestern United States. The non-marine deposits consist of sandstone and shale that originated from the deposition of stream and river sediments into the sea (Johnson, 1990). Many solution channels and caverns have developed in the gypsum and anhydrite beds of the Blaine Formation. Water chiefly occurs in these channels and caverns. The presence of these solution channels and caverns results in variable water transmissivity within the formation, with areas of high water yield located almost adjacent to areas of low water yield.

The hydrostratigraphic units for the Seymour aquifer include the Seymour Formation, Lingos Formation, and Quaternary alluvium deposits. These units make up layer 1, and the underlying Permian beds make up layer 2 of the Seymour aquifer GAM. The Permian beds dip to the west while the land surface dips to the east resulting in increasingly younger rocks from east to west. The Permian rock outcrops in bands trending north to northeast. From east to west, the Seymour aquifer overlies the Permian-age Wichita Group, Clear Fork Group, Pease River Group, Whitehorse Group, and Quartermaster Formation (see Figure 2.18). Since the hydrostratigraphic units underlying the aquifer vary across the model region, the units making up model layer 2 also vary across the model.

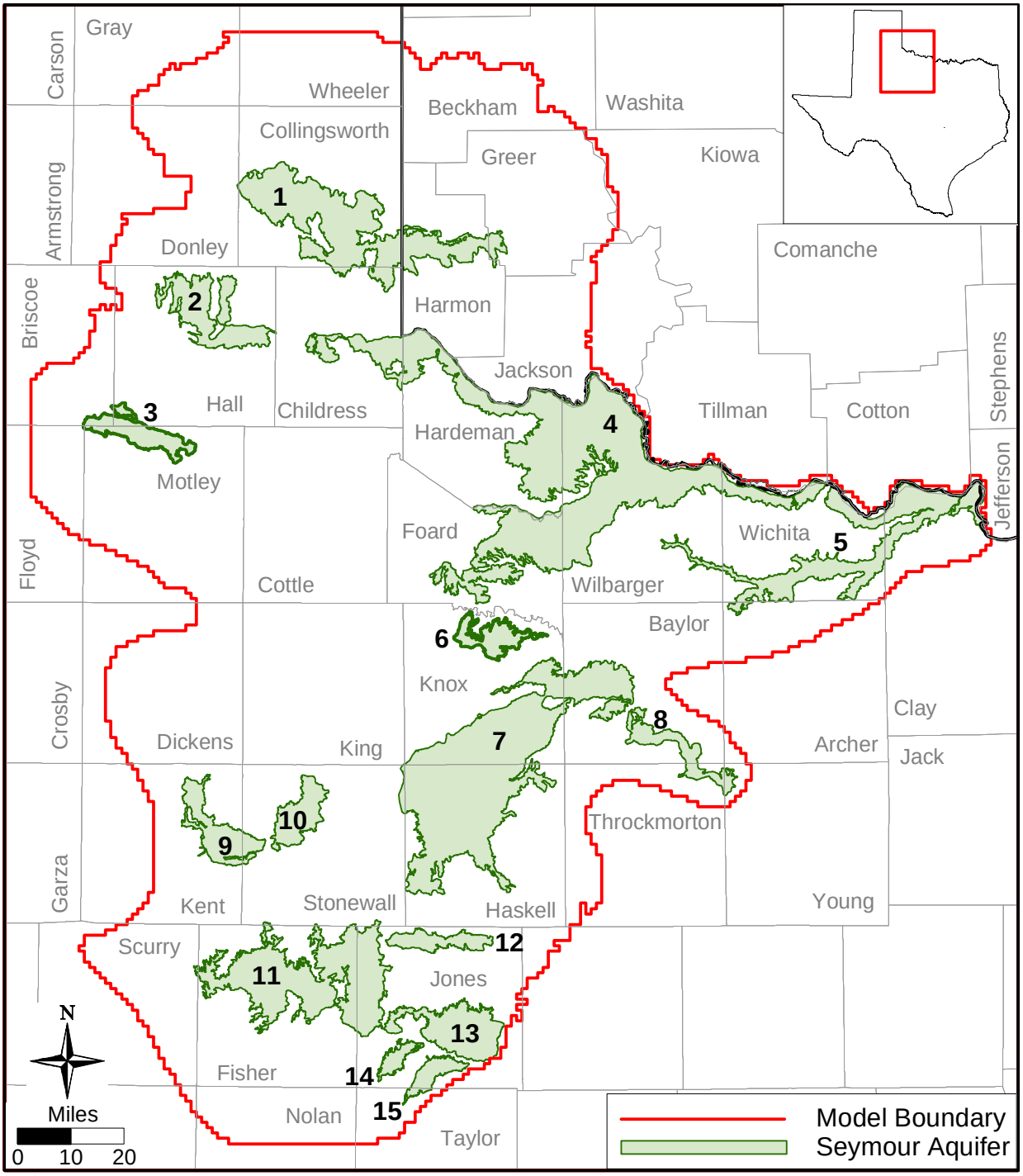

Figure 4.1.1 Pods of the Seymour aquifer.

4.2 Structure

The geologic structure of the Seymour aquifer is dominated by the character of the erosional surface of the underlying Permian beds, the character of the land surface, and the erosional characteristics of recent streams. The structure surfaces generated for the two model layers for the Seymour GAM are based on several sources as summarized in Table 4.2.1.

Table 4.2.1 Data sources for model layer elevations for the Seymour aquifer GAM.

Model Layer 1			
Data Source	**Type of Data**	**Data Use**	**Data Location**
R.W. Harden and Associates (1978)	Contours of altitude of base of Seymour Formation	Digitized and used directly	Haskell County and portions of Knox County
Price (1978)	Contours of approximate altitude of base of Seymour Formation	Digitized and used directly	Most of Jones County
Price (1979)	Contours of approximate altitude of base of Seymour Formation and Quaternary alluvium	Digitized and used directly	Lockett and Odell-Fargo areas in Wilbarger County
Preston (1978)	Contours of approximate altitude of base of Seymour Formation	Digitized and used directly	West-central Baylor County
Caran and Baumgardner (1990)	Structure-contour map of top of Permian subcrop	Digitized and used directly	Northwest Motley County, southwest corner of Hall County, and southeast corner of Briscoe County
Drillers' logs on TWDB website	Base of Seymour Formation as given in drillers' logs	Used directly as point data	Throughout model area
Well logs in TCEQ records	Base of Seymour Formation as given in drillers' logs	Used directly as point data	Throughout model area
Drillers' logs in Turner (1936a, 1936b)	Base of Seymour Formation as given in drillers' logs	Used directly as point data	Foard and Hardeman counties
Water-level data on TWDB website	Maximum depth to water for wells in the Seymour aquifer	Used indirectly to ensure that the base of layer 1 is deeper than the maximum depth to water	Throughout model area
USGS Quads	30-m DEM elevations	Calculated average DEM elevation for the center of each model grid block	Throughout model area
TWDB website	Polygon extent of Seymour aquifer	Points extracted from polygons and DEM elevations at points used as data	Throughout model area
Johnson (1985)	Contours of the base of the Blaine Formation	Digitized and used directly	Oklahoma

Table 4.2.1, continued

Model Layer 2			
Data Source	**Type of Data**	**Data Use**	**Data Location**
Maderak (1972)	Base of Blaine as determined from cross section	Used directly as point data	Hardeman County
Maderak (1973)	Base of Blaine as determined from cross section	Used directly as point data	Wheeler and Gray counties
Well casing data table on TWDB website	Base of screened interval in wells completed to formations underlying the Seymour aquifer	Used indirectly to constrain base of layer 2	Throughout model area
TWDB website	Polygon extent of Blaine outcrop	Points extracted from polygons and DEM elevations at points used as data	Throughout model area

All of the data listed in Table 4.2.1 were for specific point locations except for the data from the Texas Commission on Environmental Quality (TCEQ) and the contour maps. Well-log records filed with the TCEQ do not contain specific surface locations for wells. Rather, the records indicate in which 2.5-minute quadrangle the well is located. A 2.5-minute quadrangle corresponds to about 10 square miles. These quadrangles may contain a few wells or many wells. The latitude and longitude for the center of each quadrangle containing wells with records pertinent to the Seymour GAM were converted to GAM coordinates. Structure-related data for all wells in each quadrangle were arithmetically averaged to obtain a final value representative of the quadrangle. That final average value, applied to the quadrangle center location, was used to develop the structure surfaces for the model. The methodology used to determine and quality control/quality assurance check the structural picks from the TCEQ records is described in detail in Appendix B. This methodology was developed to ensure that no anomalous data were included in the averaging process.

To benefit from the efforts of previous studies, five contour maps of the elevation of the Seymour base and one for the Blaine base (see Table 4.2.1) were scanned, digitized, and projected into GAM coordinates. The average value of the contours intersecting each model grid block was then calculated. This value was applied to the grid-block centroid to create a dataset that could be merged with the point datasets. For all data derived from driller's logs, the basal elevations of the Seymour and Blaine aquifers were calculated from the reported depth to the base of the formation and the DEM elevation at that point. Because the elevation of land surface along the contact between an aquifer and the underlying unit describes the elevation of the base

of the aquifer, the points defining the outline of the Seymour aquifer and the Blaine aquifer outcrop were extracted from the polygons of the aquifer extents. The DEM elevations at alternate points along the Seymour outline and the eastern edge of the Blaine outcrop in Texas were then used as additional point data. The locations of the various data sources used in constructing the basal elevations of the Seymour and Blaine aquifers (as listed in Table 4.2.1) are depicted in Figures 4.2.1 and 4.2.2, respectively.

Because the points along the Seymour outline encompassed the lateral extents of each pod, it was possible to contour each of the pods (or groups of neighboring pods) separately. Prior to kriging, a linear trend removal (50 percent global, 50 percent local) was used to remove the, often significant, topographical trend across each pod. To assess how well the kriging predicts unknown values, cross-validations were plotted. The process of cross-validation involves removing a point from the dataset, predicting the elevation at that point using the remaining data, and comparing the prediction value with the actual value. Figure 4.2.3 depicts the cross validations for several of the pods containing the most data. The slope (close to 1) and correlation coefficient (close to 1) of the best-fit line for each of the cross-validation plots indicate that the Seymour basal elevation is predictable given the available data.

Considerably fewer structural data exist for the Blaine aquifer, so a slightly different method was used to contour its basal elevations. Using the contours in Oklahoma and the available point data, the Blaine aquifer thickness was interpolated by kriging. Because of the paucity of data, this represented only the approximate trend of increasing thickness to the west. This thickness was then subtracted from the DEM at points intersecting the US EPA River Reach File 1 (RF1) coverage (i.e., topographical lows) to create elevation control points throughout the domain. These control points, elevation points along the eastern edge of the Blaine outcrop, and points from the Oklahoma contour map were merged and the elevations interpolated by kriging to generate the Blaine basal elevations. For the remainder of model layer 2, the basal elevations were calculated by subtracting an arbitrary aquifer thickness of 500 feet from the elevation of the base of the Seymour, where present, or from the land surface elevation elsewhere. In order to avoid a sudden change in thickness along the eastern edge of the Blaine aquifer, a gradual increase in thickness was implemented across 10 miles on either side of the aquifer's eastern

edge. A practical minimum layer thickness of 20 feet was assumed for both layers and applied to all grid cells not initially meeting this requirement.

To calculate aquifer thicknesses, the interpolated surfaces of the Seymour and Blaine base and the 30-meter DEM raster map were first averaged onto the model grid. Once the model grid had been populated with the structure data, several additional checks were performed to ensure that the structure was reasonable and consistent with other soft data. In many wells, water-level data were available but structure data were not. For each of these wells, the minimum water level was queried from the water-level database. Where the predicted Seymour aquifer thickness was less than the maximum depth to water in a grid block, the Seymour basal elevation in that grid block was lowered. For several grid blocks, the maximum depth to water exceeded the predicted Seymour thickness by 20 feet or more. For those locations, the basal elevation for the neighboring eight grid blocks were also lowered by half of the exceeding amount. For all cases, the Blaine thickness exceeded the maximum depth to water measured and the structure was not altered.

Figures 4.2.4 through 4.2.9 depict the structure of the hydrostratigraphic layers in the model. The structure of the Seymour aquifer is dictated largely by topography. The elevation of the top of the Seymour aquifer is shown in Figure 4.2.4. The elevation of the Seymour base varies several hundred feet across a single pod, as shown in Figure 4.2.5, while the Seymour thickness is generally less than 100 feet as evident in Figure 4.2.8. The elevation of the top and bottom of layer 2 is shown in Figures 4.2.6 and 4.2.7, respectively. In contrast to the Seymour, the base of the Blaine aquifer generally dips slightly to the west as shown in Figure 4.2.7. While the thickness of the Blaine aquifer tends toward zero at the eastern outcrop of the formation, the thickness is generally several times greater than that of the Seymour as evident in Figure 4.2.9.

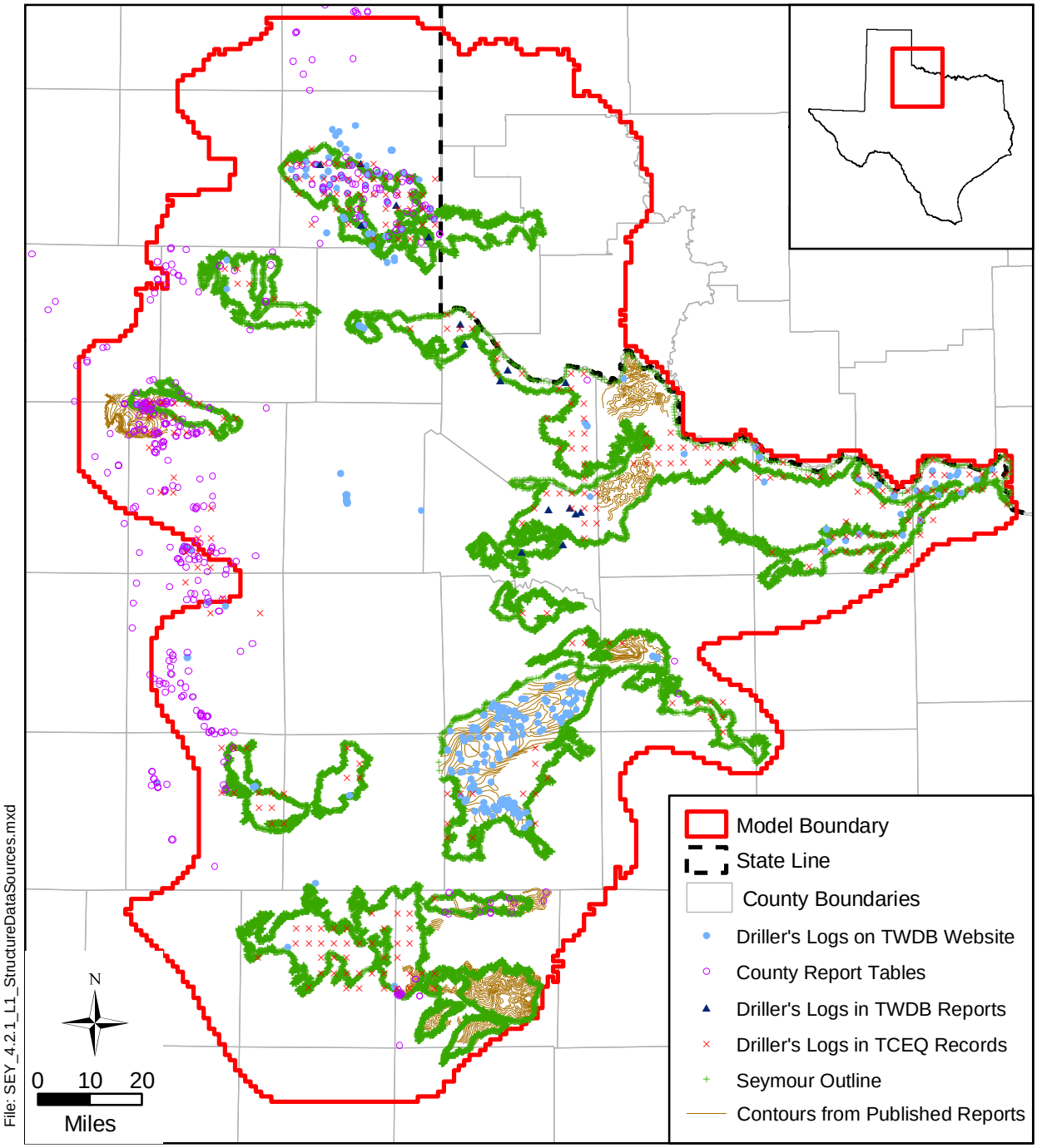

Figure 4.2.1 Data sources for the Seymour aquifer structure.

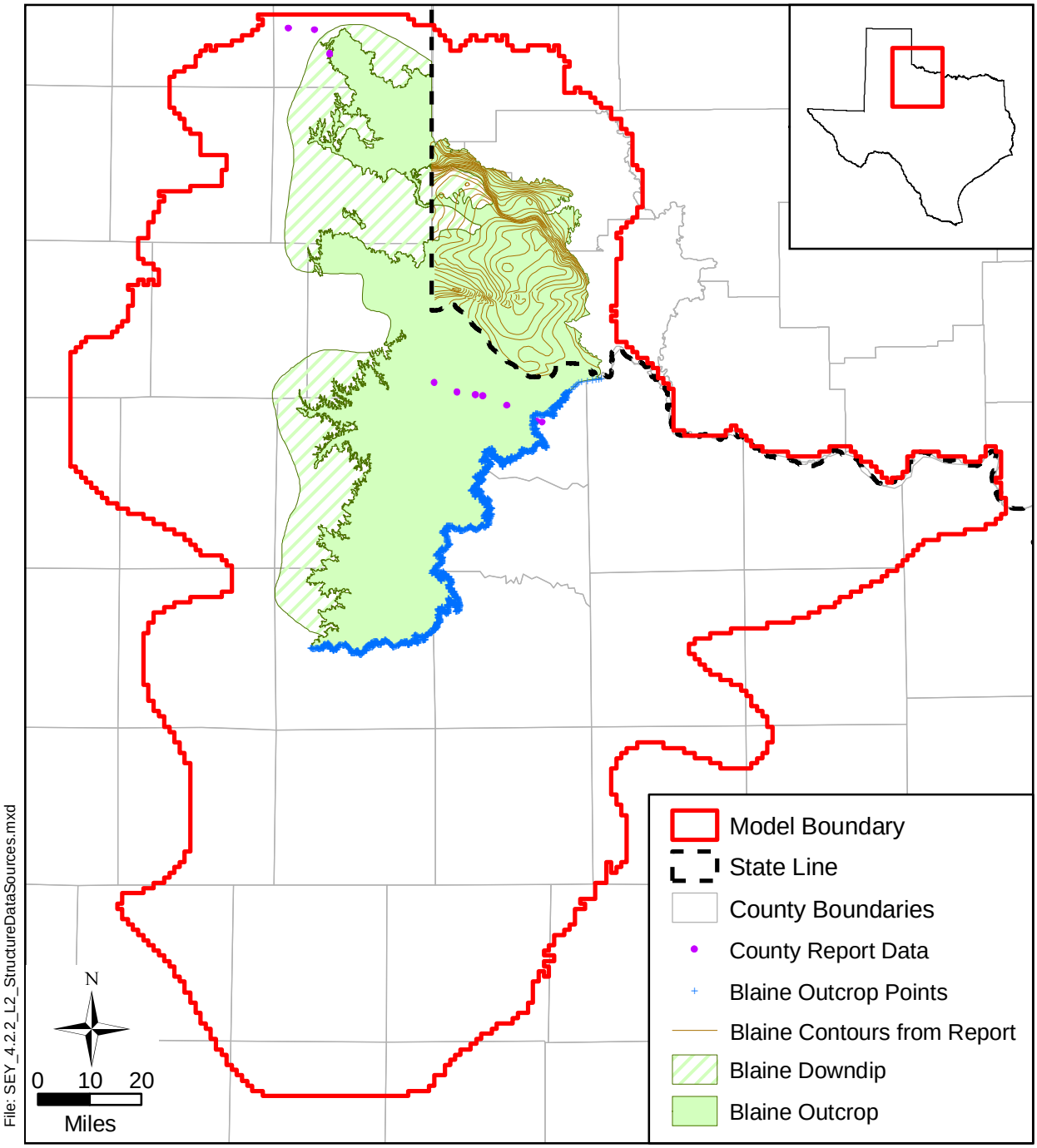

Figure 4.2.2 Data sources for the Blaine aquifer structure.

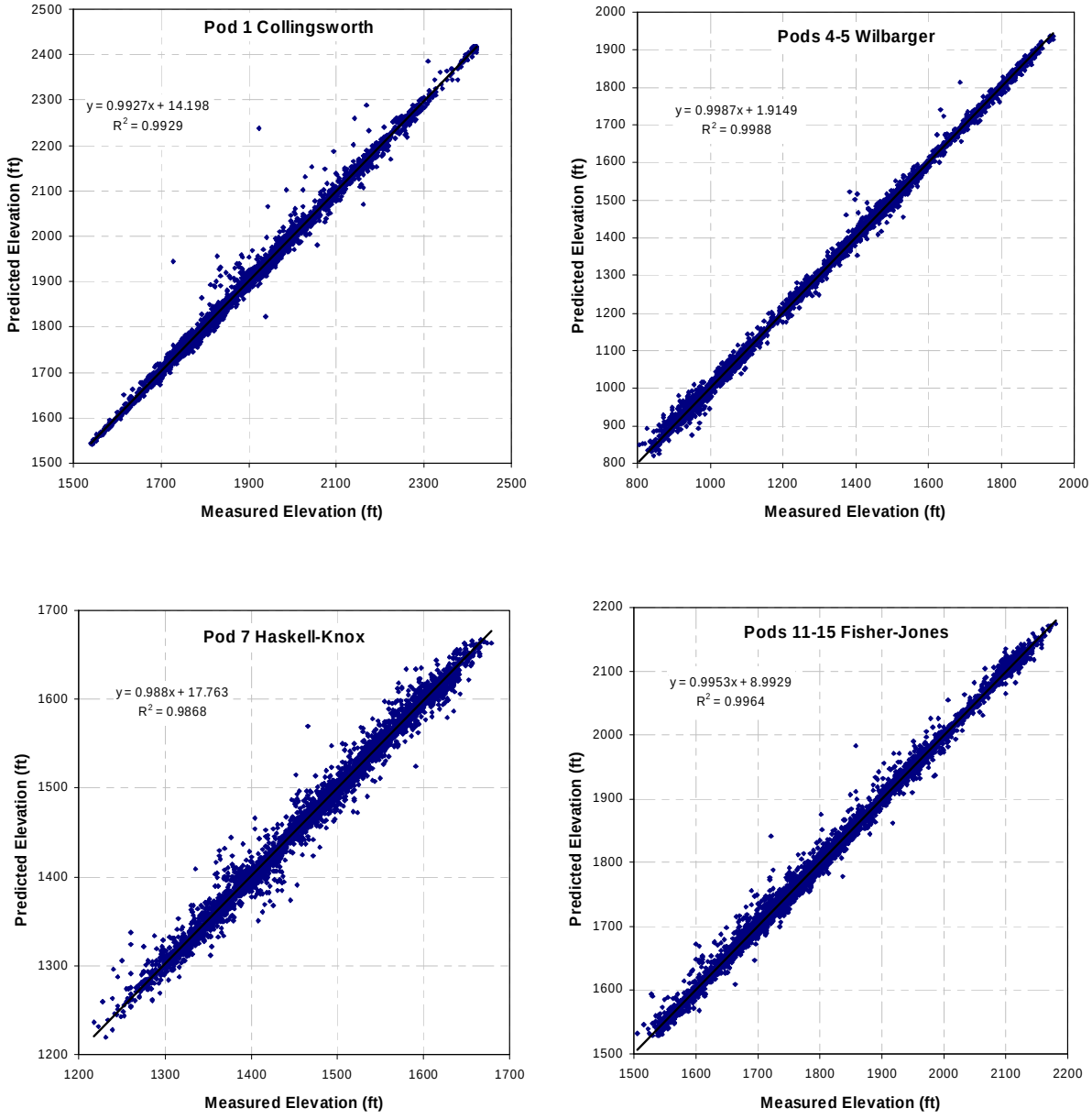

Figure 4.2.3 Cross-validation plots of the Seymour basal elevation interpolation.

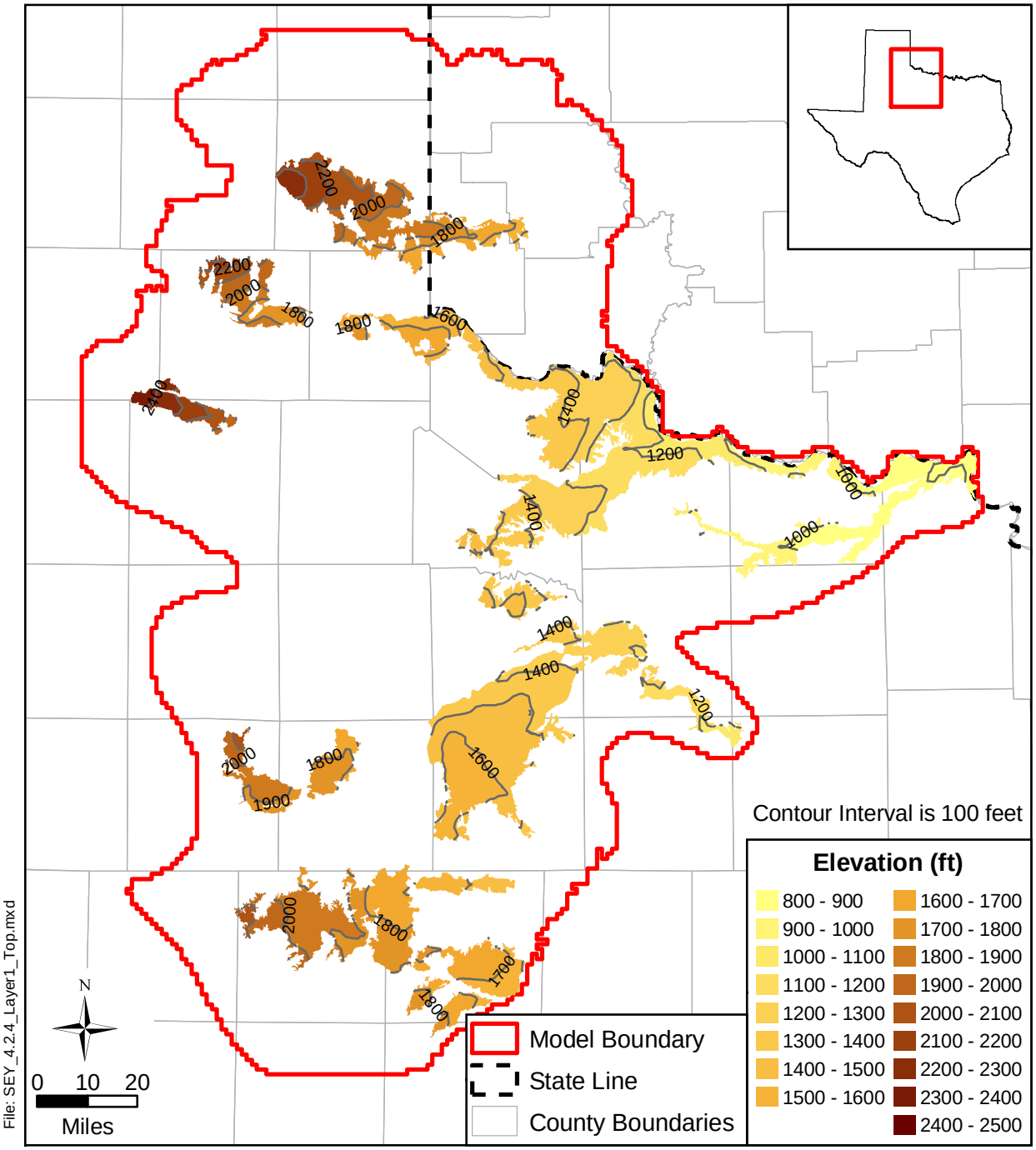

Figure 4.2.4 Structure contour map of the top of the Seymour aquifer.

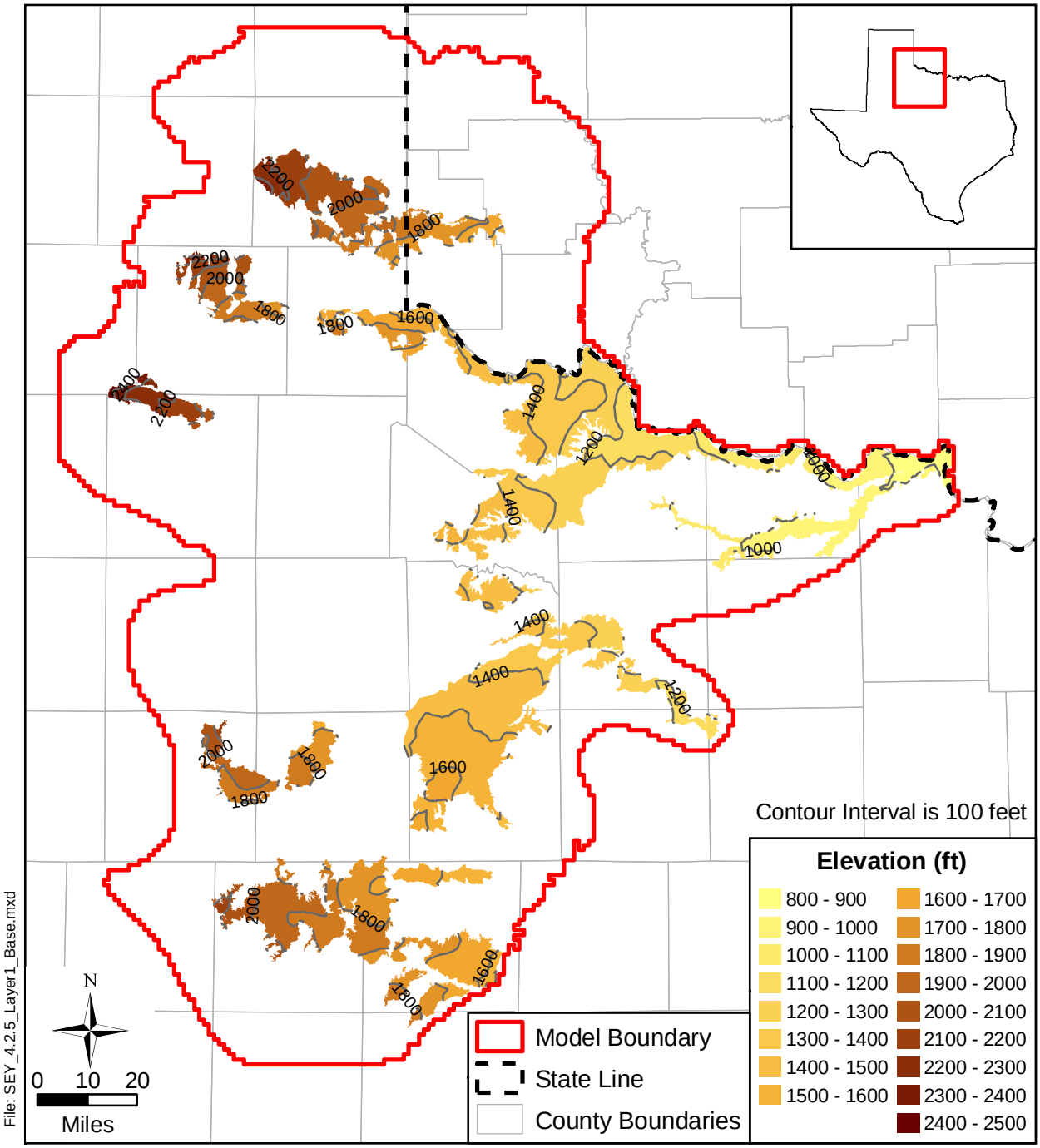

Figure 4.2.5 Structure contour map of the base of the Seymour aquifer.

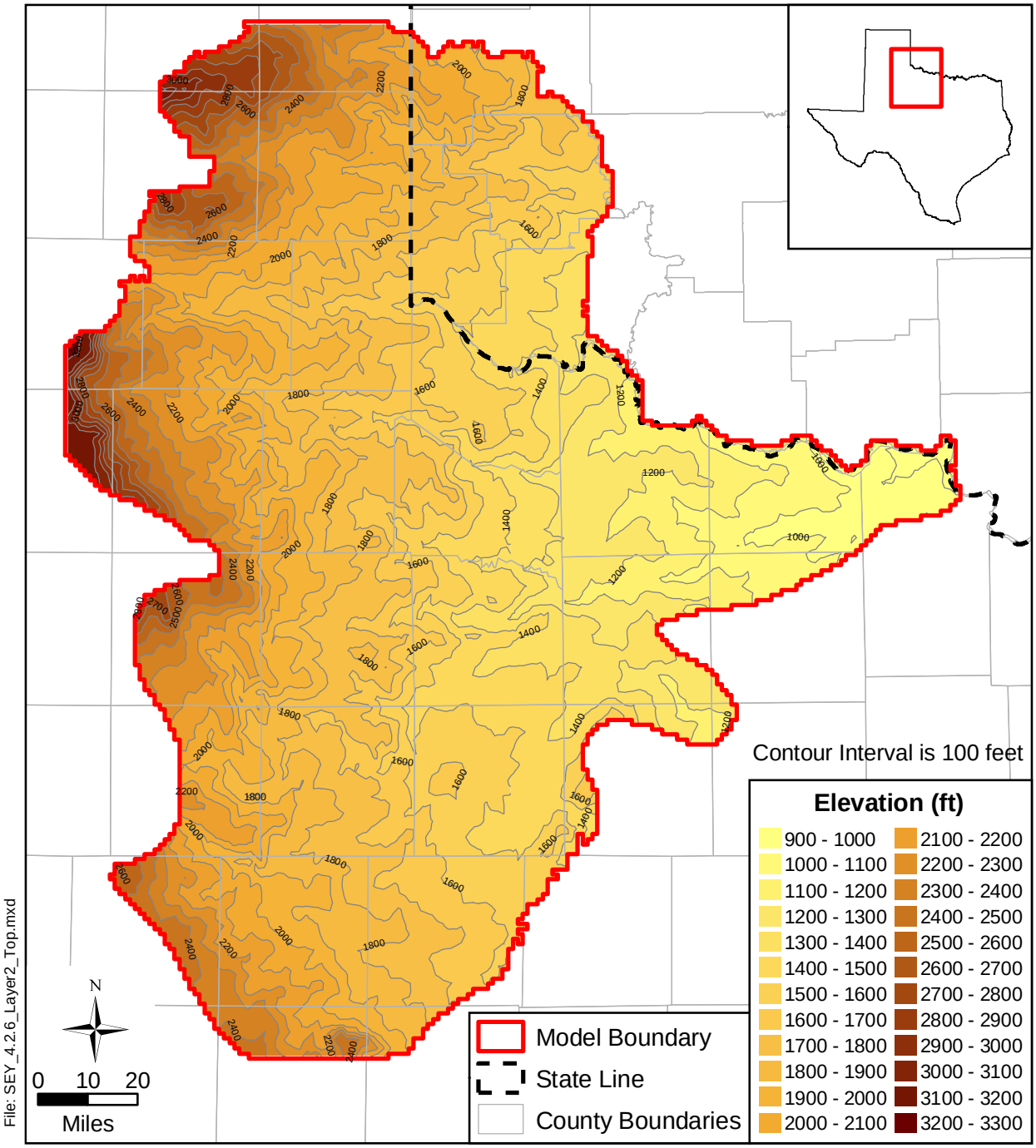

Figure 4.2.6 Structure contour map of the top of layer 2.

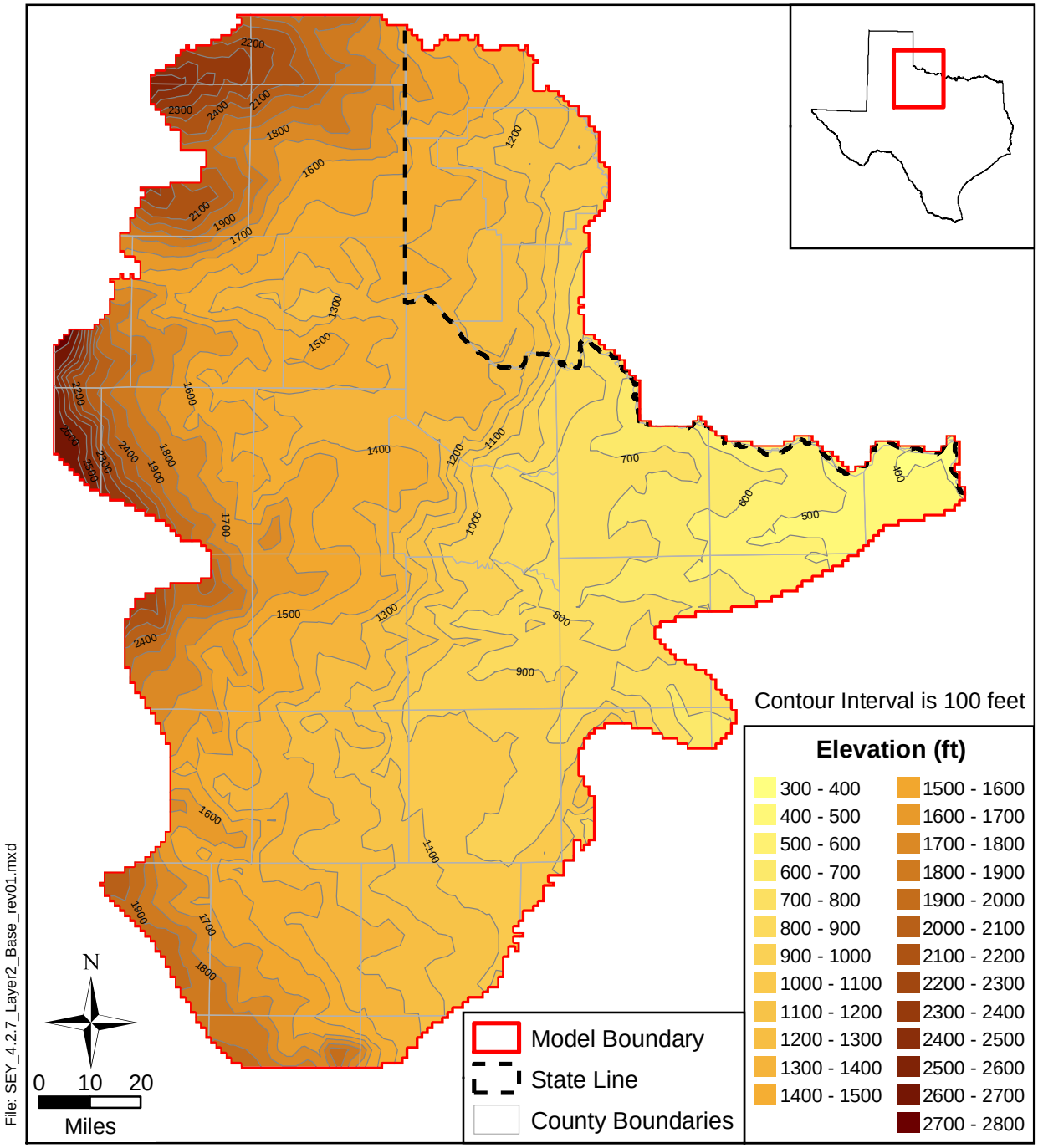

Figure 4.2.7 Structure contour map of the base of layer 2.

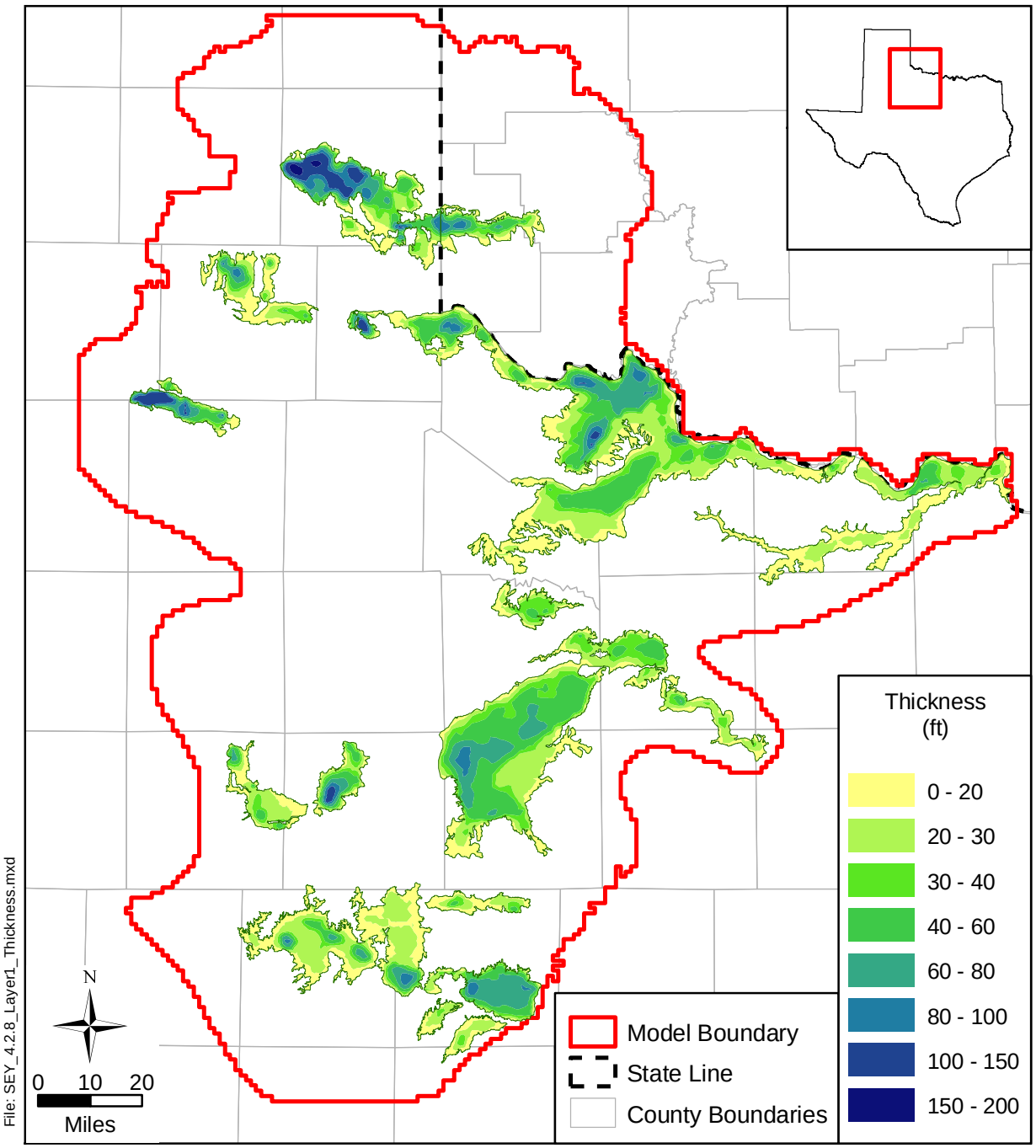

Figure 4.2.8 Isopach map of the Seymour aquifer.

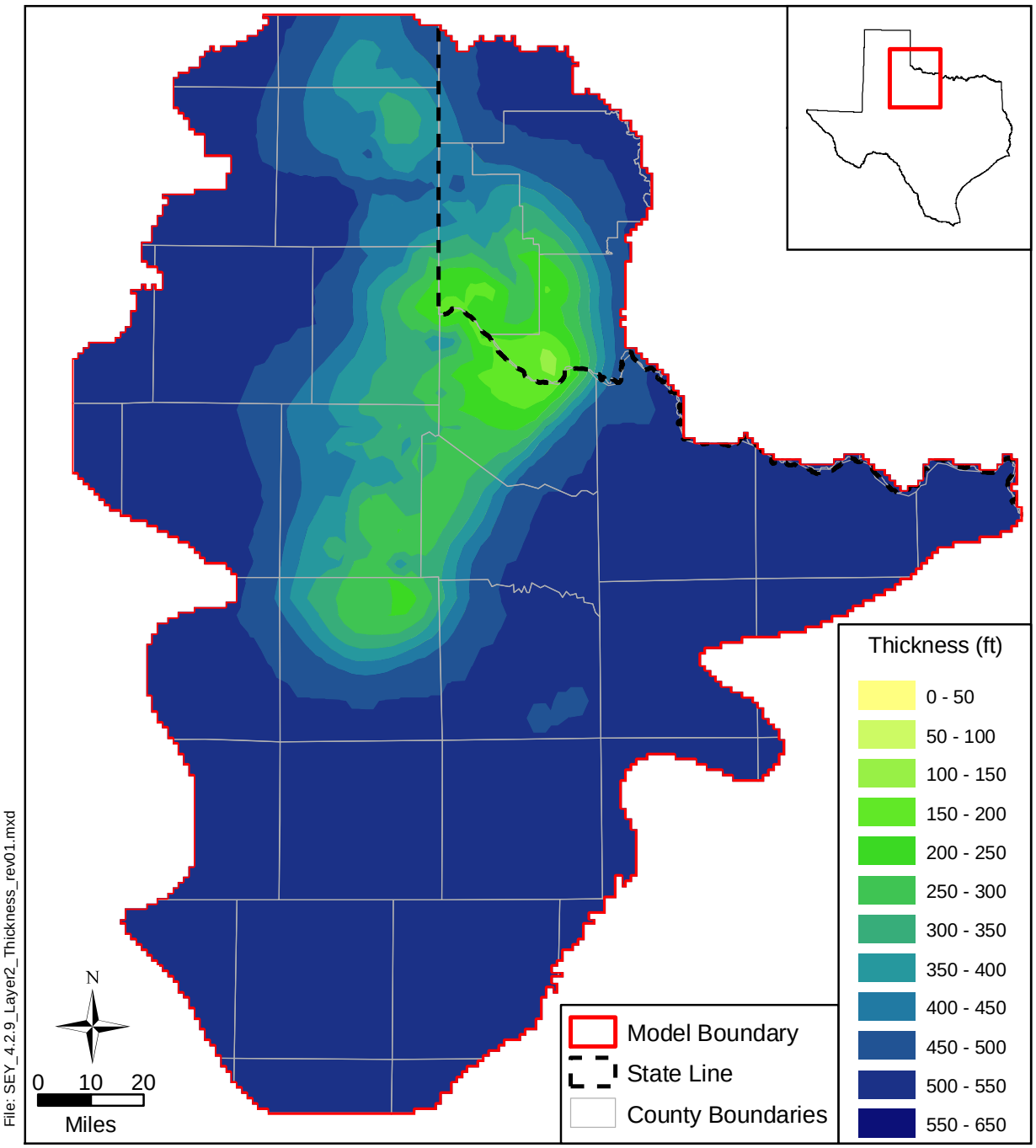

Figure 4.2.9 Isopach map of layer 2.

4.3 Water Levels and Regional Groundwater Flow

An extensive literature search was conducted to understand regional groundwater flow in the Seymour aquifer and the history of groundwater usage from the aquifer. The literature search included a review of available reports by the various past and present Texas state agencies responsible for water resources (i.e., the Texas Board of Water Engineers, the Texas Water Commission, the Texas Department of Water Resources, and the TWDB), the USGS, the Bureau of Economic Geology, and the Oklahoma Water Resources Board.

In addition, water-level data provided by the TWDB on their website were used to (1) develop water-level elevation contours for the steady-state period, the start time for the transient model (January 1980), the end of the model calibration period (December 1989), and the end of the model verification period (December 1999); (2) investigate cross-formational flow; and (3) investigate transient water-level conditions.

The Seymour aquifer consists of isolated remnants of the Seymour Formation, the Lingos Formation, and younger alluvial deposits of Quaternary age. Therefore, regional flow does not occur across the entire aquifer. Rather, each isolated pod behaves independently. In some cases, the pod consists of a single stratigraphic unit, such as the Seymour Formation in Haskell and Knox counties, and in other cases it consists of two stratigraphic units, such as the Seymour Formation and younger alluvium in Hardeman County (see Figure 2.23).

The source for the water-level data used for the Seymour and Blaine aquifers in Texas is the TWDB website[5]. Locations and hydrostratigraphic units for wells with water-level data in the Seymour aquifer are shown on Figure 4.3.1. A summary of the aquifer codes assigned to these wells is provided in Table 4.3.1. Note that none of the aquifer codes correspond to the Lingos Formation. The reason for this is unknown. It is likely, however, that the assignment of aquifer codes to wells in the model area occurred before the Lingos Formation was named. Caran and Baumgardner (1990) indicate that, at the time of their report, use of the term Lingos Formation was new. Because the Lingos Formation terminology is not used in the TWDB data, it is not used in subsequent discussions of water-level data in this report.

[5] http://rio.twdb.state.tx.us/publications/report/GroundWaterReports/GWDatabaseReports/GWdatabaserpt.htm

Table 4.3.1 Summary of aquifer codes for wells within the Seymour aquifer.

TWDB Aquifer Code	Description	Number of Wells
100ALVM	Alluvium	116
110ALVM	Quaternary Alluvium	179
110ALVP	Alluvial Plain Deposits	110
110AVTC	Alluvial Terrace and Channel Deposits	25
110AVTS	Alluvium, Terrace Deposits, and Seymour Formation	81
110TRRC	Terrace Deposits	9
112PLSC	Pleistocene Series	3
112SYMR	Seymour Formation	3046

According to the water-level data on the TWDB website, a total of 11,855 individual water-level measurements have been taken in 3,569 wells completed in the Seymour aquifer. The number of wells with water-level measurements in counties containing Seymour aquifer varies significantly as illustrated in Figure 4.3.2a. The counties having the largest number of wells are Wilbarger, Knox, Haskell, Jones, and Baylor. These are also the counties in which the majority of water-level measurements have been made (Figure 4.3.2b) because these are the counties in which the Seymour aquifer has been most extensively studied. Note that the distribution of wells (Figure 4.3.2a) and the distribution of water-level measurements (Figure 4.3.2b) are similar but not identical. The counties with the least number of wells in the Seymour are Hall, Fisher, and Stonewall and the counties with the least number of water-level measurements are Stonewall, Throckmorton, and Fisher.

In addition to varying by location, the frequency of water-level measurements has also varied with time (Figure 4.3.3). The largest number of water-level measurements was taken in the Seymour aquifer in 1956 and 1970. Prior to 1956, the lower number of water-level measurements may have been due to fewer wells completed to the aquifer. Note that the number of water levels measured around the time of the start of model calibration (1980), end of model calibration (1989), and end of model verification (1999) is low.

The sources of water levels for the Blaine aquifer were the TWDB website for data in Texas and the USGS water data website[6] for data in Oklahoma. Locations and

[6] http://waterdata.usgs.gov/ok/nwis/gw

hydrostratigraphic units for wells with water-level data in the Blaine aquifer are shown on Figure 4.3.4. In addition to water levels with the Blaine Formation designation, the TWDB database also includes water levels designated as the Blaine Formation and the Dog Creek Shale. The Dog Creek Shale overlies the Blaine Formation and, in some areas, it is difficult to distinguish between the two. In Texas, 2,941 water-level measurements have been made in the Blaine aquifer at 781 locations. In Oklahoma, 5,172 water-level measurements have been made in the Blaine aquifer at 354 locations.

4.3.1 Regional Groundwater Flow

As stated above, the Seymour aquifer consists of isolated pods (see Figure 4.1.1) of alluvial material and, because these pods are not connected, regional flow does not occur throughout the aquifer. Rather, each pod acts as its own flow system. In general, flow within the pods is from areas of recharge near topographic highs to areas of discharge in nearby major streams and/or their tributaries or to springs. The major streams associated with each pod are shown on Figure 4.3.5. Much of the following discussion of groundwater flow within each pod is taken from literature sources that provide results based on detailed investigations of groundwater conditions in the aquifer. These sources include county reports by the TWDB and associated agencies and a major study of the Seymour aquifer in Haskell and Knox counties by R.W. Harden and Associates (1978).

Groundwater flow in pod 1 located in Collingsworth County is from recharge areas in sand dunes towards the streams located to the north (Salt Fork Red River), east (Sand Creek), and south (Buck Creek) of the pod (Smith, 1970). The sand dunes associated with recharge are located in three main areas: on the western tip of the pod, northwest of the town of Wellington, and near the towns of Fresno and Dodson located in the southeastern corner of the county (Smith, 1970). In pod 2, located in Hall County, groundwater flow is toward the Prairie Dog Town Fork Red River which runs through the pod (Popkins, 1973). Consequently, north of the river, flow is to the south and south of the river, flow is to the north. Groundwater flow in pod 3, located in Motley, Hall, and Briscoe counties, is predominantly to the southeast toward the North Pease River (Smith, 1973; Popkins, 1973).

Pod 4 of the Seymour aquifer extends across the counties of Childress, Hardeman, Foard, Wilbarger, and Wichita. No studies of the Seymour aquifer in Childress County were identified

during the literature search and water-level data for this portion of the aquifer are sparse. Therefore, the direction of groundwater flow in the Seymour aquifer in Childress County is unknown, but is expected to be to the north and northeast toward the Prairie Dog Town Fork Red River located north of the pod. In Hardeman County, groundwater flow within the portion of pod 4 located adjacent to the Red River is toward the Red River. In the portion of pod 4 located along the eastern edge of Hardeman County, flow in the north is to the south and flow in the south is to the north toward Wanderers Creek (Maderak, 1972). Groundwater in the portion of pod 4 located in Foard County east and northeast of the city of Crowell flows northward and northeastward toward the Pease River (George and Johnson, 1941). Study of the Seymour aquifer in the portion of pod 4 located in Wilbarger County has predominantly been restricted to two areas: the Odell-Fargo area located in the northwestern portion of the county and the Lockett area located in the west-central portion of the county. Groundwater in the Odell-Fargo area flows (1) radially outward from two groundwater highs located in the center of the area and (2) northward and northeastward from another high located in the southwestern portion of the area (Price, 1979). In the Lockett area, groundwater generally flows northward or northwestward off of a regional high that trends to the northeast towards the Pease River (Price, 1979). No studies of the Seymour aquifer in Wichita County were identified during the literature search and water-level data for this portion of the aquifer are sparse. Therefore, the direction of groundwater flow in the portion of pod 4 located in Wichita County is unknown, but is expected to be to the north and northeast toward the Red River.

As noted above, no studies of the Seymour aquifer in Wichita County were identified during the literature search and water-level data for this portion of the Seymour aquifer are sparse. The same is true for the aquifer in Clay County. As a result, the direction of groundwater flow in pod 5 is unknown but is expected to be towards the three streams associated with this pod: the Red River to the north and Beaver Creek and the Wichita River which run through the southern fork of the pod.

No studies of the Seymour aquifer in northern Knox County (pod 6) were identified during the literature search. Water-level data in this pod are available for the years 1991 through 1993. Based on that data, flow in the pod appears to be toward the North Fork Wichita River located north of the pod and towards the South Fork Wichita River located south of the pod.

In the portion of pod 7 located in Baylor County, "the general movement of ground water is to the south and southeast following the general slope of the land surface and the slope of the underlying surface upon which the formation rests" (Preston, 1978). In the portion of pod 7 located in Haskell and Knox counties, the direction of groundwater flow is generally to the north and northeast following the slope of the ground surface and the slope of the underlying Permian beds (Ogilbee and Osborne, 1962). R.W. Harden and Associates (1978) contains a figure showing the approximate direction of groundwater flow in the portion of pod 7 that they studied assuming no pumpage effects. That figure is reproduced as Figure 4.3.6.

Although literature references to flow within pod 8 located in Baylor, Throckmorton, and Young counties were not found during the literature search, flow within this pod is most likely toward the Brazos River which runs through the pod. In the portion of pod 9 located in Kent County groundwater flow is southwestward toward Duck Creek and the Salt Fork Brazos River located along the western edge of the pod (Cronin, 1972). In the remaining portion of the pod, groundwater is expected to flow southward toward the Salt Fork Brazos River, which also wraps around the southern edge of the pod. No studies of the Seymour aquifer in Stonewall or Fisher counties were identified during the literature search, and water-level data for this portion of the aquifer (pods 10 and 11) are sparse. Therefore, the direction of groundwater flow in this area is unknown. Groundwater flow within pod 10 is most likely to the north toward the Salt Fork Brazos River, which runs along the northern tip of the pod. Groundwater flow within pod 11 is most likely toward the Clear Fork Brazos River that runs through the southern portion of the pod and toward California Creek that runs through the northern portion of the pod.

The following discussion of flow within pods 12, 13, 14, and 15 located in Jones County is taken from Price (1978). In pod 12, groundwater flows in two general directions. Flow is to the north and northeast toward tributaries of the Brazos River in the northern portion of the pod and to the south and southeast toward California Creek in the southern and eastern portions of the pod. In pod 13, flow is generally from the central portion of the pod toward the northern, eastern, and southern edges of the pod. Groundwater flows into the Clear Fork Brazos River on the southern side and to tributaries of both California Creek and the Clear Fork Brazos River on the northern side. In pods 14 and 15, flow is generally northward or northeastward to the Clear Fork Brazos River.

4.3.2 Steady-State Conditions

The predevelopment condition of the Seymour aquifer was "dry" in several counties. Ogilbee and Osborne (1962) state that water in the Seymour Formation in Haskell and Knox counties was located near the base of the formation and was hard and "gip" in the early 1900s. They indicate that as land was developed for cultivation, water levels within the Seymour Formation began to rise. Now, water in the Seymour Formation in these counties is found at shallower depths and is soft and fresh rather than hard and gip. Similar changes in water levels and quality are reported for the Seymour Formation in Jones County (Price, 1978). Price (1978) states the following,

> "The clearing of water-consuming vegetation (phreatophytes); the improved farming practices of terracing, contour plowing, and deep plowing; and the general increase in rainfall for the period from 1885 through 1941, have all been major contributing factors to the general rise in water levels."

Since a dry condition is not conducive to calibration of the steady-state model, a time period over which water levels were stable was determined to be the best condition for calibration of the steady-state model. Steady-state calibration of the Seymour aquifer considered a time period over which water levels in the pods were at relatively steady-state conditions. Determination of steady-state conditions was conducted on a pod by pod basis. All transient water-level data for wells within each pod were evaluated together. The time period over which water levels were stable for the greatest number of wells on an individual pod basis prior to the start of the transient model (January 1980) was selected as representative of steady-state conditions. The steady-state time periods determined for the pods are summarized in Table 4.3.2 and the locations of the corresponding 1,747 wells with water-level data for those time periods are provided in Figure 4.3.7. Only those wells completed to alluvium or the Seymour Formation and located within the outline of the Seymour aquifer as defined by the TWDB were used to determine water levels for the Seymour aquifer. The TWDB website was the source for all water-level data for the Seymour aquifer.

Table 4.3.2 Time periods for steady-state conditions.

Pod Number	Counties	Steady-State Time Period
1	Collingsworth	1967-1970
2	Hall	1969-1975
3	Hall	1975-1981
	Motley	1973-1977
4	Childress, Hardeman, Foard, Wilbarger, and Wichita	1968-1970
5	Wichita and Clay	1978-1979
6	Knox	(1)
7	Knox, Haskell, and Baylor	1967-1970
8	Baylor and Throckmorton	1967-1970
9	Kent and Stonewall	1972-1978
10	Stonewall	1960-1965
11	Fisher	1970-1975
	Jones	1967-1970
12	Jones	1967-1970
13	Jones	1967-1970
14	Jones	1967-1970
15	Jones	1967-1970

(1) No water-level data available prior to the start of the transient model.

Several aspects of the Seymour aquifer introduce challenges in processing the water-level data to yield representative areal water-table surfaces. First, the change in ground-surface elevation is very large (approximately 2,000 feet) across the study area from west to east and large (about 200 feet) across individual pods. Second, the changes in elevations across the pods are large compared to the thicknesses of the pods (usually less than 100 feet). Third, the areal size of the pods is small. Fourth, the amount of water-level data for any given year in some pods is sparse. The paucity of data requires use of a correlation to populate water-level data into many of the model grid blocks. Correlations of water-level to land-surface elevation have been demonstrated to be effective by others (Williams and Williamson, 1989; Sepulveda, 2003). However, for the Seymour aquifer, correlating water-level to ground-surface elevation across the entire model domain was deemed inappropriate because elevation changes are large. Although the correlation may look good, small errors resulting from the correlation can yield water-level elevations that fall outside of the upper and lower elevations of the thin Seymour pods. Relating the water-level elevation to localized topography was determined to provide a better approach.

Because the base of the Seymour was relatively smooth, this provided a datum from which a local topographical elevation could be determined. Subtracting this datum from both the land-surface elevation and the water-level elevation resulted in the depth to the base of the Seymour and the saturated thickness, respectively. A correlation between the depth to the base of the Seymour and the depth to water (Seymour thickness minus saturated thickness) was used. In this way, the conceptual model presented by Freeze and Cherry (1979), of a water table that coincides with the ground surface in the valleys and forms a subdued replica of the topography in the hills, was honored.

Once the average depth to water during the identified steady-state period was calculated for each well, these data were interpolated by kriging within pods containing enough data to warrant interpolation. For the steady-state period, this included pods 1, 4, 5, 7, 8, 12, 13, 14, and 15. This interpolated depth to water was used to calculate the steady-state saturated thickness for locations within a 2-mile radius of observed data points. Elsewhere, a correlation of depth to water versus formation thickness (Figure 4.3.8) was used to calculate the steady-state saturated thickness. The resulting steady-state saturated thickness for the Seymour aquifer is shown in Figure 4.3.9. Based on these calculations of saturated thickness, contours of the water-level elevation for the steady-state period were created (Figure 4.3.10).

Water-level data from 1968 to 1970 were used to generate water-level elevation contours representative of steady-state conditions for model layer 2 (Figure 4.3.11). These data were used for two main reasons. First, the steady-state time period for most of the Seymour pods includes the years 1968 to 1970. Second, a large number of data points were available for formations in layer 2 during this time period. These data were used to establish initial conditions in layer 2 for the steady-state model.

4.3.3 Water-Level Elevations for Model Calibration and Verification

Model calibration considers the time period from January 1, 1980 to December 31, 1989 and model verification considers the time period from January 1, 1990 to December 31, 1999. Saturated-thickness contours for the Seymour aquifer and water-level elevation contours for model layer 2 representative of the time period associated with the start of calibration were used to initialize the transient model. Saturated-thickness contours and water-level elevation contours for the end of calibration and the end of verification were generated for the Seymour aquifer and

model layer 2, respectively, for use as guidelines when assessing the ability of the transient model to reproduce observed conditions. Only those wells completed to alluvium or the Seymour Formation and located within the outline of the Seymour aquifer as defined by the TWDB were used to determine saturated thickness for the Seymour aquifer. The source for all water-level data was the TWDB website.

Data on the TWDB website are not available at regular time intervals in every well. Therefore, the coverage of water-level data for a particular month is very sparse. For example, water levels in the Seymour aquifer were measured in two wells in January 1980, none in December 1989, and 46 wells in December 1999. Considering the entire year of interest increased the number of available wells with water-level measurements to 106 for all of 1980, 119 for all of 1989, and 73 for all of 1999. Further expanding the time period to two years prior to and two years after the year of interest resulted in 162, 166, and 100 wells with water-level measurements available for 1980, 1989, and 1999, respectively. The locations of these wells are shown in Figure 4.3.12.

Since the majority of the wells completed in the Seymour aquifer shown on Figure 4.3.12 are located in only a few pods, development of representative saturated-thickness contours for the pods with little or no data is problematic. To define water-level conditions for all pods, correlations between depth to water and depth to the base of the Seymour were determined for the 1980, 1989, and 1999 data in the same manner as was done for the steady-state water levels (see Section 4.3.2). If a well had only one water-level measurement during the period of interest (1978-1982 for the start of calibration, 1987-1991 for the end of calibration, and 1997-2001 for the end of verification), that measurement was used. If a well had more than one water-level measurement during that time, the average of the water levels was used.

Once the average depth to water for 1980, 1989, and 1999 was calculated for each well, these data were interpolated by kriging within pods containing enough data to warrant interpolation. For 1980, this included pods 4, 5, 7, and 13. For 1989, this included pods 4, 6, 7, and 13. For 1999, this included pods 4, 7, and 13. This interpolated depth to water was used to calculate the saturated thickness for locations within a 2-mile radius of observed data points for each of the three time periods. Elsewhere, correlations of depth to water versus formation thickness were used to calculate the saturated thickness for the appropriate time period. The

correlations for the 1980, 1989, and 1999 water-level data are shown in Figure 4.3.13 and the resulting saturated thicknesses for the three periods are shown in Figures 4.3.14, 4.3.15, and 4.3.16, respectively. Based on these calculations of saturated thickness, contours of the water-level elevations for 1980, 1989, and 1999 were developed (Figures 4.3.17, 4.3.18, and 4.3.19, respectively).

Development of water-level elevation contours for model layer 2 representative of the start of calibration, the end of calibration, and the end of verification considered the year of interest plus two years prior to and two years after the year of interest. If a well had only one water-level measurement during the time of interest, that measurement was used. If a well had more than one water-level measurement during the time of interest, the average of the water levels was used.

Figures 4.3.20, 4.3.21, and 4.3.22 show water-level elevation contours in model layer 2 at the start of calibration, end of calibration, and end of verification, respectively. All three figures show continuity of the water-level elevations across the active model area in the different stratigraphic units making up layer 2. The water-level elevations indicate that regional flow is from topographic highs on the western side of the active model area to topographic lows on the eastern side. Local variations within the potentiometric surface are not visible on these figures due to their scale and the paucity of data.

4.3.4 Cross-Formational Flow

An exercise was conducted to investigate cross-formational flow between the Seymour aquifer and underlying Permian rocks. Vertical flow within the Seymour aquifer itself was not evaluated due to the thin nature of the aquifer and the fact that it is under water-table conditions at all locations. At several places in the active model area, wells completed separately to the Seymour and the underlying formation share a similar surface location. For those wells, water-level elevations in the wells at similar times were compared and documented in Figure 4.3.23. On this figure, the well having the highest water-level elevation is listed at the top of the table associated with each well cluster. At four locations, the water-level elevation for the underlying formation is higher than that for the Seymour aquifer. At seven locations, the water-level elevation for the Seymour aquifer is higher than that for the underlying formation. Notice that in Baylor and Jones counties, clusters showing opposite trends are located close to each other. The

difference between water-level elevations in the Seymour and underlying formations ranges from a low of 3 feet for the cluster in pod 12 to a high of 50 feet for a cluster in pod 11 and averages 25 feet. Since the differences are relatively low, the direction of indicated flow could be affected by any error in the measured LSD (land surface datum) elevation or the measured depth to water. The direction of flow between the Seymour aquifer and the underlying formations could not be conclusively determined based on this evaluation of measured data. However, the low sulfate concentration of the water in the Seymour aquifer indicates that significant cross-formational flow from the higher sulfate concentration in the Permian units does not occur. Therefore, while flow from the Permian to the Seymour may occur in some areas, the net cross-formational flow is expected to discharge from the Seymour into the Permian sediments.

4.3.5 Transient Water Levels

Transient water-level data were used to both calibrate and verify the transient model. Figure 4.3.24 shows the locations for which transient water-level data (hydrographs) are available for the Seymour aquifer based on data found on the TWDB website. On this figure, the wells for which transient data are available during the model calibration and verification time periods (January 1980 through December 1999) are indicated with open circles, the wells for which transient data are available only during the calibration period (January 1980 through December 1989) are indicated with closed circles, and the wells for which transient data are available during only the verification period (January 1990 through December 1999) are indicated with a plus sign. For the other wells in the figure, indicated with a square, the time period for the transient water-level data does not include either the calibration or verification periods.

About 30 percent of the hydrographs show stable water-level conditions over periods of time ranging from fewer than ten years to over 50 years. Stable conditions are defined as those in which water levels may fluctuate up and down but do not show any apparent increasing or decreasing trend. Fluctuations in the water levels range from lows on the order of ±5 feet to highs on the order of ±20 feet. Stable hydrographs are found for wells located in pods 1, 2, 4, 5, 7, 9, 11, and 13. Examples of stable hydrographs are shown in Figure 4.3.25.

For the hydrographs in this figure and subsequent figures, both the ground-surface and base of well elevations are shown. The base of the well is assumed to represent the base of the

Seymour aquifer because most wells were drilled only into the top few inches of the Permian redbeds underlying the aquifer. Adding this information to the figures provides a means to evaluate the changes in water-level elevation with time relative to the aquifer thickness. Most of the hydrographs are plotted with a 100-foot elevation difference on the y-axis. In some cases, the difference in water-level elevation was greater than 100 feet, and the y-axis had to be expanded. In all cases, the interval between grid lines on the y-axis is 10 feet.

About 20 percent of the hydrographs show increasing water levels during some portion of the transient record. Three types of rises are observed in the hydrographs; from least common to most common, they are increases early in the record, increases late in the record, or a continuous increase throughout the record. The magnitude of the water-level increases ranges from five to 25 feet. Hydrographs showing increasing water levels are found for wells located in pods 1, 2, 3, 4, 5, 7, 8, and 13. Examples of hydrographs with water-level increases are shown in Figure 4.3.26. A few of the wells showing increases in water-level elevation with time are located in recharge areas on topographic highs.

About 26 percent of the hydrographs show a decrease in water levels during some portion of the transient record. Three types of declines are observed in the hydrographs; from least common to most common, they are decreases early in the record, decreases late in the record, or a continuous decrease throughout the record. The majority of the wells with hydrographs having a decrease in water level early in the transient record are located in Wilbarger County. For these wells, the declines in water level ranged from 10 to 40 feet, and the water levels stopped declining in the early 1970s. One such hydrograph is shown in Figure 4.3.27. The well with the largest decline in water level is located in Childress County. The water-level elevation in that well dropped 50 feet from the mid-1940s until the late 1960s and dropped another 10 feet since that time (Figure 4.3.27). For the majority of wells showing a continuous decline in water levels, the magnitude of the decrease ranges from five to 20 feet (Figure 4.3.27). Hydrographs showing decreasing water levels with time are found for wells located in pods 3, 4, 7, 11, 12, and 13.

For the remainder of the hydrographs (about 23 percent), the transient data show cycles of increasing and decreasing water levels. An increase in water level followed by a decrease is observed for some wells while the opposite is observed for others. In several wells, more than one increasing-decreasing cycle is observed. Although wells showing this type of transient

behavior are found in pods 3, 4, 5, 7, 9, and 13, the majority are located in Wilbarger County in pod 4 and Haskell County in pod 7. For many of the wells in Haskell County, the latest trend is a drop in water level of about 20 feet between the mid-1990s and 2000. In general, the 2000 water level for these wells is at or slightly below the lowest water level ever measured in the well. Precipitation data from a gage in Haskell, Texas indicate drought conditions between the mid-1990s and 2000 (see Section 2.1) corresponding to the same time period as the observed water-level declines. The current declines are most likely associated with the drought, and water levels in these wells are expected to rise again once precipitation increases and the drought ends. Examples of hydrographs with increasing-decreasing cycles are shown in Figure 4.3.28.

Figure 4.3.29 shows the locations for which transient water-level data (hydrographs) are available for the Blaine aquifer based on data found on the TWDB and USGS websites. The transient data for the Blaine aquifer can be separated into two basic types. The first type exhibits little change (± 20 feet) in water-level elevation with time (Figure 4.3.30). Hydrographs of this type show data that remain nearly constant with time, data that increase slightly with time, and data that decrease slightly with time. The second type exhibits large and oscillating changes with time (Figure 4.3.31). For many of the wells, a large decrease in water-level elevation is observed during the 1960s, followed by an approximately 30-year increase. The degree of change varies from about 25 feet to about 90 feet in Texas and from about 20 feet to about 140 feet in Oklahoma.

Transient data were also evaluated with respect to seasonal fluctuations in the Seymour aquifer and the unconfined portion of the Blaine aquifer. Data for a total of three wells in Seymour pods 4, 7, and 13 were sufficient for this evaluation (Figure 4.3.32). Nearly monthly water-level measurements are available over approximately 10 years for well 13-46-504 in Wilbarger County and well 21-42-409 in Haskell County and over approximately 6 years for well 30-18-502 in Jones County. Water-level data for the Blaine aquifer in Texas were insufficient for evaluation of seasonal fluctuations. However, data for several wells completed to the Blaine in Oklahoma were sufficient (Figure 4.3.33).

Data for the well completed to the Seymour aquifer in Wilbarger County show an overall increase from July 1975 to about July 1977 and then an overall decrease from July 1977 through about July 1984 (see Figure 4.3.32). Fluctuations in this overall trend indicate a slight decline in

water level from about September to November 1976 and then recovery until May 1977. In general, water levels for the decreasing portion of the curve slightly increase or are stable in the late winter and spring of most years, slightly decline during the summer, and follow the overall decrease during the fall and early winter. These fluctuations are on the order of half a foot indicating small seasonal changes in water level in this well.

Water-level data for the well completed to the Seymour aquifer in Haskell County show several cycles of decreasing then increasing trends of periods ranging from about 7 years to about 1 year (see Figure 4.3.32). Imposed on the overall trend are smaller-scale fluctuations with respect to both length of time and degree of change in water level. The timing of the fluctuations does not appear to follow a seasonal pattern, with increases occurring both in the winter (e.g., January 1981) and in the summer (e.g., July 1983). Likewise, decreases are observed in both the winter (January 1983) and the summer (July 1978). Consequently, no consistent changes in water level on a seasonal basis are observed in this well.

Data for the well completed to the Seymour aquifer in Jones County show a very consistent seasonal trend over the period of record (see Figure 4.3.32). Water levels decline every late spring and summer, increase in the fall and early winter, then remain stable until declining again the next spring. The degree of fluctuation ranges from about 1.5 to 3 feet.

A consistent seasonal trend is observed in the water-level data for well 344220099441601 completed to the Blaine aquifer in Harmon County, Oklahoma (see Figure 4.3.33). Data over a 4-year period show lower water levels in the July to September time frame every year and higher water levels from about November to May. Fluctuations in the water level range from about 20 feet to about 55 feet.

Data for another well completed to the Blaine aquifer in Harmon County, Oklahoma show no correlation between season and water level (see Figure 4.3.33). Water-level data for well 343855099544501 show three cycles of increasing then decreasing water levels. These cycles, however, do not correspond to changes in season. The time period for each increase ranges from 2 to 4 months, but the time period for the decreases ranges from over 6 months to about one and a half years.

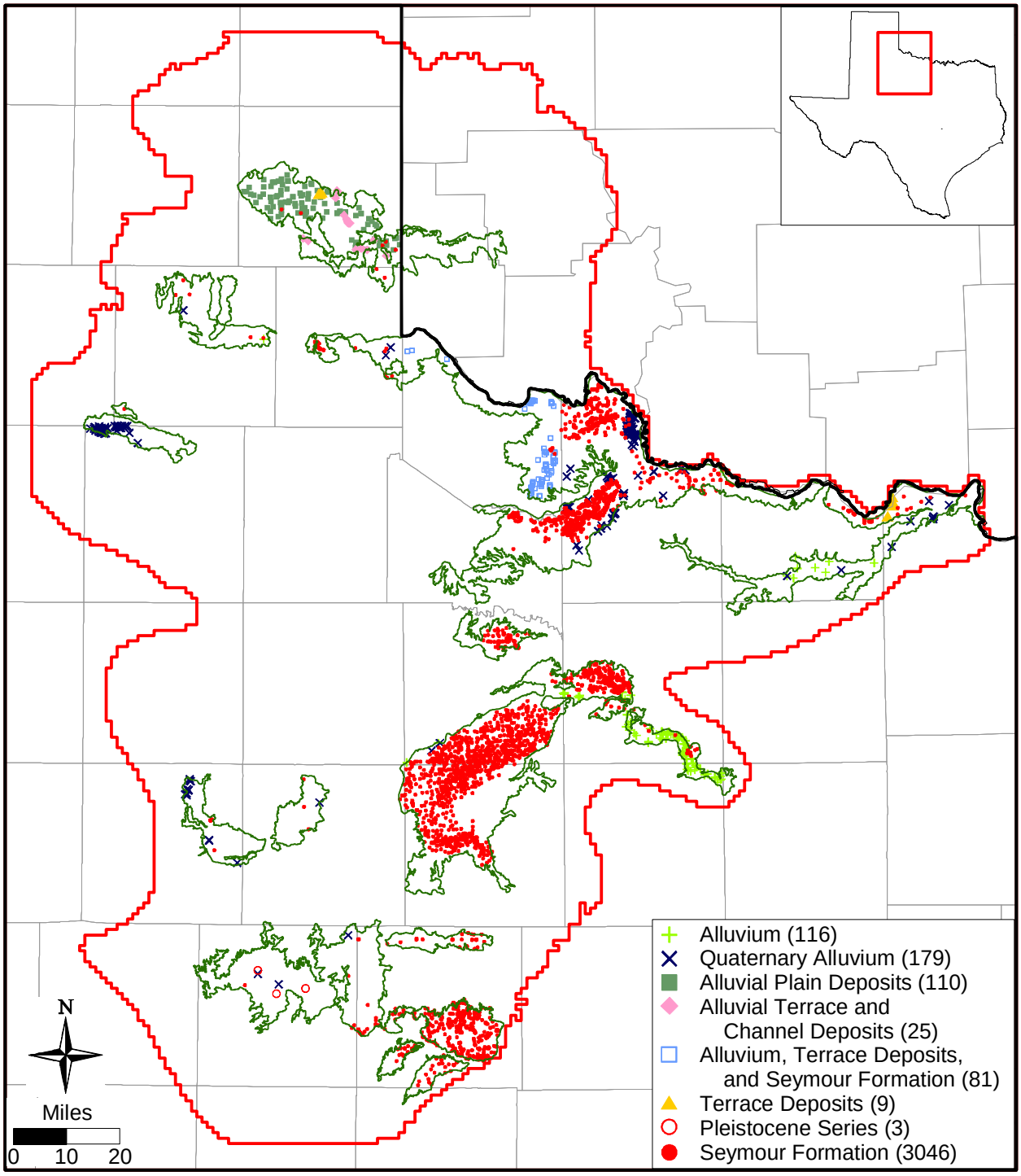

Figure 4.3.1 Water-level measurement locations for the Seymour aquifer.

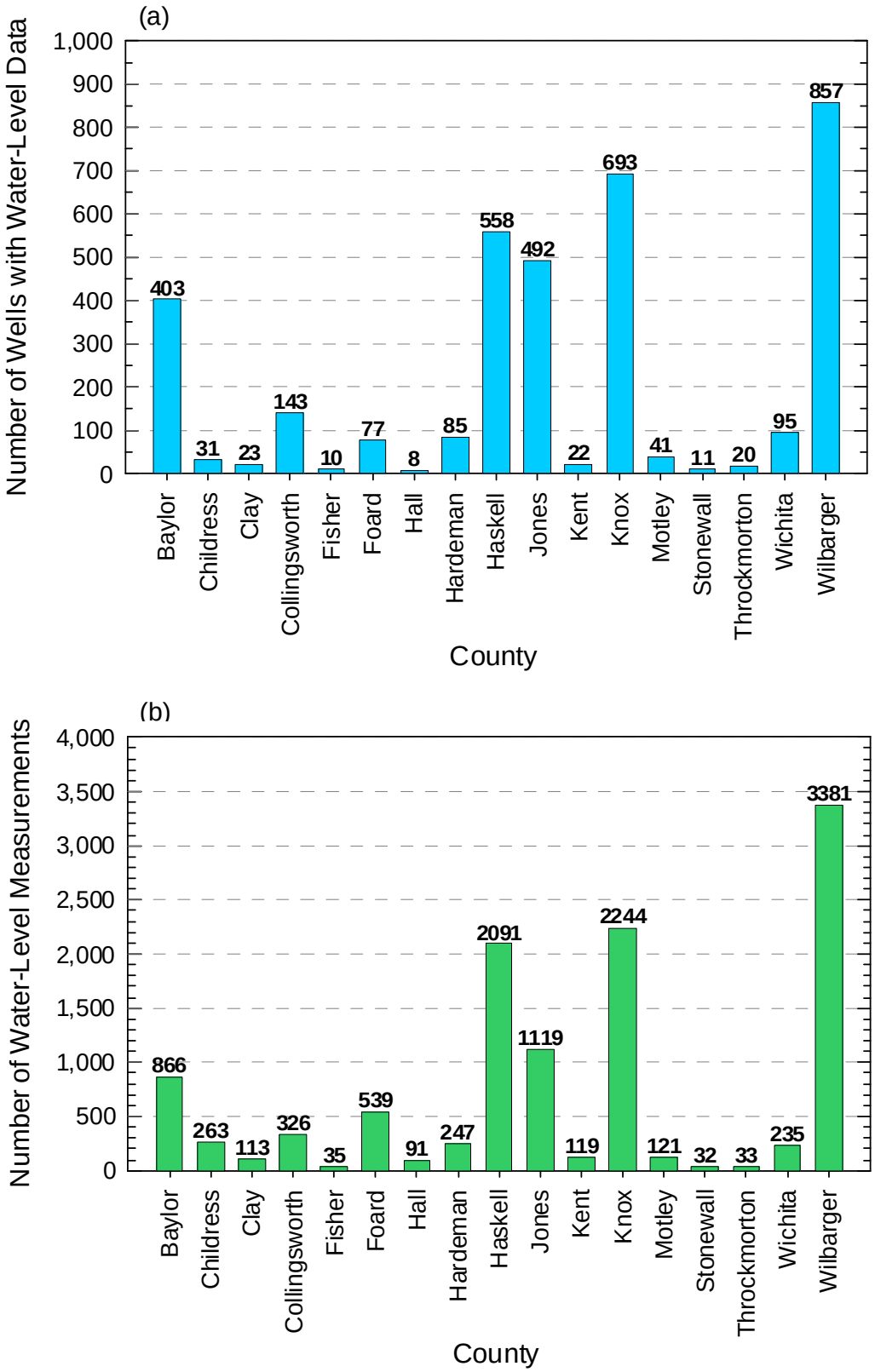

Figure 4.3.2 County data for (a) number of wells with water-level data and (b) number of water-level measurements.

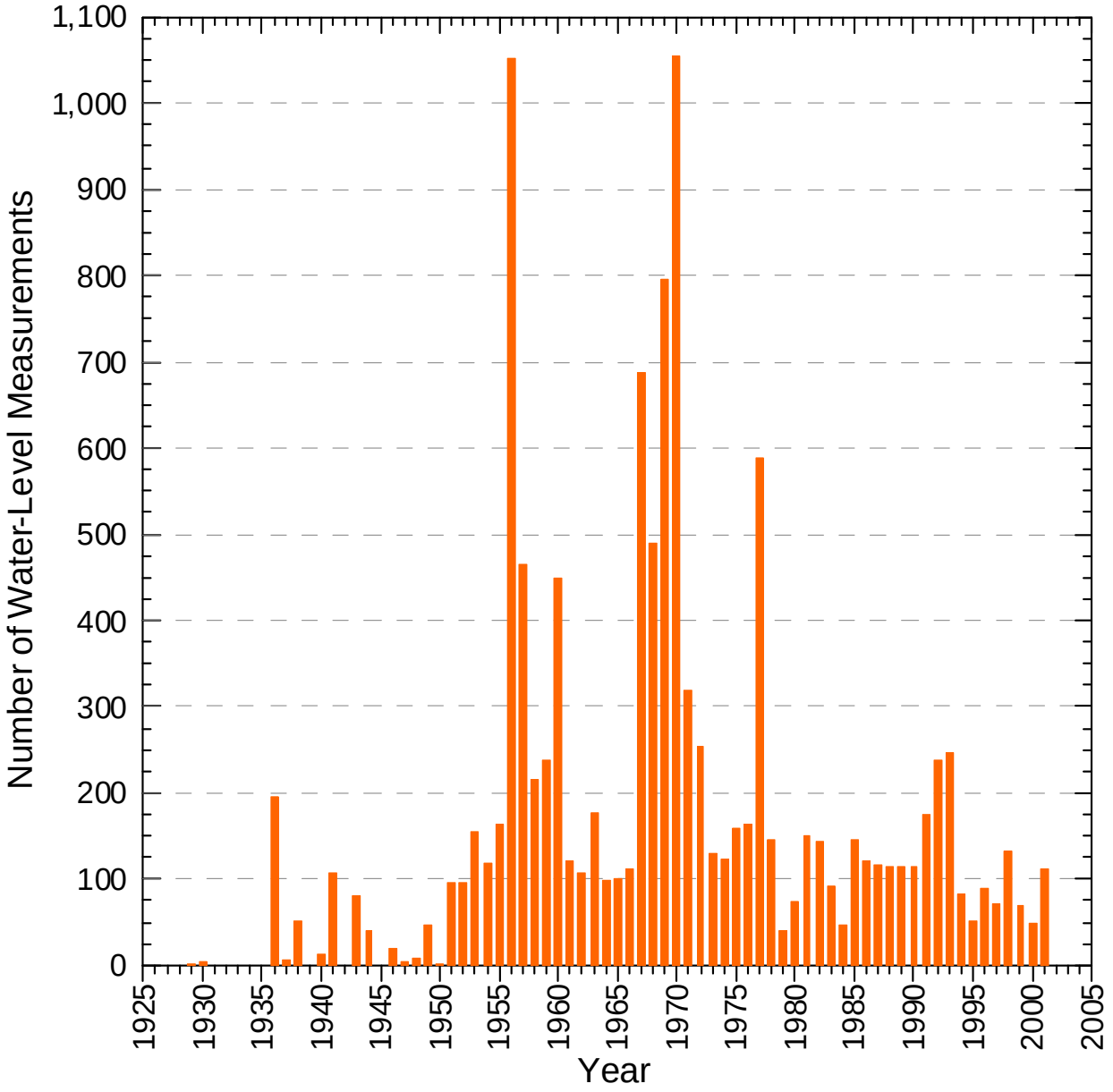

Figure 4.3.3 Temporal distribution of water-level measurements in the Seymour aquifer.

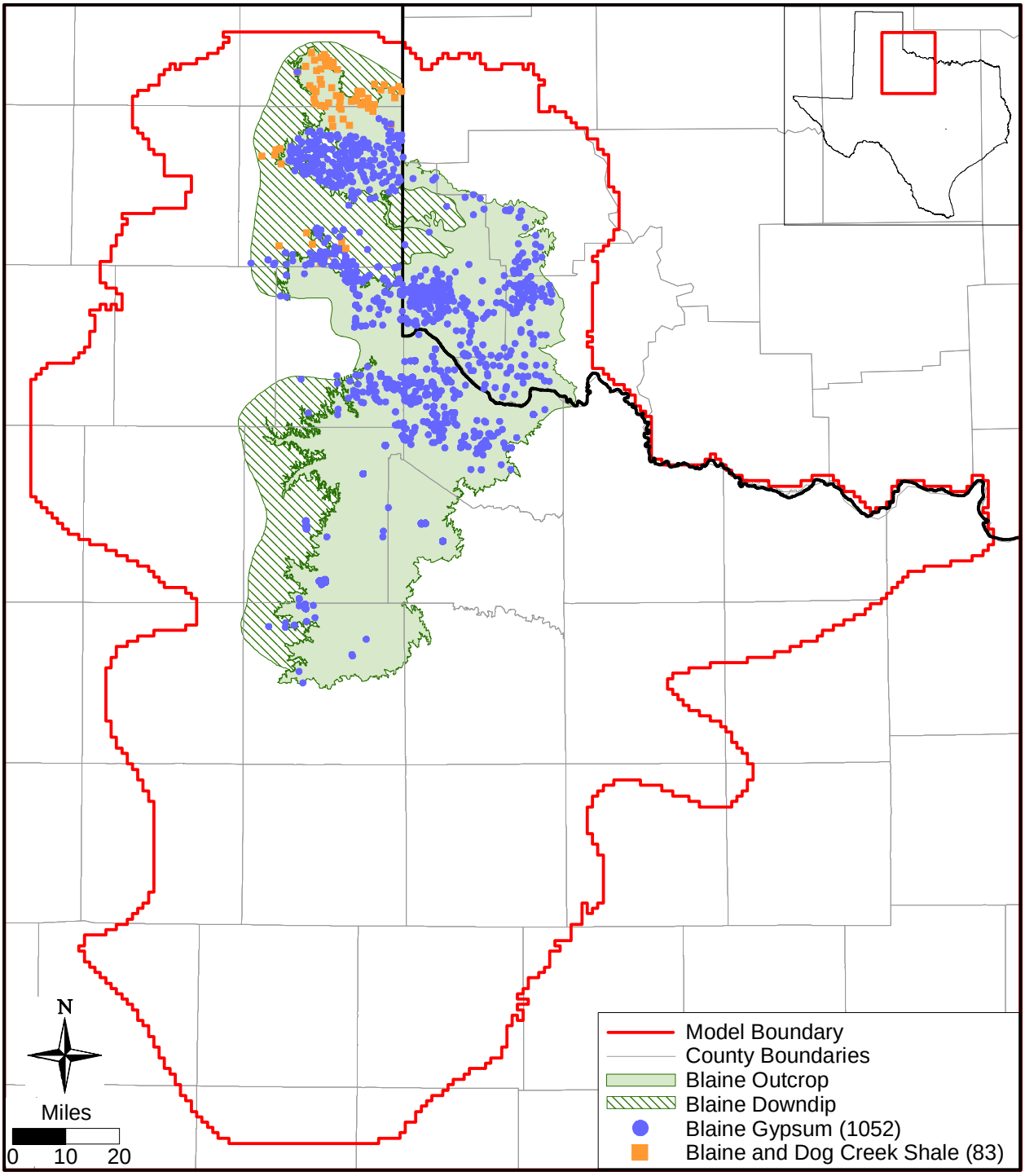

Figure 4.3.4 Water-level measurement locations for the Blaine aquifer.

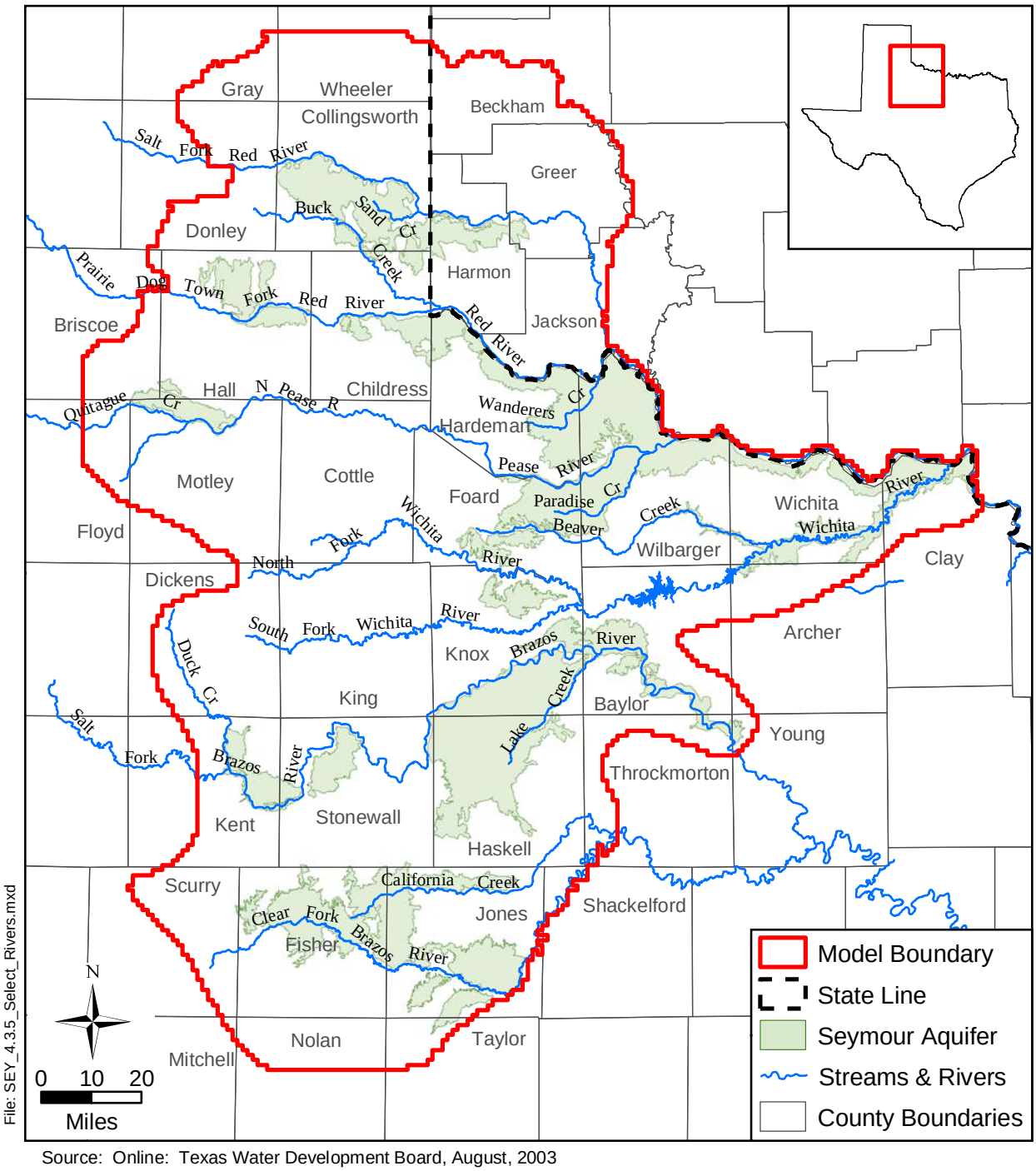

Source: Online: Texas Water Development Board, August, 2003

Figure 4.3.5 Major streams and rivers associated with each pod of the Seymour aquifer.

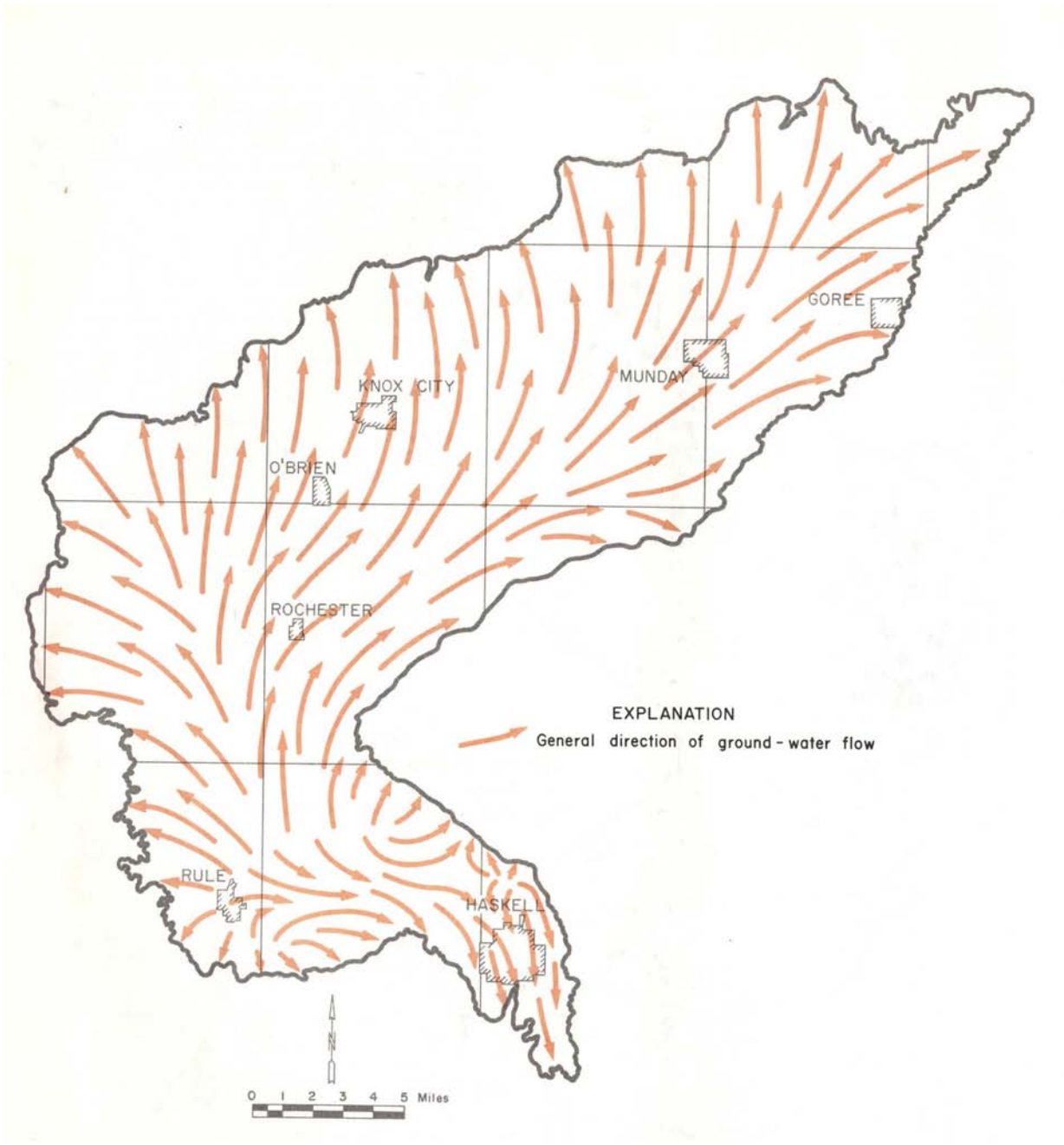

Figure 4.3.6 Groundwater flow direction in portions of pod 7 (from R.W. Harden & Associates, 1978).

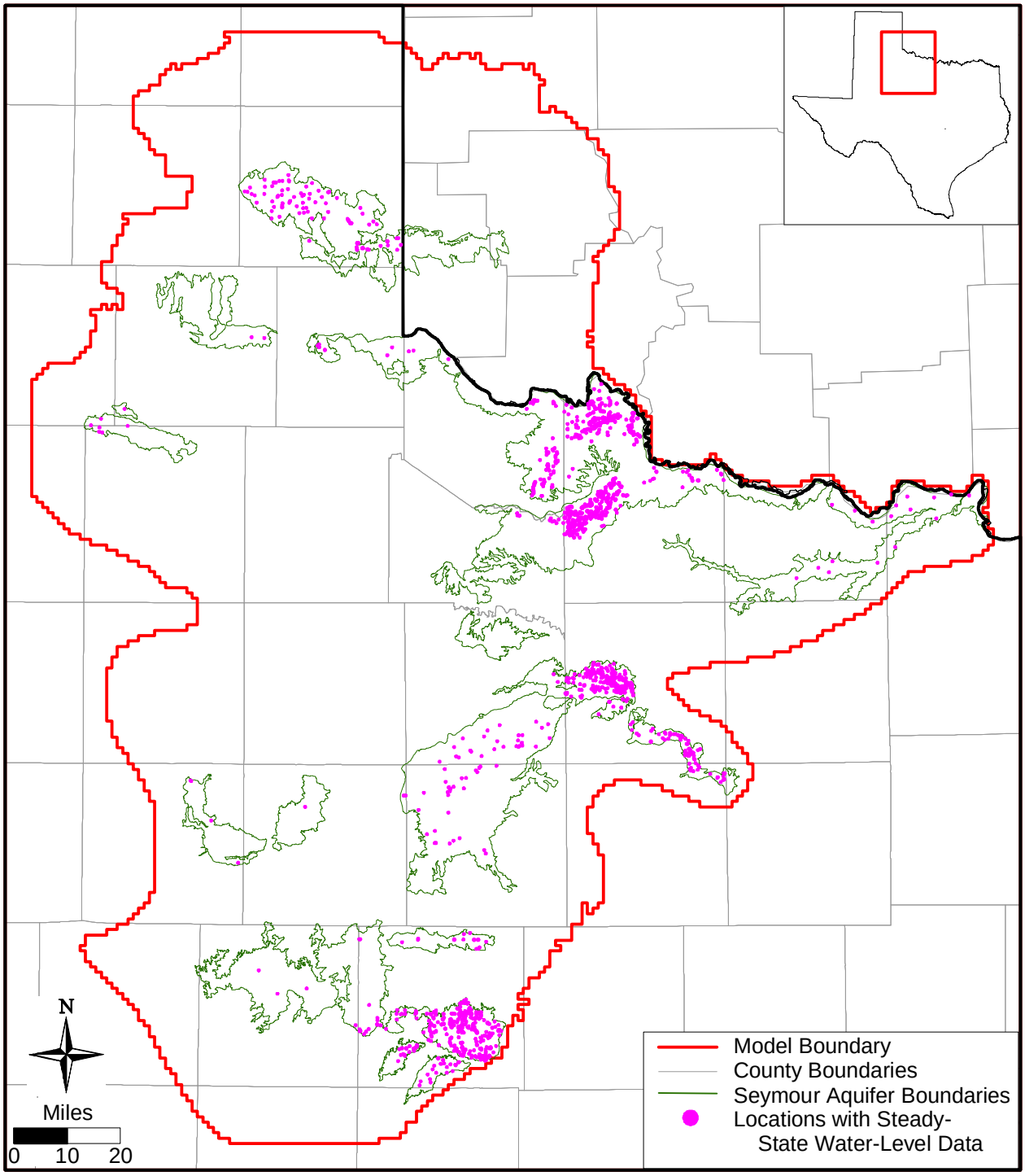

Figure 4.3.7 Locations with water-level data for steady-state conditions.

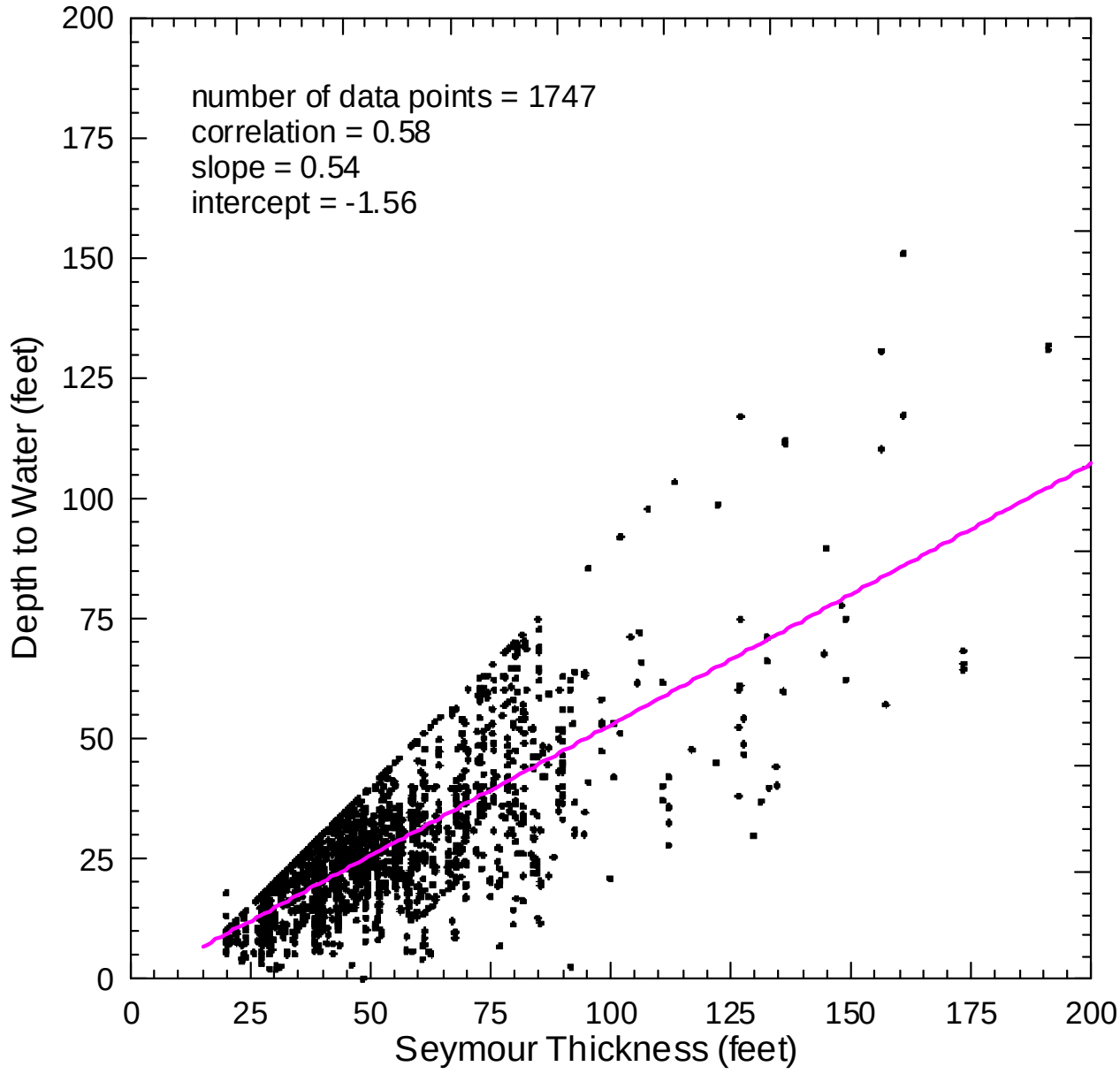

Figure 4.3.8 Correlation of Seymour thickness versus depth to water for the steady-state water-level data.

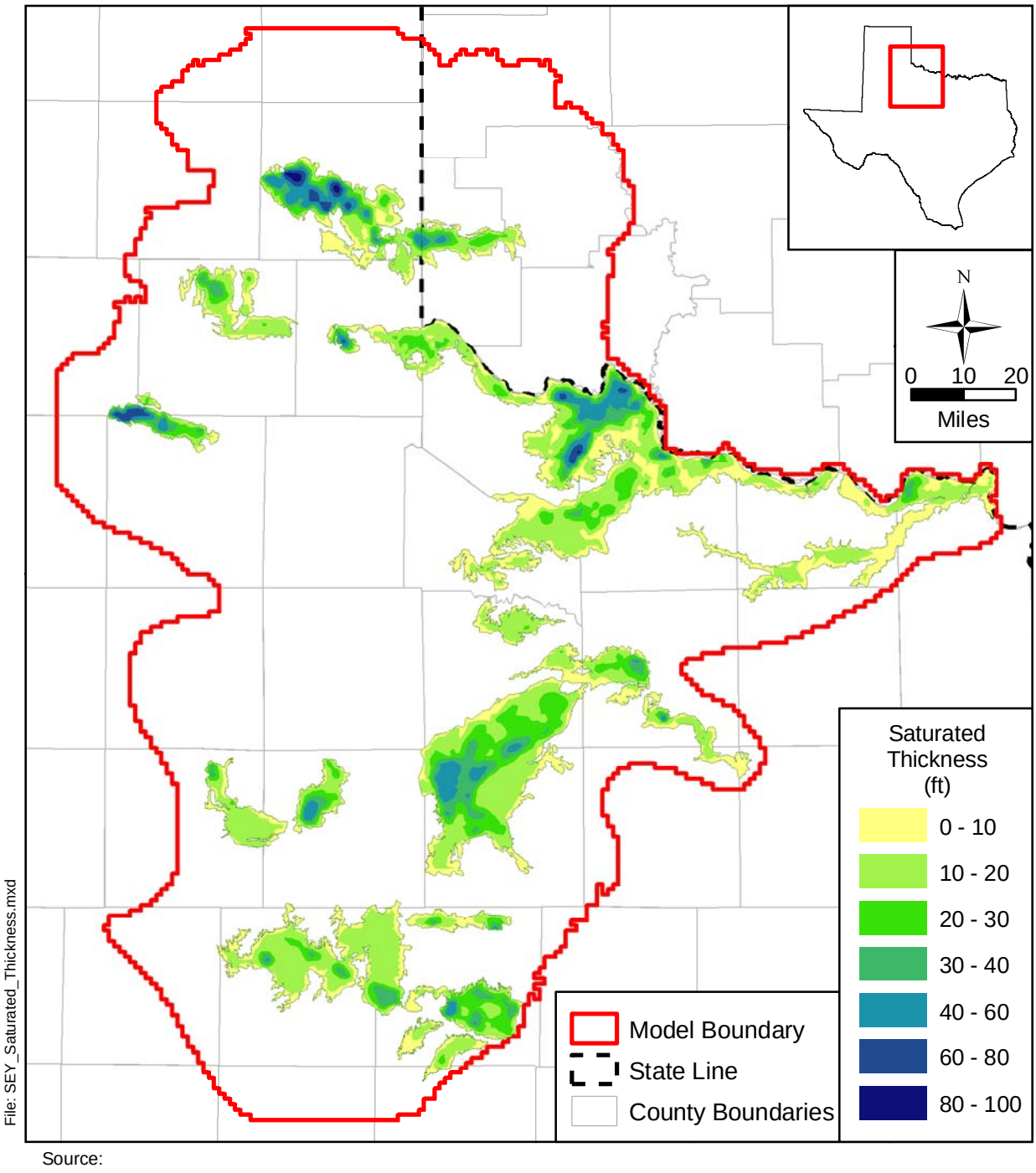

Figure 4.3.9 Estimated saturated-thickness contours for steady-state conditions in the Seymour aquifer.

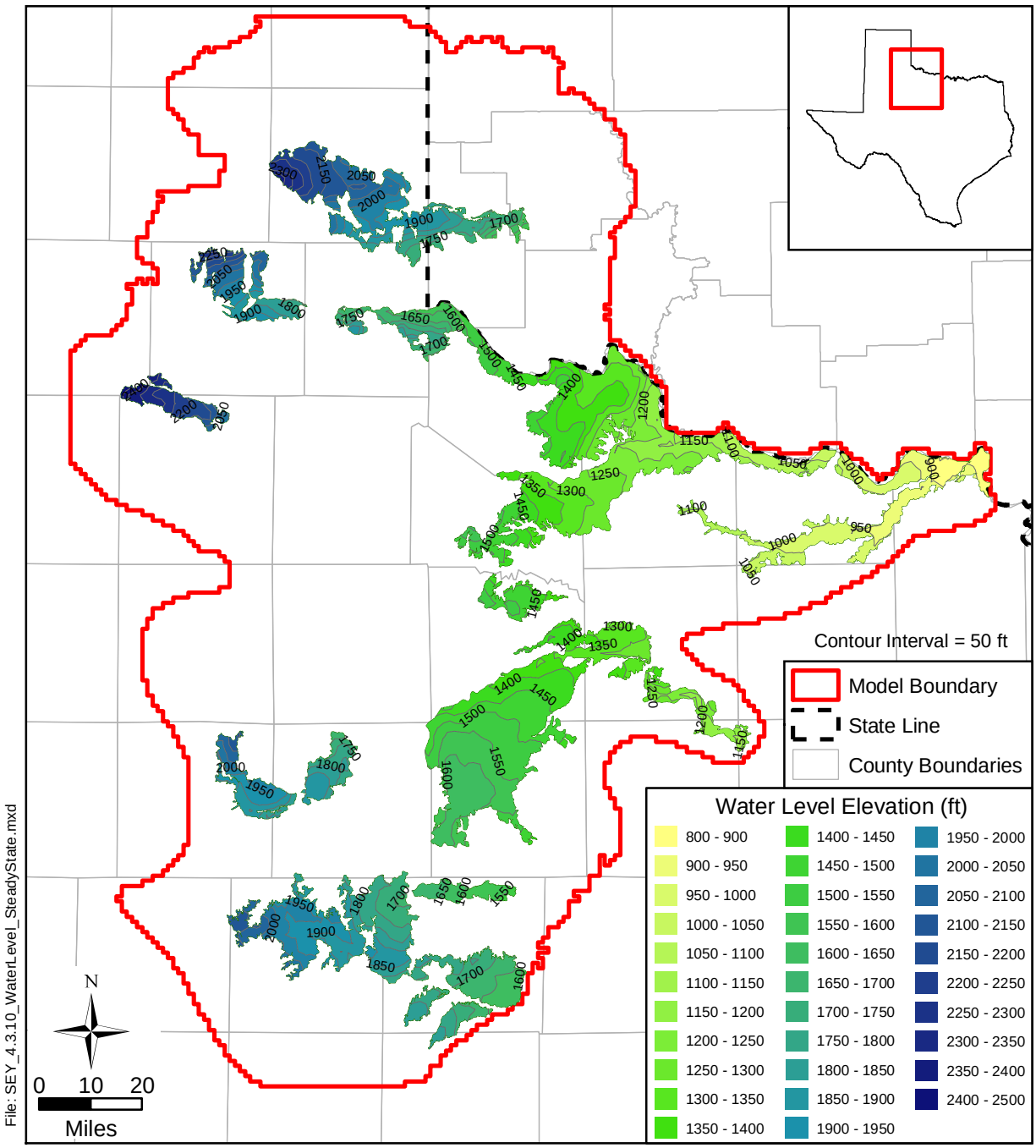

Figure 4.3.10 Estimated water-level elevation contours in the Seymour aquifer for steady-state conditions.

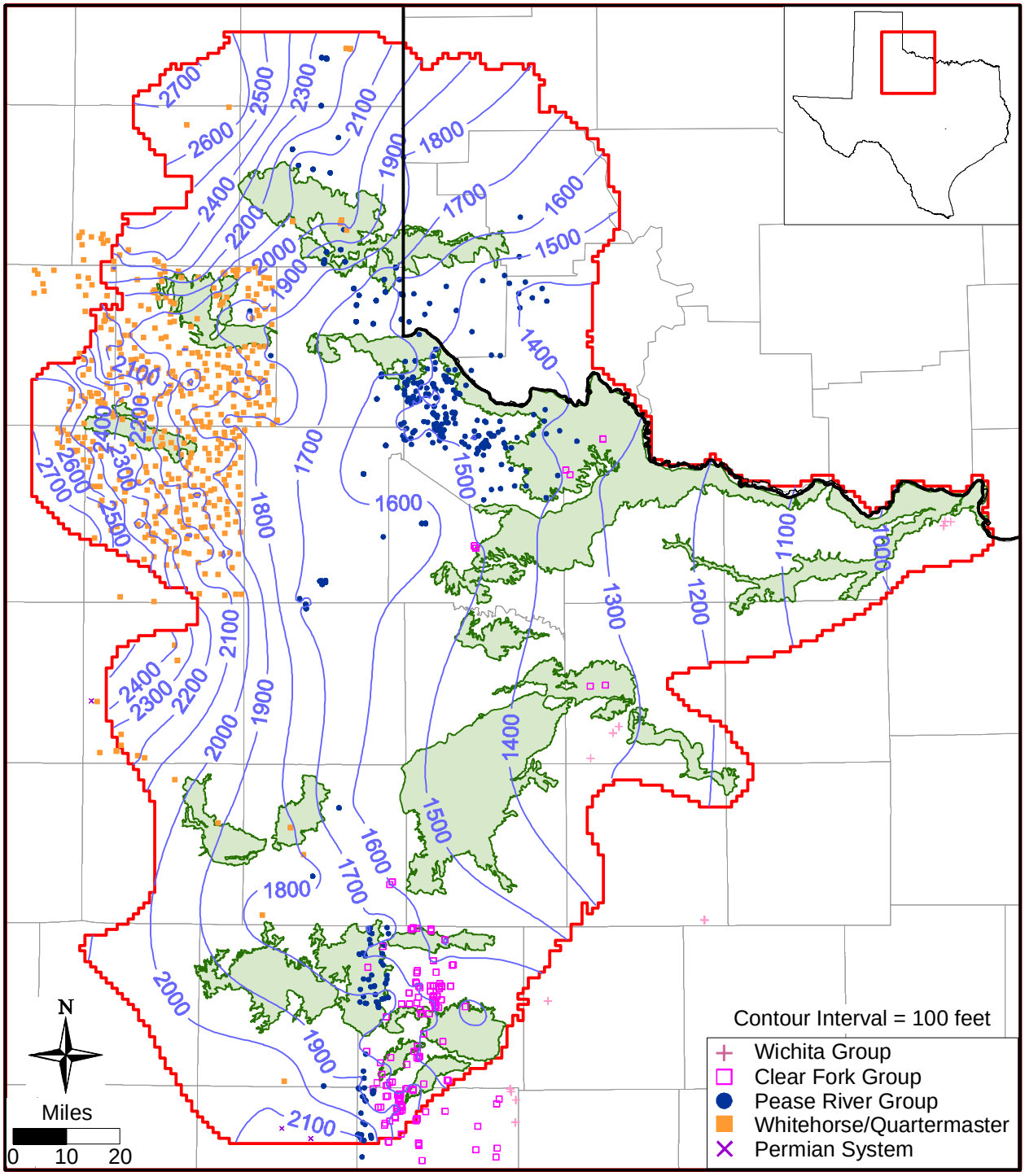

Figure 4.3.11 Estimated water-level elevation contours in model layer 2 for steady-state conditions.

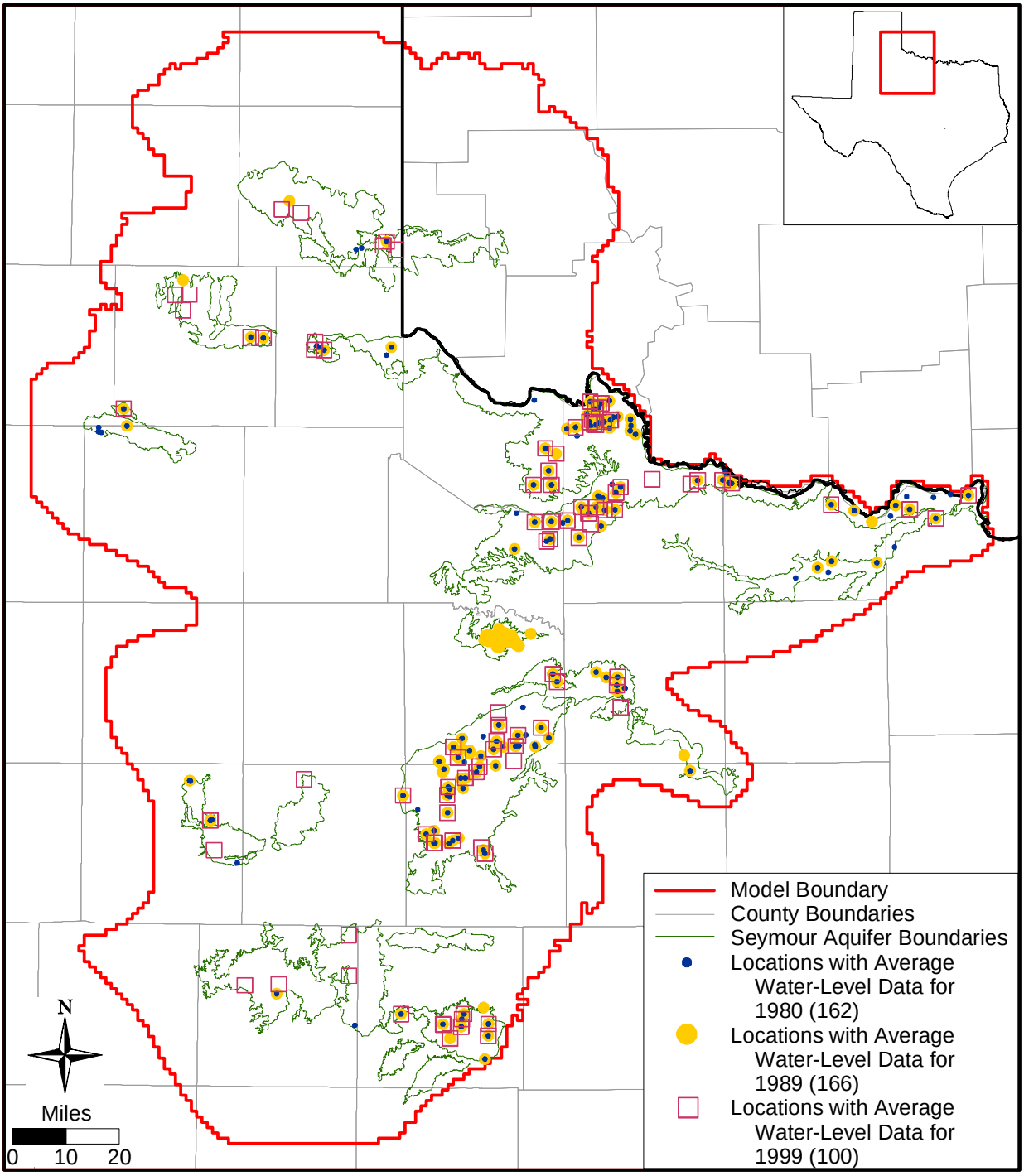

Figure 4.3.12 Locations with water-level data for the beginning of model calibration (1980), the end of model calibration (1989), and the end of model verification (1999).

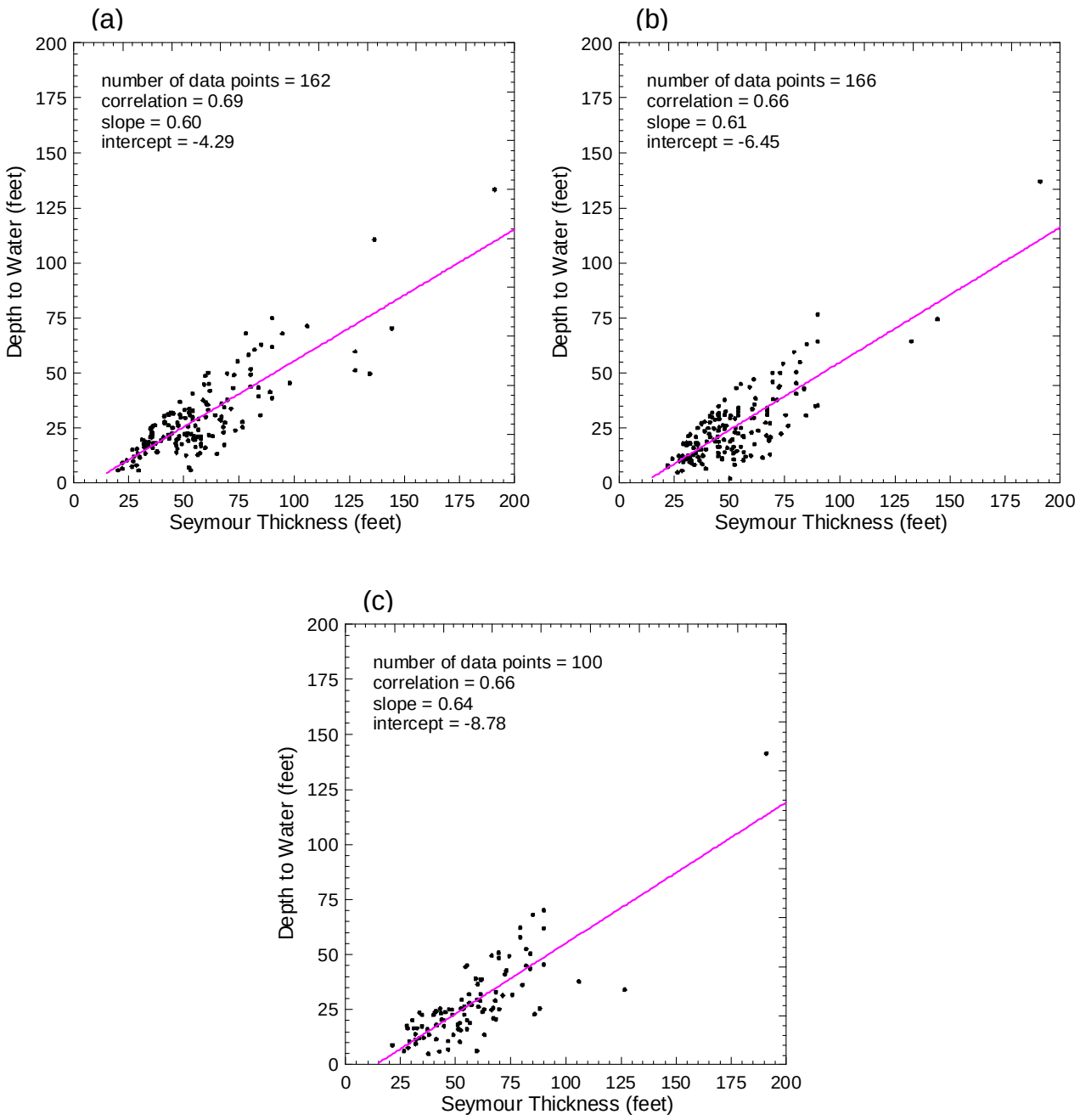

Figure 4.3.13 Correlation of Seymour thickness versus depth to water for the (a) 1980 water-level data, (b) 1989 water-level data, and (c) 1999 water-level data.

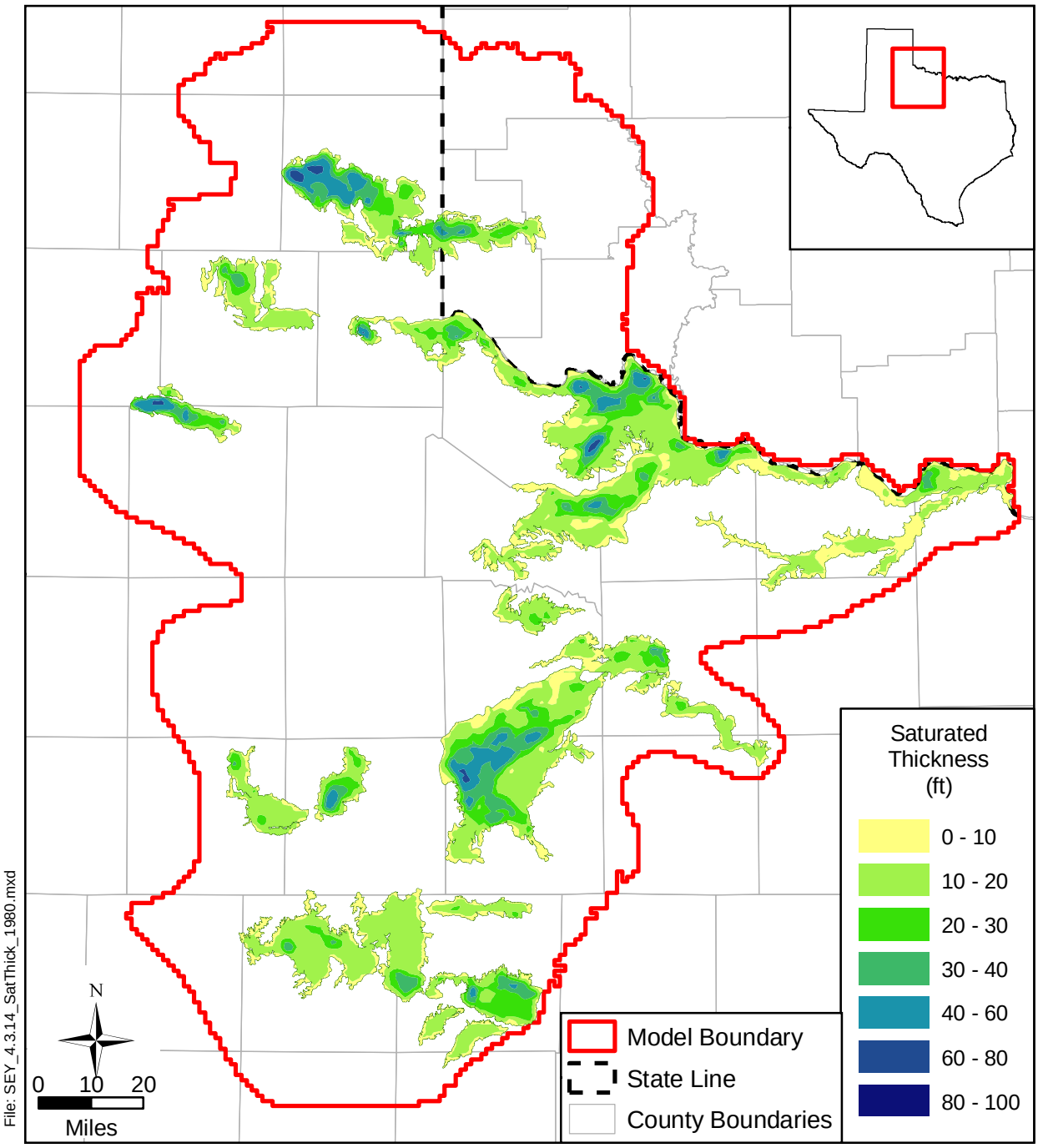

Figure 4.3.14 Estimated saturated-thickness contours for 1980 conditions in the Seymour aquifer.

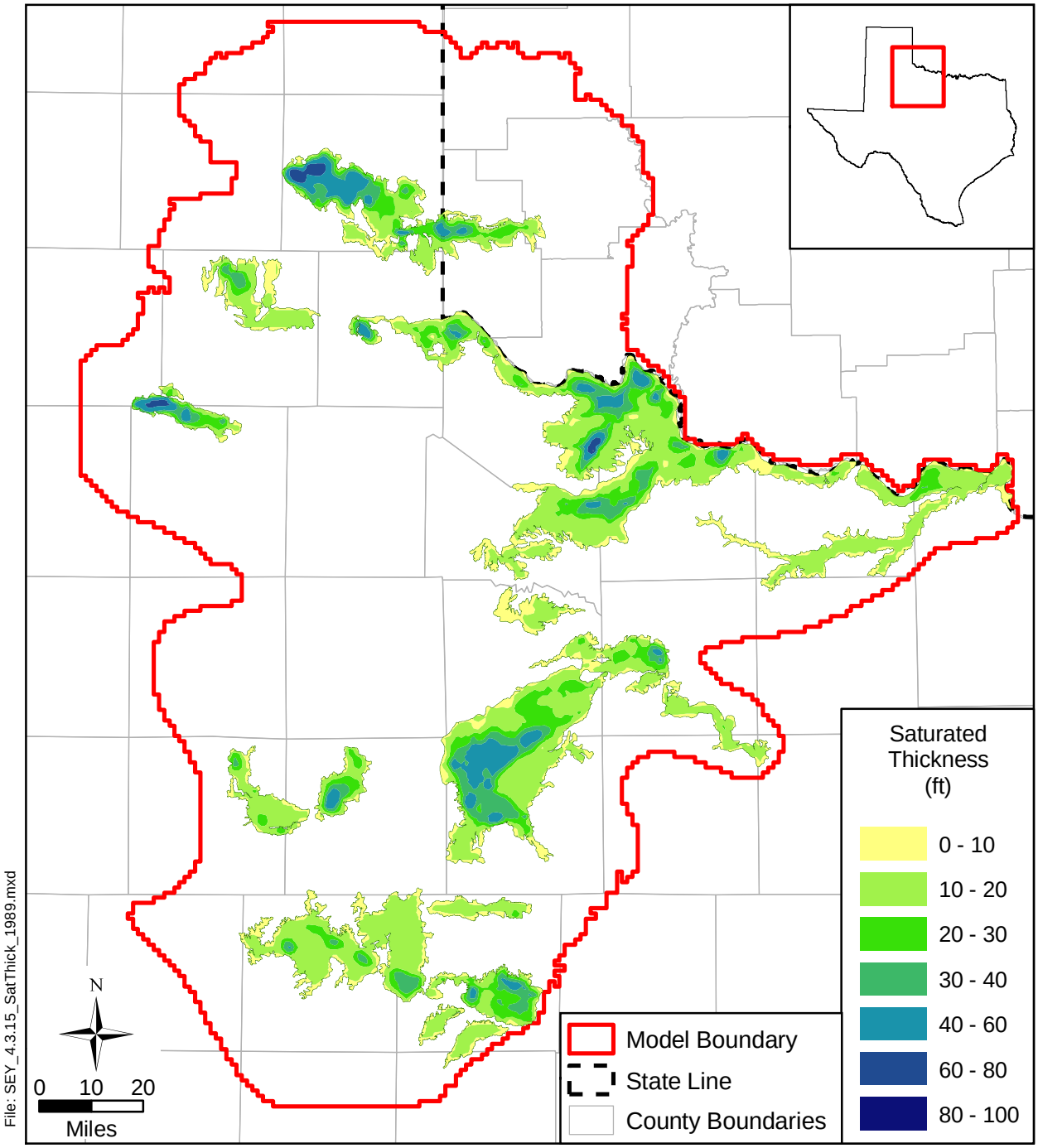

Figure 4.3.15 Estimated saturated-thickness contours for 1989 conditions in the Seymour aquifer.

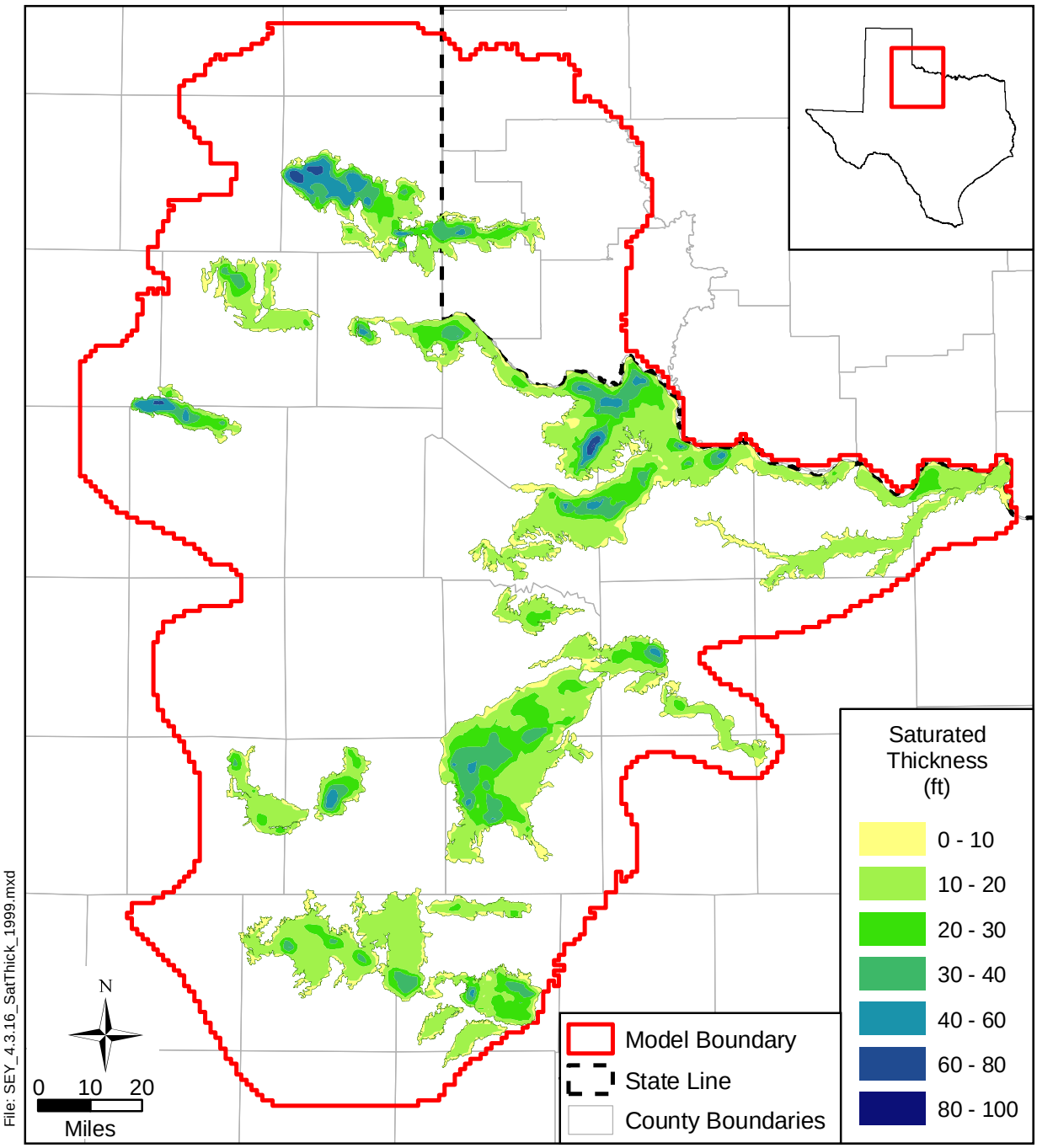

Figure 4.3.16 Estimated saturated-thickness contours for 1999 conditions in the Seymour aquifer.

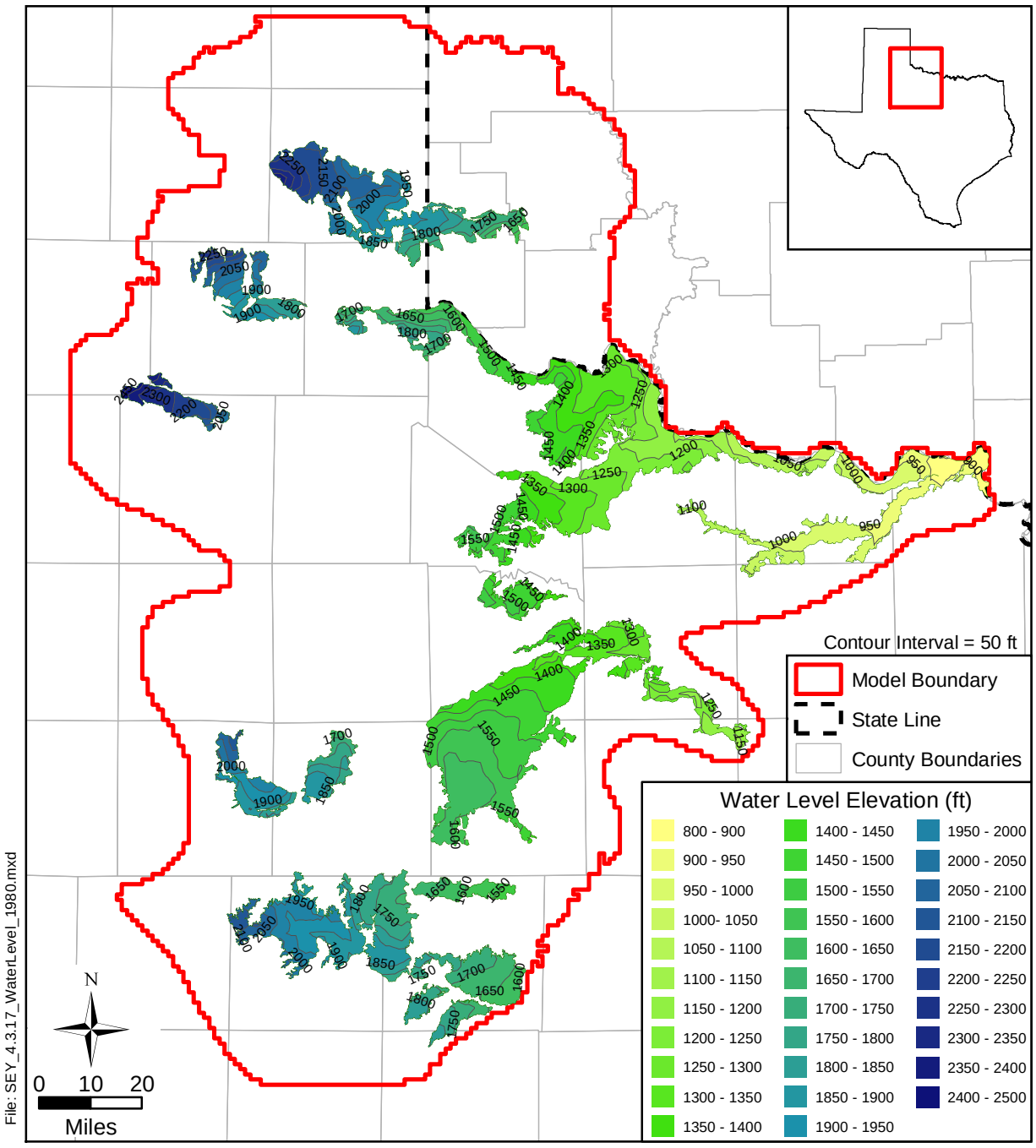

Figure 4.3.17 Estimated water-level elevation contours in the Seymour aquifer for 1980 conditions.

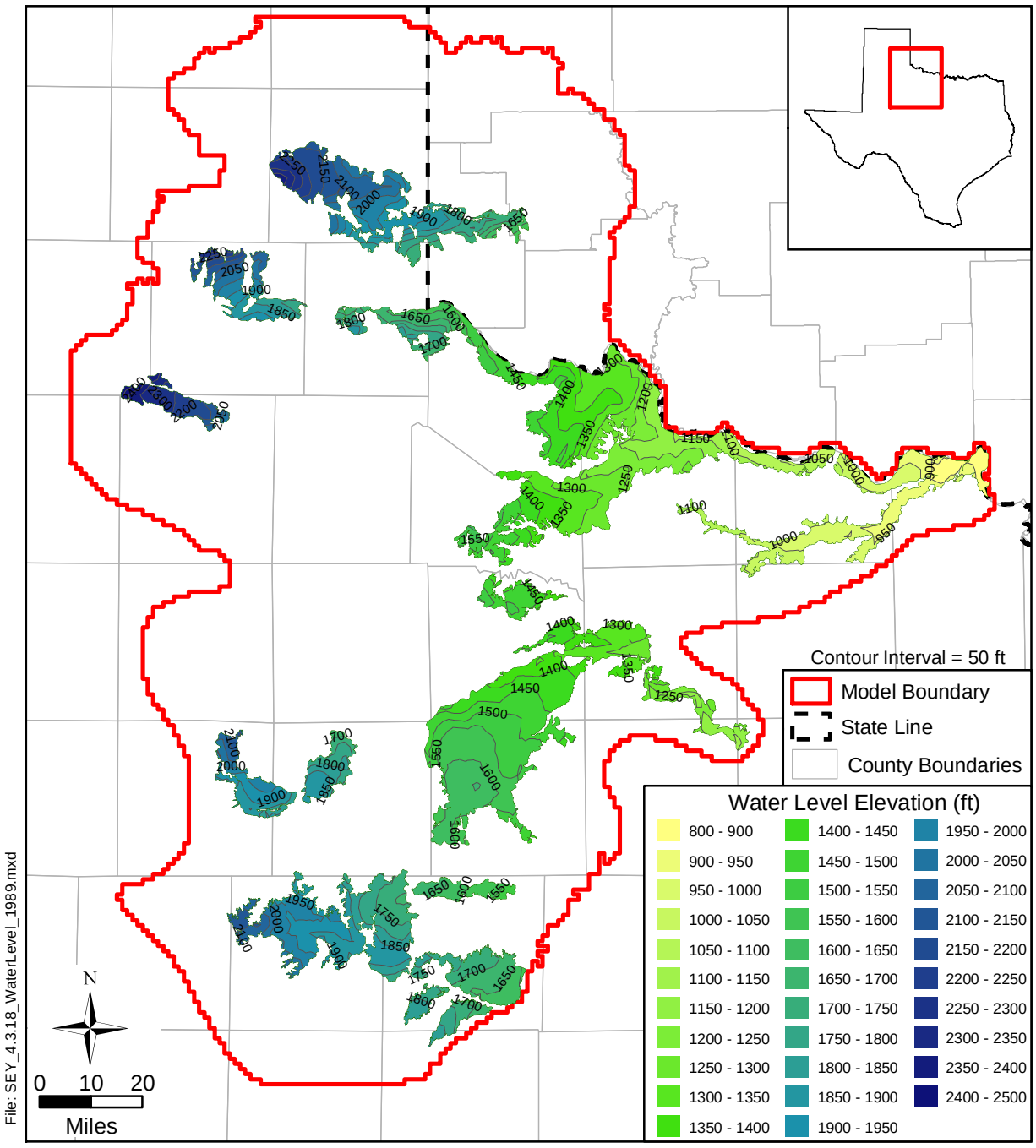

Figure 4.3.18 Estimated water-level elevation contours in the Seymour aquifer for 1989 conditions.

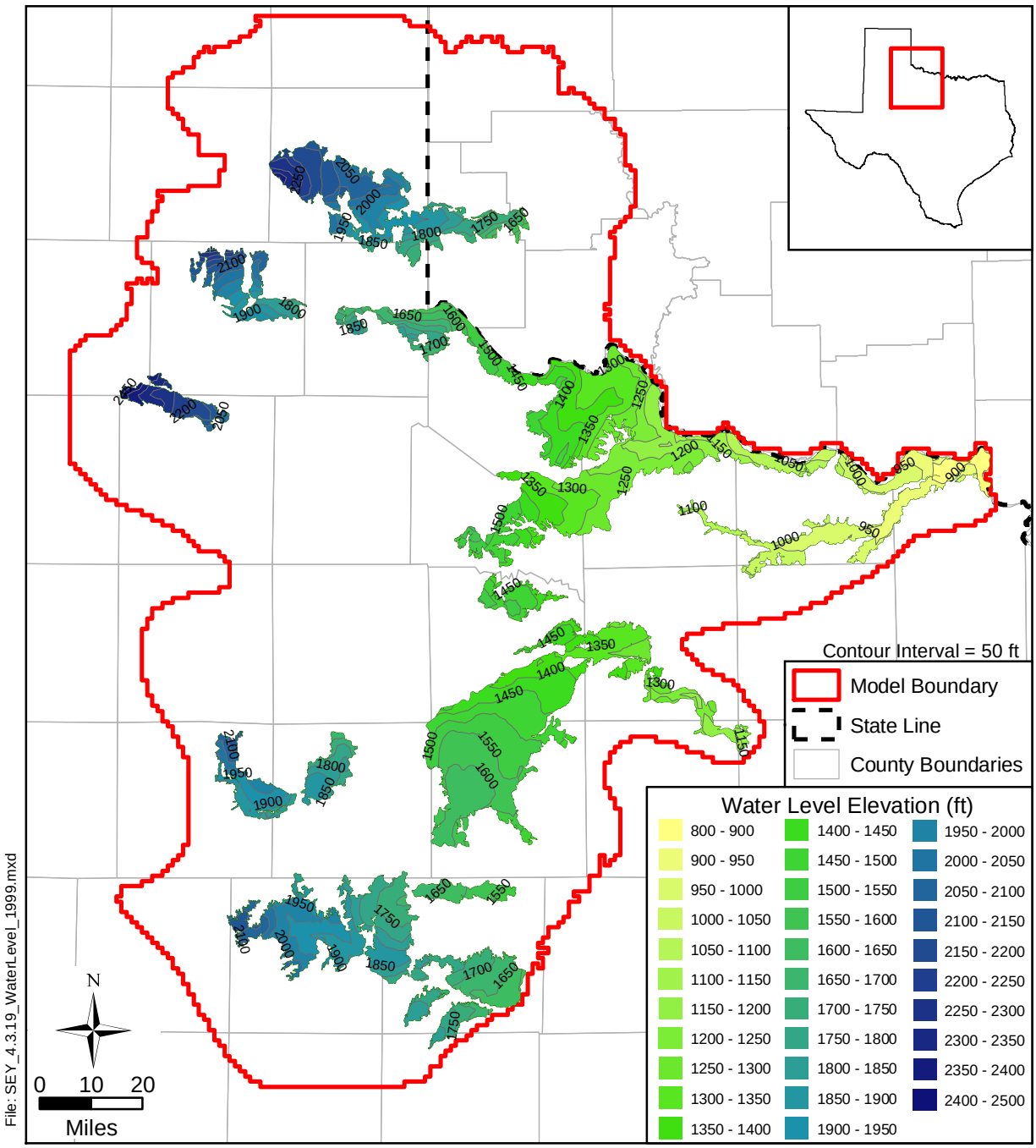

Figure 4.3.19 Estimated water-level elevation contours in the Seymour aquifer for 1999 conditions.

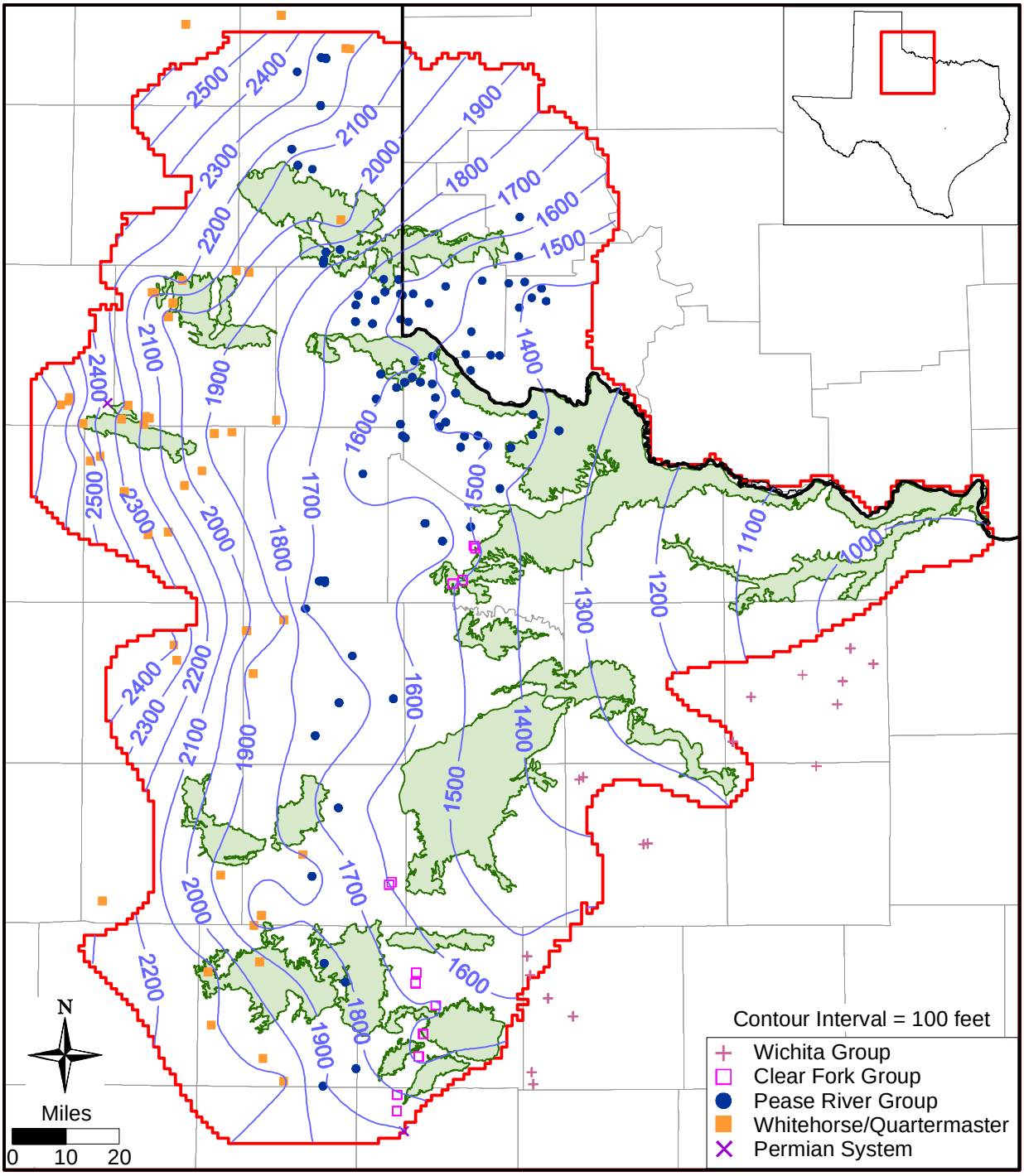

Figure 4.3.20 Estimated water-level elevation contours in model layer 2 for 1980.

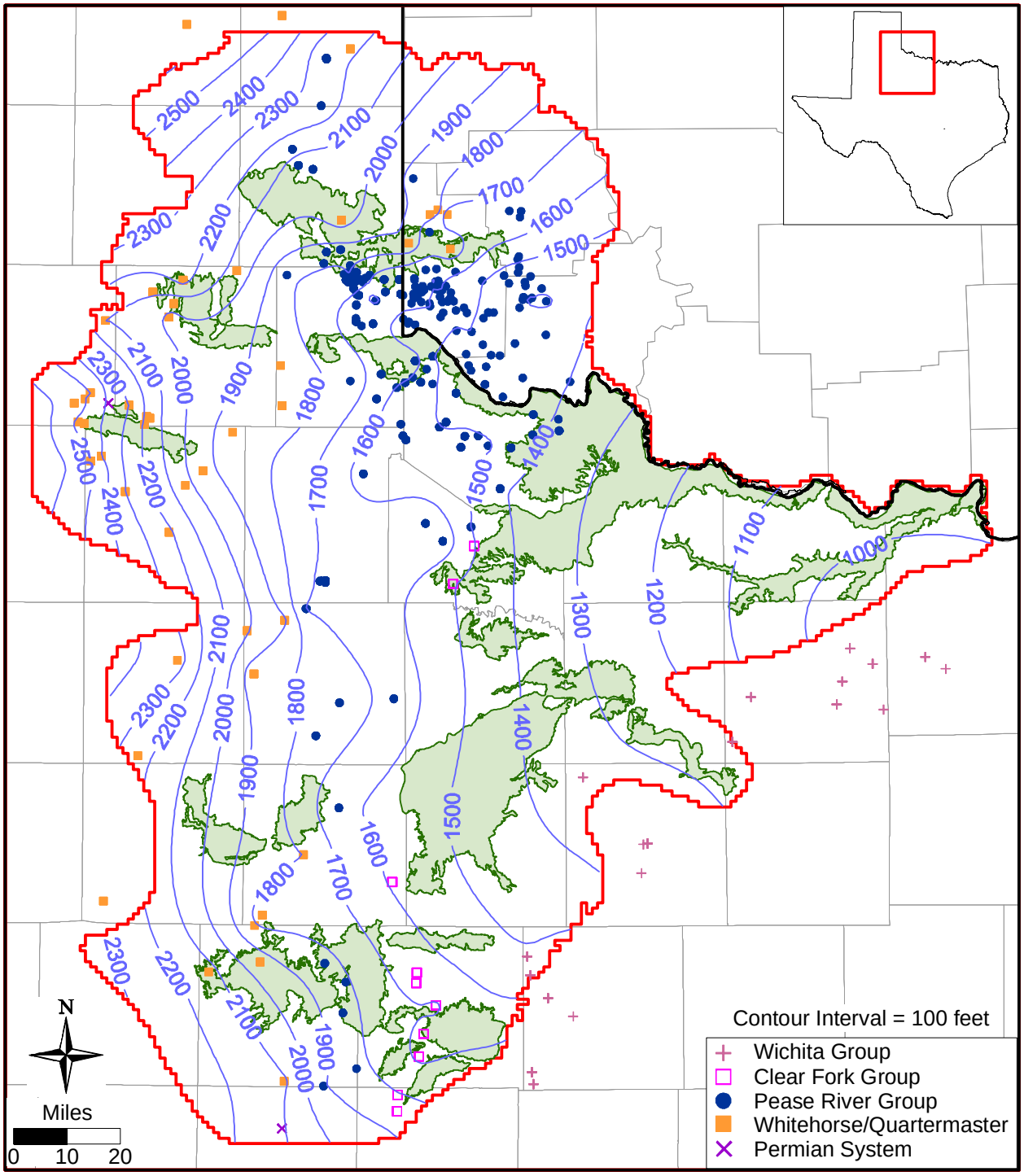

Figure 4.3.21 Estimated water-level elevation contours in model layer 2 for 1989.

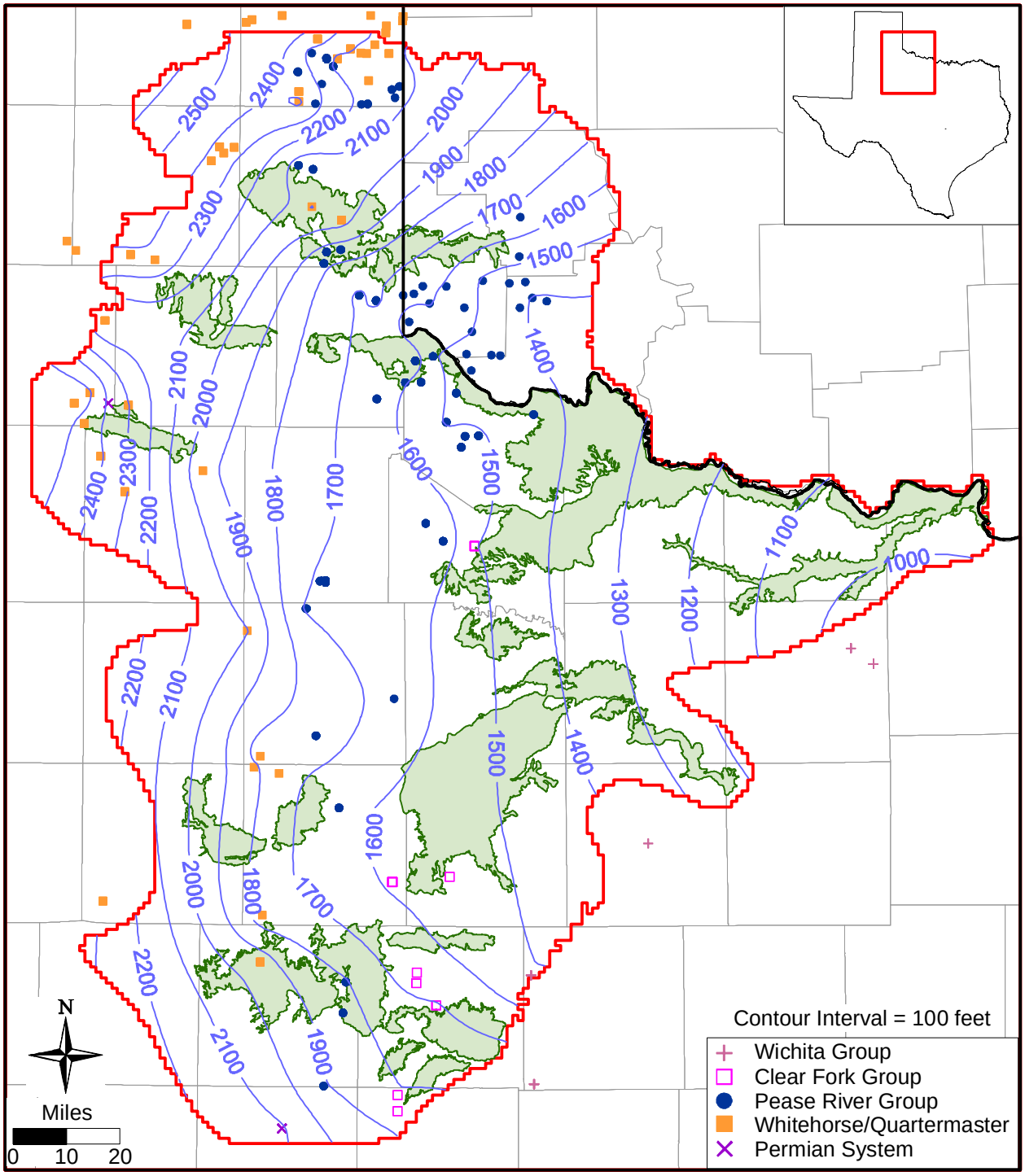

Figure 4.3.22 Estimated water-level elevation contours in model layer 2 for 1999.

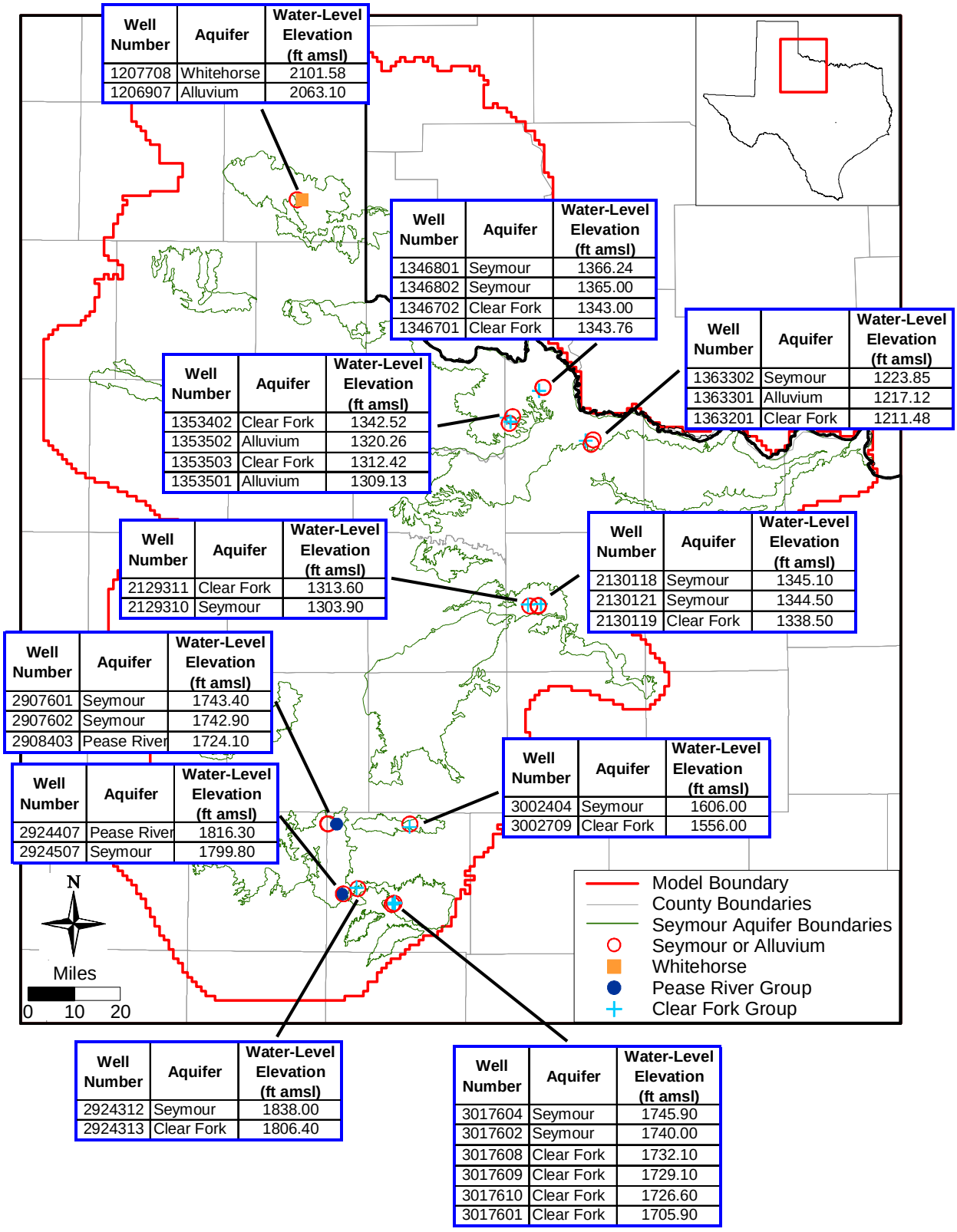

Figure 4.3.23 Comparison of water-level elevations in the Seymour aquifer and the underlying formation.

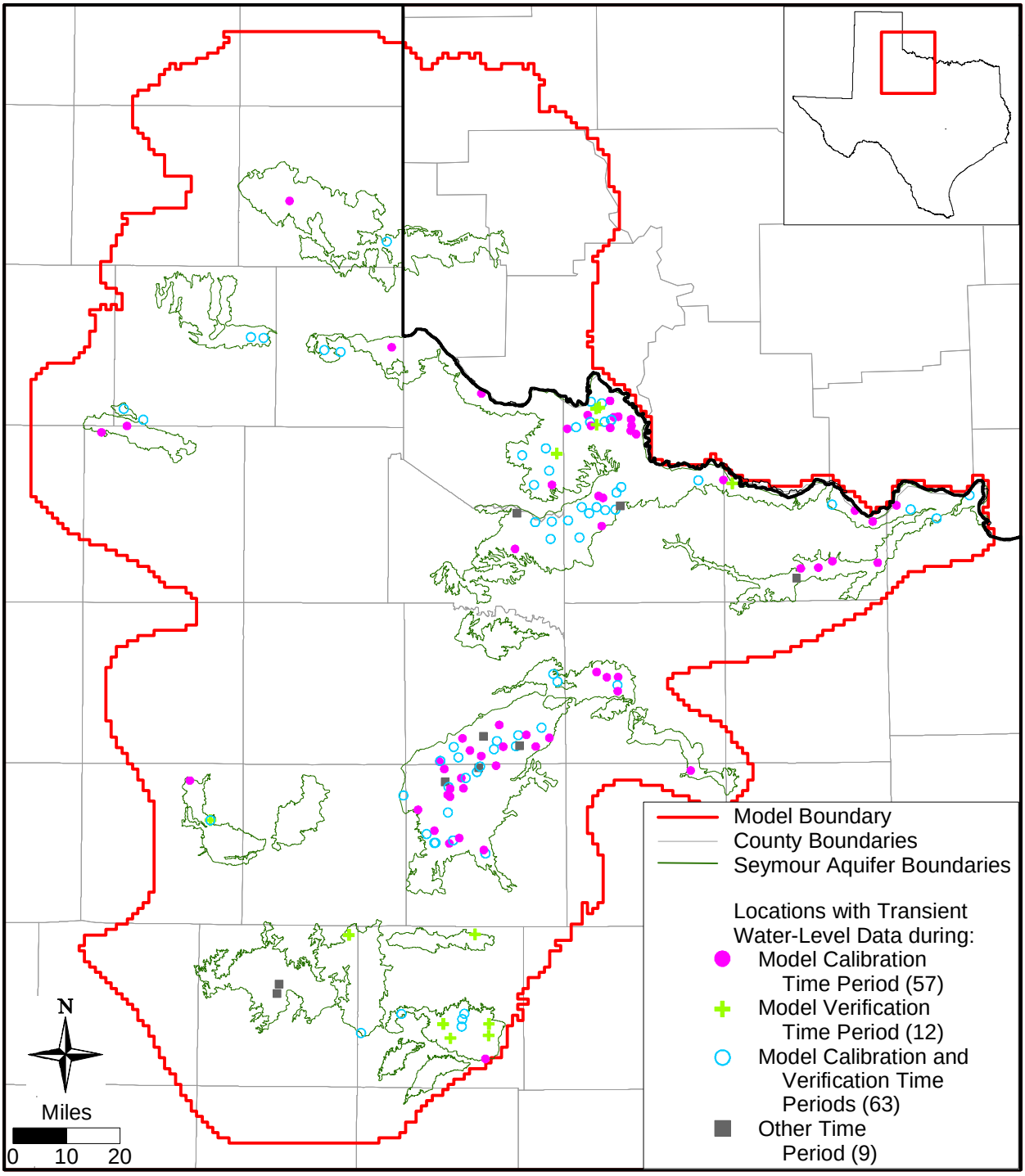

Figure 4.3.24 Locations with transient water-level data in the Seymour aquifer.

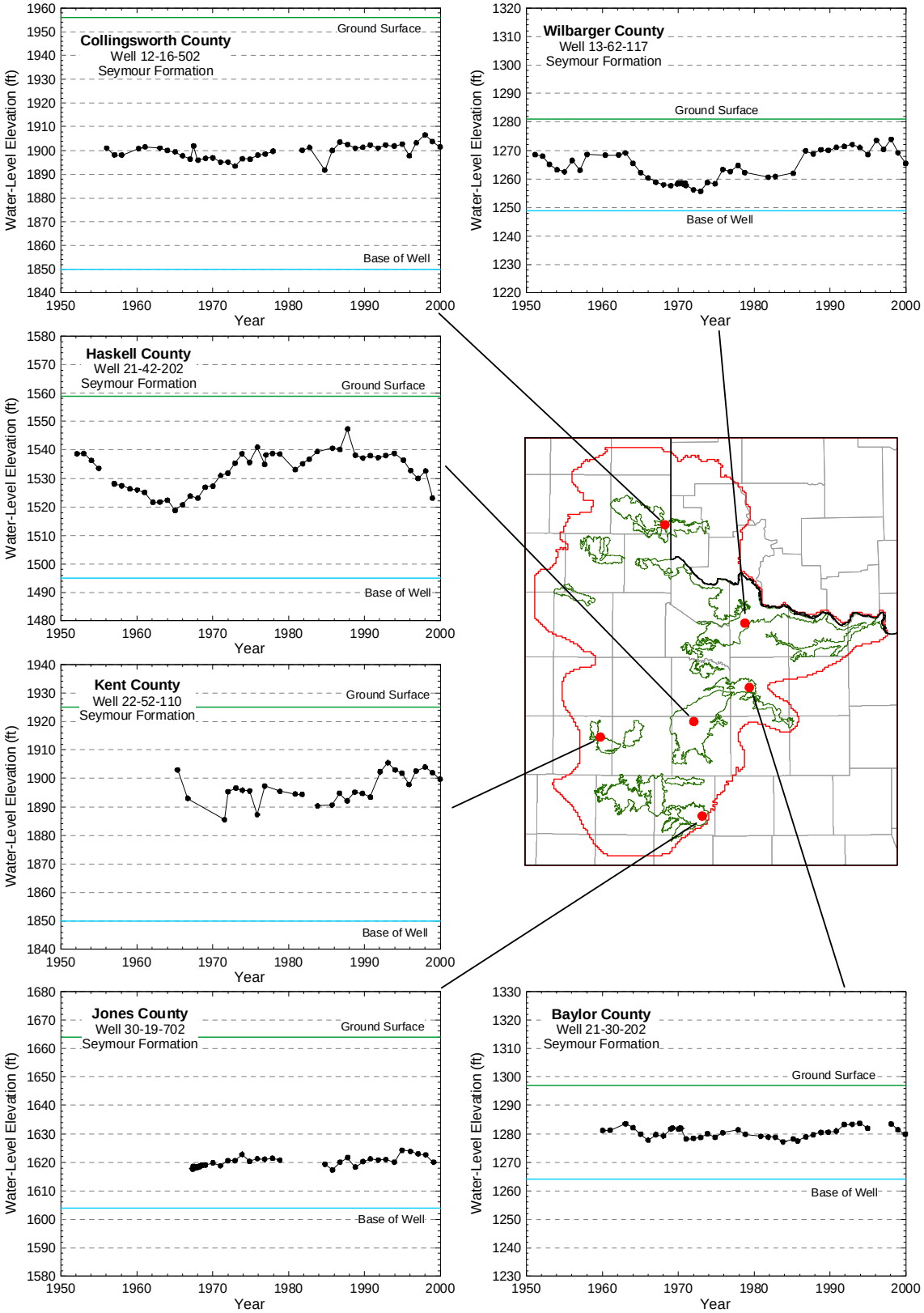

Figure 4.3.25 Example hydrographs showing stable water-level elevations with time in the Seymour aquifer.

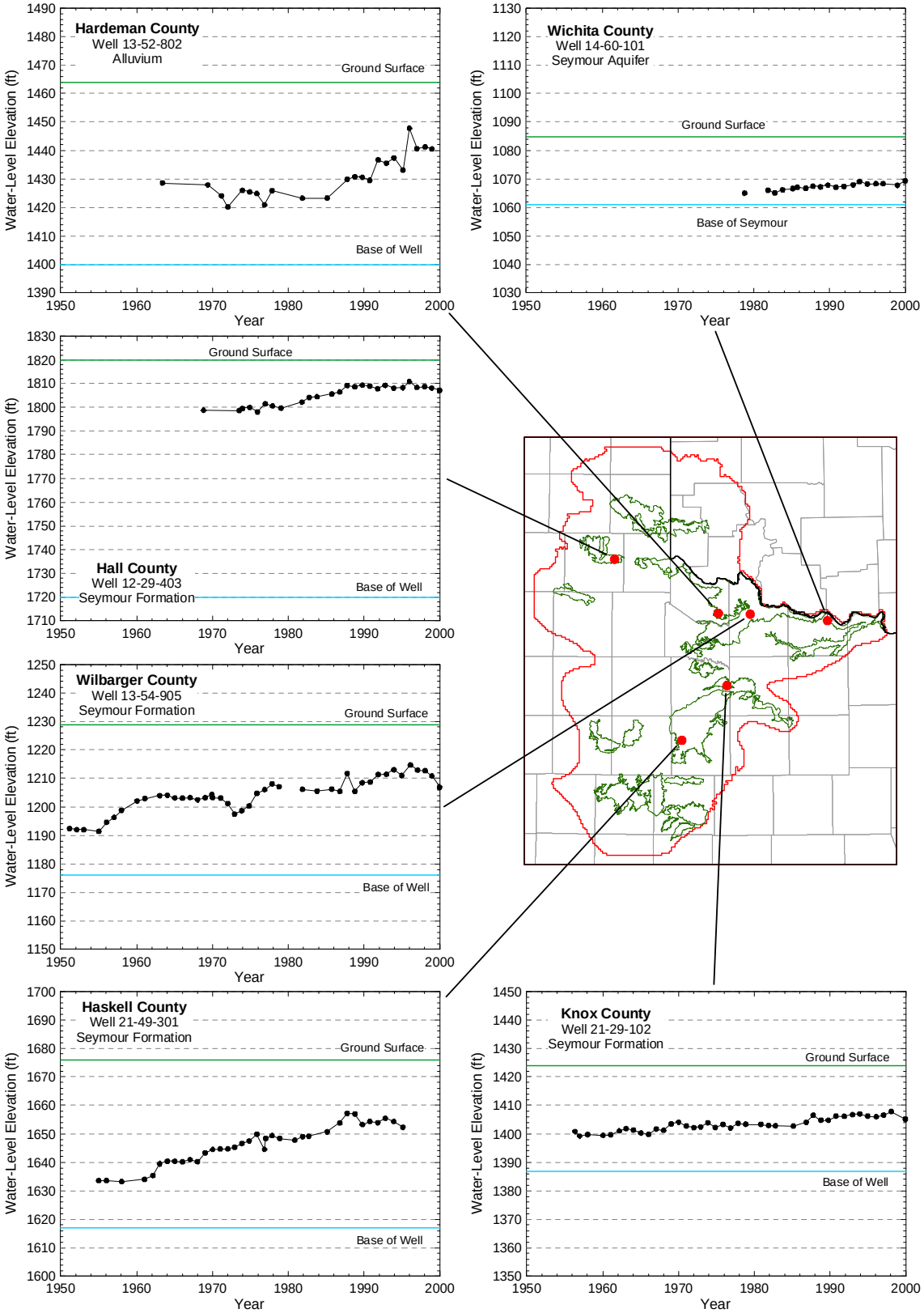

Figure 4.3.26 Example hydrographs showing increasing water-level elevations with time in the Seymour aquifer.

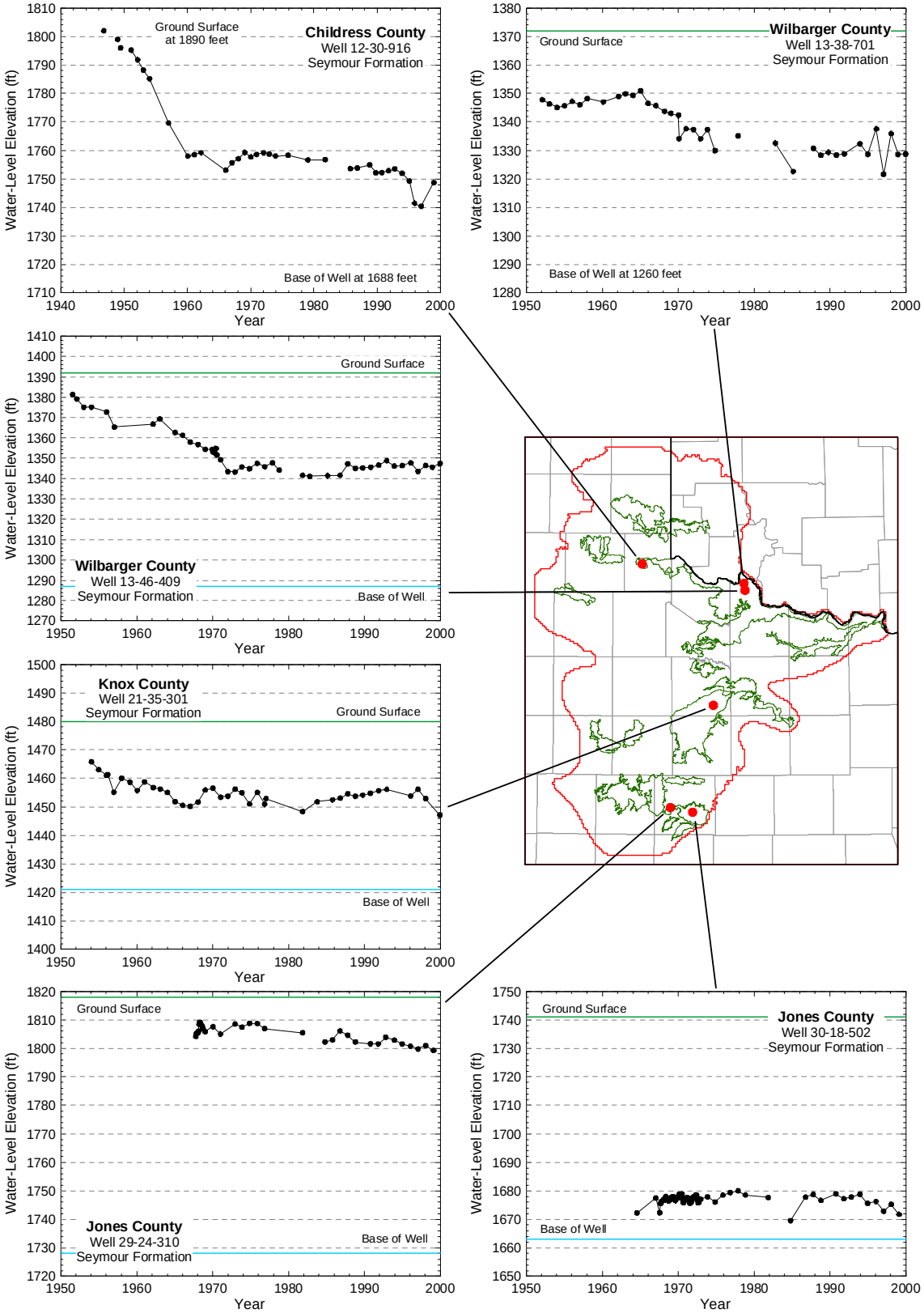

Figure 4.3.27 Example hydrographs showing decreasing water-level elevations with time in the Seymour aquifer.

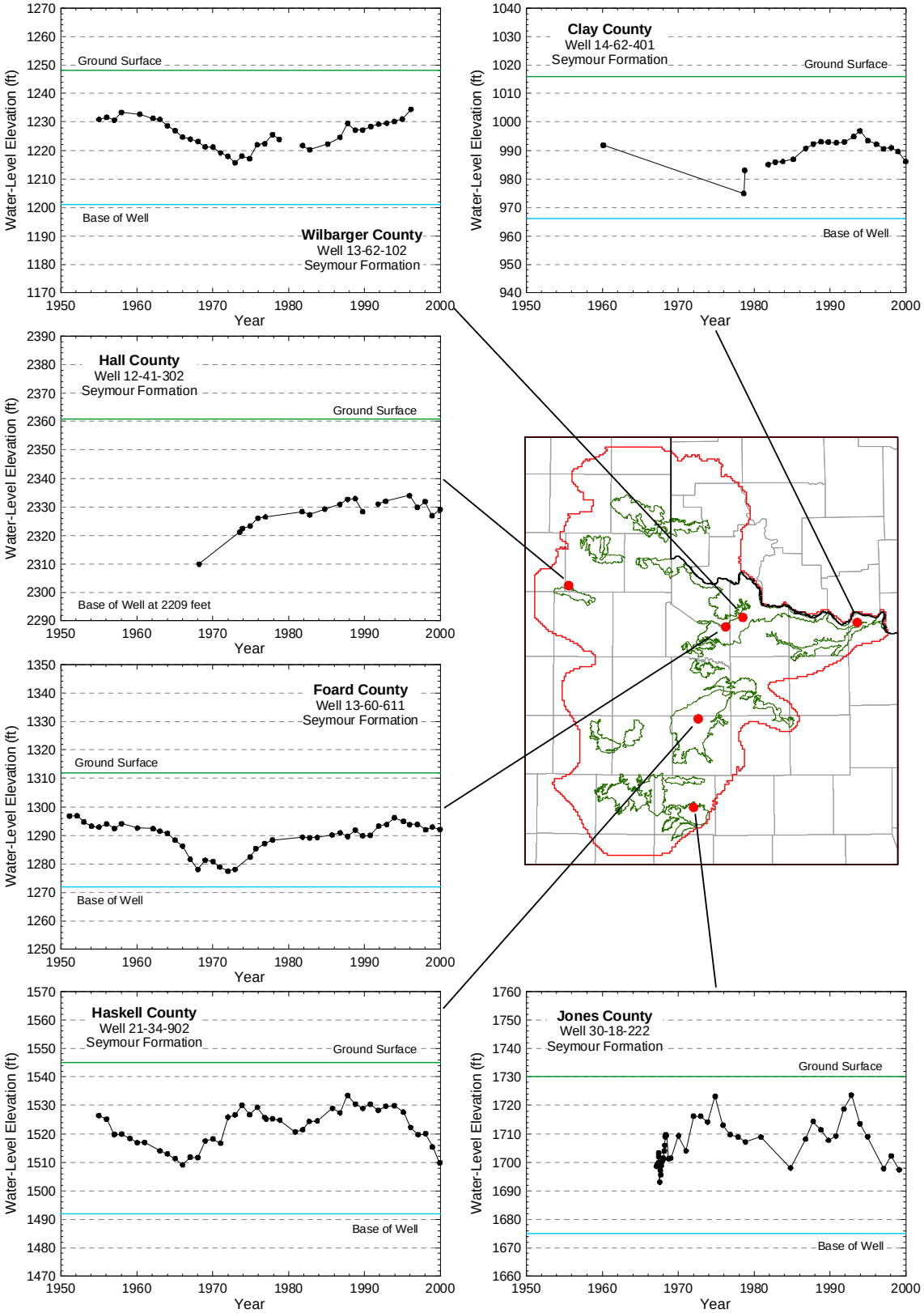

Figure 4.3.28 Example hydrographs showing cyclic water-level elevations with time in the Seymour aquifer.

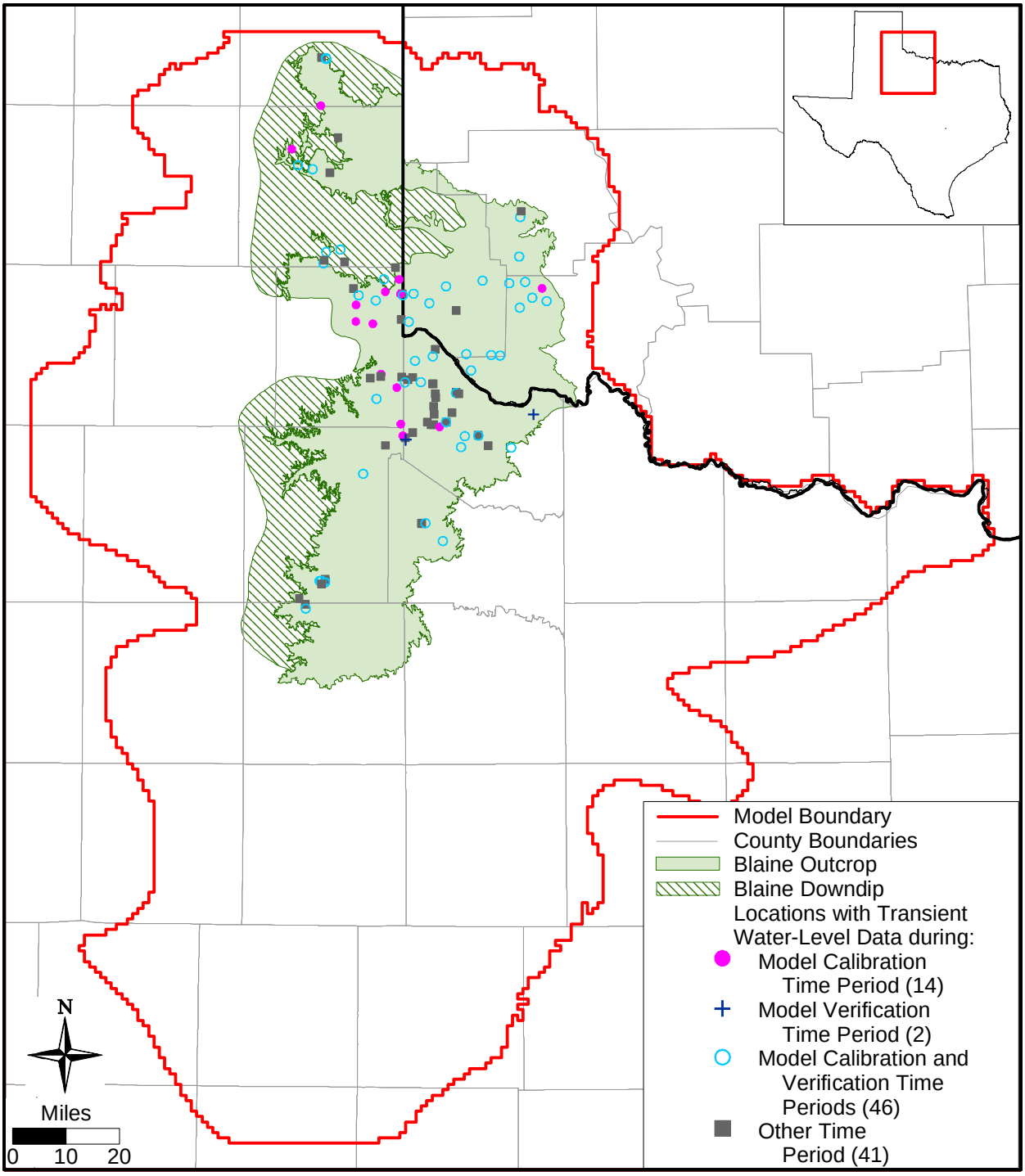

Figure 4.3.29 Locations with transient water-level data in the Blaine aquifer.

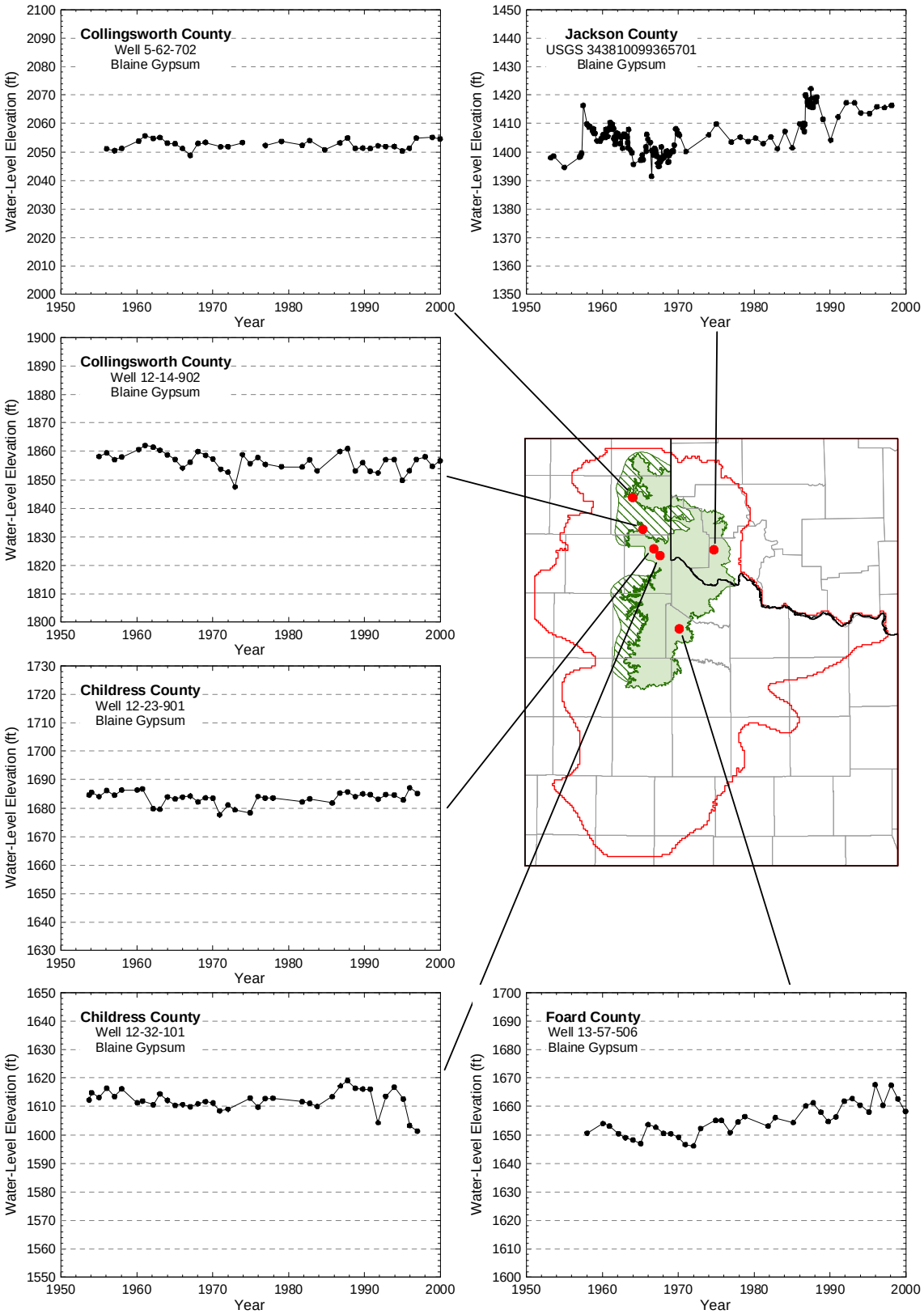

Figure 4.3.30 Example hydrographs showing small water-level changes in the Blaine aquifer.

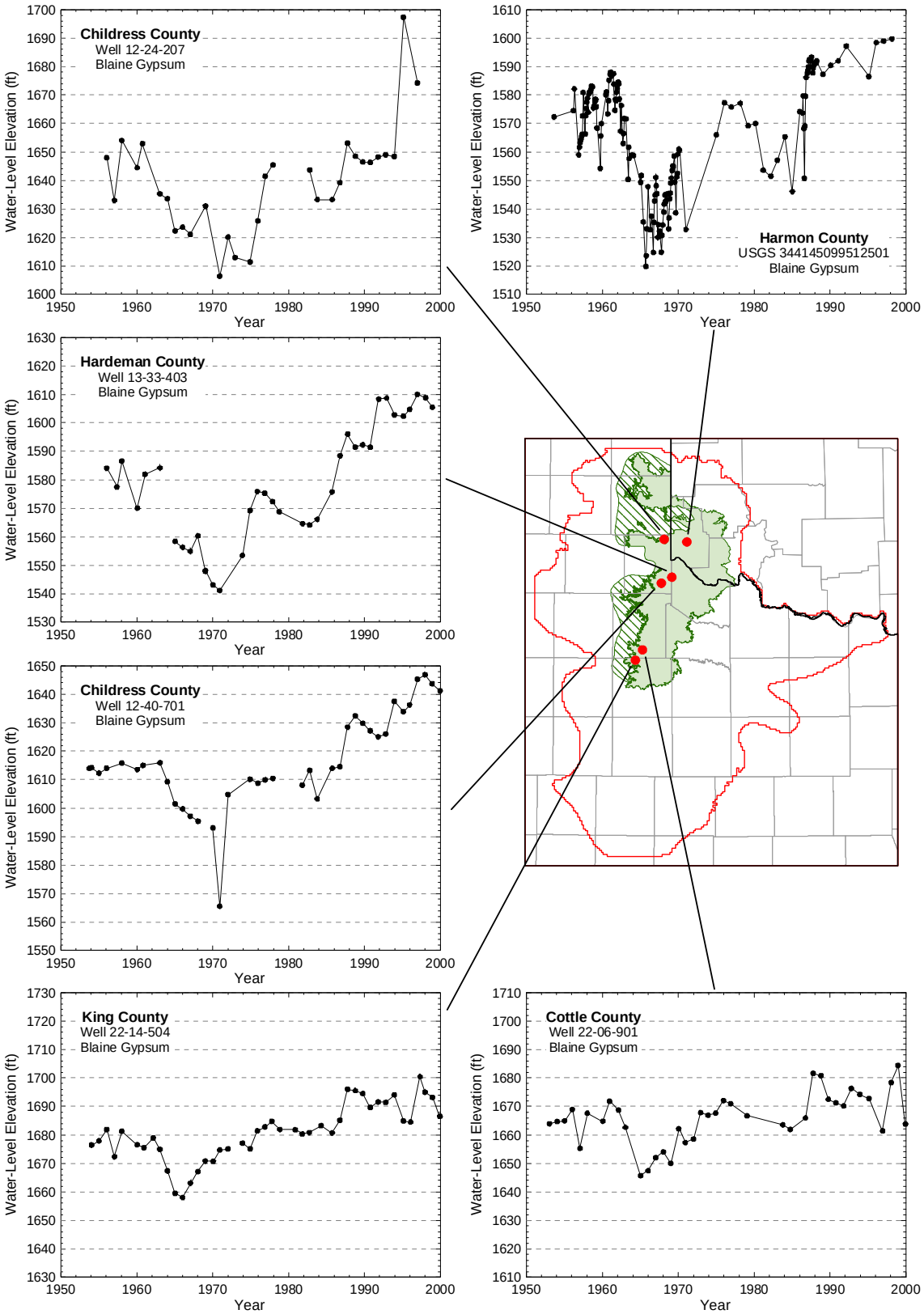

Figure 4.3.31 Example hydrographs showing large water-level changes in the Blaine aquifer.

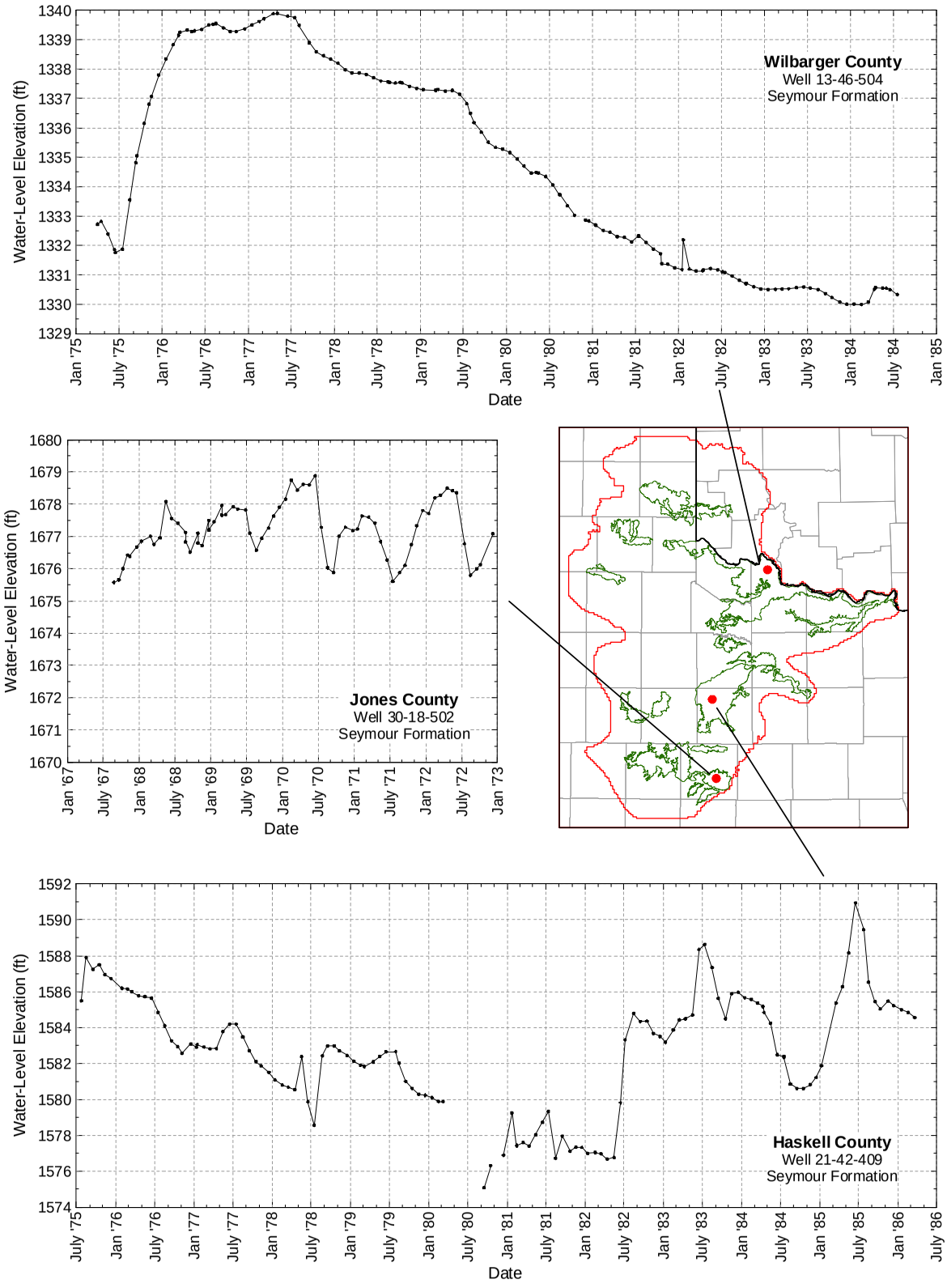

Figure 4.3.32 Evaluation of water levels for seasonal fluctuations in wells completed to the Seymour aquifer.

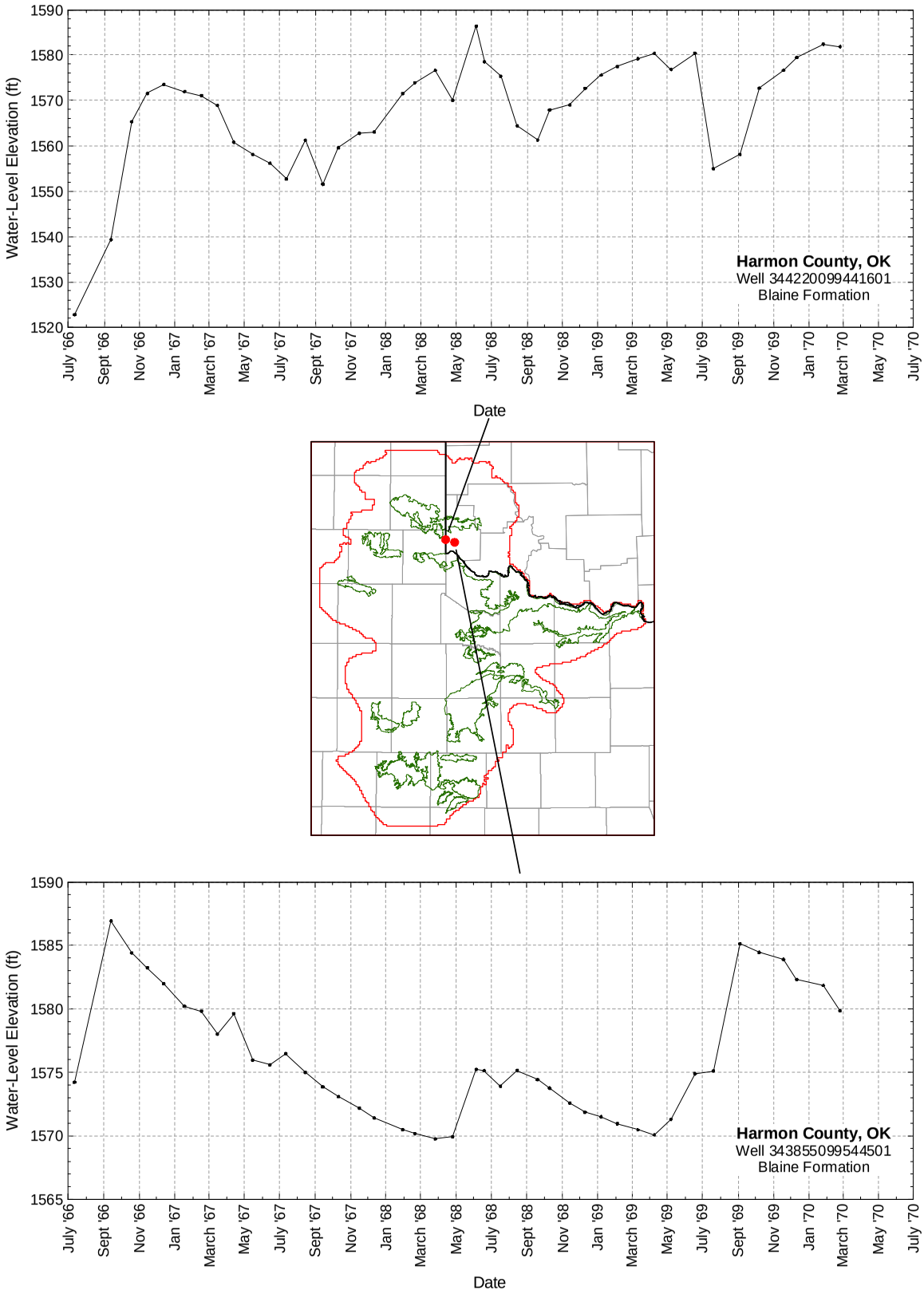

Figure 4.3.33 Evaluation of water levels for seasonal fluctuations in wells completed to the Blaine aquifer.

4.4 Recharge

Recharge can be defined as water which enters the saturated zone at the water table (Freeze, 1969). Recharge is a complex function of rate and volume of precipitation, soil type, water level, soil moisture, topography, and evapotranspiration (ET) (Freeze, 1969). Potential sources for recharge to the water table include precipitation, stream or reservoir leakage, and irrigation return flow. In the Seymour aquifer, recharge is conceptualized to occur primarily as diffuse recharge. Focused recharge along streams may also occur when the water table in the aquifer is below the stream-level elevation. This may occur in the younger Quaternary alluvium where streams are in direct contact with the Seymour aquifer. Recharge will include irrigation return flow in relevant areas.

In a natural aquifer system unaffected by anthropological activities, the aquifer system is in a long-term dynamic equilibrium condition generally referred to as steady-state conditions (or predevelopment) where aquifer recharge is balanced by aquifer discharge resulting in no net change in groundwater storage. It appears that the Seymour was generally unsaturated or locally saturated prior to anthropological activities. In this case, any precipitation that was infiltrating the soil column was being lost to ET. Recharge in the Seymour aquifer under predevelopment conditions could include areal recharge from precipitation, cross-formational flow from adjacent formations, and potentially stream losses. Areal recharge would dominate the other two potential recharge mechanisms. Discharge in the Seymour aquifer would include ET, cross-formational flow to underlying units, stream baseflow contribution, and spring flow. As previously stated, before anthropological activities recharge was balanced by ET resulting in a lack of significant saturated thickness in the Seymour.

Human activities altered the dynamic equilibrium of the predevelopment flow system through the development of land over the aquifer. ET was reduced by the removal of phreatophytes and recharge was increased by the introduction of terracing, contour plowing, and deep plowing. This caused an imbalance in the aquifer which resulted in increases in water levels. The subsequent introduction of significant pumping from the aquifer again changed its dynamics. Groundwater withdrawals due to pumping have a significant impact on aquifer hydraulics. The water removed by pumping is supplied through decreased groundwater storage (i.e., decreased water levels), reduced groundwater discharge (ET), and sometimes increased

recharge. If pumping stays relatively constant, a new steady-state condition will be established. In this new equilibrium, the source of the pumped water will be drawn completely from either reduced discharge or increased recharge. Bredehoeft (2002) terms these two volumes as capture. Bredehoeft (2002) also defines sustainable yield (pumped flow rate) as being equal to the rate of capture. For the Seymour, we expect that the pumping will be balanced primarily from decreased discharge occurring from ET, streams and springs, and cross-formational flows to the underlying strata.

Within the Seymour aquifer, effective recharge will be greatest in topographically high areas (e.g., the sand hills region in Haskell County). Because these topographical highs are generally some distance away from the natural discharge areas at the topographically lower edges of the formation, little rejected recharge is expected to occur in the Seymour Formation (R.W. Harden and Associates, 1978). In river valleys and topographically low regions characteristic of the younger Quaternary alluvium, however, effective recharge to the aquifer is reduced (more recharge is rejected) as a result of a high water table relative to land surface elevation and as a result of gaining streams.

Few estimates of recharge are available for the Seymour and Blaine aquifers. Scanlon et al. (2002) compiled recharge estimates from published reports for all of the major aquifers in Texas. Scanlon et al. (2003) calculated recharge rates of 5 to 30 mm/yr (0.20 to 1.18 in/yr) for the Seymour aquifer in Haskell County based on field measurements of chloride in the unsaturated zone. They also estimated a recharge rate of 7 mm/yr (0.28 in/yr) in Fisher/Jones counties based on unsaturated flow modeling. Table 4.4.1 lists the recharge estimates identified by Scanlon et al. (2002; 2003) for the Seymour aquifer. This table also includes a recharge estimate (Maderak, 1972) for the Blaine aquifer in Greer and Jackson counties, Oklahoma. The recharge study by Scanlon et al. (2003) is specific to the Seymour aquifer and supercedes the initial intended approach of evaluating information gathered from the USGS National Water Quality Assessment (NAWQA) program about the High Plains aquifer for analogous estimates of recharge.

Table 4.4.1 Estimated recharge rates (in/yr) for the Seymour and Blaine aquifers (after Scanlon et al., 2002).

County/Area	Aquifer	Recharge (in/yr)	Reference	Technique
Haskell and Knox counties	Seymour	2.2	R.W. Harden & Associates (1978)	water budget
Hardeman County	Seymour	1.0	Maderak (1972)	Darcy's Law
Baylor County	Seymour	2.6	Preston (1978)	baseflow discharge
Jones County	Seymour	1.8	Price (1978)	baseflow discharge
Wilbarger County	Seymour	2.5	Willis and Knowles (1953)	baseflow discharge
Haskell County	Seymour	0.20 to 1.18	Scanlon et al. (2003)	field study
Fisher/Jones counties	Seymour	0.28	Scanlon et al. (2003)	unsaturated flow modeling
Greer and Jackson counties, Oklahoma	Blaine	1.5*	Maderak (1972)	water budget
Greer, Harmon, Jackson counties, Oklahoma and Childress, Collingsworth, Hardeman counties, Texas	Blaine	1.5	Runkle and McLean (1995)	numerical model calibration parameter

* estimated as 7 percent of rainfall (annual precipitation of 22 inches assumed).

An important component of recharge to the Seymour aquifer is infiltration of precipitation. A comparison was conducted to evaluate the affects of major precipitation events on water-level elevations in wells. Water-level data collected on an approximately one month interval or less over a sufficient period of time was needed in order to conduct the comparison. Only three wells completed to the Seymour aquifer have data at this frequency. These are the same wells as discussed in Section 4.3.5 with respect seasonal fluctuations of water levels.

Figure 4.4.1 shows water-level elevations in a total of three wells in pods 4, 7, and 13 of the Seymour aquifer. Also shown for comparison are data for a precipitation gage located near the well. For the well in Jones County, a correlation between precipitation and water level could be identified if the precipitation data were shifted forward in time by 7 months (Figure 4.4.1a). The depth to water in this well averages about 64 feet. The shift in precipitation indicates that approximately 7 months is required before precipitation at the ground surfaces affects water levels at a depth of 64 feet. A rough correlation between precipitation and water level could also be identified for well 21-42-409 located in Haskell County (Figure 4.4.1b). This correlation is best seen at the time of high precipitation in the latter half of 1978 and the early summer of 1982. In order to see the correlation, no shift in precipitation data was required due to the shallow depth of the water table (9 to 25 feet) at this well. No correlation between precipitation and water level

is observed for well 13-46-504 located in Wilbarger County (Figure 4.4.1c). The depth to water in this well ranged from about 40 to 80 feet during the period with frequent water-level measurements.

Based on precipitation and water-level data at only three locations, it appears that water levels in the Seymour respond to precipitation events. The lag time between high precipitation and observed increases in water level appears to be shorter for locations with a shallow depth to water and longer for locations with a deeper depth to water. This conclusion is very general, however, due to the very limited amount of high frequency, water-level data.

An attempt was made to use a watershed scale tool to estimate diffuse recharge rates in the Seymour aquifer. The results from that tool were inconsistent with the conceptual model for the Seymour and underlying Permian formations. As a result, recharge was determined through model calibration. A complete discussion of the implementation of recharge into the model can be found in Section 6.3.4.

As stated earlier, reservoirs provide a potential site of focused recharge. There are 11 reservoirs with surface areas greater then 1 square mile located within the active model area, none of which overly the Seymour or Blaine aquifers. Table 4.4.2 lists the name, owner, and year completed for these reservoirs. Figure 4.4.2 shows the lake stage elevations for five of the reservoirs located within the active model area. Hydrograph data for four of the five lakes show changes in elevation ranging from 10 to 40 feet. These reservoirs are not potential areas of focused recharge to the aquifers of interest since they overlie Permian rock and are located some distance from the Seymour and Blaine aquifers. Lake Wichita is the only reservoir that may be a potential site of focused recharge due to its proximity to the Seymour aquifer. Data for that lake show little change in elevation, less than 3 feet, with time. The fact that little data are available for the lakes in the active model area does not impact decisions regarding model conceptualization, since most of the lakes are not a potential source of recharge to the Seymour or Blaine aquifers.

Table 4.4.2 Characteristics of reservoirs in the active model area.

Reservoir Name	Reservoir Owner	Date Impounded
Lake Davis	unknown	unknown
Lake Diversion	City of Wichita Falls and Wichita Water Improvement District No. 2	1924
Lake Kemp	City of Wichita Falls and Wichita Water Improvement District No. 2	1922
Lake Pauline	West Texas Utilities Company	1910
Lake Stamford	City of Stamford	1953
Lake Sweetwater	City of Sweetwater	1930
Lake Wichita	City of Wichita Falls	1901
Millers Creek Reservoir	North Central Texas Municipal Water Authority	1974
North Fork Buffalo Creek Reservoir	Wichita County Water Control and Improvement District No. 3	1964
Santa Rosa Lake	W. T. Waggoner Estate	1929
Truscott Brine Lake	U.S. Army Corp of Engineers	1983

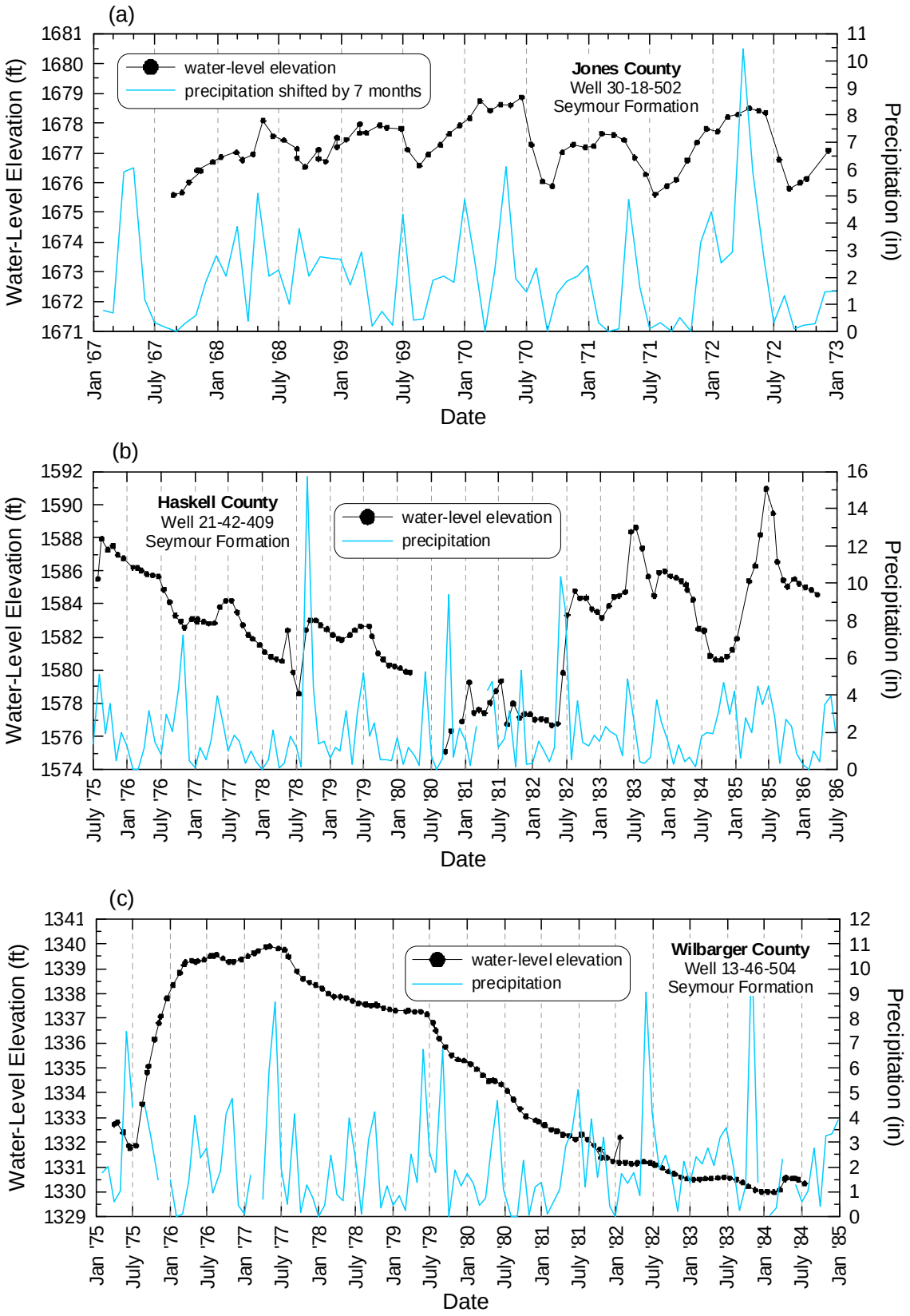

Figure 4.4.1 Correlations between precipitation events and water-level fluctuations.

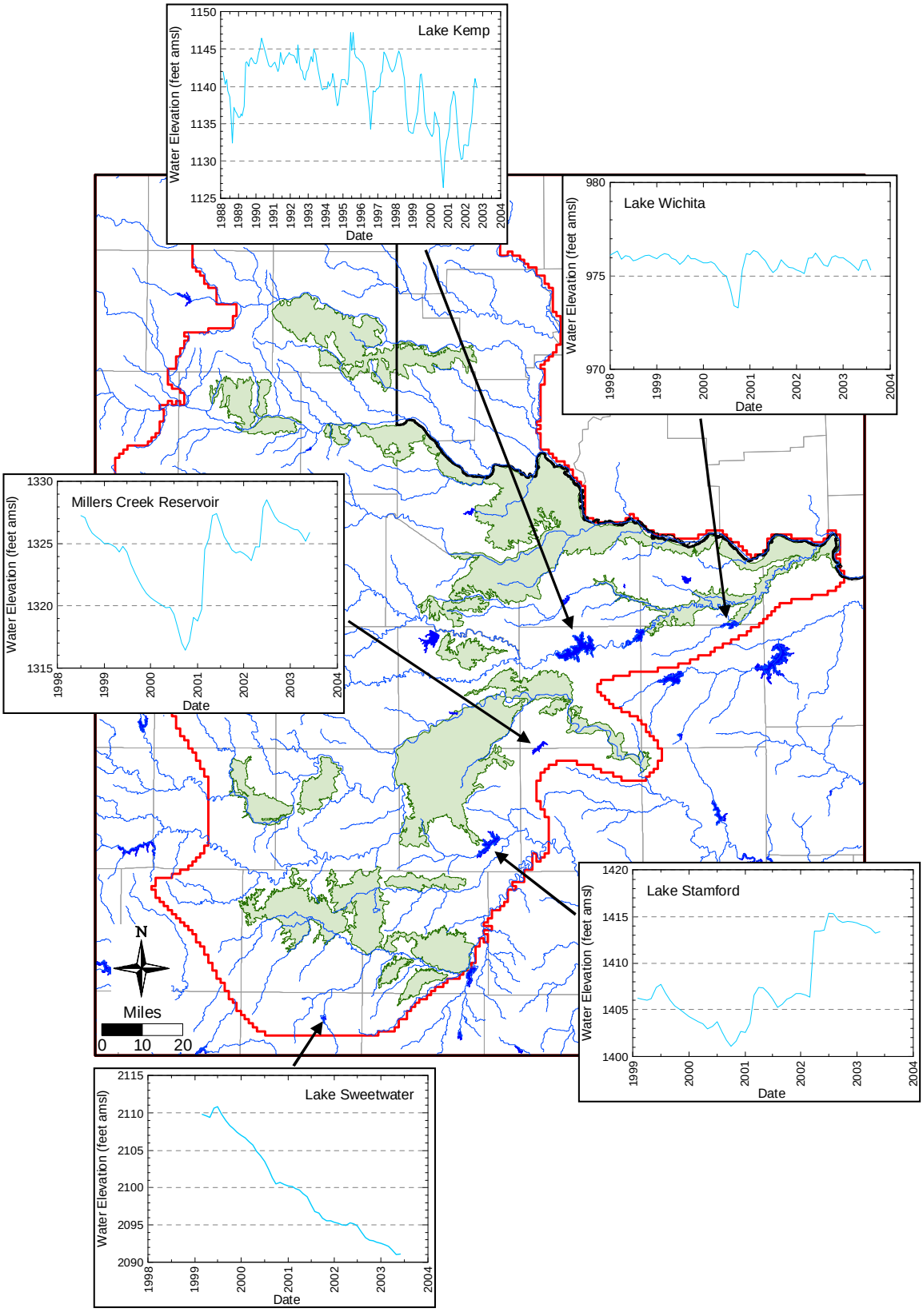

Figure 4.4.2 Hydrographs for select reservoirs in the active model area.

4.5 Natural Aquifer Discharge

Under natural conditions, groundwater flow in the Seymour aquifer is elevation driven from the higher elevations to the lower elevation stream valleys. Prior to significant resource development, recharge occurring as a result of infiltration of precipitation and stream loss was balanced by water-table ET, discharge to streams and springs, and through flow to underlying Permian formations.

The major streams intersecting the study area include the Brazos River and its major forks, the Red River and its major forks, the Pease River, and the Wichita River. Numerous other smaller streams are present in the study area. It is likely that most streams throughout the study area were gaining streams prior to significant resource development.

Base flow is the contribution of groundwater to gaining reaches of a stream. After runoff from storm events has drained away, the natural surface-water flow that continues is predominantly base flow from groundwater. Streams can have an intermittent base flow, which is usually associated with wet winters and dry, hot summers. Larger streams and rivers may have a perennial base flow. The locations of USGS stream gaging stations throughout the study area are shown in Figure 4.5.1 along with the arithmetic average of the flows measured at the gage in cubic feet per second (cfs). Figures 4.5.2 and 4.5.3 show stream flow hydrographs over the model calibration and verification periods for several streams in the study area. The spikes of low flow in the majority of the hydrographs indicate that base flow to some streams may be intermittent during drier periods. Discussion of the implementation of stream flow data in the model is presented in Section 6.3.3.

Stream interaction with underlying aquifers can be quantified through stream gain/loss studies that determine the rate of water exchange between a stream and the underlying aquifers. A low-flow gain/loss study was conducted in the winter of 1969 on the Brazos River from the Knox-Baylor county line to the bridge over the river at the city of Seymour (Preston, 1978). The study showed that this portion of the river is gaining with a yearly net gain ranging from 72.4 to 1,882.5 acre-feet. Discussions in several county reports of natural groundwater discharge indicate that rivers and streams located adjacent to the Seymour or connected to the Seymour via younger alluvium gain water from the aquifer (Cronin, 1972; Maderak, 1972; Price, 1978; Price,

1979; Smith, 1970). The Slade et al. (2002) report on gains from and losses to major and minor aquifers in Texas does not include stream gain/loss study data for the Seymour GAM study area.

An attempt was made to find supplemental stream-flow data to aid in calibration. No stream-flow data were publicly accessible through the U.S. Army Corps of Engineers website at either a national or local level (Fort Worth and Tulsa regional districts share the Seymour region). The Red River Authority (RRA) chloride control project has produced several publications, but they do not appear to contain raw stream flow information. The RRA monitors streams for water quality but no stream-flow information could be found other than the USGS gaging stations already shown on Figure 4.5.1.

Discharge also occurs in areas where the water table intersects the surface at springs or seeps. These springs usually occur in topographically low areas in river valleys or in areas where hydrogeologic conditions preferentially reject recharge. Figure 4.5.4 shows the results of a literature survey for springs located within the active model area. Source data were collected from the TWDB website, Brune (1975), Brune (1981), and USGS data from Heitmuller and Reece (2003). It should be noted that one source for spring locations (Brune, 1981) includes spring surveys for all counties in the study area except Fisher and Jones. Spring data for Oklahoma were not available. It should also be noted that there are likely thousands of undocumented smaller springs and seeps.

Of the more than 600 springs or groups of springs located in the active model area, 26 were 100 gpm (0.22 cfs) or higher based on measured flow rates (Table 4.5.1). However, since flow rates were not provided for many of the documented springs, this number may be higher. The available measured spring flow rates range from less than 0.01 cfs (7 AFY) to a high of 3.5 cfs (2,536 AFY) measured at Salt Springs in Childress County and originating from the Permian System (Brune, 1981). Springs with multiple measurements over time show that fluctuations in precipitation can strongly influence spring flow. Table 4.5.1 shows some of the variation in spring flow for the springs which have discharge over 100 gpm. For example, Jonah Spring in Childress County, which discharges from the Blaine Formation, has measured discharge variations between 491 and 1,315 gpm measured in 1974 and 1978, respectively.

Almost all of the major springs in the model area (those discharging greater than 100 gpm) are found within the Pease River Group, which includes the Dog Creek Shale, Blaine

Formation, and Flowerpot Shale. These formations are karstic due to the dissolution of halite, gypsum, and anhydrite beds commonly present in the Pease River Group. There also appears to be a concentration of large discharging springs in close proximity to the existing river systems, especially to the Red River system. Many large springs are evident in Childress and Collingsworth counties in conjunction with the Salt Fork Red River and the Prairie Dog Town Fork Red River.

Throughout much of the Permian System within the active model area, spring flows have not shown any significant decline over time. Brune (1981) notes that, throughout Texas, declining groundwater levels due to pumping and flowing wells have resulted in the drying out of thousands of smaller springs and reduced flow in many of the larger springs. However, this trend does not appear to be representative of the Permian System within the active model area.

Numerous springs and seeps with either low or unreported flows discharge from the edges of the Seymour Formation where it sits above river valleys. While the individual spring flows are comparatively low from the Seymour aquifer, aggregate flows of a few hundred gallons per minute have been noted for groups of springs in close proximity (R.W. Harden and Associates, 1978).

Some loss of groundwater from the Seymour aquifer occurs through flow to underlying formations. The amount of this flow is unknown and, in the literature (R.W. Harden and Associates, 1978; Preston, 1978), is assumed to be small due to the low permeability of the underlying Clear Fork and Wichita groups of the Permian System in the eastern portion of the active model area. Some measurable discharge from the Seymour to the Bullwagon Dolomite Member of the Vale Formation within the Clear Fork Group may occur in Jones County (Price, 1978). In the north-central region of the model domain, where the Seymour aquifer overlies the Blaine aquifer, appreciable, localized cross-formational flow to the Blaine may occur, depending largely on the thickness of the Dog Creek Shale and the location of solution channels within the Blaine Formation.

Another potential source for natural groundwater discharge from the Seymour aquifer is ET. Direct evaporation from the water table is estimated to be small and occurs only in areas where the water table is within a few feet of land surface (R.W. Harden and Associates, 1978). Total ET, however, is estimated to be a large part of the total natural discharge and considerably

larger than discharge from springs and seeps in some areas of the Seymour aquifer (R.W. Harden and Associates, 1978). High rates of plant transpiration occur primarily along the edges of the Seymour aquifer and along creeks where depths to the water table are small and native grasses, willows, and mesquite are prominent. A complete discussion of the implementation of ET in the model can be found in Section 6.3.4. This section discusses both groundwater ET and extinction depths.

Table 4.5.1 Documented springs in the active model area discharging greater than 100 gpm.

County	Spring	Formation	Max flow (lps)	Max flow (gpm)	Max flow (cfs)	Max flow (AFY)	Date of Max	Min flow (lps)	Min flow (gpm)	Min flow (cfs)	Min flow (AFY)	Date of Min	Source
Childress	Salt	Permian	99	1,569	3.5	2,533	1978	45	713	1.59	1,151	1974	Brune (1981)
Childress	Jonah	Blaine	83	1,315	2.9	2,123	1978	31	491	1.09	793	1974	Brune (1981)
Collingsworth	Baxter	Permian	88	1,395	3.11	2,252	1962 & 1963	26	412	0.92	665	1971	Brune (1981)
Collingsworth	Spring(1)	Alluvium	48	761	1.7	1,228	1968						TWDB website
Collingsworth	Wischkaemper	Permian	48	761	1.7	1.228	1967	7.1	113	0.25	182	1971	Brune (1981)
Collingsworth	Buck	Permian	48	761	1.7	1,228	1968	1.6	25	0.06	40	1977	Brune (1981)
Collingsworth	Sand	Permian	40	634	1.41	1,023	1967	2.3	36	0.08	58	1971	Brune (1981)
Collingsworth	O'Hair	Permian	37	586	1.31	946	1967	3.4	54	0.12	87	1971	Brune (1981)
Collingsworth	Cottonwood	Permian	25	396	0.88	639	1967	14	222	0.49	358	1977	Brune (1981)
Collingsworth	Spring(1)	Alluvium	14.4	229	0.51	370	1967						TWDB website
Collingsworth	Corral	Blaine	24	380	0.85	613	1967	14	222	0.49	358	1977	Brune (1981)
Collingsworth	Wills	Permian	11	174	0.39	281	1967	0.15	2	0.010	3	1977	Brune (1981)
Collingsworth	Gyp	Permian	11	174	0.39	281	1967	11	174	0.39	281	1977	Brune (1981)
Collingsworth	Hale	Permian	10	159	0.35	257	1967	1.9	30	0.07	48	1977	Brune (1981)
Collingsworth	Spring(1)	Alluvium	9.1	144	0.32	232	1967						TWDB website
Collingsworth	Cottonwood(1)	Permian	8.5	135	0.3	218	1979						Brune (1981)
Collingsworth	Big Sandy	Permian	8.1	128	0.29	207	1967	3.1	49	0.11	79	1977	Brune (1981)
Collingsworth	Baggett	Permian	7.4	117	0.26	189	1967	2.8	44	0.1	71	1977	Brune (1981)
Collingsworth	Coleman	Permian	28	444	0.99	717	1951	0.71	11	0.03	18	1956 &1957	Brune (1981)
Cottle	Otta(1)	Blaine	71	1,125	2.51	1,816	1979						Brune (1981)
Foard	Y(1)	Blaine	17	269	0.6	434	1979						Brune (1981)
Foard	Boiling	Blaine	15	238	0.53	384	1979	32	507	1.13	818	1936	Brune (1981)
Knox	Spring(1)	Seymour	6.3	100	0.22	161	1957						TWDB website
Stonewall	Salt Flat Brine	Blaine	34	539	1.2	870	1969	16	254	0.57	410	1964	Brune (1981)
Stonewall	Mc Broom(1)	Seymour	6.5	103	0.23	166	1979						Brune (1981)
Wichita	China	Alluvium	6.8	108	0.24	174	1969	6.5	103	0.23	166	1970	Brune (1981)

(1) Only one discharge rate reported for spring

lps = liters per second
gpm = gallons per minute
cfs = cubic feet per second

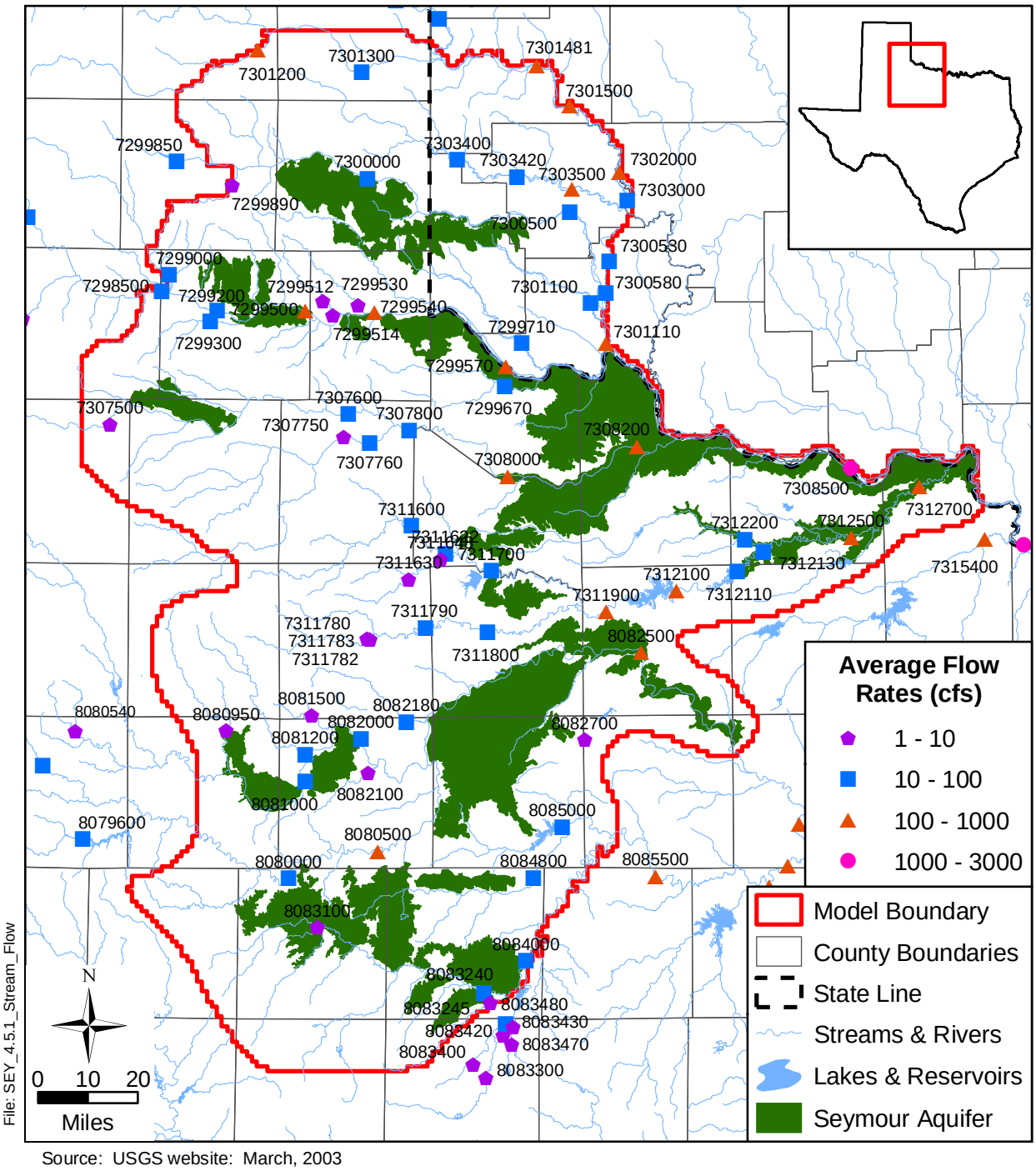

Source: USGS website: March, 2003

Figure 4.5.1 Location of stream gaging stations and average stream flows.

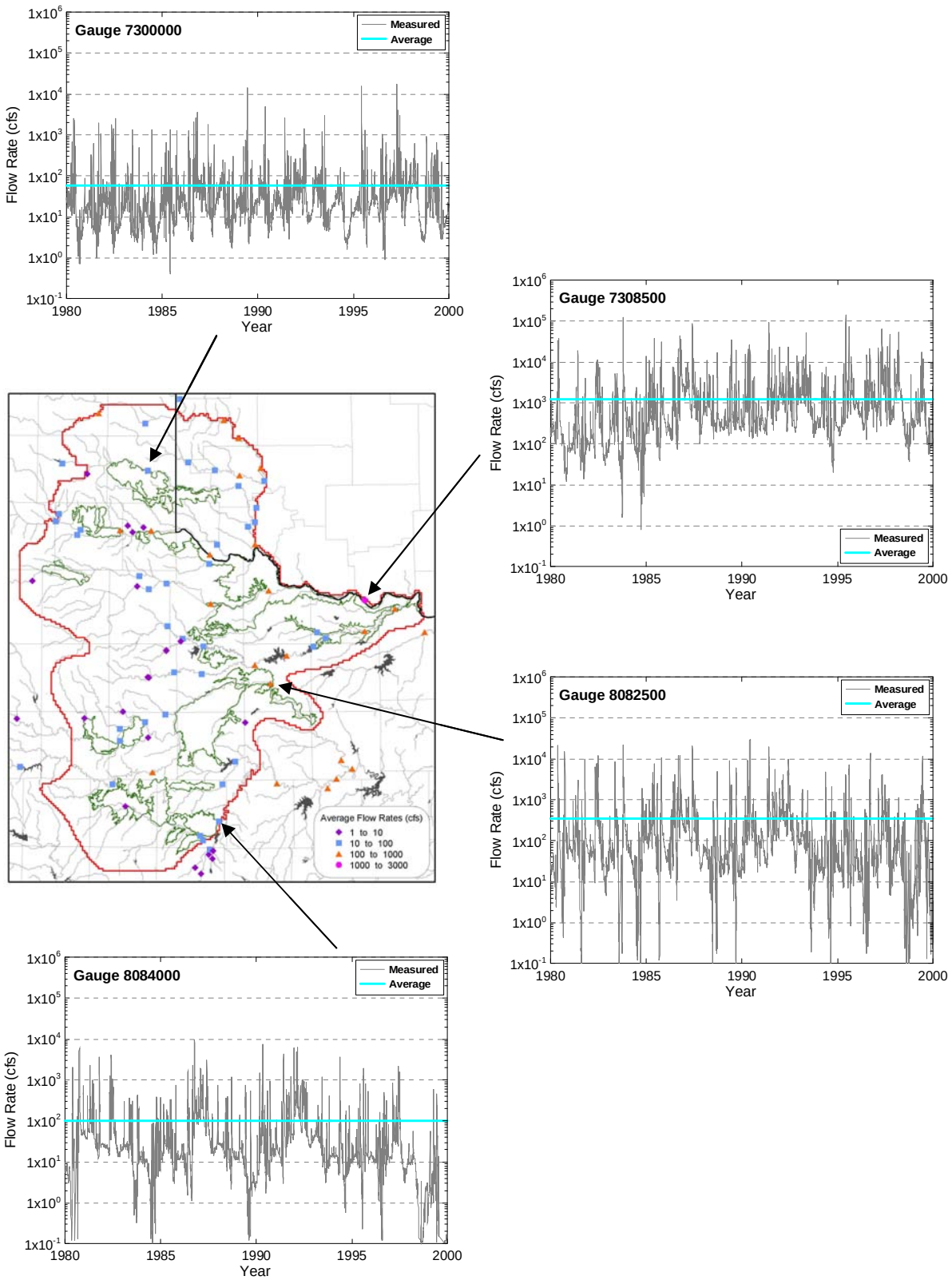

Figure 4.5.2 Example stream flow hydrographs in Collingsworth, Wichita, Baylor, and Jones counties.

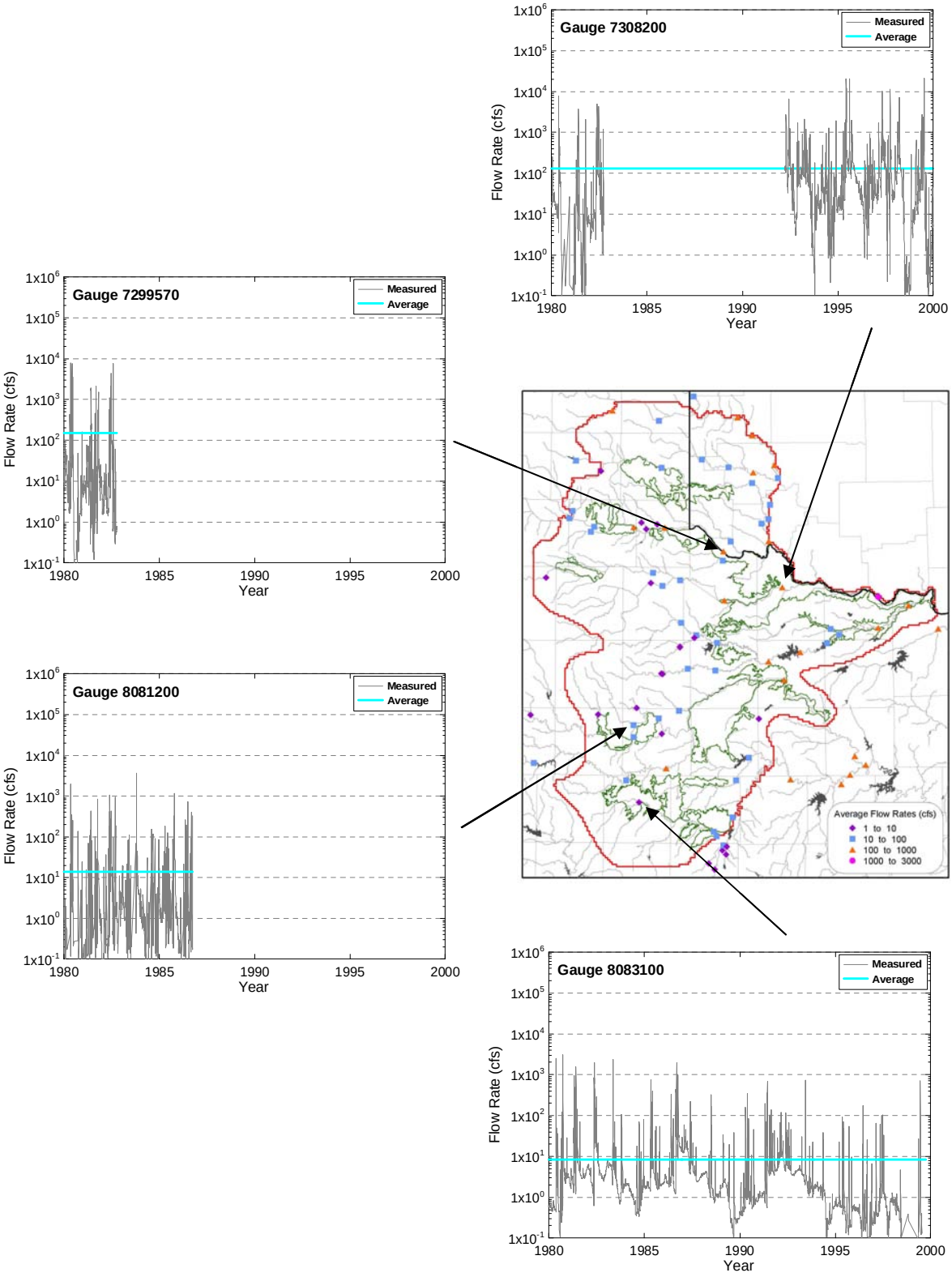

Figure 4.5.3 Example stream flow hydrographs in Hardeman, Wilbarger, Stonewall, and Fisher counties.

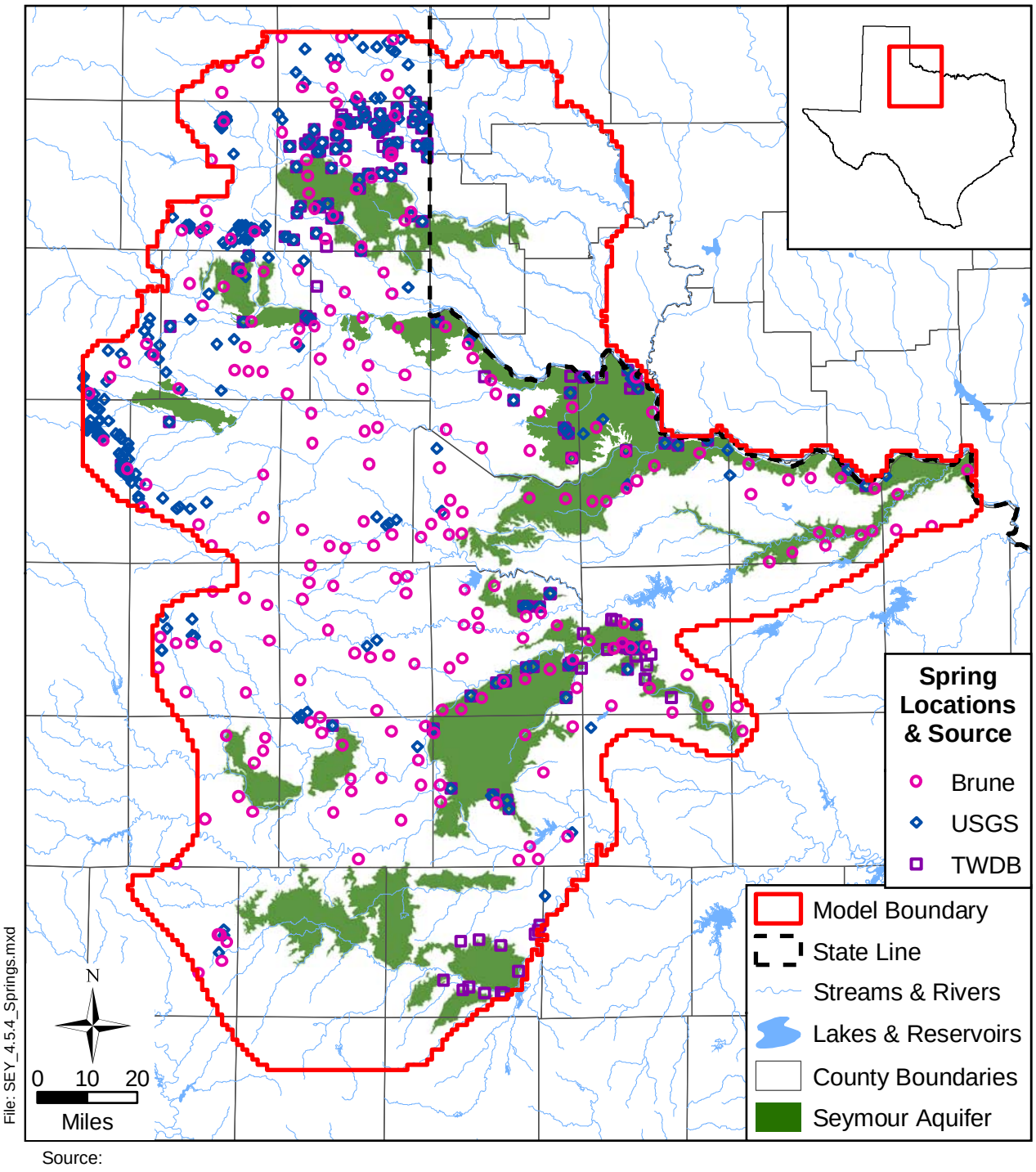

Figure 4.5.4 Documented spring locations in the study area.

4.6 Hydraulic Properties

The Seymour aquifer includes the Seymour Formation and other Quaternary age alluvium. The Seymour Formation generally consists of fluvial sheet deposits of clays, silts, sands, caliche, gravels and conglomerates that are isolated by incised river valleys. The Quaternary alluvium, which constitutes portions of the Seymour aquifer, consists of silt, sand and gravel derived primarily from the Seymour Formation. A fairly consistent deposit of sands and gravels is present near the base of the Seymour Formation over much of the model domain resulting in reasonably high permeabilities.

The Permian System, including the Wichita, Clear Fork, Pease River, and Whitehorse groups, and the Quartermaster Formation in the model domain, consists of generally low-permeability rocks with poor water transmitting characteristics. The Blaine aquifer, including the Dog Creek Shale and Blaine formations of the Pease River Group, consists of anhydrite, gypsum, shale, and dolomite and may be locally very permeable as a result of cavernous solution channels within the gypsum and anhydrite.

4.6.1 Data Sources

Development of hydraulic properties for the Seymour aquifer used transmissivity (T), hydraulic conductivity (K), field permeability (k), specific capacity (SC), and storage (S) values reported in various TWDB reports and on the TWDB website, and specific capacity data from TCEQ well records. Hydraulic properties for the Blaine aquifer and other Permian units were developed using specific capacity data from TCEQ well records. The data locations of the hydraulic property sources for the Seymour aquifer are illustrated in Figure 4.6.1.

4.6.2 Calculation of Hydraulic Conductivity from Specific Capacity

Because specific capacity is relatively easy to measure, requiring knowledge of only the pumping rate and drawdown, it is commonly reported in well records. However, hydraulic conductivity is a more useful parameter than specific capacity for regional groundwater modeling. The methodologies presented in Mace (2001) were used to estimate hydraulic conductivity from specific capacity.

For the Seymour aquifer, transmissivity and specific capacity were measured at 40 coincident locations (R.W. Harden and Associates, 1978; Price, 1978; Price, 1979; Smith, 1973). From these paired values, an empirical correlation relating transmissivity to specific capacity was established for the Seymour aquifer as depicted in Figure 4.6.2. This relationship was then used to estimate transmissivity at the locations where only specific capacity was measured.

Because the Seymour is a water-table aquifer with relatively small saturated thicknesses, the saturated thickness was used to calculate hydraulic conductivity from the transmissivity estimates. Where field permeability estimates were reported (46 locations in Haskell and Knox counties; R.W. Harden and Associates, 1978), these values were used for the hydraulic conductivity. Where saturated thicknesses were reported with the measured specific capacities (79 locations in Wilbarger County; Price, 1979), these thicknesses were used to calculate the hydraulic conductivity from the transmissivity values determined with the empirical relationship. Elsewhere (792 locations), the steady-state saturated thicknesses presented in Section 4.3.2 (see Figure 4.3.9) were used to calculate hydraulic conductivity from the transmissivities. Because the majority of hydrographs are relatively stable during the steady-state period (see Section 4.3.5), saturated thicknesses during that period were considered to be representative of the saturated thickness for all the transmissivity and specific capacity measurements. These steady-state saturated thicknesses differ somewhat from the saturated thicknesses reported during specific capacity measurements at the same locations. The geometric mean of the hydraulic conductivities determined from the 79 transmissivities with reported saturated thicknesses and from the 49 field permeabilities was calculated to be 166.6 ft/day. Using the steady-state saturated thicknesses shown in Figure 4.3.9 to calculate hydraulic conductivities at the same locations resulted in a geometric mean of 166.2 ft/day. This indicates that the use of the steady-state saturated thickness, where required, does not likely result in hydraulic conductivities that are systematically biased high or low with respect to the more straight-forward measurements of hydraulic conductivity.

No transmissivity measurements were available for the Permian units in the model domain, so no empirical relationship could be developed to estimate transmissivity from the 208 available specific capacity measurements. Instead, the analytical methodology presented in

Mace (2001) was used to estimate transmissivity for these units. Specifically, the analytical method of Theis et al. (1963) was used for all but five of the measurements, for which the method did not converge. The empirical correction for well loss according to Equation 64 of Mace (2001) was applied to the drawdowns; however, the low conductivity of the Permian sediments and the correspondingly low pumping rates resulted in negligible well losses (average of 1 percent) in most cases. Hydraulic conductivity was calculated from transmissivity using well screen length for all Permian data.

4.6.3 Analysis of the Hydraulic Property Data

Figure 4.6.3 shows a histogram of the hydraulic conductivity data for several pods of the Seymour aquifer. Only those pods where 20 or more samples were available are shown. Figure 4.6.3 shows that pod 1 has significantly lower hydraulic conductivities than do pods 4 and 5, which are similar. Pod 7 is shifted to the right, indicating the highest hydraulic conductivities among all of the pods. Figure 4.6.3 indicates that the data, as a whole, and the data subsets are close to lognormally distributed. Summary statistics of the hydraulic conductivity data for several pods of the Seymour aquifer are presented in Table 4.6.1.

Table 4.6.1 Summary statistics by pod number for Seymour hydraulic conductivity data (ft/day).

Statistic	Pod*						
	All	**1**	**2**	**3**	**4**	**5**	**6**
Number of Samples	917	179	14	25	257	284	0
Arithmetic Mean	149.2	65.7	155.8	42.7	158.1	144.2	
Median	74.6	40.3	127.1	27.5	92.7	75.4	
Geometric Mean	68.5	35.9	135.6	27.9	87.6	75.0	
Standard Deviation K	256.7	78.6	102.6	41.7	226.9	258.6	
Standard Deviation $Log_{10}(K)$	0.56	0.51	0.22	0.42	0.47	0.50	
Statistic	**Pod***						
	7	**8**	**9**	**10**	**11**	**12**	**13**
Number of Samples	60	12	8	0	73	1	4
Arithmetic Mean	463.4	143.5	71.9		129.3	4.3	184.9
Median	258.9	116.1	40.3		31.3	4.3	147.9
Geometric Mean	285.0	100.3	40.0		36.0	4.3	148.1
Standard Deviation K	507.4	117.0	91.4		233.0		141.4
Standard Deviation $Log_{10}(K)$	0.44	0.41	0.53		0.75		0.34

* see Figure 4.1.1 for pod locations

The similarity between the geometric mean and median in all of the pods indicates that the distribution of hydraulic conductivity is nearly lognormal. Many of the pods have few measurements (i.e., approximately 10 or less), so the statistics are highly uncertain. All of the pods with adequate sample sizes show relatively high median hydraulic conductivities, ranging from a low of 27.5 ft/day in pod 3 to a high of 258.9 ft/day in pod 7. The field permeabilities reported for pumping tests in the county reports are generally somewhat higher than the geometric mean shown here, which includes all hydraulic conductivities determined from the specific capacity data. Based only on reported field permeabilities from county reports (i.e., neglecting the additional values determined from specific capacity data), pod 7 in Haskell and Knox counties should have, on average, higher hydraulic conductivities than pod 13 in Jones County which, in turn, should have higher values than pod 4 in Wilbarger County. This hierarchy is in agreement with the summary values listed in Table 4.6.1.

Summary statistics of the hydraulic conductivities calculated for the Permian units are presented in Table 4.6.2. The similarity between the geometric mean and median for each Permian group and the Blaine aquifer indicate that the distribution of hydraulic conductivity is likely lognormal. As expected, the Blaine mean hydraulic conductivity values are somewhat higher than those of the other Permian units. While the Clear Fork Group exhibits the lowest mean hydraulic conductivity values, the actual value may be still lower than that presented.

Table 4.6.2 Summary statistics for Permian hydraulic conductivity data (ft/day).

Statistic	Blaine	Whitehorse	Quartermaster	Clear Fork
Number of Samples	59	106	24	19
Arithmetic Mean	39.5	12.6	10.0	6.0
Median	16.3	3.4	3.1	2.3
Geometric Mean	9.2	3.1	3.2	2.6
Standard Deviation	53.5	27.6	11.9	8.9
Standard Deviation $\log_{10}(K)$	1.0	0.78	0.84	0.71

4.6.4 Variogram Analysis of Hydraulic Conductivity

The spatial distribution of hydraulic properties can be characterized by a variogram analysis. A variogram analysis quantifies gross spatial correlation and variability (for detailed background information on geostatistics, refer to Isaaks and Srivastava, 1989). Typical

hydrogeologic properties show some spatial correlation indicated by lower variance for nearby measurements. As the distance between measurements increases, variance increases until it becomes constant. That constant value corresponds to the ensemble variance of the entire dataset. At the separation distance where the variance becomes constant, no correlation between measurements exists. The variogram describes the degree of spatial variability between observation points as a function of distance. Spatial variability is described in terms of the nugget (variance at zero separation), range (correlation length), and the sill (ensemble variance). The variogram can also be used as a tool to characterize horizontal anisotropy in hydraulic conductivity. In an aquifer with horizontal anisotropy, hydraulic conductivity is a function of horizontal direction. For a detailed explanation of directional variogram terminology and calculation, see Deutsch and Journel (1992).

All of the Seymour data were first analyzed as a whole. Next, the data from pods with an adequate number of available samples were analyzed separately. The analyses were completed on logarithmically transformed hydraulic conductivity data. For all datasets, directional variograms were calculated along 10 degree increments and compared to an omnidirectional variogram of the data to help delineate any directional trends. For the directional variograms, the search tolerance was 30 degrees. For all variograms, the lag width was from 10,000 to 20,000 feet (about 2 to 4 miles), and the total lag distance varied depending on the size of the pod. None of the data exhibited distinct directional trends. Some of the variograms changed with direction, but closer analysis revealed that these trends were likely due to the geometry of the data, rather than any data trend. In the end, omnidirectional variograms were retained for all pods.

Figures 4.6.4 and 4.6.5 show the experimental variograms calculated for the Seymour pods and the entire Seymour aquifer. In general, the practical range of the variograms is approximately 8 miles and the nugget is approximately half of the sill. Pod 7 shows the largest range at over 10 miles. The initial slope of the variogram for this pod appears almost linear, although this may be an artifact of the data spacing. Several of the variograms show sensitivity to a few wide ranging hydraulic conductivity values, with pods 1, 4, and 11 having significant perturbations at distances at or beyond the range. The variogram for the combined Seymour data (Figure 4.6.5) is relatively smooth in comparison.

Figures 4.6.4 and 4.6.5 also show model variogram fits for each of the data subsets. Two types of variogram models were used, exponential and spherical. The equation for the exponential variogram model is:

$$\gamma(h) = C_0 + C_1 \exp(\frac{-h}{A}) \tag{4.6.1}$$

where C_0 is the nugget, C_1 is the scale (basically, sill minus nugget), A is the range parameter, and h is the lag distance. The equation for the spherical model is:

$$\gamma(h) = \begin{cases} C_0 + C_1(1.5\frac{h}{A} - 0.5\left(\frac{h}{A}\right)^3) & h < A \\ C_0 + C_1 & h \geq A \end{cases} \tag{4.6.2}$$

Note that for the exponential model the "practical range", or distance where the variogram value closely approaches the sill, is approximately 3A. Table 4.6.3 shows a summary of the variogram parameters for each of the model fits.

Table 4.6.3 Variogram model parameters for the Seymour aquifer.

	Model	C_0	C_1	A
All	Spherical	0.13	0.13	9.5
1	Spherical	0.16	0.1	7.6
4	Exponential	0.09	0.12	2.3
5	Spherical	0.145	0.08	8.0
7	Spherical	0.09	0.12	11.4
11	Exponential	0.18	0.33	2.1

A variogram analysis was attempted for the Blaine aquifer hydraulic conductivity data. However, no correlation trends were observed in the variogram. Figure 4.6.5 shows an omnidirectional experimental variogram for the Blaine aquifer hydraulic conductivity data.

4.6.5 Spatial Distribution of Hydraulic Conductivity

The hydraulic conductivity data from each pod were kriged using the variogram models described above. For pods where sufficient data were unavailable, the variogram model for the overall Seymour dataset was used. The resulting spatial distribution of hydraulic conductivity

within the Seymour aquifer is depicted in Figure 4.6.6. Although the kriging tends to smooth the irregularities in the sampled data, hydraulic conductivity still varies approximately two orders of magnitude (from 10 to 1,000 ft/day) over all pods in the model area. Consistent with the summary statistics (Table 4.6.1), pod 7 shows the highest values of hydraulic conductivity. In general, the hydraulic conductivity within a given pod does not vary over more than one order of magnitude.

Based on a post plot of the Blaine aquifer hydraulic conductivities (Figure 4.6.7), in which no clear spatial trends are apparent, and the variogram (see Figure 4.6.5), which indicated no spatial correlation between data, it was concluded that the karstic nature of the Blaine aquifer results in heterogeneity in hydraulic conductivity at a scale smaller than the distribution of the data. Therefore, a spatially variable distribution of hydraulic conductivity could not be developed given the data. A single value was used for the hydraulic conductivity of the Blaine aquifer. The geometric means summarized in Table 4.6.2 were used for each Permian unit in the model.

Hydraulic conductivity zones and geometric means for the Permian units are shown in Figure 4.6.8. The zones were developed based on the surface geology across the active model area. The entirety of the Pease River Group, including the outcrop and downdip portions of the Blaine aquifer, was assigned the geometric mean calculated for the Blaine aquifer. Because no hydraulic conductivity data were found for the Wichita Group, it was assumed that the hydraulic conductivity in the Wichita Group was similar to that in the Clear Fork Group. In developing the hydraulic conductivity zones, geologic formations outcropping over only a small portion near the extreme edges of the active model area were grouped with the more prevalent neighboring formations. A representative literature value of hydraulic conductivity (geometric mean of 14.8 ft/day and standard deviation of $\log_{10}(K)$ of 0.47; Dutton et al., 2001) for the Ogallala aquifer was used for the portion of that aquifer intersecting the northwest region of the active model area.

4.6.6 Vertical Hydraulic Conductivity

No vertical hydraulic conductivity data for the hydrogeologic units in the model were found in the literature review. The stratified nature of sediments will likely result in some degree

of anisotropy in hydraulic conductivity. While horizontal hydraulic conductivity is dominated by the higher permeability sediments, vertical hydraulic conductivity will be dominated by the lower permeability strata and will tend to be lower than the horizontal hydraulic conductivity. Domenico and Schwartz (1998) list values of horizontal to vertical hydraulic conductivity ratios that range from 2 to 10 for materials similar to sediments in the study area. At the regional scale of the Seymour GAM, higher anisotropy ratios may exist.

In MODFLOW (the groundwater model specified by the TWDB for all GAMs), the parameter dictating vertical flow of water between two layers is the leakance between those layers. The leakance between two layers (L_{12}) can be calculated from the weighted harmonic mean of the vertical conductivities of the two layers:

$$L_{12} = \frac{K_V}{\Delta z} = \frac{1}{\frac{\Delta z_1}{K_{V1}} + \frac{\Delta z_2}{K_{V2}}} \qquad (4.6.3)$$

where Δz is the layer thickness, K_V is the vertical hydraulic conductivity, and the subscripts 1 and 2 refer to the model layers. The hydraulic conductivity in the Permian units is roughly an order of magnitude lower and the Permian layer thicknesses are roughly an order of magnitude higher than those for the Seymour aquifer. Thus, the leakance and, therefore, the vertical flow of water between the two model layers, will be governed primarily by the vertical hydraulic conductivity of the Permian units. The model will be largely insensitive to perturbations in the vertical hydraulic conductivity of the Seymour aquifer.

4.6.7 Storativity

For unconfined aquifers, the storativity is referred to as the specific yield and is defined as the volume of water an unconfined aquifer releases from storage per unit surface area of aquifer per unit decline in the water table (Freeze and Cherry, 1979). A literature review was conducted for specific yield of the Seymour aquifer (Table 4.6.4). Specific yield ranged from 0.03 to 0.30 and the arithmetic means reported for four studies ranged from 0.11 to 0.15. An average specific yield value of 0.14 is considered representative of the Seymour aquifer. Figure 4.6.1 shows the locations of specific yield estimates. Domenico and Schwartz (1998) list values of specific yield that range from 0.03 to 0.28 for materials similar to the sediments of the

Seymour aquifer in the active model area. Lohman (1972) gives 0.1 and 0.3 as general limits for the specific yield of unconfined aquifers. Originally, augmenting specific capacity values with inferred porosity data was considered. This idea was later deemed inferior to using measured data for the Seymour aquifer and was dismissed. Specific yields were assumed to be approximately 0.15 for all of the Permian units. Based on the values plotted in Figure 21 in Dutton et al. (2001), a specific yield of 0.15 was used for the Ogallala aquifer.

Table 4.6.4 Storage values for the Seymour aquifer from the literature.

County	Well Number	Storage		Reference
		Point	Average	
Baylor	2130387	0.03	0.11	Preston, 1978
Baylor	2130385	0.04		
Baylor	2122911	0.04		
Baylor	2122912	0.06		
Baylor	2122913	0.08		
Baylor	2121941	0.16		
Baylor	2121940	0.18		
Baylor	2130386	0.30		
Jones	3018206	0.11	0.15	Price, 1978
Jones	2923606	0.18		
Haskell-Knox	-	-	0.15	R.W. Harden & Associates, 1978
Wilbarger	-	-	0.14	Price, 1979

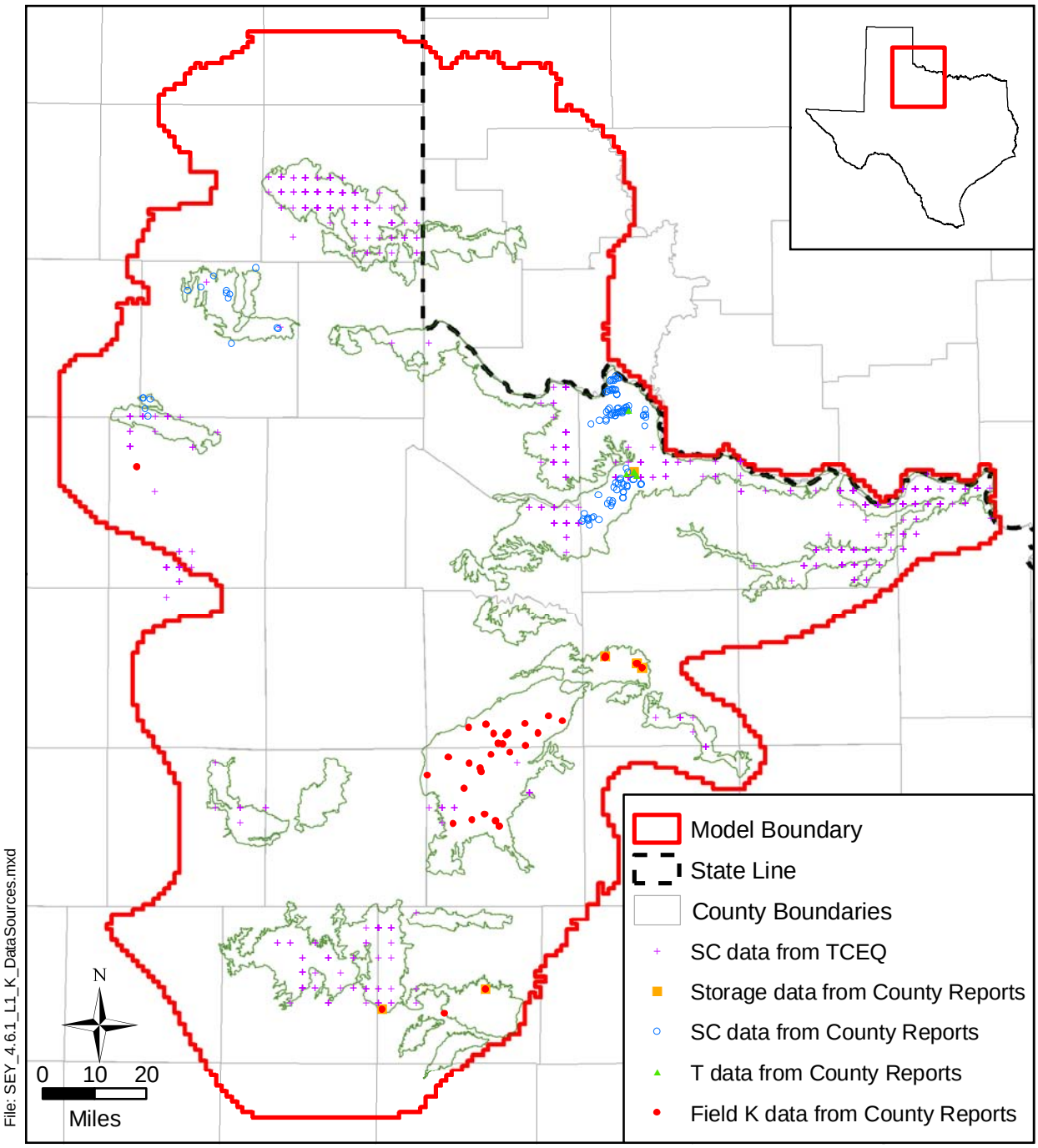

Figure 4.6.1 Location of data sources for Seymour aquifer hydraulic properties.

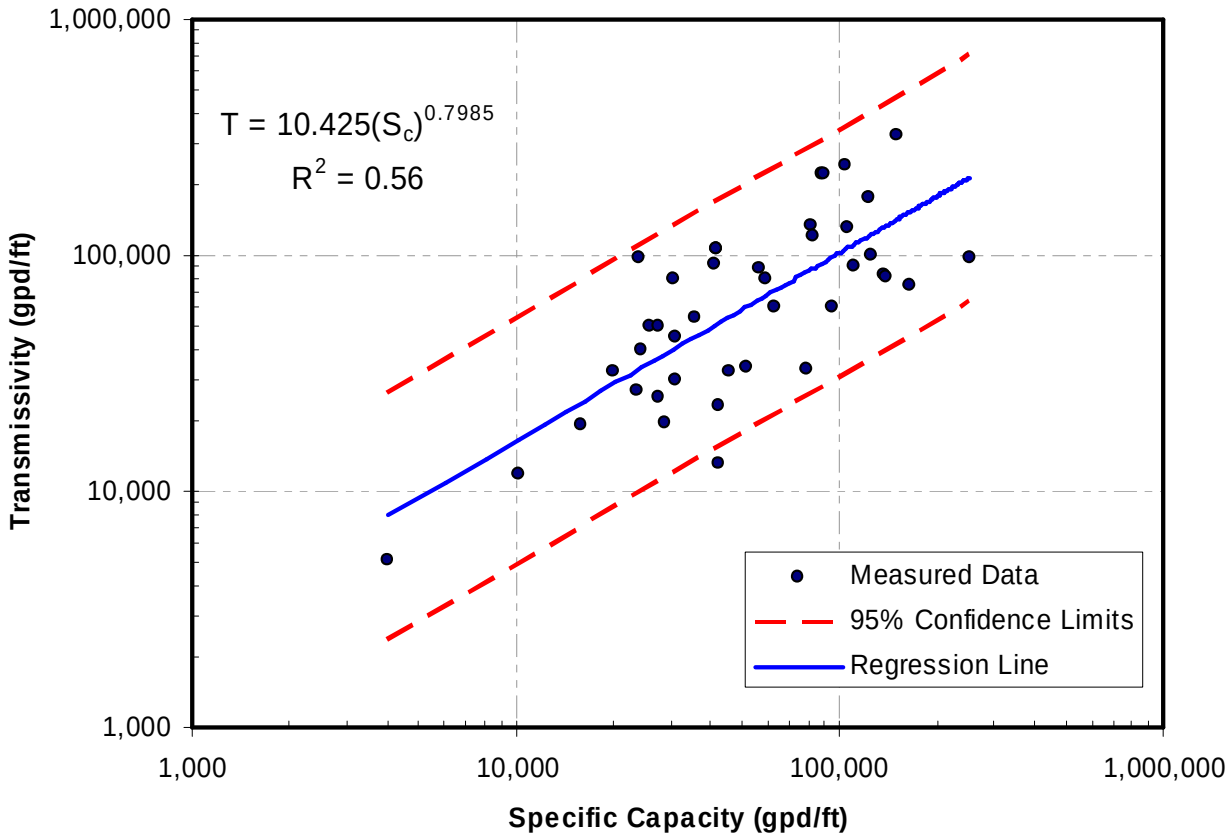

Figure 4.6.2 Empirical correlation between transmissivity and specific capacity for the Seymour aquifer.

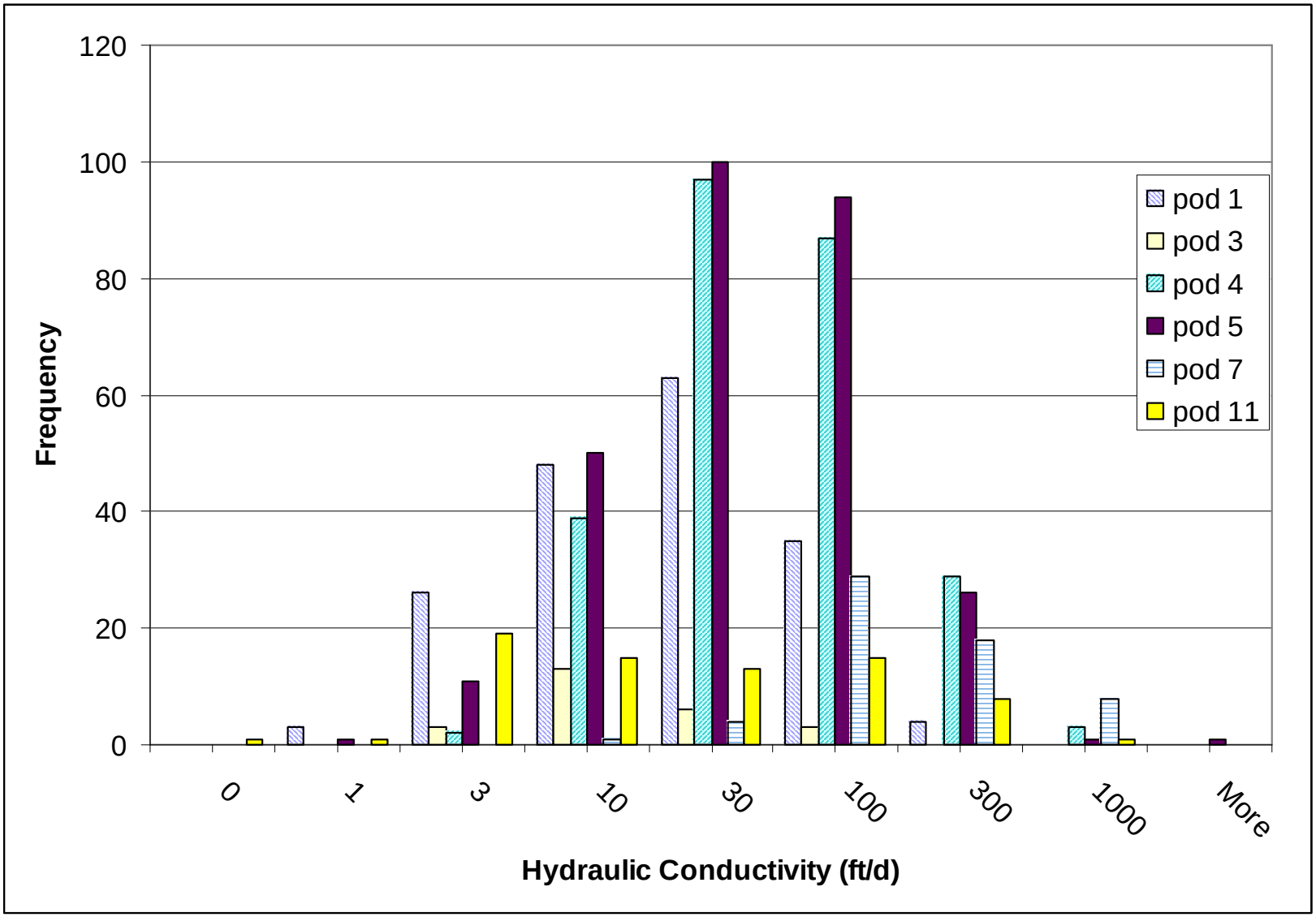

Figure 4.6.3 Histogram of hydraulic conductivity data for Seymour aquifer pods.

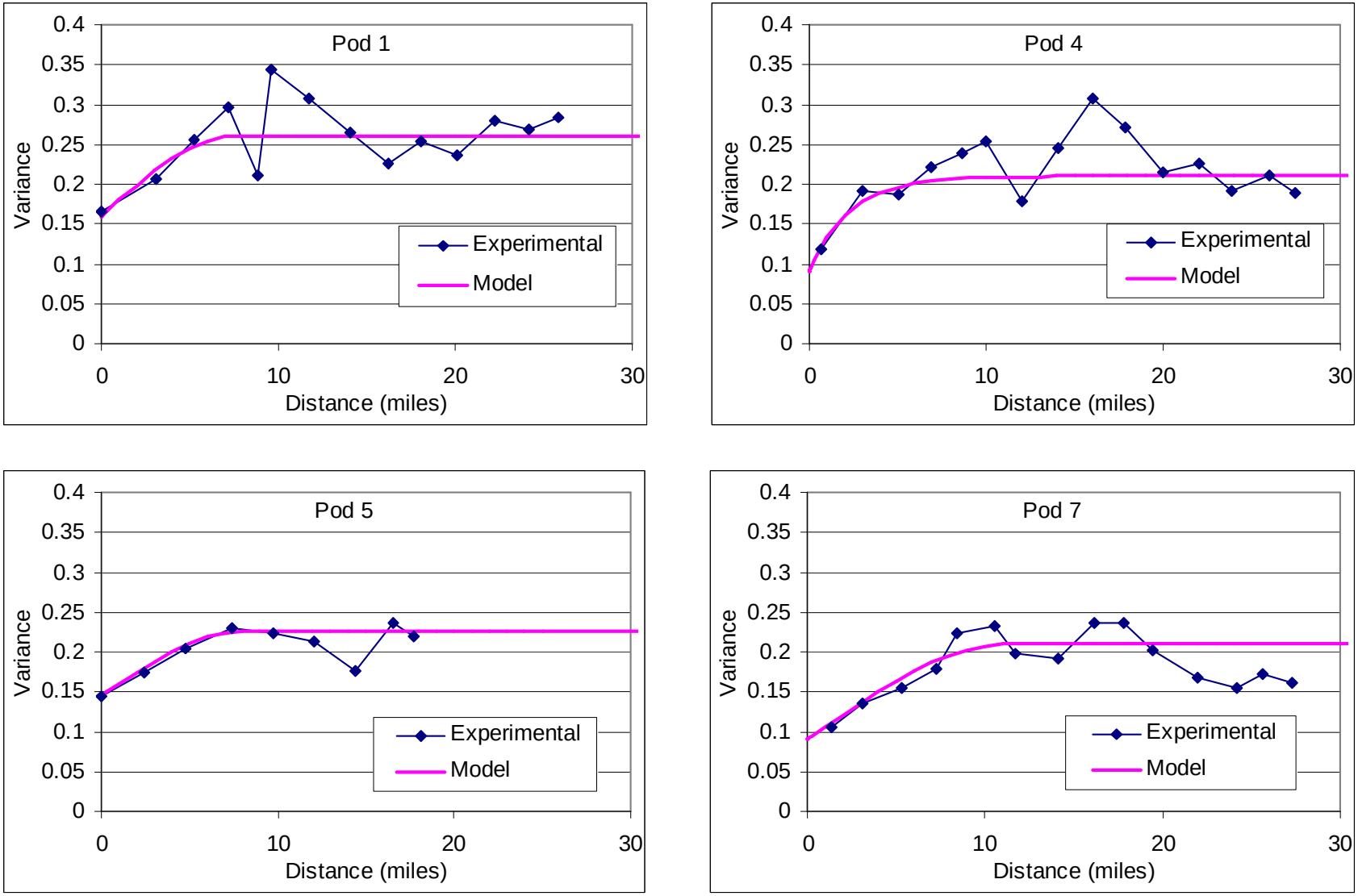

Figure 4.6.4 Experimental variogram of hydraulic conductivity for Seymour aquifer pods 1, 4, 5, and 7.

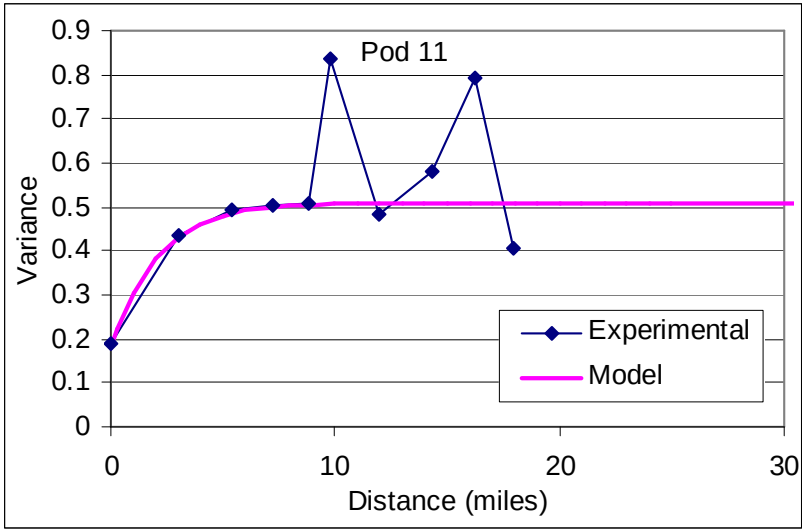

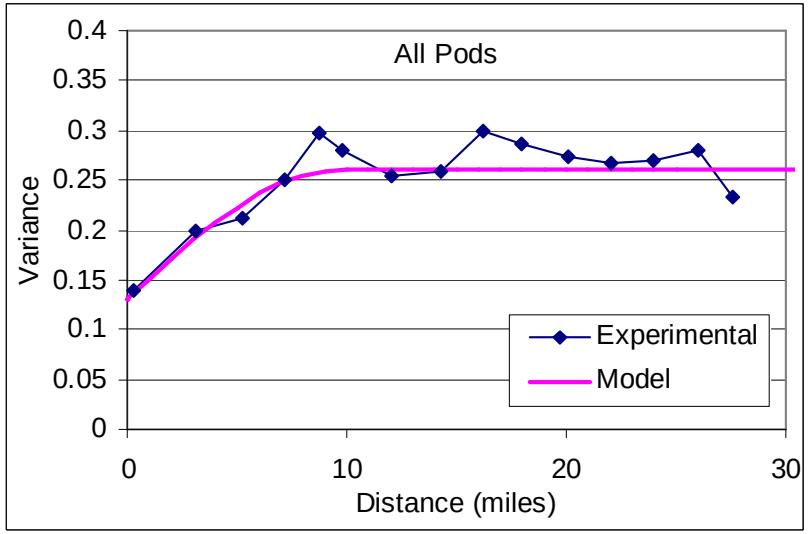

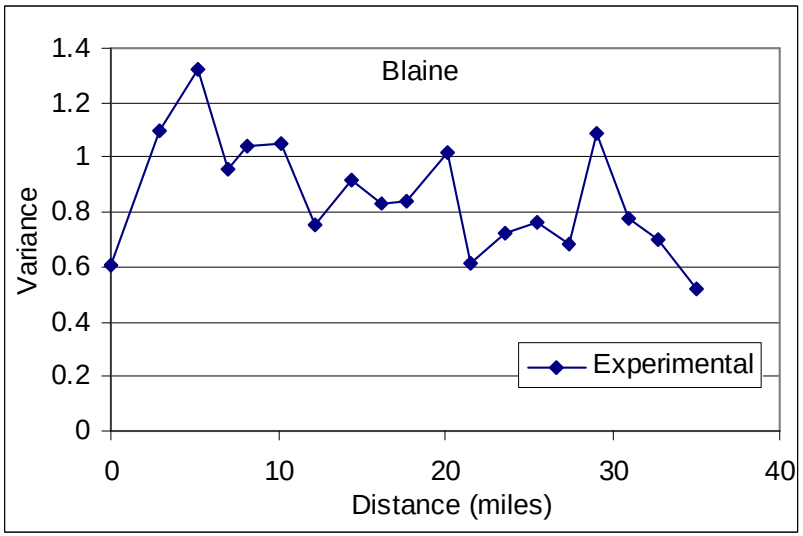

Figure 4.6.5 Experimental variogram of hydraulic conductivity for Seymour pod 11, the entire Seymour aquifer, and the Blaine aquifer.

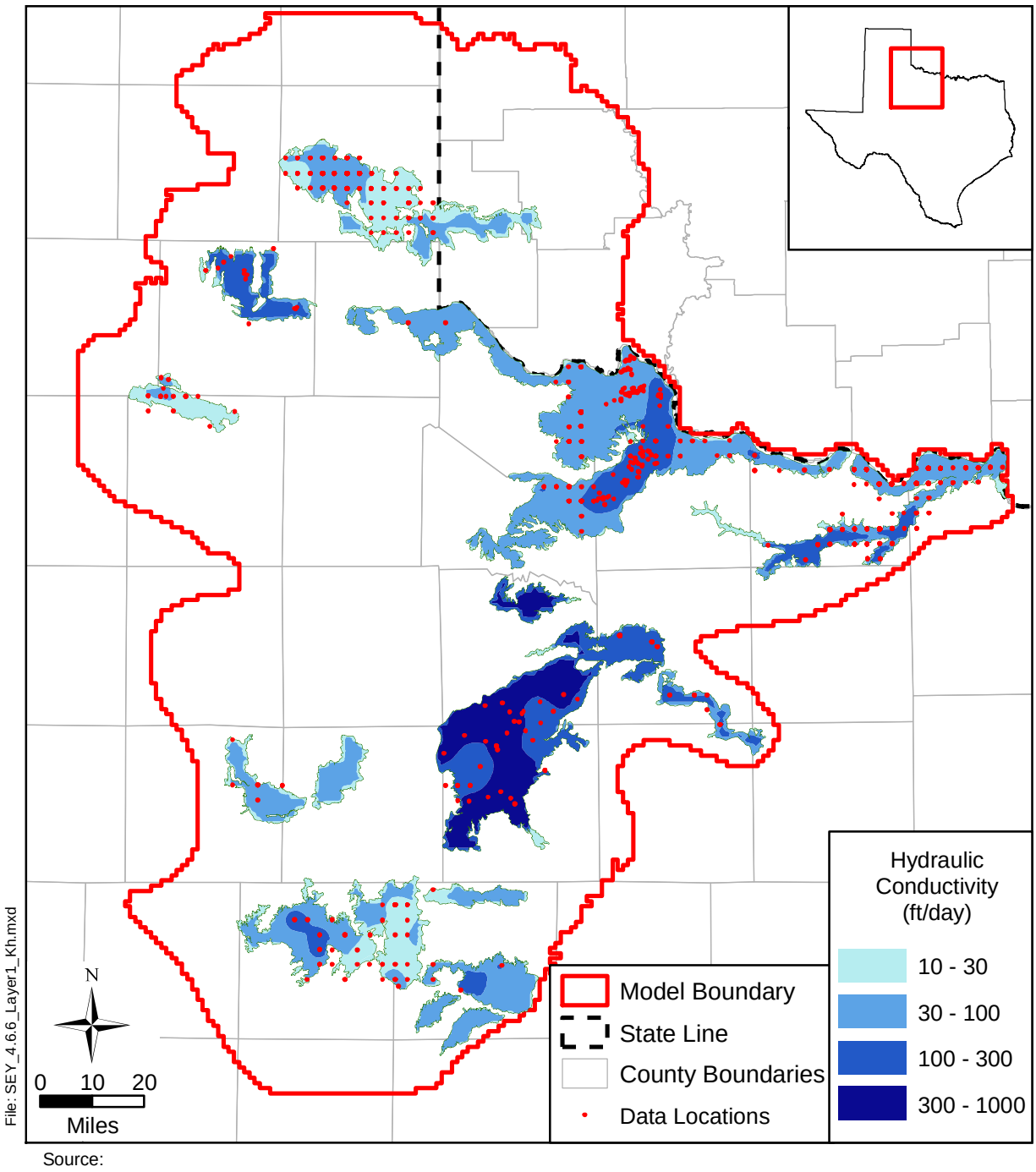

Figure 4.6.6 Kriged map of hydraulic conductivity for the Seymour aquifer.

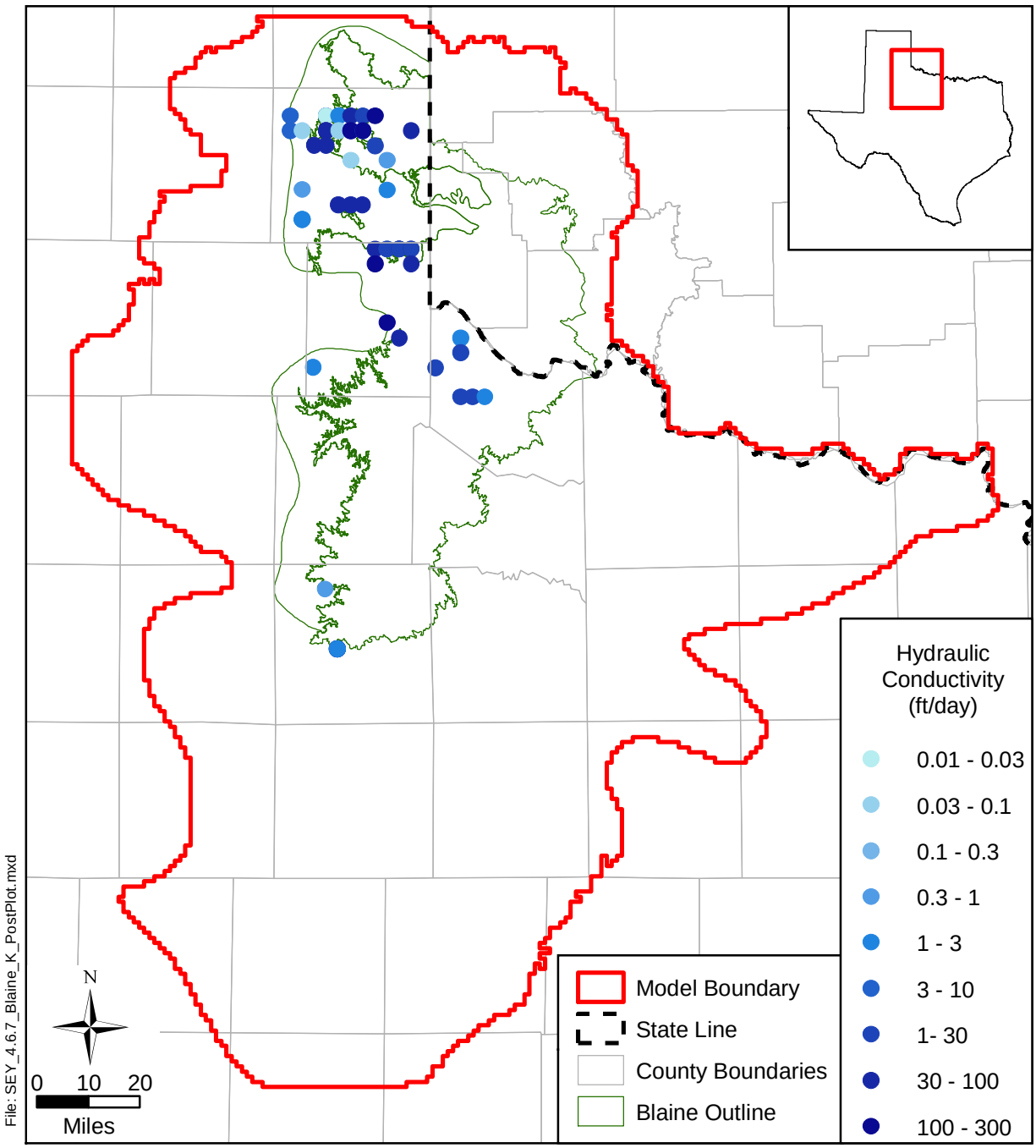

Figure 4.6.7 Post plot of Blaine aquifer hydraulic conductivity data.

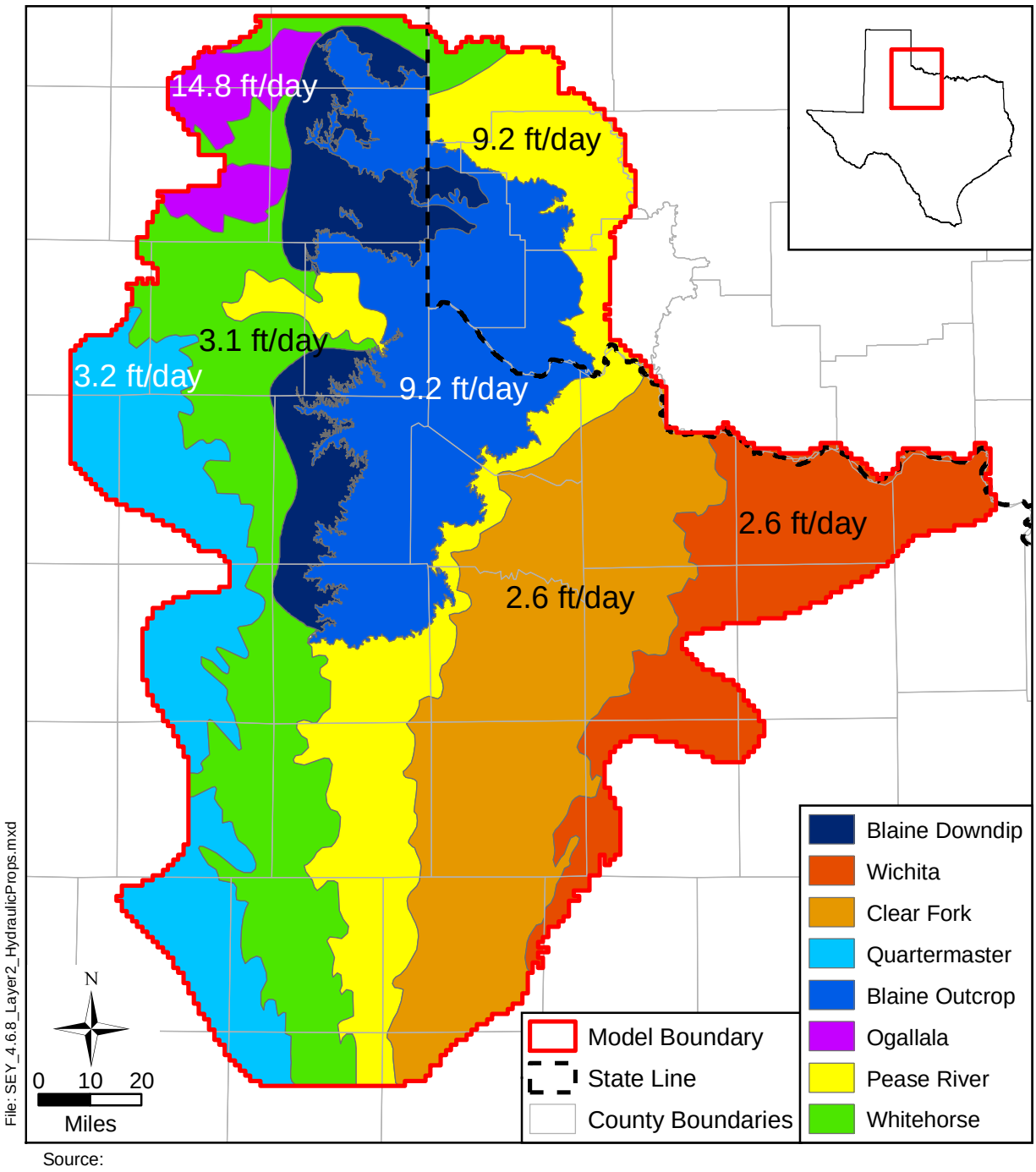

Figure 4.6.8 Hydraulic conductivity zones and geometric means for the Permian System.

4.7 Aquifer Discharge Through Pumping

Pumping discharge estimates for each model cell must be developed for both the steady-state model and the transient model, which includes the historical period (1980 through 1999) and the predictive period (2000 through 2050). Historical estimates of groundwater pumping throughout Texas have been compiled by the TWDB as a water use survey database. Municipal, manufacturing, mining, and power pumping estimates are available for 1980 through 2000. Livestock, irrigation, and county-other pumping estimates are available for 1980 through 1997. Predictive estimates of groundwater pumping throughout Texas are also available in a form similar to the historical pumping database from the TWDB. The TWDB predicted groundwater pumping for the period 2000 through 2050 are based on projected water demands reported by the RWPGs as part of Senate Bill 1 planning (TWDB, 2002). The seven water use categories defined in the TWDB database are city-municipal (MUN), manufacturing (MFG), steam electric power generation (PWR), mining (MIN), livestock (STK), irrigation (IRR), and county-other (C-O), which consists primarily of rural domestic water use. The methodology used to distribute the pumping estimates for each aquifer is described below.

The time period for which historical and predictive pumping estimates are available from the TWDB coincide with the time period for the transient model but not with the time periods for the steady-state model, which are generally in the 1960s and 1970s (see Section 4.3.2). Therefore, estimates of pumpage during the transient model were taken from the TWDB water use survey database and estimates of pumpage during the steady-state period were taken from literature sources.

The literature sources used to develop estimates of pumping for the steady-state model consisted of TWDB county reports for Baylor (Preston, 1978), Collingsworth (Smith, 1970), Hall (Popkin, 1973), Hardeman (Maderak, 1972), Jones (Price 1978), and Wilbarger (Price, 1979) counties; the R.W. Harden and Associates (1978) report on the Seymour aquifer in Haskell and Knox counties; and a report summarizing the results of irrigation surveys conducted in 1958, 1964, 1969, 1974, 1979, 1984, 1989, and 1994 (TWDB, 1996). In cases where the literature contained more than one value during the steady-state period, those values were averaged to obtain a single value for use in the model. In some instances, the pumpage volume reported in

the literature for a specific use applied to pumpage from all aquifer sources within the county. That pumpage volume was modified by the ratio of the number of Seymour or Blaine wells with that use to the total number of wells with that use to get the steady-state pumpage for the model. For example, if the use was irrigation, the total irrigation pumping volume would be multiplied by the number of Seymour irrigation wells divided by the total number of irrigation wells in the county to get estimated irrigation pumping for the Seymour. In instances when no literature data were found, steady-state pumping was set equivalent to 1980 pumping from the TWDB water use survey database. Tables 4.7.1 and 4.7.2 summarize pumpage volumes assigned to the steady-state model and the source for those volumes for the Seymour and Blaine aquifers, respectively. Figures 4.7.1 and 4.7.2 show the distribution of steady-state pumping by county for the Seymour and Blaine aquifers, respectively.

The following sections briefly summarize procedures used to spatially and temporally (transient model only) distribute groundwater pumpage for modeling purposes, in accordance with TWDB Technical Memorandum 02-02 (http://www.twdb.state.tx.us/gam/GAM_documents/GAM_memo_02_02_pumpage.pdf). Specific methodologies are described in detail in Appendix C for the historical period of 1980 to 2000, and in Appendix D for the predictive period of 2000 to 2050. Note that several minor pods of the Seymour aquifer were not modeled as per TWDB direction. Thus, pumpage from these pods was not included in the model, and pumping summaries for model grid cells do not match the historical totals from the water use surveys or predicted periods. The unmodeled pods are located in Cottle, Crosby, Dickens, Kent, Motley, and Wheeler counties (see Figure 2.2).

Pumping during the historical period of the transient model (1980 through 1999) was taken from the TWDB water use survey database. Each water use record in that database carries an aquifer identifier that was used to select pumping records for the Seymour and Blaine aquifers. For the municipal, manufacturing, mining, and power water uses, pumping estimates are actual water use records reported by the water user. In cases where only the total annual pumping was reported, the average monthly distribution of annual pumping for the same water use category in the same county-basin, or an adjacent county-basin, was used. A county-basin is a geographic unit created by the intersection of county and river basin boundaries. For example, Baylor County, which is intersected by both the Red River Basin and the Brazos River Basin,

contains two county-basins. The TWDB database of pumpage from the Seymour aquifer in Motley County includes municipal pumpage by the City of Matador. This pumpage is not included in the model because its source is portions of the Seymour aquifer and Quartermaster Formations not included in the Seymour GAM (see Figure 2.2 for unmodeled pods of the Seymour and Figure 2.3 for city locations).

Annual pumping estimates for livestock, irrigation, and county-other (primarily unreported domestic water use) uses are available in the TWDB database for the years 1980 through 1997 for each county-basin (the 1981 to 1983 estimates for livestock and irrigation were developed by the TWDB using linear regression since it did not develop water use summaries for this period). Annual pumping estimates for the years 1998 through 1999 were developed by linear regression based on statistically significant relationships between reported pumping and (1) average annual temperature, (2) total annual rainfall measured at the nearest weather station, and (3) the year, for each water use category. In the case that no significant relationship was found, or if the annual pumpage totals exhibited a substantial step-like change in recent years that limited the ability of the relationship to predict pumpage for 1998 through 1999, the water use for the last year reported (1997) was used.

The monthly distribution of county-other water use was assumed to be similar to that of municipal use. The average monthly distribution of municipal water use for a given year within the same (if possible) or adjacent county-basin was used to estimate how much of the annual total county-other usage was pumped in each month. Annual livestock water use was distributed uniformly across all twelve months, in accordance with TWDB guidance. Annual irrigation water use was distributed among months using predicted monthly water deficits, based on rainfall deficit and crop evapotranspiration estimates for each Texas Crop Reporting District, using the approach of Borrelli et al. (1998).

The methodology used to distribute the historical pumping estimates for each aquifer into the model grid blocks for the transient model varied depending on the use category. The distribution of pumping for the steady-state model was assumed to be the same as that for the year 1980 in the transient model. Reported historical pumping for municipal, manufacturing, mining, and power water uses was matched to the specific wells from which it was pumped to identify the location in the aquifer from which it was drawn (latitude, longitude, and depth below

mean sea level) based on the well's reported properties. The well properties were obtained by compiling data from the TWDB's state well database, the TCEQ's Public Water System database, the USGS's National Water Information System, the TWDB's follow up survey with water users, and various other minor sources. When more than one well was associated with a given water user, groundwater withdrawals were divided evenly among those wells, after eliminating wells in different aquifers, wells that were not drilled until a later date, unused wells, and wells used for different water use categories.

Livestock pumping totals within each county-basin were distributed uniformly over the rangeland within the county-basin that overlies active model cells of the source aquifer. Rangeland was identified based on the USGS 1:250,000 Global Land Information System (GLIS) land use land cover maps, using the Anderson Level II categories "herbaceous rangeland", "shrub and brush rangeland", and "mixed rangeland".

County-other pumping was spatially distributed within each county-basin based on population density (Figure 4.7.3), after excluding reservoirs and urban areas which would generally be served by municipal water suppliers, using the 1990 federal block-level census data for the years 1980-1990, and the 2000 census data for the years 1991-1999. County-other pumping was assigned to model layer 1 where active Seymour model cells are present and to model layer 2 where active layer 2 model cells are present, but active Seymour model cells are not. In areas where neither model layer 1 or 2 are active, county-other pumpage was not included in the model.

Irrigation pumping within each county-basin was spatially distributed to the portions of the irrigated farms mapped from the irrigated farmlands surveys performed in 1989 and 1994 by the Natural Resource Conservation Service of the U.S. Department of Agriculture that also (1) match the land use categories "row crops", "orchard/vineyard", or "small grains" from the National Land Cover Database, and (2) overly the source aquifer. The irrigation pumping was not uniformly distributed to these areas, but in proportion to the reported area irrigated in the irrigated farmlands survey. The 1989 irrigation survey was used for pumping between 1980 and 1989; the 1994 survey was used for pumping from 1990 to 1999.

Groundwater pumping estimates for the part of the study area in Oklahoma were derived from data provided by the Oklahoma Water Resources Board (OWRB). The OWRB provided annual groundwater pumping estimates for 1980 through 2001 for Beckham, Greer, Harmon, and Jackson counties, Oklahoma, portions of which were included in the model domain. These estimates provided a specific permit number, source aquifer, and water use category for each water user. The pumping was spatially distributed by linking the permit number for each water user to separate data provided by the OWRB that identified the locations of wells or dedicated lands for each permit. The pumping was temporally distributed among months using the temporal distribution factors for the same water use category from the nearest adjacent Texas county-basin.

Pumping for the Seymour and Blaine aquifers has been summed by county for each aquifer and summed over the entire study area in Texas. Data for those portions of the study area in Oklahoma have not been summarized. Historical groundwater withdrawals by county (Texas only) for the years 1980, 1985, 1990, 1995, and 1999 are listed in Tables 4.7.3 through 4.7.7 for the Seymour aquifer and Tables 4.7.8 through 4.7.11 for the Blaine aquifer. Projected total water use from the Seymour and Blaine aquifers in 1999 was 132,763 and 17,170 AFY, respectively. Comparing these numbers to the totals in Tables 4.7.3 through 4.7.11 indicates that irrigation accounts for about 94 percent of Seymour pumping and about 97 percent of Blaine pumping. Figures 4.7.4 and 4.7.5 show the 1980-1999 average pumping demands by county for the Seymour and Blaine aquifers, respectively. Figure 4.7.4 shows that the heaviest pumping from the Seymour aquifer occurs in Haskell, Knox, and Wilbarger counties. For the Blaine aquifer, the main pumping centers are in the Collingsworth and Hardeman county areas (Figure 4.7.5).

Figures 4.7.6 through 4.7.37 show the 1980-1999 pumping demands by water use category for the Seymour and Blaine aquifers in Texas. From these figures, it appears that total pumping from the Seymour and Blaine aquifers declined between 1980 and 1986, but since that time has increased slightly from the Seymour aquifer, and increased substantially from the Blaine aquifer. These changes are caused by increases in irrigation pumping. Municipal pumping from the Seymour has remained relatively constant. Groundwater from the Blaine aquifer is not used for municipal purposes due to its high dissolved solids levels. Livestock and

county-other water use from the Seymour and Blaine aquifers has remained relatively unchanged over this time period. Only a few acre-feet per year of water pumped from the Seymour and Blaine aquifers are reported to have been used for manufacturing and mining uses, and no water was reported pumped for use in power generation.

Recall that not all pods of the Seymour aquifer are included in the Seymour GAM (see Figure 2.2). As a result, pumpage for the GAM is less than pumpage reported by the TWDB for several counties in the model area. Specifically, none of the pods in Cottle, Crosby, Dickens, or Wheeler counties are included in the Seymour GAM. Therefore, no pumpage from these counties was modeled or is reported in Tables 4.7.3 through 4.7.7 and Figures 4.76 and 4.7.8 through 4.7.28. In addition, pumpage in the model as listed in these tables and shown in these figures is less than that reported by the TWDB for Motley and Kent counties because not all Seymour pods in those counties are included in the Seymour GAM (see Figures 2.2). Therefore, comparing county-wide historical pumpage for the entire Seymour aquifer to model pumpage in the Seymour GAM is not applicable.

Predictive estimates of groundwater pumping throughout Texas for the period 2000 through 2050 were assembled by the TWDB from the 2002 State Water Plan, based on projected water demand reported by RWPGs as part of Senate Bill 1 planning (TWDB, 2002). These pumping estimates were provided in a format similar to the historical pumping database. As with the historical pumping database, pumping is provided for each of the seven use categories and each water use record carries an aquifer identifier. The RWPG water demand projections were available for the years 2000, 2010, 2020, 2030, 2040, and 2050. Intervening year projections were developed by linear interpolation. In some cases, the RWPGs identified new well field locations for developing new water supplies. In such instances, the specific location of the future well fields, as identified in the RWPG reports, was used to spatially distribute the groundwater pumping forecasts. However, in the absence of any data indicating otherwise, it was assumed that the most recent past spatial distribution of groundwater pumping represents the best available estimate of the locations of future groundwater withdrawals.

In most cases, predicted municipal groundwater use for 2000 though 2050 for each public water supplier was matched to the same wells reportedly used for that water user in the period 1995 through 2000. Recall that the source for pumpage by the City of Matador in Motley

County is not part of the Seymour GAM and, therefore, the predictive pumpage for this city is not included in the model. For manufacturing, mining, and power generation, predicted future water pumping totals by county-basin were distributed among the same wells and locations used by those water users in the period 1995 through 2000.

In some cases, the 2002 State Water Plan (TWDB, 2002) allocated predictive pumping from the Seymour or Blaine aquifers for water user groups not pumping from these aquifers during the historical period (according to the TWDB's historical water use surveys) without an indication that new wells would provide this supply. The procedures for spatially distributing this pumpage were similar to those for historical pumpage, and are described in detail in Appendix D. This condition occurred for water used by the City of Aspermont in Stonewall County. Historical pumping records show that the source of water for this city is Seymour-aquifer wells located in neighboring Haskell County, state wells 21-49-212, 21-49-317, and 21-49-503. The predictive pumping records indicate that the Seymour aquifer in Stonewall County will be the source for future pumping by the City of Aspermont. However, the predictive pumping records do not indicate a new source or new wells being drilled in Stonewall County, nor does the regional water plan indicate a new source. Therefore, predictive pumping for the City of Aspermont was assigned to the same wells as for historical pumping, and those wells are located in Haskell County.

If the water management strategy listed in the State Water Plan indicated a quantity of groundwater to be purchased from another supplier in the predictive period, that pumping was spatially allocated to the wells used by the water supplier rather than those of the water user. In other cases, the State Water Plan indicated that new groundwater supplies would be developed with new wells or through re-developing existing well fields, and the location of the new well fields were identified by examination of maps and other files submitted with the regional water planning reports. Some changes in water supply for the predictive period that affected the Seymour aquifer are listed in the following table.

Water User Group ID	County-Basin	Use Category	Water Management Strategy Name
021001244	Wilbarger-Red	Manufacturing	Purchase water from City of Vernon – Seymour aquifer
020930000	Wilbarger-Red	Vernon	Develop new groundwater supply – Seymour aquifer
020277000	Wichita-Red	Electra	Develop groundwater supply – expand and redevelop existing well field – Seymour aquifer

Irrigation, county-other, and livestock pumping estimates for each county-basin from 2000 to 2050 also used the 2000 spatial distribution within county-basins. The average monthly use factors for each county-basin and water use for 1980 though 2000 were applied to distribute future annual totals among months.

Estimates of projected Oklahoma groundwater pumping for 2000 through 2050 are not available. Municipal and county-other pumping totals for future years were predicted by multiplying the per capita consumption for the period 1995 to 2000 by the projected future county populations supplied by the state demographers. Predicted future pumping for other water use categories in Oklahoma were not projected. Instead, we assumed that pumping in future years will equal the average pumping for the period 1995 to 2000.

Predictive withdrawals by county (Texas only) for the years 2000, 2010, 2020, 2030, 2040, and 2050 are listed in Tables 4.7.12 through 4.7.16 for the Seymour aquifer and Tables 4.7.17 through 4.7.20 for the Blaine aquifer. Comparing the aquifer totals for all water uses to the totals for individual uses indicates that irrigation accounts for the largest percentage of total pumpage for both the Seymour and Blaine aquifers. Total pumpage from both aquifers declines throughout the 50-year period from 2000 to 2050. Because not all Seymour-aquifer pods are included in the Seymour GAM (see Figure 2.2), no predictive pumpage is included in the model or reported here for Cottle, Crosby, Dickens, and Wheeler counties and model predictive pumpage in Motley and Kent counties is less than that reported by the TWDB. Therefore, comparing county-wide predictive pumpage for the entire Seymour aquifer to model pumpage in the Seymour GAM is not applicable.

Model predictive pumpage for the Blaine aquifer in Wheeler County is about 14 AFY higher than that estimated by the TWDB. This overage is in the county-other use category and spread across a large area. Since the model includes more predictive pumping in the Blaine aquifer for Wheeler County than has been estimated by the TWDB, the model predictions of future drawdown in this portion of the aquifer are conservative.

Tables 4.7.21 and 4.7.22 summarize total pumpage from the Seymour and Blaine aquifers, respectively, for the steady-state model and for 1980, 1990, 2000, 2010, 2020, 2030, 2040, and 2050 pumping in the transient model. For the Seymour aquifer, pumping during

steady-state is lower than at all other times and pumpage during 1980 is significantly higher than any other year listed. For the Blaine aquifer, pumping during steady-state is higher than at all other times and pumpage during 1980 and 1990 is a little greater than half that predicted to occur from 2000 through 2050. Figures 4.7.38 through 4.7.60 show bar charts of total pumping by county from the Seymour and Blaine aquifers in Texas by year from 1980 through 2050.

Table 4.7.1 Summary of steady-state pumpage from the Seymour aquifer.

County	Municipal (AFY)	Irrigation (AFY)	Industrial (AFY)	Livestock (AFY)	County-Other (AFY)	Total (AFY)
Archer	0[1]	0[1]	nr	0[1]	1.4[1]	1.4
Baylor	685[2]	3,240[2]	150[2]	310[2]		4,385
Briscoe	0[1]	0[1]	nr	0[1]	2.4[1]	2.4
Childress	0[1]	0[3]	nr	36[1]	5[1]	41
Clay	136[1]	162[3]	nr	35[1]	91[1]	424
Collingsworth	4,530[4]	4,440[4]	1,530[4]	30[1]	120[1]	10,650
Fisher	0[1]	925[3]	nr	24[1]	127[1]	1,076
Foard	0[1]	2,470[3]	nr	46[1]	57[1]	2,573
Hall	140[1 & 5]	9,505[3]	nr	19[1]	70[1]	9,734
Hardeman	560[6]	4,000[6]	nr	8[1]	72[1]	4,640
Haskell	1,170[7]	20,500[7]	nr	38[1]	203[1]	21,911
Jones	0[8]	1,255[8]	77[8]	435[8]		1,767
Kent	149[1]	530[3]	nr	1[1]	7[1]	687
Knox	630[7]	17,555[7]	nr	30[1]	169[1]	18,384
Motley	0[1]	1,585[3]	nr	6[1]	7[1]	1,598
Stonewall	0[1]	300[3]	nr	8[1]	14[1]	322
Taylor	0[1]	0[1]	nr	0[1]	17[1]	17
Throckmorton	0[1]	0[1]	nr	0[1]	3[1]	3
Wichita	1,343[1]	0[3]	nr	56[1]	356[1]	1,755
Wilbarger	4,500[9]	1,533[9]	9[9]	150[9]		6,192
Young	0[1]	0[1]	nr	0[1]	0.8[1]	0.8
Total	**13,843**	**68,000**	**1,766**	**337**	**895**	**1,323**	**86,164**

nr – none reported

Sources:

1. TWDB water use survey database
2. Occurrence and Quality of Ground Water in Baylor County, Texas (Preston, 1978)
3. Surveys of Irrigation in Texas 1958, 1964, 1969, 1974, 1979, 1984, 1989, and 1994 (TWDB, 1996)
4. Ground-Water Resources of Collingsworth County, Texas (Smith, 1970)
5. Ground-Water Resources of Hall and Eastern Briscoe Counties (Popkin, 1973)
6. Ground-Water Resources of Hardeman County, Texas (Maderak, 1972)
7. The Seymour Aquifer – Ground-Water Quality and Availability in Haskell and Knox Counties, Texas Volume I (R.W. Harden and Associates, 1978)
8. Occurrence, Quality, and Availability of Ground Water in Jones County, Texas (Price, 1978)
9. Occurrence, Quality, and Quantity of Ground Water in Wilbarger County, Texas (Price, 1979)

Table 4.7.2 Summary of steady-state pumpage from the Blaine aquifer.

County	Municipal (AFY)	Irrigation (AFY)	Industrial (AFY)	Livestock (AFY)	County-Other (AFY)	Total (AFY)
Childress	nr	7,750[2]	nr	0[1]	108[1]	7,858
Collingsworth	nr	8,205[3]	1,020[3]	43[1]	64[1]	9,332
Cottle	nr	5,463[2]	nr	0[1]	87[1]	5,550
Foard	nr	110[2]	nr	6[1]	4[1]	120
Hall	nr	0[2]	nr	nr	21[1]	21
Hardeman	0[4]	5,900[4]	nr	28[1]	86[1]	6,014
King	nr	500[1]	nr	7[1]	21[1]	528
Knox	0[1]	0[1]	nr	0[1]	2[1]	2
Wheeler	nr	1,324[1]	nr	57[1]	97[1]	1,478
Total	**0**	**29,252**	**1,020**	**141**	**490**	**30,903**

nr – none reported

Sources:

[1] TWDB water use survey database

[2] Surveys of Irrigation in Texas 1958, 1964, 1969, 1974, 1979, 1984, 1989, and 1994 (TWDB, 1996)

[3] Ground-Water Resources of Collingsworth County, Texas (Smith, 1970)

[4] Ground-Water Resources of Hardeman County, Texas (Maderak, 1972)

Table 4.7.3 Rate of groundwater withdrawal (AFY) from the Seymour aquifer for counties within the active model area – all water use categories.

County	1980	1985	1990	1995	1999
Archer	1	2	1	1	1
Baylor	6,947	2,572	2,514	1,424	1,187
Briscoe	2	2	2	2	1
Childress	10,041	7,283	5,876	134	91
Clay	462	701	580	860	896
Collingsworth	3,057	6,750	16,950	11,810	25,157
Fisher	2,151	3,040	2,203	1,747	2,915
Foard	5,103	2,971	3,663	3,171	3,842
Hall	21,690	9,175	12,755	10,331	11,518
Hardeman	3,416	2,449	2,481	185	197
Haskell	39,297	11,049	22,210	32,519	27,805
Jones	2,212	2,008	2,257	4,038	2,972
Kent	527	1,074	770	836	960
Knox	50,235	30,979	32,547	31,654	26,213
Motley	3,454	2,818	3,776	4,728	1,868
Stonewall	363	315	353	632	745
Taylor	17	16	12	14	13
Throckmorton	3	4	3	3	3
Wichita	1,756	1,841	1,716	2,184	2,330
Wilbarger	26,589	22,163	19,543	20,051	24,048
Young	1	1	1	1	1
TOTALS	**177,324**	**107,213**	**130,213**	**126,325**	**132,763**

All withdrawals rounded to the nearest 1 AFY.

Table 4.7.4 Rate of groundwater withdrawal (AFY) from the Seymour aquifer for counties within the active model area – municipal and manufacturing uses.

County	1980	1985	1990	1995	1999
Archer	0	0	0	0	0
Baylor	786	846	690	734	631
Briscoe	0	0	0	0	0
Childress	0	0	0	0	0
Clay	136	153	151	145	158
Collingsworth	668	653	575	483	504
Fisher	0	0	0	0	0
Foard	0	0	0	0	0
Hall	100	127	128	81	82
Hardeman	200	194	109	94	108
Haskell	150	135	95	64	63
Jones	0	0	0	0	0
Kent	149	142	146	138	144
Knox	39	46	0	44	65
Motley	0	0	0	0	0
Stonewall	281	197	180	182	185
Taylor	0	0	0	0	0
Throckmorton	0	0	0	0	0
Wichita	1,343	1,478	1,249	1,179	1,260
Wilbarger	3,413	3,115	2,477	2,804	3,537
Young	0	0	0	0	0
TOTALS	**7,265**	**7,086**	**5,800**	**5,948**	**6,737**

All withdrawals rounded to the nearest 1 AFY.

Table 4.7.5 Rate of groundwater withdrawal (AFY) from the Seymour aquifer for counties within the active model area – irrigation use.

County	1980	1985	1990	1995	1999
Archer	0	0	0	0	0
Baylor	5,998	1,532	1,630	472	405
Briscoe	0	0	0	0	0
Childress	10,000	7,250	5,834	81	35
Clay	200	433	306	587	609
Collingsworth	2,239	5,959	16,260	11,205	24,547
Fisher	2,000	2,905	2,073	1,626	2,800
Foard	5,000	2,917	3,600	3,102	3,774
Hall	21,501	8,969	12,560	10,184	11,380
Hardeman	3,136	2,164	2,281	0	0
Haskell	38,906	10,697	21,873	32,190	27,443
Jones	1,785	1,534	1,792	3,590	2,549
Kent	370	918	610	678	797
Knox	49,998	30,695	32,323	31,365	25,948
Motley	3,441	2,806	3,764	4,717	1,858
Stonewall	60	90	154	426	538
Taylor	0	0	0	0	0
Throckmorton	0	0	0	0	0
Wichita	0	0	0	461	503
Wilbarger	22,800	18,621	16,678	16,807	20,075
Young	0	0	0	0	0
TOTALS	**167,434**	**97,490**	**121,738**	**117,491**	**124,261**

All withdrawals rounded to the nearest 1 AFY.

Table 4.7.6 Rate of groundwater withdrawal (AFY) from the Seymour aquifer for counties within the active model area – livestock use.

County	1980	1985	1990	1995	1999
Archer	0	0	0	0	0
Baylor	64	78	93	110	46
Briscoe	0	0	0	0	0
Childress	36	28	39	50	53
Clay	35	15	19	18	19
Collingsworth	30	15	15	24	23
Fisher	24	13	14	11	9
Foard	46	5	7	8	9
Hall	19	17	20	18	18
Hardeman	8	6	32	35	40
Haskell	38	24	43	70	108
Jones	64	33	23	39	49
Kent	1	4	5	12	11
Knox	29	41	45	75	38
Motley	6	6	5	4	3
Stonewall	8	12	8	13	12
Taylor	0	0	0	0	0
Throckmorton	0	0	0	0	0
Wichita	57	49	52	60	47
Wilbarger	66	57	66	98	95
Young	0	0	0	0	0
TOTALS	**531**	**403**	**486**	**645**	**580**

All withdrawals rounded to the nearest 1 AFY.

Table 4.7.7 Rate of groundwater withdrawal (AFY) from the Seymour aquifer for counties within the active model area – county-other use.

County	1980	1985	1990	1995	1999
Archer	1	2	1	1	1
Baylor	100	116	102	108	105
Briscoe	2	2	2	2	1
Childress	5	5	3	3	3
Clay	91	100	104	110	109
Collingsworth	120	123	99	98	83
Fisher	127	122	116	110	106
Foard	57	49	56	61	59
Hall	70	62	47	48	39
Hardeman	72	85	59	56	50
Haskell	203	193	199	194	190
Jones	363	441	442	409	374
Kent	7	10	9	8	7
Knox	169	197	179	171	161
Motley	7	7	7	7	7
Stonewall	14	16	11	10	9
Taylor	17	16	12	14	13
Throckmorton	3	4	3	3	3
Wichita	356	314	416	483	520
Wilbarger	311	370	323	342	341
Young	1	1	1	1	1
TOTALS	**2,096**	**2,235**	**2,191**	**2,239**	**2,182**

All withdrawals rounded to the nearest 1 AFY.

Table 4.7.8 Rate of groundwater withdrawal (AFY) from the Blaine aquifer for Texas counties within the active model area – all water use categories.

County	1980	1985	1990	1995	1999
Childress	108	105	92	7,286	3,141
Collingsworth	2,906	1,575	4,126	3,892	7,312
Cottle	86	80	60	1,019	2,565
Foard	10	15	18	26	28
Hall	21	19	12	12	10
Hardeman	6,582	4,587	4,896	3,777	3,966
King	528	781	79	50	48
Knox	2	2	0	0	0
Wheeler	1,478	922	749	104	100
TOTALS	**11,721**	**8,086**	**10,032**	**16,166**	**17,170**

All withdrawals rounded to the nearest 1 AFY.

Table 4.7.9 Rate of groundwater withdrawal (AFY) from the Blaine aquifer for Texas counties within the active model area – irrigation use.

County	1980	1985	1990	1995	1999
Childress	0	0	0	7,194	3,053
Collingsworth	2,799	1,490	4,064	3,818	7,245
Cottle	0	0	0	961	2,517
Foard	0	0	0	0	0
Hall	0	0	0	0	0
Hardeman	6,468	4,462	4,703	3,577	3,755
King	500	750	50	20	20
Knox	0	0	0	0	0
Wheeler	1,324	800	655	10	12
TOTALS	**11,091**	**7,502**	**9,472**	**15,580**	**16,602**

All withdrawals rounded to the nearest 1 AFY.

Table 4.7.10 Rate of groundwater withdrawal (AFY) from the Blaine aquifer for Texas counties within the active model area – livestock use.

County	1980	1985	1990	1995	1999
Childress	0	0	0	0	0
Collingsworth	43	20	20	33	32
Cottle	0	0	0	0	0
Foard	6	12	14	21	24
Hall	0	0	0	0	0
Hardeman	28	23	122	132	152
King	7	9	9	10	10
Knox	0	0	0	0	0
Wheeler	57	14	11	16	16
TOTALS	**141**	**78**	**176**	**212**	**234**

All withdrawals rounded to the nearest 1 AFY.

Table 4.7.11 Rate of groundwater withdrawal (AFY) from the Blaine aquifer for Texas counties within the active model area – county-other use.

County	1980	1985	1990	1995	1999
Childress	108	105	92	92	87
Collingsworth	64	65	42	41	35
Cottle	86	80	60	58	48
Foard	4	3	4	5	5
Hall	21	19	12	12	10
Hardeman	86	102	71	68	60
King	21	22	20	20	18
Knox	2	2	0	0	0
Wheeler	97	108	83	78	72
TOTALS	**489**	**506**	**384**	**374**	**335**

All withdrawals rounded to the nearest 1 AFY.

Table 4.7.12 Predictive pumping estimates for the Seymour aquifer (AFY) – all water use categories.

County	2000	2010	2020	2030	2040	2050
Archer	0	0	0	0	0	0
Baylor	1,806	1,695	1,536	1,440	1,392	1,353
Briscoe	4,063	4,063	4,063	1,821	1,821	1,821
Childress	64	65	70	71	72	73
Clay	803	745	722	714	721	723
Collingsworth	14,135	14,124	14,125	14,120	14,112	14,110
Fisher	3,325	3,195	3,228	3,139	3,074	3,028
Foard	5,025	4,875	4,730	4,590	4,455	4,321
Hall	8,317	8,302	8,288	8,276	8,269	8,266
Hardeman	401	395	392	388	385	383
Haskell	21,972	21,281	20,647	20,032	19,437	18,870
Jones	4,045	3,888	3,767	3,658	3,560	3,470
Kent	1,625	1,212	999	875	786	725
Knox	26,247	26,242	26,285	26,289	25,650	25,035
Motley	2,065	2,003	1,943	1,885	1,828	1,774
Stonewall	1,258	1,189	1,109	1,035	967	935
Taylor	0	0	0	0	0	0
Throckmorton	0	0	0	0	0	0
Wichita	1,873	2,058	2,070	2,085	2,099	2,096
Wilbarger	23,349	22,806	22,281	21,823	21,374	20,989
Young	0	0	0	0	0	0
Total	**120,373**	**118,138**	**116,255**	**112,241**	**110,002**	**107,972**

All withdrawals rounded to the nearest 1 AFY.

Table 4.7.13 Predictive pumping estimates for the Seymour aquifer (AFY) – municipal, manufacturing, and mining uses.

County	2000	2010	2020	2030	2040	2050
Archer	0	0	0	0	0	0
Baylor	764	689	560	491	463	444
Briscoe	0	0	0	0	0	0
Childress	0	0	0	0	0	0
Clay	465	374	343	325	320	321
Collingsworth	614	593	580	571	561	553
Fisher	564	524	509	511	525	541
Foard	23	24	24	25	26	27
Hall	118	114	111	110	110	113
Hardeman	69	67	66	66	65	65
Haskell	202	149	144	132	122	122
Jones	289	237	217	208	205	208
Kent	893	499	306	203	132	89
Knox	95	93	91	96	95	97
Motley	0	0	0	0	0	0
Stonewall	414	366	312	261	216	204
Taylor	0	0	0	0	0	0
Throckmorton	0	0	0	0	0	0
Wichita	993	1,146	1,127	1,112	1,090	1,089
Wilbarger	3,658	3,662	3,687	3,764	3,838	3,943
Young	0	0	0	0	0	0
Total	**9,161**	**8,537**	**8,077**	**7,875**	**7,768**	**7,816**

All withdrawals rounded to the nearest 1 AFY.

Table 4.7.14 Predictive pumping estimates for the Seymour aquifer (AFY) – irrigation use.

County	2000	2010	2020	2030	2040	2050
Archer	0	0	0	0	0	0
Baylor	707	685	666	646	626	607
Briscoe	4,063	4,063	4,063	1,821	1,821	1,821
Childress	37	37	37	37	37	37
Clay	217	252	262	273	287	287
Collingsworth	13,343	13,352	13,368	13,373	13,379	13,385
Fisher	2,304	2,235	2,168	2,103	2,041	1,979
Foard	4,956	4,808	4,664	4,523	4,388	4,256
Hall	8,072	8,072	8,073	8,073	8,073	8,073
Hardeman	103	100	97	94	91	88
Haskell	21,579	20,937	20,315	19,711	19,125	18,557
Jones	3,517	3,412	3,311	3,211	3,116	3,023
Kent	646	628	611	593	577	561
Knox	25,867	25,867	25,867	25,866	25,231	24,611
Motley	2,065	2,003	1,943	1,885	1,828	1,774
Stonewall	518	502	487	473	458	446
Taylor	0	0	0	0	0	0
Throckmorton	0	0	0	0	0	0
Wichita	591	610	639	673	712	712
Wilbarger	19,071	18,499	17,944	17,406	16,884	16,377
Young	0	0	0	0	0	0
Total	**107,656**	**106,062**	**104,515**	**100,761**	**98,674**	**96,594**

All withdrawals rounded to the nearest 1 AFY.

Table 4.7.15 Predictive pumping estimates for the Seymour aquifer (AFY) – livestock use.

County	2000	2010	2020	2030	2040	2050
Archer	0	0	0	0	0	0
Baylor	95	95	95	95	95	95
Briscoe	0	0	0	0	0	0
Childress	24	25	30	31	32	33
Clay	100	100	100	100	100	100
Collingsworth	18	19	21	21	22	23
Fisher	140	140	140	140	140	140
Foard	0	0	0	0	0	0
Hall	15	15	16	16	17	17
Hardeman	192	192	192	192	192	192
Haskell	175	175	175	175	175	175
Jones	239	239	239	239	239	239
Kent	63	63	63	63	63	63
Knox	71	71	71	71	71	71
Motley	0	0	0	0	0	0
Stonewall	201	201	201	201	201	201
Taylor	0	0	0	0	0	0
Throckmorton	0	0	0	0	0	0
Wichita	71	71	71	71	71	71
Wilbarger	156	156	156	156	156	156
Young	0	0	0	0	0	0
Total	**1,560**	**1,562**	**1,570**	**1,571**	**1,574**	**1,576**

All withdrawals rounded to the nearest 1 AFY.

Table 4.7.16 Predictive pumping estimates for the Seymour aquifer (AFY) – county–other use.

County	2000	2010	2020	2030	2040	2050
Archer	0	0	0	0	0	0
Baylor	240	226	215	208	208	207
Briscoe	0	0	0	0	0	0
Childress	3	3	3	3	3	3
Clay	21	19	17	16	14	15
Collingsworth	160	160	157	154	150	149
Fisher	317	296	411	386	369	368
Foard	46	43	42	42	41	38
Hall	112	101	89	78	70	62
Hardeman	37	36	37	37	37	38
Haskell	16	19	13	14	15	17
Jones	0	0	0	0	0	0
Kent	23	21	19	15	14	12
Knox	214	211	256	256	253	256
Motley	0	0	0	0	0	0
Stonewall	125	120	109	100	92	84
Taylor	0	0	0	0	0	0
Throckmorton	0	0	0	0	0	0
Wichita	218	231	232	229	226	224
Wilbarger	464	490	495	497	497	513
Young	0	0	0	0	0	0
Total	**1,996**	**1,976**	**2,095**	**2,035**	**1,989**	**1,986**

All withdrawals rounded to the nearest 1 AFY.

Table 4.7.17 Predictive pumping estimates for the Blaine aquifer (AFY) in Texas – all water use categories.

County	2000	2010	2020	2030	2040	2050
Childress	3,755	3,743	3,740	3,737	3,735	3,734
Collingsworth	4,532	4,524	4,511	4,505	4,499	4,494
Cottle	4,782	4,630	4,477	4,334	4,188	4,047
Foard	25	24	24	23	22	22
Hall	28	25	22	19	17	15
Hardeman	4,841	4,696	4,559	4,423	4,292	4,165
King	344	341	339	337	336	335
Knox	1,333	1,333	1,333	1,333	1,300	1,268
Wheeler[a]	50	48	48	48	47	49
Total	**19,690**	**19,364**	**19,053**	**18,759**	**18,436**	**18,129**

All withdrawals rounded to the nearest 1 AFY.

[a] Values are approximately 14 AFY higher than those estimated by the TWDB.

Table 4.7.18 Predictive pumping estimates for the Blaine aquifer (AFY) in Texas – irrigation use.

County	2000	2010	2020	2030	2040	2050
Childress	3,654	3,653	3,654	3,653	3,652	3,650
Collingsworth	4,441	4,432	4,417	4,412	4,406	4,399
Cottle	4,377	4,246	4,118	3,995	3,875	3,759
Foard	22	21	20	20	19	19
Hall	0	0	0	0	0	0
Hardeman	4,797	4,653	4,514	4,379	4,247	4,119
King	20	20	20	20	20	20
Knox	1,333	1,333	1,333	1,333	1,300	1,268
Wheeler	15	15	15	15	15	16
Total	**18,659**	**18,373**	**18,091**	**17,827**	**17,534**	**17,250**

All withdrawals rounded to the nearest 1 AFY.

Table 4.7.19 Predictive pumping estimates for the Blaine aquifer (AFY) in Texas – livestock use.

County	2000	2010	2020	2030	2040	2050
Childress	0	0	0	0	0	0
Collingsworth	25	26	29	30	30	32
Cottle	0	0	0	0	0	0
Foard	0	0	0	0	0	0
Hall	0	0	0	0	0	0
Hardeman	0	0	0	0	0	0
King	49	49	49	49	49	49
Knox	0	0	0	0	0	0
Wheeler	11	12	13	14	15	15
Total	**85**	**87**	**91**	**93**	**94**	**96**

All withdrawals rounded to the nearest 1 AFY.

Table 4.7.20 Predictive pumping estimates for the Blaine aquifer (AFY) in Texas – county–other uses.

County	2000	2010	2020	2030	2040	2050
Childress	101	90	86	84	82	84
Collingsworth	67	67	65	64	62	62
Cottle	405	384	359	339	313	288
Foard	3	3	3	3	3	3
Hall	28	25	22	19	17	15
Hardeman	45	43	45	45	45	46
King	275	272	270	268	267	266
Knox	0	0	0	0	0	0
Wheeler[a]	23	21	20	19	18	18
Total	**947**	**905**	**870**	**841**	**807**	**782**

All withdrawals rounded to the nearest 1 AFY.

[a] Values are approximately 14 AFY higher than those estimated by the TWDB.

Table 4.7.21 Summary of total Seymour pumpage (AFY).

County	SS	1980	1990	2000	2010	2020	2030	2040	2050
Archer	1	1	1	0	0	0	0	0	0
Baylor	4,385	6,947	2,514	1,806	1,695	1,536	1,440	1,392	1,353
Briscoe	2	2	2	4,063	4,063	4,063	1,821	1,821	1,821
Childress	41	10,041	5,876	64	65	70	71	72	73
Clay	424	462	580	803	745	722	714	721	723
Collingsworth	10,650	3,057	16,950	14,135	14,124	14,125	14,120	14,112	14,110
Fisher	1,076	2,151	2,203	3,325	3,195	3,228	3,139	3,074	3,028
Foard	2,573	5,103	3,663	5,025	4,875	4,730	4,590	4,455	4,321
Hall	9,734	21,690	12,755	8,317	8,302	8,288	8,276	8,269	8,266
Hardeman	4,640	3,416	2,481	401	395	392	388	385	383
Haskell	21,911	39,297	22,210	21,972	21,281	20,647	20,032	19,437	18,870
Jones	1,767	2,212	2,257	4,045	3,888	3,767	3,658	3,560	3,470
Kent	687	527	770	1,625	1,212	999	875	786	725
Knox	18,384	50,235	32,547	26,247	26,242	26,285	26,289	25,650	25,035
Motley	1,598	3,454	3,776	2,065	2,003	1,943	1,885	1,828	1,774
Stonewall	322	363	353	1,258	1,189	1,109	1,035	967	935
Taylor	17	17	12	0	0	0	0	0	0
Throckmorton	3	3	3	0	0	0	0	0	0
Wichita	1,755	1,756	1,716	1,873	2,058	2,070	2,085	2,099	2,096
Wilbarger	6,192	26,589	19,543	23,349	22,806	22,281	21,823	21,374	20,989
Young	1	1	1	0	0	0	0	0	0
Total	**86,164**	**177,324**	**130,213**	**120,373**	**118,138**	**116,255**	**112,241**	**110,002**	**107,972**

All withdrawals rounded to the nearest 1 AFY.

Table 4.7.22 Summary of total Blaine pumpage (AFY) in Texas.

County	SS	1980	1990	2000	2010	2020	2030	2040	2050
Childress	7,858	108	92	3,755	3,743	3,740	3,737	3,735	3,734
Collingsworth	9,332	2,906	4,126	4,532	4,524	4,511	4,505	4,499	4,494
Cottle	5,550	86	60	4,782	4,630	4,477	4,334	4,188	4,047
Foard	120	10	18	25	24	24	23	22	22
Hall	21	21	12	28	25	22	19	17	15
Hardeman	6,014	6,582	4,896	4,841	4,696	4,559	4,423	4,292	4,165
King	528	528	79	344	341	339	337	336	335
Knox	2	2	0	1,333	1,333	1,333	1,333	1,300	1,268
Wheeler	1,478	1,478	749	50[a]	48[a]	48[a]	48[a]	47[a]	49[a]
Total	**30,903**	**11,721**	**10,032**	**19,690**	**19,364**	**19,053**	**18,759**	**18,436**	**18,129**

All withdrawals rounded to the nearest 1 AFY.

[a] Values are approximately 14 AFY higher than those estimated by the TWDB.

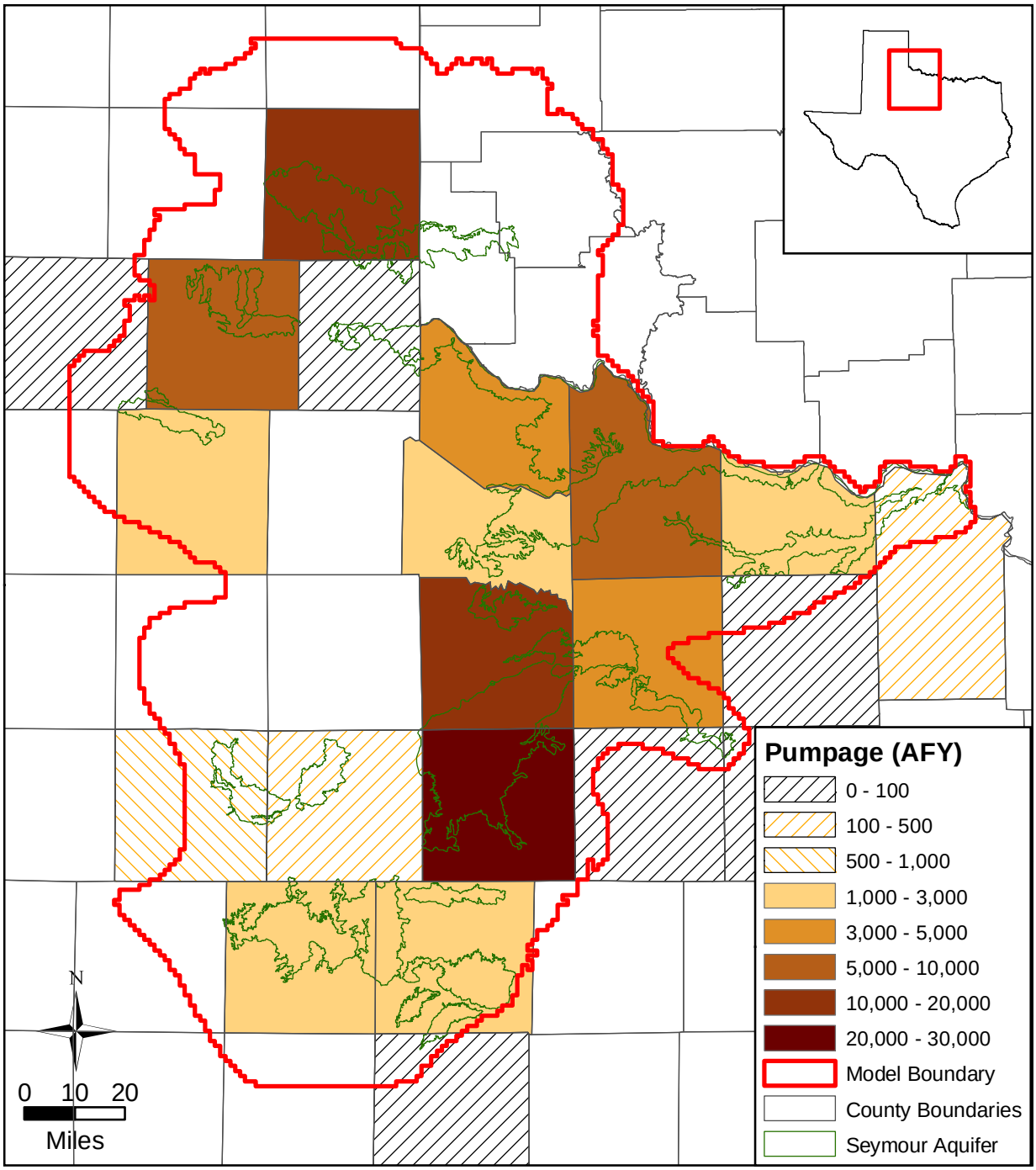

Figure 4.7.1 Steady-state pumping for the Seymour aquifer.

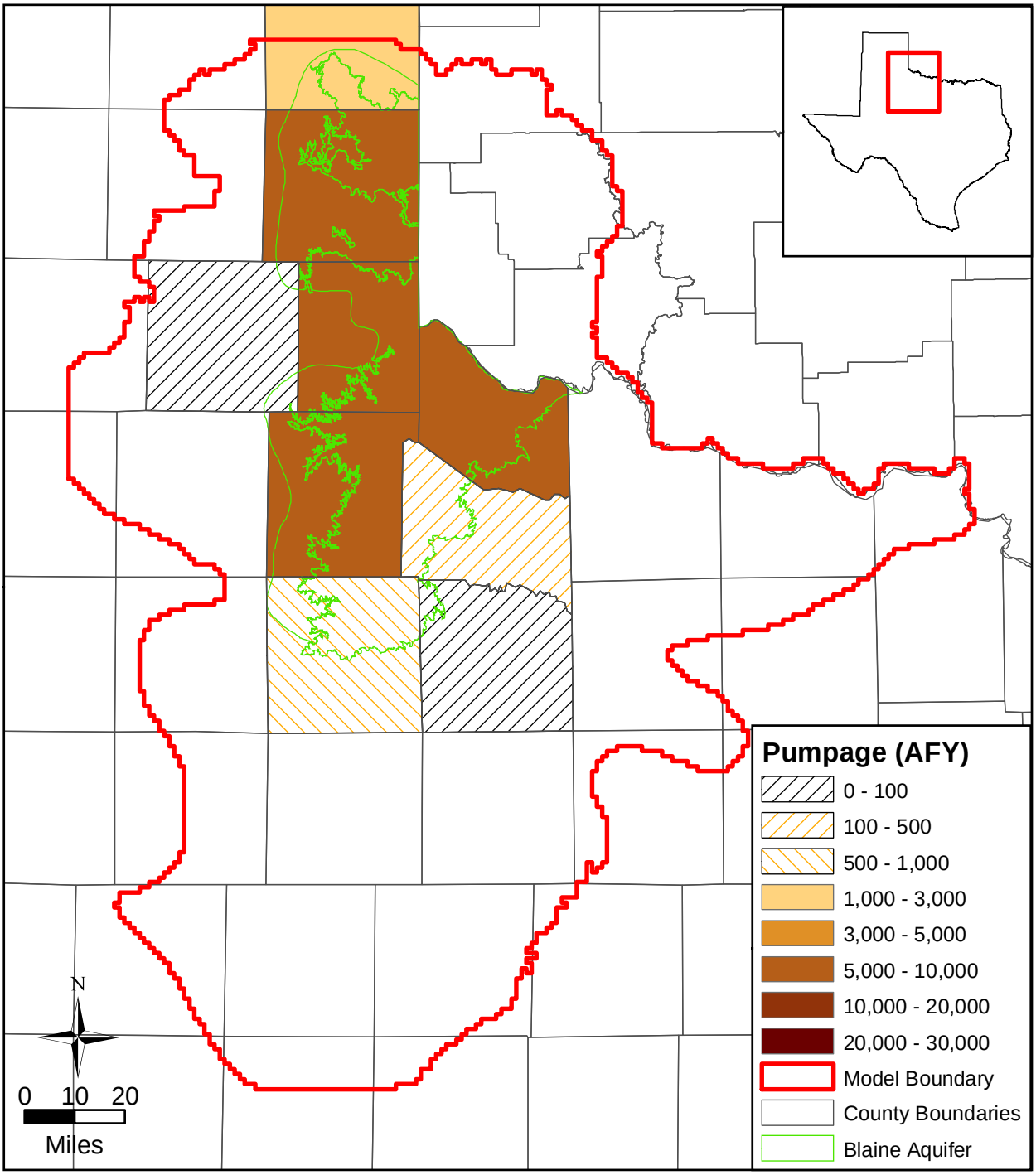

Figure 4.7.2 Steady-state pumping for the Blaine aquifer.

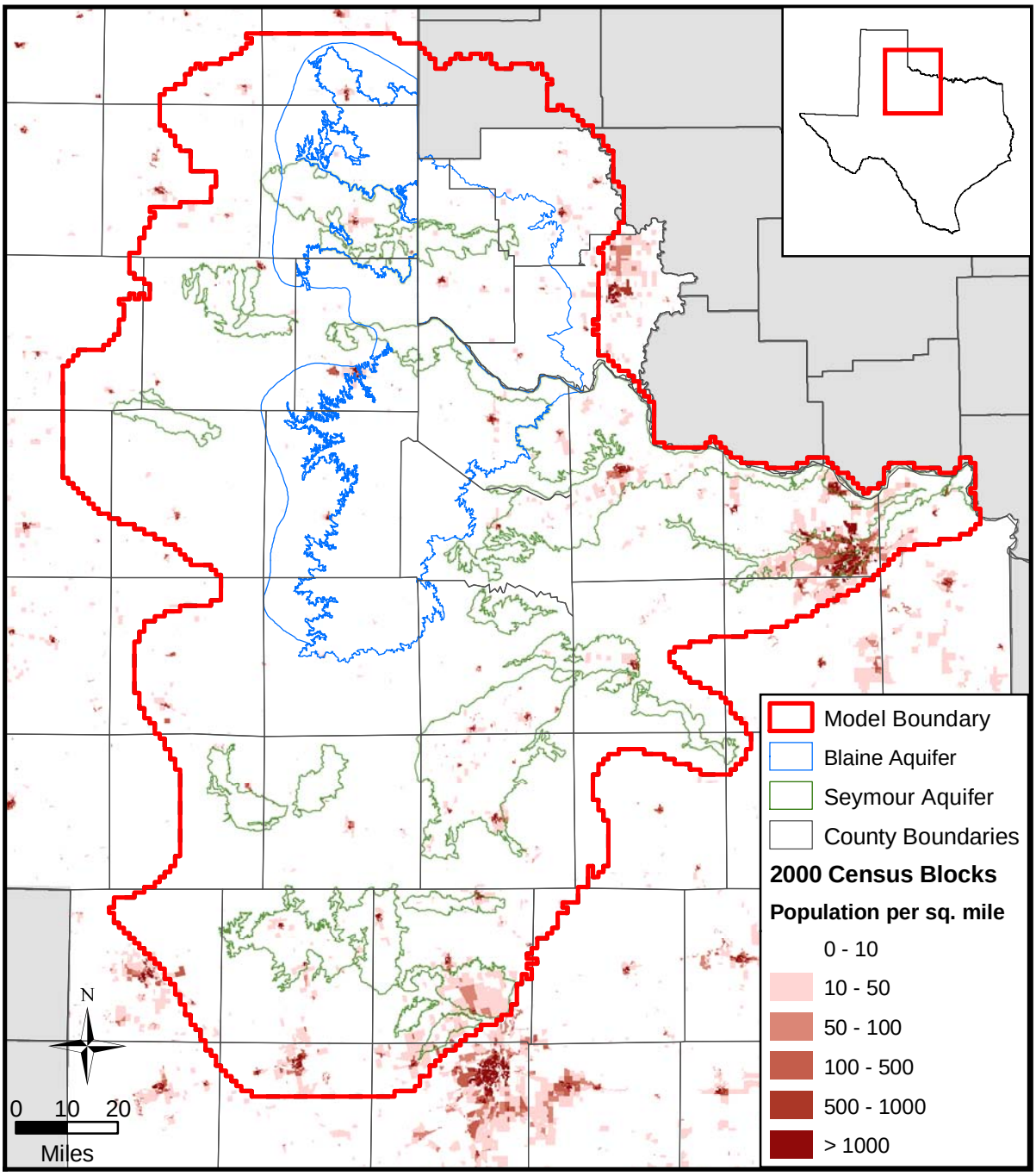

Figure 4.7.3 Population density for the study area.

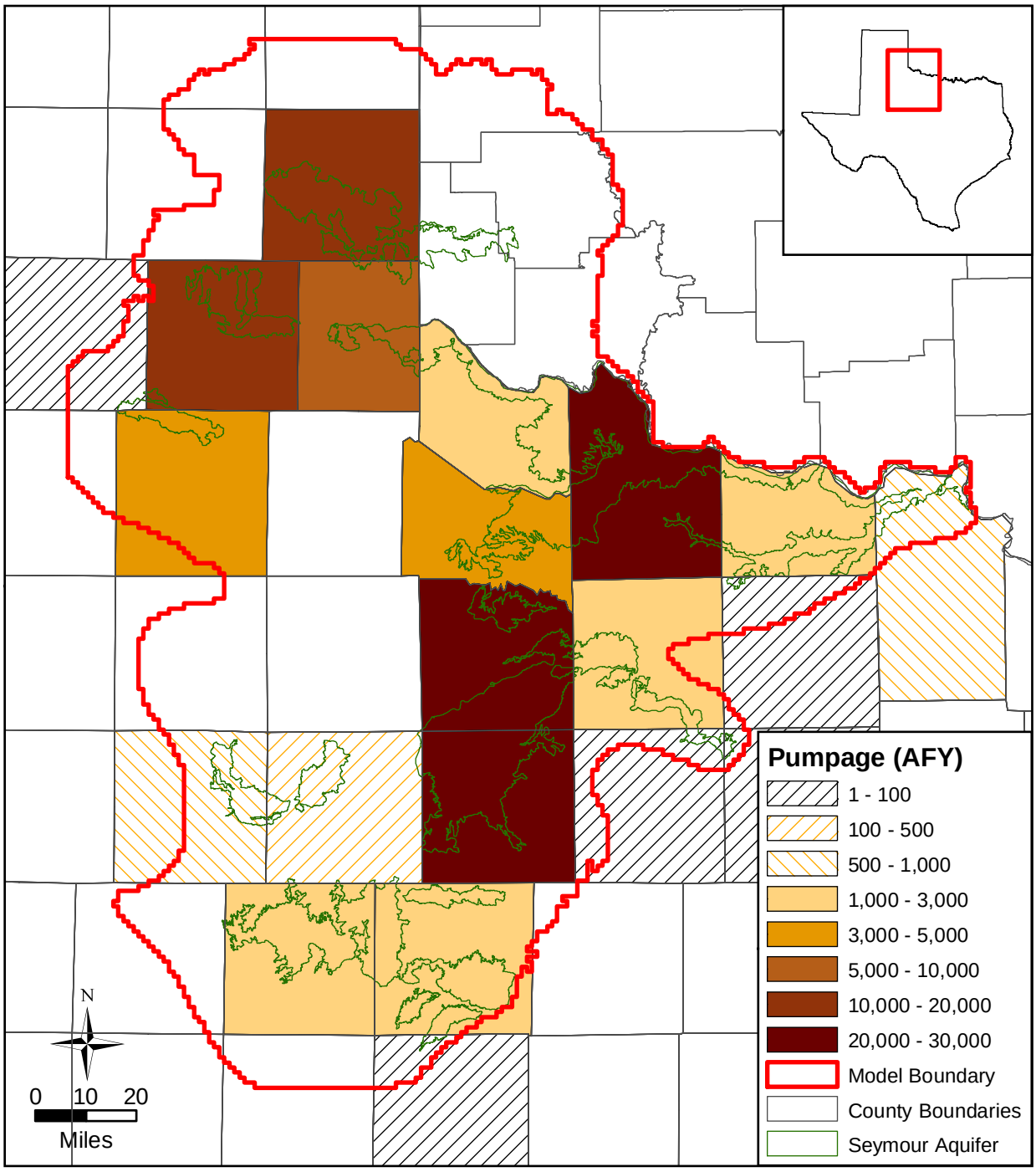

Figure 4.7.4 Yearly average pumping rate for the Seymour aquifer for 1980-1999.

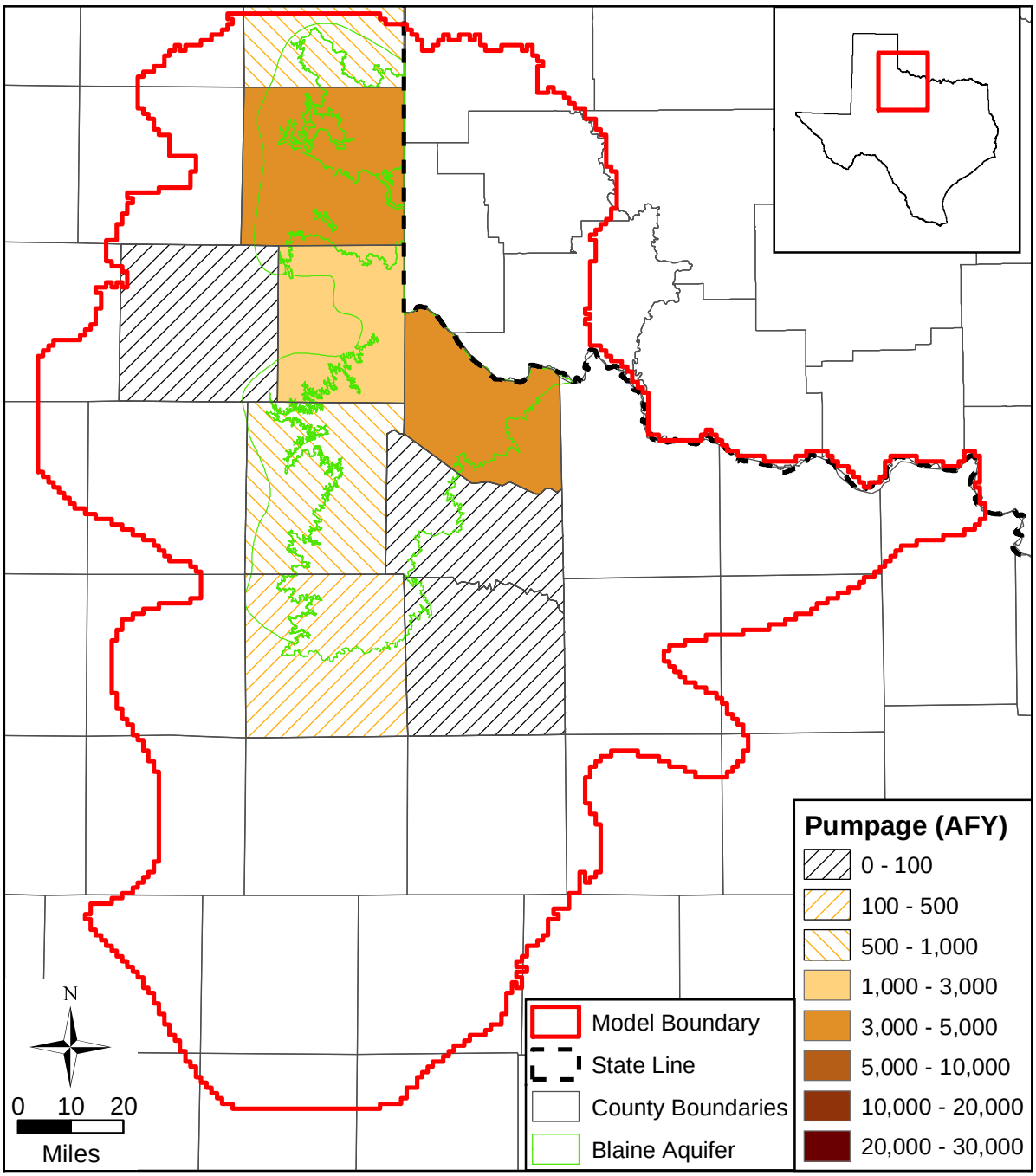

Figure 4.7.5 Yearly average pumping rate for the Blaine aquifer for 1980-1999.

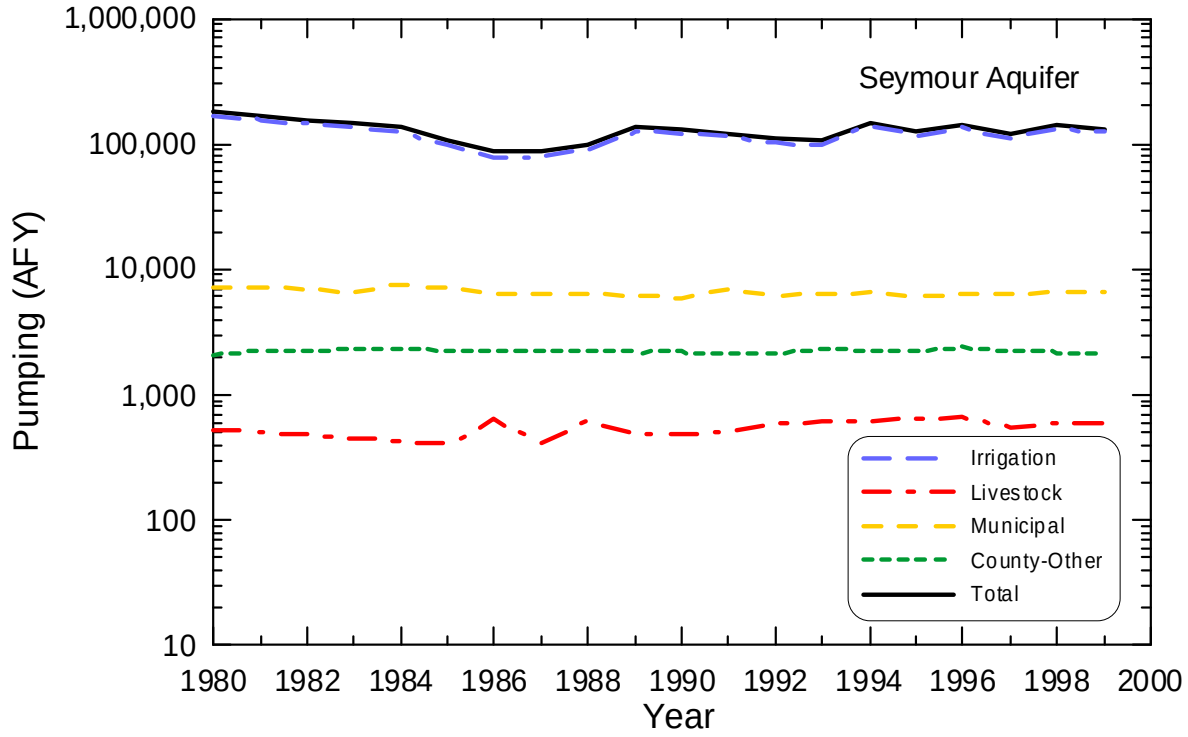

Figure 4.7.6 Groundwater withdrawals for the Seymour aquifer for 1980-1999.

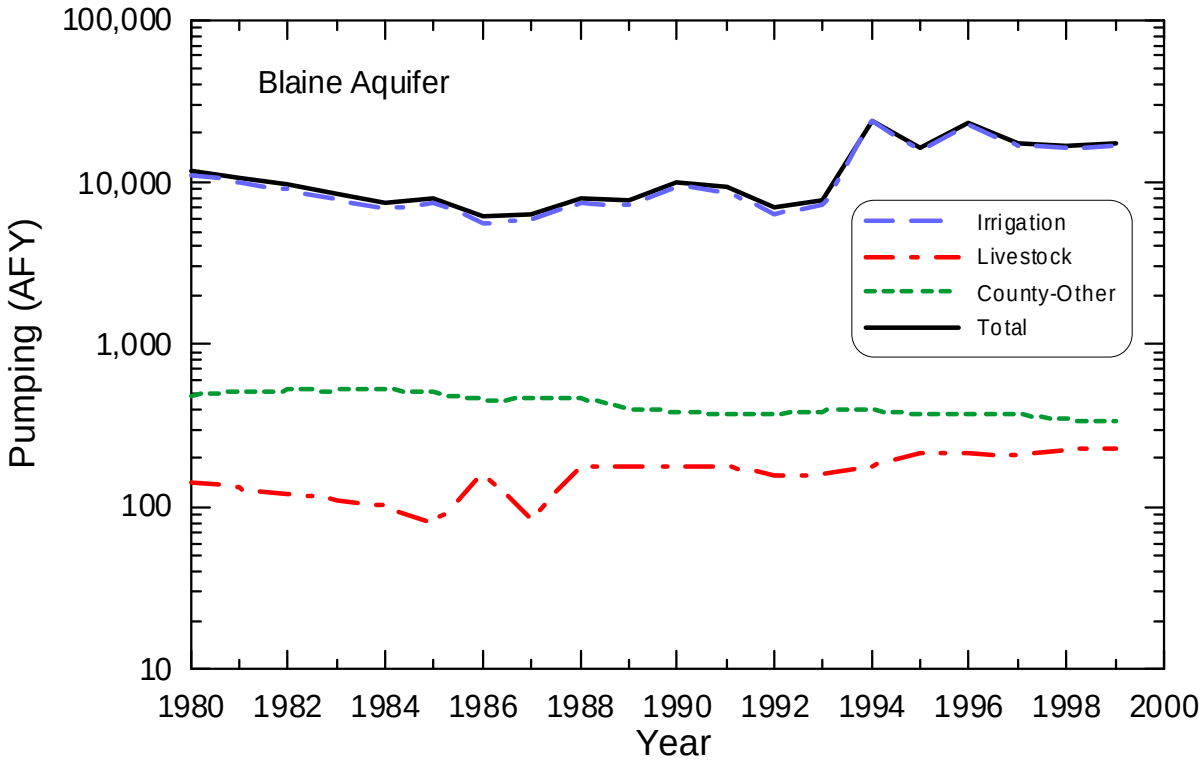

Figure 4.7.7 Groundwater withdrawals for the Blaine aquifer in Texas for 1980-1999.

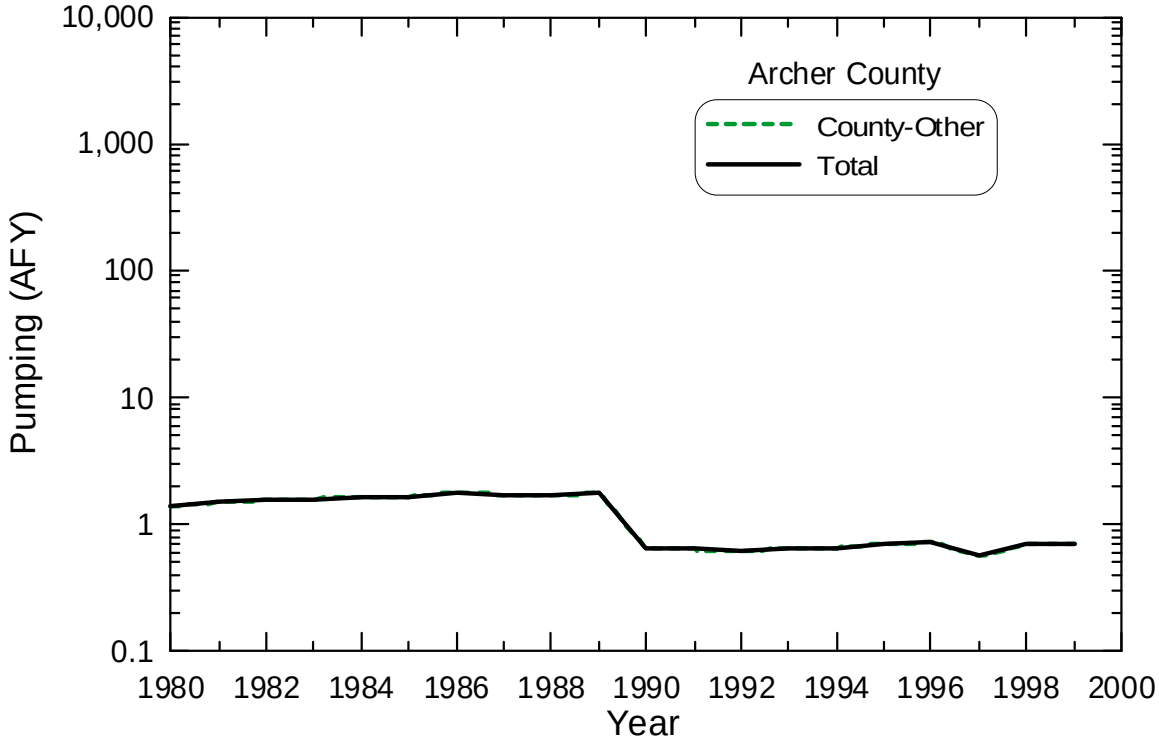

Figure 4.7.8 Groundwater withdrawals for Archer County from the Seymour aquifer for 1980-1999.

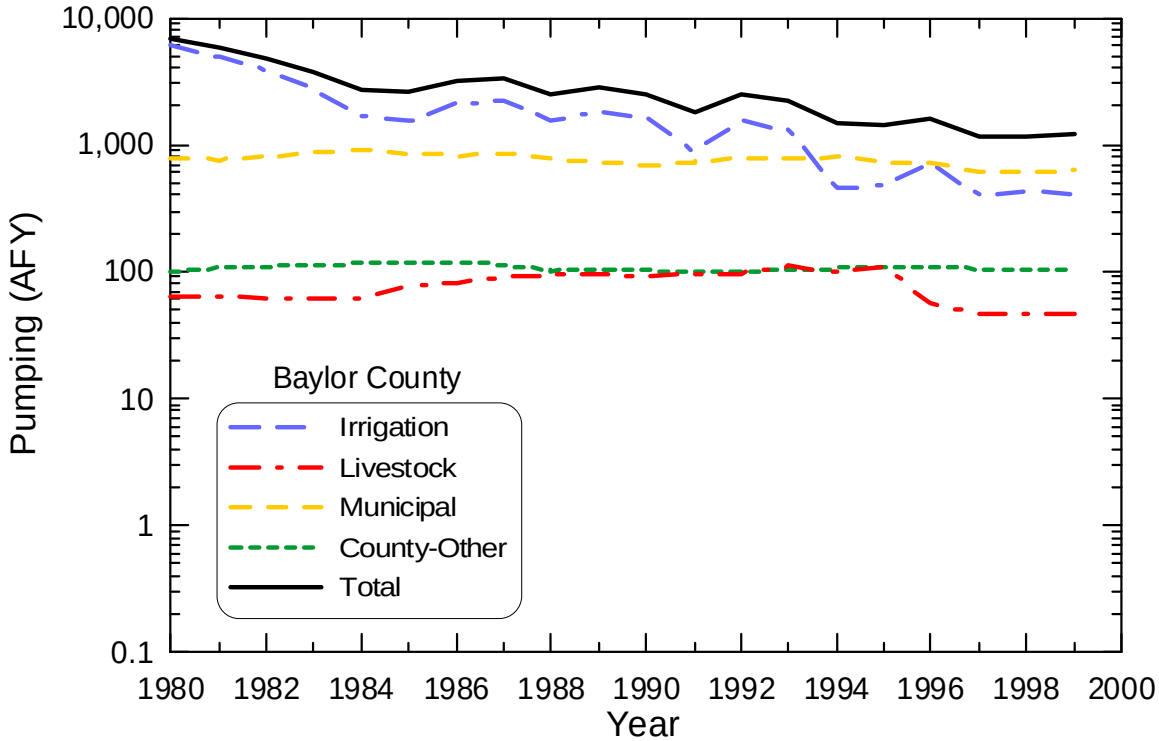

Figure 4.7.9 Groundwater withdrawals for Baylor County from the Seymour aquifer for 1980-1999.

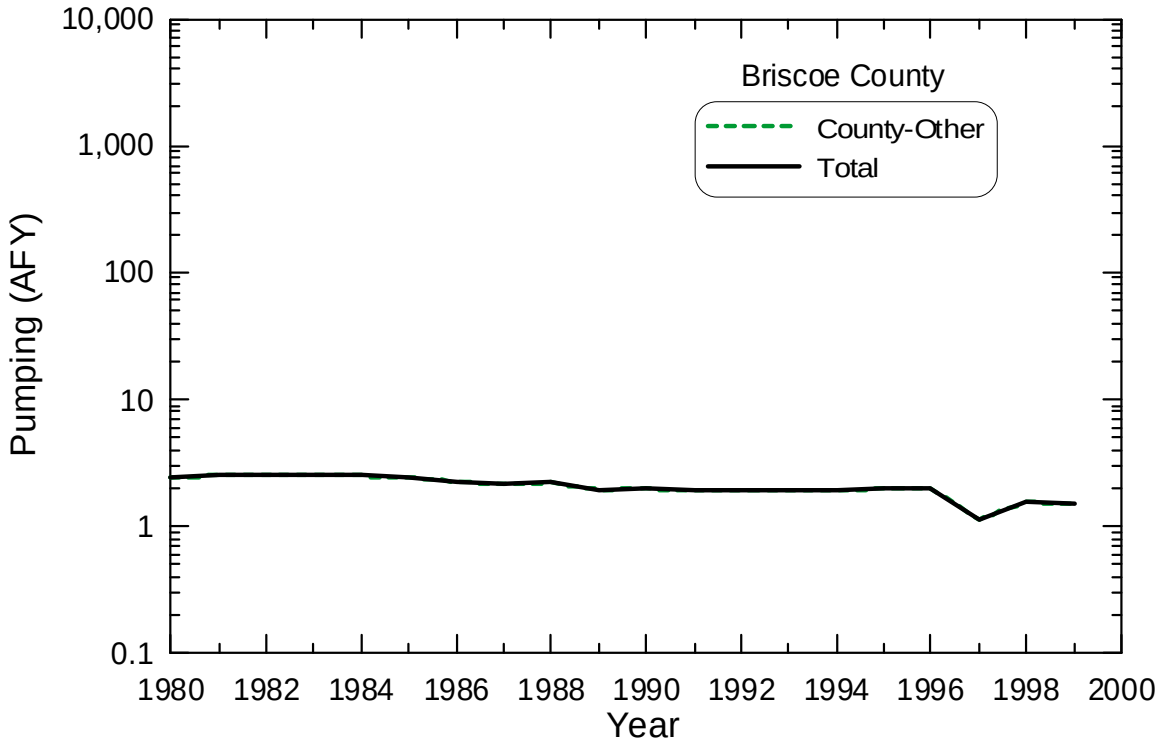

Figure 4.7.10 Groundwater withdrawals for Briscoe County from the Seymour aquifer for 1980-1999.

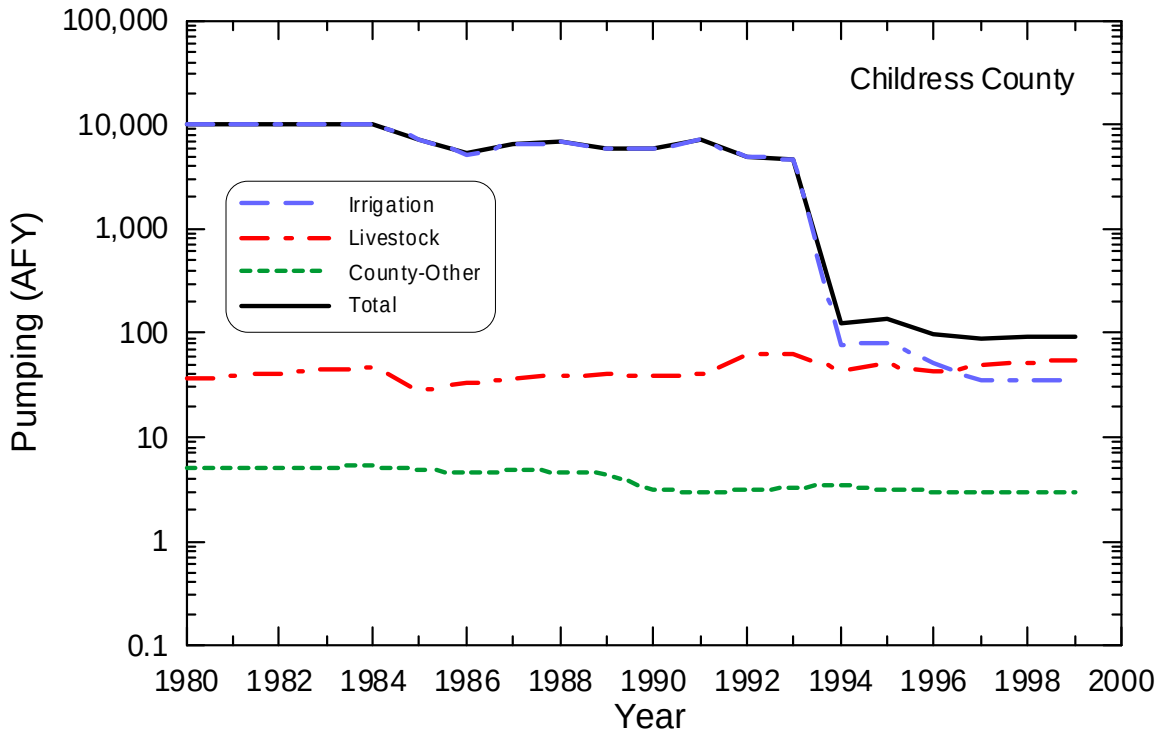

Figure 4.7.11 Groundwater withdrawals for Childress County from the Seymour aquifer for 1980-1999.

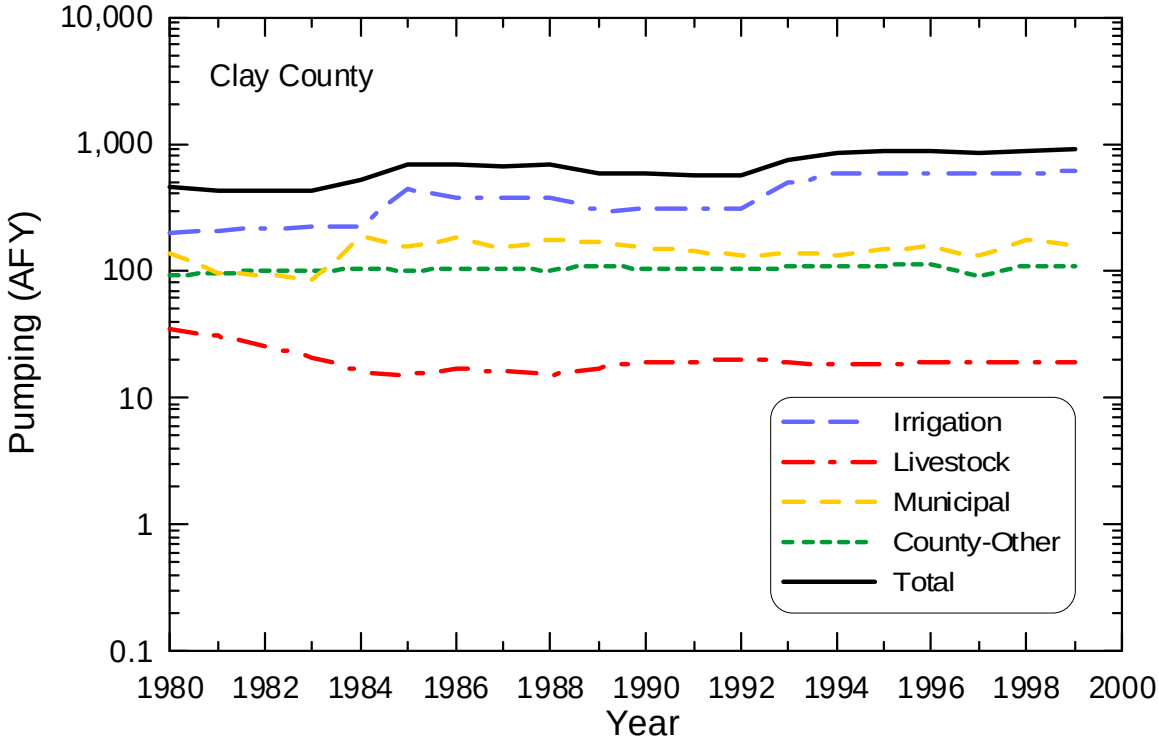

Figure 4.7.12 Groundwater withdrawals for Clay County from the Seymour aquifer for 1980-1999.

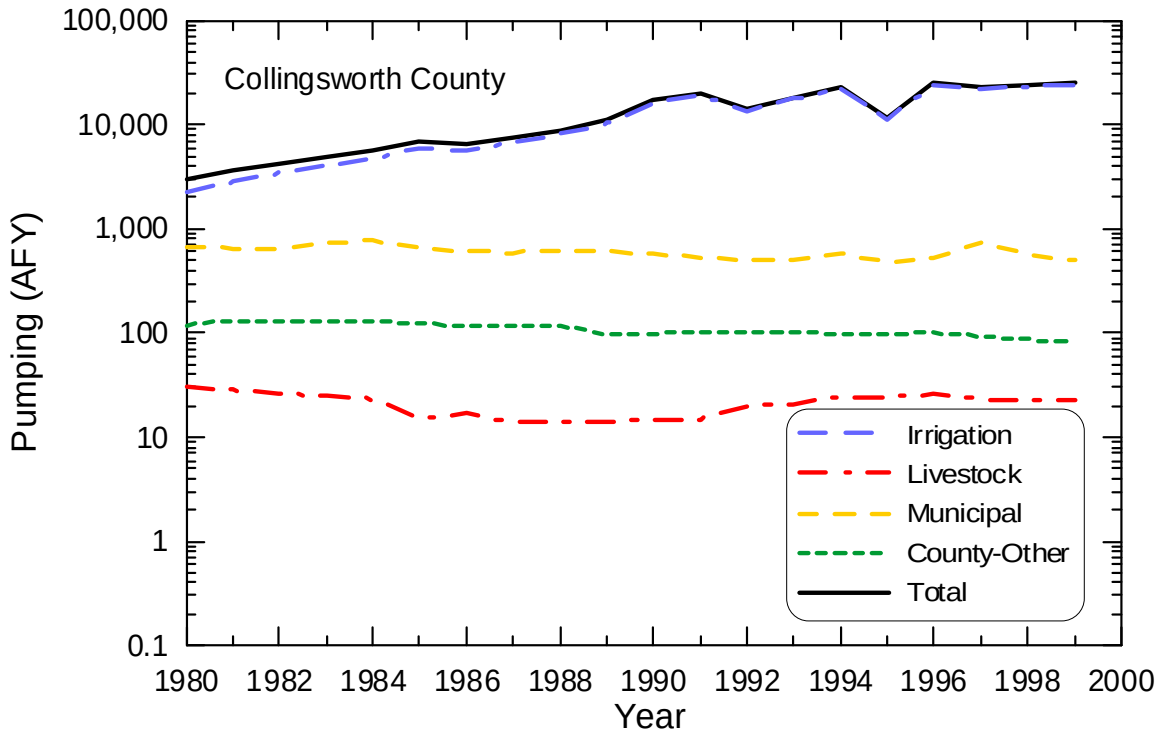

Figure 4.7.13 Groundwater withdrawals for Collingsworth County from the Seymour aquifer for 1980-1999.

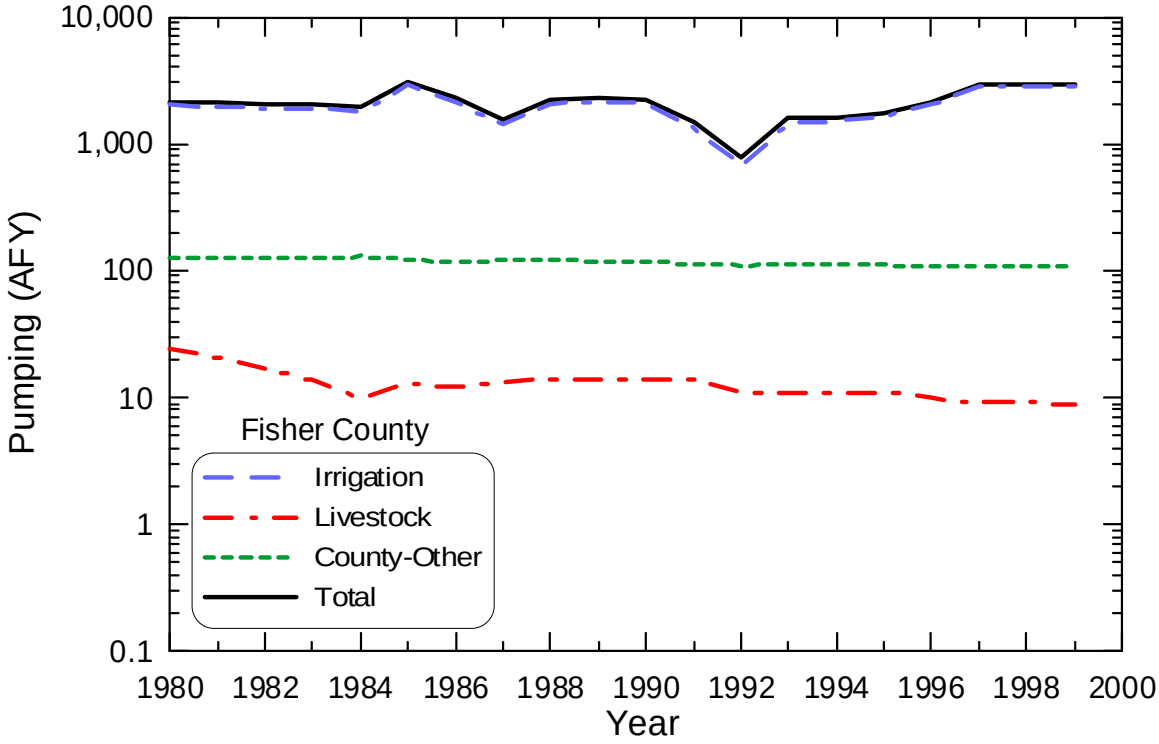

Figure 4.7.14 Groundwater withdrawals for Fisher County from the Seymour aquifer for 1980-1999.

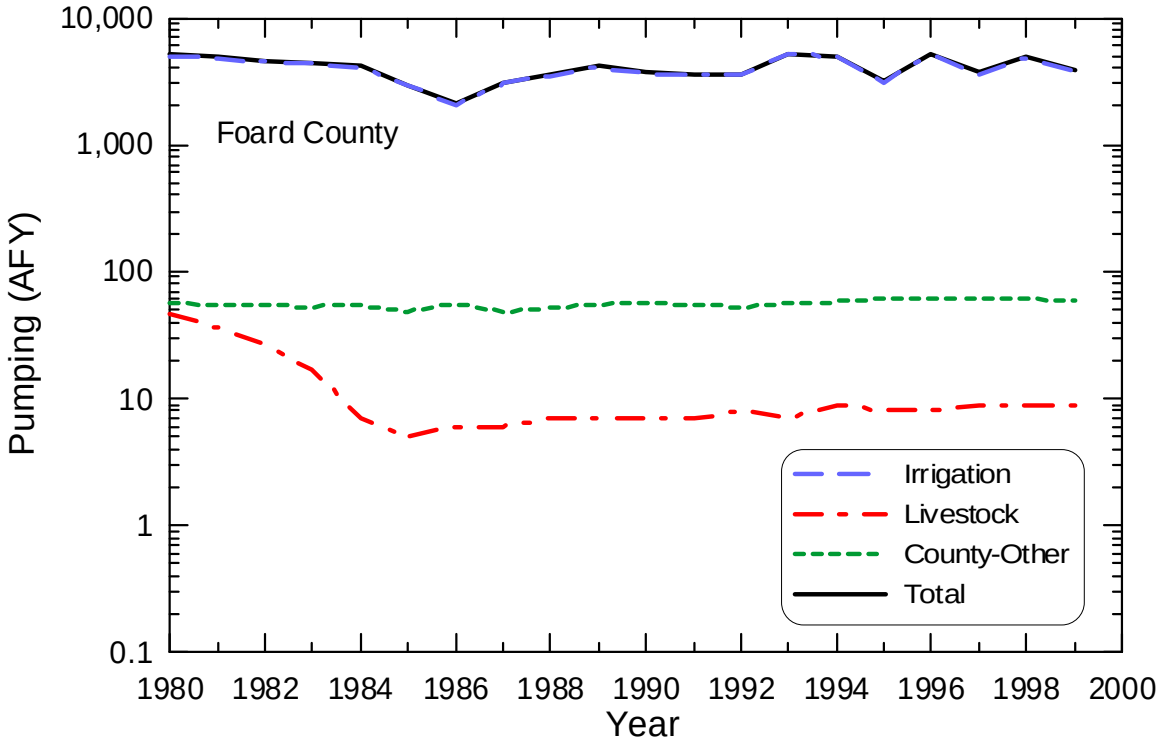

Figure 4.7.15 Groundwater withdrawals for Foard County from the Seymour aquifer for 1980-1999.

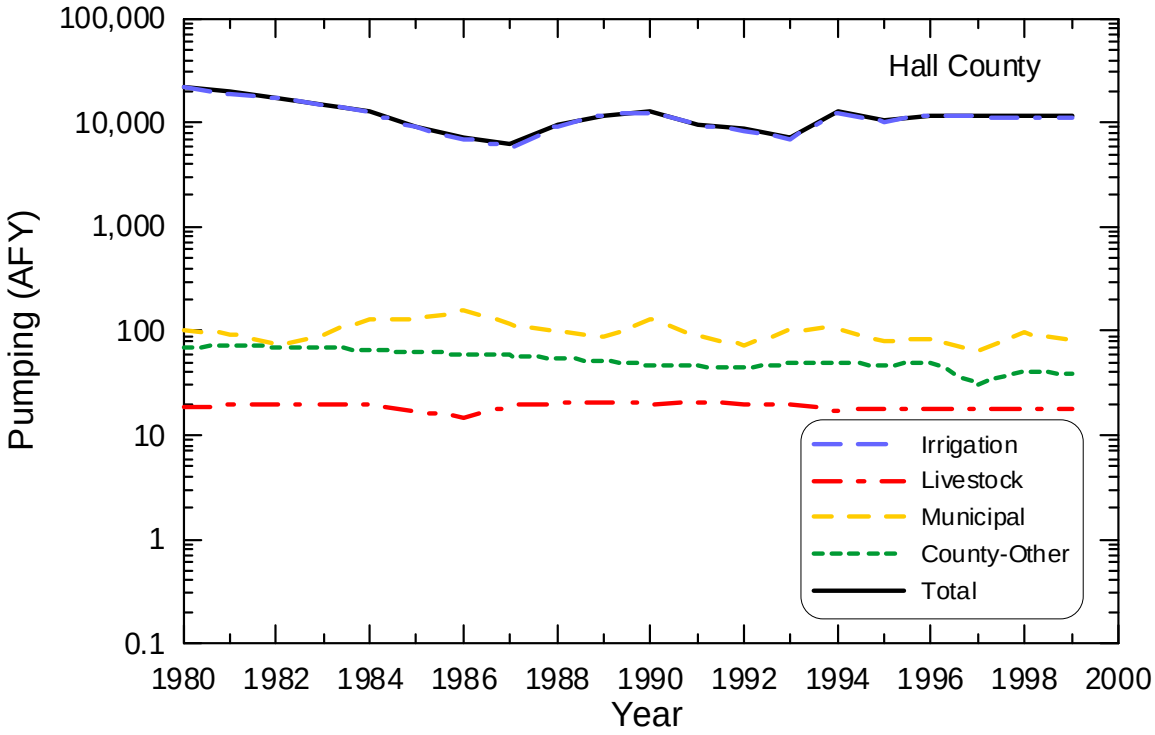

Figure 4.7.16 Groundwater withdrawals for Hall County from the Seymour aquifer for 1980-1999.

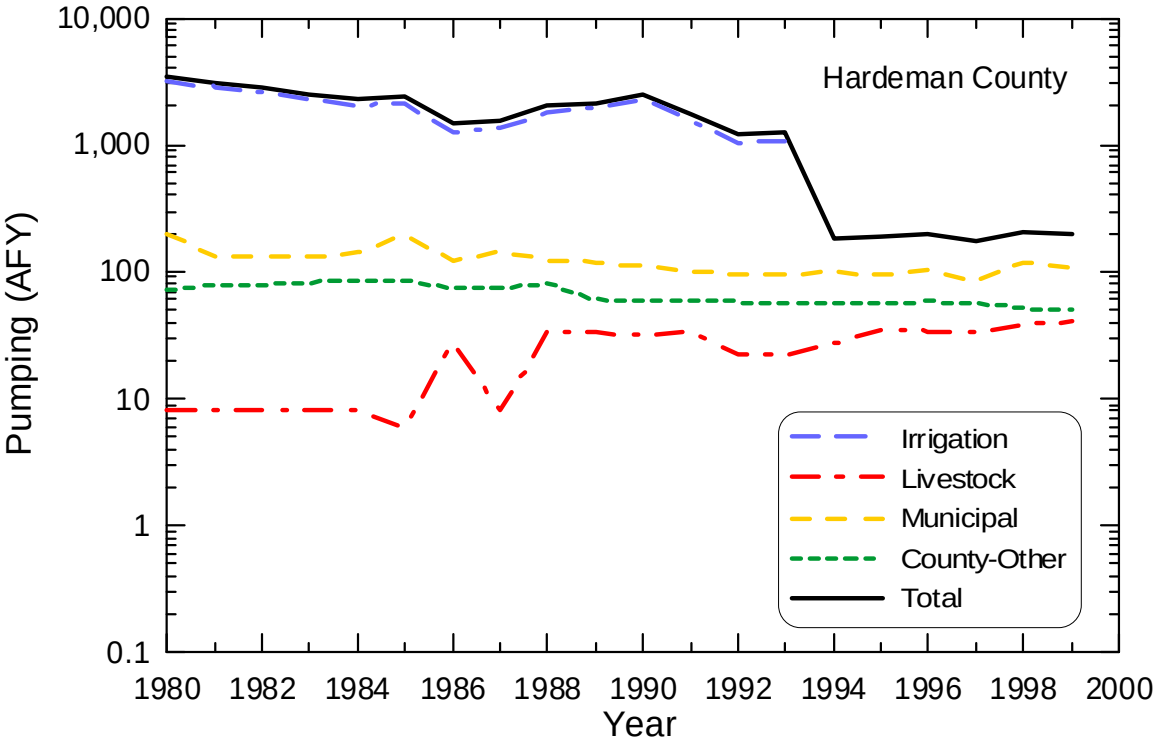

Figure 4.7.17 Groundwater withdrawals for Hardeman County from the Seymour aquifer for 1980-1999.

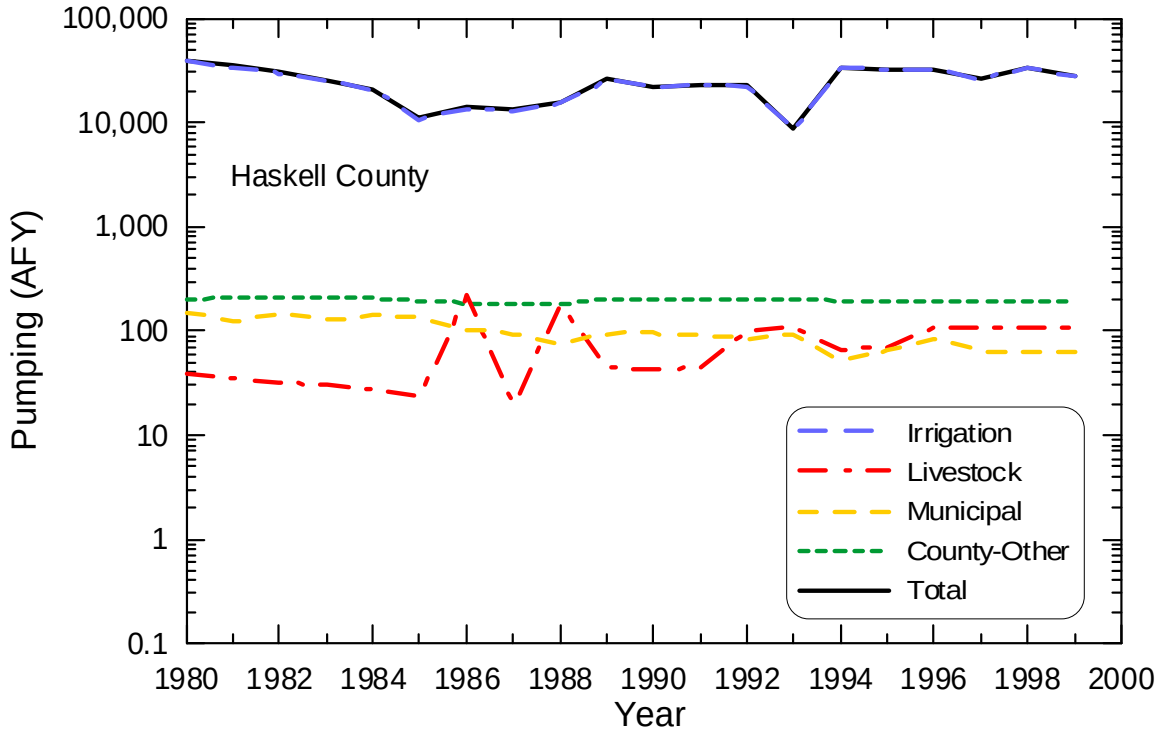

Figure 4.7.18 Groundwater withdrawals for Haskell County from the Seymour aquifer for 1980-1999.

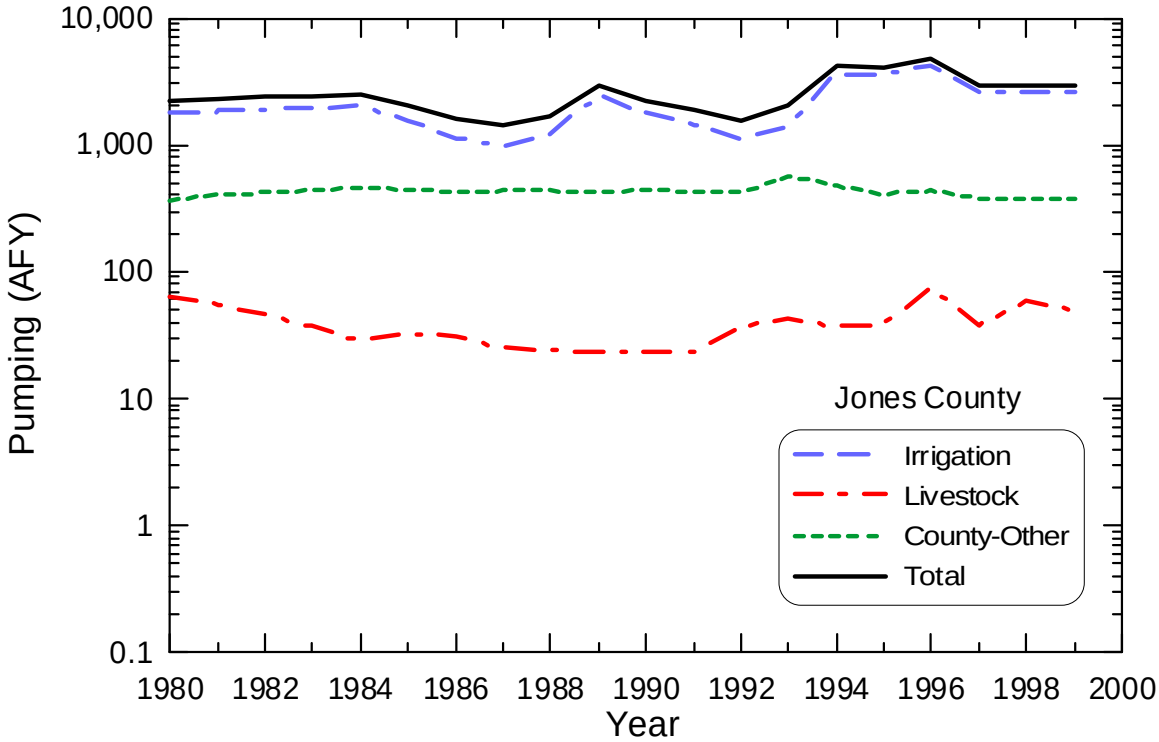

Figure 4.7.19 Groundwater withdrawals for Jones County from the Seymour aquifer for 1980-1999.

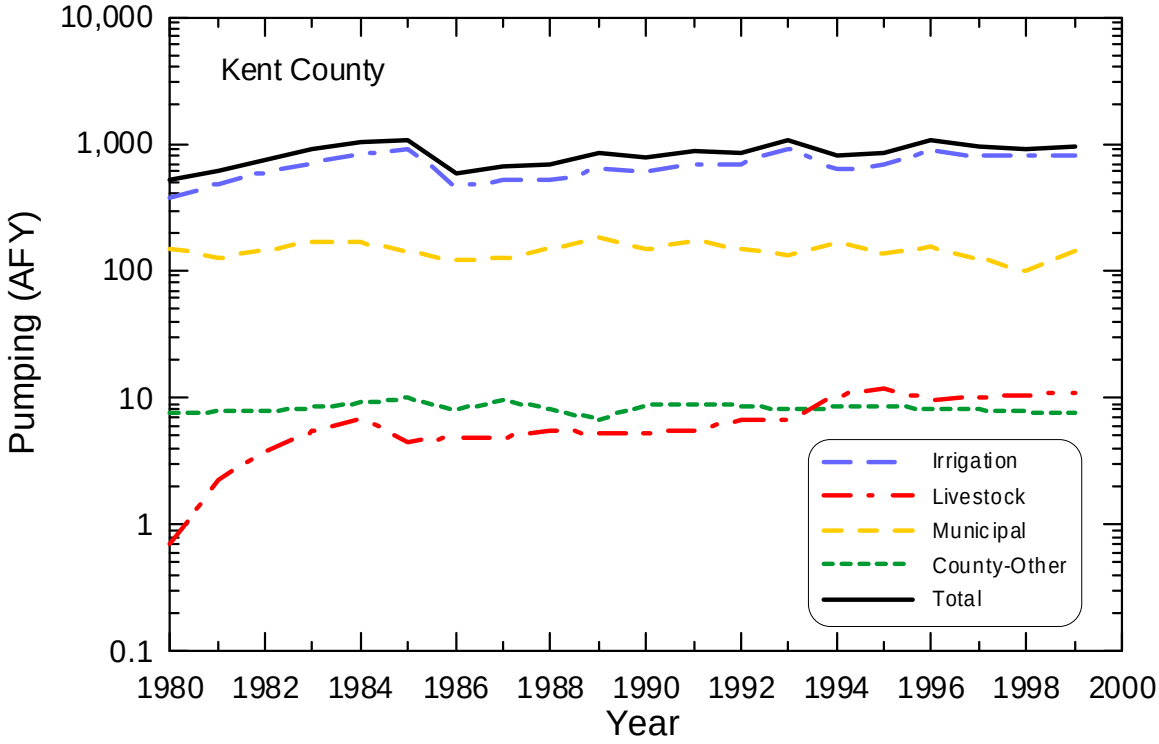

Figure 4.7.20 Groundwater withdrawals for Kent County from the Seymour aquifer for 1980-1999.

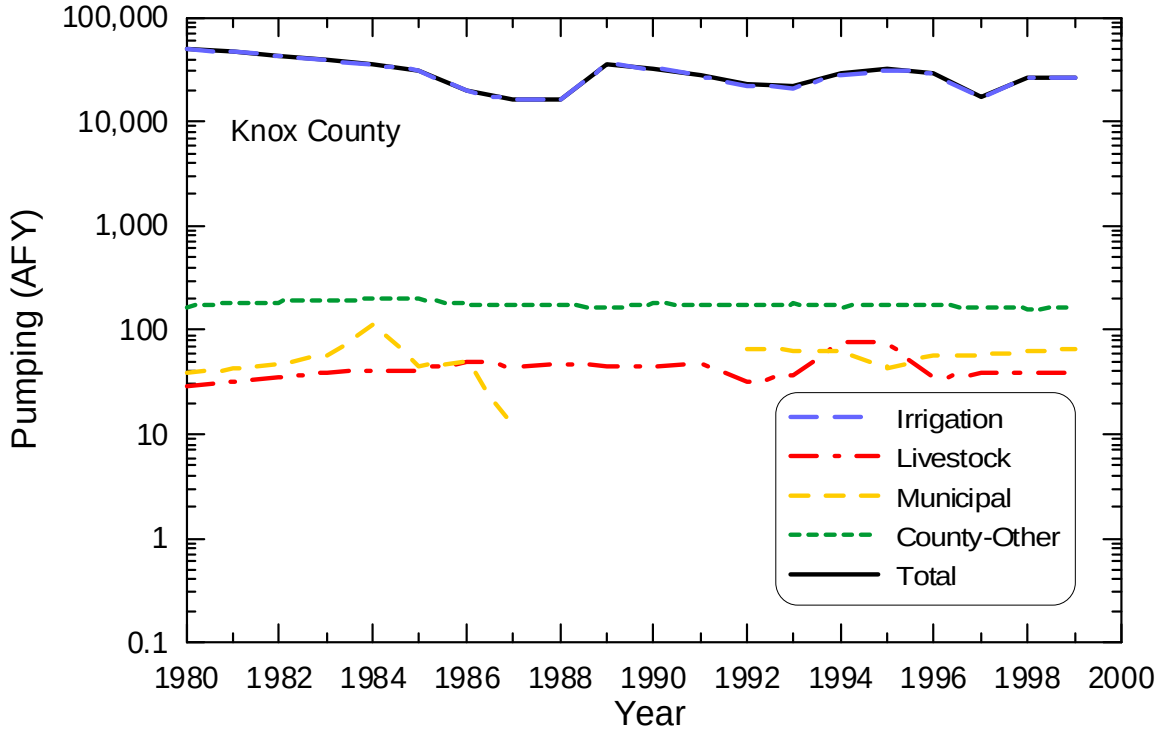

Figure 4.7.21 Groundwater withdrawals for Knox County from the Seymour aquifer for 1980-1999.

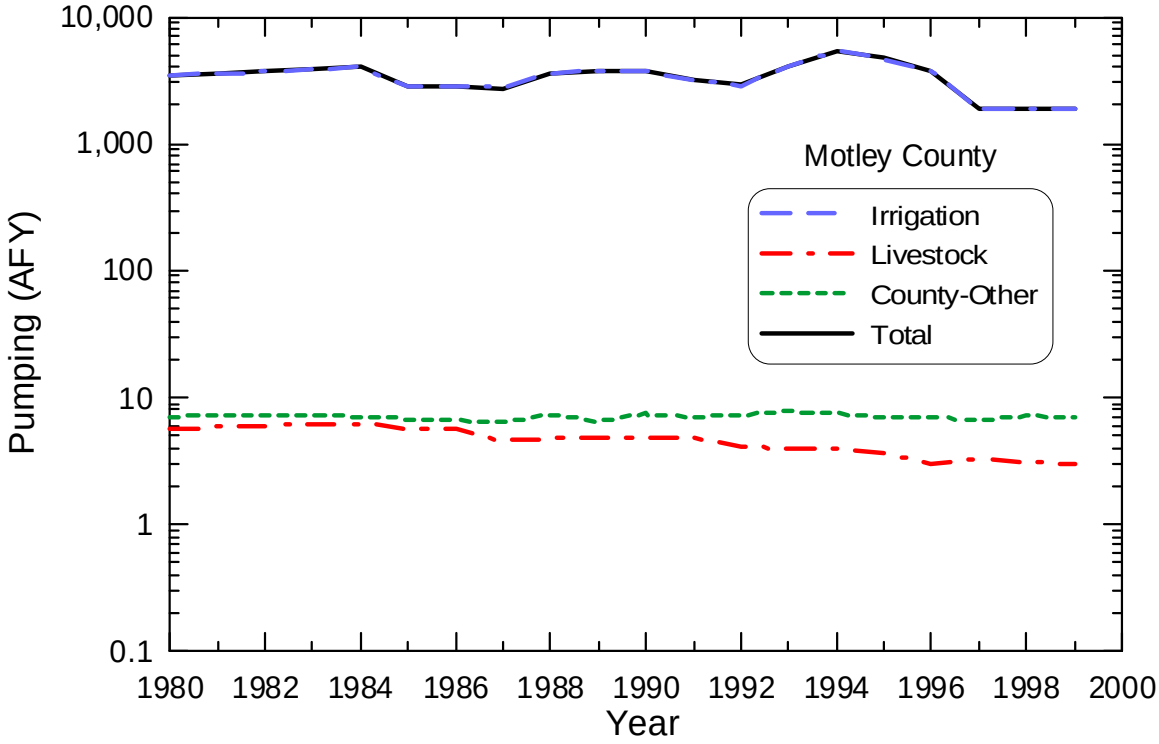

Figure 4.7.22 Groundwater withdrawals for Motley County from the Seymour aquifer for 1980-1999.

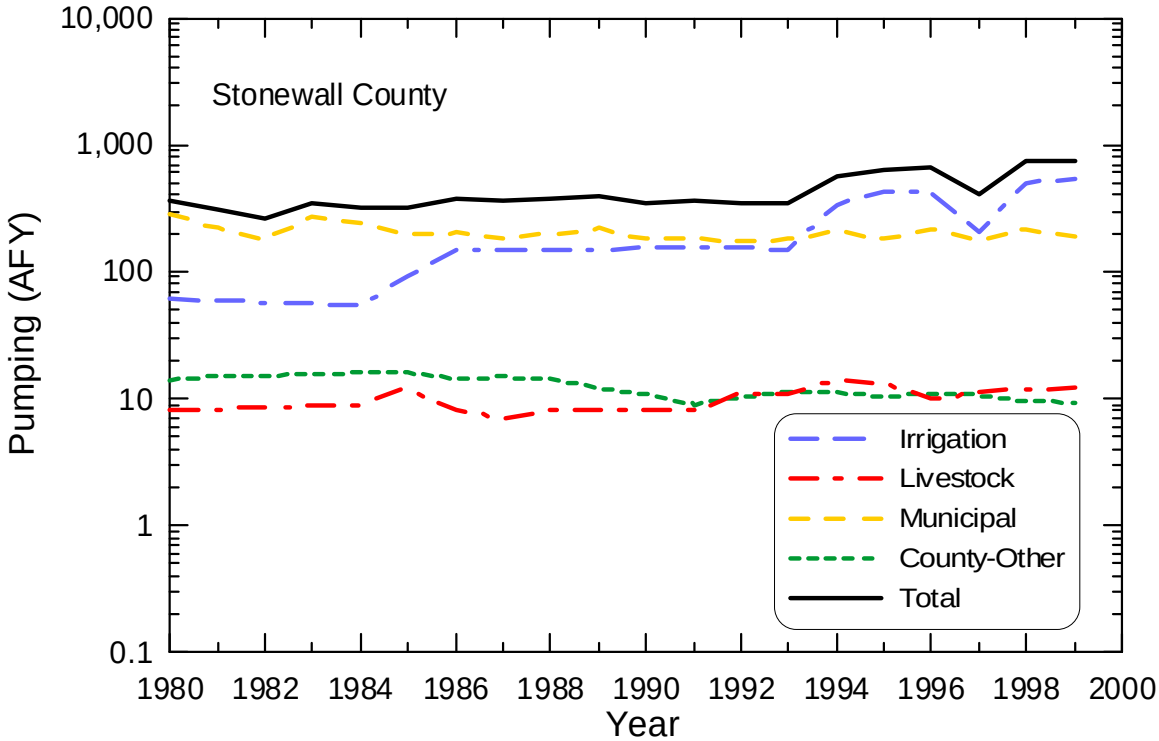

Figure 4.7.23 Groundwater withdrawals for Stonewall County from the Seymour aquifer for 1980-1999.

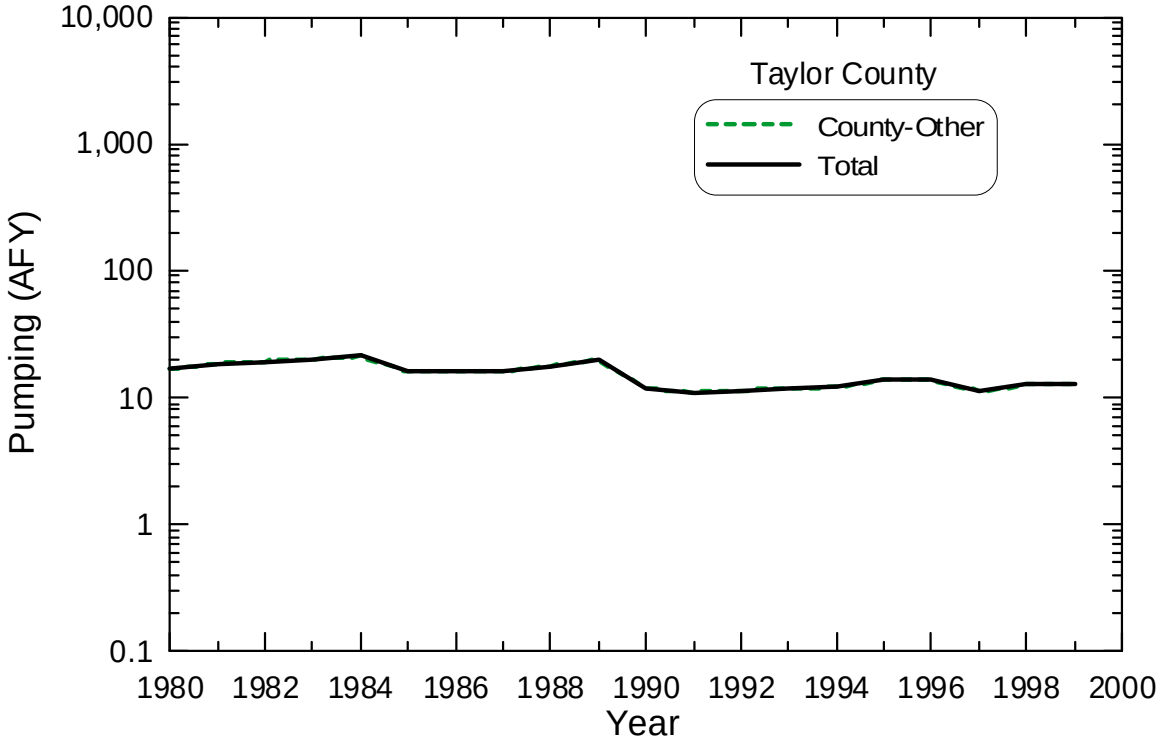

Figure 4.7.24 Groundwater withdrawals for Taylor County from the Seymour aquifer for 1980-1999.

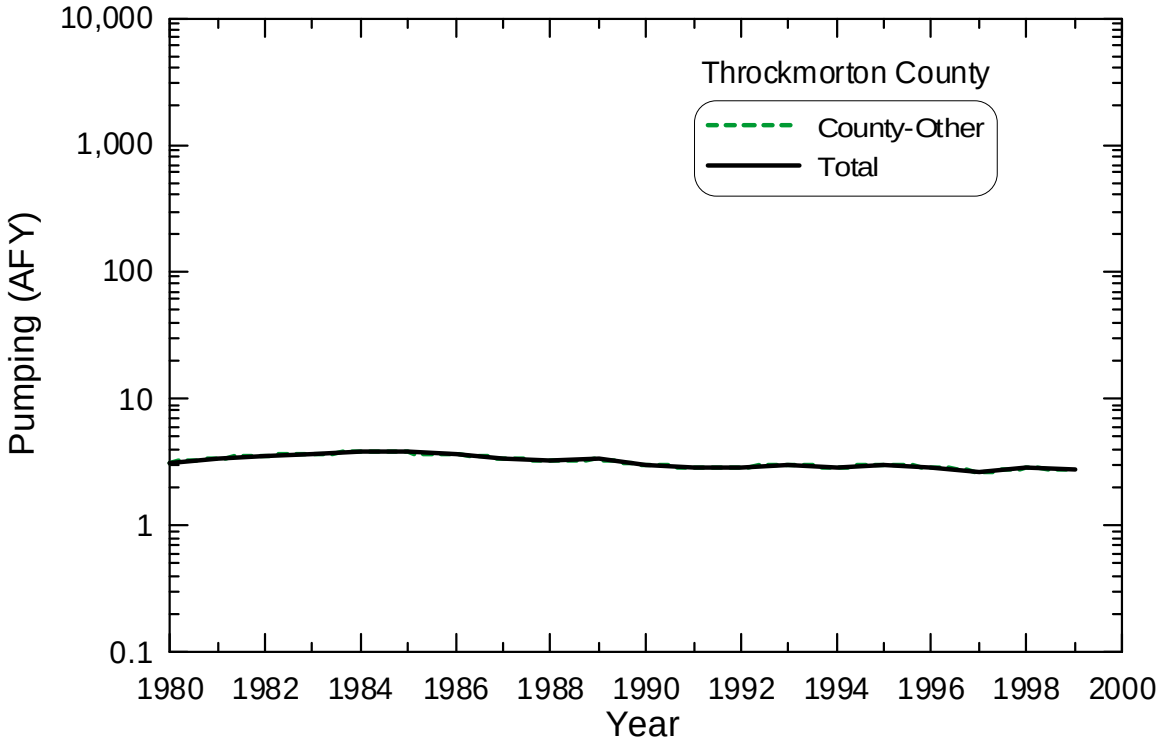

Figure 4.7.25 Groundwater withdrawals for Throckmorton County from the Seymour aquifer for 1980-1999.

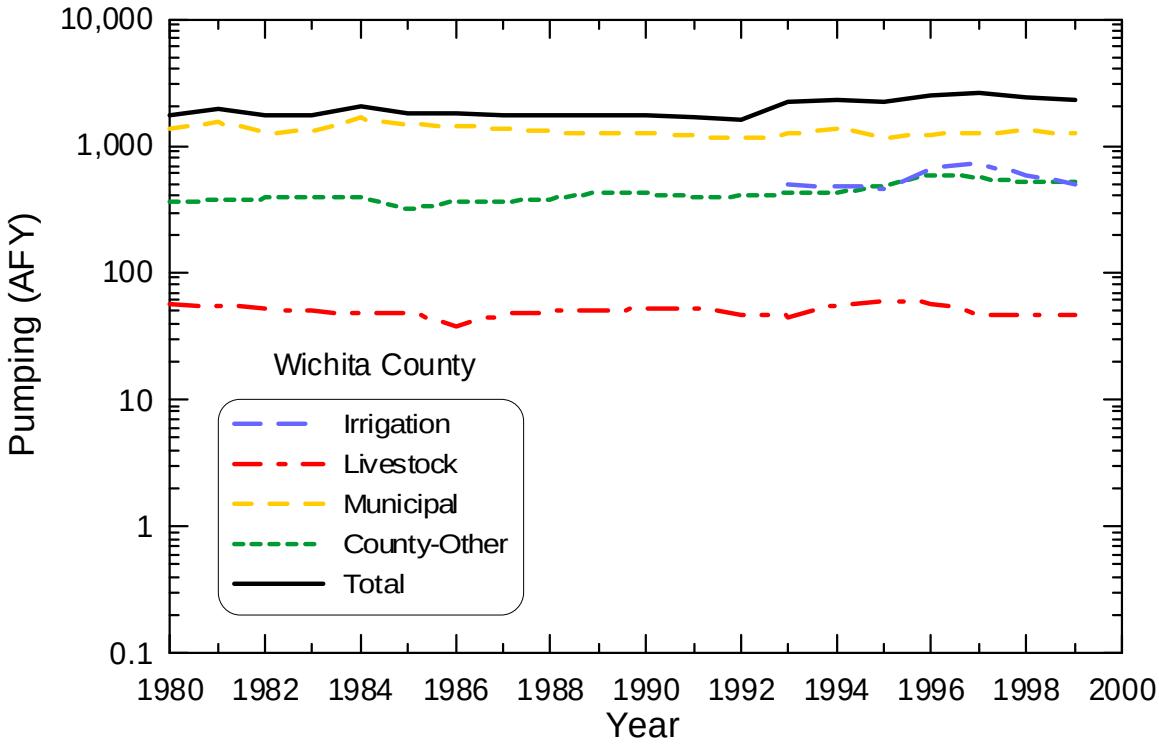

Figure 4.7.26 Groundwater withdrawals for Wichita County from the Seymour aquifer for 1980-1999.

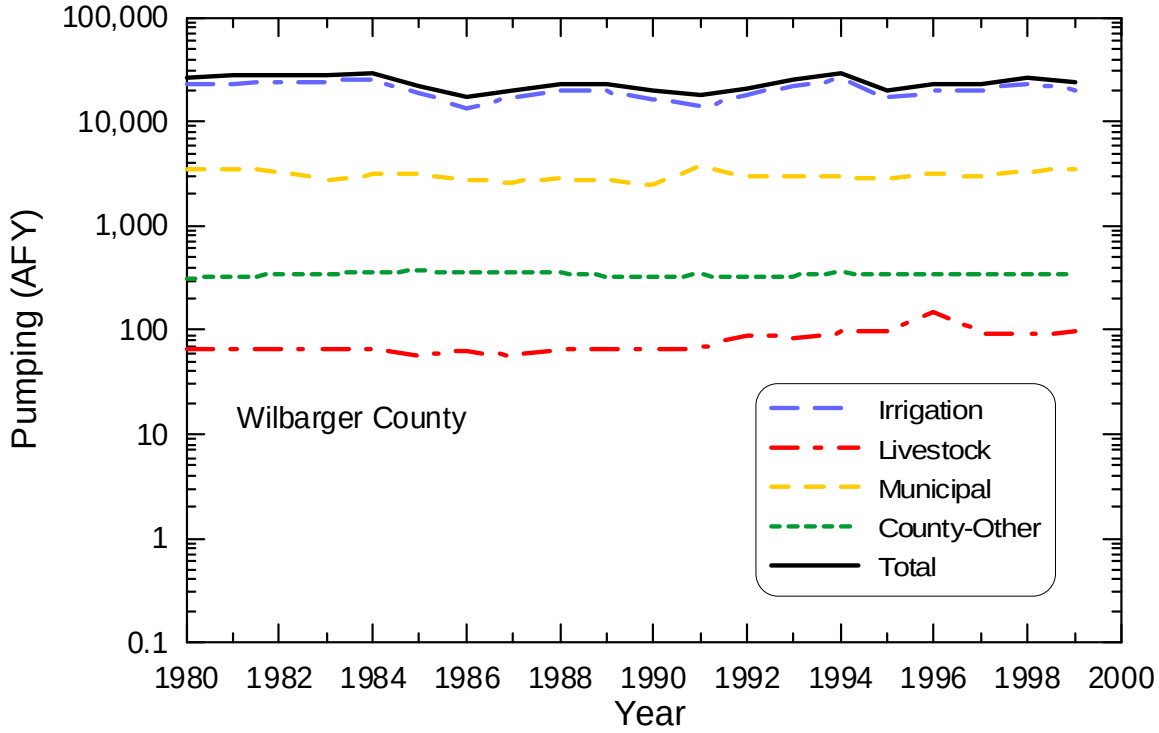

Figure 4.7.27 Groundwater withdrawals for Wilbarger County from the Seymour aquifer for 1980-1999.

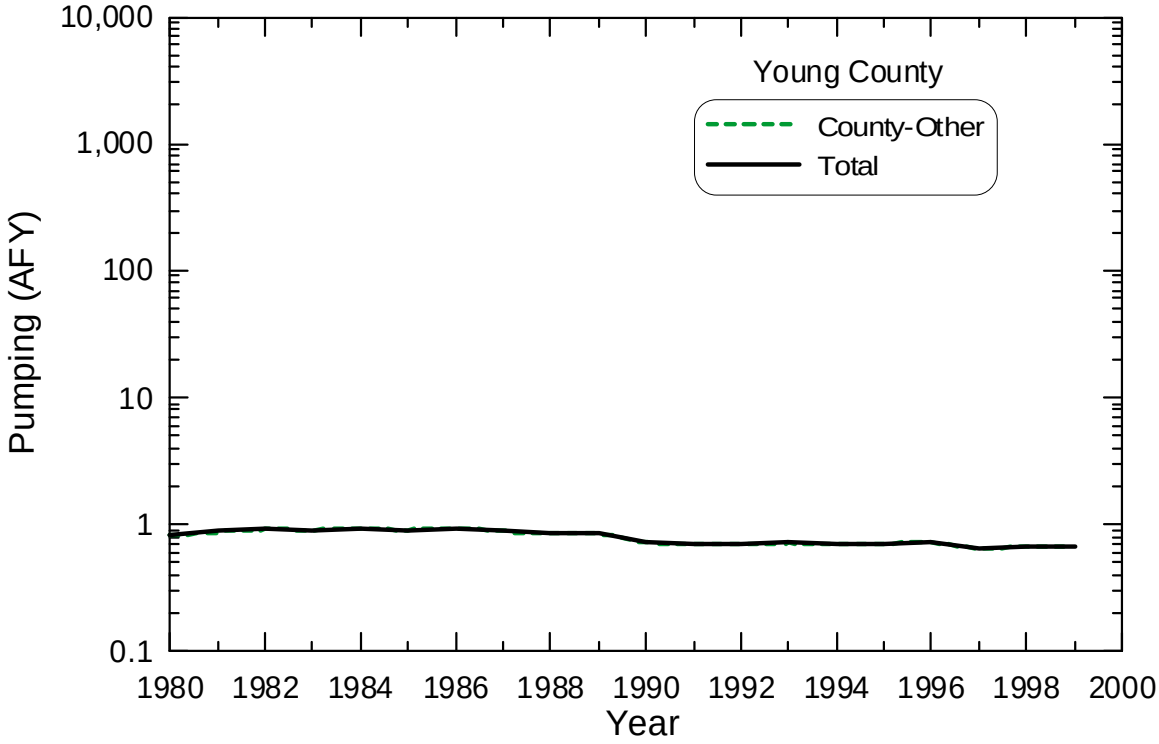

Figure 4.7.28 Groundwater withdrawals for Young County from the Seymour aquifer for 1980-1999.

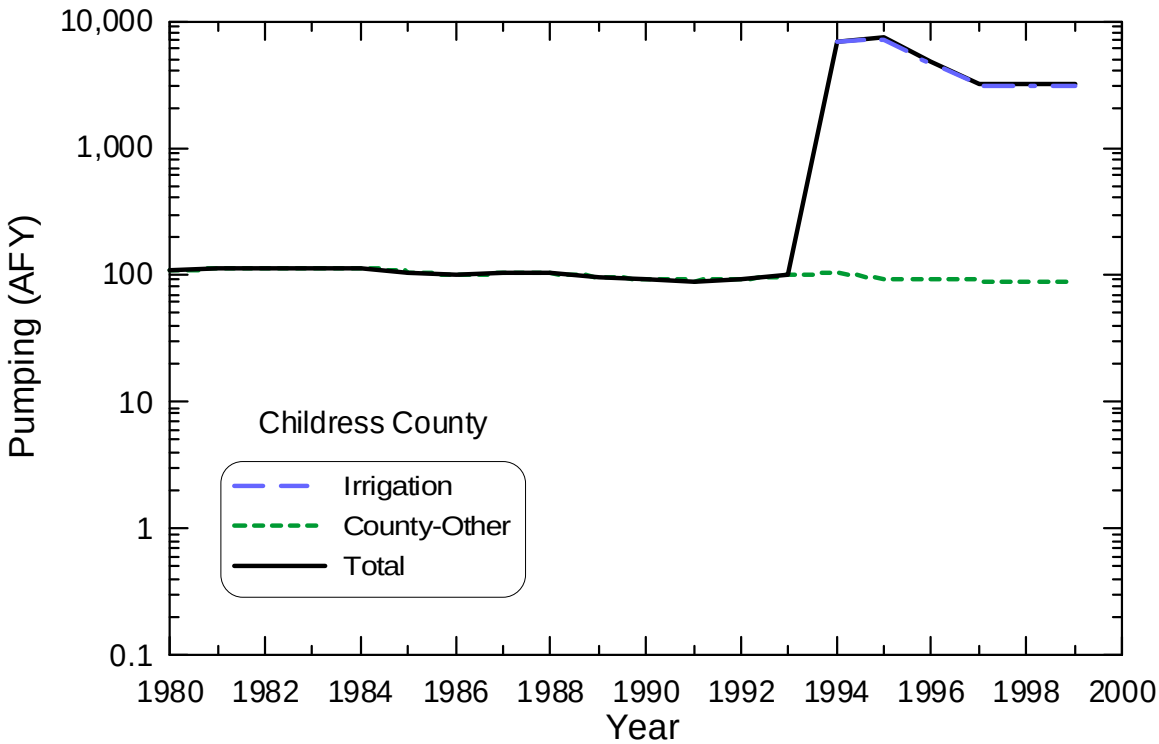

Figure 4.7.29 Groundwater withdrawals for Childress County from the Blaine aquifer for 1980-1999.

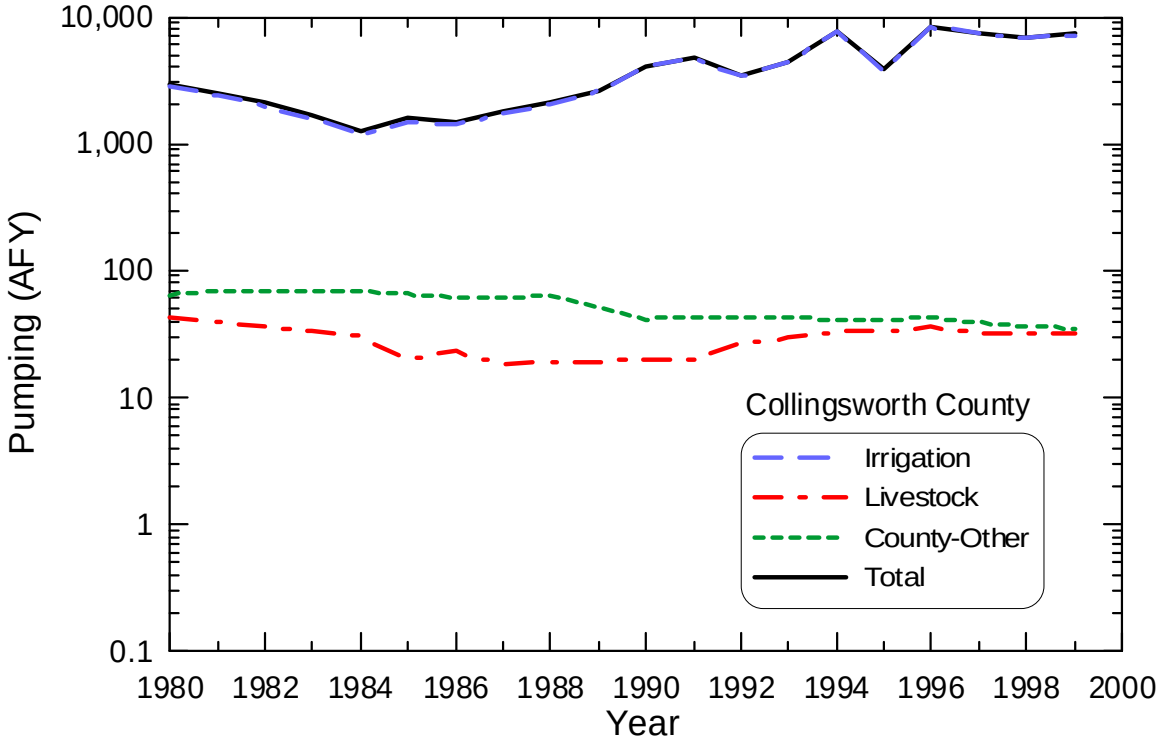

Figure 4.7.30 Groundwater withdrawals for Collingsworth County from the Blaine aquifer for 1980-1999.

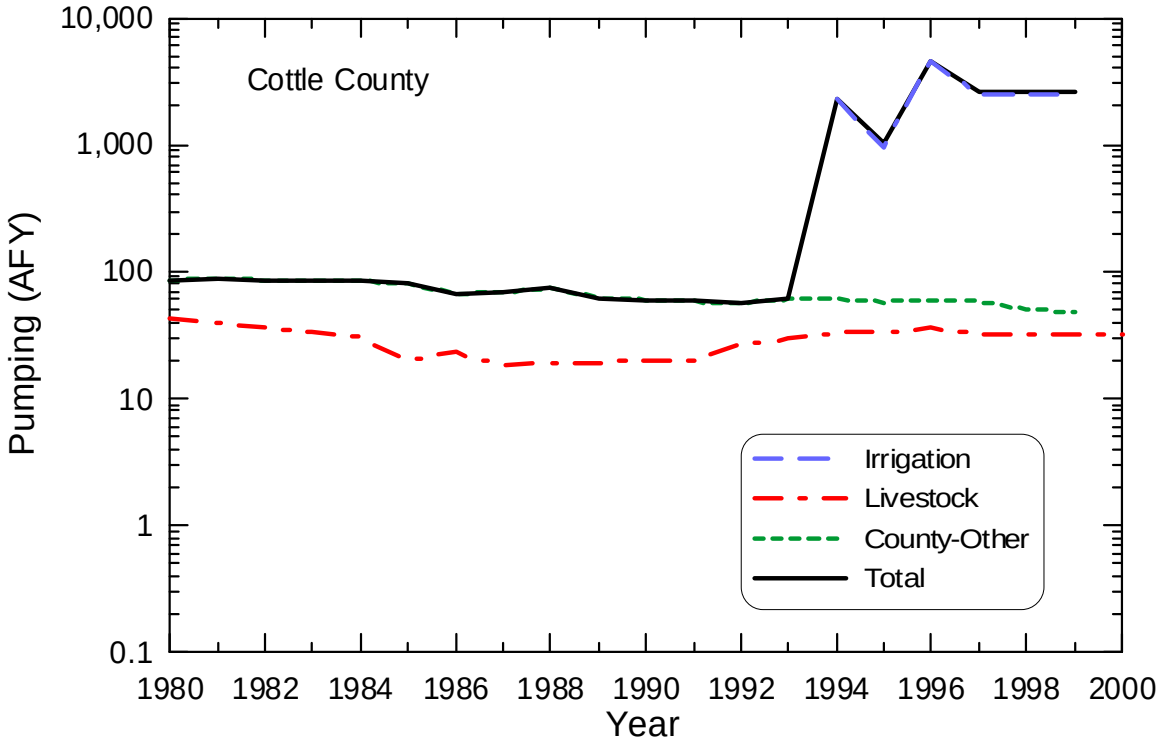

Figure 4.7.31 Groundwater withdrawals for Cottle County from the Blaine aquifer for 1980-1999.

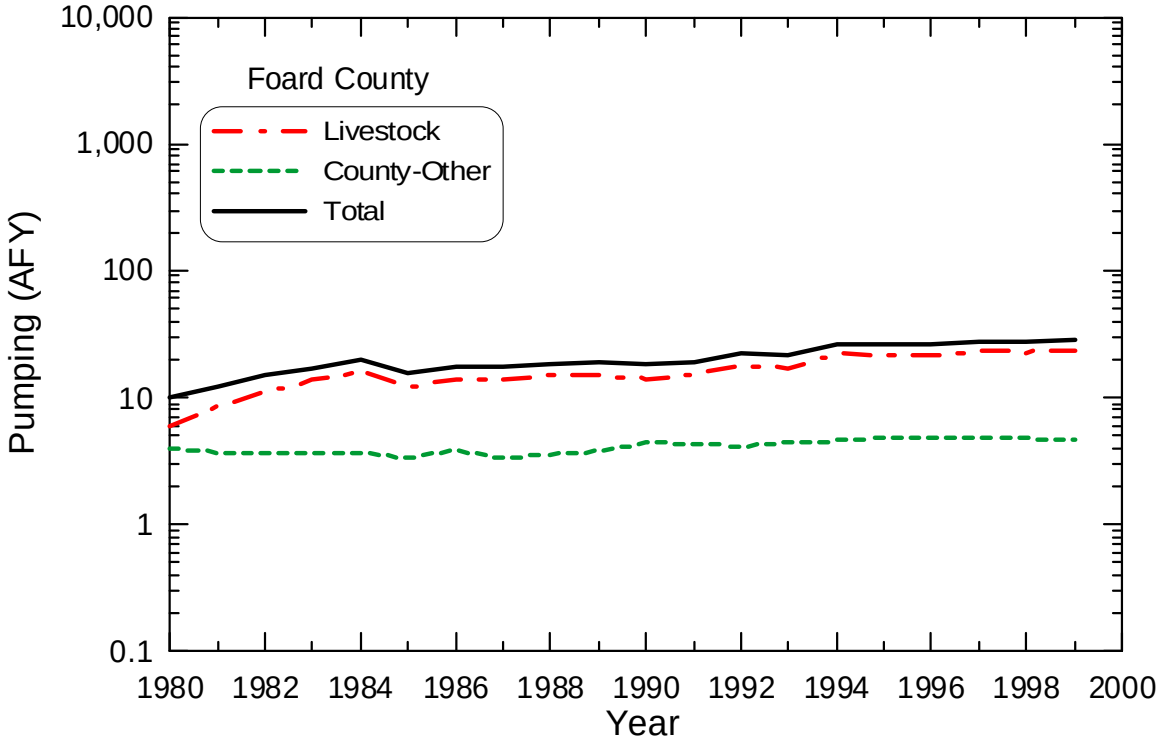

Figure 4.7.32 Groundwater withdrawals for Foard County from the Blaine aquifer for 1980-1999.

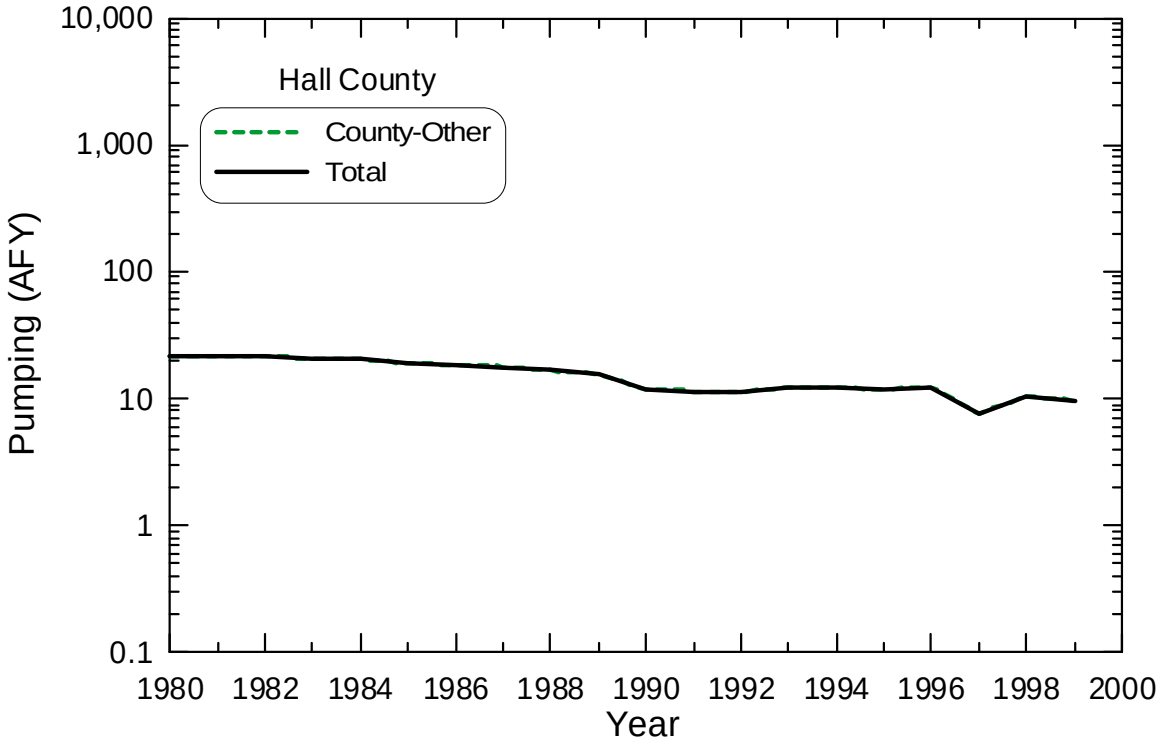

Figure 4.7.33 Groundwater withdrawals for Hall County from the Blaine aquifer for 1980-1999.

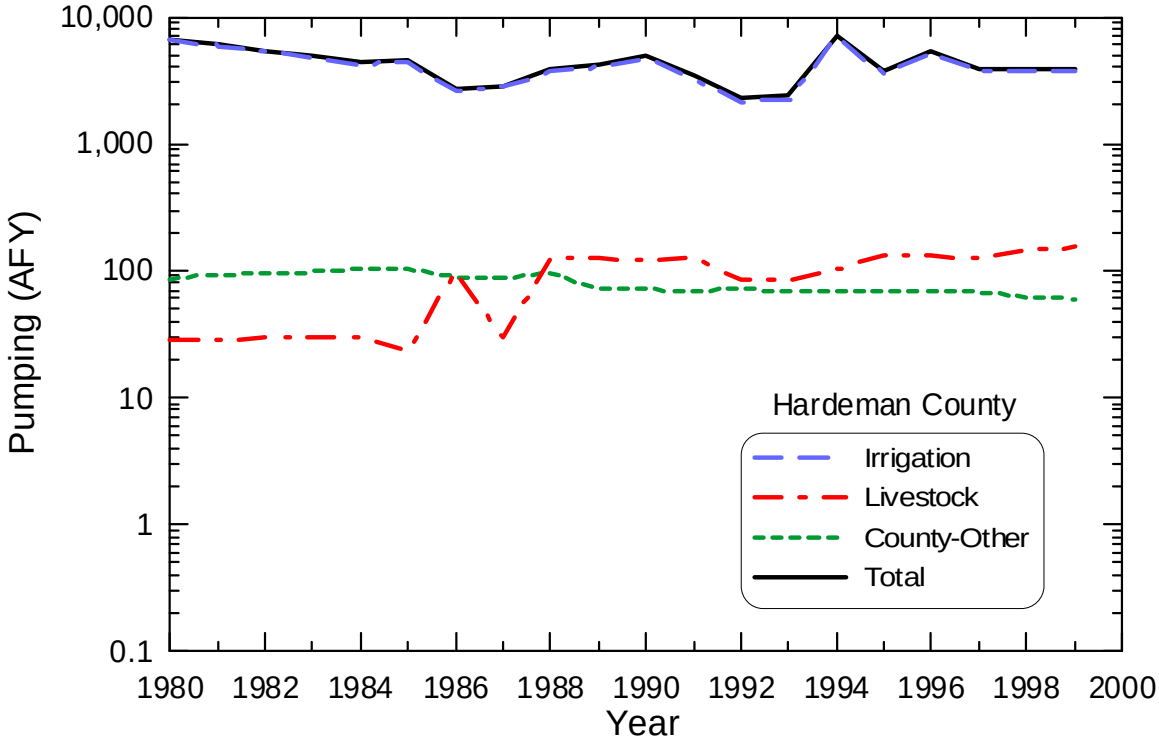

Figure 4.7.34 Groundwater withdrawals for Hardeman County from the Blaine aquifer for 1980-1999.

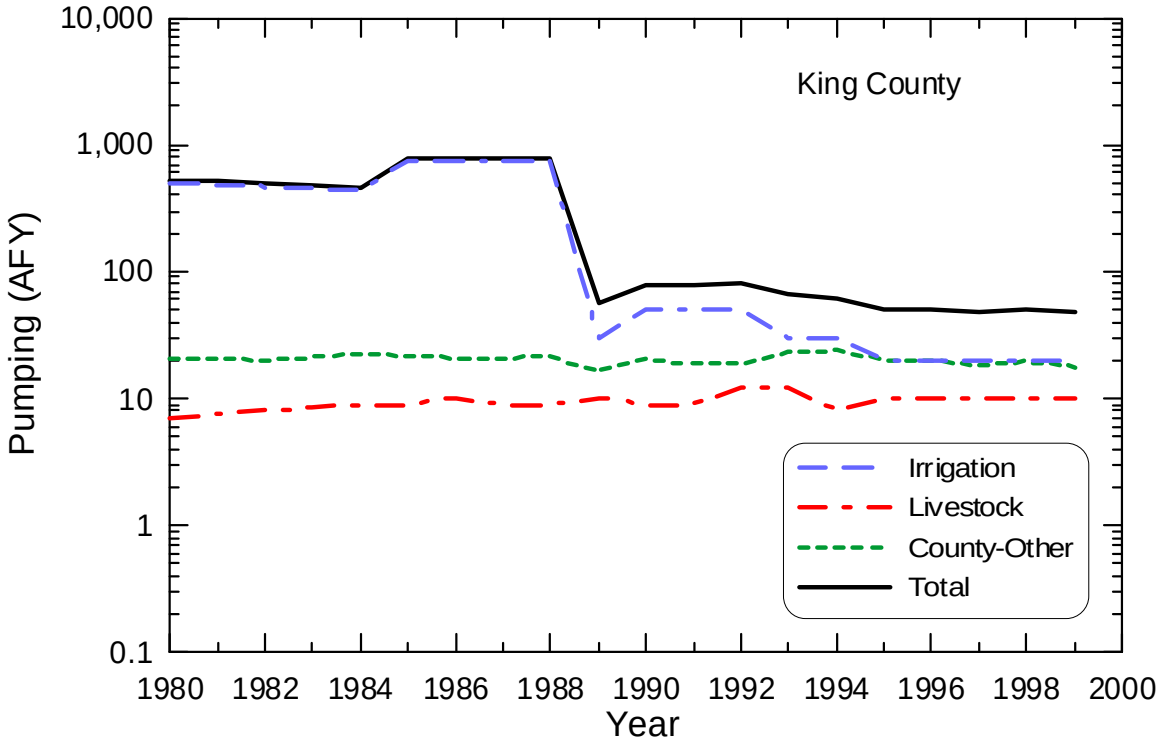

Figure 4.7.35 Groundwater withdrawals for King County from the Blaine aquifer for 1980-1999.

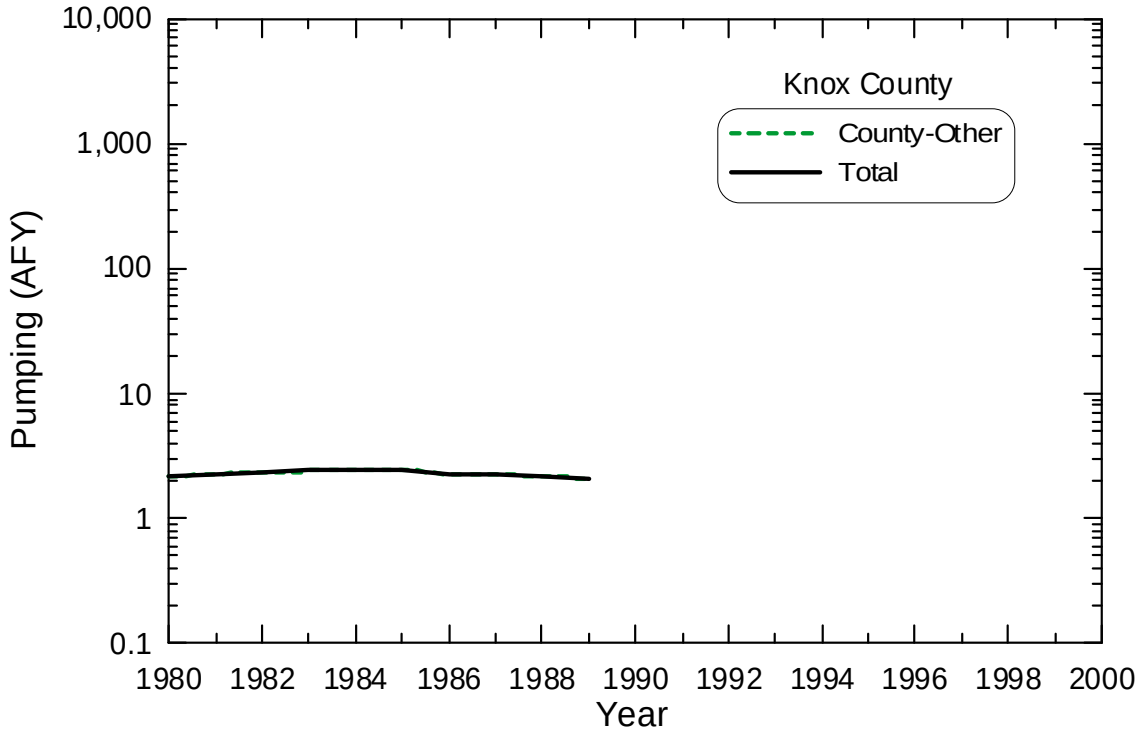

Figure 4.7.36 Groundwater withdrawals for Knox County from the Blaine aquifer for 1980-1999.

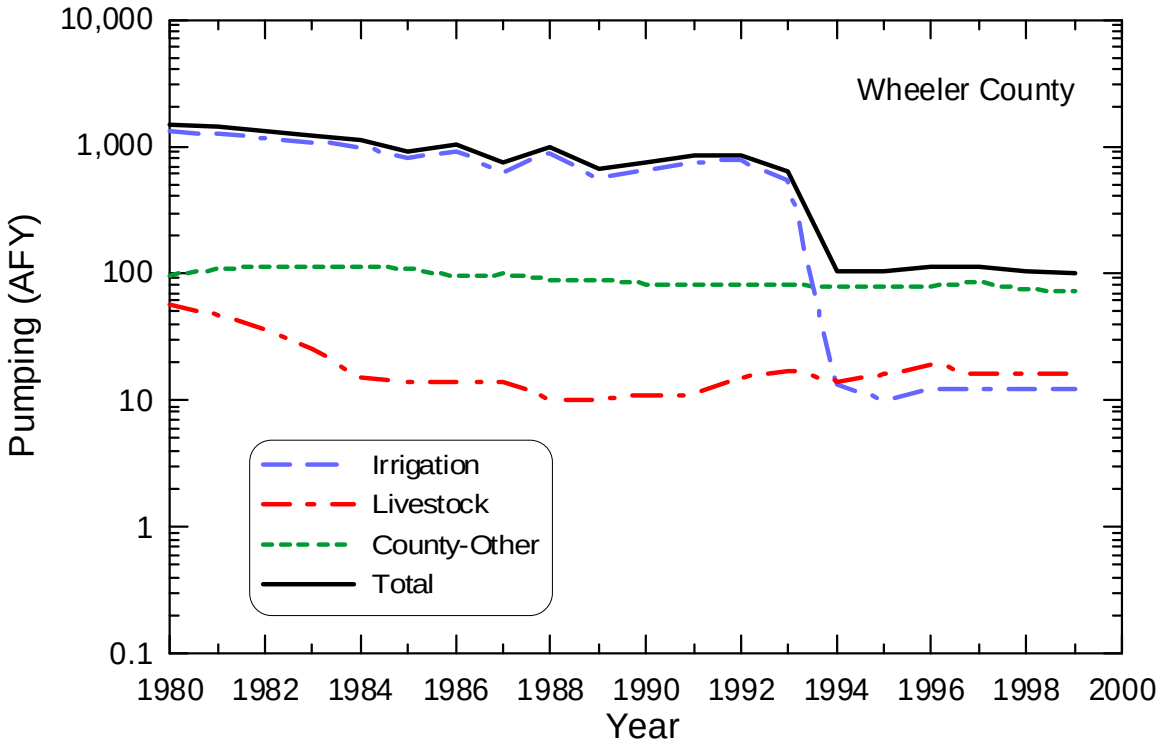

Figure 4.7.37 Groundwater withdrawals for Wheeler County from the Blaine aquifer for 1980-1999.

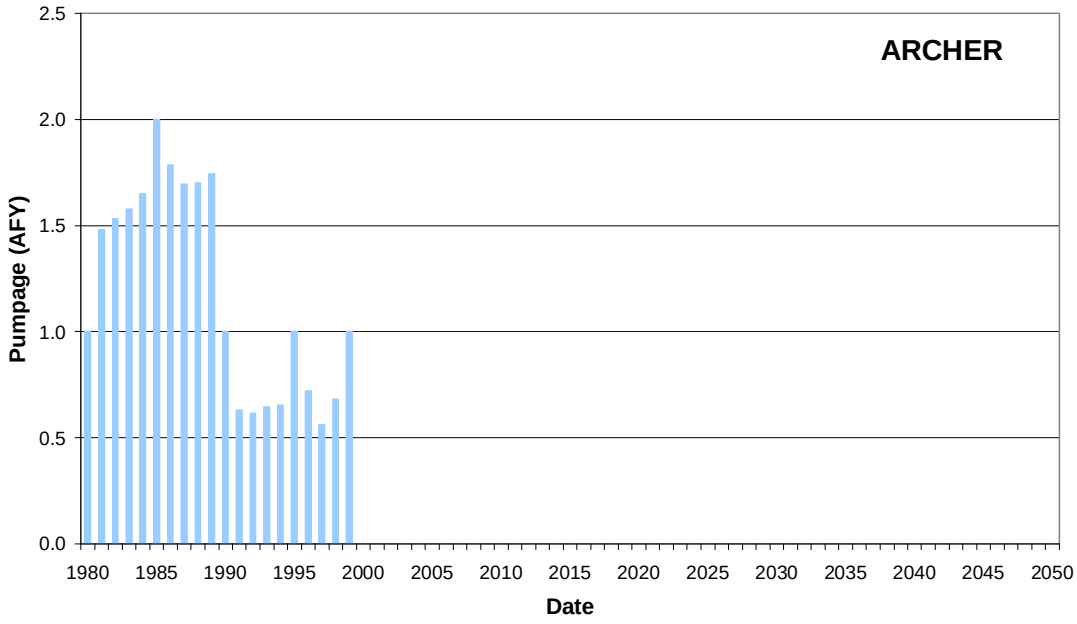

Figure 4.7.38 Seymour aquifer yearly pumpage (AFY) from 1980 through 2050 for Archer County.

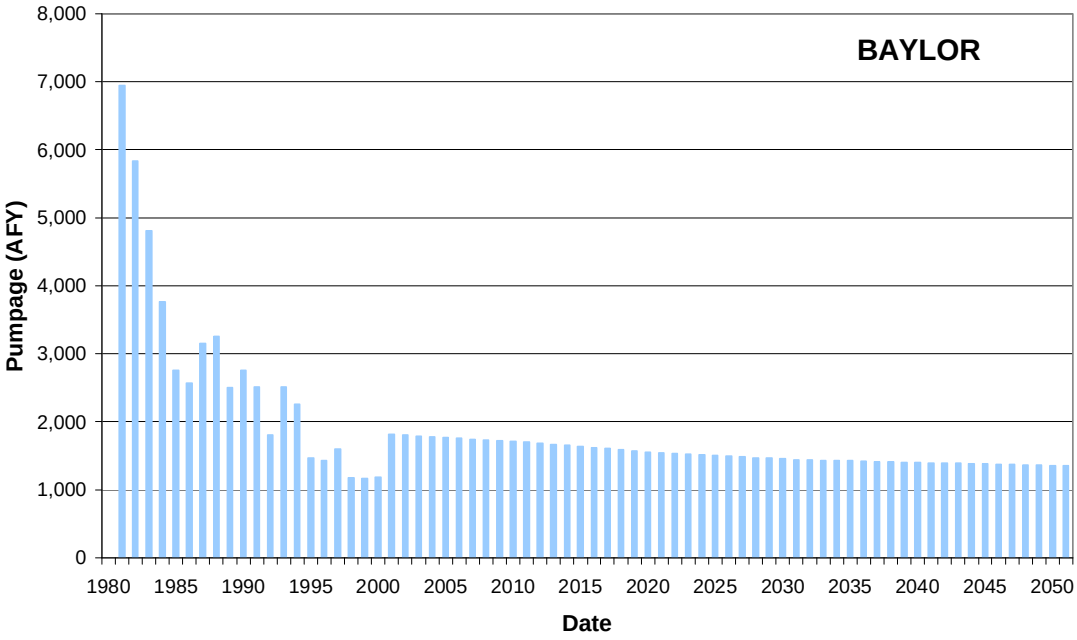

Figure 4.7.39 Seymour aquifer yearly pumpage (AFY) from 1980 through 2050 for Baylor County.

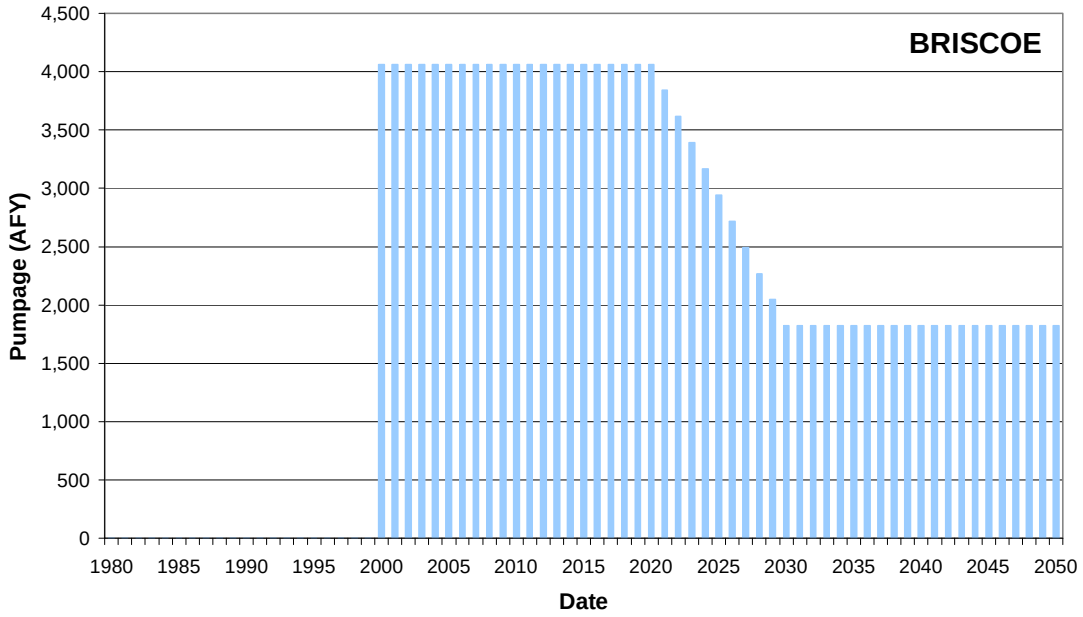

Figure 4.7.40 Seymour aquifer yearly pumpage (AFY) from 1980 through 2050 for Briscoe County.

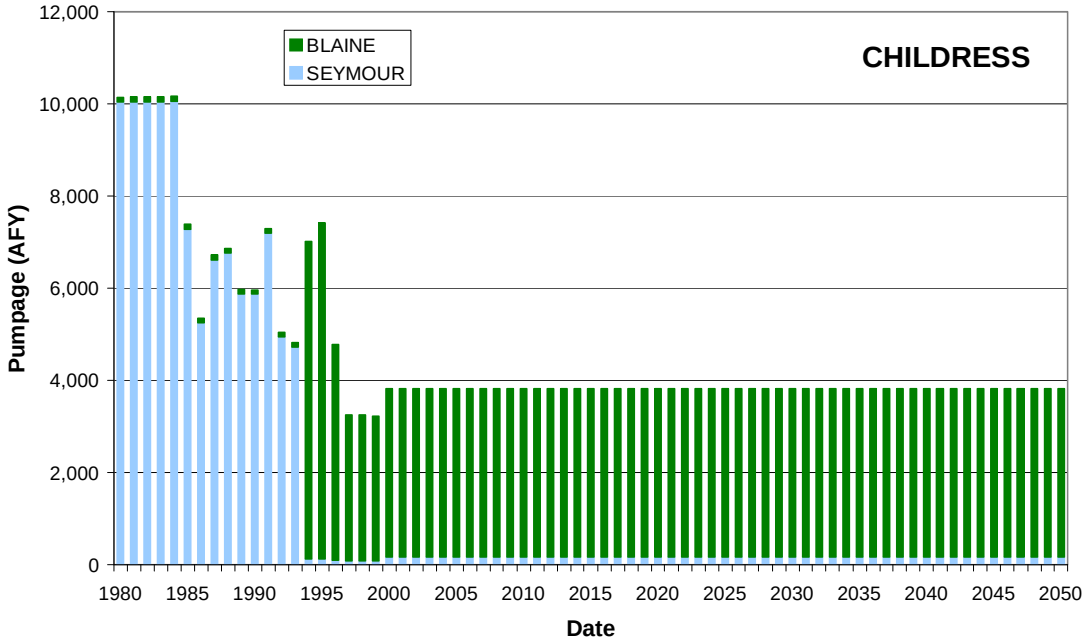

Figure 4.7.41 Seymour and Blaine aquifer yearly pumpage (AFY) from 1980 through 2050 for Childress County.

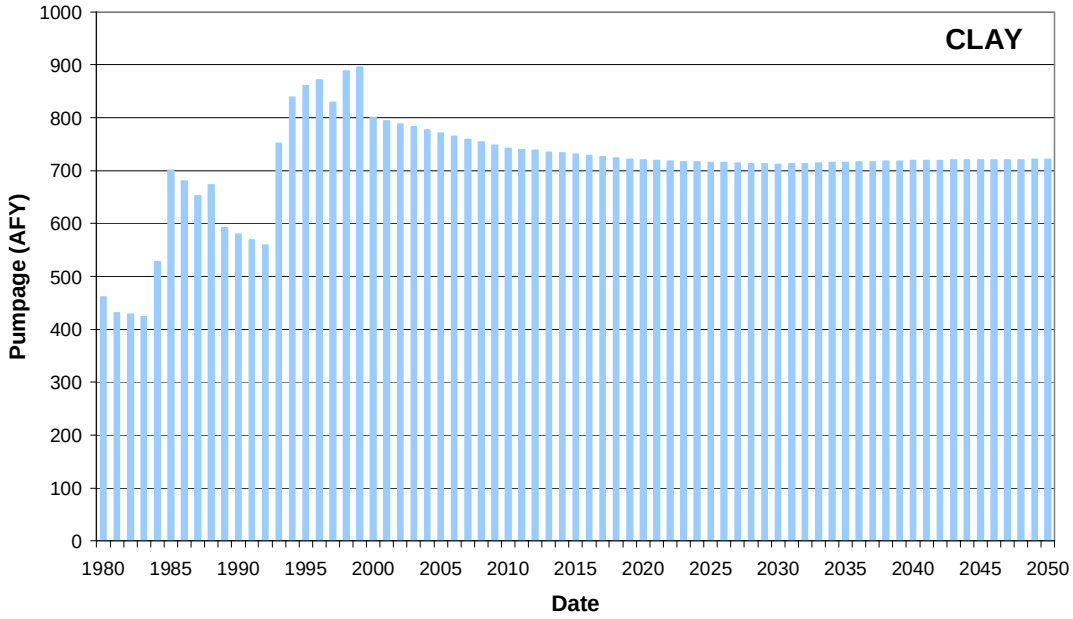

Figure 4.7.42 Seymour aquifer yearly pumpage (AFY) from 1980 through 2050 for Clay County.

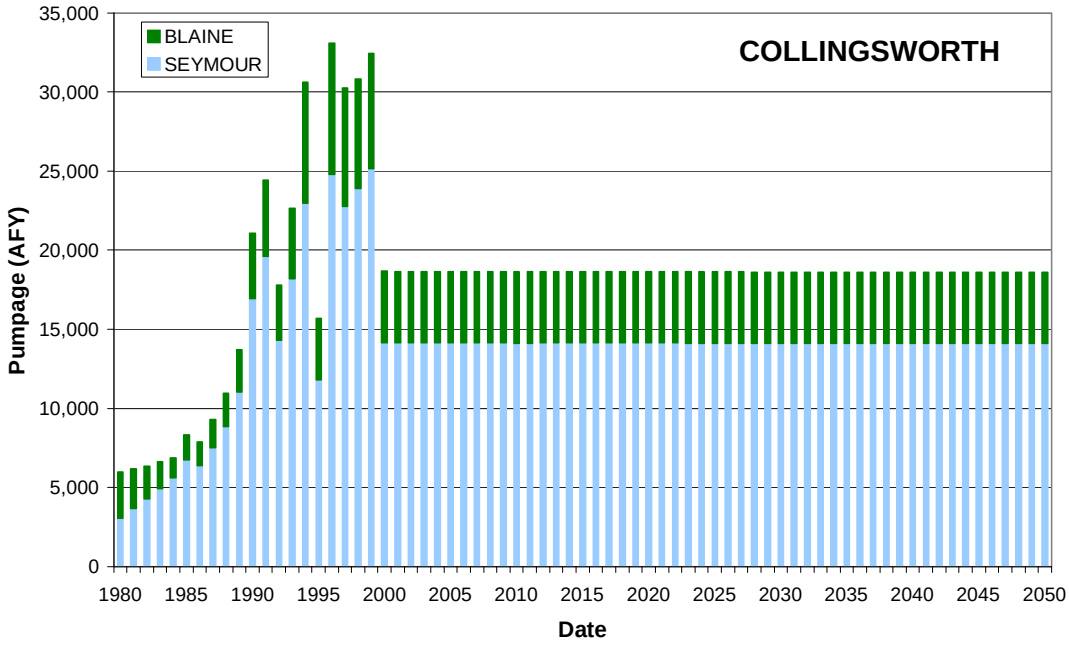

Figure 4.7.43 Seymour and Blaine yearly pumpage (AFY) from 1980 through 2050 for Collingsworth County.

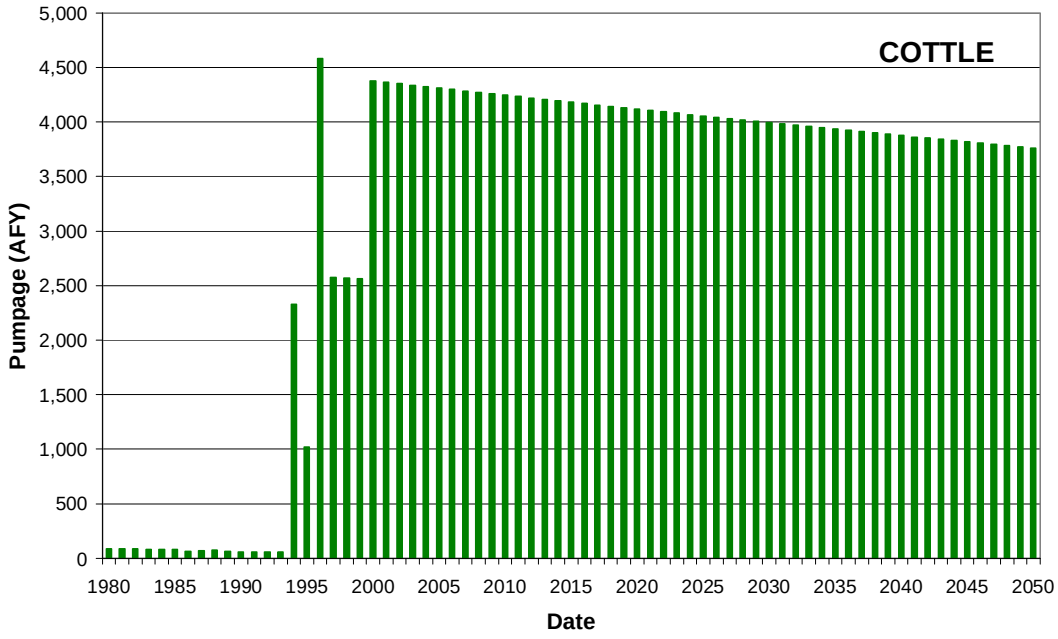

Figure 4.7.44 Blaine aquifer yearly pumpage (AFY) from 1980 through 2050 for Cottle County.

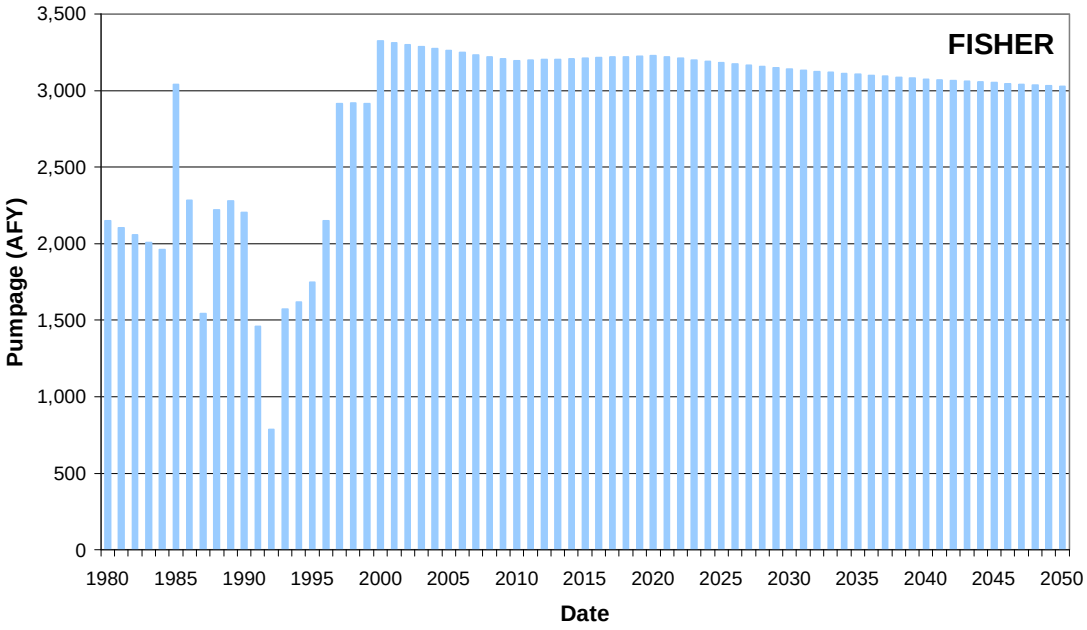

Figure 4.7.45 Seymour aquifer yearly pumpage (AFY) from 1980 through 2050 for Fisher County.

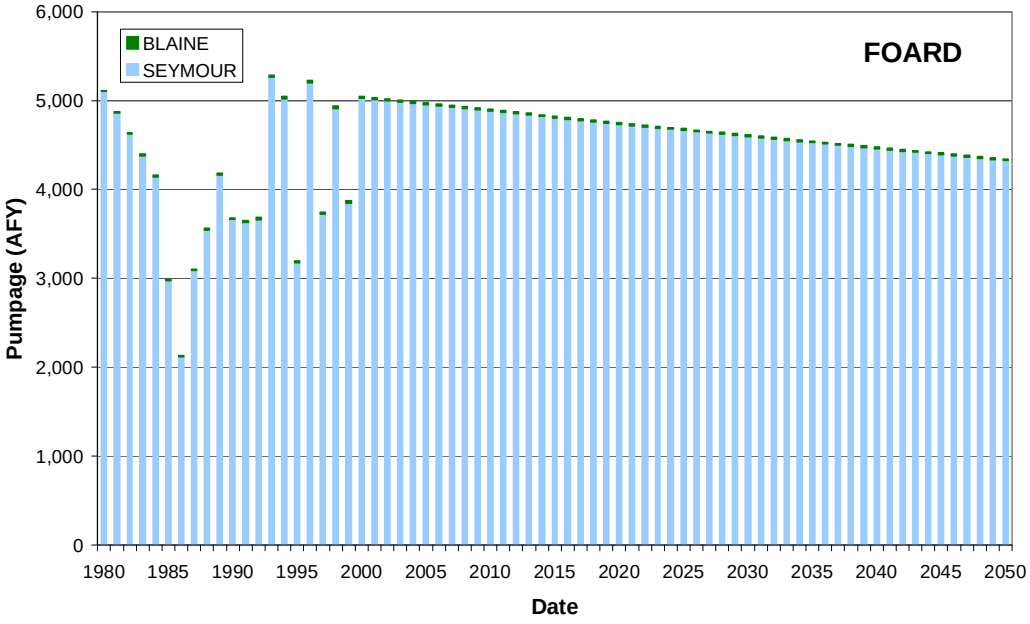

Figure 4.7.46 Seymour and Blaine aquifer yearly pumpage (AFY) from 1980 through 2050 for Foard County.

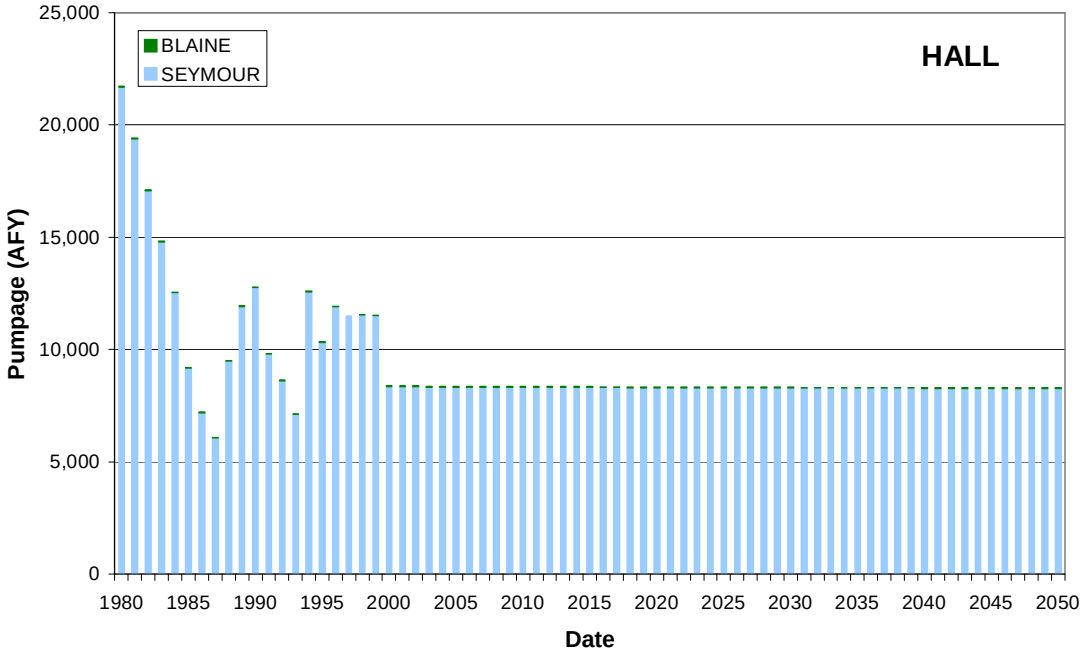

Figure 4.7.47 Seymour and Blaine aquifer yearly pumpage (AFY) from 1980 through 2050 for Hall County.

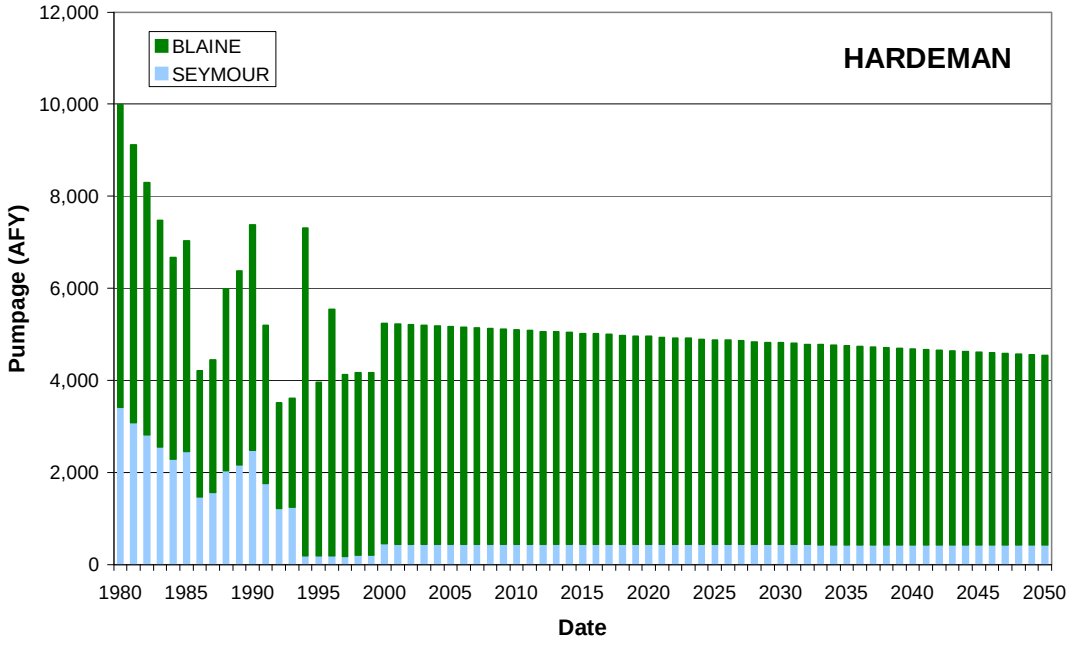

Figure 4.7.48 Seymour and Blaine aquifer yearly pumpage (AFY) from 1980 through 2050 for Hardeman County.

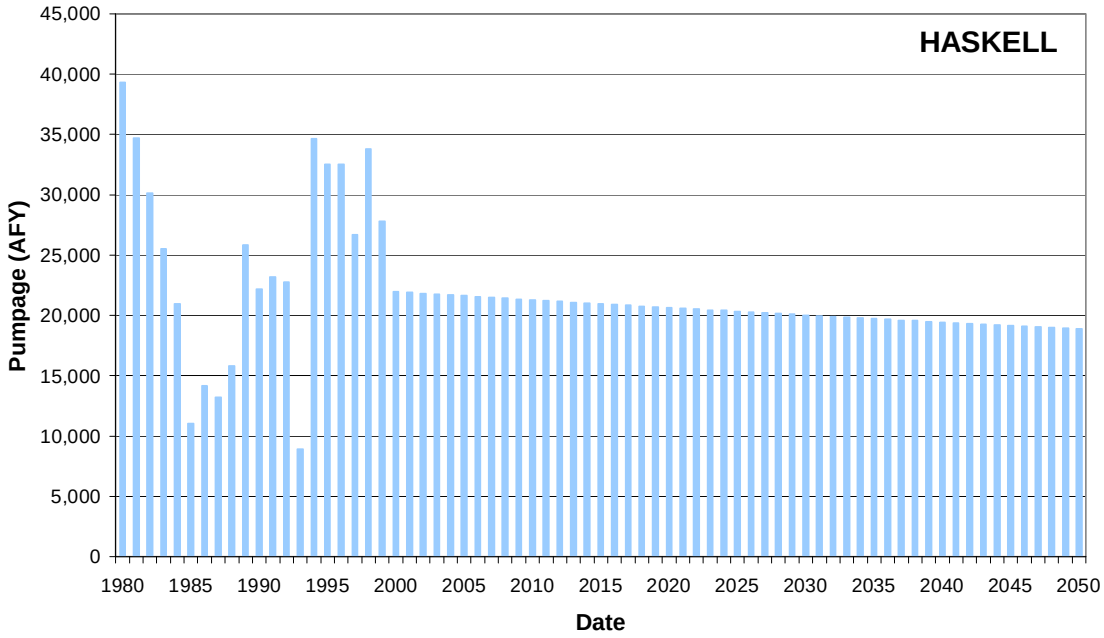

Figure 4.7.49 Seymour aquifer yearly pumpage (AFY) from 1980 through 2050 for Haskell County.

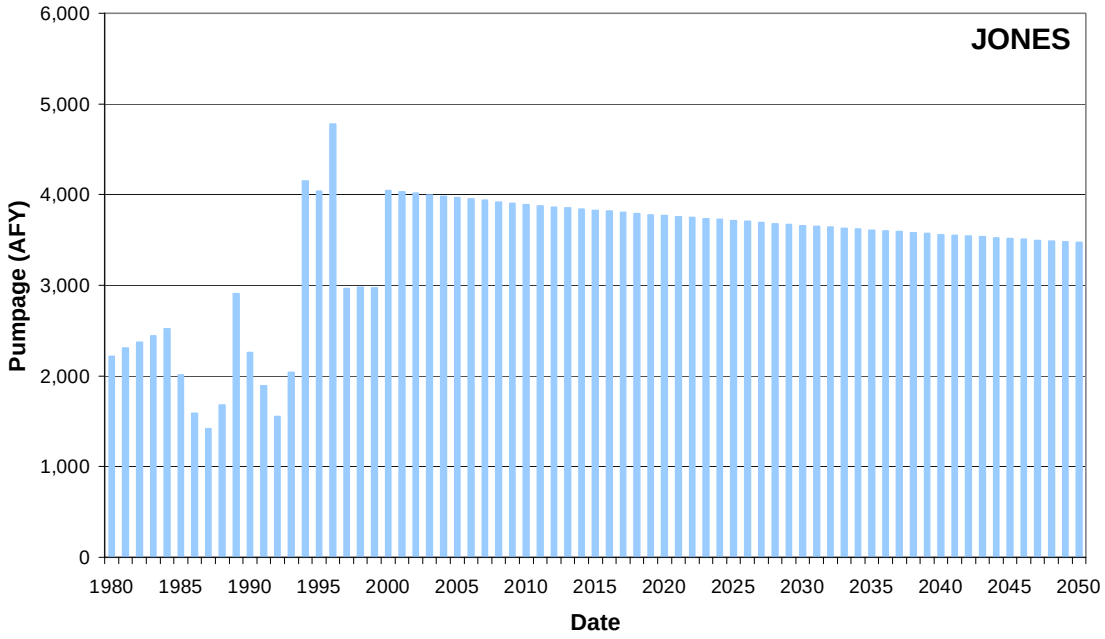

Figure 4.7.50 Seymour aquifer yearly pumpage (AFY) from 1980 through 2050 for Jones County.

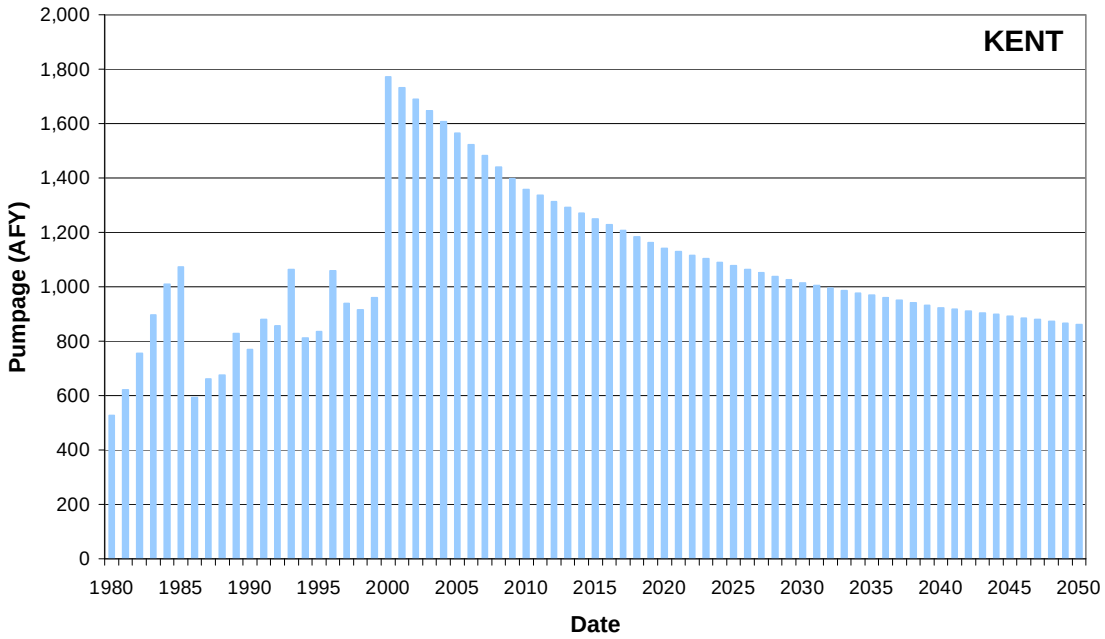

Figure 4.7.51 Seymour aquifer yearly pumpage (AFY) from 1980 through 2050 for Kent County.

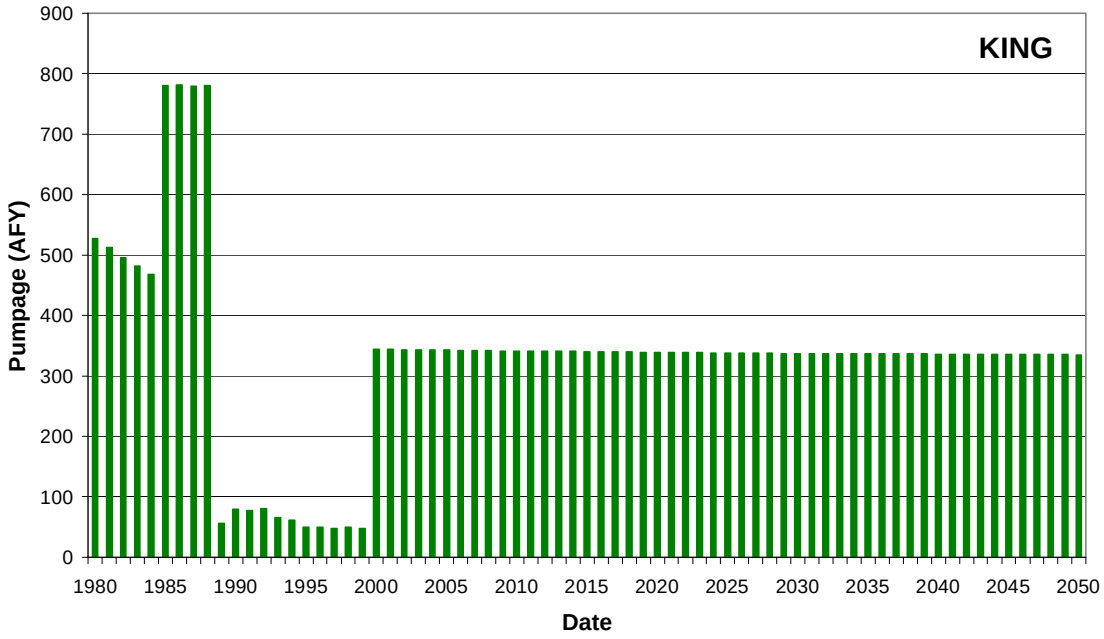

Figure 4.7.52 Blaine aquifer yearly pumpage (AFY) from 1980 through 2050 for King County.

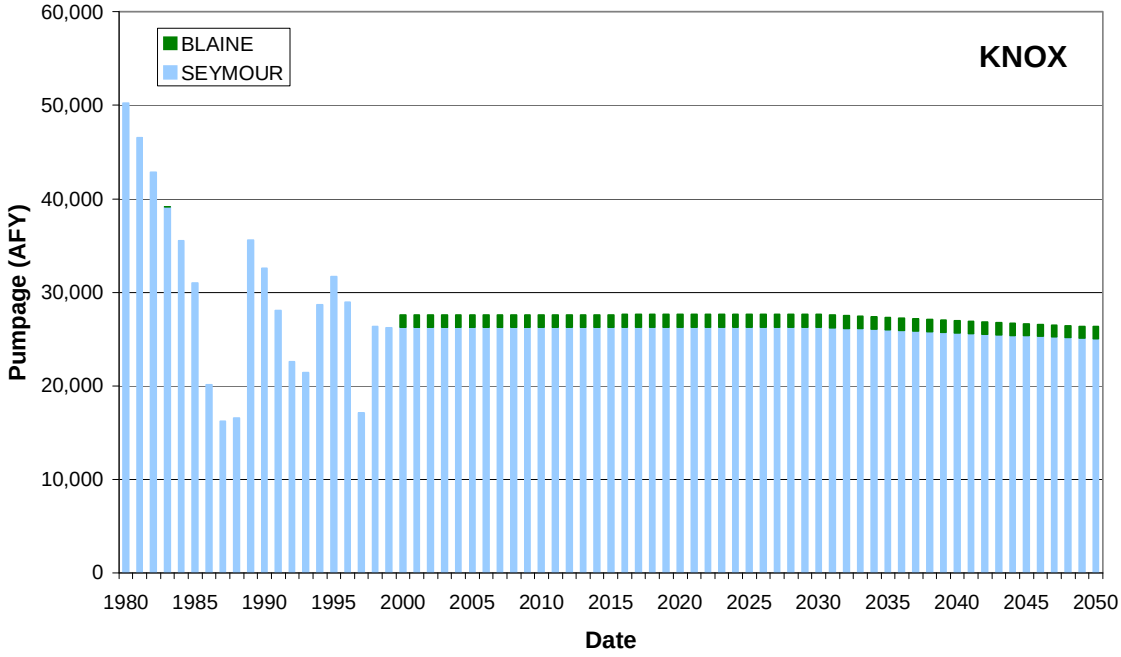

Figure 4.7.53 Seymour and Blaine aquifer yearly pumpage (AFY) from 1980 through 2050 for Knox County.

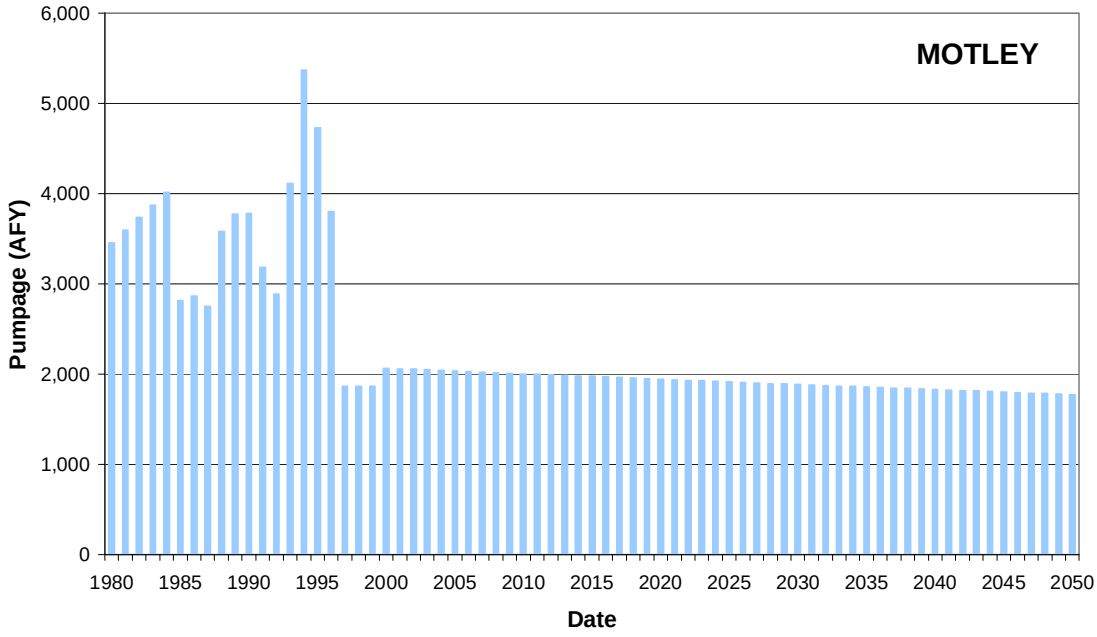

Figure 4.7.54 Seymour aquifer yearly pumpage (AFY) from 1980 through 2050 for Motley County.

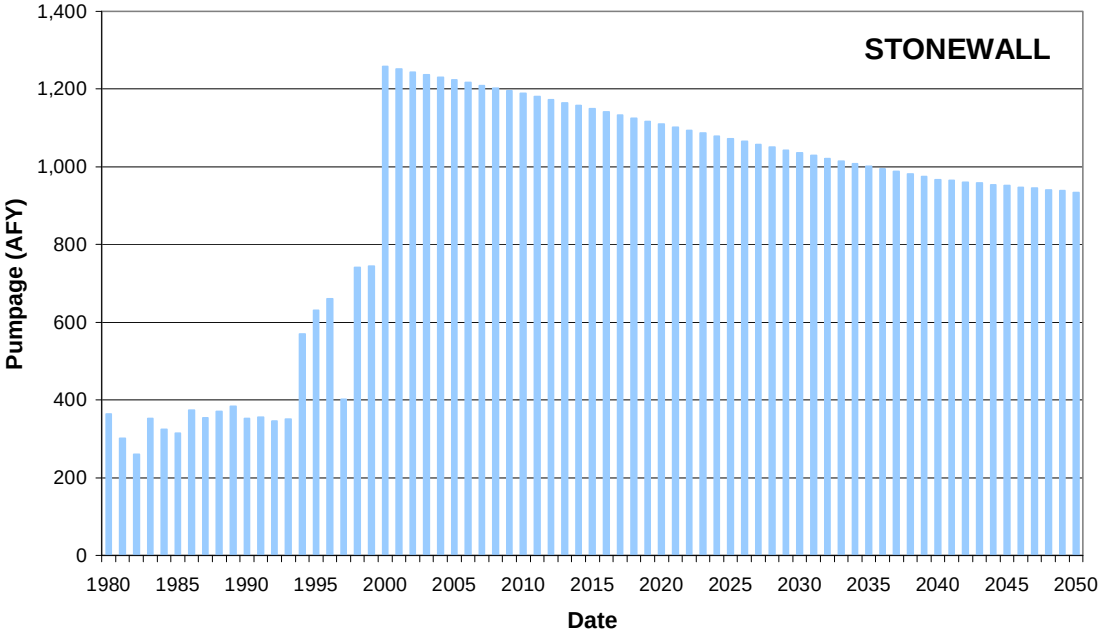

Figure 4.7.55 Seymour aquifer yearly pumpage (AFY) from 1980 through 2050 for Stonewall County.

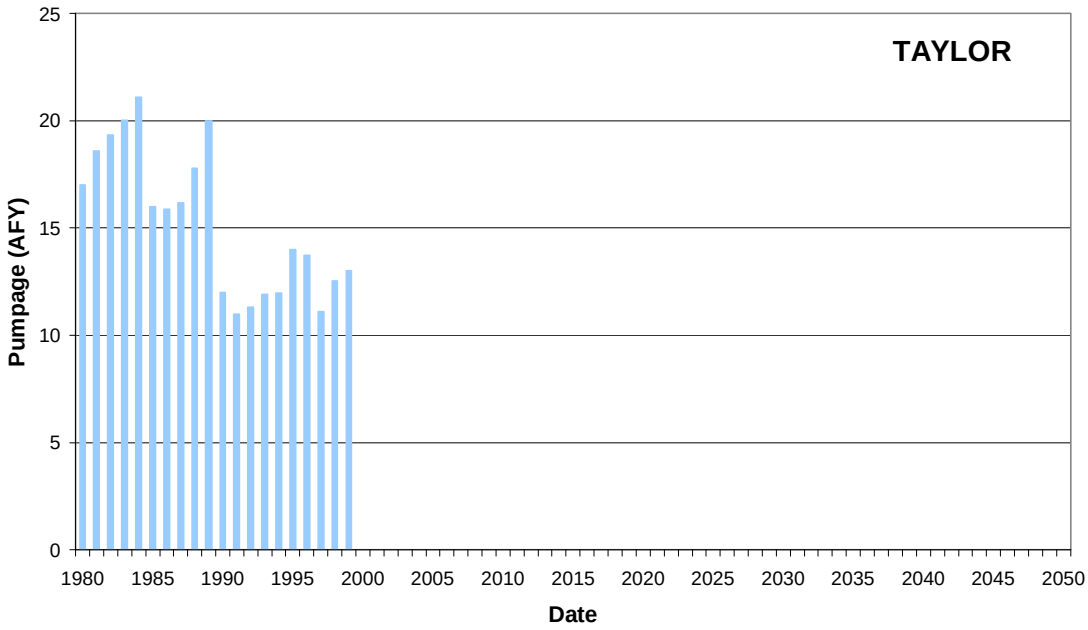

Figure 4.7.56 Seymour aquifer yearly pumpage (AFY) from 1980 through 2050 for Taylor County.

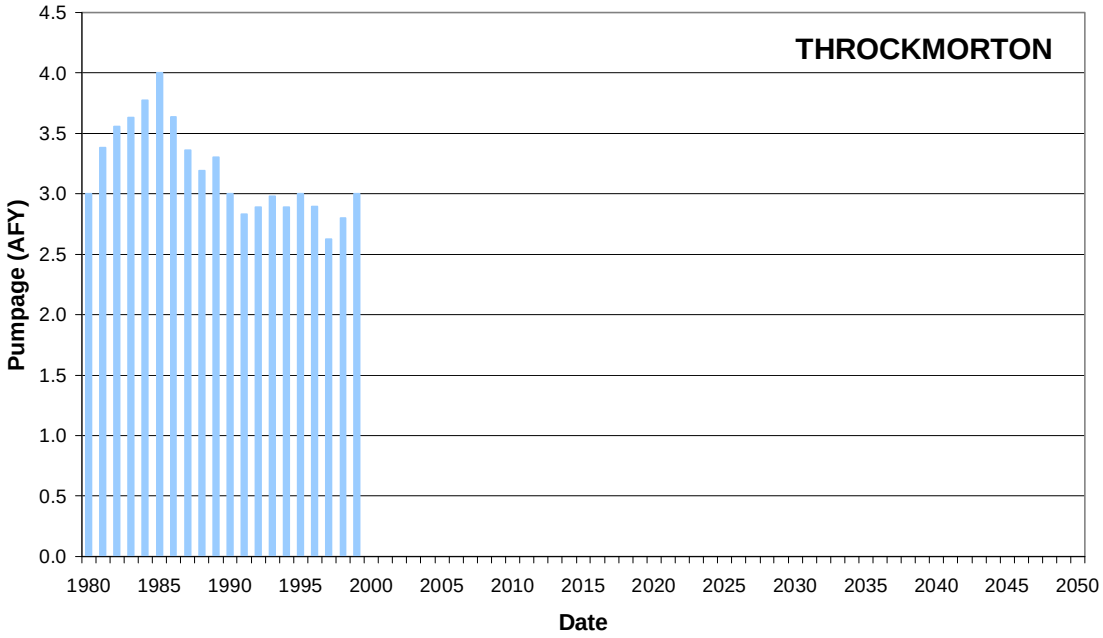

Figure 4.7.57 Seymour aquifer yearly pumpage (AFY) from 1980 through 2050 for Throckmorton County.

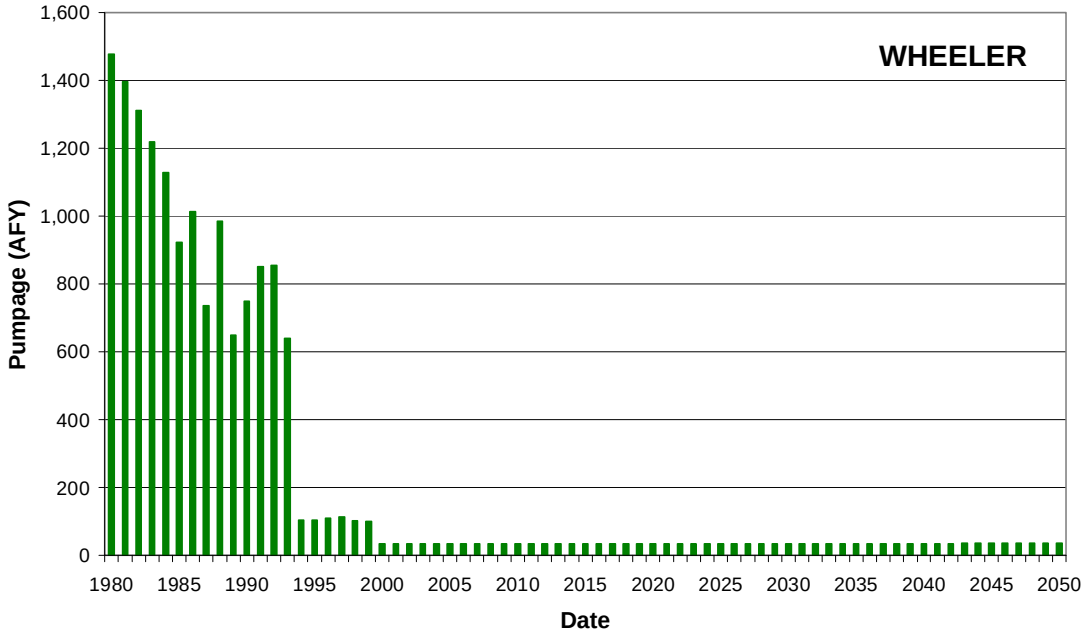

Figure 4.7.58 Blaine aquifer yearly pumpage (AFY) from 1980 through 2050 for Wheeler County.

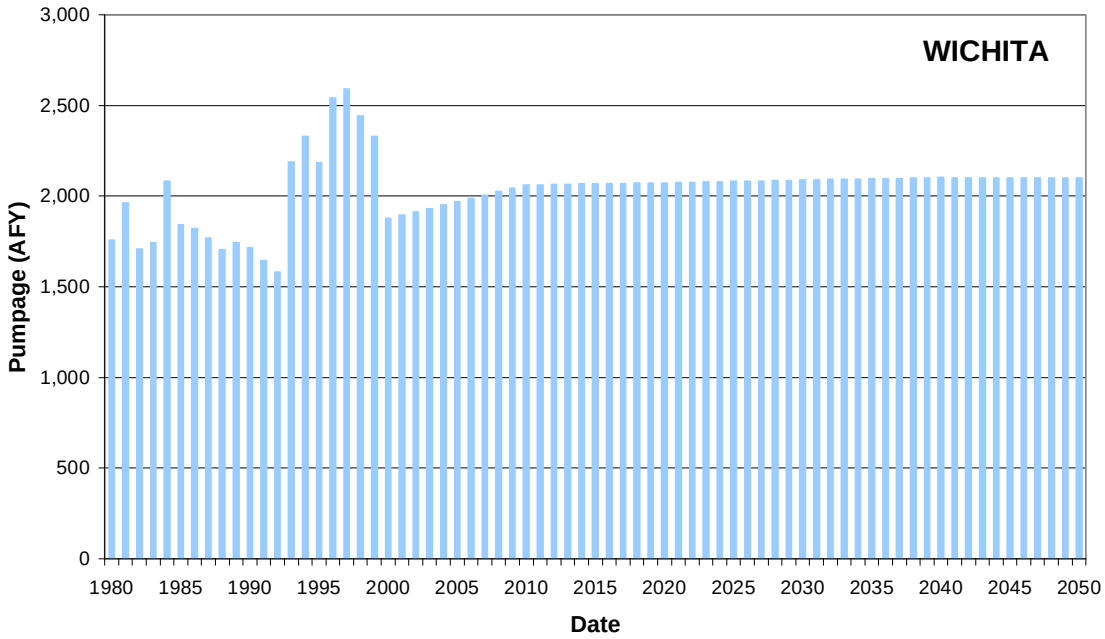

Figure 4.7.59 Seymour aquifer yearly pumpage (AFY) from 1980 through 2050 for Wichita County.

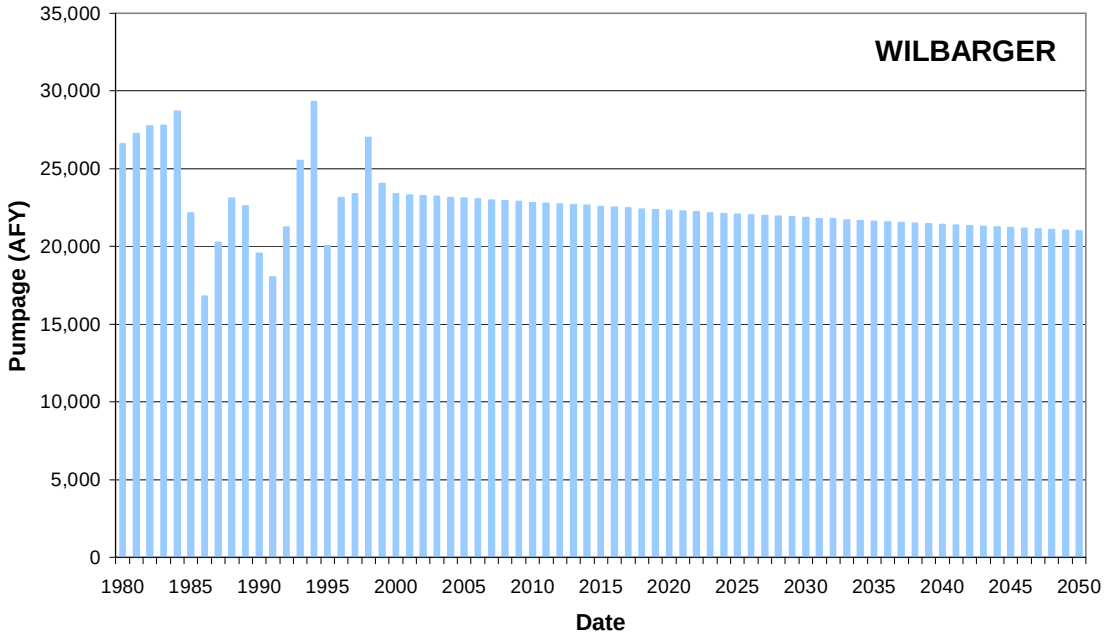

Figure 4.7.60 Seymour aquifer yearly pumpage (AFY) from 1980 through 2050 for Wilbarger County.

4.8 Water Quality in the Seymour and Blaine Aquifers

Groundwater in the Seymour and Blaine aquifers was evaluated for its quality as a drinking water supply and for irrigation of crops by comparing the measured chemical and physical properties of the water to screening levels. Water quality measurements were retrieved for the entire available historical record, from 1907 through 2001, from databases maintained by the TWDB, the USGS, and the TCEQ. Data that were considered unreliable, as indicated by the data reliability code in the TWDB dataset, were excluded from the analysis. The temporal distribution of the available water quality measurements for the Seymour and Blaine aquifers is shown in Figure 4.8.1. The percentage of wells in the Seymour and Blaine aquifers with one or more measurements exceeding individual screening levels are illustrated in Tables 4.8.1 and 4.8.2, respectively.

4.8.1 Drinking Water Quality

Screening levels for drinking water supply are based on the maximum contaminant levels (MCLs) established in the Texas Administrative Code (Title 30 Chapter 290). Primary MCLs are legally enforceable standards that apply to public water systems to protect human health from contaminants in drinking water. Secondary MCLs are non-enforceable guidelines for drinking water contaminants that may cause aesthetic effects (taste, color, odor, foaming), cosmetic effects (skin or tooth discoloration), and technical effects (e.g., corrosivity, expensive water treatment, plumbing fixture staining, scaling, and sediment).

High levels of nitrate are common in the Seymour aquifer, with more than half the wells exhibiting one or more measurements exceeding the primary MCL of 10 mg/L as nitrogen (Figure 4.8.2). In the Blaine aquifer, 12 percent of the wells exceed the primary MCL for nitrate (Figure 4.8.3). High concentrations of nitrate nitrogen can cause serious illness in infants younger than 6 months old. These high nitrate levels may be due in part to domestic sewage contamination, the use of nitrate fertilizers on croplands, or leaching from soil following conversion of former grasslands and mesquite groves to cropland, but also the shallow and permeable nature of the Seymour aquifer (Price, 1979).

Fluoride is a naturally-occurring element found in most rocks. At very low concentrations, fluoride is a beneficial nutrient. At a concentration of 1 mg/L, fluoride helps to prevent dental cavities. However, at concentrations above the secondary MCL of 2 mg/L, fluoride can stain children's teeth. Approximately 14 percent of wells in the Seymour aquifer (Figure 4.8.4), and 0.5 percent of the wells in the Blaine aquifer (Figure 4.8.5), have exceeded this level. At concentrations above the primary MCL of 4 mg/L, fluoride can cause a type of bone disease. Almost 2 percent of the wells in the Seymour have exceeded 4 mg/L fluoride, while none of the wells in the Blaine have exceeded this MCL.

Alpha particles are one type of naturally-occurring radionuclide that can cause cancer. Alpha activity that exceeds the primary MCL of 15 pCi/L were recorded in almost 5 percent of the wells in the Seymour aquifer, and almost 8 percent of the wells in the Blaine aquifer. The radioactive MCL exceedances were found in Childress, Jones, and Baylor counties.

Selenium is a natural trace element that may cause a variety of adverse health effects at high concentrations. Selenium concentrations have exceeded the primary MCL of 0.05 mg/L in four of the 36 wells in which it has been measured in the Blaine aquifer, and in two of 153 wells in the Seymour aquifer. Other contaminants exceeding primary MCLs in a single well in the Seymour aquifer include the trace elements antimony, thallium, and lead.

Total dissolved solids (TDS) is a measure of water saltiness, the sum of concentrations of all dissolved ions (such as sodium, calcium, magnesium, potassium, chloride, sulfate, carbonates) plus silica. Some dissolved solids, such as calcium, give water a pleasant taste, but most make water taste salty, bitter, or metallic. Dissolved solids can also increase the corrosiveness of water. TDS levels have exceeded the Texas secondary MCL in approximately 41 percent of the wells in the Seymour aquifer (Figure 4.8.6), and 94 percent of the wells in the Blaine aquifer (Figure 4.8.7). Concentrations of sulfate, a major component of TDS, have exceeded secondary MCLs in 17 percent of wells in the Seymour, and 96 percent of the wells in the Blaine aquifer. Concentrations of chloride, another major component of TDS, have exceeded the secondary MCL of 300 mg/L in 29 percent of Seymour wells (Figure 4.8.8), and 26 percent of Blaine wells (Figure 4.8.9).

Elevated levels of iron and manganese adversely impact water quality in approximately 15 and 10 percent, respectively, of the wells in the Seymour aquifer, and 23 and 8 percent, respectively, of the wells in the Blaine aquifer. Water containing iron and manganese in excess of the secondary MCL of 0.3 mg/L and 0.05 mg/L, respectively, may cause reddish-brown or blackish-gray stains on laundry, utensils, and plumbing fixtures, as well as color, taste, and odor problems. Other water quality constituents affecting the suitability of water from the Seymour and Blaine aquifers as a drinking water supply in limited areas include pH and aluminum.

In summary, the utility of water from the Seymour aquifer as a drinking water supply is limited in many areas for health reasons, primarily due to elevated nitrate concentrations, and for taste reasons due to saltiness. The unpalatability of water from the Blaine aquifer severely limits its use for drinking water, primarily due to high sulfate concentrations.

4.8.2 Irrigation Water Quality

The utility of groundwater from the Seymour and Blaine aquifers for crop irrigation was evaluated based on its salinity hazard, sodium hazard, and concentrations of boron and chloride.

Saline irrigation waters limit the ability of plants to take up water from soils. Various crops differ in their tolerance of high salinity. Salinity is often measured by the TDS content or electrical conductivity of the water. The salinity hazard classification system of the U.S. Salinity Laboratory (1954) indicates that waters with electrical conductivity over 750 micromhos present a high salinity hazard, and those with electrical conductivity over 2,250 micromhos present a very high salinity hazard. Of the wells in the Seymour aquifer, 91 percent have exhibited a high salinity hazard scale, and 30 percent of the wells have exhibited a very high salinity hazard (Figure 4.8.10). For the Blaine aquifer, 100 percent of the wells have exhibited a high salinity hazard, and 90 percent of the wells have exhibited a very high salinity hazard (Figure 4.8.11).

Irrigation water containing large amounts of sodium causes a breakdown in the physical structure of soil such that movement of water and air through the soil is restricted. The sodium hazard was calculated based on the classification system developed by the U.S. Salinity Laboratory (1954). The sodium absorption ratio (SAR) is an indication of the sodium hazard to soils. Waters with a SAR above 18 are considered to present a high sodium hazard, generally considered unsuitable for continuous use in irrigation. Waters with a SAR above 26 are

considered to represent a very high sodium hazard. Less than 1 percent of the wells in either the Seymour or Blaine aquifers have exhibited a high sodium hazard.

Boron may cause toxicity to many plants at levels above 2 mg/L (Van der Leeden et al., 1990). Some investigators (Lemon and McFarland, 2002) have found reductions in peanut yields at boron levels above 0.75 mg/l. Boron levels in the Seymour aquifer have exceeded 0.75 mg/L in approximately 13 percent of wells, and have exceeded 2 mg/L in approximately 2 percent of wells (Figure 4.8.12). In the Blaine aquifer, boron levels have exceeded 0.75 mg/L in 36 percent of wells, and have exceeded 2 mg/L in 9 percent of wells (Figure 4.8.13).

Most crops cannot tolerate chloride levels above 1,000 mg/L for an extended period of time (Tanji, 1990). This level has been exceeded in about 6 percent of wells in the Seymour aquifer and 8 percent of wells in the Blaine aquifer.

Table 4.8.1 Occurrence and levels of some commonly-measured groundwater quality constituents in the Seymour aquifer.

Constituent	Number of Wells	Screening Level (mg/L)	Type	Percent Of Wells Exceeding Screening Level*
Nitrate Nitrogen	2200	10	MCL[1]	56%
Fluoride	2081	4	MCL[1]	1.9%
Alpha Activity, pCi/L	63	15	MCL[1]	4.8%
Nitrite Nitrogen	141	1	MCL[1]	1.4%
Selenium	153	0.05	MCL[1]	1.3%
Antimony	89	0.006	MCL[1]	1.1%
Thallium	88	0.002	MCL[1]	1.1%
Arsenic	153	0.05	MCL[1]	0.0%
Lead	155	0.015	Action level	0.6%
Chromium	124	0.1	MCL[1]	0.0%
Beryllium	89	0.004	MCL[1]	0.0%
Cadmium	151	0.005	MCL[1]	0.0%
Barium	170	2	MCL[1]	0.0%
Copper	155	1.3	Action level	0.0%
Mercury	76	0.002	MCL[1]	0.0%
Total Dissolved Solids	2070	1,000	MCL[2]	41%
Chloride	2438	300	MCL[2]	29%
Sulfate	2290	300	MCL[2]	17%
Fluoride	2081	2	MCL[2]	14%
Iron	321	0.3	MCL[2]	15%
Manganese	314	0.05	MCL[2]	10%
pH	2015	>7	MCL[2]	3.4%
Aluminum	133	0.2	MCL[2]	1.5%
Zinc	153	5	MCL[2]	0.0%
Copper	155	1.0	MCL[2]	0.0%
Silver	75	0.1	MCL[2]	0.0%
Salinity Hazard	2103	Very High (Sp. Cond. >2,250)	Irrigation	30%
		High (Sp. Cond. > 750)	Irrigation	91%
Sodium Hazard	2057	Very High (SAR > 26)	Irrigation	0.10%
		High (SAR > 18)		0.49%
Boron	602	2	Irrigation	2.0%
		0.75		13%
Chloride	2438	1,000	Irrigation	5.6%

* percentage of wells with one or more measurements of the parameter that exceeded the screening level

[1] refers to National Primary Drinking Water Regulations

[2] refers to National Secondary Drinking Water Regulations

Table 4.8.2 Occurrence and levels of some commonly-measured groundwater quality constituents in the Blaine aquifer.

Constituent	Number Of Wells	Screening Level (mg/L)	Type	Percent Of Wells Exceeding Screening Level*
Nitrate Nitrogen	286	10	MCL[1]	12%
Selenium	36	0.05	MCL[1]	11%
Alpha Activity, pCi/L	26	15	MCL[1]	7.7%
Arsenic	35	0.05	MCL[1]	0.0%
Chromium	13	0.1	MCL[1]	0.0%
Fluoride	182	4	MCL[1]	0.0%
Lead	35	0.015	Action level	0.0%
Beryllium	26	0.004	MCL[1]	0.0%
Cadmium	20	0.005	MCL[1]	0.0%
Barium	39	2	MCL[1]	0.0%
Copper	36	1.3	Action level	0.0%
Antimony	25	0.006	MCL[1]	0.0%
Mercury	10	0.002	MCL[1]	0.0%
Nitrite Nitrogen	10	1	MCL[1]	0.0%
Thallium	25	0.002	MCL[1]	0.0%
Total Dissolved Solids	363	1,000	MCL[2]	94%
Sulfate	428	300	MCL[2]	96%
Chloride	429	300	MCL[2]	26%
Iron	47	0.3	MCL[2]	23%
Manganese	39	0.05	MCL[2]	7.7%
pH	247	>7	MCL[2]	14%
Aluminum	32	0.2	MCL[2]	6.2%
Fluoride	182	2	MCL[2]	0.5%
Zinc	36	5	MCL[2]	0.0%
Copper	36	1.0	MCL[2]	0.0%
Silver	10	0.1	MCL[2]	0.0%
Salinity Hazard	229	Very High (Sp. Cond. >2,250)	Irrigation	90%
		High (Sp. Cond. > 750)		100%
Sodium Hazard	317	Very High (SAR > 26)	Irrigation	0.3%
		High (SAR > 18)		0.6%
Boron	55	2	Irrigation	9.0%
		0.75		36%
Chloride	429	1,000	Irrigation	8.4%

* percentage of wells with one or more measurements of the parameter that exceeded the screening level

[1] refers to National Primary Drinking Water Regulations

[2] refers to National Secondary Drinking Water Regulations

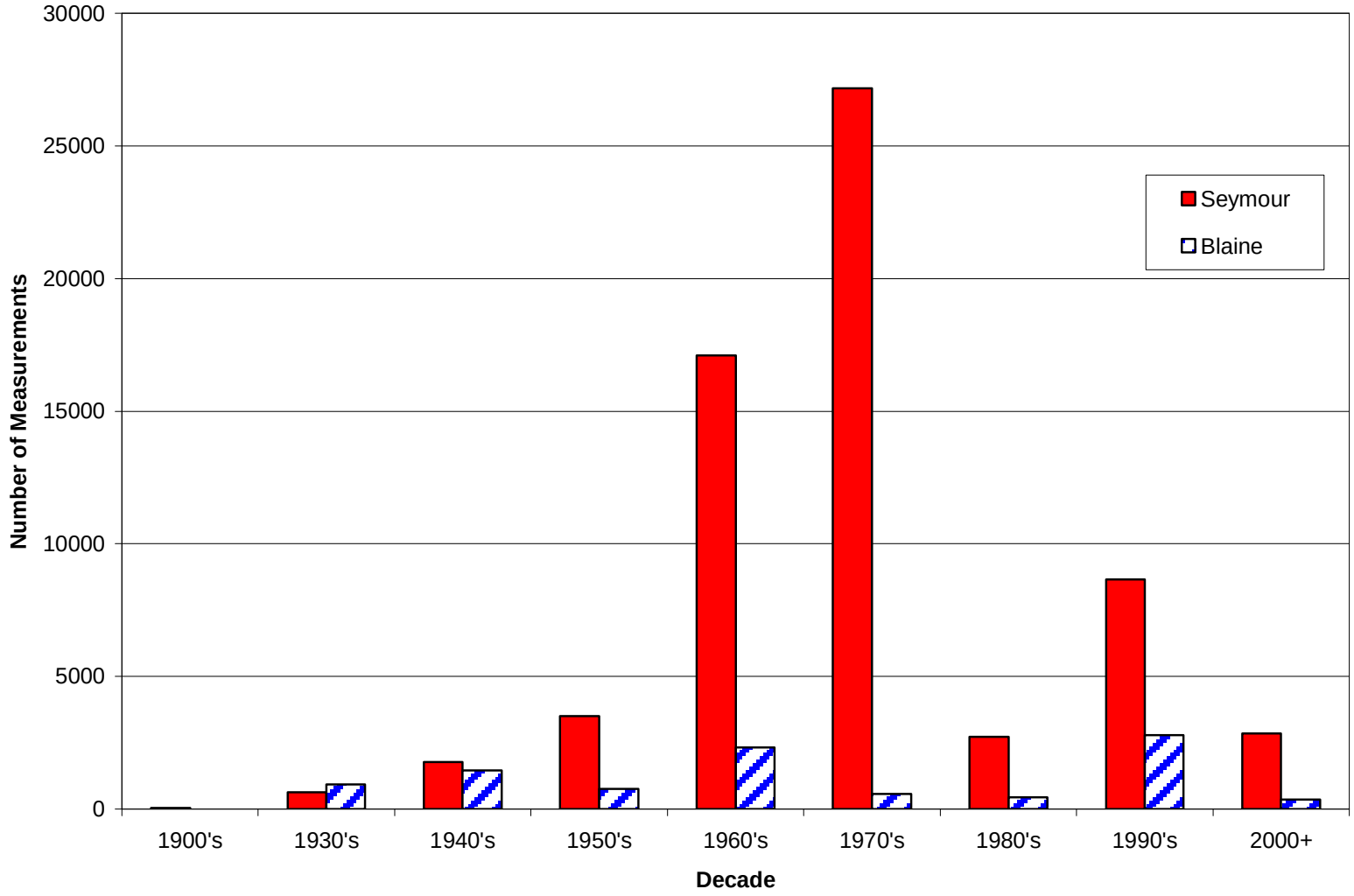

Figure 4.8.1 Temporal distribution of water quality measurements in the Seymour and Blaine aquifers.

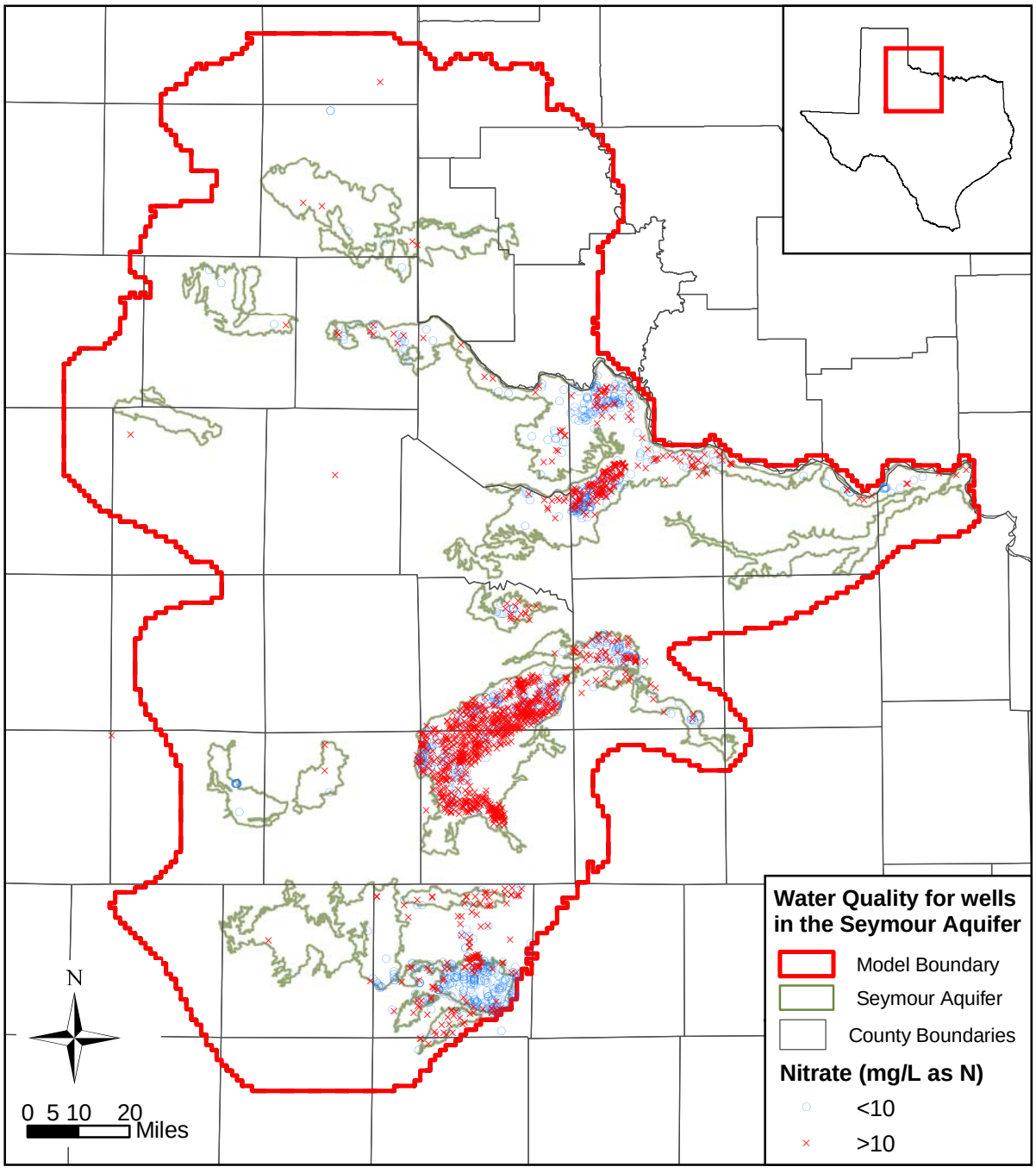

Figure 4.8.2 Nitrate concentrations in the Seymour aquifer.

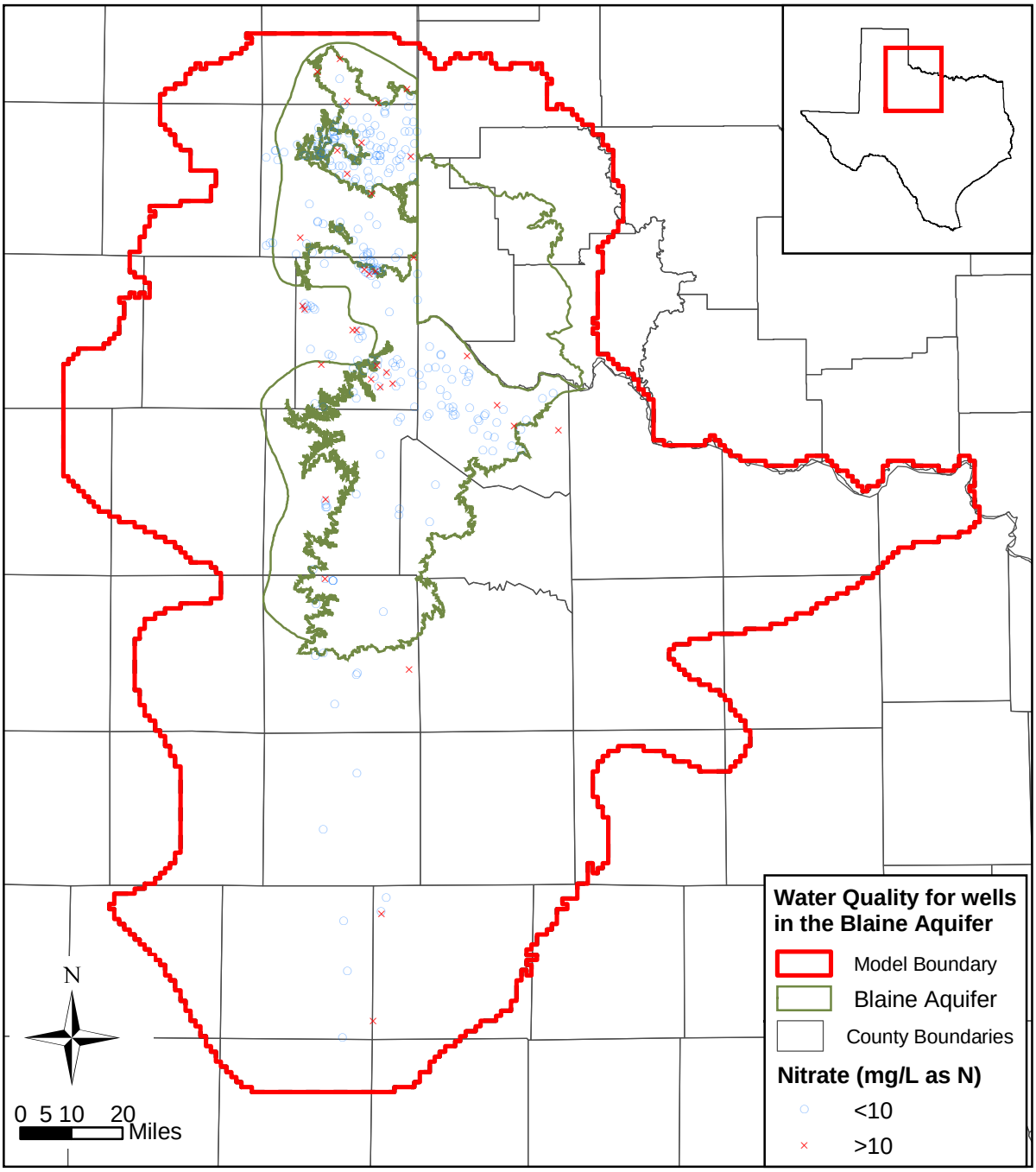

Figure 4.8.3 Nitrate concentrations in the Blaine aquifer.

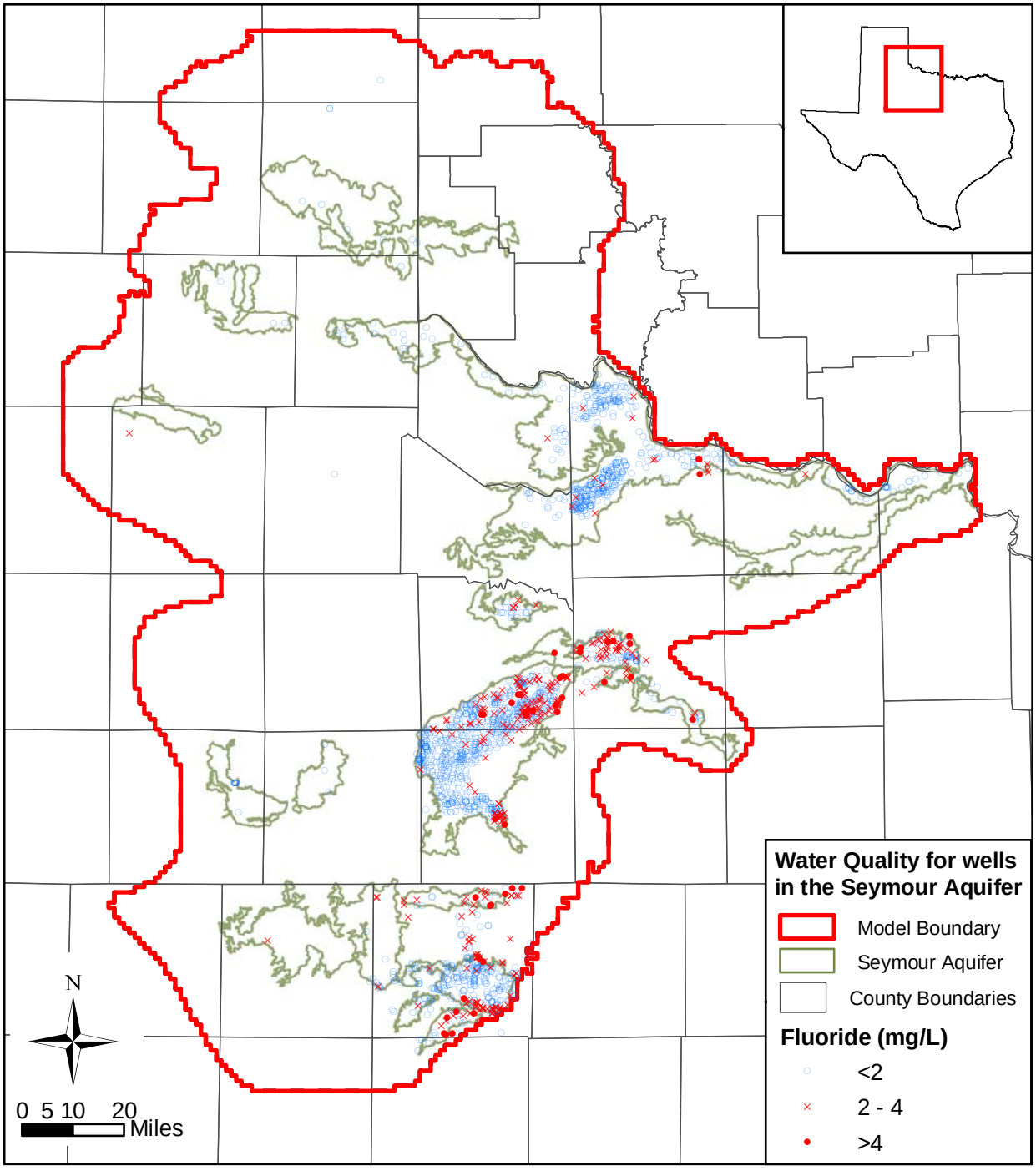

Figure 4.8.4 Fluoride concentrations in the Seymour aquifer.

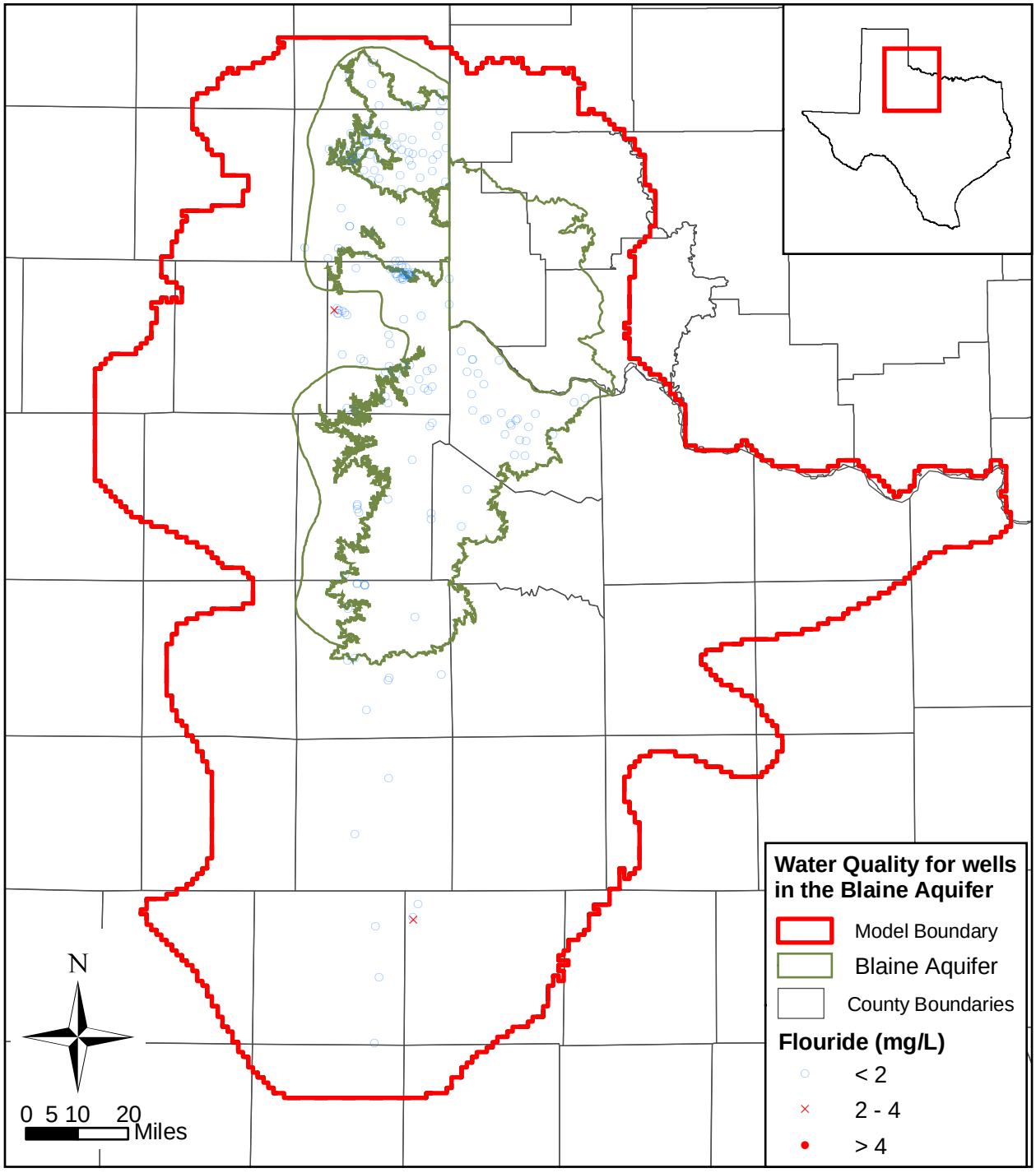

Figure 4.8.5 Fluoride concentrations in the Blaine aquifer.

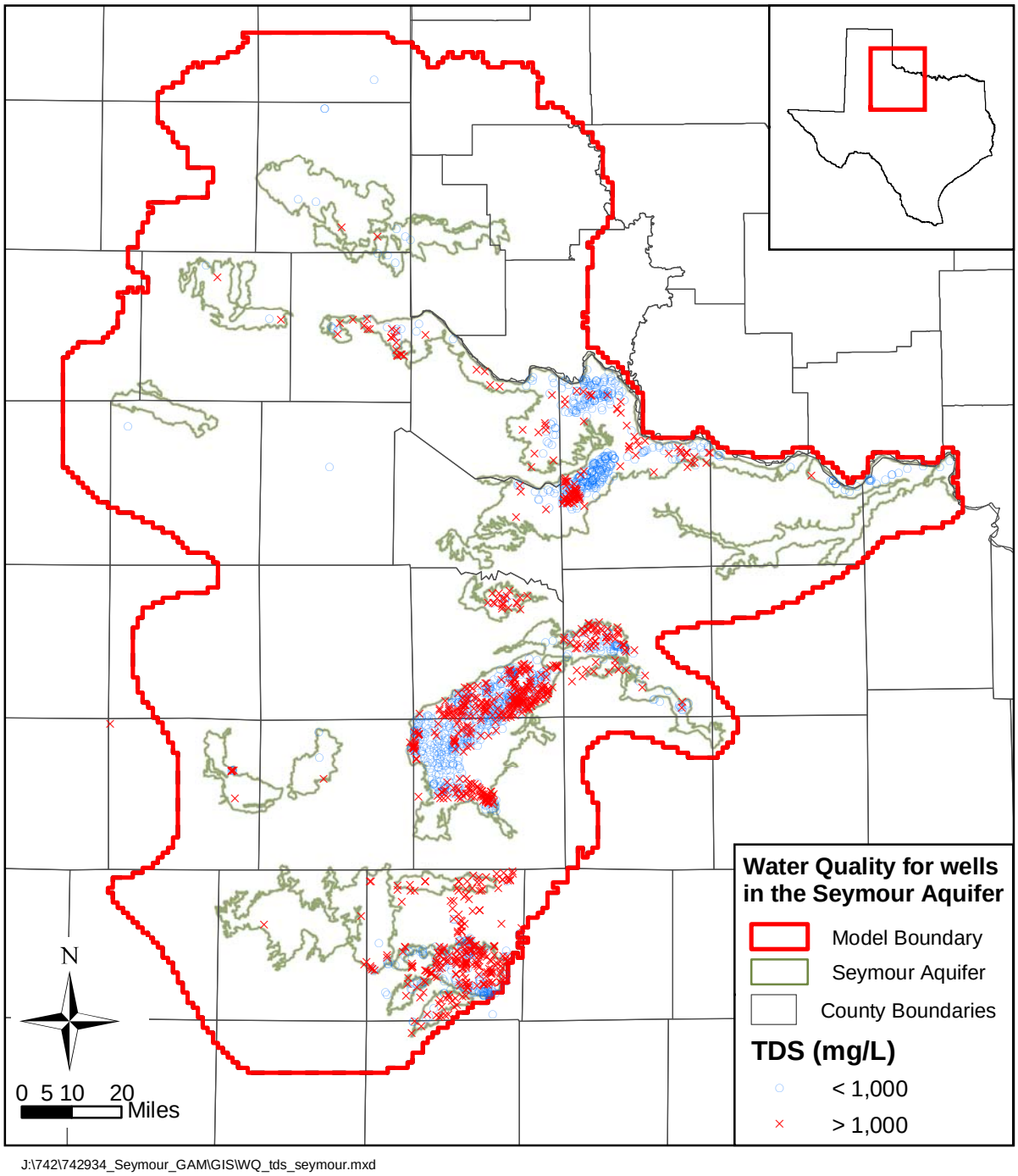

Figure 4.8.6 Total dissolved solids in the Seymour aquifer.

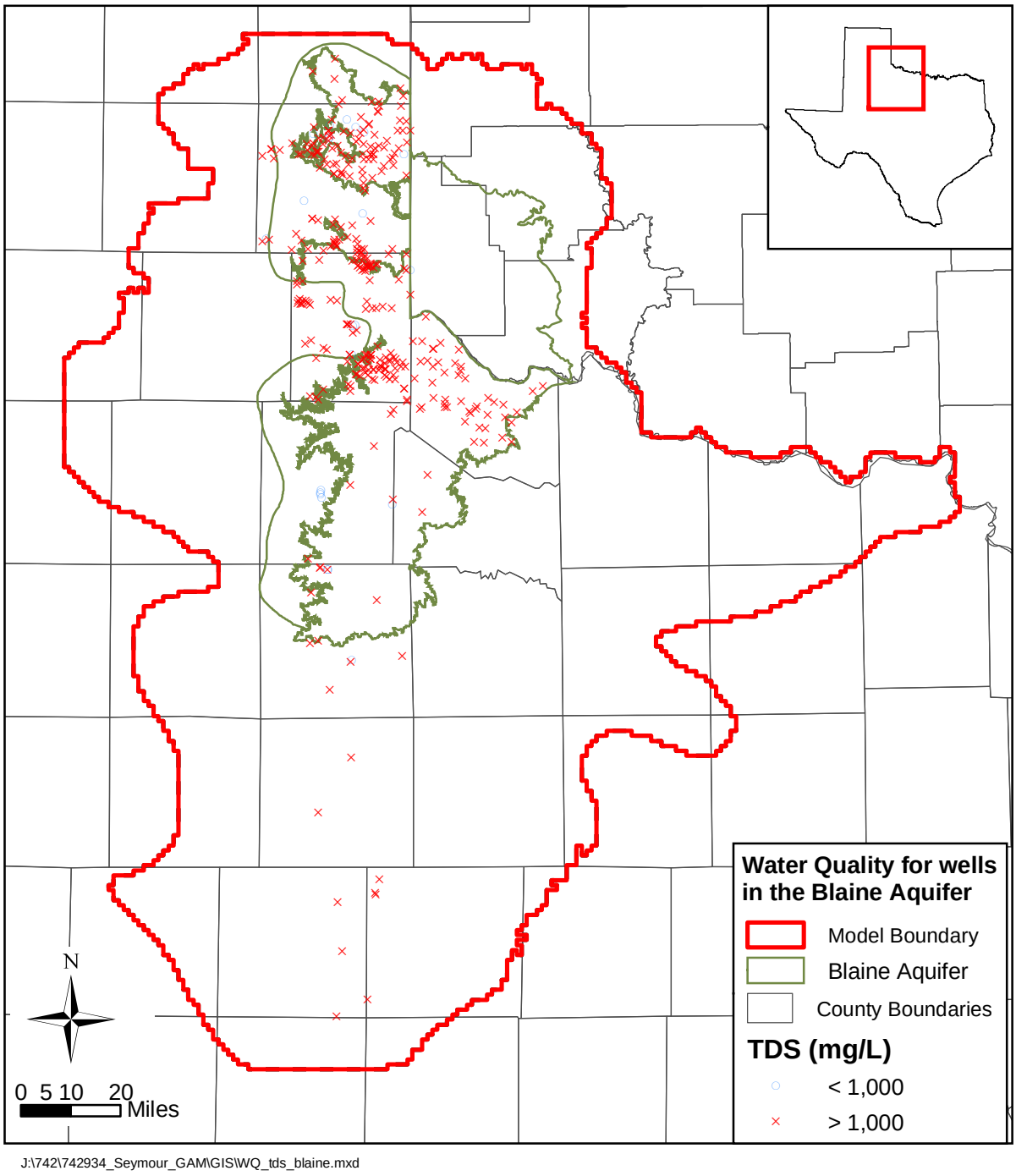

Figure 4.8.7 Total dissolved solids in the Blaine aquifer.

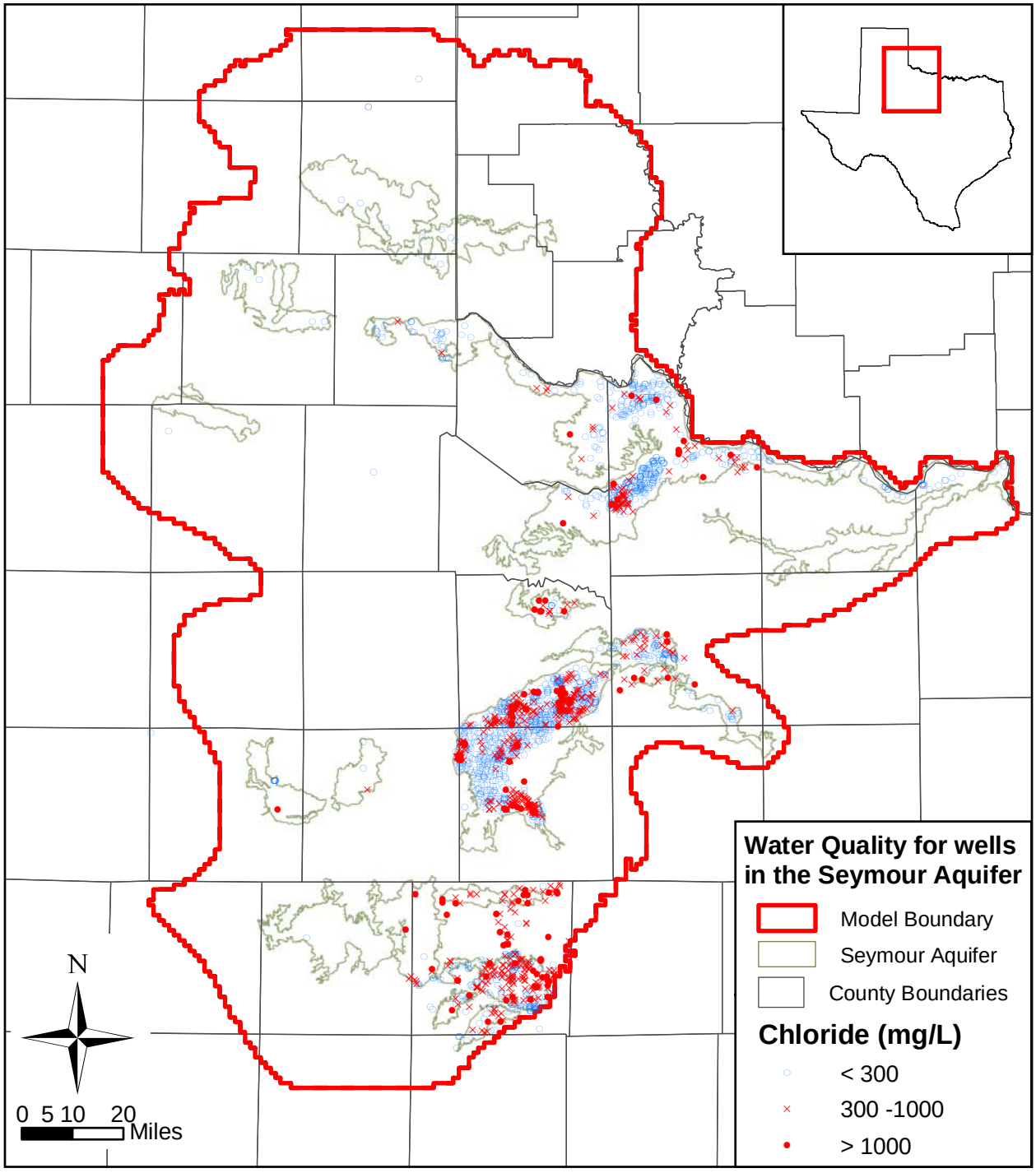

Figure 4.8.8 Chloride concentrations in the Seymour aquifer.

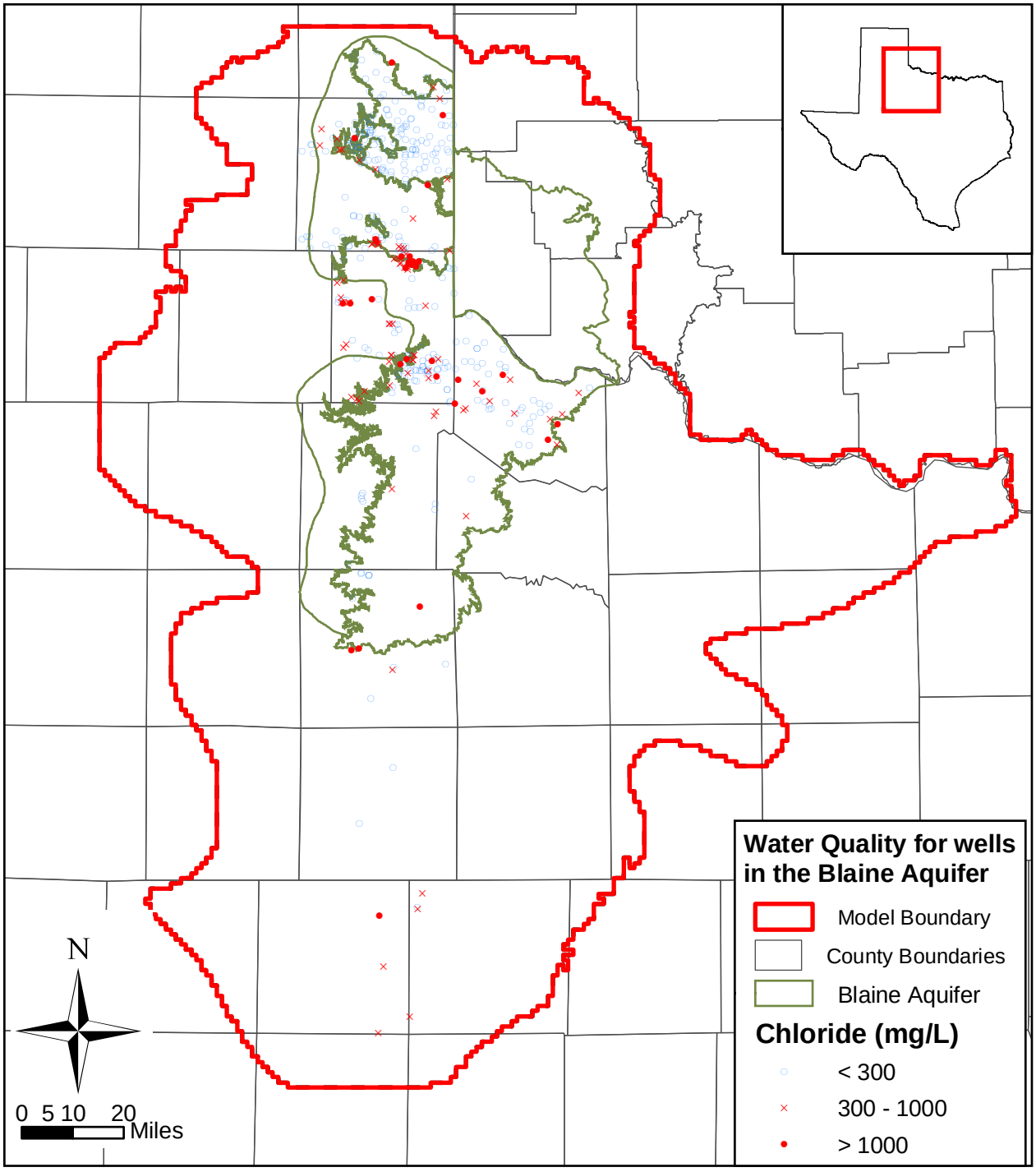

Figure 4.8.9 Chloride concentrations in the Blaine aquifer.

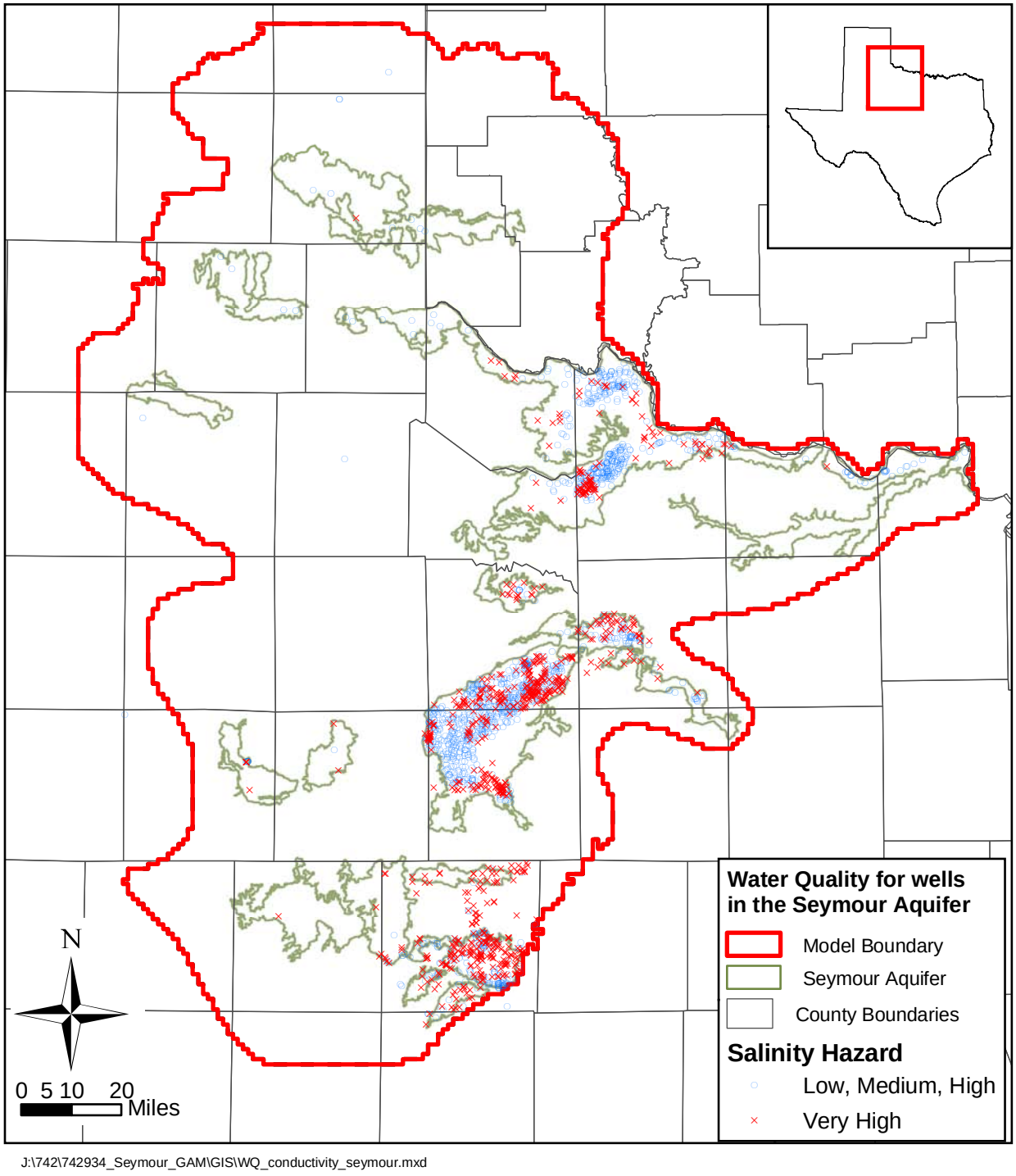

Figure 4.8.10 Salinity hazard in the Seymour aquifer.

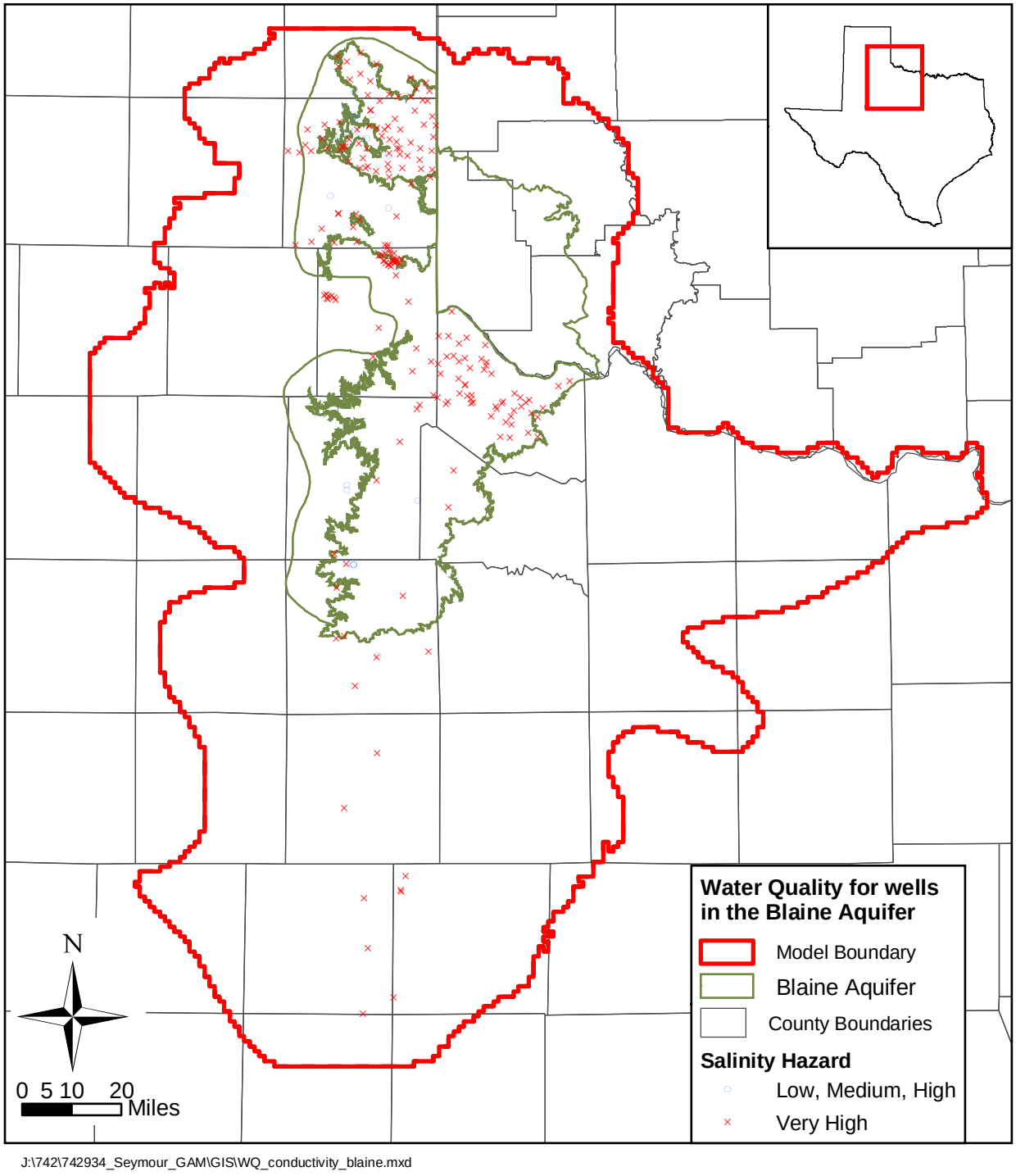

Figure 4.8.11 Salinity hazard in the Blaine aquifer.

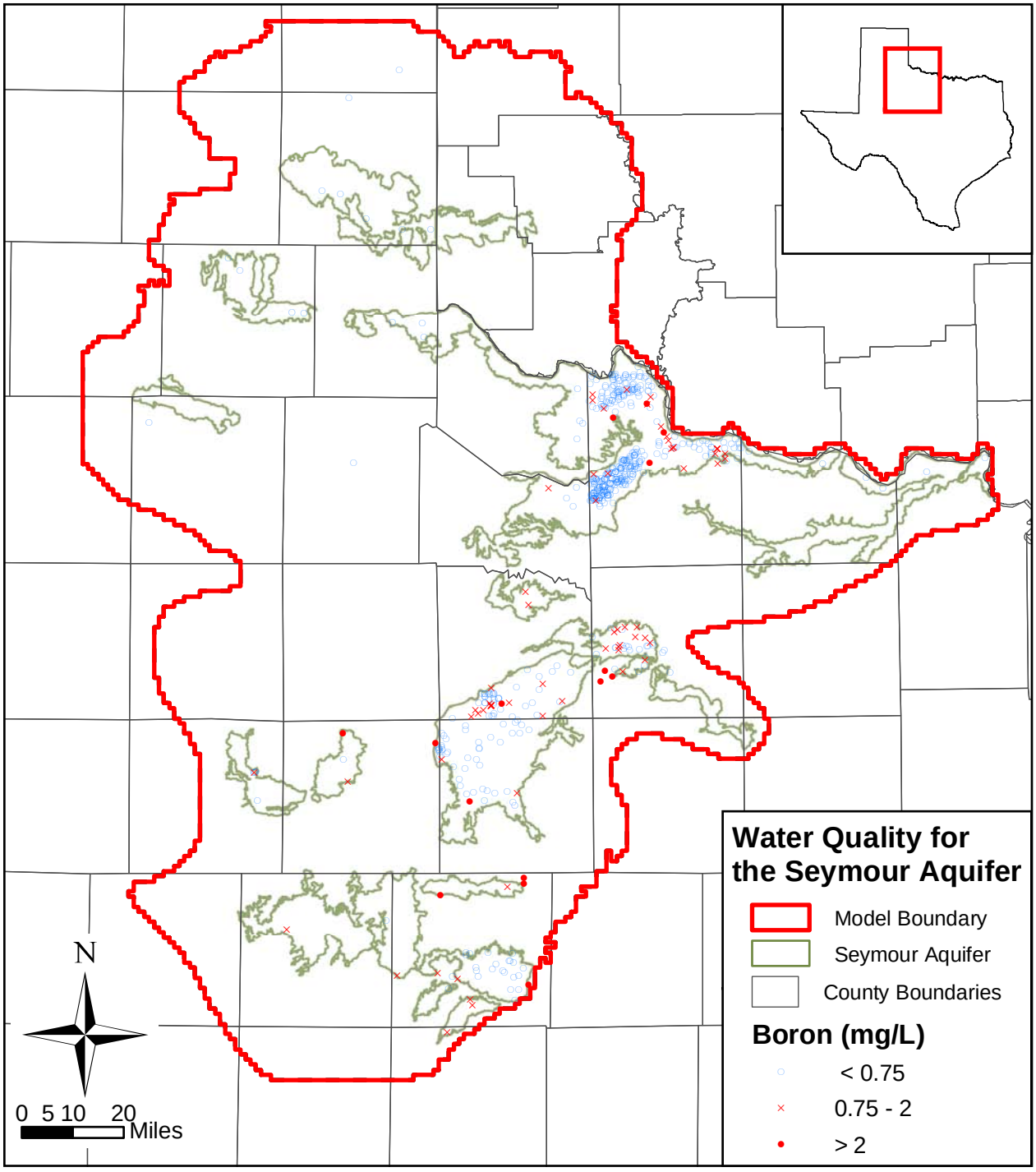

Figure 4.8.12 Boron concentrations in the Seymour aquifer.

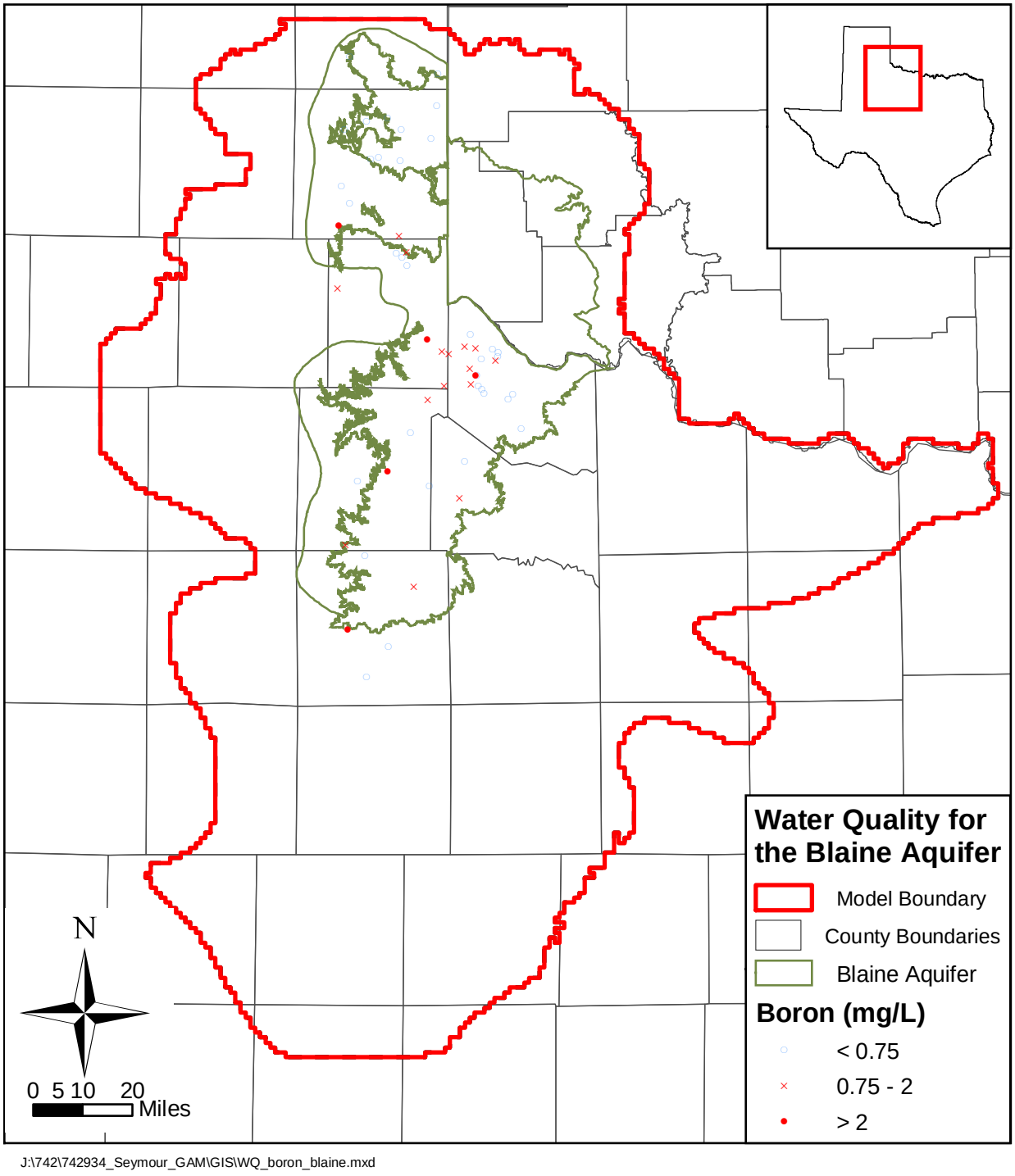

Figure 4.8.13 Boron concentrations in the Blaine aquifer.

This page intentionally left blank.

5.0 CONCEPTUAL MODEL OF GROUNDWATER FLOW FOR THE SEYMOUR GAM

The conceptual model for groundwater flow in the Seymour and Blaine aquifers is based on the hydrogeologic setting, described in Section 4.0. The conceptual model is a simplified representation of the hydrogeological features which govern groundwater flow in the aquifers. These include the hydrostratigraphy, hydraulic properties, stresses such as pumping and recharge, and the boundaries. Each of the elements of our conceptual model is described below. The schematic diagram in Figure 5.1 depicts the conceptual hydrogeologic model of groundwater flow in the Seymour and Blaine aquifers.

The conceptual model for the Seymour and Blaine aquifers defines two layers. The upper layer represents the Seymour aquifer, consisting of the Seymour Formation and other younger Quaternary alluvium. The Seymour aquifer is the most productive groundwater zone in the model. The lower layer represents the Blaine aquifer, consisting of the Blaine Formation and the Dog Creek Shale of the Pease River Group, and other shallow portions of the Permian System. Productivity of the Blaine aquifer is highly variable and productivity of the other Permian units is generally low. In addition to the Permian System, small portions of the Ogallala and Dockum formations outcrop in the westernmost edge of the active model area.

In addition to identifying the hydrostratigraphic layers of the aquifer, the conceptual model defines the mechanisms of recharge and discharge, as well as groundwater flow through the aquifer. Recharge occurs over the entire extent of the Seymour aquifer and in the outcrop portions of the Permian sediments. Additional recharge to the Permian subcrop may also occur as a result of discharge from the overlying Seymour aquifer (Figure 5.1). Cross-formational flow may redistribute groundwater between the two model layers as a result of variations in hydraulic properties, hydraulic heads, and topography (Figure 5.1).

Most of the precipitation falling on the land surface runs off into the small creeks, which discharge through major streams out of the model area. In addition to runoff, a significant portion of the precipitation is lost by evapotranspiration (ET), leaving only a small fraction of the precipitation to infiltrate into the subsurface and recharge the aquifer. Before anthropological activities, it is believed that most infiltration from precipitation to the Seymour was consumed in the vadose zone by ET. Diffuse recharge occurs preferentially in topographically higher

interstream areas. Focused recharge along streams can occur when the water table in the aquifer is below the stream-level elevation. If stream levels are lower than surrounding groundwater levels, groundwater discharges to the streams resulting in gaining streams. In the case of gaining streams, water levels in the valleys are typically close to land surface and some of the shallow groundwater in this area can be lost to evapotranspiration. Direct precipitation is the only recharge mechanism occurring in the isolated sections of the Seymour aquifer which sit at elevations higher than the stream valleys. In the younger Quaternary alluvium portion of the Seymour aquifer, focused recharge from streams and flood flow may periodically recharge the aquifer in addition to infiltration from direct precipitation.

Recharge is a complex function of precipitation, soil type, geology, water level and soil moisture, topography, and ET. Precipitation, ET, water-table elevation, and soil moisture vary spatially and temporally, whereas soil type, geology, and topography vary spatially. In addition to natural phenomena, groundwater levels are affected by pumping and man-made surface-water reservoirs and lakes which, in turn, affect recharge. Under undisturbed conditions (e.g., prior to pumping), groundwater recharge is balanced by natural groundwater discharge. It is reported that prior to significant land clearing and farming, the Seymour was not a productive aquifer with adequate saturated thickness to support pumping. However, after land use changes were made, ET losses as a result of vegetation decreased resulting in the evolution of adequate saturated thickness in the Seymour.

When the Seymour developed an adequate saturated thickness to support pumping, aquifer development began. With aquifer development, the water removed by pumping is supplied through decreased groundwater storage (i.e., decreased water levels), reduced groundwater discharge, and sometimes increased recharge. If pumping stays relatively constant, a new steady-state condition will be established. In this new equilibrium, the source of the pumped water will be drawn completely from either reduced discharge or increased recharge with the latter component usually being relatively small. Bredehoeft (2002) terms these two volumes as capture. Bredehoeft (2002) also defined sustainable yield (pumped flow rate) as being equal to the rate of capture. For a given production volume to be sustainable (i.e., groundwater levels return to a new steady-state), there must be enough groundwater capture volume to balance the pumping volume. If pumping exceeds the potential available capture volume for a basin, that basin will experience water-level declines until there are no recoverable

groundwater reserves. This is equivalent to the 'unstable' basin concept discussed by Freeze (1971).

The sources of capture as a result of pumping of the Seymour are expected to be primarily from capture of aquifer discharge with little to no potential for capture of additional recharge. Because the majority of the streams in the model domain are in valleys at elevations beneath the neighboring Seymour Formation, little or no increased capture potential can be expected as a result of pumpage from these areas. Pumpage from the Blaine Formation, on the other hand, may result in increased capture of stream discharge. Lowering the water table, as a result of pumping, beneath the extinction depth of phreatophyte root systems may lead to discharge capture through the reduction in groundwater ET. The distribution of rooting depths throughout the Seymour aquifer is not well characterized and difficult to define for 1-mile by 1-mile grid cells, however. The unconfined-confined system of the Blaine aquifer will exhibit a delayed water-table response in the outcrop to pumpage in the confined sections.

Our conceptual model of the Seymour and Blaine aquifers is that of stable groundwater aquifers where historical groundwater pumpage volumes can be satisfied by groundwater capture. We do not believe that there is much potential for capture of additional recharge as a result of pumping in the Seymour because the areas of high recharge (i.e., sandy soils in topographic highs) are generally distant from areas of natural discharge (i.e., topographic lows at the edge of the formation) from the Seymour (R.W. Harden and Associates, 1978).

Groundwater from the Seymour aquifer discharges to springs and seeps, local creeks, and major streams throughout the area, contributing to the baseflow of the streams. Springs and seeps occur along much of the boundary of the Seymour Formation. Discharge directly to streams occurs in the younger Quaternary alluvium portions of the Seymour aquifer where the aquifer is in direct contact with the streams. In addition, discharge from the Seymour aquifer occurs by cross-formational flow into the underlying units. Cross-formational flow from the Seymour aquifer is expected to be lowest in the eastern portion of the model domain where the Seymour aquifer overlies the Wichita and Clear Fork groups of the Permian System. Some measurable discharge from the Seymour to the Bullwagon Dolomite Member of the Vale Formation within the Clear Fork Group may occur in Jones County (Price, 1978). In the north-central region of the model domain, where the Seymour aquifer overlies the Blaine aquifer,

appreciable, localized cross-formational flow to the Blaine may occur, depending largely on the thickness of the Dog Creek Shale and the location of solution channels within the Blaine Formation. The largest fraction of natural discharge, however, is anticipated to be ET, due to the shallow nature of the water table and existence of phreatophytes throughout portions of the aquifer (R.W. Harden and Associates, 1978). This is expected to be especially important in the younger Quaternary alluvium portions of the Seymour aquifer where depths to the water table are smallest and phreatophyte density is highest.

Groundwater flow within the Seymour aquifer pods is controlled by topography, structure, and permeability variation. A map showing the inferred groundwater flow pattern within a portion of pod 7 in Haskell and Knox counties is shown in Figure 4.3.6. This figure shows the high recharge area in the topographically high, sand hills region in the southwestern portion of the pod. Groundwater flow generally follows the topographical gradient along the major axis of the pod and discharges laterally to springs, seeps, and alluvium leading to the Brazos River to the north and Lake Creek to the south. Similar mechanisms can be expected within the majority of the other pods with the exception of areas consisting of younger Quaternary alluvium where flow will be more directly governed by streams.

The boundaries for the Seymour GAM are represented conceptually in Figure 5.1. The boundary beneath the Seymour aquifer is the erosion surface of the Permian System through which some groundwater discharges. The boundary beneath the Blaine aquifer in the northern-central portion of the model domain corresponds to the Flowerpot Shale Formation (considered a no-flow boundary) at the base of the Pease River Group. The boundary beneath the lower model layer describing the remaining portions of the Permian System is assumed to represent horizontal flow lines (considered a no-flow boundary).

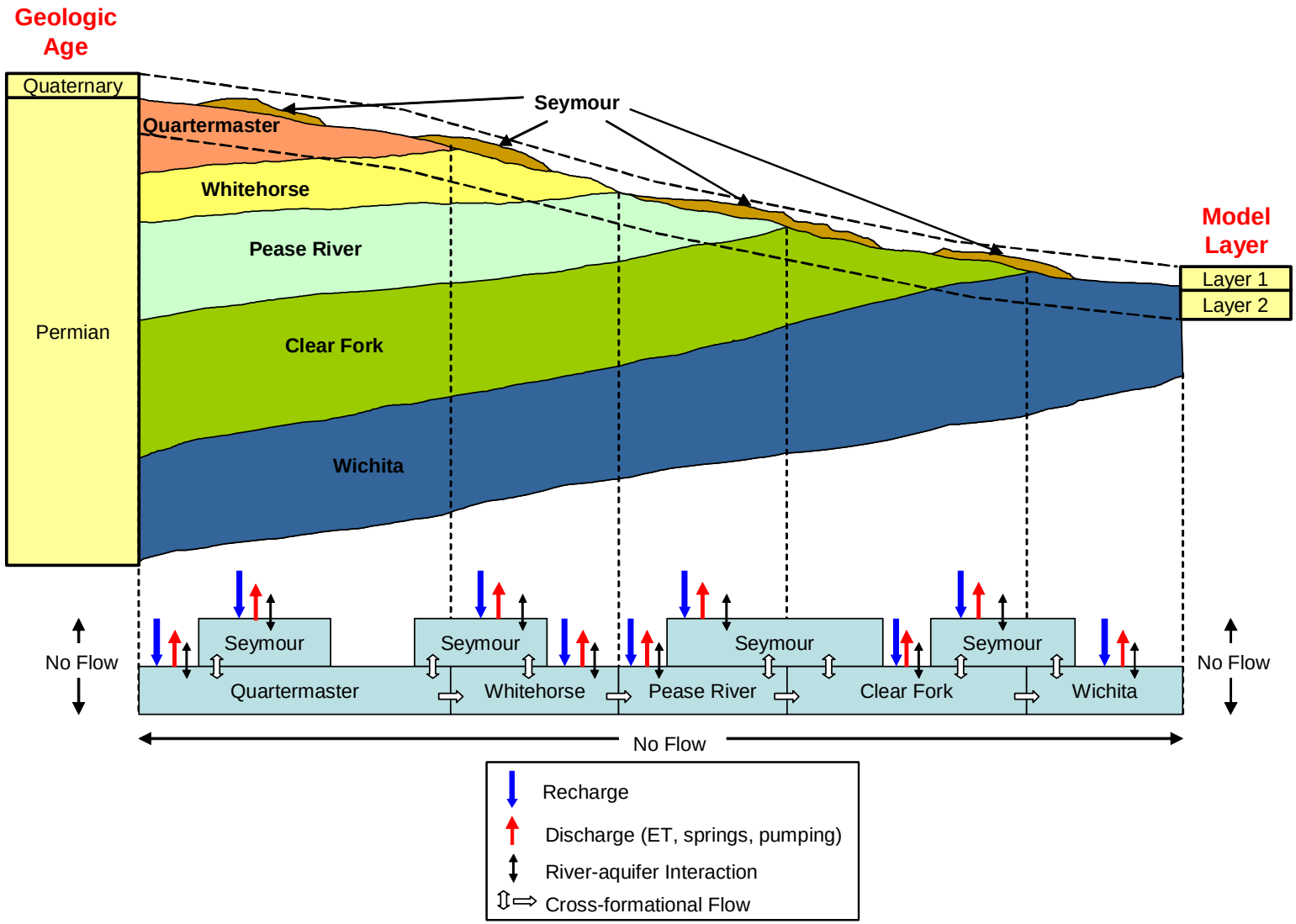

Figure 5.1 Conceptual groundwater flow model for the Seymour GAM.

This page intentionally left blank.

6.0 MODEL DESIGN

Model design represents the process of translating the conceptual model for groundwater flow in the aquifer (Section 5) into a numerical representation which is generally described as the model. The conceptual model for flow defines the required processes and attributes for the code to be used. In addition to selection of the appropriate code, model design includes definition of the model grid and layer structure, the model boundary conditions, and the model hydraulic parameters. Each of these elements of model design and their implementation are described in this section.

6.1 Code and Processor

The code selected for the GAMs developed by or for the TWDB is MODFLOW-96 (Harbaugh and McDonald, 1996). MODFLOW-96 is a multi-dimensional, finite-difference, block-centered, saturated groundwater flow code which is supported by enhanced boundary condition packages to handle recharge, ET, streams (Prudic, 1988), springs, and reservoirs (Fenske et al., 1996). Difficulties were encountered in model convergence for some sensitivity cases when using the solvers available in MODFLOW-96. Using the GMG solver (Wilson and Naff, 2004) written for MODFLOW-2000 (Harbaugh et al., 2000) ameliorated these convergence issues. Therefore, MODFLOW-2000 was used for all calibration, verification, and predictive simulations for the Seymour GAM.

The benefits of using MODFLOW for the Seymour GAM include: (1) MODFLOW incorporates the necessary physics represented in the conceptual model for flow described in Section 5 of this report, (2) MODFLOW is the most widely accepted groundwater flow code in use today, (3) MODFLOW was written and is supported by the USGS and is public domain, (4) MODFLOW is well documented (McDonald and Harbaugh, 1988; Harbaugh and McDonald, 1996), (5) MODFLOW has a large user group, and (6) there are a plethora of graphical user interface programs written for use with MODFLOW.

To the extent possible, we have developed the MODFLOW data sets to be compatible with Processing MODFLOW for Windows (PMWIN) Version 5.3 (Chiang and Kinzelbach, 1998). The size of the GAM and the complexity of the Seymour GAM application (e.g., number

of stream segments) precludes 100-percent compatibility with PMWIN, as well as many other interfaces.

We have executed the model on x86 compatible (i.e., Pentium or Athlon) computers equipped with the Windows 2000 operating system. MODFLOW is not typically a memory-intensive application in its executable form. However, if any preprocessor (such as PMWIN) is used for this size and complexity of model, at least 256MB of RAM is recommended.

6.2 Model Layers and Grid

Consistent with the model hydrostratigraphy described in Section 4.1 and the conceptual flow model detailed in Section 5, the Seymour GAM is divided into two model layers. The top layer (layer 1) consists of the isolated pods of the Seymour aquifer which are composed of sediments of the Seymour Formation and other younger Quaternary alluvium. The bottom layer (layer 2) consists of the upper portion of the Permian sediments, including the Blaine aquifer where present, which underlie the Seymour aquifer. From east to west, these Permian sediments make up the Wichita, Clear Fork, Pease River, and Whitehorse groups and the Quartermaster and Ogallala formations. The model layers are shown with the corresponding hydrostratigraphic units in Figure 5.1.

The upper boundary of the model is defined by ground surface. Where the Blaine aquifer is present, the lower boundary of the model is defined by the base of the Blaine aquifer, which is confined from below by the Flowerpot Shale. Where the Blaine is not present, an arbitrary base was defined assuming a uniform thickness of 500 feet for the remainder of layer 2. In order to avoid an abrupt change in the thickness of layer 2 at the eastern edge of the Blaine aquifer, the thickness of layer 2 was gradually increased to 500 feet across 10 miles on both sides of the aquifer's eastern edge (see Section 4.2). A thickness of 500 feet was selected because it was considered large enough to represent the Permian units in the sense that small changes in water-level elevation would not greatly affect the transmissivity within the layer.

MODFLOW requires a rectilinear grid. Typically, one axis of the model grid is aligned parallel to the primary direction of flow. While no single flow direction could be defined for all of the Seymour pods, a general primary flow direction following the topographical dip over the model domain from west to east was assumed. The model area was determined by imposing the

preceding constraints with the additional constraint of minimizing the number of model grid cells intersecting the Seymour aquifer outline. In this way, an attempt was made to minimize the number of model grid cells containing only a small portion of the Seymour aquifer. The model grid origin is located at GAM coordinates 20,093,600 feet north and 4,554,160 feet east with the x-axis oriented east-west. The GAM standard requires that grid cells be squares with a uniform lateral dimension of no greater than 1 mile (area of 1 square mile). The model has 180 columns and 208 rows for a total of 37,440 grid cells per layer. As discussed below, not all of these grid cells are active in the model. Figure 6.2.1 shows the entire model grid and includes an inset with an enlargement of Foard County to demonstrate the model grid at the county scale.

The active area of layer 1 (the Seymour aquifer) was defined by intersecting the layer grid with the outline of the aquifer. If the aquifer outline covered 50 percent or more of a grid cell area, that grid cell was defined as active. Because MODFLOW is a finite-difference model where flow occurs only through grid cell faces, groups of four or fewer Seymour blocks isolated laterally from other cell faces were also made inactive. This resulted in the removal of a total of 40 cells. The active area of layer 2 was determined by the hydrologic boundaries surrounding the Seymour and Blaine aquifers. After clipping the layers to their proper dimensions, layers 1 and 2 have 3,436 and 20,001 active grid cells, respectively. The total number of active grid cells in the model is 23,437.

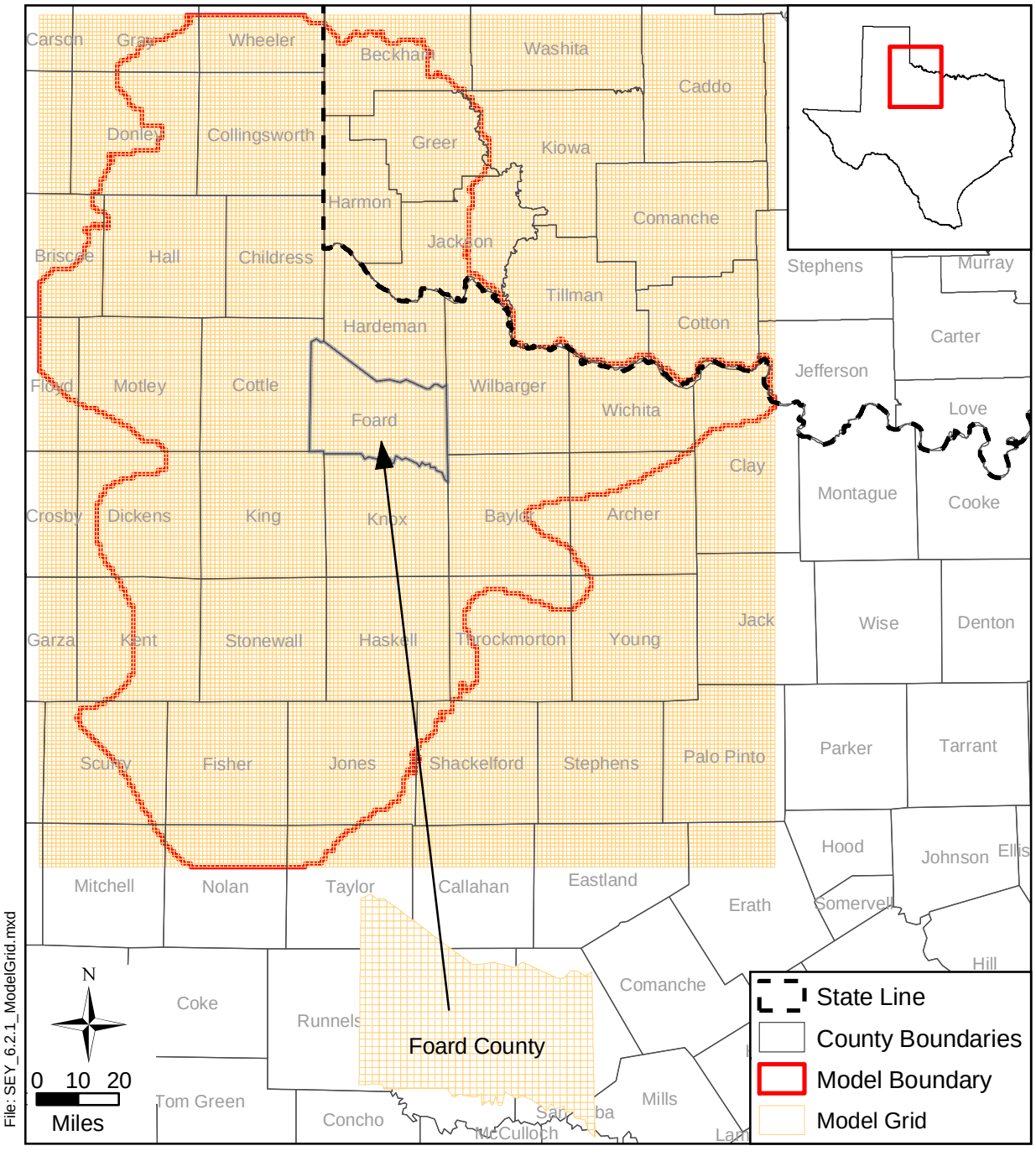

Figure 6.2.1 Model grid for the Seymour GAM.

6.3 Boundary Condition Implementation

A boundary condition can be defined as a constraint put on the active model grid to characterize the interaction between the active simulation grid domain and the surrounding environment. There are generally three types of boundary conditions: specified head (First Type or Dirichlet), specified flow (Second Type or Neumann), and head-dependent flow (Third Type or Cauchy). The no-flow boundary condition is a special case of the specified flow boundary condition.

Boundaries can be either time independent or time dependent. An example of a time-dependent boundary is a pumping flow boundary (e.g., grid cell with a well) or a reservoir stage elevation. Because many boundaries require time-dependent (transient) specification, the stress periods used by MODFLOW must be specified. A stress period in MODFLOW defines the time period over which boundary and model stresses remain constant. Each stress period may have a number of computational time steps which are some fraction of the stress period. For the transient model calibration and verification periods, the stress periods were set at one month. Therefore, transient boundaries in the model cannot change over a period of less than one month. For the predictive period of 2000 through 2050, yearly stress periods were used until the last ten years, which includes the 76-month drought-of-record, when monthly stress periods were used.

Boundaries requiring specification include: lateral and vertical boundaries for each layer, surface-water boundaries, recharge boundaries, and discharge boundaries, including ET and pumping. Specified flow (no-flow, Second Type) boundary conditions were assigned to the lateral and vertical boundaries. Surface-water boundaries, including streams and springs (drains), are head-dependent flow boundaries (Third Type). Recharge is a specified flow boundary (Second Type). ET is a head-dependent flow boundary (Third Type). Pumping discharge is a specified flow boundary (Second Type).

Figures 6.3.1 and 6.3.2 show the active and inactive grid cells along with the model boundary conditions for model layers 1 and 2, respectively. Implementation of the boundary conditions for the Seymour GAM is described below.

6.3.1 Lateral Model Boundaries

For layer 1 (the Seymour aquifer), the lateral model boundaries have been defined by the extents of the formation. Beyond the extents of the Seymour aquifer outline, grid cells in layer 1 were set as inactive, creating a no-flow boundary laterally. For layer 2, numerous hydrologic divides – either drainage divides at topographical highs or river divides at topographical lows – were used to define the lateral model boundaries. Where these hydrologic divides may not always represent regional hydrologic boundaries, the boundary was placed at a great enough distance (tens of miles) from the Seymour and Blaine aquifers that any underflow beneath these divides was assumed to have an insignificant effect on the flow systems of the Seymour and Blaine aquifers.

6.3.2 Vertical Boundaries

The model has a no-flow boundary at the bottom of layer 2. Where the Blaine aquifer is present, this no-flow boundary represents the Flowerpot Shale of the Pease River Group (Smith, 1970). Elsewhere, this no-flow boundary is arbitrary but exceeds the assumed depth extent of primarily lateral flow within the Permian sediments. The recharge and ET boundary conditions that define the top of the model are discussed in Section 6.3.4.

6.3.3 Surface Water Implementation

Surface water acts as a head-dependent flow (Third Type) boundary condition for the top boundary of the active model grid cells. The stream package (Prudic, 1988) is a head-dependent flow boundary condition that offers a first-order approximation of surface water/groundwater interaction. The stream-routing package allows for stream-related discharge during gaining conditions and for stream-related recharge during losing conditions. When pumping affects water levels near stream/aquifer connections, streams may change from gaining to losing or become more strongly losing. Although several reservoirs are located within the model area, they were not included in the model because they do not interact with the Seymour or Blaine aquifers.

The stream-routing package requires designation of segments and reaches. A reach is the smallest division of the stream network and is comprised of an individual grid cell. A segment is a collection of reaches which are contiguous and do not have contributing or diverting

tributaries. In MODFLOW, the hydraulic connection (conductance) between the stream and the aquifer must be defined.

INTERA developed a GIS-based method for creating the reach and segment data coverages for MODFLOW. Figures 6.3.1 and 6.3.2 show the grid cells that contain stream reaches in the model domain. Required physical properties of the reaches, including stream width, bed thickness, and roughness, are taken from the EPA River Reach dataset (http://www.epa.gov/region02/gis/atlas/rf1.htm).

The stream-routing package also requires specification of a stream flow rate at the starting reach of each headwater segment at each stress period. For steady-state conditions and the historical period, no representative stream gage data exist for the majority of the stream segments. For the steady-state simulation, mean flow rates from the EPA RF1 dataset were used to specify the flow rate entering each model headwater segment. The EPA RF1 dataset contains mean flow rates estimated along the entire stream and coinciding with all of the modeled stream segments.

For the transient simulations, stream flows are based on historical records. However, because the stream gage coverage is sparse, stream flow rates required estimation at the majority of the stream segments. The approach employed to develop ungaged stream segment flow rates has the following assumptions: (1) gages in close proximity behave similarly, (2) the RF1 average stream segment stream flow estimates are accurate, (3) a gage's distribution of monthly stream flow is lognormal, and (4) the standard deviation of the log of the monthly flow rate at an ungaged location is equal to the standard deviation of the log of the monthly flow rate at a nearby gaged location. Assumptions 1 through 3 have been verified to generally hold for the model region. Assumption 4 cannot be definitively established in the current domain, due to a lack of data for cross validation.

After conducting several simulations it became clear that the model was insensitive to stream flow. In the stream package, discharge to or from a stream cell is governed by the gradient (the difference between the stream stage and the water-level elevation in that cell) and the streambed conductance. In general, changes in the stream stage resulting from changes in the stream flow were very small compared to the gradient as a whole. It was, therefore, deemed

unnecessary to pursue more rigorous methods of implementing stream flow such as those being studied by the USGS (Lanning-Rush, 2002).

To calculate the flow rates at each monthly stress period for the ungaged stream segments, the monthly distribution of log flow rate at the gaged stream locations were constructed and the standard deviation of that distribution was calculated. From the EPA RF1 dataset, the mean flow rates for all segments are obtained. If, for stress period one, the gaged monthly stream flow was equal to the 75^{th} percentile of the distribution, the mean flow rate from the EPA RF1 dataset was used with the standard deviation taken from the actual gaged flow distribution to estimate the 75^{th} percentile flow rate at the ungaged segment. This technique maintains the proper magnitude of flows at ungaged locations as constrained by the EPA RF1 mean flow estimates while superposing the flow variability based upon the nearest gaged data.

Spring discharge records were reviewed for application in the Seymour GAM as drain boundary conditions (Type 3). Table 4.5.1 summarizes the documented springs in the model discharging at greater than 100 gpm. The cumulative effect of the numerous spring and seeps is unknown and will be evaluated. Therefore, an attempt to include all documented springs in the model domain was made. The lateral scale of the grid blocks resulted in many springs sharing a grid block with another spring or coinciding with stream cells. Springs that were coincident with stream cells were not included in the model because streams provide a sufficiently similar type of boundary condition. For multiple springs occurring in one gridblock, the minimum elevation was used and only one drain boundary condition was applied to that cell. This resulted in a total of 253 drain boundary conditions being included in the model. The elevation of the drain was calculated by taking the elevation from the 30-meter DEM at the reported spring location.

6.3.4 Implementation of Recharge and Evapotranspiration

Because an evaluation of groundwater availability is largely dependent upon recharge (Freeze, 1971), it is an important model input parameter warranting careful examination and meaningful implementation. In typical model applications, recharge is either homogeneously defined as a percentage of the yearly average precipitation or calibrated as an unknown parameter. Unfortunately, recharge and hydraulic conductivity can be correlated parameters preventing independent estimation when using only head data constraints. Another compounding problem is that recharge is a complex function of precipitation rate and volume,

soil type, water level and soil moisture, topography, and ET (Freeze, 1969). Precipitation, ET, water-table elevation, and soil moisture are areally and temporally variable. Soil type, geology, and topography are spatially variable. For the GAM, recharge requires specification for steady-state conditions, transient conditions from 1980 through 1999, and transient drought of record and average conditions from 2000 through 2050. Reliable tools for specification of recharge at the watershed scale, or the regional-model scale (thousands of square miles for the GAMs) do not currently exist.

The initial approach for dealing with recharge at the scale of this model was to use SWAT (Soil Water Assessment Tool) to estimate diffuse recharge rates. SWAT was developed for the USDA Agricultural Research Service by the Blacklands Research Center in Temple, Texas. Downloads and code-specification documentation for SWAT, a public-domain model, can be found at http://www.brc.tamus.edu/swat/. SWAT provides a GIS-driven, watershed scale tool to estimate regional soil water balances, incorporating soils data (USDA/NRCS STATSGO) with the USGS Multi-Resolution Land Characteristics (MRLC) data. SWAT uses standard techniques to track water after it reaches the ground as precipitation. SWAT uses the SCS Curve Number Method (accounting for antecedent moisture conditions) to partition precipitation into runoff and infiltration. Infiltrating water either increases the soil moisture, is lost through ET, or continues down to the water table. The Hargreaves Method for estimating Potential ET was used because it only requires estimates of monthly mean minimum and maximum temperatures which are available for the study area. Average daily net radiation is available within SWAT for month and degrees of latitude. The Hargreaves Method is considered accurate for simulation periods that are equal to, or larger than, one month. This is consistent with one-month stress periods and the assumptions underlying the NRCS curve-number method for estimating runoff. The potential ET is converted to an actual ET based on the vegetation size and type (determines maximum ET) and soil water availability (determines actual ET).

SWAT is used to estimate several model inputs for MODFLOW. SWAT simulations were completed using daily timesteps with output data summarized monthly. For each month, SWAT calculates (1) the recharge rate for the recharge package, (2) the ET maximum for the ET package, and (3) the extinction depth for the ET package. The SWAT estimate of shallow recharge corresponds to recharge flux in MODFLOW. SWAT accounts for ET which may occur in the vadose zone. However, in the selected method of implementation, SWAT does not

account for groundwater transpiration. To account for groundwater ET, the "surplus" ET from SWAT (ET potential – ET actual) was applied as ET maximum in the ET package in MODFLOW. For each month simulated, SWAT calculates a rooting depth representative of the season, vegetative cover, and soil type. This rooting depth is passed through to MODFLOW as the extinction depth in the MODFLOW ET package. As a result, ET from groundwater will occur when the water table (as simulated by MODFLOW) is above the extinction depth and there is "surplus" ET for that particular stress period.

SWAT was simulated for the time period from 1980 through 1999 to coincide with the calibration and verification periods in the transient model simulation. The temporally averaged spatial distribution of recharge estimated by SWAT is depicted in Figure 6.3.3. The overall average recharge estimated by SWAT for the Seymour model layer (2.0 in/yr) was consistent with that found in the literature. However, SWAT appeared to estimate too much recharge in the valleys where the water table is near land surface and too little recharge in hills where the water table is at a greater depth. This is contrary to expected trends of higher recharge in hills and less in valleys for systems with primarily gaining streams (Meyboom, 1966; Tóth, 1966). In addition, the estimated recharge from SWAT for the Permian sediments (1.5 in/yr), which have low hydraulic conductivities, seemed to be too high. These inconsistencies likely result from the fact that SWAT fails to account for (1) differences in underlying soil permeability and (2) subsurface infiltration gradients. Therefore, the SWAT estimates of the spatial distribution of recharge were not used in the GAM. However, because the SWAT-estimated average recharge was found to be consistent with literature values and SWAT accounts for the effects of temporal variations in precipitation on recharge, the temporal variation in recharge predicted by SWAT was used in the transient GAM.

For the steady-state and transient models, recharge was determined through model calibration using an average recharge value for each layer and pod. A spatially varying recharge distribution was used for the steady-state model and, for the transient model, this spatial distribution was varied as a function of time with the monthly average from the SWAT simulations. For systems with primarily gaining streams, like the Seymour aquifer system, higher recharge can be expected to occur in hills and less recharge can be expected to occur in valleys (Meyboom, 1966; and Tóth, 1966). Accordingly, a relationship between recharge and local topography was developed. Because the base of the Seymour was considered to be

relatively smooth and a good surrogate for the regional elevation trend, the Seymour formation thickness was used as a surrogate for local topographical elevation. In the thicker (higher relative elevation) areas, the recharge was increased, and in the thinner (lower relative elevation) areas, recharge was decreased. The following equation was applied to calculate recharge on a cell-by-cell basis:

$$R_{[i,j]} = R_{AVG} \cdot \frac{\left(\Delta Z_{[i,j]} - \Delta Z_{AVG}\right) \cdot DF + \Delta Z_{AVG}}{\Delta Z_{AVG}}, \qquad 0 \le DF \le 1 \qquad (6.3.1)$$

where $R_{[i,j]}$ is the recharge for a cell, R_{AVG} is the average recharge for a pod, $\Delta Z_{[i,j]}$ is the cell thickness, ΔZ_{AVG} is the average cell thickness for a pod, and *DF* is a damping factor. When *DF* = 0, the average recharge would be used in all cells and, when *DF* = 1, recharge would vary most strongly with thickness and a thickness of zero would result in zero recharge. A *D*F of 0.75 was chosen initially for all pods. In this way, the average recharge for a pod was held constant and the recharge for a given cell was altered up or down based on the thickness of the cell with respect to the mean formation thickness of the Seymour in that pod. The variation of recharge is discussed further in Sections 8 and 9. A uniform value of recharge was used for layer 2.

Groundwater ET, as provided by the SWAT results, was input and applied as ET maximum in the model. Naturally, ET occurs at ground surface, within the vadose zone, and within the saturated zone. It is important to note that the ET maximum taken from SWAT and applied to MODFLOW is groundwater ET not vadose zone ET (which was already considered in the SWAT results). The ET surface was set to ground surface, so groundwater ET varied linearly starting from a maximum at ground surface and decreasing linearly to zero at the extinction depth. Figure 6.3.4 shows how the groundwater ET maximum, averaged over the transient period, varies across the model region. The median groundwater ET maximum for the study area was 1.2 in/yr.

The SWAT estimates of ET maximum and ET extinction depth were applied on a monthly basis from 1980 through 1999 in the transient model calibration and verification. For the steady-state model, the ET maximum estimates from the 1980 through 1999 SWAT simulation were temporally averaged for input into the MODFLOW ET package. The maximum extinction depth for each cell was used for input into the MODFLOW ET package for the steady-

state model. This is shown in Figure 6.3.5. The median rooting depth for the study area was 5.8 feet.

For the predictive simulations, the average recharge from the calibration and verification periods was used with seasonal variations. To estimate recharge during the drought-of-record, a relationship between precipitation and recharge was developed using precipitation measurements and recharge estimates from the calibration and verification periods. Recharge conditions for the drought-of-record were estimated using this precipitation-recharge relationship and the precipitation measured during the drought of record. A discussion of the drought of record is given in Section 10 (predictive simulations).

6.3.5 Implementation of Pumping Discharge

Pumping discharge is a primary stress on the steady-state, transient (1980 through 1999), and predictive (2000 through 2050) models. Pumping discharge is a cell dependent specified flow boundary. The procedural techniques used in estimating and allocating pumping are provided in Section 4.7 and Appendices C and D. For procedural details on how the historical or predictive pumping was derived, the reader is referred to those appendices. Once the pumping had been estimated for each of the seven user groups (municipal, manufacturing, power generation, mining, livestock, irrigation, and county-other), it was summed across all user groups for a given model cell (row, column, layer). This process was repeated for all active cells in the model domain for the steady-state model and for each active cell and each stress period in the transient and predictive models. As discussed above, the stress period length used in the transient simulations was one month. In the predictive simulations, a combination of yearly and monthly stress periods was used. Therefore, there are different MODFLOW well-package datasets for the steady-state, the transient, and the six various predictive models. For the transient and predictive models, the well-package datasets have a specified flow boundary condition for each stress period, for each active grid cell within which pumping occurs.

The model for the Seymour GAM consists of regularly spaced one-mile square grid cells. These cells do not coincide with county or basin boundaries. Therefore, grid cells straddling those boundaries will always be comprised of two or more counties or basins, respectively. All pumpage that is spatially distributed within a particular grid cell is summed and assigned to the centroid of that cell. For grid cells located across county boundaries, this can lead to pumpage in

one county being assigned at a centroid located in another county. This is, in fact, the case for pumpage in pod 3. Irrigation pumpage in the portion of Motley County located adjacent and directly south of Briscoe County was distributed evenly over the portions of Motley County where irrigated cropland overlay the Seymour aquifer. This pumpage was assigned at the centroids of the grid bocks straddling the boundary between these two counties. For several of these grid blocks, the centroid is located in Briscoe County. Therefore, assuming that all pumpage for a particular grid block occurs in the county containing the grid-block centroid is not always correct. Consequently, analyzing model pumpage by assigning it to the county containing the grid-block centroid will result in error. The error is exacerbated when there is a significant difference in pumpage for the counties sharing a grid block, as is the case for pumpage in Motley and Briscoe counties.

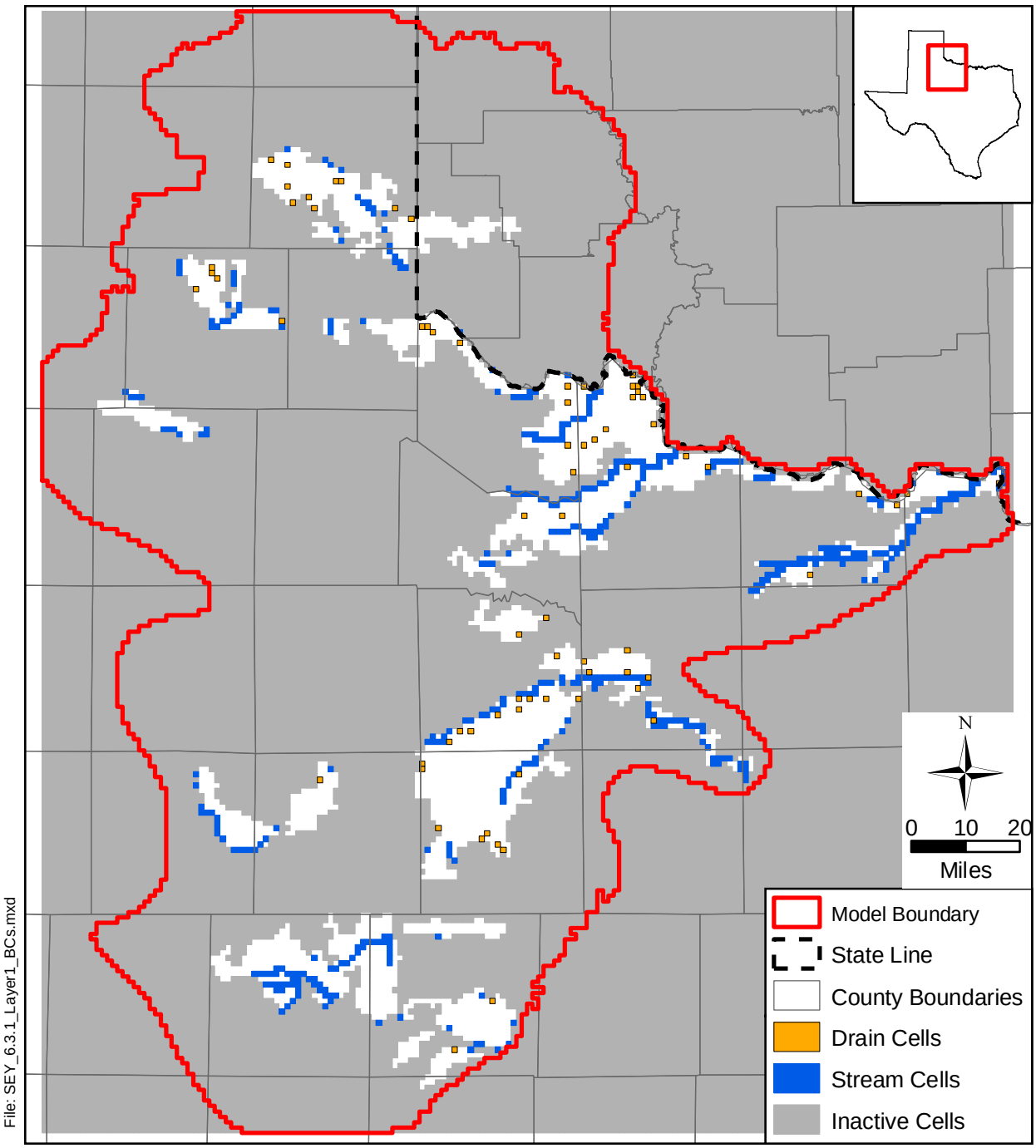

Figure 6.3.1 Layer 1 boundary conditions and active/inactive cells.

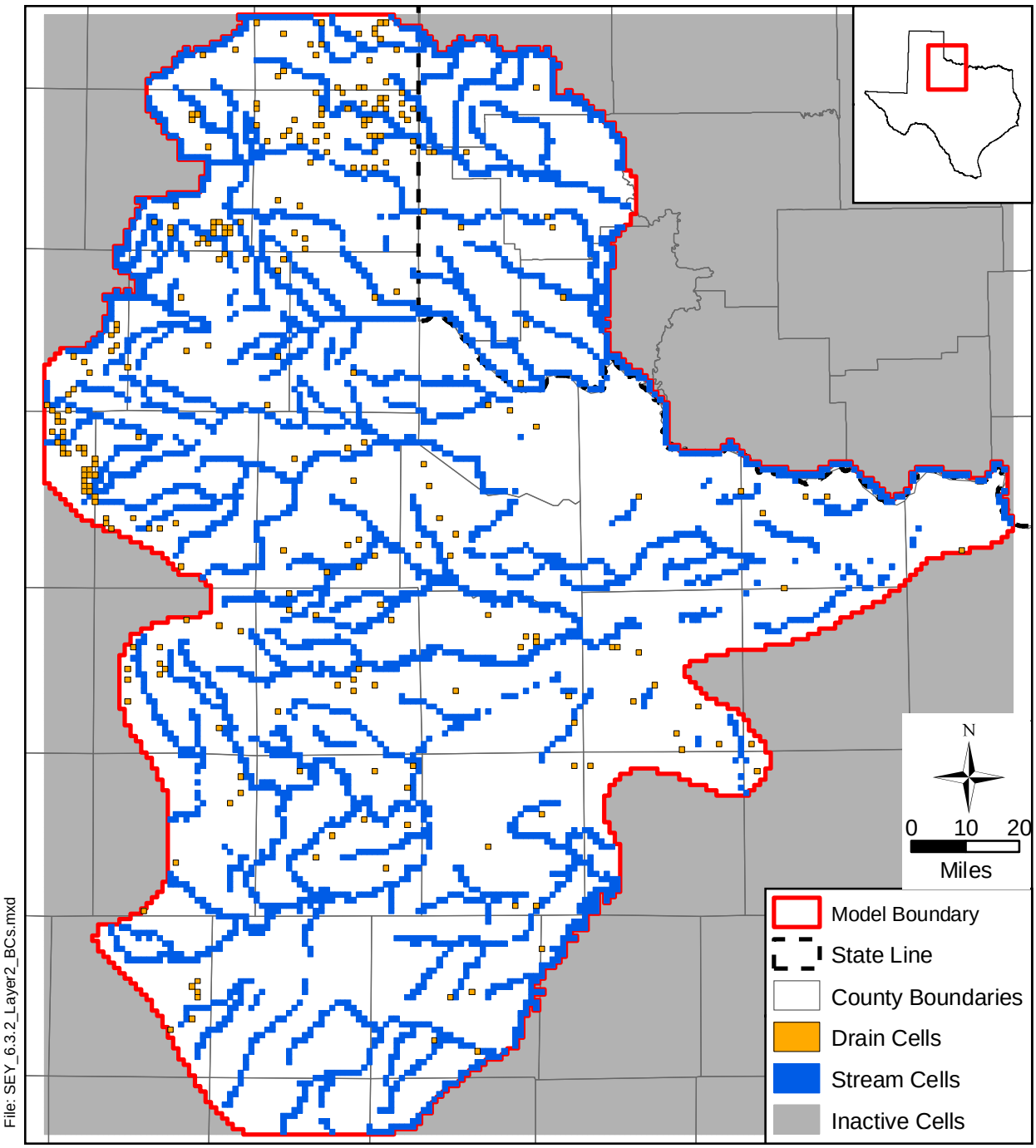

Figure 6.3.2 Layer 2 boundary conditions and active/inactive cells.

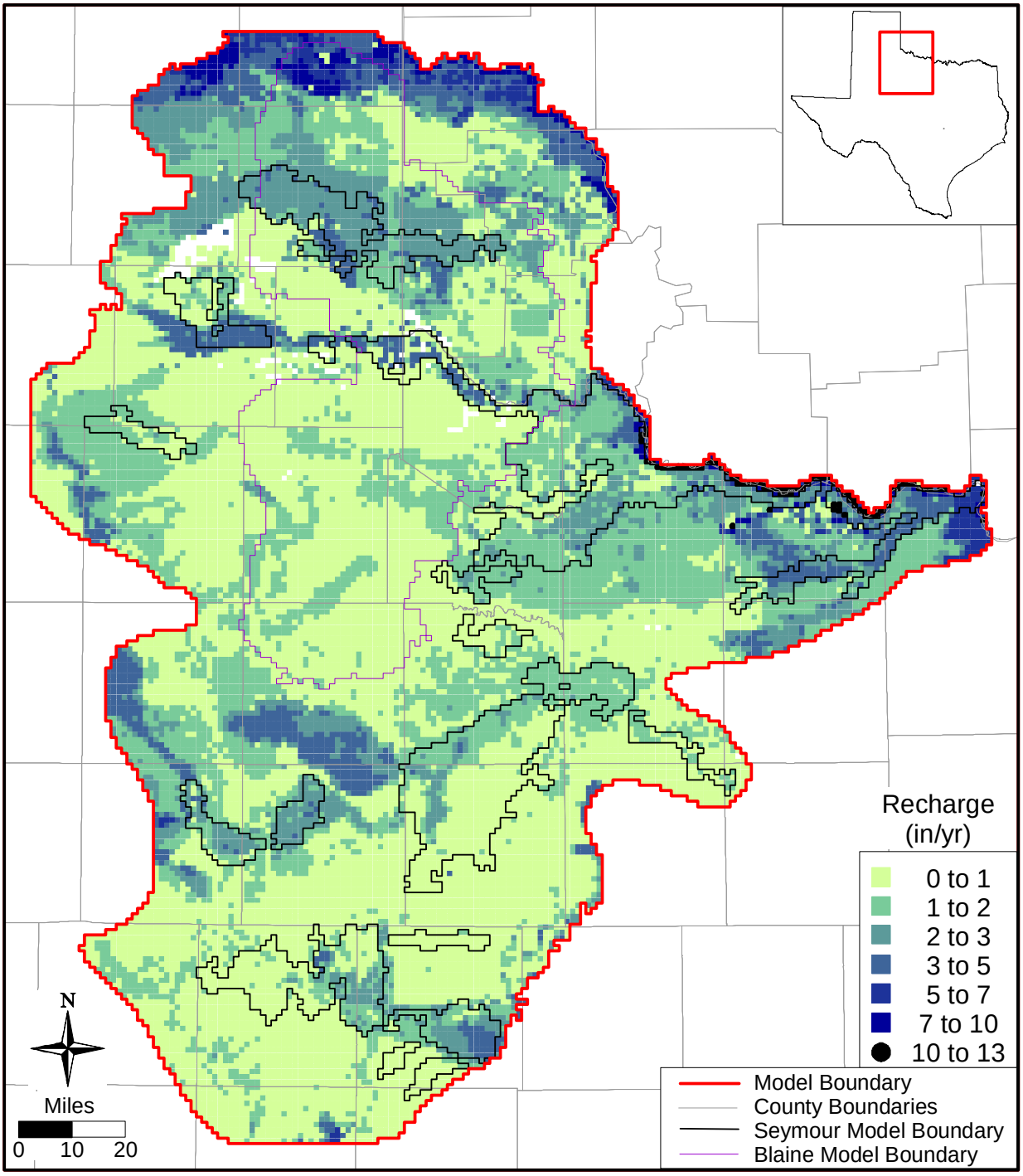

Figure 6.3.3 Temporally averaged spatial distribution of recharge estimated by SWAT. (not used in model)

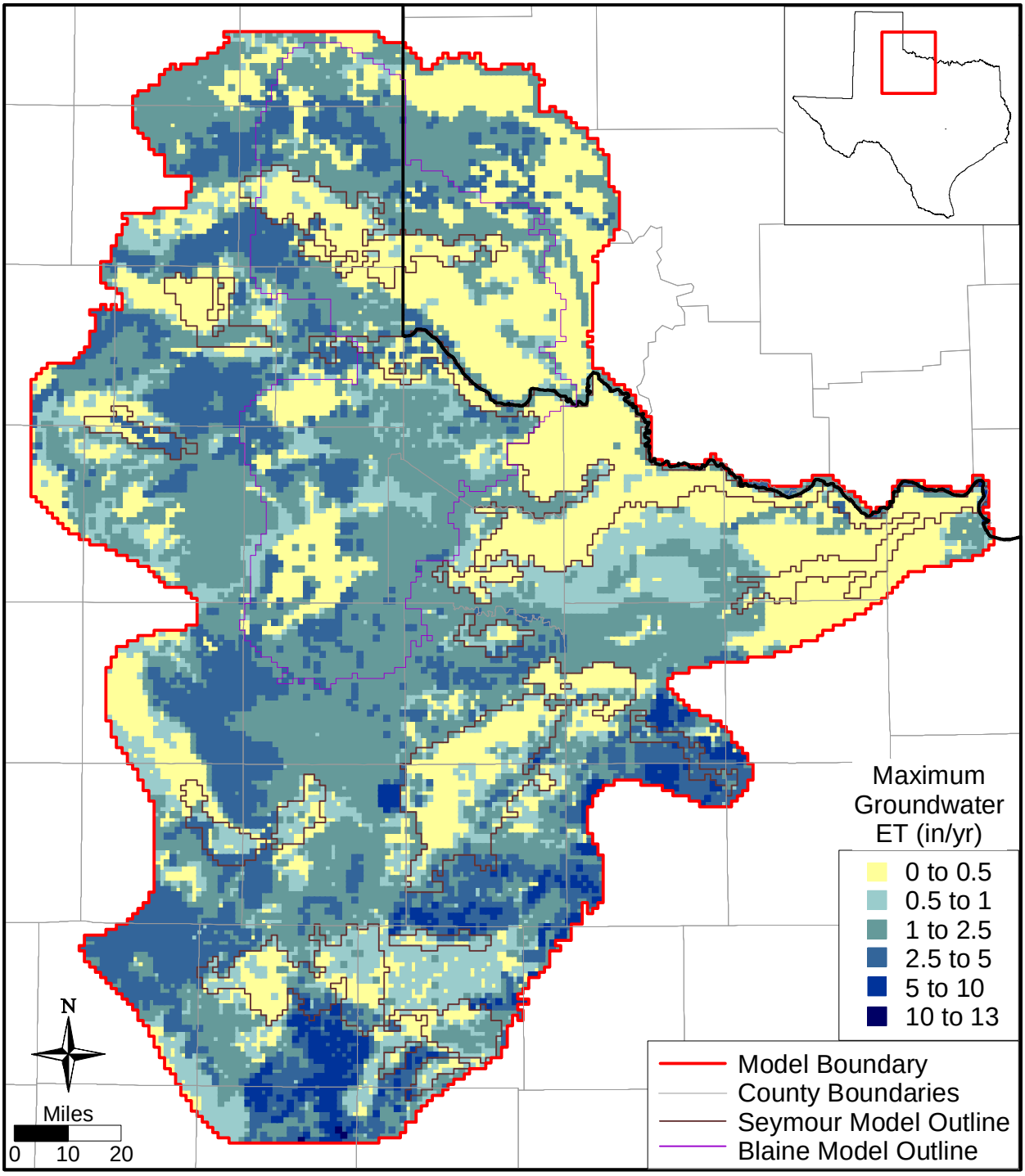

Figure 6.3.4 Groundwater ET maximum rate distribution averaged over the transient period.

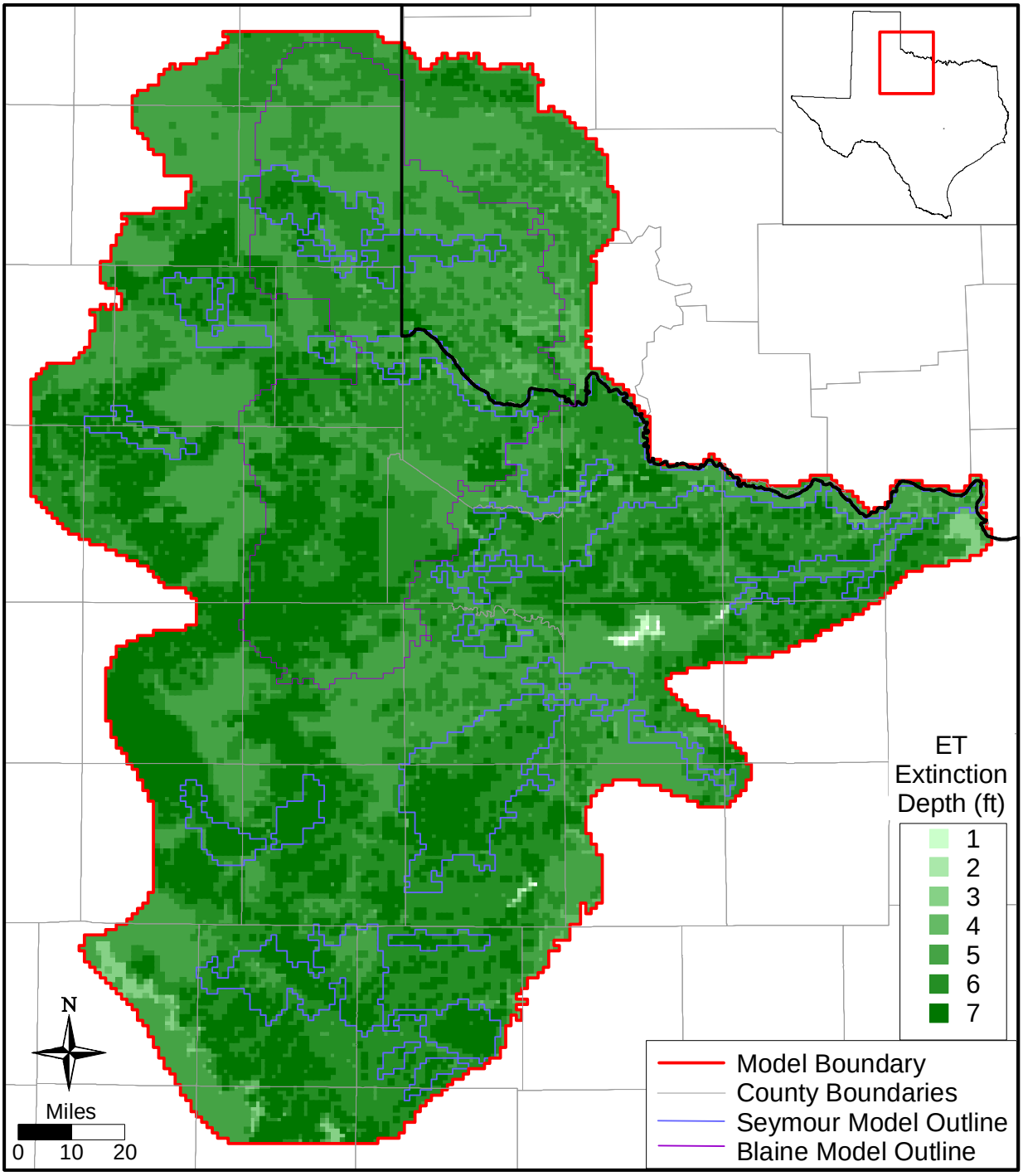

Figure 6.3.5 Maximum ET extinction depth distribution.

6.4 Model Hydraulic Parameters

For the steady-state model, the primary hydraulic parameter to be estimated and distributed across the model grid is hydraulic conductivity. For the transient and predictive models, the storage coefficient must also be included. The following sections describe the method used for distributing hydraulic conductivity and storage in the model domain.

6.4.1 Hydraulic Conductivity

In the GAM, model properties are constant within a given grid block. Each grid block is one square mile in area and varies in thickness from a minimum of 20 feet to hundreds of feet. One of the challenges in constructing a regional model is the development of an accurate "effective" hydraulic conductivity field that is representative of the different lithologies present in each grid cell. The effective hydraulic conductivity depends on the geometry, individual hydraulic conductivities, and the correlation scale relative to the grid and simulation scales of the various lithologies present in a grid cell (Freeze, 1975).

Many investigations exist regarding estimating average effective hydraulic conductivity given assumptions for flow dimension, layer geometry, and correlation scales (Warren and Price, 1961; Gutjahhr et al., 1978). For one-dimensional flow in lithologies combined in parallel (i.e., layered), the appropriate effective hydraulic conductivity would be the weighted arithmetic mean. For one-dimensional flow in lithologies combined in series, the effective hydraulic conductivity is the weighted harmonic mean. Hydraulic conductivity has been found to be a lognormally distributed parameter in many studies. In two-dimensional uniform flow, assuming that the hydraulic conductivity is lognormally distributed and randomly juxtaposed, the effective hydraulic conductivity is exactly the geometric mean (de Marsily, 1986).

The distribution of data available for determining hydraulic conductivity in the Seymour aquifer and the analysis of that data are discussed in Section 4.6. Directional variograms of the hydraulic conductivity data revealed little horizontal anisotropy. The spatial distribution of horizontal hydraulic conductivity was determined by kriging using the pod data and its associated variogram model for pods with sufficient data and using the variogram model for the overall Seymour dataset for pods with insufficient data.

Little hydraulic conductivity data are available for the Permian sediments. A variogram analysis was attempted using hydraulic conductivity data for the Blaine aquifer, however, no correlation trends were observed in the variogram. Also, a post plot of the data for the Blaine aquifer showed no clear spatial trends. These findings indicate that the karstic nature of the Blaine results in heterogeneity in hydraulic conductivity at a scale smaller than the distribution of the data. Therefore, a spatially variable distribution of hydraulic conductivity could not be developed, and a single value was used for the hydraulic conductivity of the Blaine aquifer. Single values were also assumed for each of the other Permian formations.

Vertical hydraulic conductivity is not measurable on a regional model scale and is therefore, generally a parameter that is calibrated within predefined limits. Typical vertical anisotropy ratios (K_h/K_v) are on the order of 1 to 1,000 determined from model applications (Anderson and Woessner, 1992). Domenico and Schwartz (1998) list values of horizontal to vertical hydraulic conductivity ratios that range from 2 to 10 for materials similar to sediments in the study area. At the regional scale of the Seymour GAM, higher anisotropy ratios may exist. A single anisotropy ratio (K_h/K_v) equal to 10^4 was assumed for the model area with vertical hydraulic conductivity varying according to the spatial distribution of the horizontal hydraulic conductivity. This value was based primarily on previous studies of a similar lateral scale (Fryar et al., 2003; Deeds et al., 2003).

6.4.2 Storativity

A specific yield value of 0.14 was used for the sediments of the Seymour aquifer based on a literature review of measurements. For the Permian sediments, a specific yield of 0.15 was used in the unconfined portions. The confined storativity of 1.0 was assigned to outcrop portions of the Permian to account for ponding water conditions, which may occur in stream valleys. For the portions of the Permian overlain by the Seymour aquifer, a homogeneous confined storativity of 1×10^{-2} was used. For the Blaine aquifer, this represents a combination of confined and unconfined conditions due to the karstic nature of the Blaine. The same value was assumed to be representative of the other Permian sediments.

7.0 MODELING APPROACH

The modeling approach included model calibration, model verification, model sensitivity analysis, and model predictions. In the context of groundwater modeling, model calibration can be defined as the process of producing an agreement between model simulated water levels and aquifer discharge, and field measured water levels and aquifer discharge through the adjustment of independent variables. Generally accepted practice for groundwater calibration includes performance of a sensitivity analysis and, if the model is going to be used for predictive purposes, a verification analysis. A sensitivity analysis entails the systematic variation of the calibrated parameters and stresses with re-simulation of aquifer conditions. Those parameters which strongly change the simulated aquifer water levels and discharges would be important parameters to the calibration. It is important to note that a standard "one-off" sensitivity analysis does not estimate parameter uncertainty, since limited parameter space is investigated and parameter correlation is not considered. A verification analysis helps determine the adequacy of the calibration and the suitability of the model for use as a predictive tool. This analysis is performed by using the model to predict aquifer conditions during a period which was not used in the model calibration. Once the model is calibrated and verified, predictive simulations are performed.

7.1 Calibration

Groundwater models are inherently non-unique, meaning that multiple combinations of hydraulic parameters and aquifer stresses can reproduce measured aquifer water levels. To reduce the impact of non-uniqueness, a calibration method described by Brown (1996) was employed. This method includes (1) calibrating the model using parameter values (i.e., hydraulic conductivity, storage coefficient, recharge) that are consistent with measured values, (2) calibrating to multiple hydrologic conditions, and (3) using multiple calibration performance measures such as water levels and discharge rates to assess calibration. Each of these elements is discussed below.

PEST (Parameter Estimation) (Doherty, 2002) was evaluated for use in automating the calibration process. As described in Section 6.1, however, considerable difficulties were encountered in model convergence and it was necessary to use the GMG solver written for

MODFLOW-2000. Even with the GMG solver, when model parameters were changed appreciably, the parameters in the solver package had to be adjusted in order to obtain model convergence. This manual adjustment of solver parameters precluded the use of an automated parameter estimation tool such as PEST. As PEST attempts to adjust model parameters over a meaningful range, non-convergence would occur, terminating the calibration run. As a result, a manual calibration of the model was necessary.

Measured hydraulic conductivity and storage coefficient data for the Seymour aquifer and measured hydraulic conductivity and literature storage coefficient values for the Permian units were used to initially estimate model parameters. The analysis of hydraulic parameters in Section 4.6 indicates that adequate hydraulic conductivity data for the Seymour aquifer are available for developing initial model values. Minimal hydraulic conductivity measurements are available for the Blaine aquifer and other members of the Permian System. It is important to note that, while some data exist for the structure of the Blaine aquifer, the structure of the remainder of layer 2 is a construct (i.e., an approximate uniform thickness of 500 feet was assumed). Accordingly, a significant degree of uncertainty exists in the hydraulic properties in layer 2. Vertical hydraulic conductivity is not measurable at the model scale and, thus, cannot be well constrained. Specific yield for the Seymour aquifer was based on measurements and the specific yield of the Permian units was reasonably well constrained within literature values. However, storativity within the portions of layer 2 overlain by the Seymour aquifer is poorly constrained due to the semi-confined nature of the Permian units and the arbitrary assignment of aquifer thickness to the majority of the layer. Although estimates of recharge are available in the study area, they serve primarily as reasonable bounds for average recharge and dictate little with respect to the spatial or temporal distribution of recharge. Adjustment of all model parameters were held to within plausible ranges based upon the available data and relevant literature. Adjustments to aquifer parameters from initial estimates were minimized to the extent possible to meet the calibration criteria. As a general rule, parameters with few measurements were adjusted preferentially as compared to properties with good supporting data.

The model was calibrated over two time periods, one representing steady-state conditions and the other representing transient conditions. Ideally, the steady-state calibration would consider a “predevelopment” time period prior to extensive aquifer development. As discussed in Section 4.3.2, the predevelopment condition of the Seymour aquifer was dry in several

counties. Therefore, a time period prior to 1980 (the start of the transient simulations) during which the Seymour aquifer appeared to be at steady state was selected for use for the steady-state model. Selection of the steady-state time period and steady-state water levels is described in Section 4.3.2. Pumping estimates for the steady-state time period were taken from the literature or from the TWDB water use survey database as described in Section 4.7.

The transient calibration period ran from 1980 through 1989 consistent with GAM requirements. The actual transient simulation involved a 5-year equilibration period to initialize the model prior to 1980. Section 4.3.3 describes the aquifer water levels and how they were derived for use in the transient calibration period. Pumping estimates based upon historical records were applied on a monthly time scale in the transient calibration period. Likewise, recharge and stream flow were estimated on a monthly time basis and set as input through the transient calibration period. The time period from 1990 through 1999 was used as the verification period to assess the predictive ability of the model. Like the calibration period, transient stresses or boundary conditions were determined on a monthly time scale. Unlike the calibration period, parameters were not adjusted in the verification process.

The model was calibrated through a wide range of hydrological conditions. The steady-state model represents a period of equilibrium where aquifer recharge and aquifer discharge are in balance. The calibration and verification periods (1980 through 1999) represent a time of transient aquifer behavior. The calibration and verification periods also help constrain the model parameterization because a wide range of hydrologic conditions are encountered and simulated. The sensitivity of the transient model to certain parameters differs from that of the steady-state model.

Calibration requires development of calibration targets and specification of calibration measures. To address the issue of non-uniqueness, it is best to use as many types of calibration targets as possible. The primary type of calibration target is hydraulic head (water level). We also qualitatively used stream leakages. Simulated water levels were compared to measured water levels at specific observation points through time (hydrographs) to ensure that model water levels are consistent with hydrogeologic interpretations.

Simulated stream flow rates were compared with measured stream flows at key stream gages in the model area. Stream gain/loss data were not available in the model area for the

calibration period. Therefore, only a qualitative comparison of model gain/loss for streams against RF1 data could be conducted. The RF1 dataset contains the mean streamflow for each stream segment in the model domain. The simulated gain/loss for major streams is expected to be a small fraction of the mean streamflow and for headwaters is expected to be less than or nearly equal to the mean streamflow. Furthermore, the model needs to be in agreement with the conceptual model in that the majority of the streams are gaining with the smallest gains/losses generally occurring in the headwater segments. These qualitative constraints provided bounds for the overall recharge rate and the streambed conductances.

Springs constitute a small portion of the total discharge from the model domain. Because of the scale of the model grid cells, gross averaging of elevations occurs within each model cell. Depending on the location of the spring within the model cell, this can result in a high or low bias of the water-level elevation with respect to the spring elevation. This makes a direct comparison of simulated and observed flows in individual springs difficult. Instead, simulated spring flows were only checked in a qualitative manner to ensure that the total simulated spring flow approximated the total observed spring flow. The model was insensitive to the drain conductance and this parameter was not adjusted during calibration.

Based on chloride measurements, the age of the groundwater in the Seymour aquifer in Haskell County has been estimated to range from 35 to 132 years in areas where dryland farming is conducted and to average 33 years in natural sites (Scanlon et al., 2003). Based on tritium/helium-3 tracer ($^3H/^3He$) measurements in the sand dunes area of Haskell County, the groundwater is estimated to range in age from 2 to 23 years (Scanlon et al., 2003). The discretization of the model – 1 layer for the Seymour aquifer and typical widths of only several grid blocks across a given pod – coupled with MODFLOW accounting only for saturated zone flow preclude conducting meaningful particle tracking simulations for comparison to the groundwater age estimates.

Traditional calibration measures (Anderson and Woessner, 1992), such as the mean error, the mean absolute error, and the root mean square error, quantify the average error in the calibration process. The mean error (ME) is the mean of the differences between measured heads (h_m) and simulated heads (h_s):

$$ME = \frac{1}{n} \sum_{i=1}^{n} \left(h_m - h_s\right)_i \tag{7.1}$$

where n is the number of calibration measurements. The mean absolute error (MAE) is the mean of the absolute value of the differences between measured heads (h_m) and simulated heads (h_s):

$$MAE = \frac{1}{n} \sum_{i=1}^{n} \left|\left(h_m - h_s\right)_i\right| \tag{7.2}$$

where n is the number of calibration measurements. The root mean square (RMS) error is the average of the squared differences between measured heads (h_m) and simulated heads (h_s):

$$RMS = \left[\frac{1}{n} \sum_{i=1}^{n} \left(h_m - h_s\right)_i^2\right]^{0.5} \tag{7.3}$$

where n is the number of calibration measurements. The difference between the measured hydraulic head and the simulated hydraulic head is termed a residual.

We used the RMS as the basic measure of calibration for heads. For the GAMs, the required calibration criterion for heads is a RMS that is equal to or less than 10 percent of the observed head range in the aquifer being simulated. To provide information on model performance with time, the RMS was calculated for the calibration period (1980 through 1989) and the verification period (1990 through 1999). The RMS is useful for describing model error on an average basis but, as a single measure, it does not provide insight into spatial trends in the distribution of the residuals.

An examination of the distribution of residuals is necessary to determine if they are randomly distributed over the model grid and not spatially biased. Post plots of head residuals for both model layers were used to check for spatial bias by indicating the magnitude and direction of mismatch between observed and simulated heads. Finally, plots of simulated versus observed water-level elevations and residual versus observed water levels were used to determine if the head residuals are biased based on the magnitude of the observed head surface.

7.2 Calibration Target Uncertainty

Calibration targets are uncertain. In order to not "over-calibrate" a model, which is a stated desire for the GAMs, the calibration criteria should be defined consistent with the

uncertainty in calibration targets. The primary calibration target in groundwater modeling is hydraulic head. Uncertainty in head measurements can be the result of many factors including measurement error, scale errors, and various types of averaging errors that are both spatial and temporal. The calibration criteria for head is a RMS less than or equal to 10 percent of the head variation within the aquifer being modeled. Head differences across the Seymour and Blaine aquifers in the study area are on the order of 1,550 and 1,100 feet, respectively. This leads to an acceptable RMS of 155 and 110 feet. Comparison of this RMS to an estimate of the head target errors indicates what level of calibration the underlying head targets can support.

Measurement errors are typically on the order of tenths of feet and, at the GAM scale, can be considered insignificant. However, measuring point elevation errors can be significant. The error (standard deviation) in averaging ground-surface elevations available on a 30-meter grid to a one-mile grid averages 13 feet and exceeds 30 feet in areas with higher topographic slopes (primarily along the edges of the Seymour pods and in river valleys). Another error is caused by combining several sediment types into single one square mile grid blocks represented by one simulated head. Horizontal gradients relative to the grid scale can account for errors averaging 4 feet and exceeding 20 feet in some areas, based on multiple steady-state target values in a single grid block. This error can be even greater near pumping centers. When these errors are added up, the average error in model heads could easily equal 20 to 30 feet. Calibrating to RMS values significantly less than 30 feet would constitute over calibration of the model and parameter adjustments to reach that RMS are not supported by the hydraulic head uncertainty.

7.3 Sensitivity Analysis

A sensitivity analysis was performed on the steady-state and transient calibrated models to determine the impact of changes in a calibrated parameter on the results of the calibrated model. A standard “one-off” sensitivity analysis was performed. This means that hydraulic parameters or stresses were adjusted from their calibrated “base case” values one by one while all other hydraulic parameters remained unperturbed.

As described in Section 7.1, model convergence issues precluded the use of PEST as a calibration tool. For the same reasons, PEST was not used to calculate the Jacobian Matrix. Consequently, the original intention of calculating parameter sensitivities based on the inverse solution of the Jacobian Matrix was not possible.

7.4 Predictions

Once the transient model satisfied the calibration criteria for both the calibration and verification periods, the model was used for predictive simulations. The predictive simulations have different simulation periods. Simulations were run from 2000 to 2010, 2020, 2030, 2040, and 2050. Average climatic conditions were applied for each predictive simulation with the simulation ending with a drought-of-record. Yearly stress periods were used for the predictive period with the exception of the final ten years (including the drought-of-record) of the simulation, during which monthly stress periods were implemented. Where monthly stress periods were used, stream flow rates and recharge were applied with seasonal variation. Pumping stresses were based upon the Regional Water Plans as described in Section 4.7 and Appendix D.

This page intentionally left blank.

8.0 STEADY-STATE MODEL

Much of the Seymour aquifer was dry under predevelopment conditions. As a result, the steady-state model developed for the Seymour aquifer represents a period during which some pumping occurred but water levels in the aquifer appeared to be relatively constant. This section details calibration of the steady-state model and presents the steady-state model results. The sensitivity of the steady-state model to various hydrologic parameters is also described.

8.1 Calibration

This section describes the steady-state calibration targets and calibrated parameters including horizontal and vertical hydraulic conductivity, vertical conductance, recharge, ET, pumping, and stream conductance.

8.1.1 Calibration Targets

Water-level measurements are needed as targets for steady-state calibration. Selection of water-level measurements representative of steady-state conditions was discussed in Section 4.3.2. Steady-state targets included water-level measurements from 579 well locations in the Seymour aquifer and 274 well locations in the Blaine aquifer. For the Seymour aquifer, 331 grid blocks contained multiple steady-state targets. The number of targets in these grid blocks ranges from 2 to 19 and the difference in water levels for the targets in these grid blocks ranges from 0.03 to 58.5 feet. The standard deviations of the water levels for grid blocks with multiple Seymour targets are shown on Figure 8.1.1. For the Blaine aquifer, 15 grid blocks contained two steady-state targets. The difference in water levels for the targets in these grid blocks ranges from 2.2 to 36.2 feet. The standard deviations of the water levels for grid blocks with two Blaine targets are shown on Figure 8.1.2. For the grid blocks containing multiple steady-state water levels, the average water level was selected as the calibration target. To avoid introducing additional errors by using a surveyed ground-surface elevation at each well, the water-level elevation for the steady-state targets was calculated using the measured depth to water and the grid-block averaged elevation from the model.

8.1.2 Horizontal and Vertical Hydraulic Conductivities

Section 6.4.1 described the determination of initial horizontal and vertical hydraulic conductivities for the model. Figure 8.1.3 depicts the final calibrated horizontal hydraulic conductivity field of the Seymour aquifer for the steady-state model, which did not require modification from its initial estimates. Hydraulic conductivity and recharge can be correlated parameters preventing independent estimation when using only water-level data constraints. Because a large amount of data was available for estimating hydraulic conductivity in the Seymour aquifer (see Section 4.6) when compared to only a few estimates of recharge, the hydraulic conductivity field was considered to be the better constrained parameter. In addition, the water levels in both the Seymour and Blaine aquifers were less sensitive to the Seymour hydraulic conductivity than to recharge. Accordingly, during calibration of the steady-state model, horizontal hydraulic conductivity of the Seymour aquifer was held constant and recharge was varied. The hydraulic conductivity range for layer 1 and the final hydraulic conductivity value for each of the Permian units of layer 2 for the steady-state model are summarized in Table 8.1.1.

The horizontal hydraulic conductivities for the Permian formations of layer 2 were varied by formation but not within a formation (i.e., a single value was used for each formation) during the steady-state calibration. In all cases, lower hydraulic conductivity values were required in layer 2 in order to maintain the water levels in layer 1 at high enough values to match observed water levels. Lowering the hydraulic conductivities in layer 2 reduced drainage from layer 1 to layer 2 and increased gradients within layer 2. The final calibrated hydraulic conductivities for layer 2 are illustrated in Figure 8.1.4 and summarized in Table 8.1.1.

In the steady-state model, vertical leakance of groundwater from layer 1 to layer 2 is controlled more by the horizontal conductivity of layer 2 than the vertical hydraulic conductivity. Even at extreme anisotropy values of K_h/K_v equal to 10^6, water flowed freely from the Seymour to the Permian in the model. In addition, simulated water levels in the Seymour and cross-formational flow were very insensitive to the vertical conductivity. In contrast, water levels in both layers 1 and 2 were sensitive to the horizontal conductivity of layer 2. For the calibrated steady-state model, a uniform anisotropy ratio (K_h/K_v) of 10^4 was used with vertical hydraulic conductivities varying according to the spatial distribution of the horizontal hydraulic

conductivity. This value was based primarily on previous studies of a similar lateral scale (Fryar et al., 2003; Deeds et al., 2003).

8.1.3 Recharge

The SWAT simulations performed for this study had some limitations in predicting recharge as discussed in Section 6.3.4. The spatial distribution of recharge was, therefore, considered a calibration parameter constrained by the few available literature estimates. Initially, different uniform values of recharge were assigned to each pod of the Seymour aquifer and a single uniform value was assigned to model layer 2. This provided an initial estimate of the average recharge required in each pod and layer to roughly match the measured water levels and honor the conceptual model of gaining streams with average stream leakages less than or equal to the mean stream flow given in the RF1 dataset. However, a uniform recharge value for each pod in the Seymour aquifer resulted in spatially biased errors in water level with the model overpredicting heads in the lower elevation areas (water table near ground surface) and underpredicting heads in the higher elevations areas (water table farther below ground surface). To account for variations in subsurface infiltration gradients resulting from differences in depth to the water table, a relationship between local topography and recharge was applied which varied recharge spatially across the Seymour (see Section 6.3.4). The recharge was increased in the higher elevation areas and decreased in the lower elevation areas, with the average recharge maintained in each pod. The resulting distribution significantly improved calibration to observed water levels.

During the subsequent transient calibration (see Section 9), it was necessary to increase the average amount of recharge in the Seymour aquifer, especially in pods 1, 2, 3, 4, and 7, from the values initially derived during the steady-state calibration, to keep areas with observed groundwater from going dry and to fit the transient water levels. This increase was necessary because pumping from the Seymour was higher during the transient period than during the steady-state period, but observed water levels remained constant or, in some instances, increased during the transient period. The only way to maintain or increase water levels at the same time additional water is withdrawn from the system, is to increase water supplied to the system through recharge. This increase in recharge across the Seymour aquifer had an adverse effect on the calibration statistics of the steady-state model. However, the number of hydrologic

conditions tested by the transient model and questions surrounding the true steady-state nature of pumping and water levels in the steady-state model warranted preferentially honoring the transient water levels.

Because the Blaine aquifer has a higher water yield and higher hydraulic conductivity than the other Permian sediments in the model (with the possible exception of the Ogallala which constitutes only a small portion of the western area of the model domain), a slightly higher uniform recharge value was assigned to this portion of layer 2. Calibration of both the steady-state and transient models was possible maintaining a single value of recharge across the other Permian sediments.

The spatial distribution of calibrated recharge for the steady-state model is presented in Figure 8.1.5. This figure also represents the temporally averaged distribution of calibrated recharge for the transient model. The calibrated recharge distribution averaged 1.9 in/yr in layer 1 and 0.30 in/yr in layer 2 (0.38 in/yr for the Blaine portion) with an overall average of 0.57 in/yr for the entire active model area. Average recharge rates for the individual Seymour pods ranged from 0.8 to 2.5 in/yr, within the range reported in the various studies that are summarized in Table 4.4.1.

In pod 1, where the Seymour aquifer overlies the Blaine and Whitehorse, the base of the Seymour is more uncertain and irregular (less smooth) than in other pods, and the dependence of recharge on the Seymour thickness was reduced by using a damping factor, *DF*, (see Section 6.3.4) of 0.6. Similarly, in pods 10 and 11, where the structure of the Seymour is also uncertain, the dependence of recharge on formation thickness was reduced by using a *DF* of 0.3. In pods 4 and 7, where higher average recharge rates were used, the dependence of recharge on topography was increased by using a *DF* of 0.95. This increase in the *DF* was an attempt to honor the water-level observations without having unreasonable discharge to streams resulting from too much recharge applied to the topographical lows near stream cells.

The steady-state model is sensitive to recharge for two reasons: (1) recharge is the primary input source for water and (2) the model is at steady-state where inflow balances outflow with no change in storage or time dependence. In a steady-state model, where there is no net change in storage, a balance must be found between the input recharge and all other flow

in the model. It follows that the behavior of the model will be sensitive to the input recharge rate.

8.1.4 Pumping

Estimates of pumpage for the Seymour and Blaine aquifers during the steady-state time period were taken from the literature. In instances when no literature data were found, steady-state pumping was set equivalent to 1980 pumping from the TWDB water use survey database. For a complete discussion of the development of pumping for the steady-state model, see Section 4.7. The pumping distribution for the steady-state model is shown in Figures 8.1.6 and 8.1.7 for model layers 1 and 2, respectively. The largest concentration of pumping in the Seymour aquifer occurs in Haskell and Knox counties (pod 7). Several isolated spots of high pumpage are located in Collingsworth County (pod 1), Hall County (pod 3), Wilbarger County (pod 4), and Baylor, Knox, and Haskell counties (pod 7). Over the majority of the aquifer, pumping is less than 100 AFY. Pumping from the Blaine aquifer in Texas is also less than 100 AFY over the majority of the aquifer. However, localized areas of high pumpage are found throughout the Blaine aquifer.

8.1.5 Stream Conductances

Because streams act as a major point of discharge in the model, simulated water levels in both layers 1 and 2 were somewhat sensitive to stream conductances. The stream conductance was decreased uniformly until the total leakage to and from each stream segment was approximately equal to or less than the RF1 mean stream flow in that segment (see Section 8.2). This resulted in a uniform stream conductance of 1,000 ft^2/day for all stream segments corresponding to an average streambed conductivity of 0.25 ft/day.

Table 8.1.1 Calibrated hydraulic conductivity ranges for the steady-state model.

	Horizontal Hydraulic Conductivity K_h (ft/day)	Anisotropy Ratio (K_h/K_v)
Layer 1 (Seymour)	10 – 1,000	10,000
Layer 2		
(Wichita)	0.52	10,000
(Clear Fork)	0.82	
(Pease River)	2.9	
(Blaine)	4.6	
(Whitehorse)	1.6	
(Quartermaster)	1.6	
(Ogallala)	7.4	

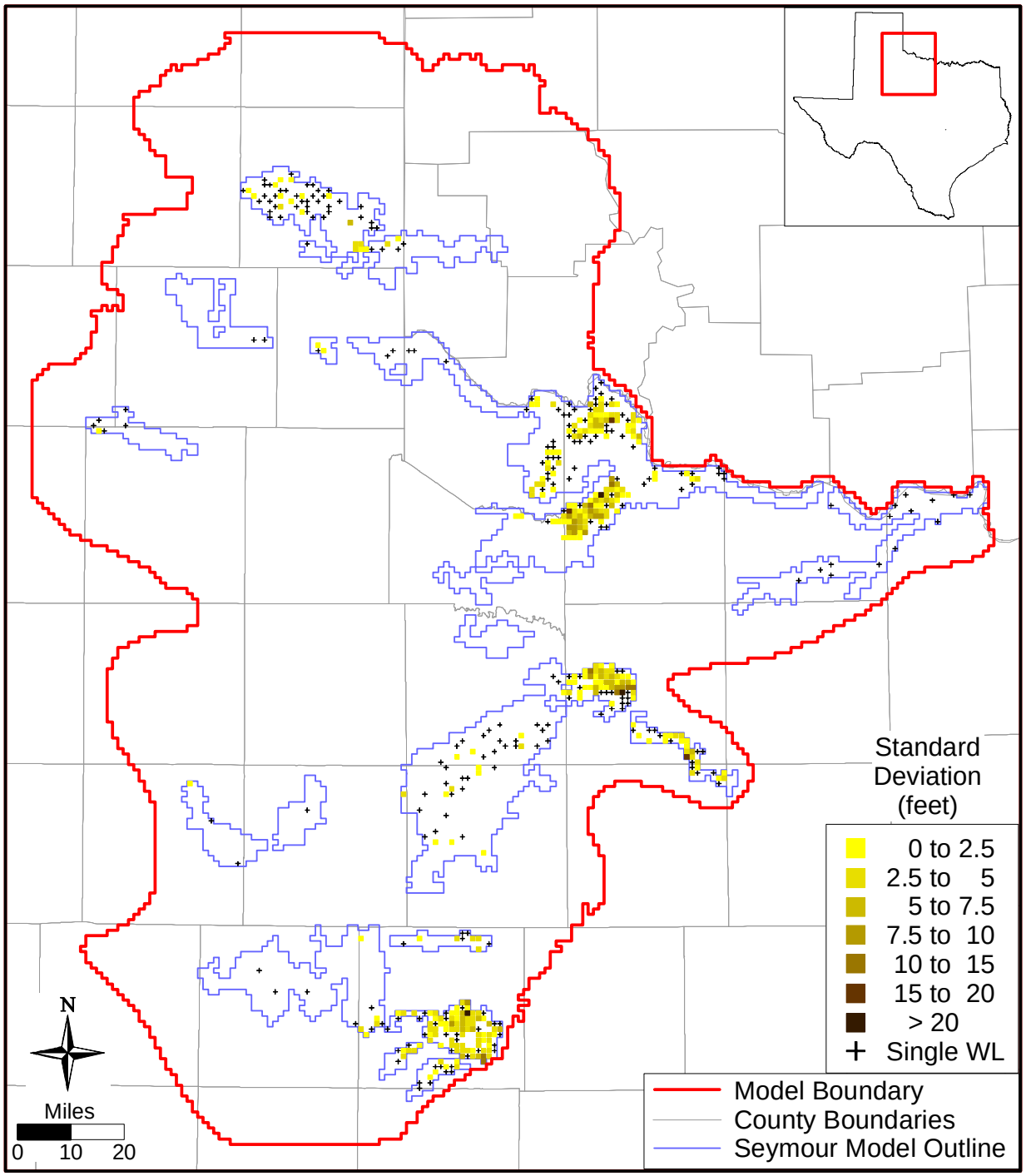

Figure 8.1.1 Standard deviation of water levels at targets in the Seymour aquifer.

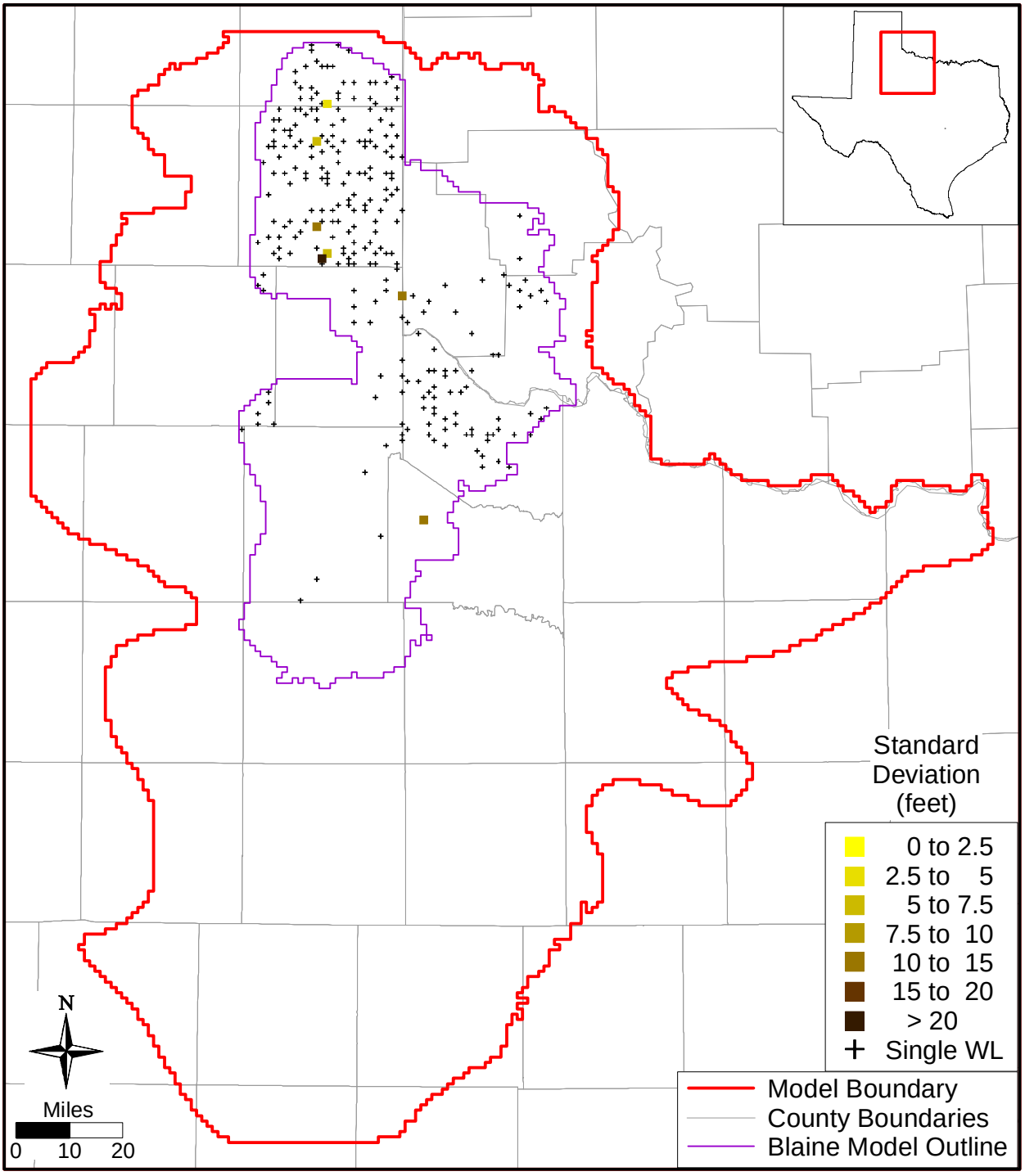

Figure 8.1.2 Standard deviation of water levels at targets in the Blaine aquifer.

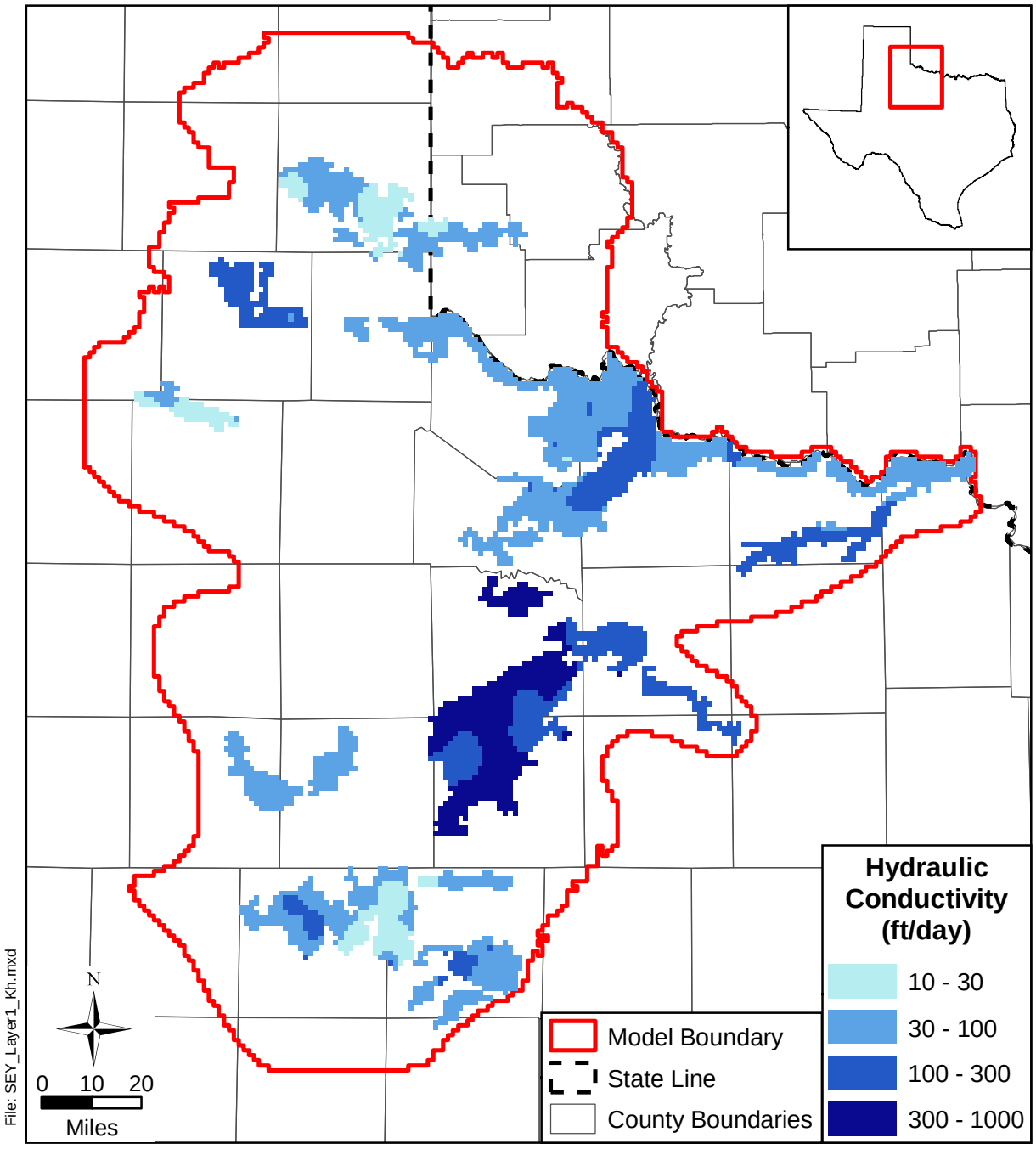

Figure 8.1.3 Calibrated horizontal hydraulic conductivity for the Seymour aquifer.

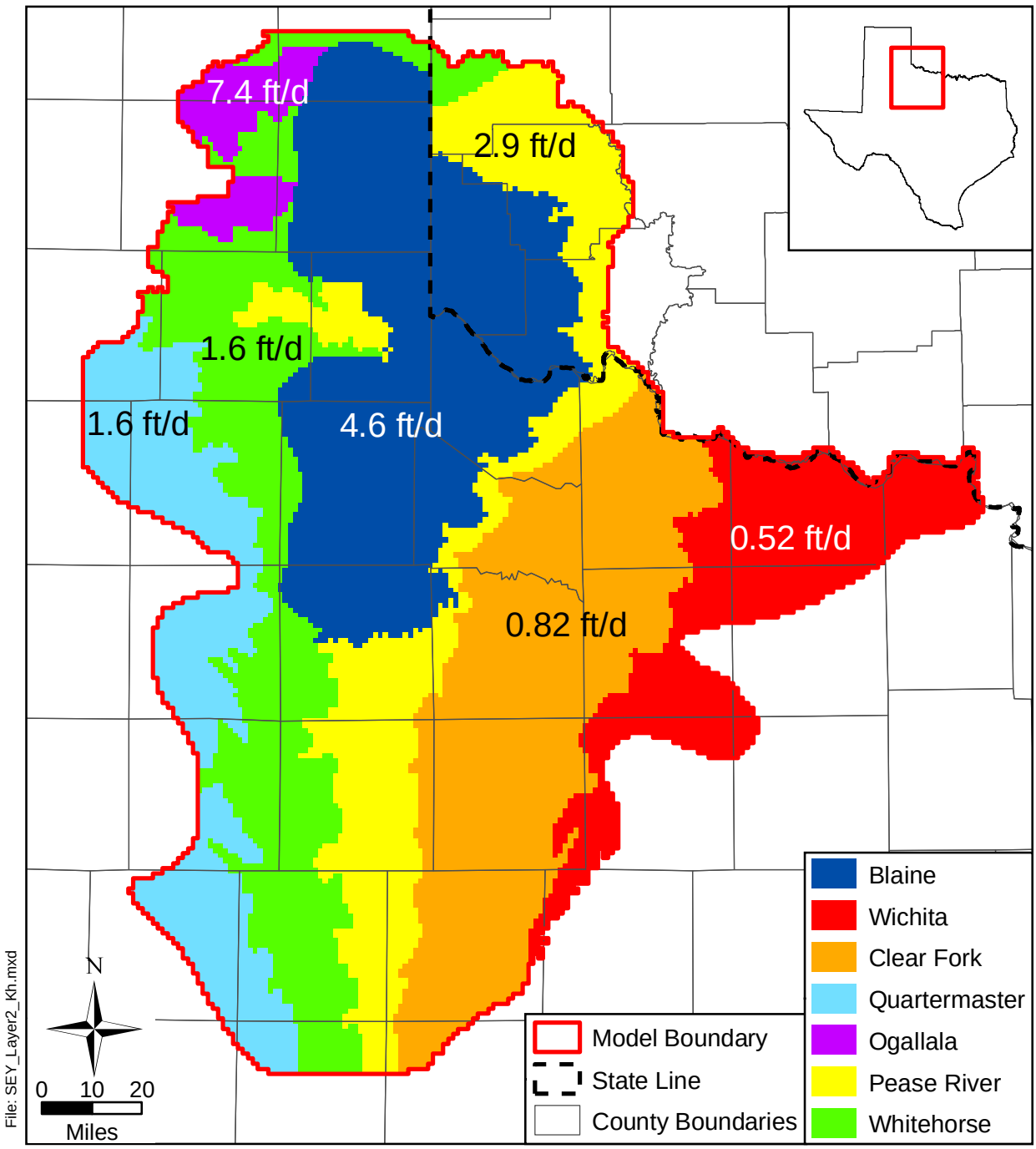

Figure 8.1.4 Calibrated horizontal hydraulic conductivities for the Permian sediments of layer 2.

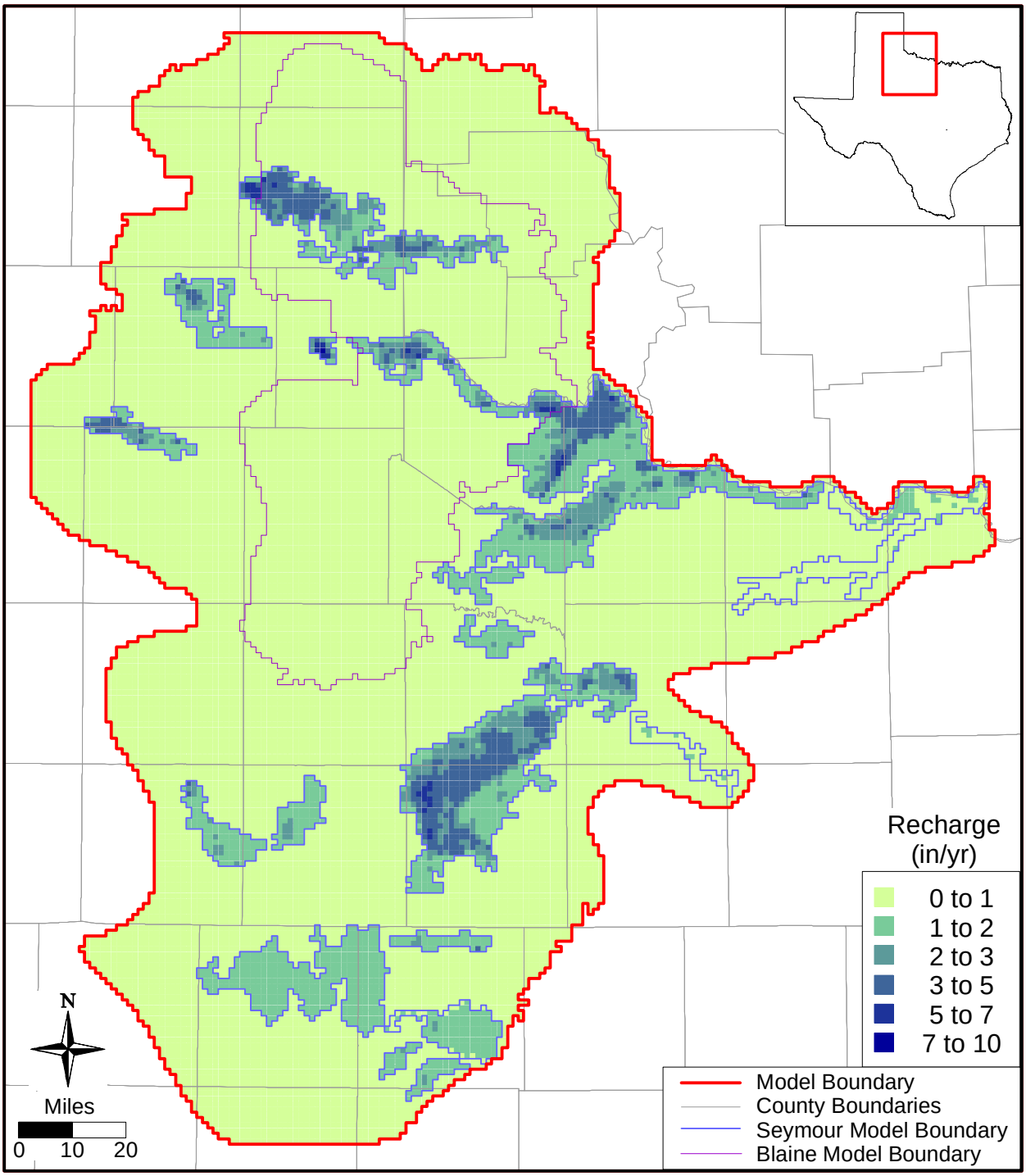

Figure 8.1.5 Calibrated recharge distribution for the steady-state and transient models.

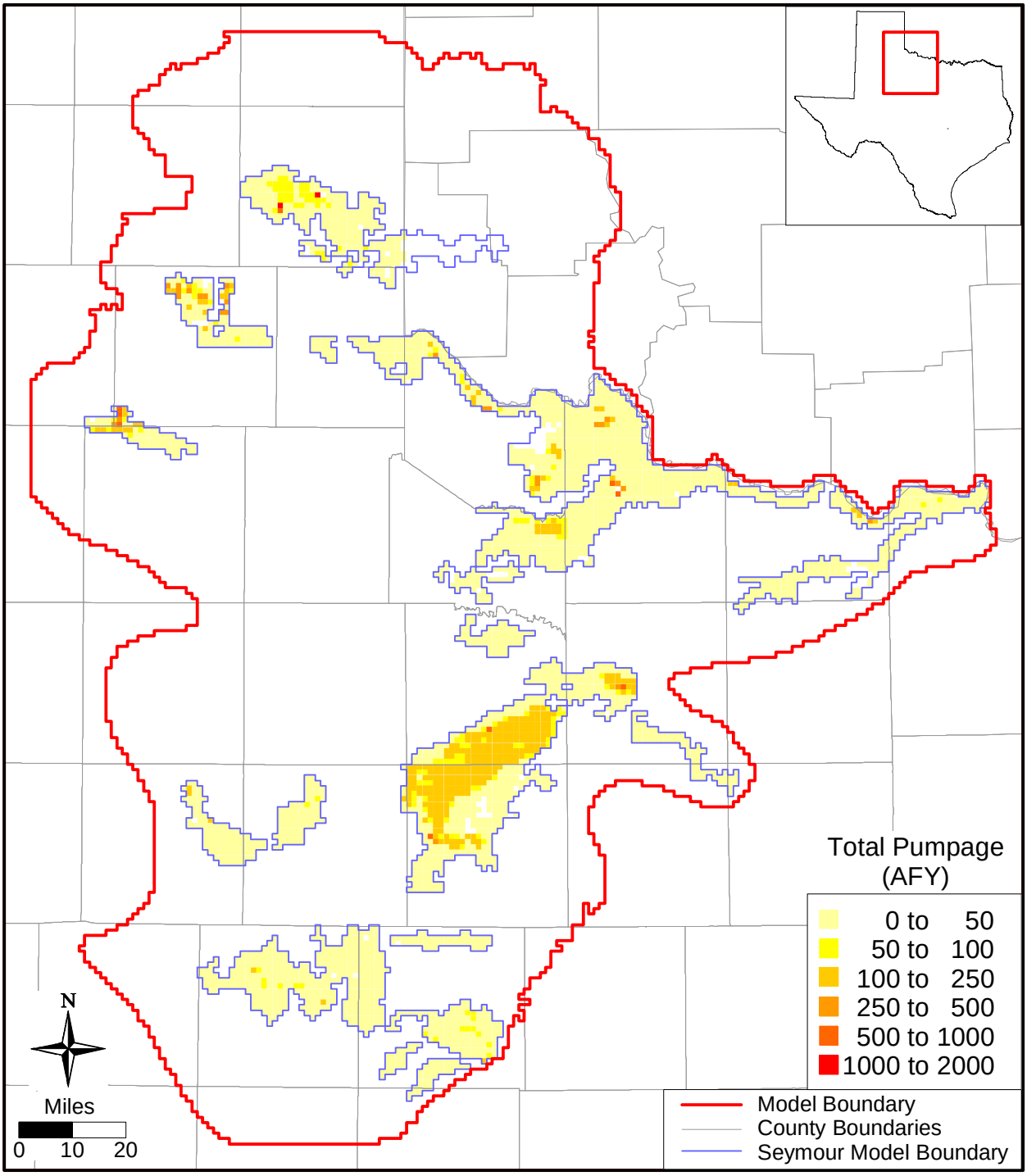

Figure 8.1.6 Distribution of pumping in layer 1 for the steady-state model.

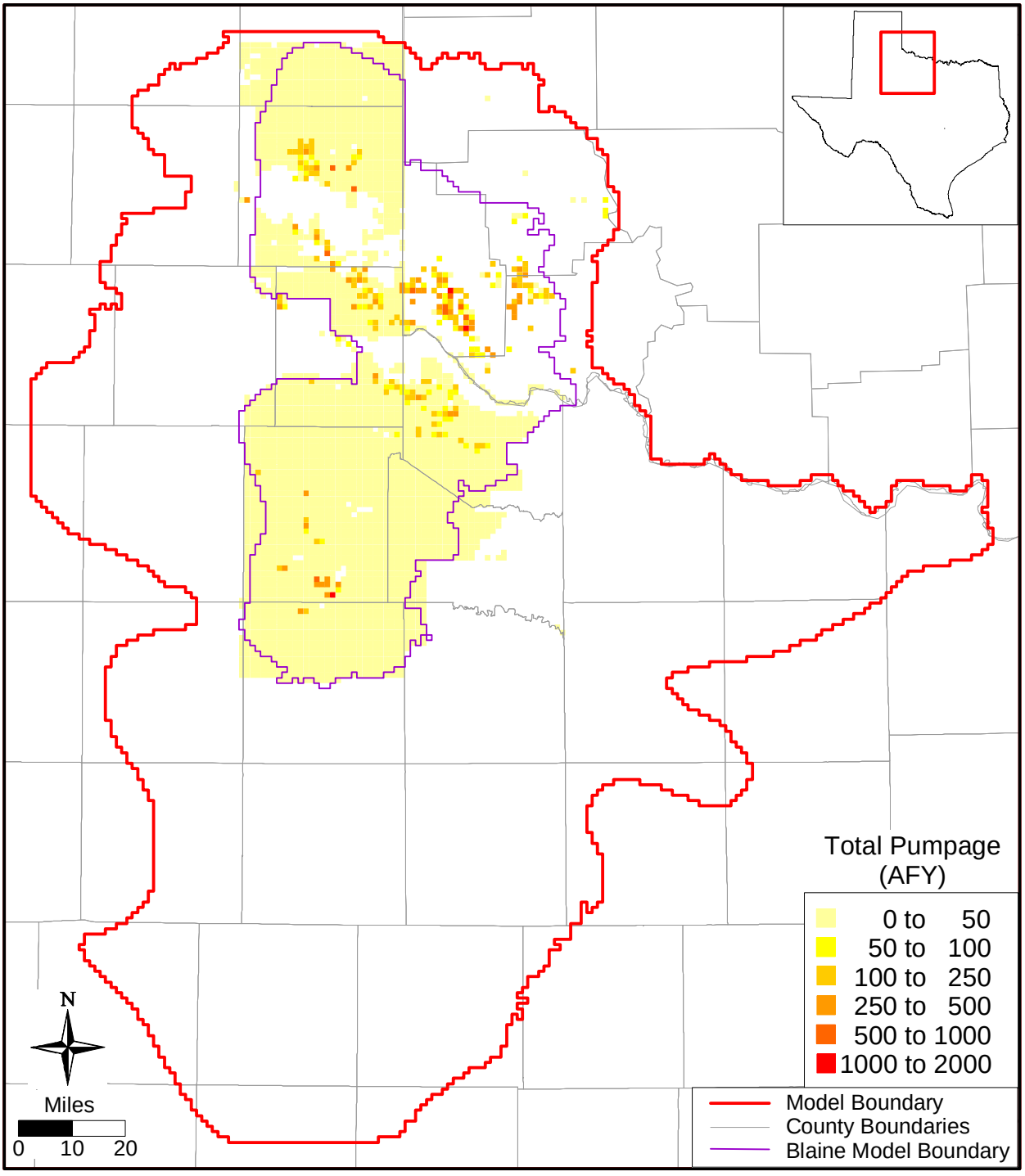

Figure 8.1.7 Distribution of pumping in layer 2 for the steady-state model.

8.2 Simulation Results

Calibration of the steady-state model is not unique. Calibrated results can be obtained by numerous combinations of recharge and vertical and horizontal hydraulic conductivities. Overall, the steady-state model is most sensitive to recharge. This is expected because recharge is the primary input source of water for the model. Streams, which can serve as a major source of inflow or outflow to the model, were constrained (by lowering the streambed conductance) to honor the conceptual model of gaining streams with leakages less than or nearly equal to the observed mean stream flow.

8.2.1 Water-Level Elevation

Figures 8.2.1a and 8.2.2a show the simulated water-level elevations for model layers 1 and 2, respectively. These figures show a general west to east groundwater gradient following the topographical gradient. Additionally, localized gradients are apparent from the center of Seymour pods towards the edges and toward river valleys within the Permian sediments. A comparison of simulated and observed water levels and residuals versus observed water levels are shown in Figure 8.2.1b for layer 1 and in Figure 8.2.2b for layer 2, where residuals are defined as:

$$residual = head_{measured} - head_{simulated} \quad (8.2.1)$$

A positive residual indicates that the model has underpredicted the hydraulic head, while a negative residual indicates overprediction. For layer 1, different symbols are used for each pod to allow for comparison on a pod by pod basis. More than half of the data fall above the unit-slope line, indicating simulated water levels for the Seymour aquifer are biased somewhat higher than those observed. Residuals in layer 1 range from –129 to 69 feet with 90 percent falling between –60 and 30 feet. The majority (73 percent) of residuals for the Seymour aquifer are negative indicating that simulated heads are greater than observed heads for the steady-state model. The comparison of simulated versus observed water-level elevations for the Blaine aquifer shows deviation from the unit-slope line. At lower water-level elevations, the model-predicted values are greater than the observed values and, at higher water-level elevations, the model-predicted values are less than the observed values. Residuals for the Blaine aquifer range from –161 to 168 feet with the majority (74 percent) falling between –80 and 80 feet. The model

overpredicts water-level elevation at 46 percent of the targets and underpredicts water-level elevation at 54 percent of the targets.

Post plots of residuals are found in Figures 8.2.1c and 8.2.2c for layers 1 and 2, respectively. In general, the model overpredicts water-level elevations in pod 4, the portion of pod 7 located in Baylor County, pod 8, and the southeastern portion of pod 13. Water-level elevations are, in general, underpredicted in pod 1, pod 7, and northwestern pod 13. The number designation for each pod is shown in Figure 4.1.1.

The calibration statistics for the individual layers are summarized in Table 8.2.1. The adjusted root mean square (RMS) error (i.e., RMS divided by the range in observed water levels) is 2 percent for the entire Seymour aquifer and 6 percent for the Blaine aquifer. Within the Seymour aquifer, the adjusted RMS is less than or equal to 10 percent for pods 1, 2, 3, 4, 7, 8, 9, 11, and 15 and between 11 and 16 percent for pods 5, 12, 13, and 14.

Some grid cells exhibited dry conditions in the steady-state simulation. The rewetting option in MODFLOW was used for the steady-state model to prevent cells from going dry purely due to convergence oscillations. Out of 20,001 active outcrop cells, 762 (3.8 percent) were dry. The majority of these dry cells are located at the edges of Seymour pods where the Seymour aquifer is thin. These dry cells may be indicative of actual subsurface conditions or limitations in the model caused by averaging structure and water level to 1-mile grid blocks. Areas with a larger percentage of dry cells occur in pods 1, 9, and 10. Generally, these dry areas coincide with areas of little or no pumping or water-level measurements which, in turn, may be a direct reflection of these portions of the Seymour bearing little or no groundwater. The portion of pod 1 where the majority of pumping and water-level measurements occur tends to remain wet. In the Blaine aquifer, 14 cells were dry. These dry cells occur in an area within Oklahoma where significant amounts of pumping were applied to the steady-state model.

Because no pre-development period could be used for the steady-state model (see Section 4.3.2) the steady-state period includes estimates of pumping. An attempt was made to find a period representative of steady-state conditions where water levels remained constant over several years while pumping occurred. Errors in the estimated pumping during this period, however, would cause errors in the steady-state model results. Pumping from the Seymour is generally lower in the steady-state model when compared to the transient model (see

Section 9.1). Relatively stable water levels were observed in some extensively pumped areas during the transient period. Therefore, recharge had to be increased from initial steady-state values to obtain simulated water levels consistent with water levels observed during the transient period when pumping rates were higher.

While observed water levels appear to be stable during the several years used for the steady-state period, even small trends in water levels would limit how representative the period is of true steady-state conditions. For this reason, the steady-state model was used primarily as a means of estimating the approximate recharge distribution and horizontal hydraulic conductivity in layer 2 that fit measured water levels and stream conductances while honoring the conceptualization of flow to streams.

8.2.2 Streams and Springs

Stream gain/loss data are not available in the model area. Therefore, only a qualitative comparison of model gain/loss for streams against RF1 data could be conducted. The gain/loss distribution for the steady-state model is depicted in Figure 8.2.3. In agreement with the conceptual model, Figure 8.2.3 shows that the majority of the streams are gaining with the smallest gains/losses generally occurring in the headwater segments. Model gain/loss for major streams is expected to be a small fraction of streamflow and for headwaters is expected to be less than or nearly equal to streamflow. Comparison of the total leakage into or out of each stream segment to RF1 mean streamflow in that segment is shown in Figure 8.2.4.

As discussed in Section 6.3.3, many of the springs in the steady-state model area coincided with stream cells and were not explicitly accounted for separately in the model. Of the remaining 253 springs, only 69 exhibited flow in the steady-state model as depicted in Figure 8.2.5. The majority of the spring flow occurs in the vicinity of the Seymour pods where recharge is highest. Overall, spring flow is insignificant in the model (see water budget given in Section 8.2.3) and, as discussed in Section 8.3, model water levels are insensitive to springs.

8.2.3 Water Budget

Tables 8.2.2a and 8.2.2b summarize the water budget for the steady-state model in terms of total volume and as a percentage of total inflow and outflow. The overall mass balance error for the steady-state simulation is -0.06 percent, well under the GAM requirement of one percent.

The predominant input source is recharge, which accounts for 94 percent of the total inflow to the model. Water discharging from the model is mainly through the streams (48 percent), followed by ET (31 percent) and pumping (19 percent).

Streams in the model are generally gaining with a net gain equivalent to 45 percent of the total recharge to the model. The majority of this discharge occurs in the Permian sediments where the majority of the stream valleys are located. The majority of the discharge through ET also occurs in the Permian sediments primarily because they constitute the majority (83 percent) of the model outcrop area.

Cross-formational flow between the Seymour aquifer and Permian sediments is primarily downward with the net discharge from the Seymour to the Permian equal to 27 percent of the recharge to the Seymour. This amount is comparable to the discharge from the Seymour aquifer through pumping (25 percent of recharge to the Seymour) and the net discharge to streams actually in model layer 1 (27 percent of recharge to the Seymour). ET constitutes a discharge equal to 14 percent of the recharge to the Seymour aquifer. Discharge to springs is relatively insignificant, comprising only 3 percent of the Seymour recharge. However, spring discharge is incorporated into the stream discharge for the springs that coincide with stream cells.

Overall, the water budget is in agreement with the conceptual model of the Seymour aquifer. Average calibrated recharge rates are within the bounds of those presented by others. Direct precipitation is the predominant form of recharge to the Seymour with little or no recharge occurring from streams. The net cross-formational flow, as expected, is from the Seymour to the underlying Permian sediments and streams in the model are predominantly gaining. ET constitutes a smaller portion of the natural discharge than initially anticipated. However, the majority of the ET was conceptually anticipated to occur in the lower elevation river valleys which, in the model, are coincident with stream cells and much of this ET is assimilated into the stream discharge portion of the water budget.

Table 8.2.1 Calibration statistics for the steady-state model.

Aquifer/Pod	Number	ME (ft)	MAE (ft)	RMS (ft)	Range (ft)	Adjusted RMS
Seymour Aquifer	537	-19.4	26.7	35.8	1566	0.02
Blaine Aquifer	278	12.8	54.7	67.5	1096	0.06
Pod 1	45	2.9	19.5	26.0	437	0.06
Pod 2	2	-11.1	11.1	11.6	386	0.03
Pod 3	6	-6.5	16.6	20.4	428	0.05
Pod 4	206	-38.0	39.0	48.8	671	0.07
Pod 5	16	-10.9	15.5	19.4	184	0.11
Pod 6[1]						
Pod 7	101	-2.0	14.8	18.7	378	0.05
Pod 8	30	-9.0	13.6	16.5	175	0.09
Pod 9	3	-15.0	18.9	26.6	263	0.10
Pod 10[2]						
Pod 11	11	-11.5	17.6	20.5	378	0.05
Pod 12	7	-0.4	12.7	14.2	133	0.11
Pod 13	88	-20.0	29.7	34.4	217	0.16
Pod 14	8	-5.5	9.6	11.4	79	0.14
Pod 15	14	-4.0	8.4	11.2	155	0.07

Number = number of targets
ME = mean error
MAE = mean absolute error
RMS = root mean square error
Note: ME, MAE, and RMS are defined in equations in Section 7.1.
[1] no steady-state targets
[2] only one steady-state target

Table 8.2.2a Water budget for the steady-state model (all rates reported in AFY).

IN	Layer	Recharge	Streams	Top	Bottom	Wells	Springs
	1	303,092	1,778	0	51,122		
	2	301,430	38,135	132,873	0		
	Sum	604,521	39,913	132,873	51,122		
OUT	**Layer**	**ET**	**Streams**	**Top**	**Bottom**	**Wells**	**Springs**
	1	43,189	83,869	0	132,873	77,255	9,496
	2	154,013	225,605	51,122	0	47,685	3,716
	Sum	197,202	309,474	51,122	132,873	124,940	13,212

Table 8.2.2b Water budget for the steady-state model with values expressed as a percentage of inflow or outflow.

IN	Layer	Recharge	Streams		
	1	47%	0%		
	2	47%	6%		
	Sum	94%	6%		
OUT	**Layer**	**ET**	**Streams**	**Wells**	**Springs**
	1	7%	13%	12%	1%
	2	24%	35%	7%	1%
	Sum	31%	48%	19%	2%

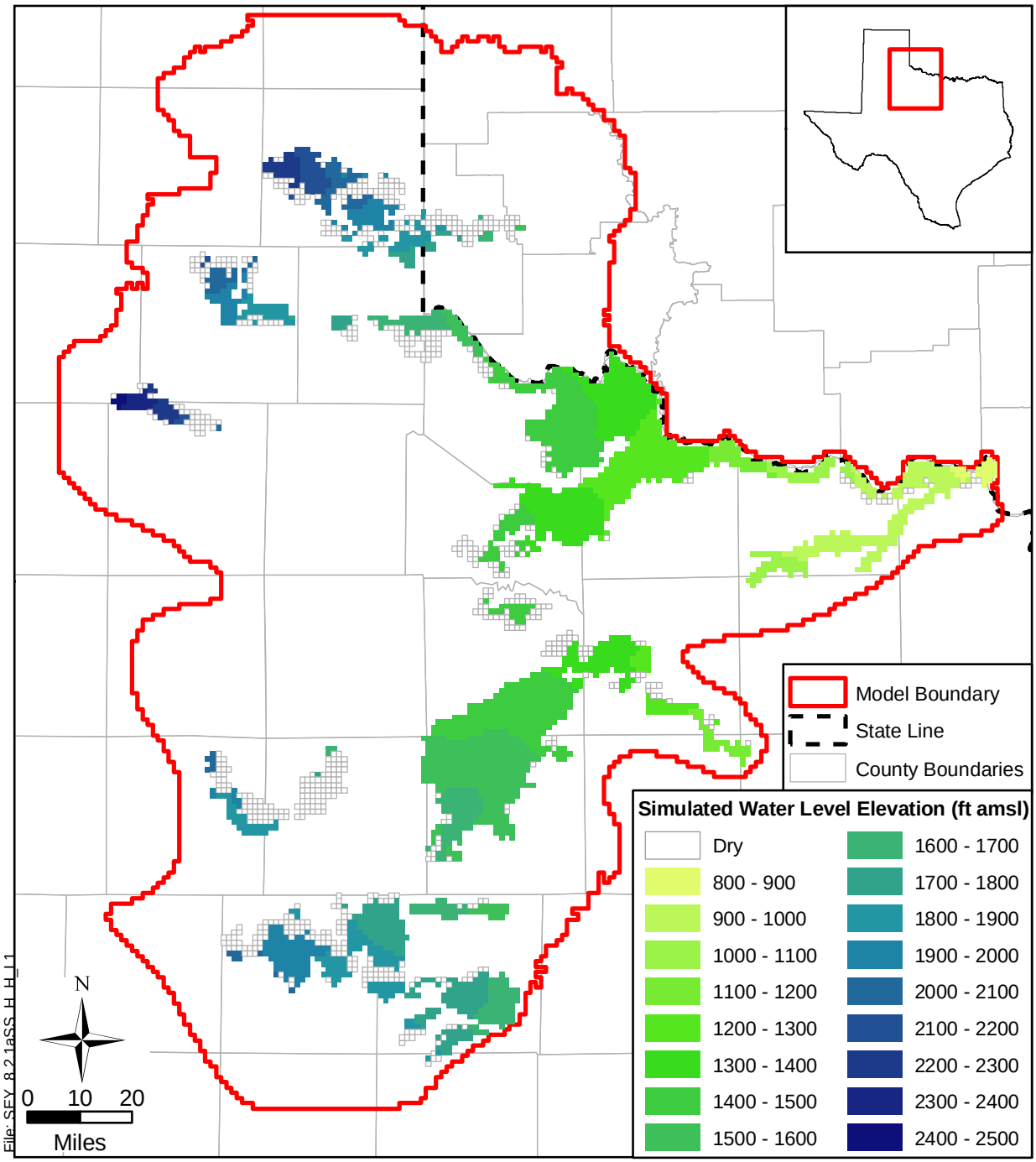

Figure 8.2.1a Simulated steady-state water-level elevations for layer 1.

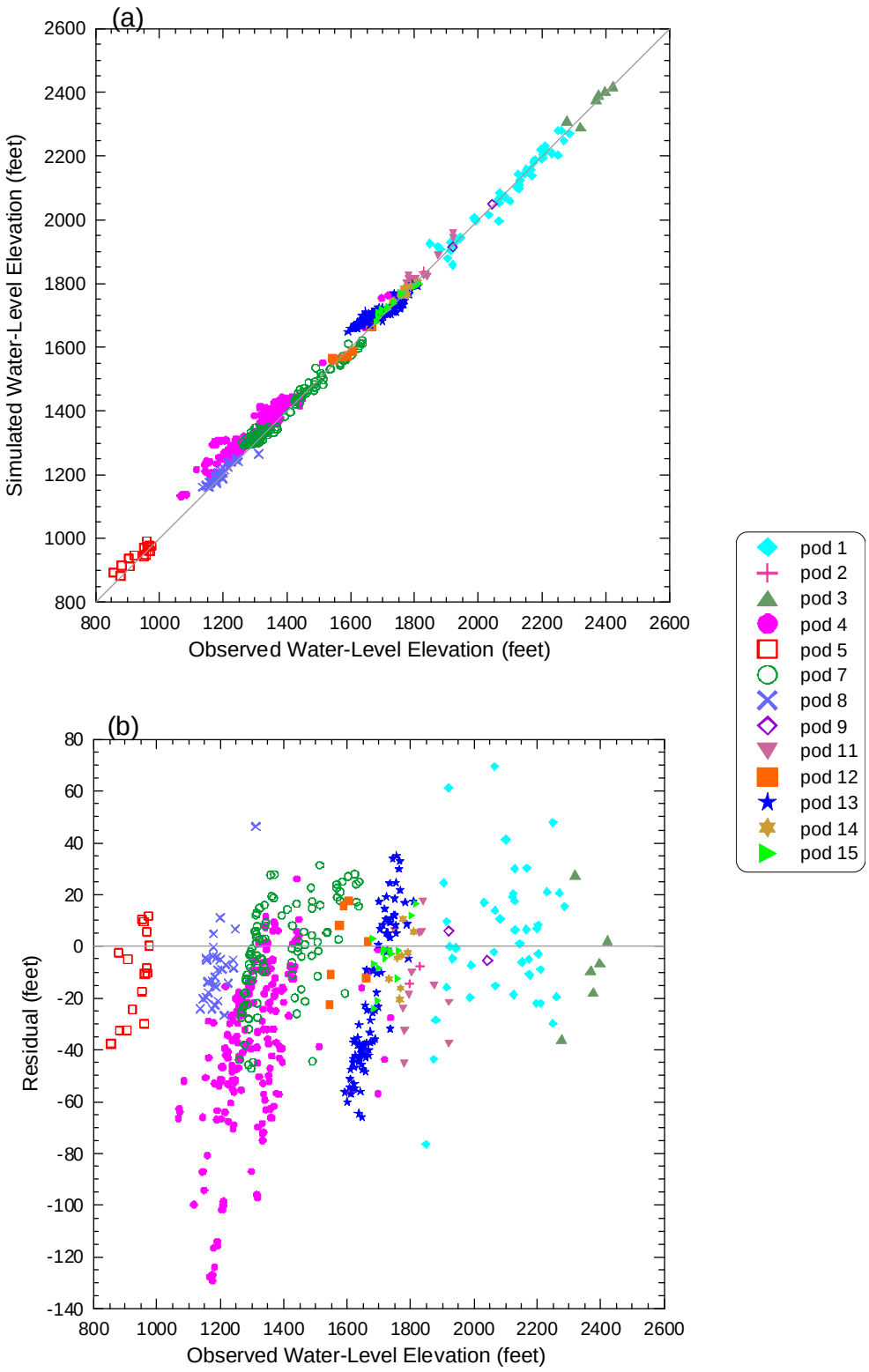

Figure 8.2.1b Plots of (a) simulated versus observed water-level elevations and (b) residual versus observed water-level elevation for the Seymour aquifer in the steady-state model.

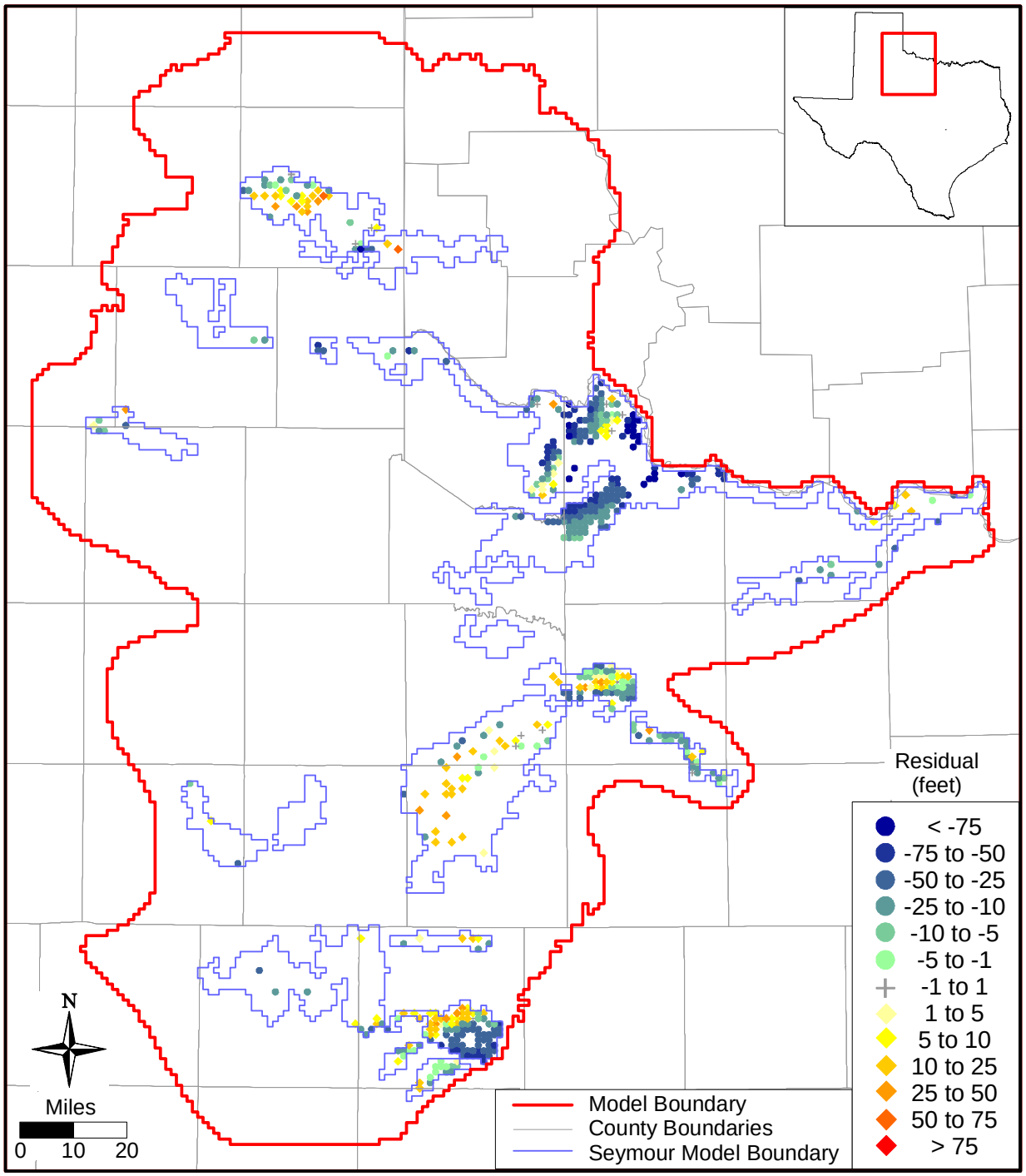

Figure 8.2.1c Residuals at target wells in the Seymour aquifer for the steady-state model.

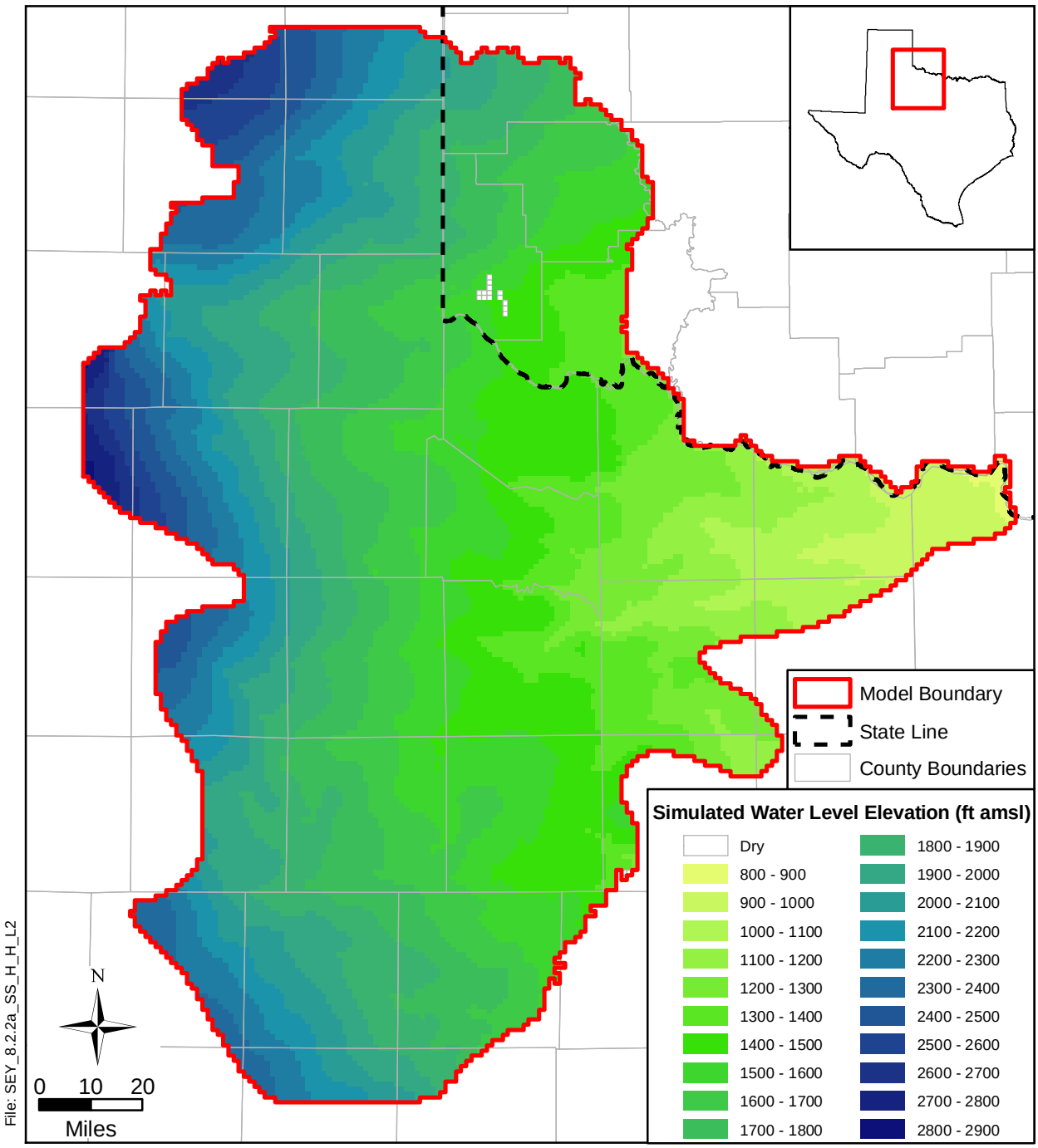

Figure 8.2.2a Simulated steady-state water-level elevations for layer 2.

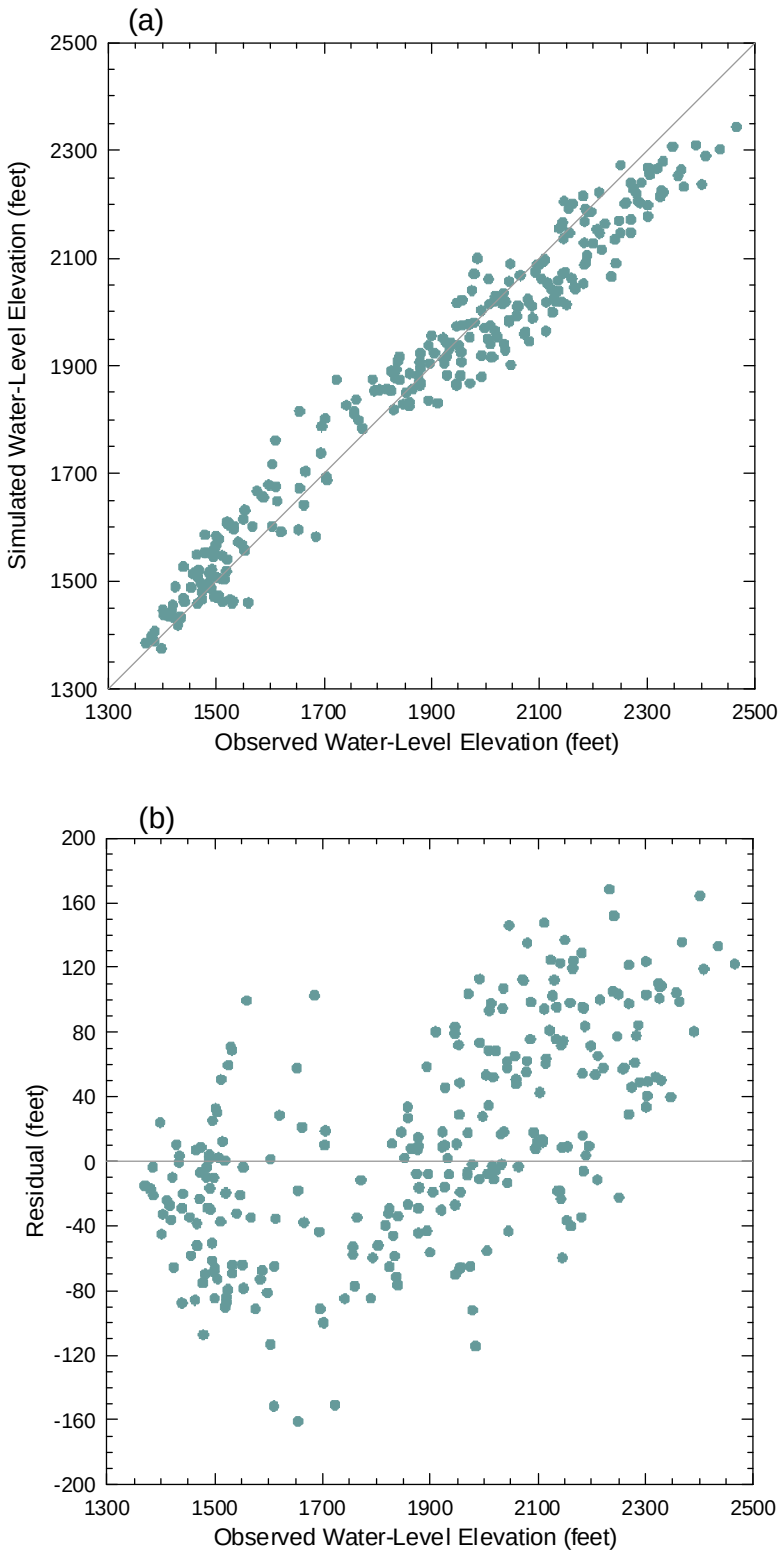

Figure 8.2.2b Plots of (a) simulated versus observed water-level elevations and (b) residual versus observed water-level elevation for the Blaine aquifer in the steady-state model.

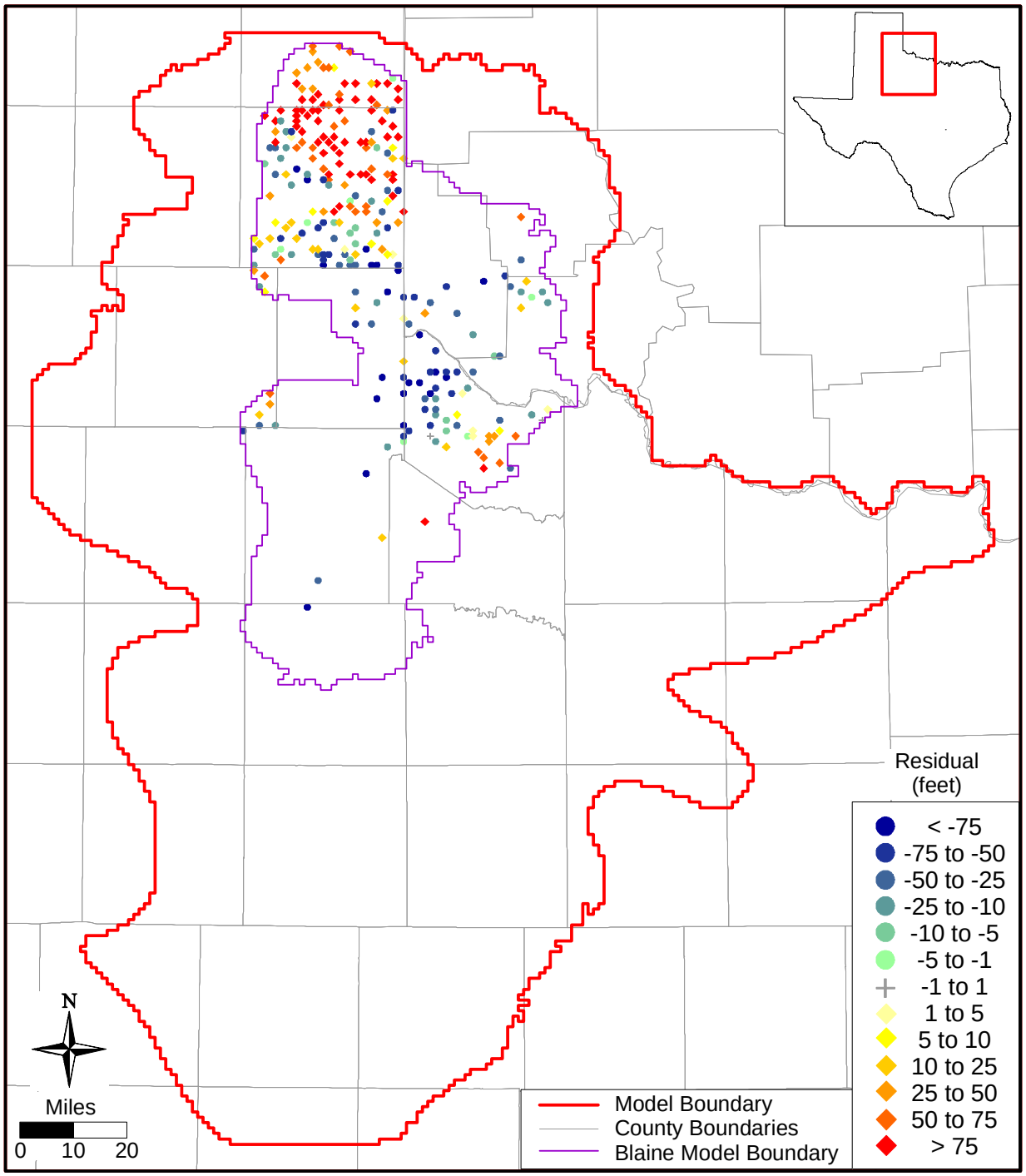

Figure 8.2.2c Residuals at target wells in the Blaine aquifer for the steady-state model.

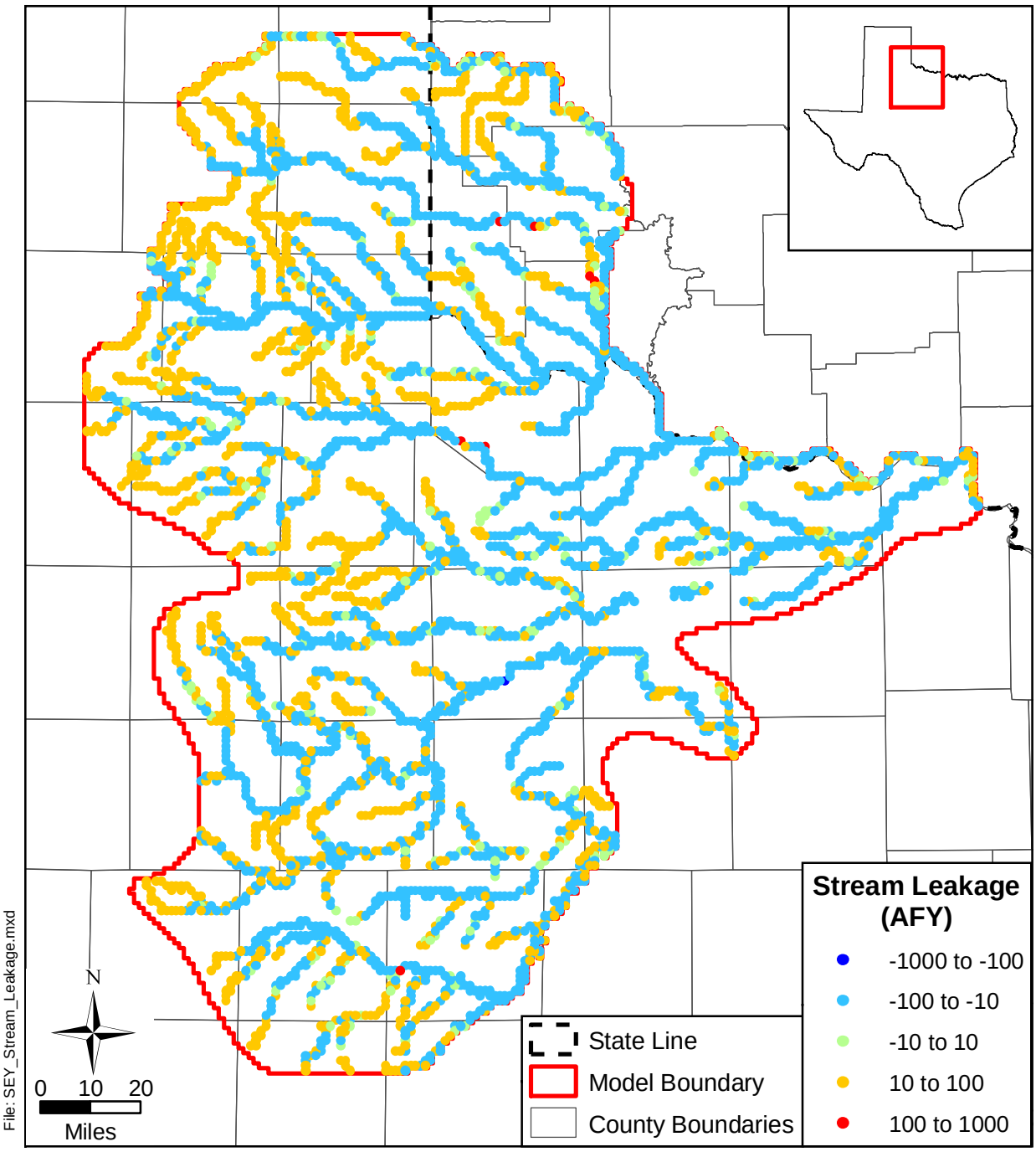

Figure 8.2.3 Steady-state model stream gain/loss (negative values denote gaining streams).

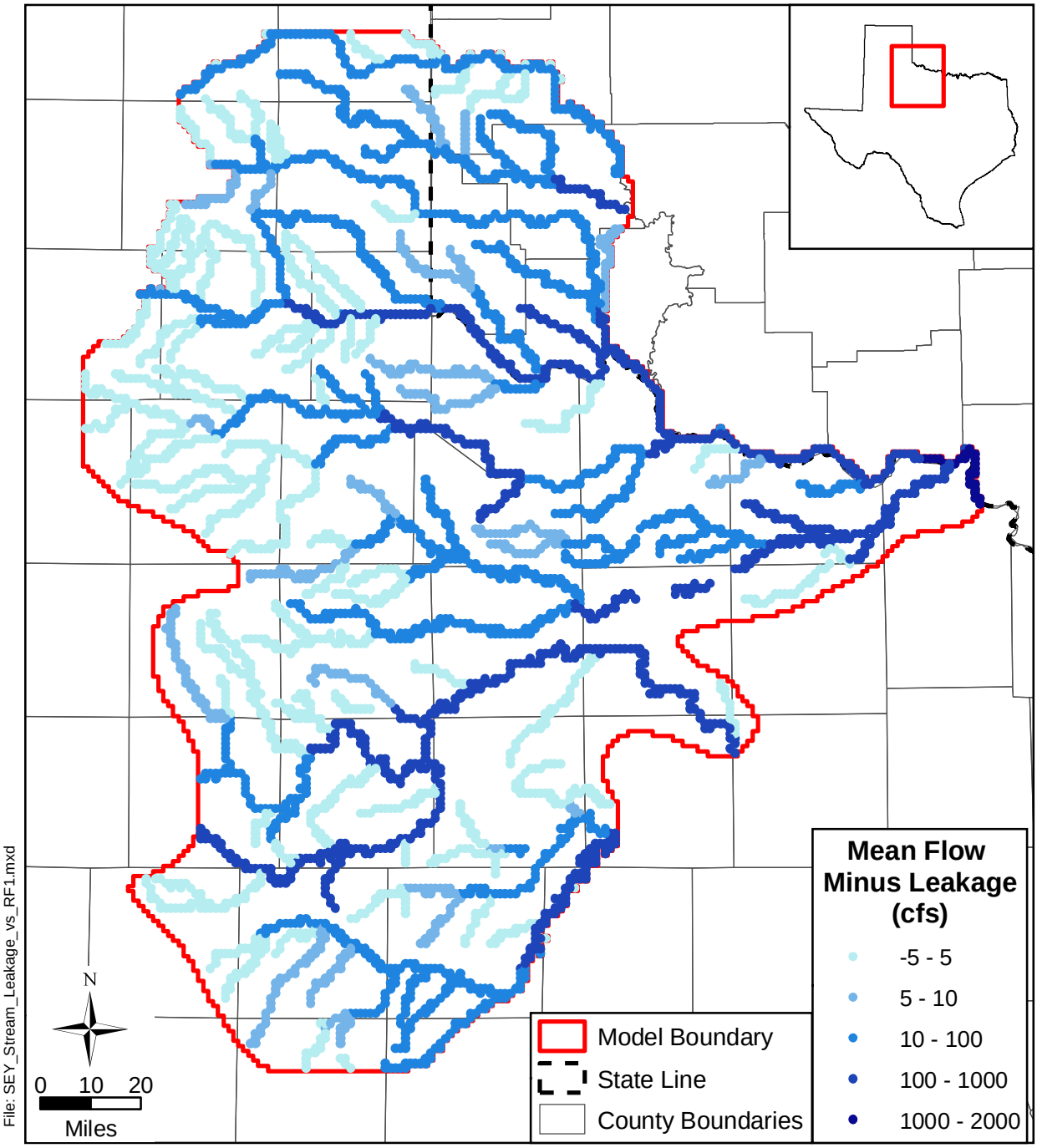

Figure 8.2.4 Steady-state simulated stream gain/loss compared to RF1 mean flow.

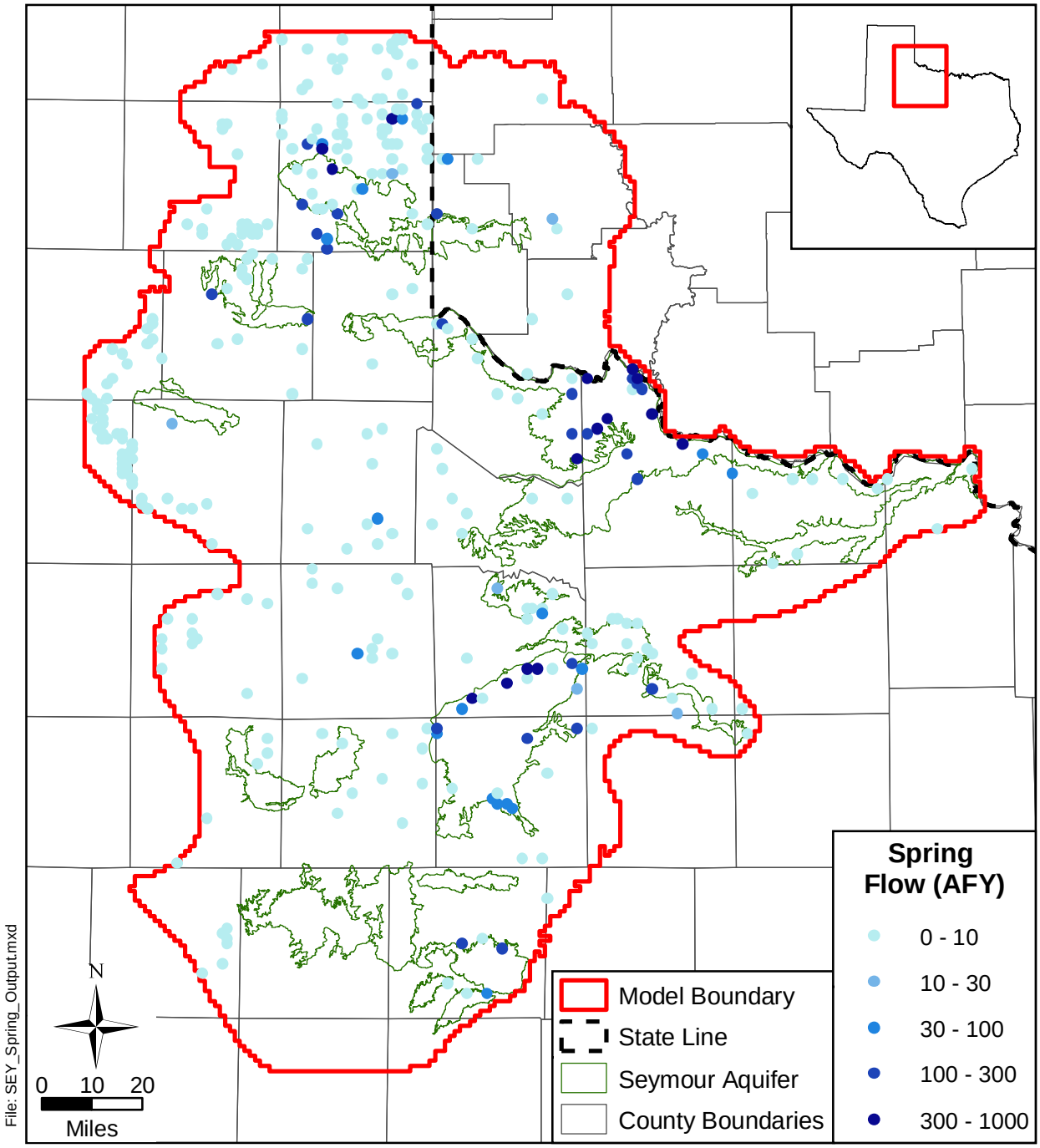

Figure 8.2.5 Spring flow in the steady-state model.

8.3 Sensitivity Analysis

A sensitivity analysis was performed on the calibrated steady-state model. A sensitivity analysis provides a means of formally describing the impact of varying specific parameters or groups of parameters on model outputs. In this sensitivity analysis, input parameters were systematically increased and decreased from their calibrated values while the change in water-level elevation was recorded. Four simulations were completed for each parameter sensitivity, where the input parameters were varied either according to:

$$\text{(new parameter)} = \text{(old parameter)} * \text{factor} \tag{8.3.1}$$

or

$$\text{(new parameter)} = \text{(old parameter)} * 10^{(\text{factor} - 1)} \tag{8.3.2}$$

and the factors were 0.8, 0.9, 1.1, and 1.2. Parameters such as recharge were varied linearly using equation (8.3.1). For parameters such as hydraulic conductivity, which are typically thought of as log-varying, equation (8.3.2) was used. For the output variable, we calculated the mean difference (*MD*) between the base simulated head and the sensitivity simulated head:

$$MD = \frac{1}{n}\sum_{i=1}^{n}\left(h_{sens,i} - h_{cal,i}\right) \tag{8.3.3}$$

where

$h_{sens,i}$ = sensitivity simulation head at active grid block i,

$h_{cal,i}$ = calibrated simulation head at active grid block i, and

n = number of active grid blocks.

Two approaches to applying Equation 8.3.3 to the sensitivity of output heads were considered. First, we compared the heads in all active grid blocks between the sensitivity output and the calibrated output. Second, we compared the heads only at grid blocks where measured targets were available (i.e., n = number of targets in that layer). A comparison between these two methods can provide information about the absence of bias in the target locations (i.e., a similar result indicates adequate target coverage).

For the steady-state analysis, we completed seven parameter sensitivities:

1. Horizontal hydraulic conductivity of layer 1,

2. Horizontal hydraulic conductivity of layer 2,
3. Vertical hydraulic conductivity in layer 1 (leakance between layers 1 and 2),
4. Recharge, model-wide,
5. Pumping, model-wide,
6. Streambed conductance, model-wide, and
7. Spring conductance, model-wide.

Equation 8.3.1 (varying linearly) was used for sensitivities 4 and 5 and Equation 8.3.2 was used for the other sensitivities.

Figures 8.3.1a and 8.3.2a show the results of the sensitivity analyses for layers 1 and 2, respectively, with *MDs* calculated from just the grid blocks where targets are available. In comparison, Figures 8.3.1b and 8.3.2b show the corresponding sensitivity results with *MDs* calculated for all active cells in layers 1 and 2, respectively. Note that the two figures show similar trends in sensitivities, indicating adequate target coverage. Figures 8.3.1 and 8.3.2 indicate that the change in water-level elevation in the Seymour aquifer and the Permian sediments for the steady-state model is most positively correlated with recharge. This is to be expected since the Seymour is a water-table aquifer and the majority of the Permian sediments outcrop in the model. Water-level elevations in the Seymour aquifer show a negative correlation to stream conductance, horizontal hydraulic conductivity in layer 2, pumping, and horizontal hydraulic conductivity in layer 1, with stream conductance being most negatively correlated. Water-level elevations in the Seymour aquifer are essentially insensitive to spring conductance and vertical conductivity. Water-level elevations in layer 2 show a negative correlation to the horizontal hydraulic conductivity of layer 2, pumping, and stream conductance, with horizontal hydraulic conductivity of layer 2 being most important. Water-level elevations in layer 2 are essentially insensitive to horizontal hydraulic conductivity in layer 1, spring conductance, and vertical hydraulic conductivity.

As described in Section 7.1, model convergence issues precluded the use of PEST as a calibration tool. For the same reasons, PEST was not used to calculate the Jacobian Matrix. Consequently, the original intention of calculating parameter sensitivities based on the inverse solution of the Jacobian Matrix was not possible.

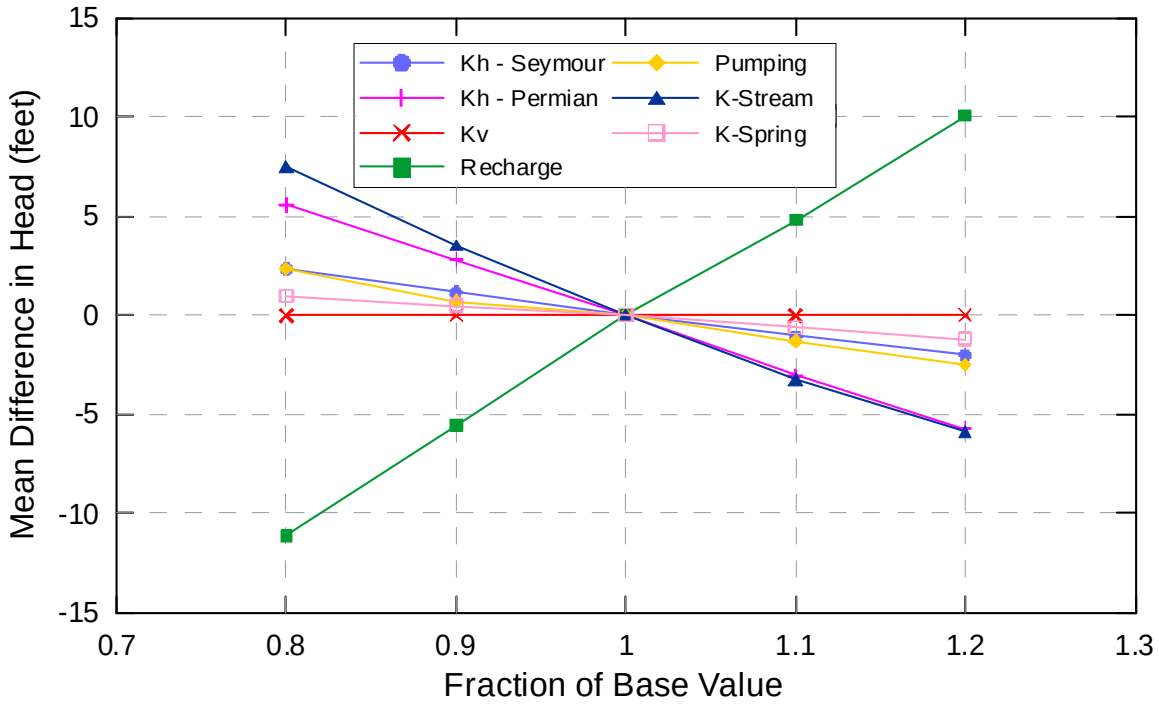

Figure 8.3.1a Steady-state sensitivity results for layer 1 using target locations.

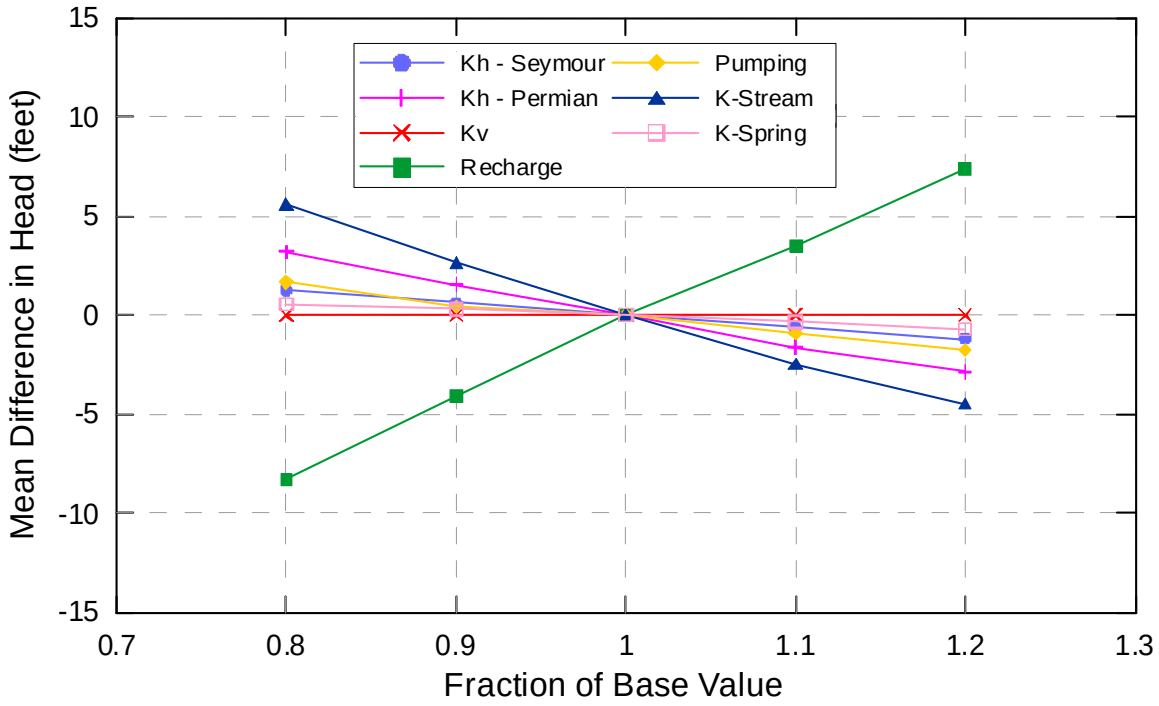

Figure 8.3.1b Steady-state sensitivity results for layer 1 using all active grid blocks.

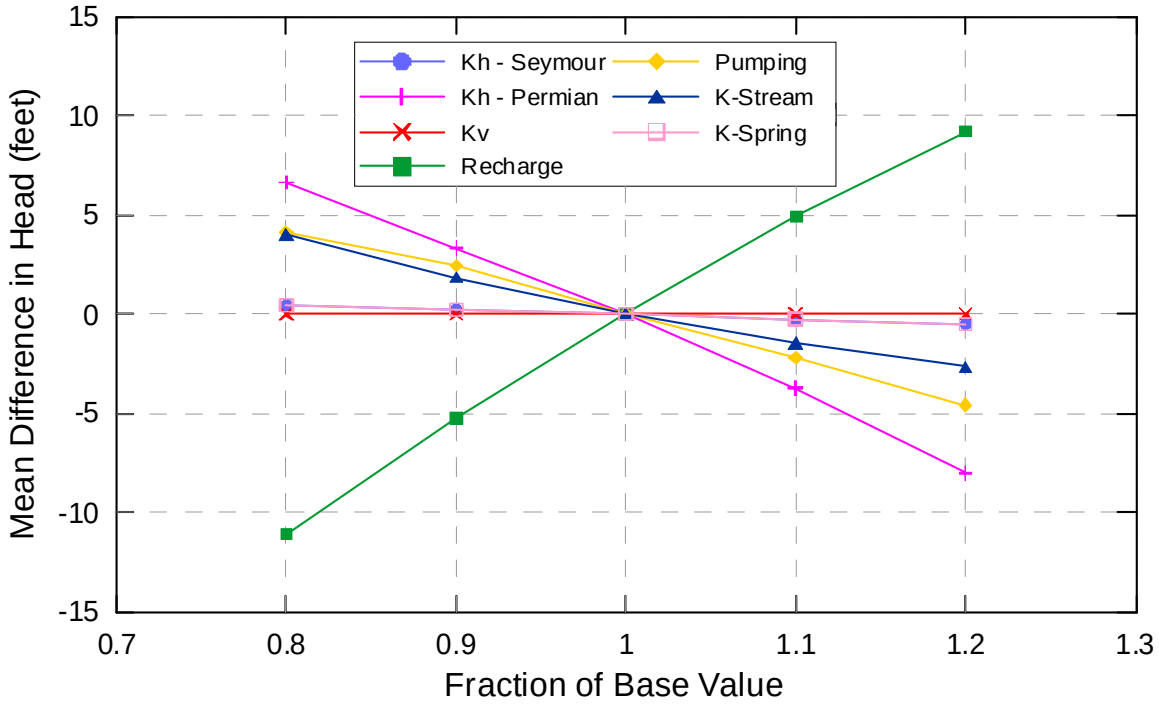

Figure 8.3.2a Steady-state sensitivity results for layer 2 using target locations.

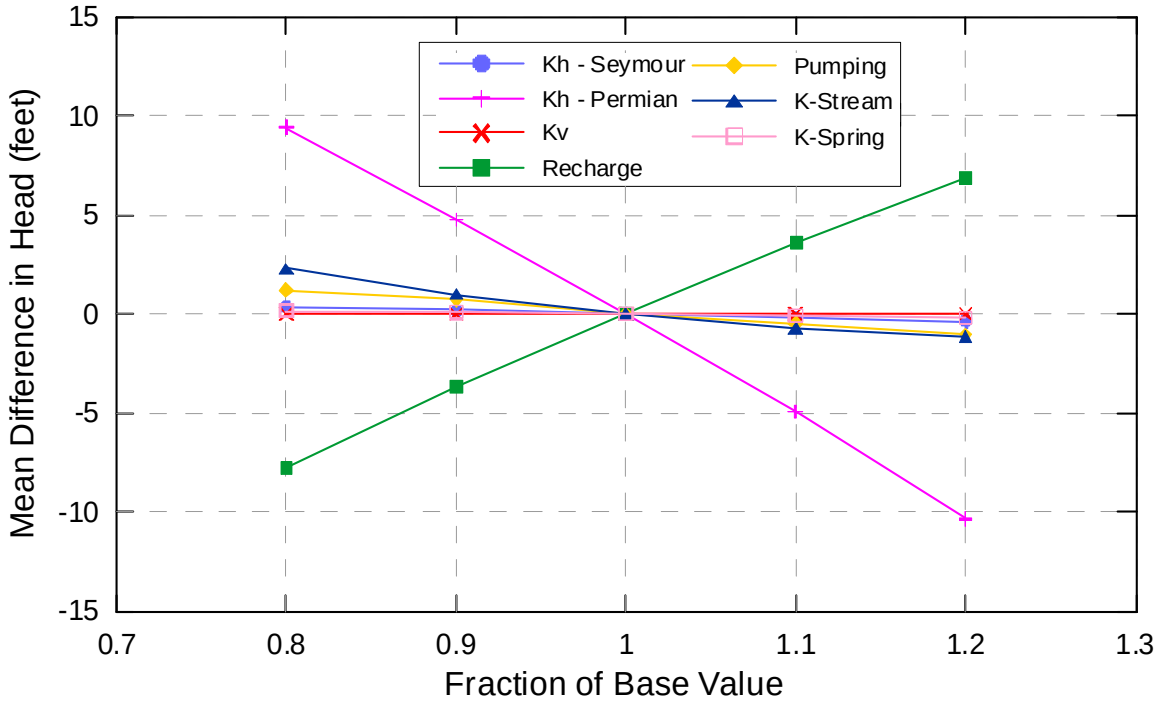

Figure 8.3.2b Steady-state sensitivity results for layer 2 using all active grid blocks.

9.0 TRANSIENT MODEL

This section describes calibration and verification of the transient model, presents the transient model results, and describes a sensitivity analysis for the transient model. The transient model included an initialization period from 1975 to 1980, a calibration period from 1980 through 1989, and a verification period from 1990 through 1999. Section 9.1 describes the model calibration. Section 9.2 presents model results for the calibration and verification time periods. Section 9.3 presents the sensitivity analysis results.

9.1 Calibration

All properties or parameters common with the steady-state model were identical in the transient model. Section 8.1 contains the discussion of hydraulic properties in the steady-state and transient models. A discussion of important inputs and new properties (such as storage estimates) follows. Figures 9.1.1 and 9.1.2 show the distribution of calibration targets (water-level elevation measurements) for the Seymour and Blaine aquifers, respectively, used for the transient model calibration.

Figures 9.1.3a and 9.1.4a show the distribution of pumping in layer 1 during the first year of model calibration (1980) and during the first year of model verification (1990), respectively. Over much of the aquifer, pumping is less than 50 AFY in both 1980 and 1990. Most of the pumpage from the Seymour aquifer occurs in Haskell, Knox, and Wilbarger counties. Pumping in these three counties decreased from 1980 to 1990. Pumping in parts of Collingsworth County increased significantly between 1980 and 1990. Of the water pumped from the Seymour aquifer, the largest volume is used for irrigation purposes. The difference between pumping in layer 1 during steady state and during 1980 and 1990 is illustrated in Figures 9.1.3b and 9.1.4b, respectively. In these figures, a negative value indicates that steady-state pumping was less than the 1980 or 1990 pumping and a positive value indicates that steady-state pumping was greater than the 1980 or 1990 pumping. Pumping in 1980 was significantly greater than that during steady state in portions of pods 2, 3, 4, and 7 and significantly less than that during steady state in small portions of pod 1. The number designation for each pod is shown in Figure 4.1.1. Overall, pumping from the Seymour aquifer during 1980 was substantially greater than during

any other time period (see Table 4.7.21). Large differences between steady-state and 1990 pumping occur in only a few grid blocks in pods 1, 2, 4, and 7.

Pumping in layer 2 for 1980 and 1990 is illustrated in Figures 9.1.5a and 9.1.6a, respectively. Pumping is less than 50 AFY over the majority of the aquifer in Texas. In general, pumping from the Blaine aquifer in Texas slightly decreased from 1980 to 1990 (see Table 4.7.22). The largest volumes of groundwater are removed from the Blaine aquifer in Oklahoma. Figures 9.1.5b and 9.1.6b show the difference between Blaine pumping during steady state and during 1980 and 1990, respectively. In general, pumping differences between the two time periods fall within ±100 AFY. Pumping during steady state is greater than that during 1980 in a few small areas in Collingsworth, Childress, and Cottle counties. A larger difference is observed between steady-state and 1990 pumping. The largest differences indicate greater pumping during steady state in localized areas in Collingsworth and Cottle counties, Texas and Harmon County, Oklahoma. In a few localized areas in Hardeman County, Texas and Harmon County, Oklahoma, steady-state pumping was over 500 AFY less than 1990 pumping.

Primary and secondary storage (also called storativity and specific yield) are properties in a transient model that are not needed in a steady-state model. All of the Seymour aquifer and 83 percent of the Permian are unconfined. Consequently, storage properties are defined by specific yield. For the Seymour aquifer, a uniform specific yield of 0.14, based on the average of measured values from literature, was used. This value was not altered during calibration. For the Permian sediments, a literature estimate of 0.15 was used for specific yield. No measurements of storativity are available for the portions of the Permian sediments overlain by the Seymour aquifer. Freeze and Cherry (1979) indicate that confined aquifers have storativity values ranging from 5×10^{-3} to 5×10^{-5}. The karstic nature of the Blaine aquifer results in areas where the transmissive portions of the Blaine are separated from the Seymour aquifer by confining material and other areas where the two are in hydraulic communication. As a result, a combination of unconfined and confined conditions exist between the Blaine and Seymour aquifers. Therefore, an unconfined specific yield was not appropriate for use for the Blaine aquifer but neither was a storativity representative of completely confined conditions. As a compromise, a storativity value falling between these two extremes was used. Simulations were conducted using several intermediate values until a value was found that minimized cross-

formational flow upward from layer 2 to layer 1, in keeping with the conceptual model of cross-formational flow. This resultant value, 10^{-2}, was applied uniformly across the Blaine aquifer and the remaining Permian sediments.

Because we lacked stream gain/loss targets, stream behavior was assessed only qualitatively and a uniform stream bed conductance was used. The stream bed conductance arrived at during steady-state calibration was found to be consistent with the conceptual model of stream leakages being equal to or less than observed stream flows and was not altered during the transient model calibration.

Similar to the steady-state calibration, recharge was critical for the transient calibration. The spatial distribution of recharge from the steady-state model (see Figure 8.1.5) was used for the transient model; when averaged temporally, the transient recharge distribution is identical to that of the steady-state model. The overall mean recharge (averaged temporally and spatially) between 1980 and 2000 from the SWAT simulations (2.0 in/yr) was consistent with the calibrated average recharge in the Seymour aquifer (final calibrated value of 2.1 in/yr) during the same time period. Therefore, the time-varying average from SWAT was used to vary the transient recharge temporally. This way, seasonal variations and periods of low or high precipitation were accounted for in the transient recharge. A plot illustrating the average monthly recharge from 1980 to 2000 in layers 1 and 2 is shown in Figure 9.1.7.

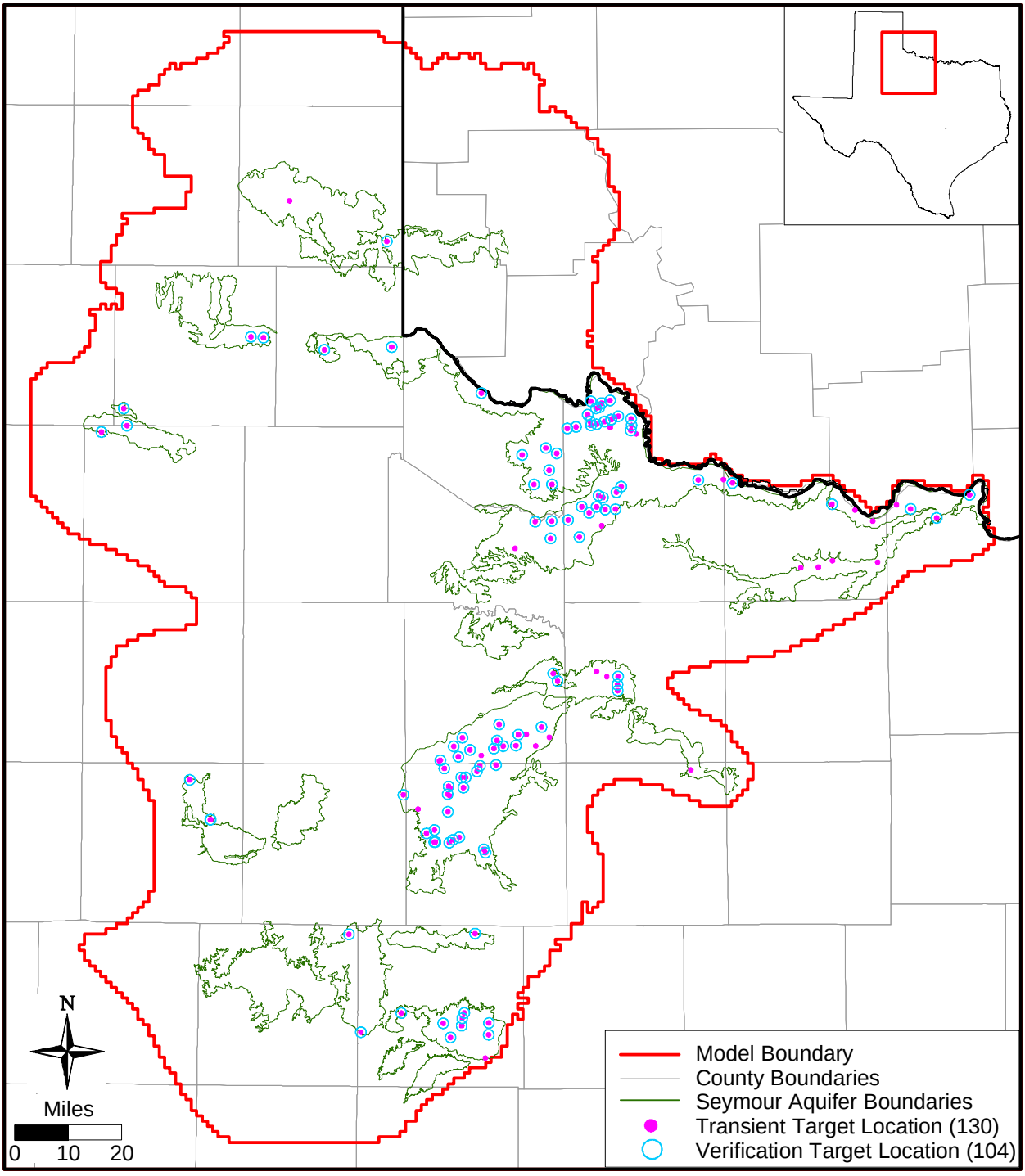

Figure 9.1.1 Target well locations in the Seymour aquifer for transient calibration.

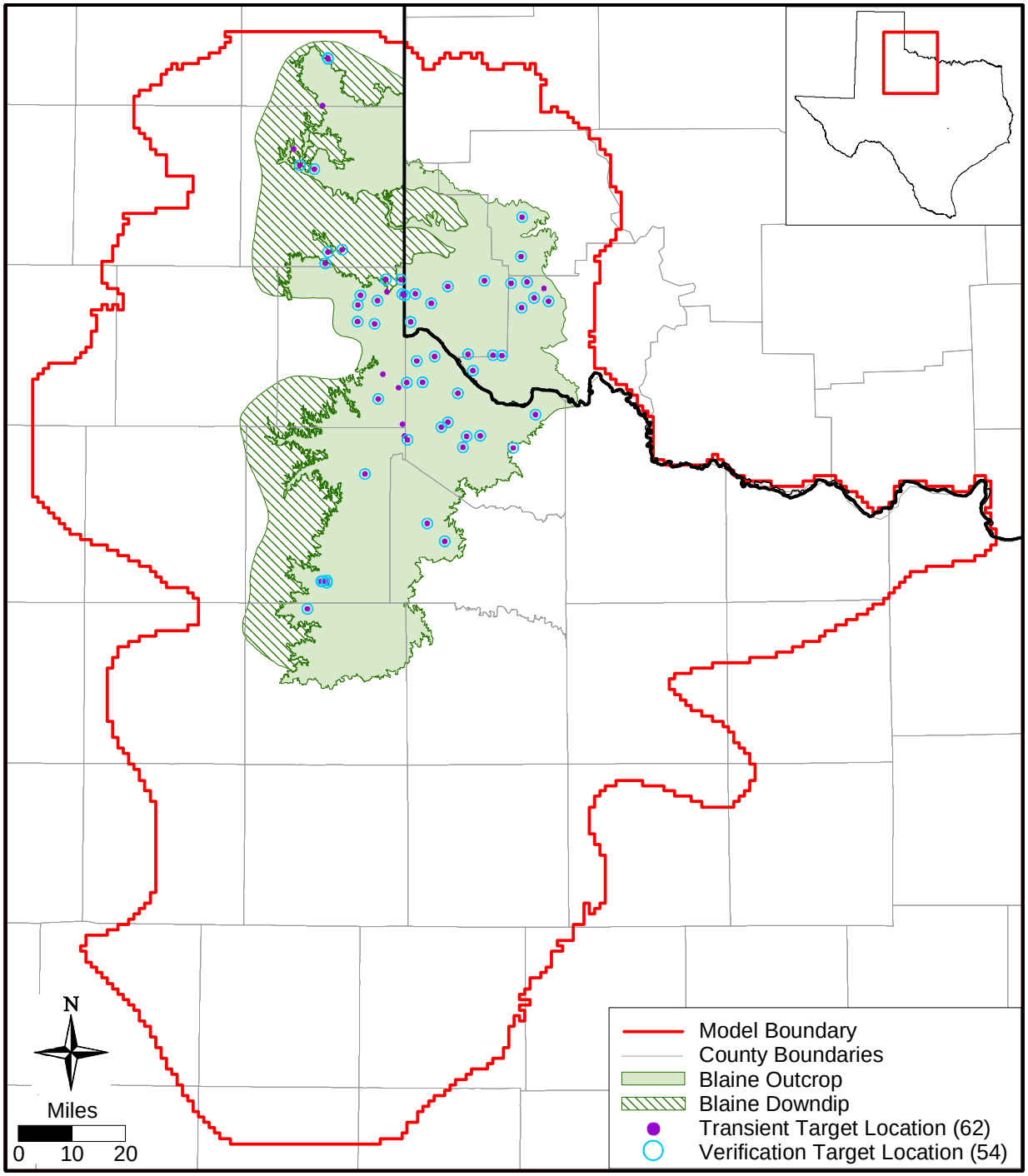

Figure 9.1.2 Target well locations in the Blaine aquifer for transient calibration.

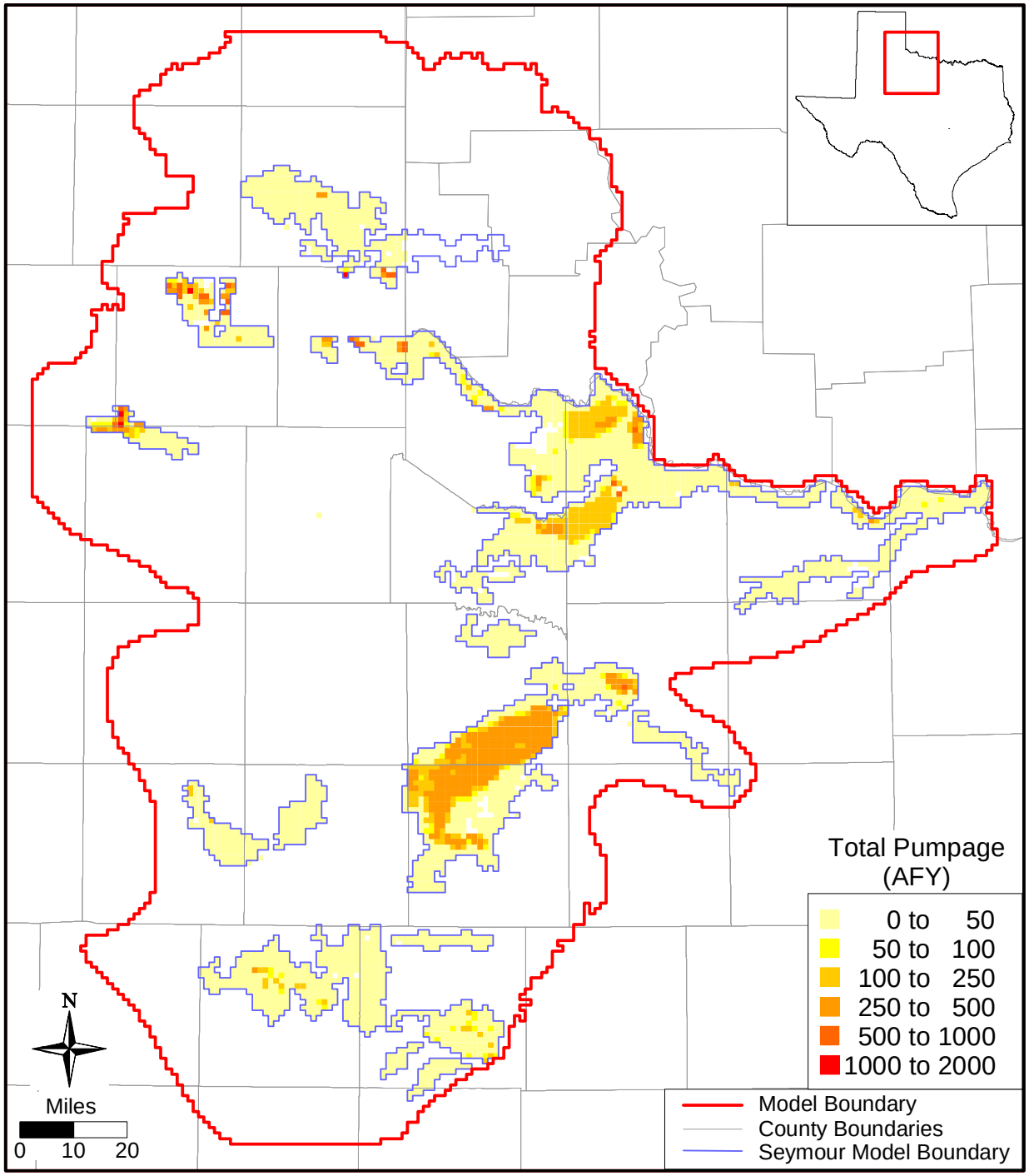

Figure 9.1.3a Pumping distribution in layer 1 in 1980.

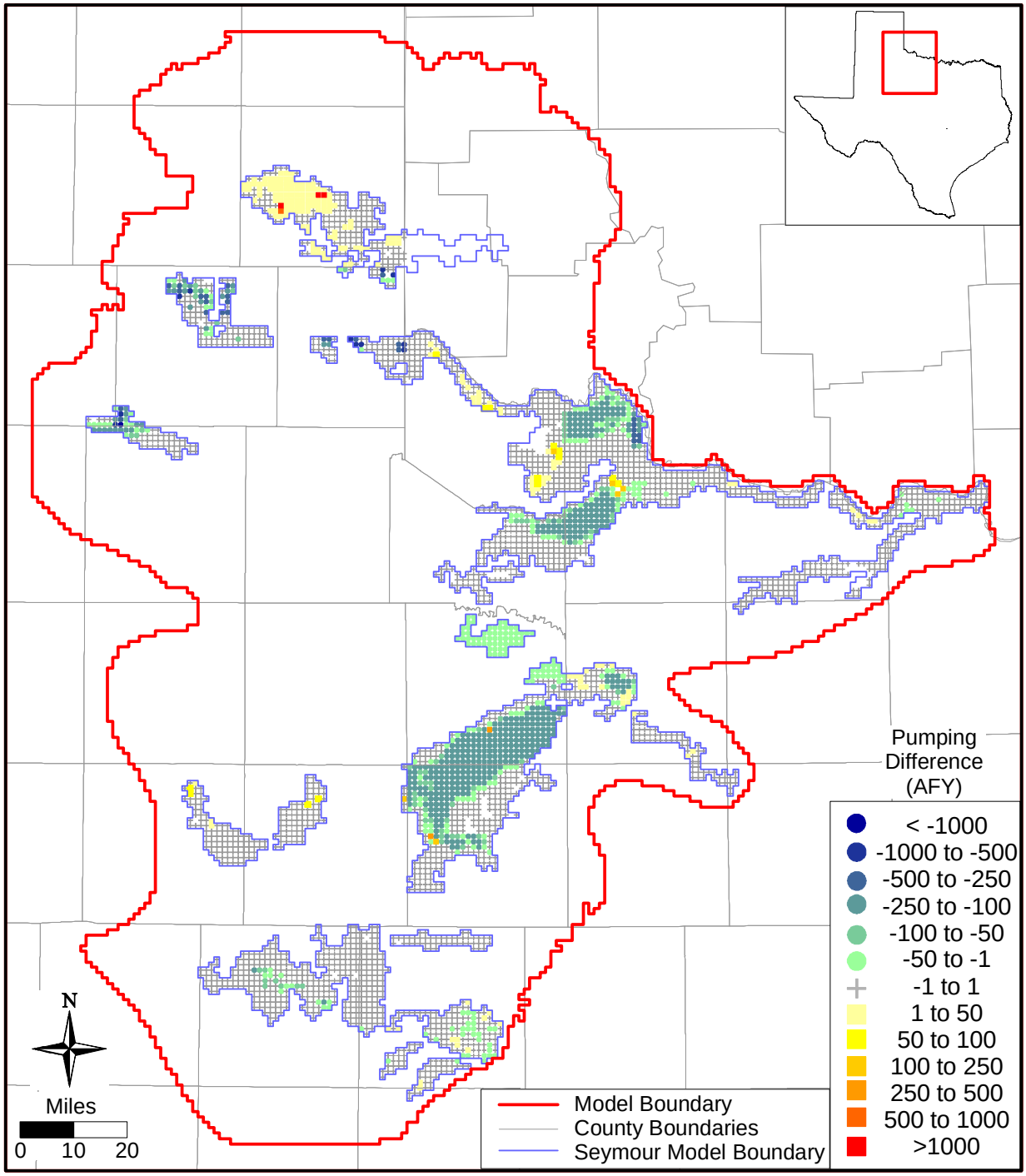

Figure 9.1.3b Difference between steady-state and 1980 pumping in layer 1.

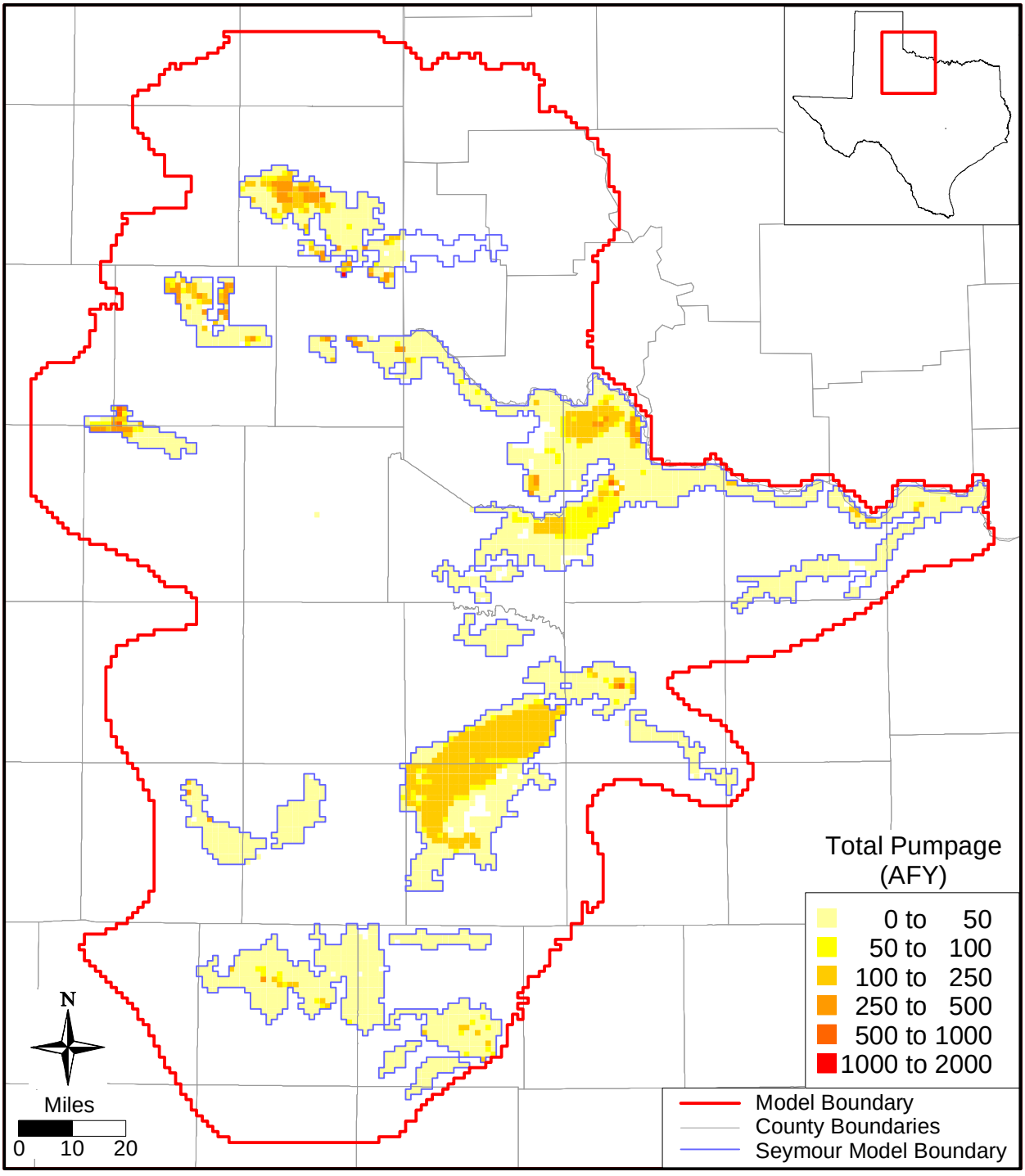

Figure 9.1.4a Pumping distribution in layer 1 in 1990.

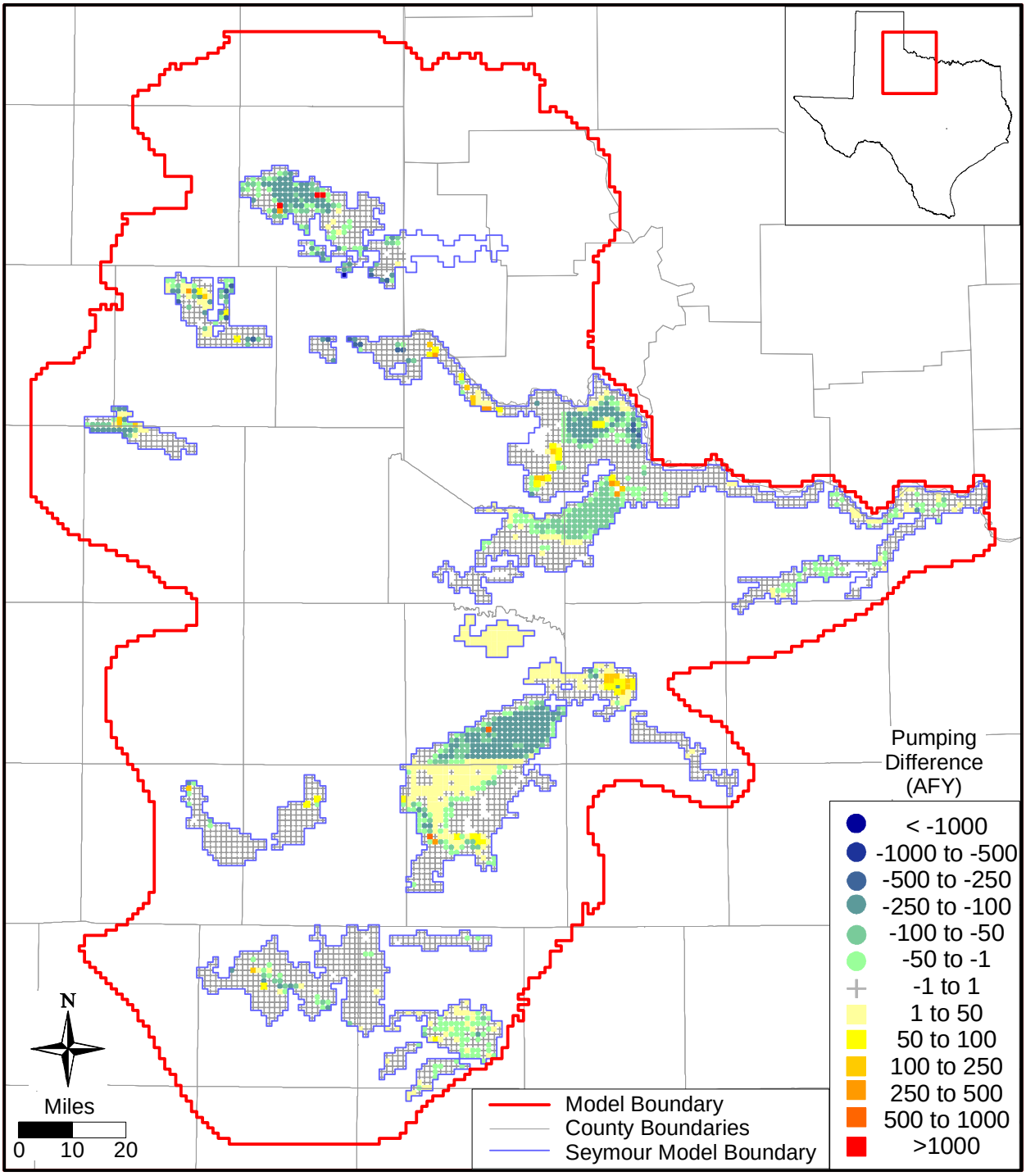

Figure 9.1.4b Difference between steady-state and 1990 pumping in layer 1.

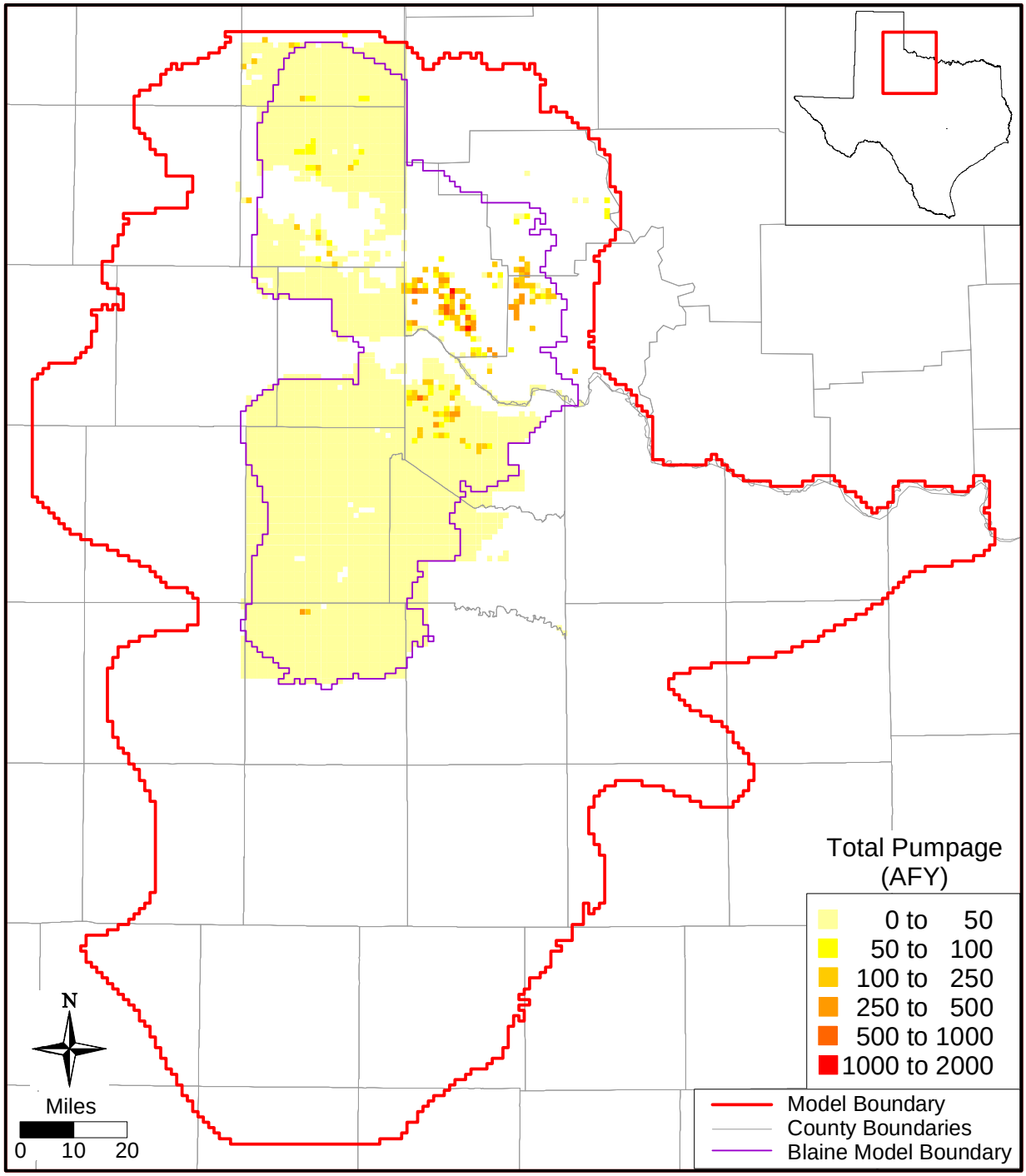

Figure 9.1.5a Pumping distribution in layer 2 in 1980.

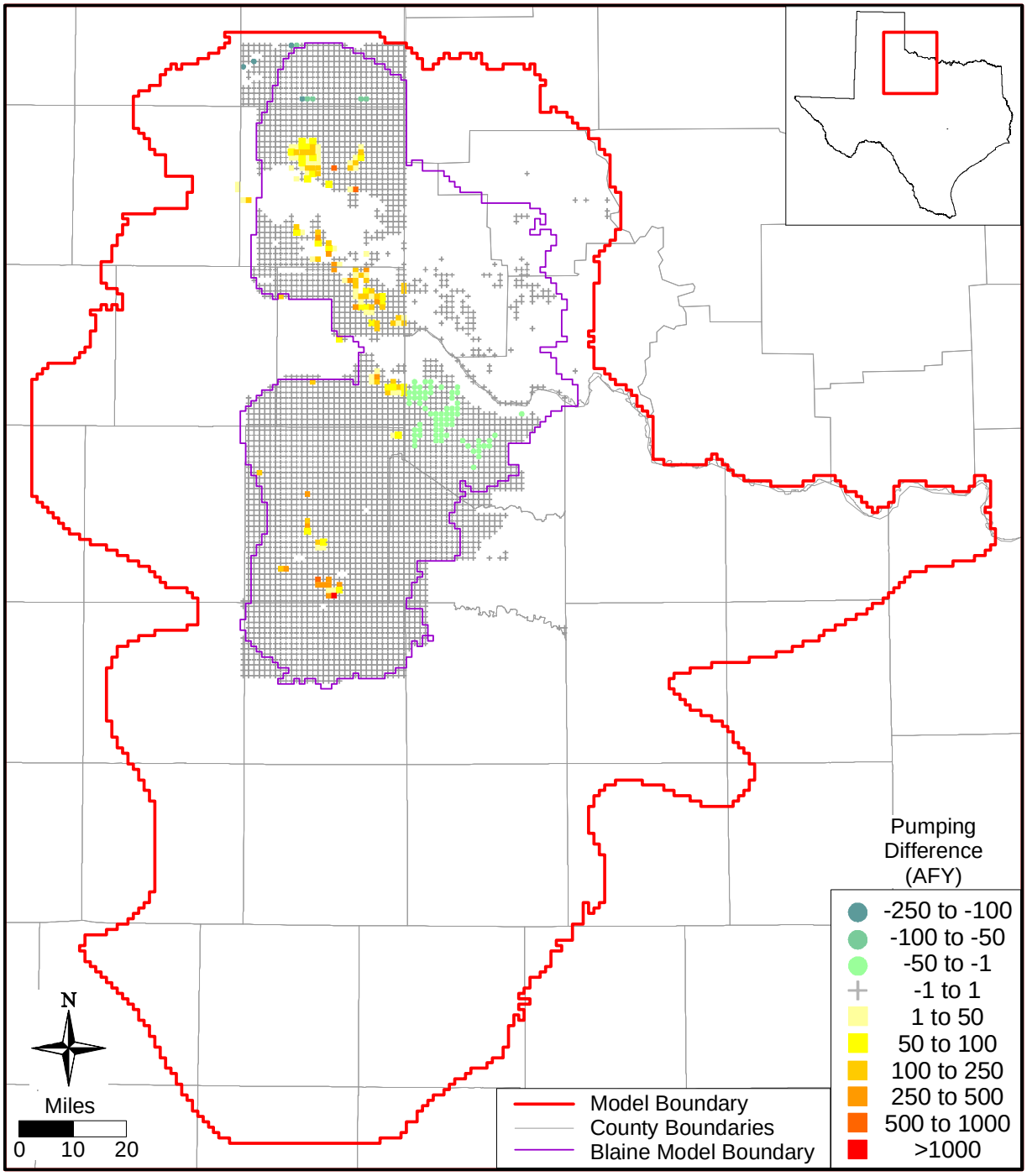

Figure 9.1.5b Difference between steady-state and 1980 pumping in layer 2.

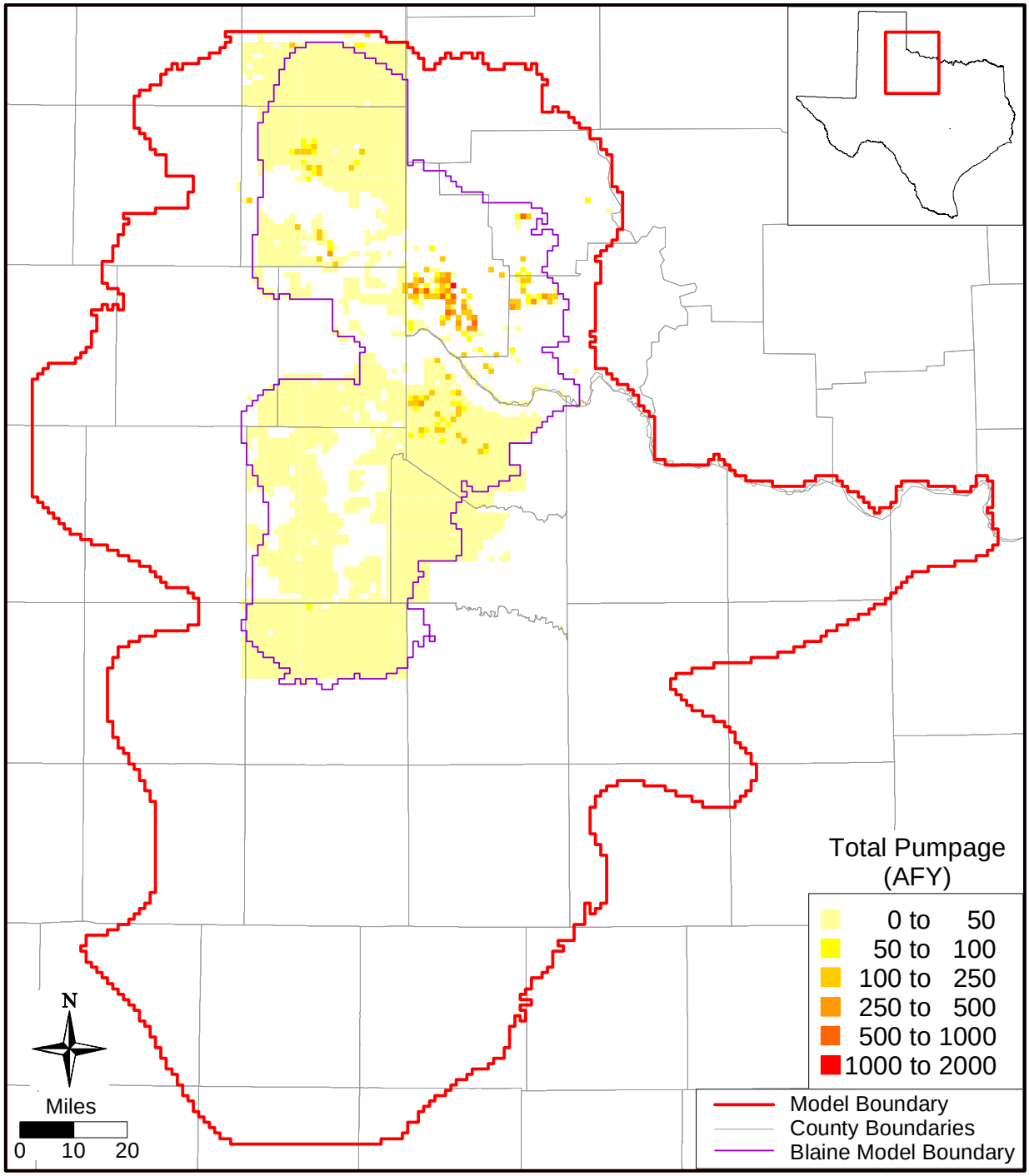

Figure 9.1.6a Pumping distribution in layer 2 in 1990.

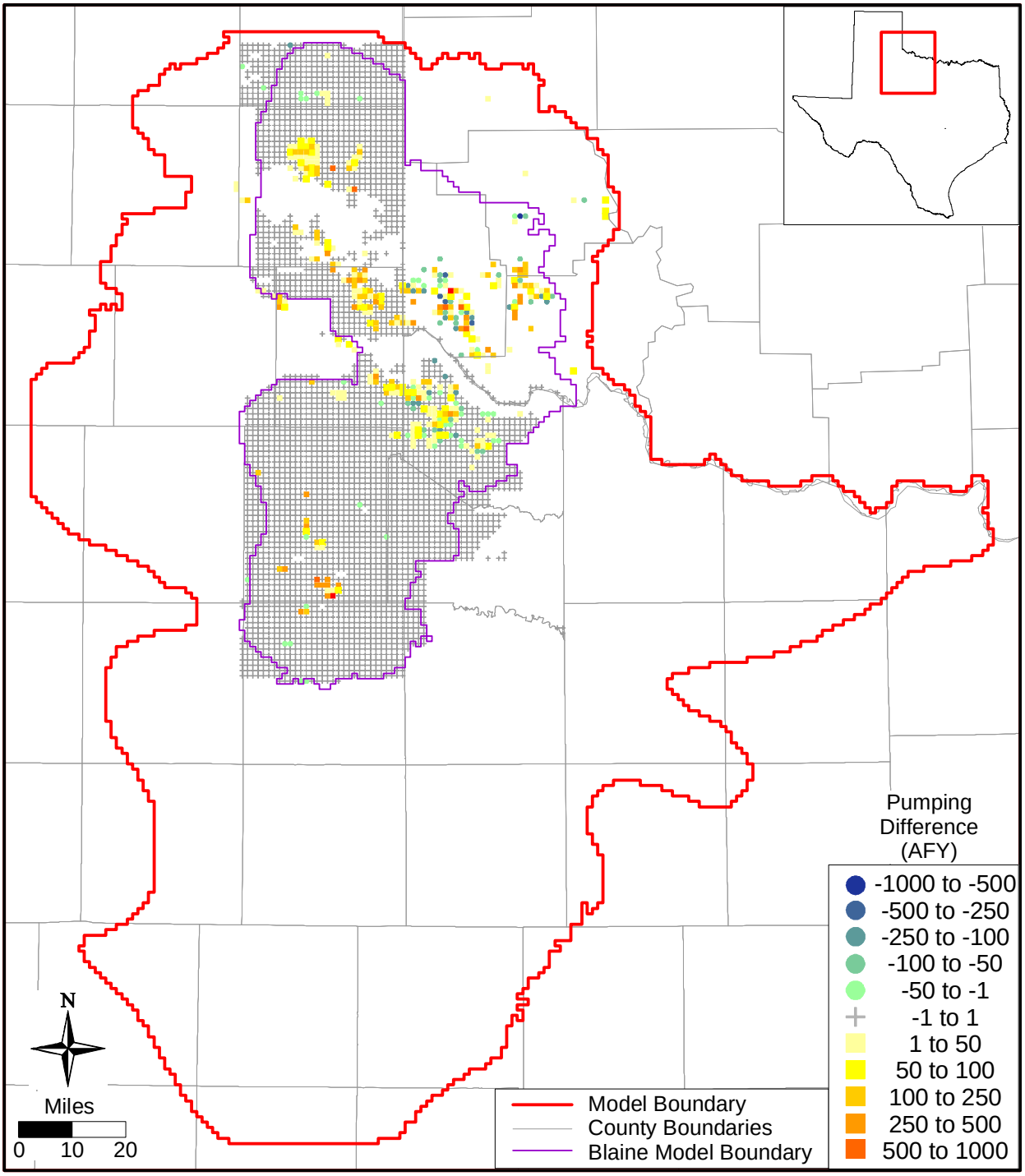

Figure 9.1.6b Difference between steady-state and 1990 pumping in layer 2.

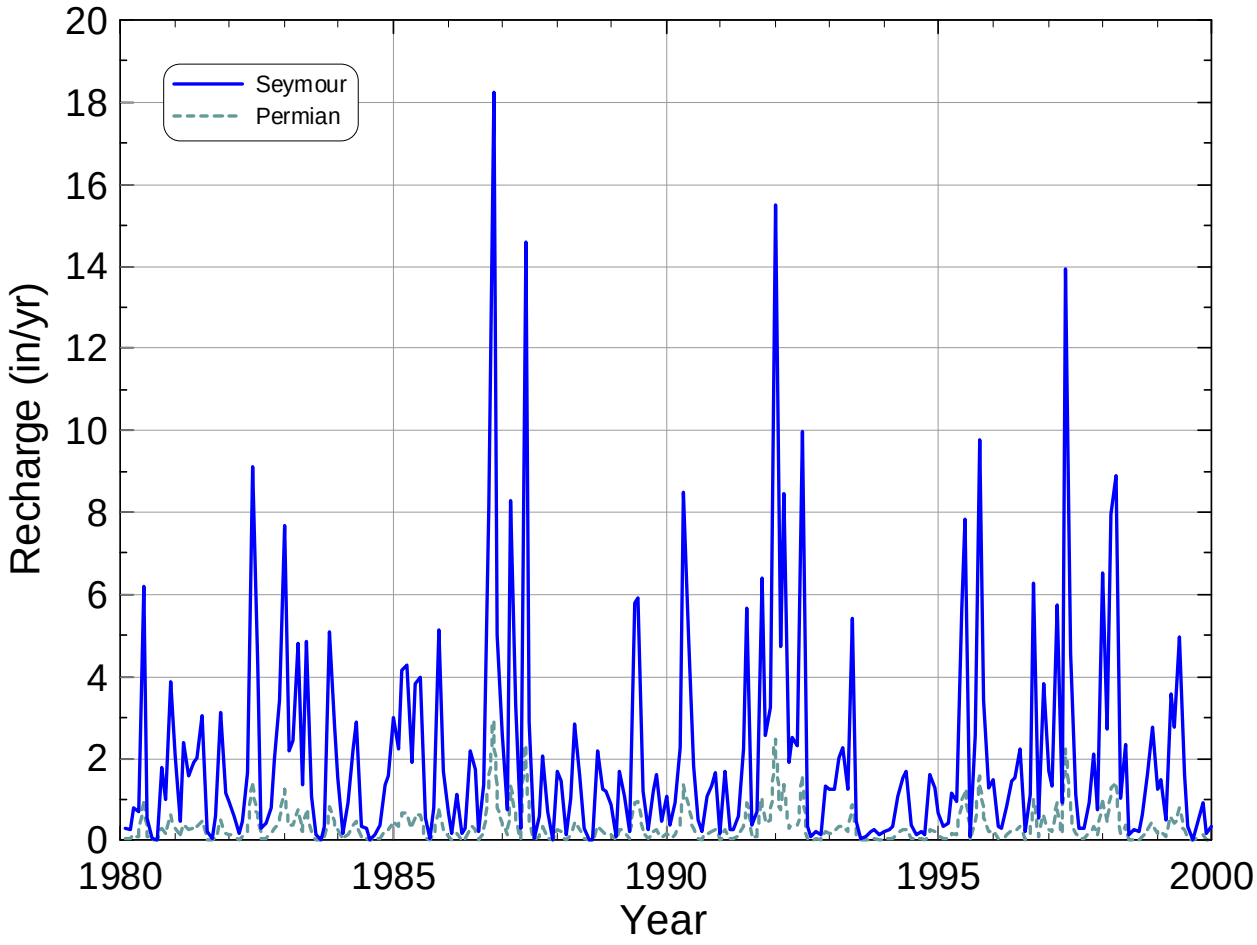

Figure 9.1.7 Temporal distribution of spatially averaged recharge in layers 1 and 2.

9.2 Simulation Results

Results for the transient model are presented in this section. Simulated water-level elevations are compared to measured values, and stream and spring leakances and water budgets are discussed. The calibration metrics were also applied to the verification period to provide an indication of the model's predictive capability.

9.2.1 Water-Level Elevations

The transient modeling is divided into a calibration period (1980 through 1989) and a verification period (1990 through 1999). Results for the calibration period are described first, followed by the performance of the model during the verification period. Table 9.2.1 provides the summary statistics of the transient model calibration and verification for the Seymour and Blaine aquifers. Summary statistics by Seymour pod are also provided in this table for both transient time periods. The adjusted root mean square (RMS) error for the entire Seymour aquifer is 1 percent for both the calibration and verification periods and the adjusted RMS for the Blaine aquifer is 2 percent for the calibration period and 3 percent for the verification period. For both aquifers and both time periods, the adjusted RMS is well below the GAM criteria of 10 percent. This is also true for each pod of the Seymour aquifer with the exception of pod 13, which has an adjusted RMS of just over 10 percent for the transient verification period (see Table 9.2.1).

Figures 9.2.1 and 9.2.2 show the simulated water-level elevations for model layers 1 and 2, respectively, at the end of transient model calibration. Posted average residuals between observed and simulated water levels for the calibration period are provided on Figure 9.2.3 for the Seymour aquifer and Figure 9.2.4 for the Blaine aquifer. A positive residual indicates that the model has underpredicted the water-level elevation, while a negative residual indicates overprediction. The model underpredicts water-level elevations in the Seymour aquifer at 69 percent of the target locations and overpredicts at 31 percent of the target locations. The model overpredicts water-level elevations at 55 percent of the targets and underpredicts water levels at 45 percent of the targets in the Blaine aquifer.

Comparisons of simulated versus observed water levels and residuals versus observed water levels at the target wells for the Seymour and Blaine aquifers for model calibration (1980 through 1989) are shown in Figures 9.2.5 and 9.2.6, respectively. For the Seymour aquifer, data

on the plots are distinguished by pod. The plot of simulated versus observed water levels for the Seymour aquifer (Figure 9.2.5a) shows that the majority of the data fall slightly below the unit-slope line, indicating simulated water levels slightly lower than observed water levels. This trend is also indicated in the plot of residuals versus observed water levels (Figure 9.2.5b) where 66 percent of residuals are greater than zero, meaning the model underpredicts water levels. For the Seymour aquifer, the maximum and minimum residuals are 41.2 and -52.5 feet, respectively. The majority of the residuals for this aquifer (89 percent) fall between –20 and 30 feet. The simulated versus observed water-level data for the Blaine aquifer (Figure 9.2.6a) show mostly uniform scatter around the unit-slope line, indicating no particular trend in the simulated results. This lack of trend is also seen in the plot of residuals versus observed water levels which shows about 58 percent of residuals greater than zero and 42 percent less than zero. For the Blaine aquifer, the maximum and minimum residuals are 66.8 and -66.4 feet, respectively. The majority of the residuals for this aquifer (94 percent) fall between –40 and 40 feet.

Comparisons of simulated and observed water-level elevations and residuals versus observed water levels at target wells for the Seymour and Blaine aquifers for model verification (1990 through 1999) are shown in Figures 9.2.7 and 9.2.8, respectively. Similar to the results for the calibration period, the model generally slightly underpredicts water levels in the Seymour aquifer during the verification period. This is evident by slightly more data falling below the unit-slope line on the plot of simulated versus observed water levels (Figure 9.2.7a) and more residuals greater than zero (65 percent) than less than zero (35 percent) on the plot of residuals versus observed water levels (Figure 9.2.7b). For the Seymour aquifer, the maximum and minimum residuals are 47.1 and -59.5 feet, respectively. The majority of the residuals for this aquifer (89 percent) fall between –30 and 30 feet. The data on the plot of simulated versus observed water levels for the Blaine aquifer show mostly uniform scatter around the unit-slope line (Figure 9.2.8a), indicating no particular trend in the simulated results. This lack of trend can also be seen in the plot of residuals versus observed water levels (Figure 9.2.8b), which shows similar numbers of residuals above zero (58 percent) as below zero (42 percent). For the Blaine aquifer, the maximum and minimum residuals are 72.8 and -59.5 feet, respectively. The majority of residuals for this aquifer (83 percent) fall between –40 and 40 feet.

Water-level elevations based on the simulated heads at the end of the verification period (December 1999) are shown in Figures 9.2.9 and 9.2.10 for layers 1 and 2, respectively. Plots of

average residuals for model verification (1990 through 1989) are posted on Figure 9.2.11 for the Seymour aquifer and Figure 9.2.12 for the Blaine aquifer. Sixty-five percent of the residuals for targets in the Seymour aquifer are positive indicating a slight underprediction of water levels by the model.

In the following discussion, selected hydrographs of simulated and observed water-level elevations are presented which describe the general model response in the two aquifers. Table 9.2.2 lists the calibration statistics for these hydrographs. All hydrographs for the Seymour and Blaine aquifers are shown on a 100-foot and 200-foot vertical scale, respectively, for consistency. All hydrographs for the transient model can be found in Appendix E for the Seymour targets and Appendix F for the Blaine targets. Figure 9.2.13 shows hydrographs for wells located in pods 1 and 2 of the Seymour aquifer. In Collingsworth County, the simulated water levels are lower than those observed and show a stronger decreasing trend than is observed. The simulated water levels for well 1229511 in Hall County are in excellent agreement with the observed water levels in both value and trend. For the other well in Hall County, the simulated water levels are slightly lower than those observed and have a stronger decreasing trend. Figure 9.2.14 shows hydrographs for wells in pod 3. For well 1241302 in Hall County, the trend of the simulated water levels is very near that of the observed data although the simulated water levels are lower than those observed. The simulated water levels for the two wells in Motley County show an increasing trend whereas the observed water levels show a somewhat scattered but roughly stable trend.

Six hydrographs are shown for wells in pod 4 in Figure 9.2.15. For all hydrographs, the trend of the simulated water levels is very similar to that of the observed data. In five of the six hydrographs, the simulated water-level values closely match the observed values. One of the hydrographs for Wilbarger County shows simulated water levels along with observed water levels for three target wells located within the same grid block. This hydrograph shows a variation of 40 feet between the observed water levels in the different wells, and illustrates the potential for uncertainty in the observed data due to spatial averaging across 1-mile grid blocks.

Figure 9.2.16 shows hydrographs for target wells in pod 5. In four of the hydrographs, the simulated and observed water levels match fairly well. In the hydrograph for well 2005501,

the model predicts increasing water levels with time while the observed data show a mostly stable water level with time.

Hydrographs for target wells located in pod 7 are shown in Figure 9.2.17. Simulated and observed water levels closely match in both magnitude and trend in five of the six hydrographs. Two of the hydrographs for Haskell County show two sets of observed data, which vary up to 15 feet. Again, this shows the potential uncertainty associated with the observed data. In general, the trends of the simulated water levels are consistent with the trends of the observed data for these hydrographs.

Hydrographs for target wells in pod 8 (Figure 9.2.18) and pods 9 and 11 (Figure 9.2.19) show very good agreement between the simulated and observed water levels in both magnitude and trend. Figure 9.2.20 shows hydrographs for target wells located in pod 13. Two of these hydrographs show good agreement in magnitude and trend between the simulated and observed water levels. Of the other four hydrographs shown, two show simulated water levels decreasing with time and two show simulated water levels increasing in time. For the former, the observed data also decrease but not at quite the same rate as is simulated. For the latter, the observed water levels are stable or decrease only slightly.

Simulated and observed water levels for several target wells in the Blaine aquifer are shown in Figure 9.2.21. In general, the simulated and observed water levels match fairly well, although the slight inflections in the observed data are not captured with the model. For well 1224307 located in Childress County, the model slightly overpredicts water levels but does a good job of reproducing the 30-foot rise in water level seen in the observed data.

To allow dry cells to resaturate over time, the rewet option in MODFLOW was used. Of the 118 grid cells containing wells with water-level measurements in the Seymour aquifer, one grid cell in Collingsworth County (pod 1) begins going dry in the transient model simulation toward the end of the verification period and one grid cell in Knox County (pod 7) goes intermittently dry in the model simulation during the calibration period before remaining saturated during the verification period. All other grid cells containing observation wells remain saturated in the model over the entire calibration and verification periods. All of the model cells remain saturated in layer 2 throughout model calibration and verification. A total of 716 cells are dry in December 1989 and 723 are dry in December of 1999. The majority of the dry cells

occur at the edges of the Seymour pods and may represent actual subsurface conditions or limitations in the model caused by areally averaging structure and water levels to 1-mile grid blocks. Greater numbers of dry cells exist around the edges of pod 1 in Collingsworth County and throughout the portion of this pod located in Oklahoma, the edges of pod 2, the eastern portion of pod 3, portions of pod 4 in Childress and western Hardeman counties, the eastern edge of pod 9, the edges of pod 10, and portions of pod 11. Comparison of the location of these dry cells with water-level measurement locations (see Figure 4.3.1) shows that, generally, the dry cells occur in areas with no observation wells. Because the presence of observation wells presumably corresponds to the presence of accessible groundwater, the dry cells in the model may be representative of actual subsurface conditions. The only exception may be pod 1 where simulated water levels generally appear to be low compared to measurements.

9.2.2 Stream and Spring Leakance

Consistent with the conceptual model, the streams in the transient model are predominantly gaining although conditions vary based on climatic changes. Figures 9.2.22 and 9.2.23 show the simulated stream leakance indicating the gains and losses along the major streams in the area at two different times, representing relatively wet and dry conditions, respectively. The stream leakance during July of 1984 indicates more losing stream segments during relatively wet conditions when stream stages are highest (Figure 9.2.22), whereas the plotted stream leakance during the drier conditions of October of 1986 indicates predominantly gaining stream segments (Figure 9.2.23). The stream leakance is consistent with expectations in that model gain/loss is smallest at the headwater segments and larger in the major river valleys at lower topographical elevations.

A comparison of simulated streamflow to stream gages in the model area was performed and showed consistency between the model and measurements. This is expected because headwater streamflow rates were based upon the available gage data. Figure 9.2.24 depicts a comparison of simulated and measured streamflows at a gage on the Brazos River at the eastern end of pod 7 in Baylor county. While the model tends to capture the time of the peak flows, it tends to be lower in magnitude because surface runoff is not simulated.

As discussed in Section 6.3.3, many of the springs in the model area coincided with stream cells and are not explicitly accounted for in the model. Of the remaining 253 springs,

only 78 exhibited flow at some time during the calibration and verification periods. The average flow at each spring from 1980 through 1999 is depicted in Figure 9.2.25. The majority of the spring flow occurs in the vicinity of the Seymour pods where recharge is highest. Overall, spring flow is insignificant in the model (as shown in Section 9.2.3) and model water levels are insensitive to springs (as shown in Section 9.3).

9.2.3 Water Budget

Table 9.2.3 shows the water budget for the transient model totaled for years 1980, 1988 (drought year for the calibration period), 1989, and 1999. Table 9.2.4 summarizes the water budgets for the decades corresponding to the periods of calibration and verification. The overall mass balance error for the transient simulation was -0.02 percent, well under the GAM requirement of one percent. In model layer 1, the greatest influx of water consistently occurs from recharge, and the greatest outflow of water is through pumping. Streams, groundwater ET, and, in most cases, cross-formational discharge to layer 2 are also significant forms of outflow from layer 1. In model layer 2, the largest influx of water is again through recharge and the largest outflow of water is through streams and ET. Pumping is significantly greater in layer 1 while ET and discharge to streams are much greater in layer 2.

During the drought year of 1988, recharge decreases noticeably. Overall outflow from pumping decreased from approximately 186,000 AFY in 1980 to 162,000 AFY in 1999. Groundwater ET rates show relatively large changes from hot summers (e.g., 1980) to more temperate summers (e.g., 1989). The seasonal variations in totals for stream recharge/discharge, diffuse recharge, groundwater ET, and pumping over the transient simulation period (1980 through 1999) are summarized in Figure 9.2.26. Generally, cross-formational flow shows a net discharge of water from the Seymour aquifer to the underlying Permian sediments. For several years (e.g., 1980) when pumping as at its highest, discharge to the Permian decreases significantly and a small net cross-formation flow upward into the Seymour is observed. However, summary water budgets over a decade (Table 9.2.4) indicate that, overall, the Seymour discharges to the Permian. The summary water budgets over a decade also show that discharge to springs is relatively insignificant, comprising only about 1 percent of the Seymour recharge. Discharge from the Seymour aquifer through pumping is 34 percent of recharge to the Seymour.

Overall, the water budget is in agreement with the conceptual model of the Seymour aquifer. Average calibrated recharge rates are within the bounds of those presented by others. Direct precipitation is the predominant form of recharge to the Seymour with little or no recharge occurring from streams. The net cross-formational flow, as expected, is from the Seymour to the underlying Permian sediments and streams in the model are predominantly gaining. ET constitutes a smaller portion of the natural discharge than initially anticipated. However, the majority of the ET was conceptually anticipated to occur in the lower elevation river valleys which, in the model, are coincident with stream cells and much of this ET is assimilated into the stream discharge portion of the water budget.

Table 9.2.1 Calibration statistics for the transient model.

Calibration Period (1980 through 1989)						
Layer/Pod	**Number of Targets**	**ME**	**MAE**	**Total RMS**	**Range**	**Adjusted RMS**
Seymour aquifer	1004	4.8	13.3	16.2	1486	0.01
Blaine aquifer	737	5.5	19.1	22.7	956	0.02
Pod 1	14	15.1	15.1	16.2	716	0.02
Pod 2	15	4.5	4.8	5.9	405	0.01
Pod 3	15	13.9	16.6	18.1	449	0.04
Pod 4	387	-0.3	13.9	17.0	678	0.03
Pod 5	74	-1.7	10.4	12.2	195	0.06
Pod 6[1]						
Pod 7	430	10.6	13.7	16.7	383	0.04
Pod 8	8	0.4	0.8	0.9	152	0.01
Pod 9	14	0.6	3.1	4.0	248	0.02
Pod 10[1]						
Pod 11[1]						
Pod 12[2]						
Pod 13	47	1.5	14.7	16.7	184	0.09
Pod 14[1]						
Pod 15[1]						
Verification Period (1990 through 1999)						
Layer/Pod	**Number of Targets**	**ME**	**MAE**	**Total RMS**	**Range**	**Adjusted RMS**
Seymour aquifer	880	4.0	16.2	19.6	1487	0.01
Blaine aquifer	409	3.4	20.5	26.4	905	0.03
Pod 1	9	27.0	27.0	27.5	715	0.04
Pod 2	20	6.3	7.6	9.7	401	0.02
Pod 3	18	7.5	18.1	20.0	452	0.04
Pod 4	372	-0.2	17.5	21.1	5669	0.03
Pod 5	57	1.2	14.0	16.1	194	0.08
Pod 6[1]						
Pod 7	302	10.0	16.1	19.5	378	0.05
Pod 8	3	1.2	1.2	1.3	121	0.01
Pod 9	23	3.2	6.4	7.1	243	0.03
Pod 10[1]						
Pod 11	5	-0.5	2.1	2.6	400	0.01
Pod 12[1]						
Pod 13	71	-0.7	16.6	19.2	179	0.11
Pod 14[1]						
Pod 15[1]						

[1] no transient targets during this period
[2] only one transient target during this period
Note: ME, MAE and RMS are defined in equations in Section 7.1

Table 9.2.2a Calibration statistics for the Seymour aquifer hydrographs shown in Figures 9.2.13 – 9.2.20.

Well	Layer	Count	ME (ft)	MAE (ft)	RMS (ft)	Figure Number
1206401	1	6	10.15	10.15	10.55	9.2.13
1216502	1	8	18.87	18.87	19.44	9.2.13
1229403	1	8	7.57	7.57	7.81	9.2.13
1229511	1	7	0.91	1.59	2.03	9.2.13
1241302	1	7	23.85	23.85	23.88	9.2.14
1241410	1	4	13.66	13.66	13.71	9.2.14
1241604	1	4	-3.34	6.82	6.85	9.2.14
1232901	1	8	-4.37	4.37	4.53	9.2.15
1338701	1	5	5.48	5.48	6.20	9.2.15
1346209	1	7	35.76	35.76	35.83	9.2.15
1346504	1	68	-5.49	5.49	5.55	9.2.15
1346505	1	5	8.05	8.05	8.29	9.2.15
1353102	1	4	-19.16	19.16	19.57	9.2.15
1360611	1	8	2.00	2.47	2.77	9.2.15
1362115	1	7	4.74	4.74	4.85	9.2.15
1460614	1	7	-7.48	7.48	7.66	9.2.16
1461306	1	7	5.87	5.87	5.96	9.2.16
1462604	1	9	-21.77	21.77	21.92	9.2.16
1463301	1	9	-4.19	4.19	4.24	9.2.16
2004401	1	3	-3.47	3.47	3.49	9.2.16
2005501	1	9	-11.53	11.53	11.94	9.2.16
2122703	1	10	4.24	5.03	5.08	9.2.17
2135602	1	8	6.64	6.64	6.79	9.2.17
2135702	1	8	7.39	7.39	7.78	9.2.17
2136201	1	9	11.11	11.11	11.17	9.2.17
2142104	1	8	27.89	27.89	28.03	9.2.17
2142402	1	7	12.45	12.45	12.82	9.2.17
2151702	1	7	1.84	1.84	2.41	9.2.17
2151710	1	8	2.03	2.11	2.47	9.2.17
2140806	1	8	0.37	0.85	0.94	9.2.18
2243202	1	6	-2.39	2.82	3.72	9.2.19
2252107*						9.2.19
2252110	1	8	2.85	3.26	4.16	9.2.19
2907501*						9.2.19
2924310	1	6	17.81	17.81	17.91	9.2.20
3018428	1	5	5.06	5.06	5.16	9.2.20
3018502	1	5	-21.93	21.93	22.18	9.2.20
3018510	1	7	17.74	17.74	17.95	9.2.20
3018702	1	6	-23.32	23.32	23.54	9.2.20
3019405	1	6	1.62	1.62	2.16	9.2.20

*Missing portion of data within the calibration period.

Note: ME, MAE, and RMS are defined in equations in Section 7.1

Table 9.2.2b Calibration statistics for the Blaine aquifer hydrographs shown in Figure 9.2.21.

Well	Layer	Count	ME (ft)	MAE (ft)	RMS (ft)	Figure Number
1224307	2	8	-49.84	49.84	50.88	9.2.21
1240701	2	8	-1.50	8.16	8.80	9.2.21
1334802	2	7	-6.70	6.87	7.66	9.2.21
1342806	2	8	-5.02	5.02	6.20	9.2.21
2206905	2	8	6.96	8.91	10.92	9.2.21
344220099355501	2	31	8.84	10.01	10.92	9.2.21

Note: ME, MAE, and RMS are defined in equations in Section 7.1

Table 9.2.3 Water budget for the transient model (all rates reported in AFY).

Year	Layer	Recharge	ET	Wells	Springs	Streams	Top	Bottom	Storage
1980	**1**	229,475	-30,095	-148,491	-2,720	-25,245	0	2,640	6,570
	2	244,315	-157,549	-37,374	4,730	-129,242	-2,640	0	54,003
	Sum	473,790	-187,644	-185,865	-7,450	-154,487	-2,640	2,640	60,573
1988*	**1**	173,294	-26,260	-87,086	-3,522	-45,479	0	-26,425	37,919
	2	177,437	-150,394	-33,917	-4,953	-180,694	26,425	0	143,201
	Sum	350,731	-176,654	-121,003	-8,474	-226,173	26,425	-26,425	181,120
1989	**1**	274,269	-15,840	-118,606	-3,536	-46,166	0	-30,063	-34,435
	2	283,228	-114,355	-31,059	-4,964	-175,934	30,063	0	-11,747
	Sum	557,497	-130,195	-149,665	-8,500	-222,100	30,063	-30,063	-46,182
1999	**1**	232,599	-24,498	-120,094	-4,259	-56,528	0	-56,671	34,247
	2	232,259	-93,339	-41,804	-5,086	-198,922	56,671	0	45,370
	Sum	464,858	-117,837	-161,898	-9,345	-255,450	56,671	-56,671	79,616

*Drought year for calibration period

Table 9.2.4 Water budget for calibration and verification periods (all volumes reported in acre-ft).

Years	Layer	Recharge	ET	Wells	Springs	Streams	Top	Bottom	Storage
1980 through 1989	**1**	3,240,161	-220,665	-1,102,586	-30,664	-351,702	0	-219,675	-1,036,375
	2	3,396,700	-1,131,210	-292,564	-48,325	-1,470,865	219,675	0	-943,931
	Sum	6,636,860	-1,351,876	-1,395,150	-78,989	-1,822,567	219,675	-219,675	-1,980,306
1990 through 1999	**1**	3,507,445	-273,557	-1,165,452	-39,496	-512,808	0	-627,860	-808,571
	2	3,544,255	-1,266,024	-362,747	-50,389	-1,851,228	627,860	0	-730,105
	Sum	7,051,700	-1,539,581	-1,528,199	-89,886	-2,364,035	627,860	-627,860	-1,538,676

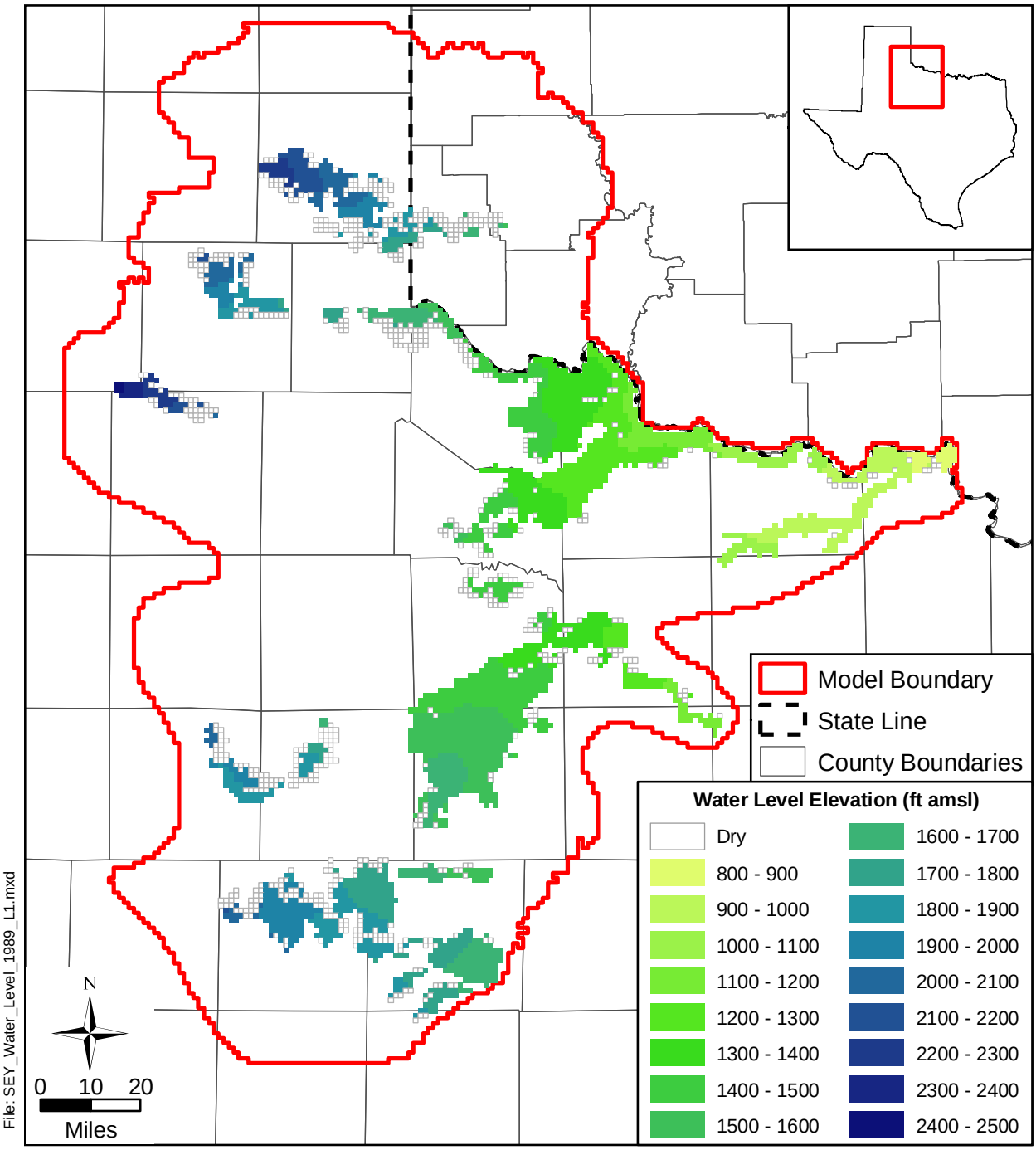

Figure 9.2.1 Simulated water-level elevations for layer 1 at the end of transient model calibration (December 1989).

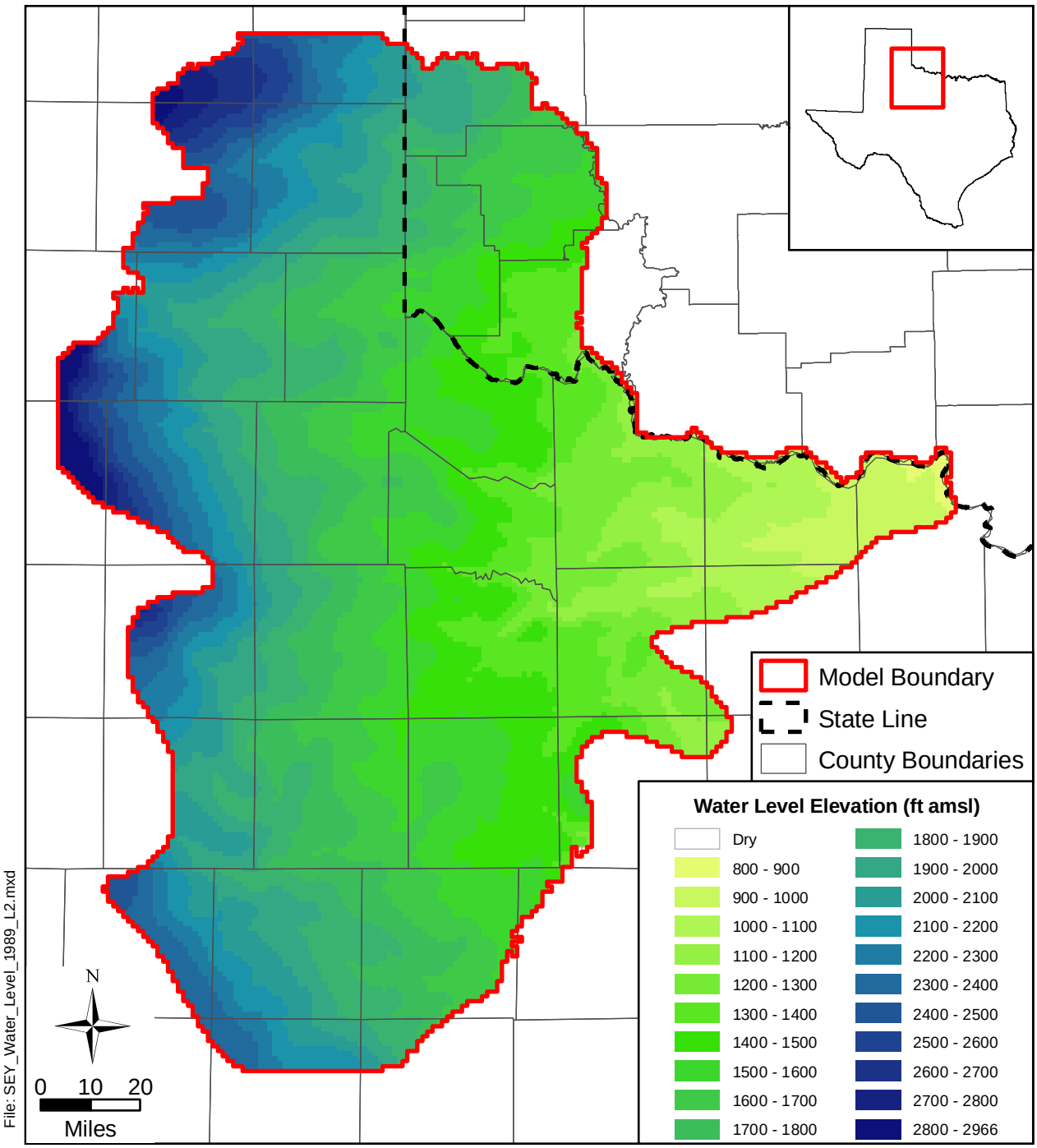

Figure 9.2.2 Simulated water-level elevations for layer 2 at the end of transient model calibration (December 1989).

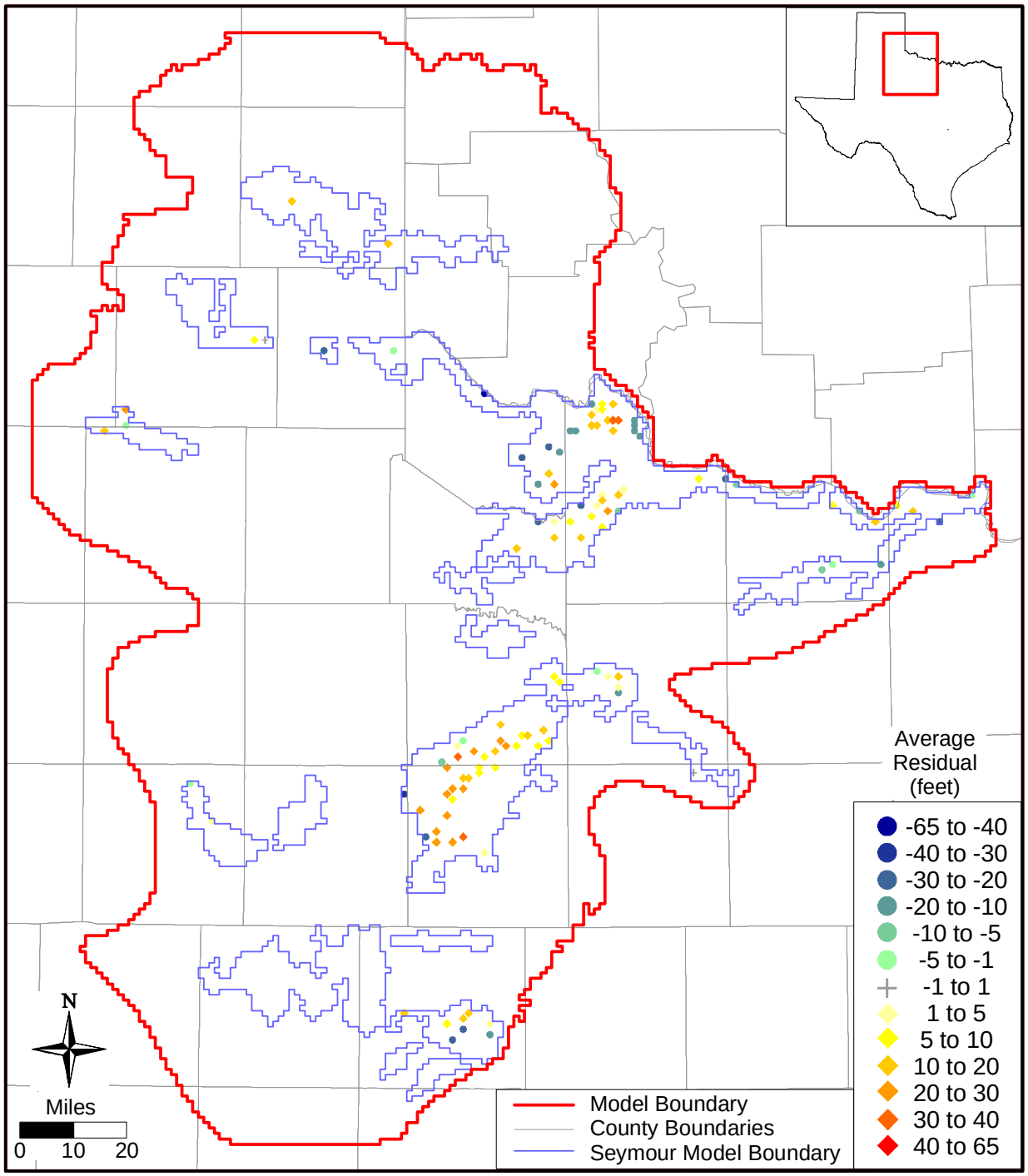

Figure 9.2.3 Average residuals at target wells for the Seymour aquifer for transient model calibration (1980 through 1989).

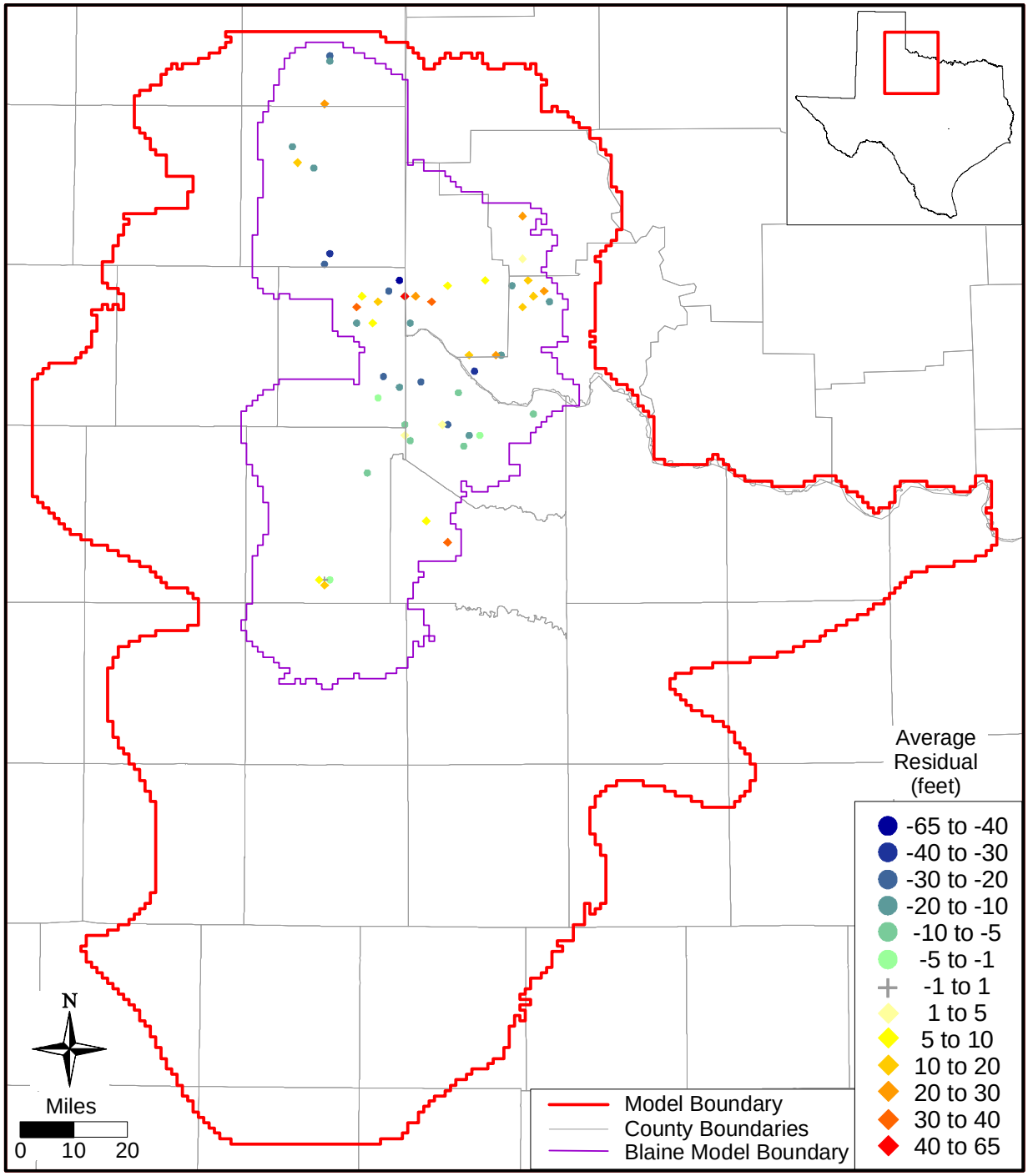

Figure 9.2.4 Average residuals at target wells for the Blaine aquifer for transient model calibration (1980 through 1989).

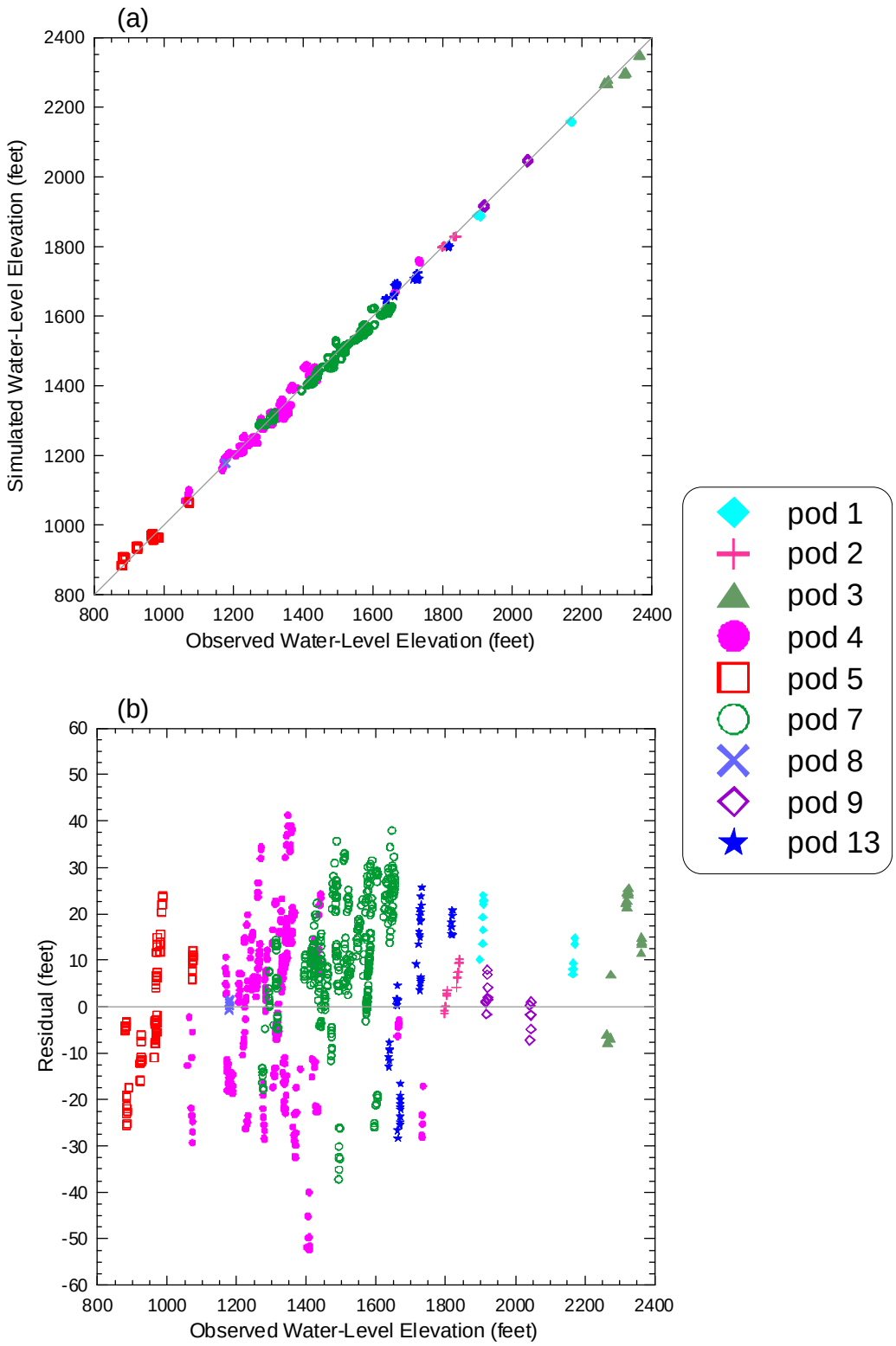

Figure 9.2.5 **Plots of (a) simulated versus observed water-level elevations and (b) residual versus observed water-level elevation for the Seymour aquifer for transient model calibration (1980 through1989).**

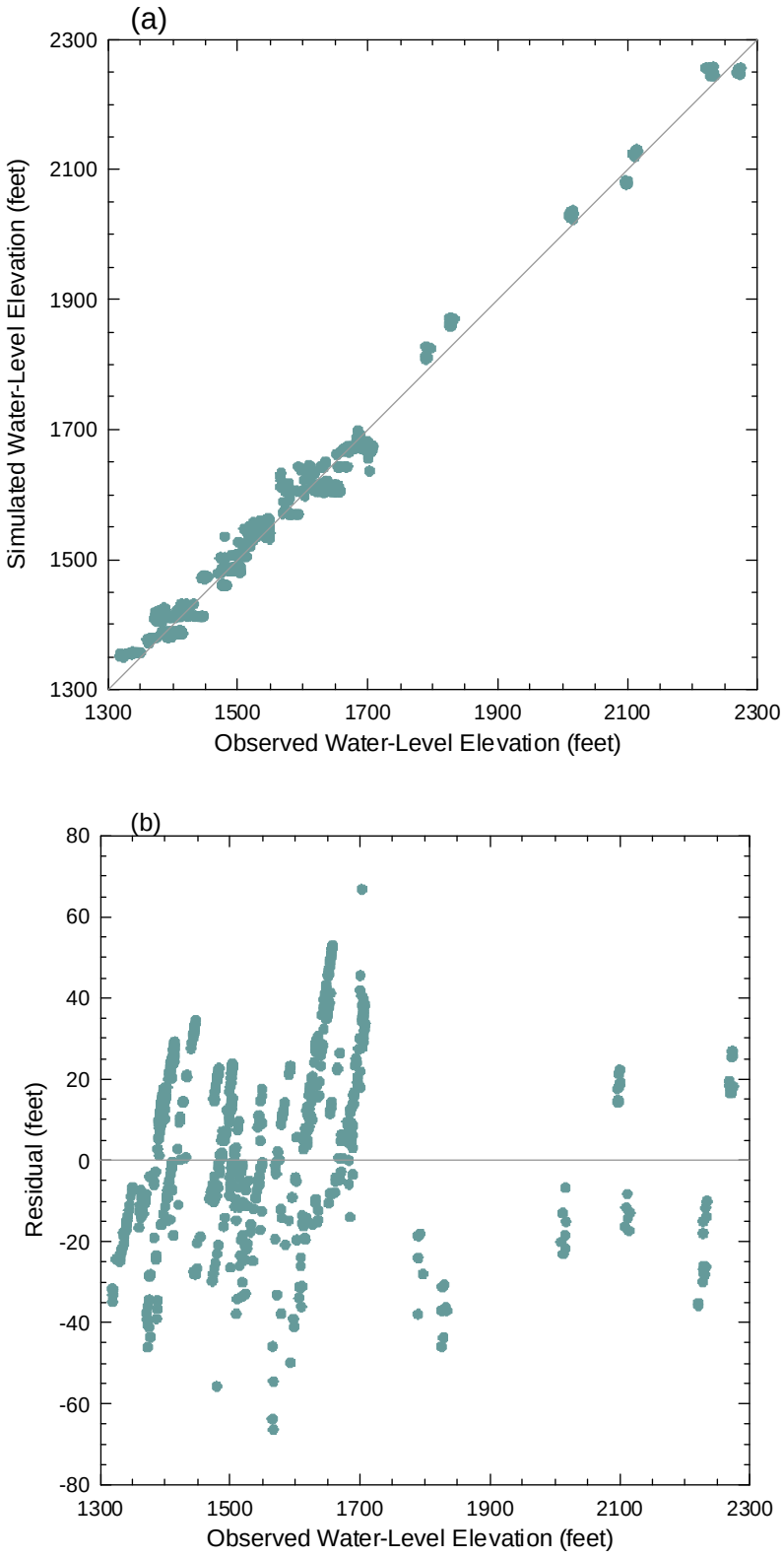

Figure 9.2.6 **Plots of (a) simulated versus observed water-level elevations and (b) residual versus observed water-level elevation for the Blaine aquifer for transient model calibration (1980 through 1989).**

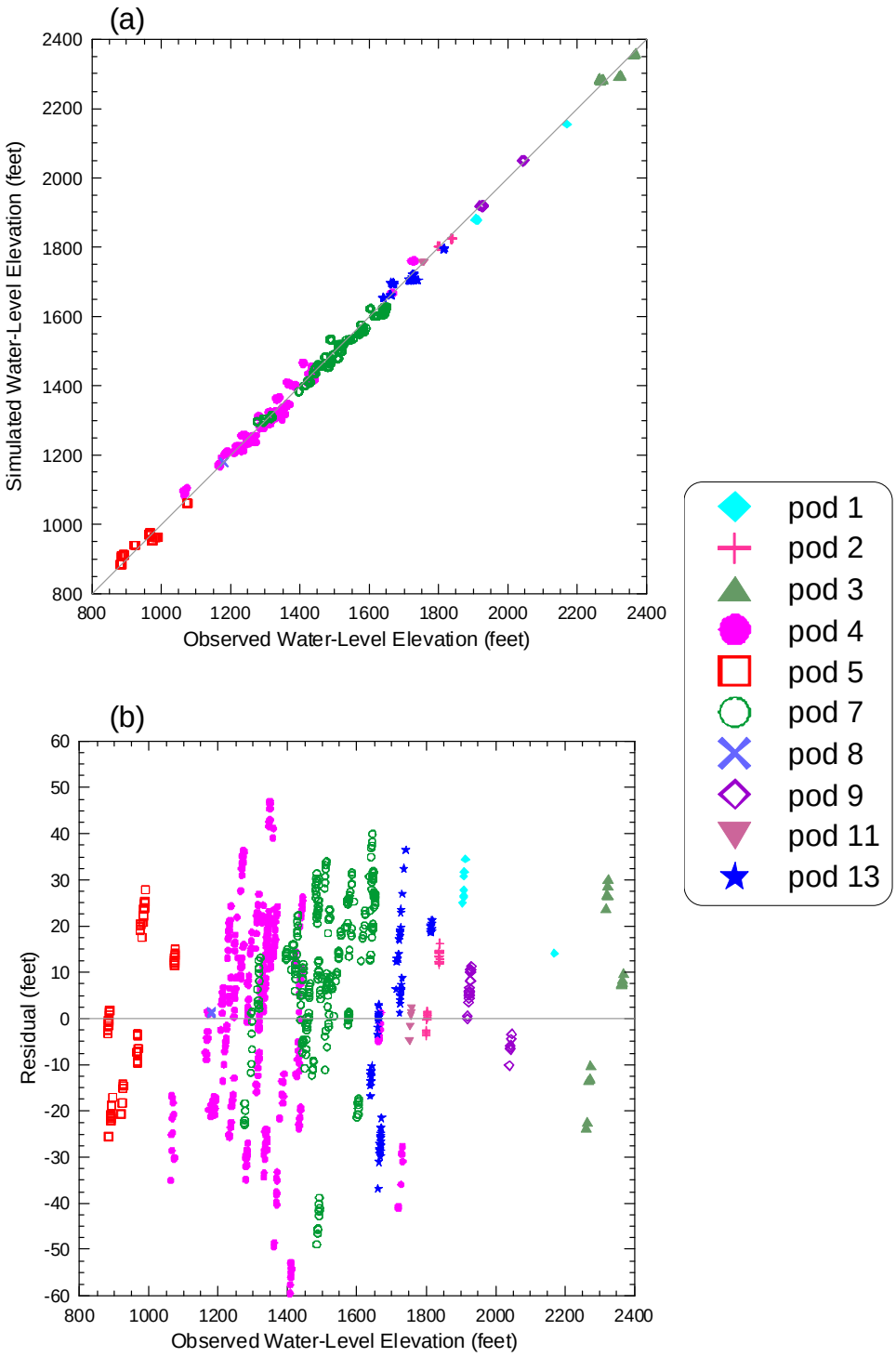

Figure 9.2.7 Plots of (a) simulated versus observed water-level elevations and (b) residual versus observed water-level elevation for the Seymour aquifer for transient model verification (1990 through 1999).

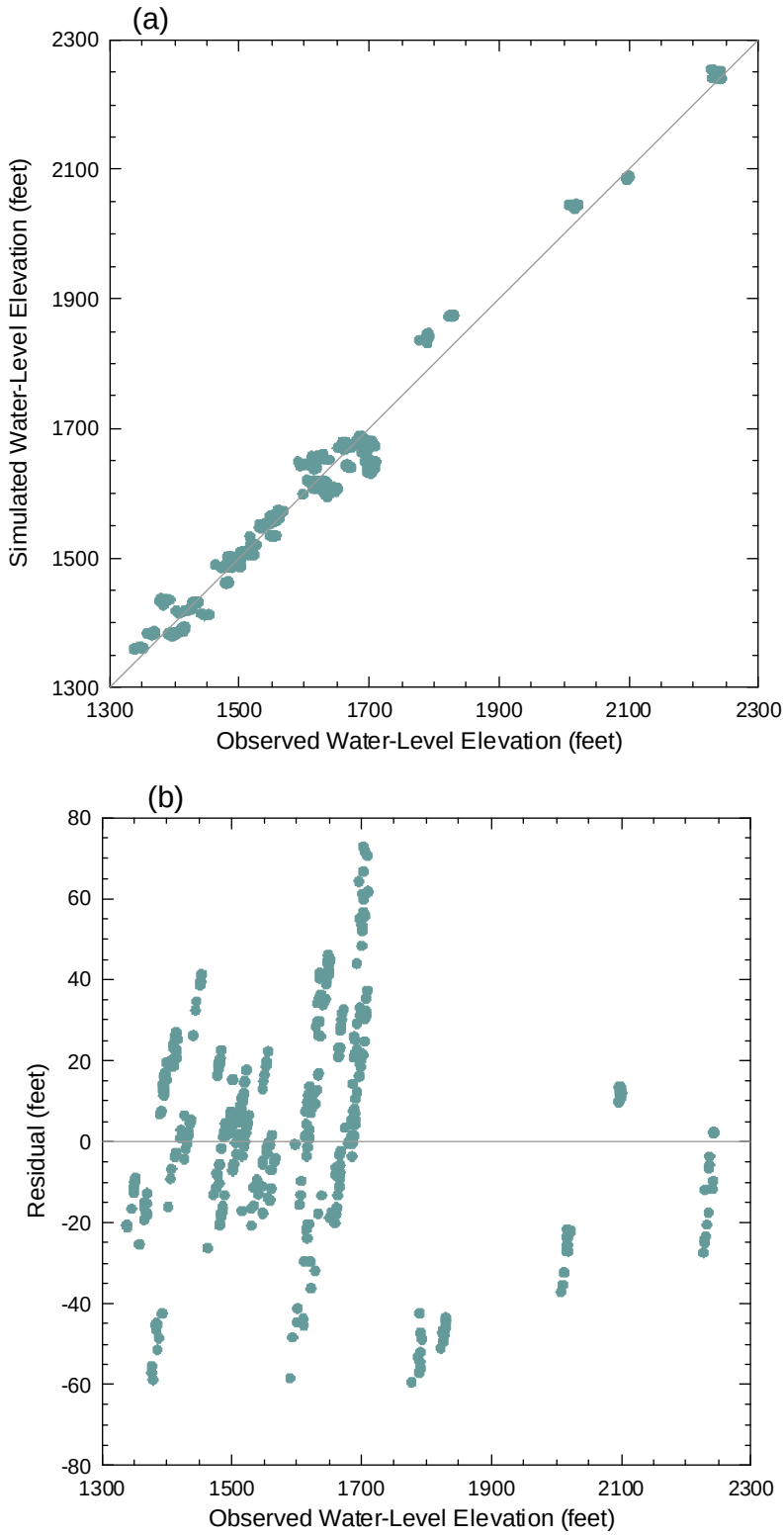

Figure 9.2.8 **Plots of (a) simulated versus observed water-level elevations and (b) residual versus observed water-level elevation for the Blaine aquifer for transient model verification (1990 through 1999).**

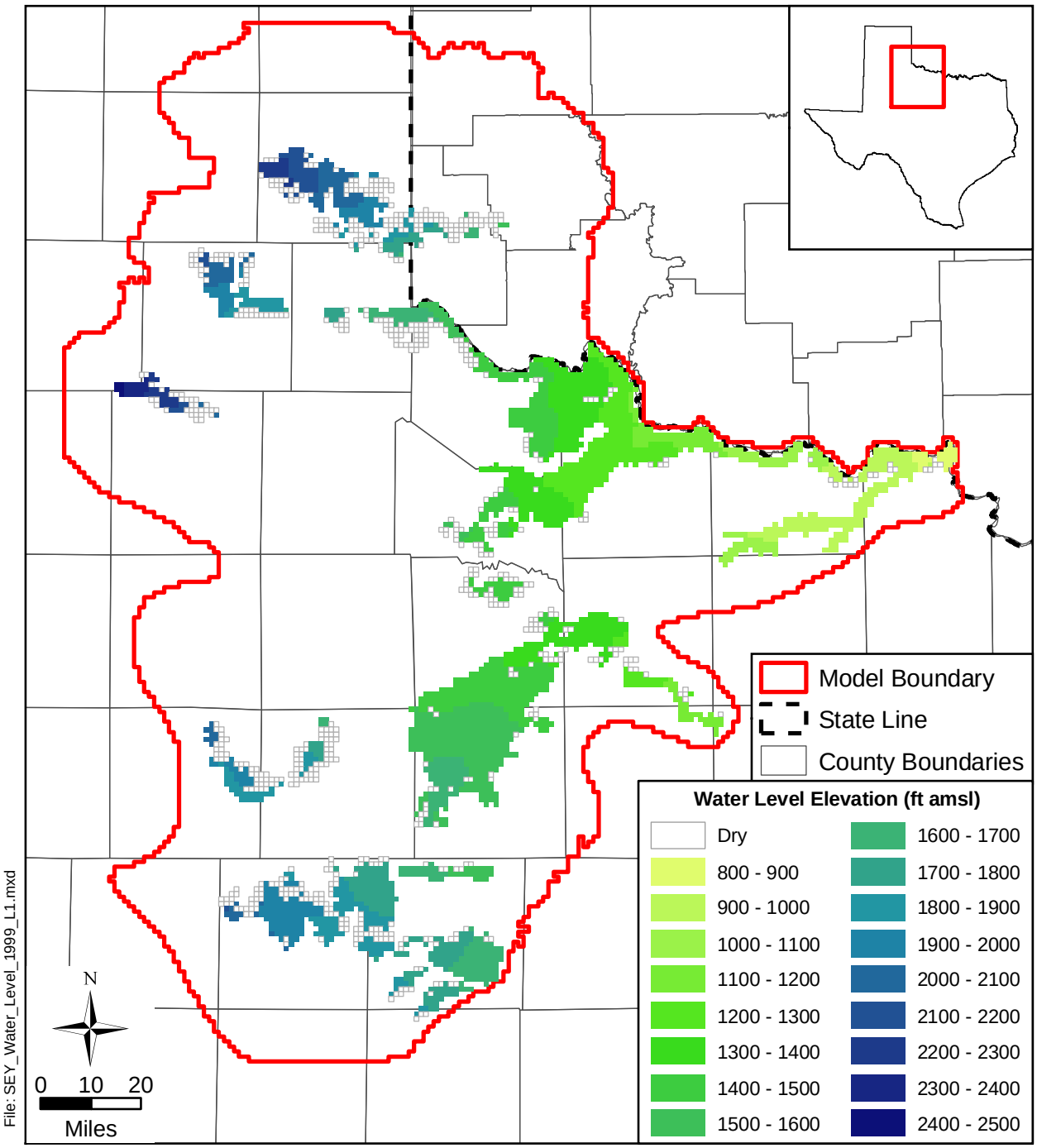

Figure 9.2.9 Simulated water-level elevations for layer 1 at the end of the transient model verification (December 1999).

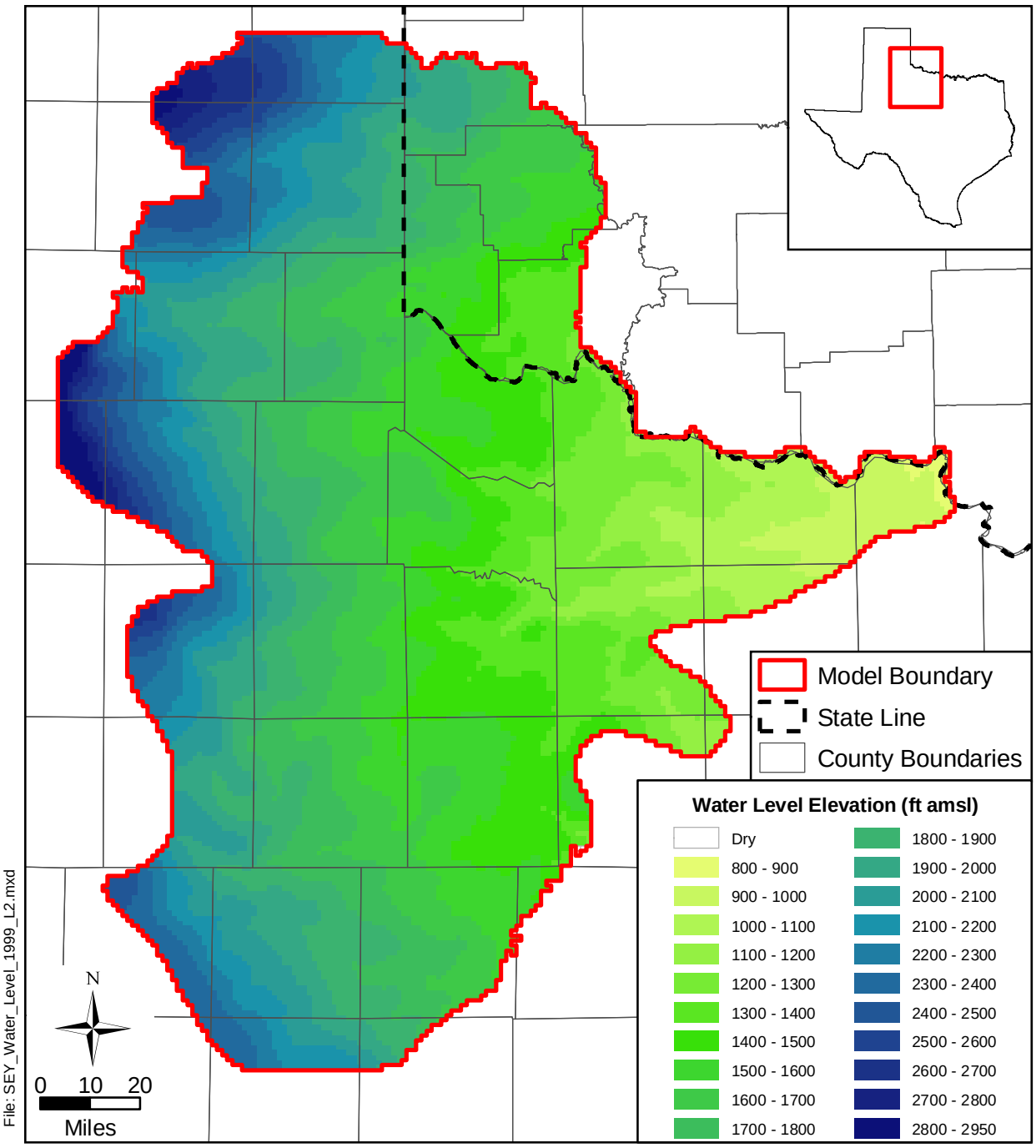

Figure 9.2.10 Simulated water-level elevations for layer 2 at the end of the transient model verification (December 1999).

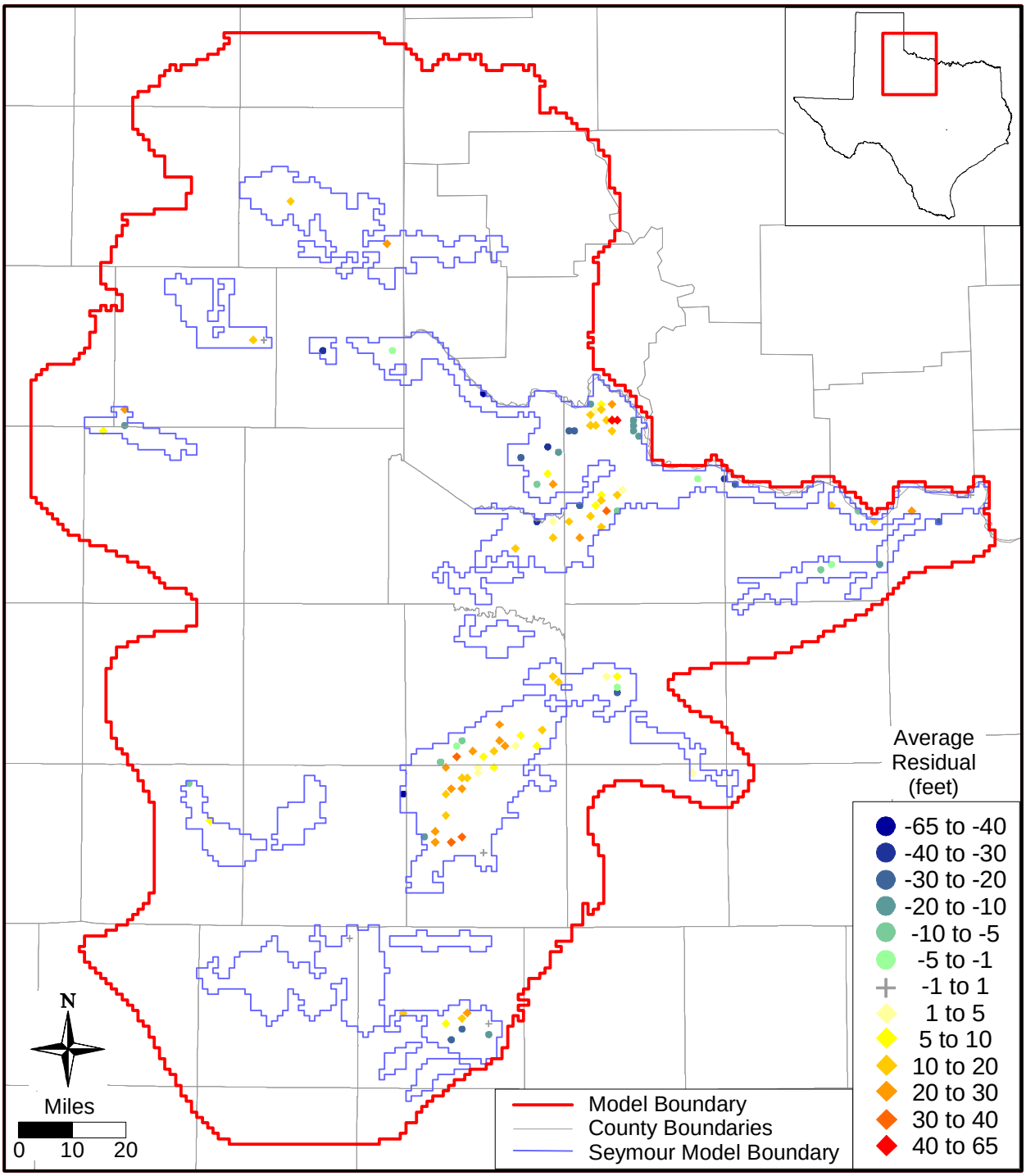

Figure 9.2.11 Average residuals at target wells for the Seymour aquifer for transient model verification (1990 through 1999).

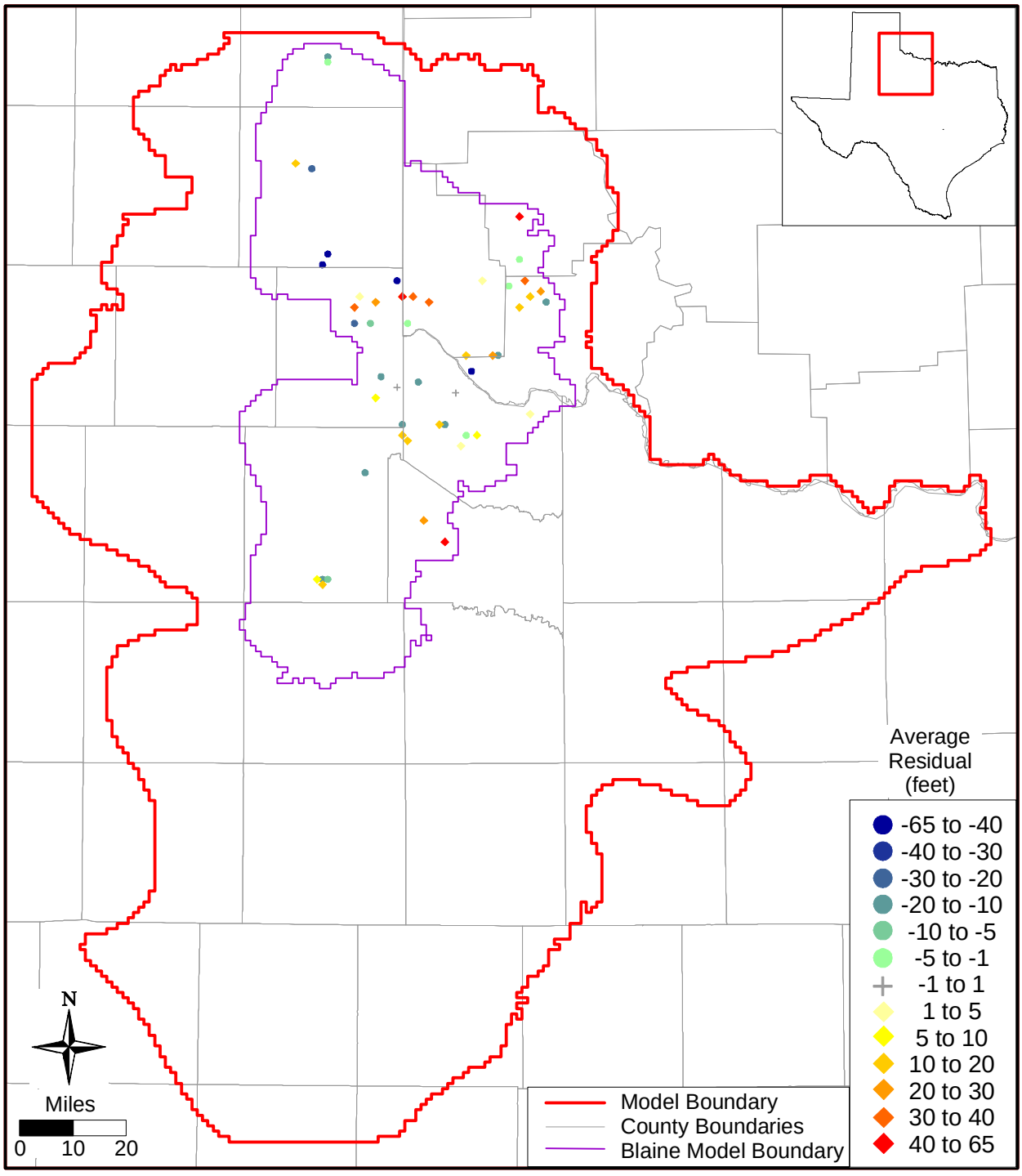

Figure 9.2.12 Average residuals at target wells for the Blaine aquifer for transient model verification (1990 through 1999).

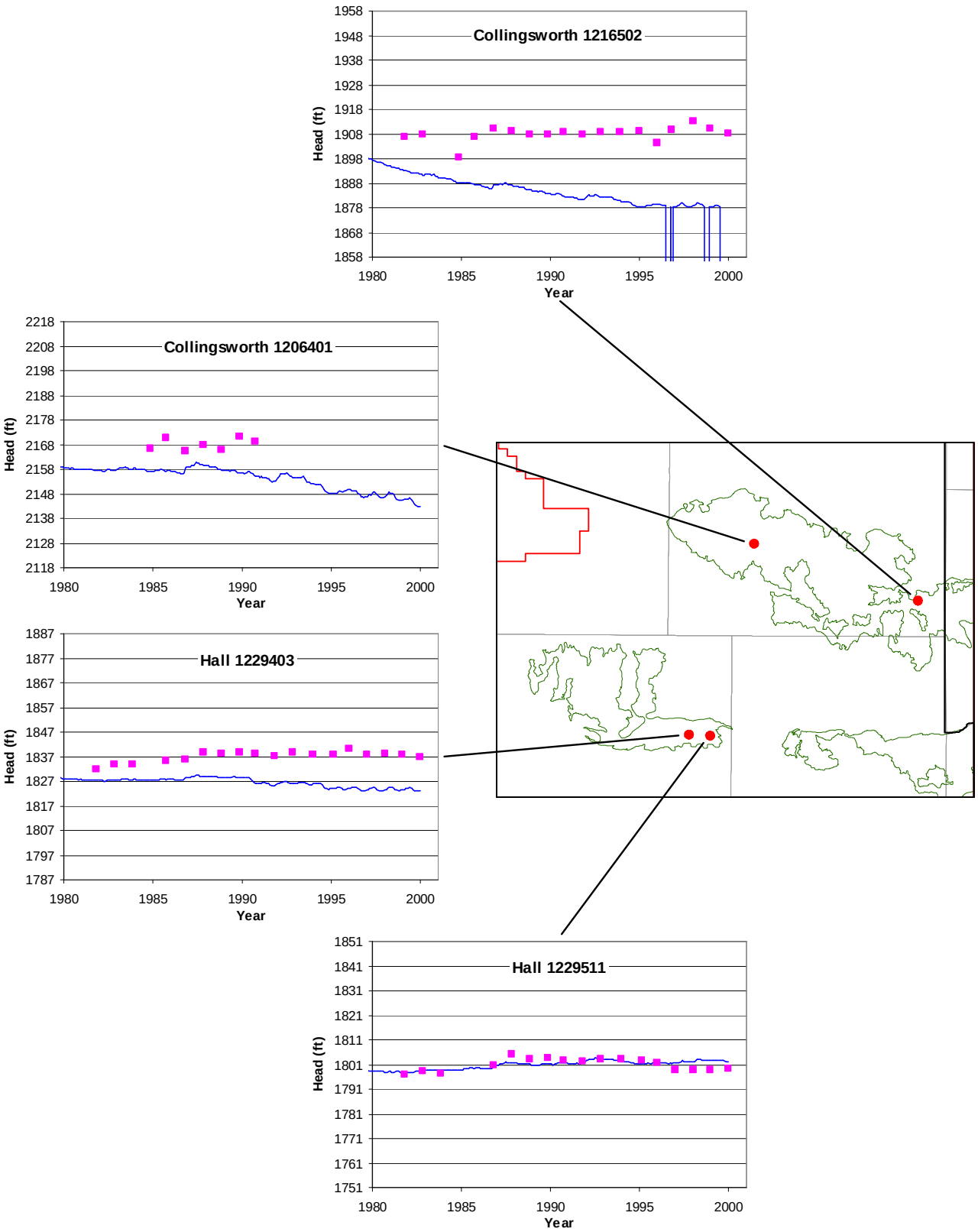

Figure 9.2.13 Selected hydrographs of simulated (lines) and measured (points) water-level elevations in Seymour pods 1 and 2.

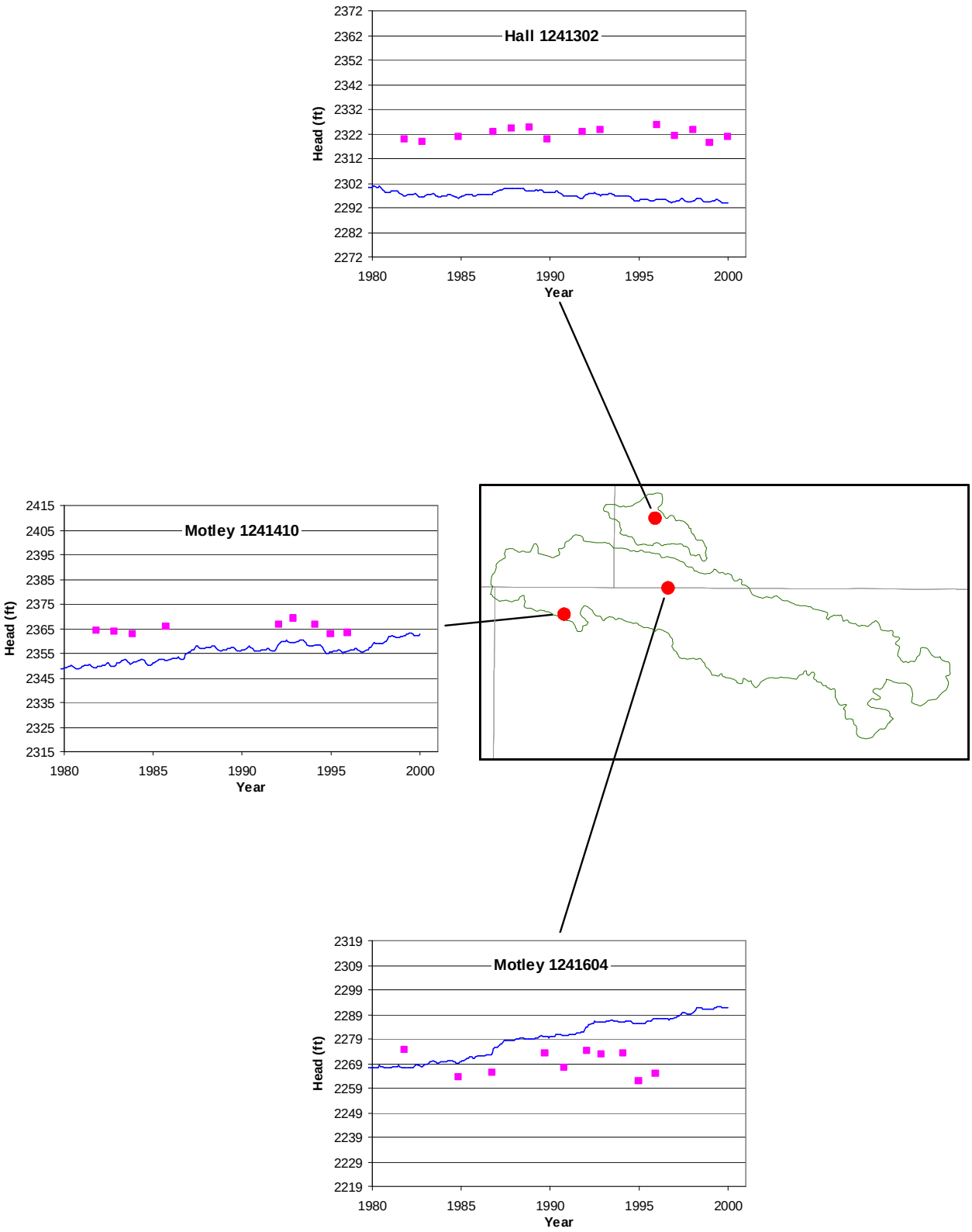

Figure 9.2.14 Selected hydrographs of simulated (lines) and measured (points) water-level elevations in Seymour pod 3.

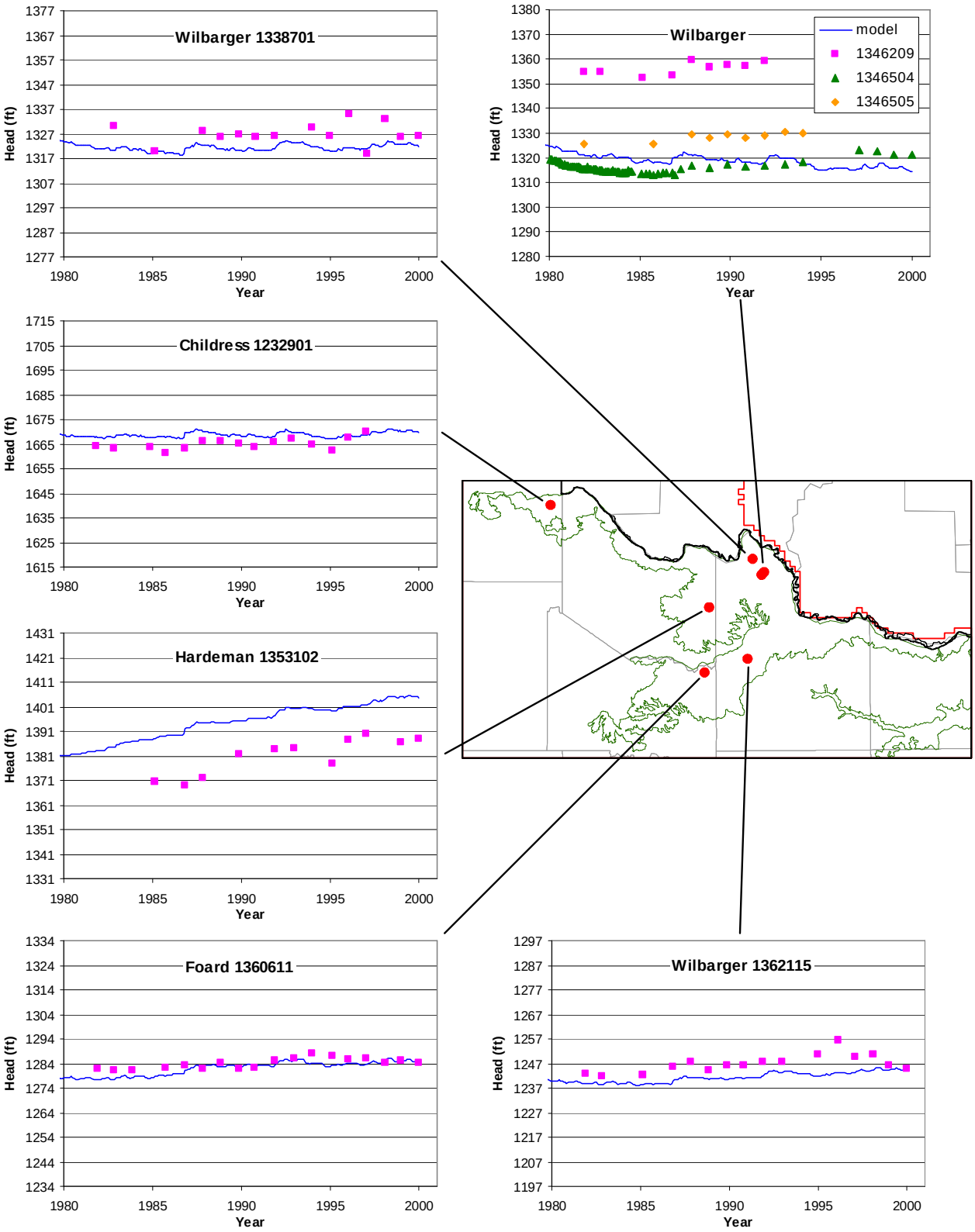

Figure 9.2.15 Selected hydrographs of simulated (lines) and measured (points) water-level elevations in Seymour pod 4.

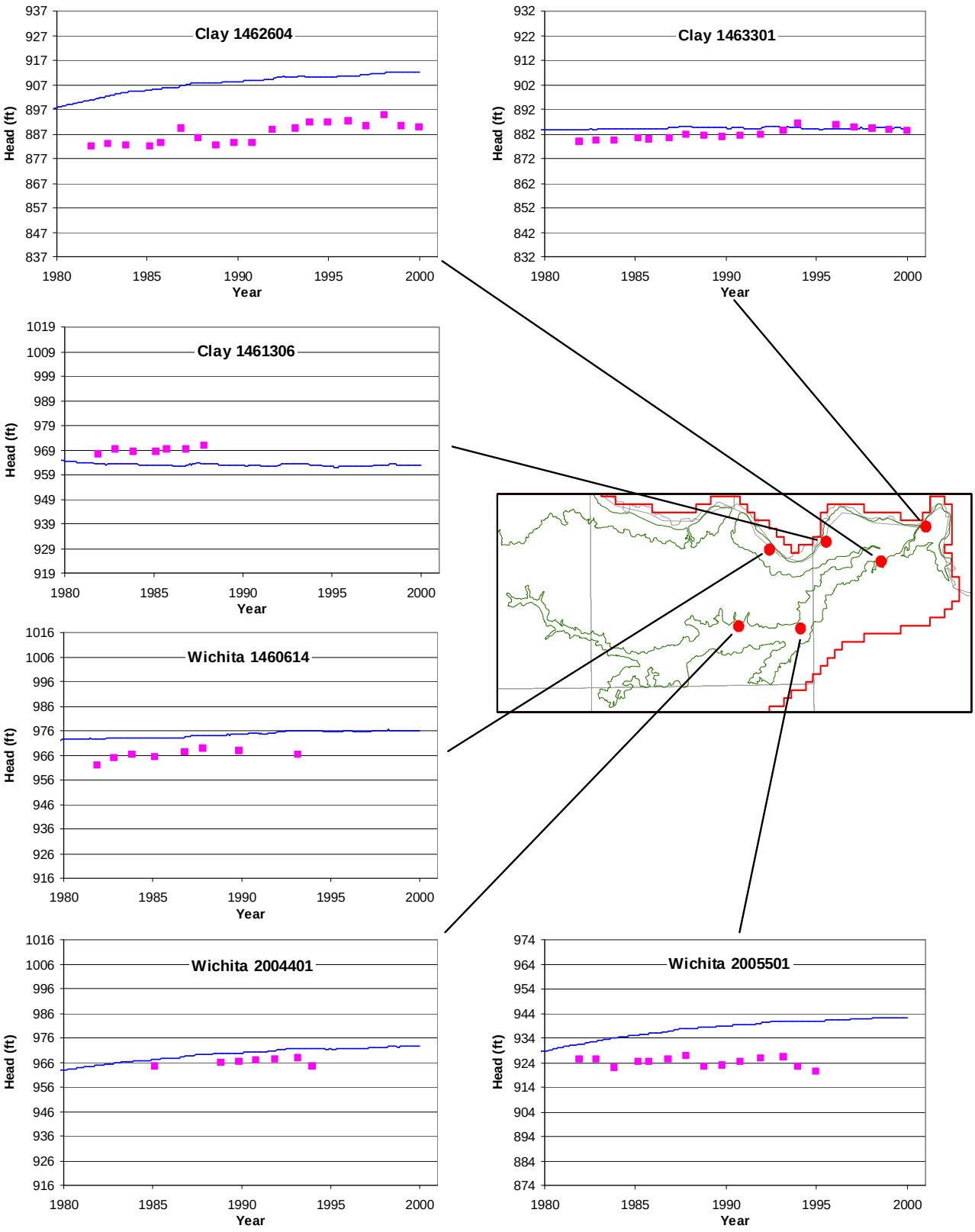

Figure 9.2.16 Selected hydrographs of simulated (lines) and measured (points) water-level elevations in Seymour pod 5.

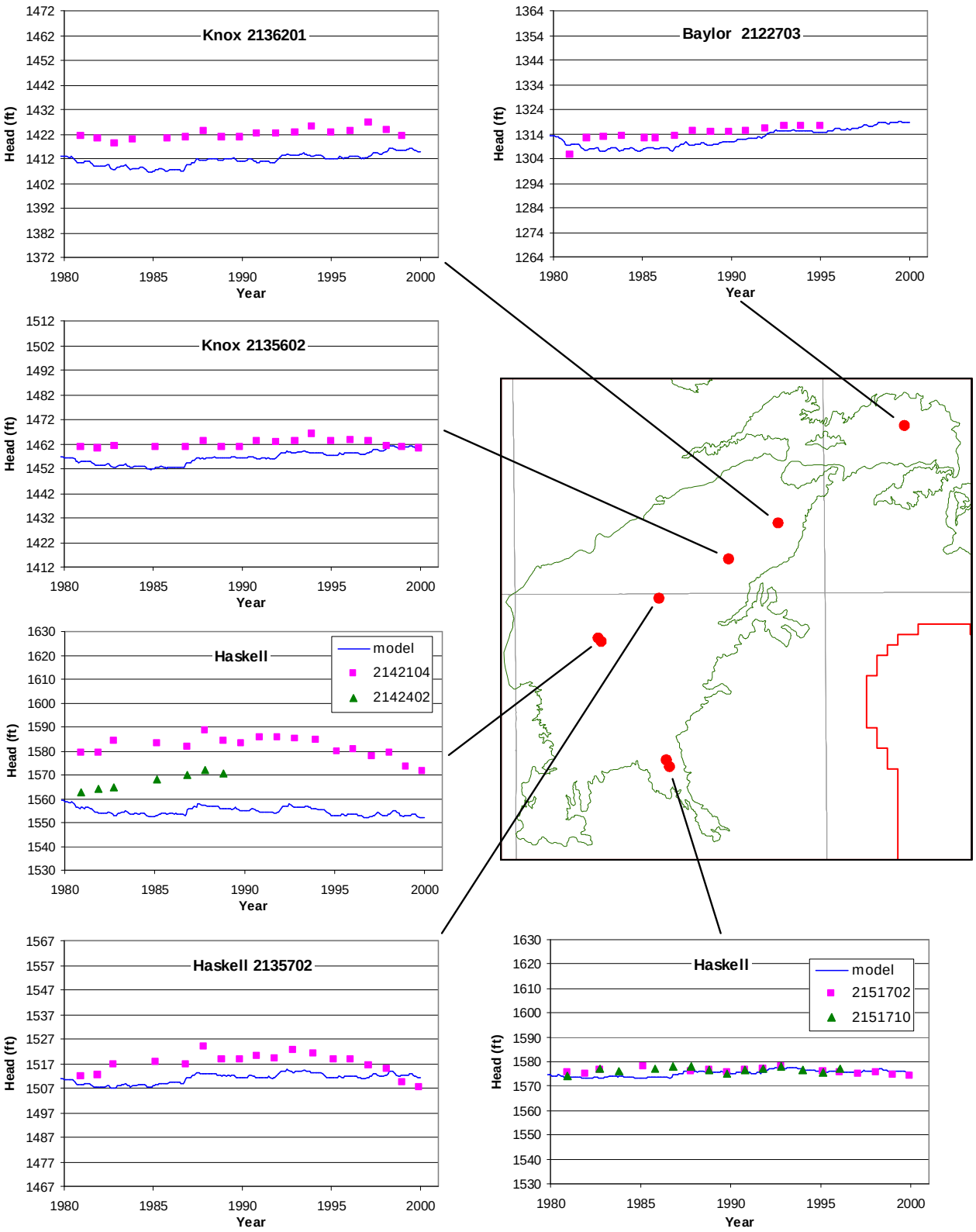

Figure 9.2.17 Selected hydrographs of simulated (lines) and measured (points) water-level elevations in Seymour pod 7.

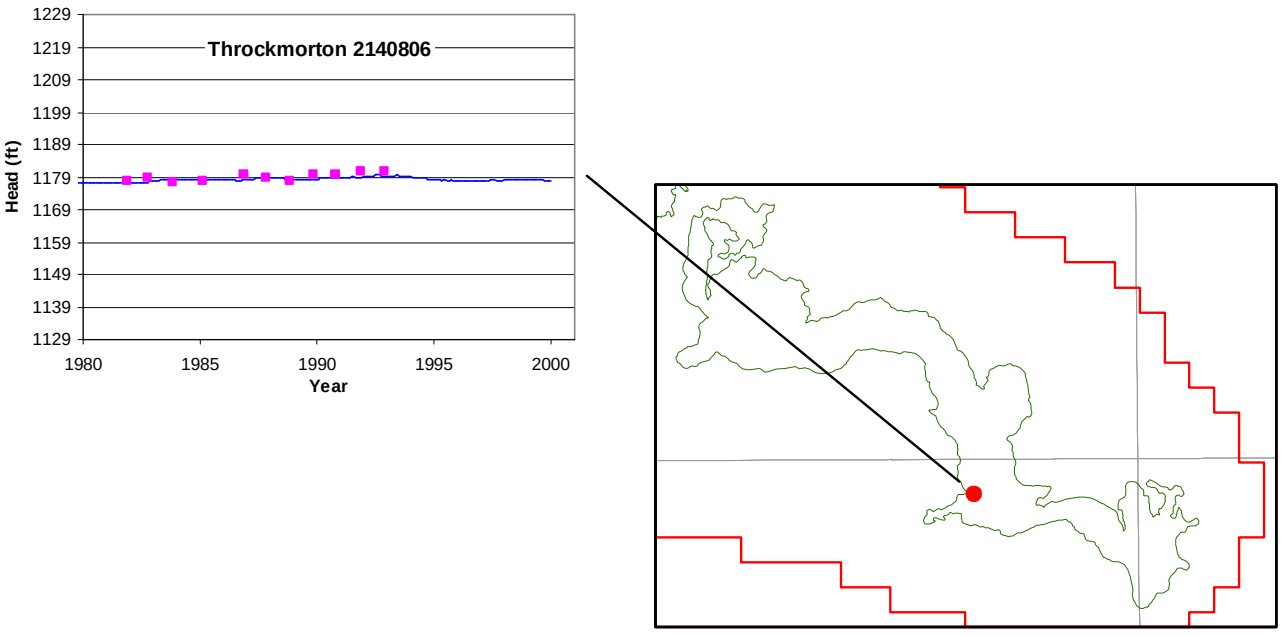

Figure 9.2.18 Selected hydrograph of simulated (line) and measured (points) water-level elevations in Seymour pod 8.

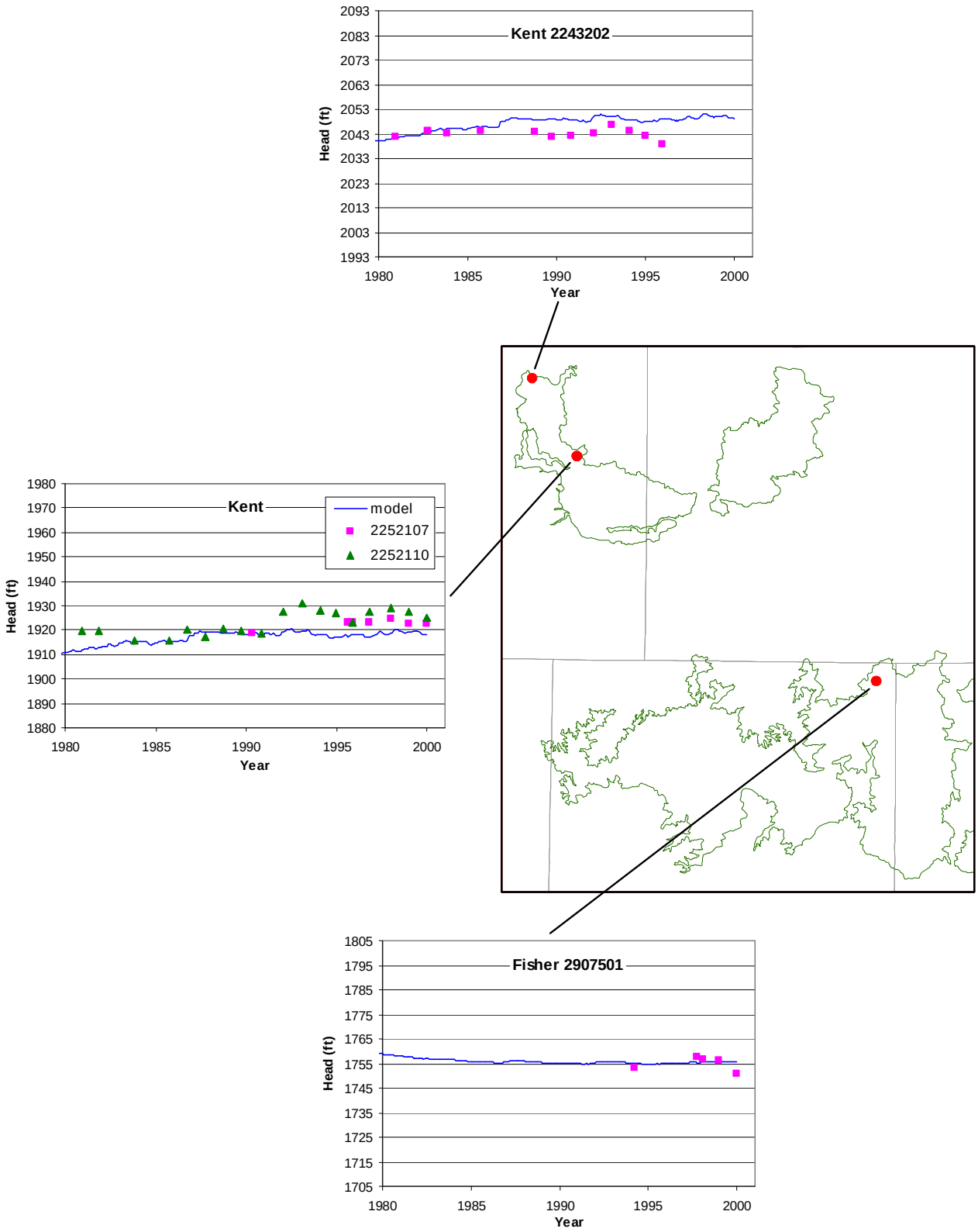

Figure 9.2.19 Selected hydrographs of simulated (lines) and measured (points) water-level elevations in Seymour pods 9 and 11.

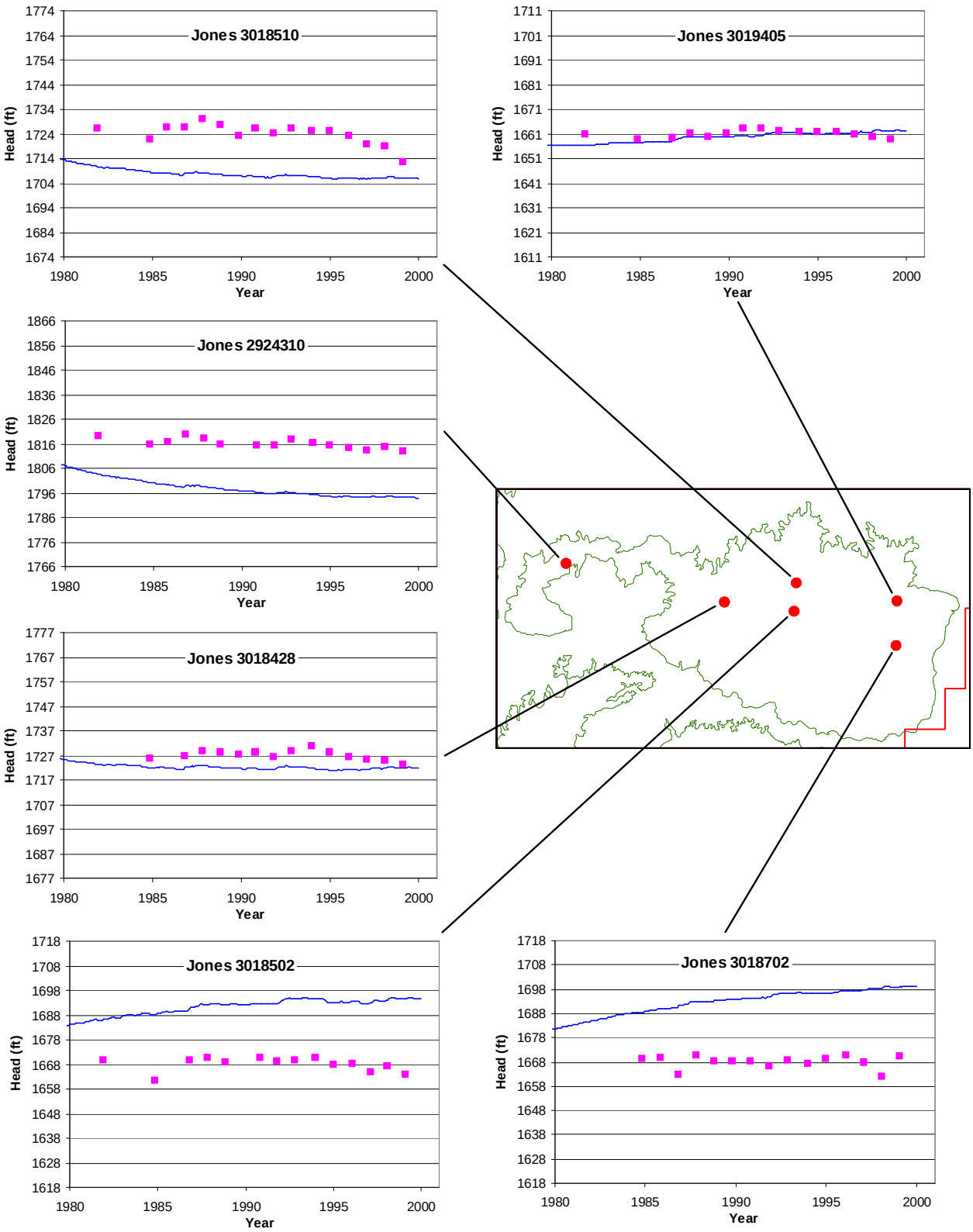

Figure 9.2.20 Selected hydrographs of simulated (lines) and measured (points) water-level elevations in Seymour pod 13.

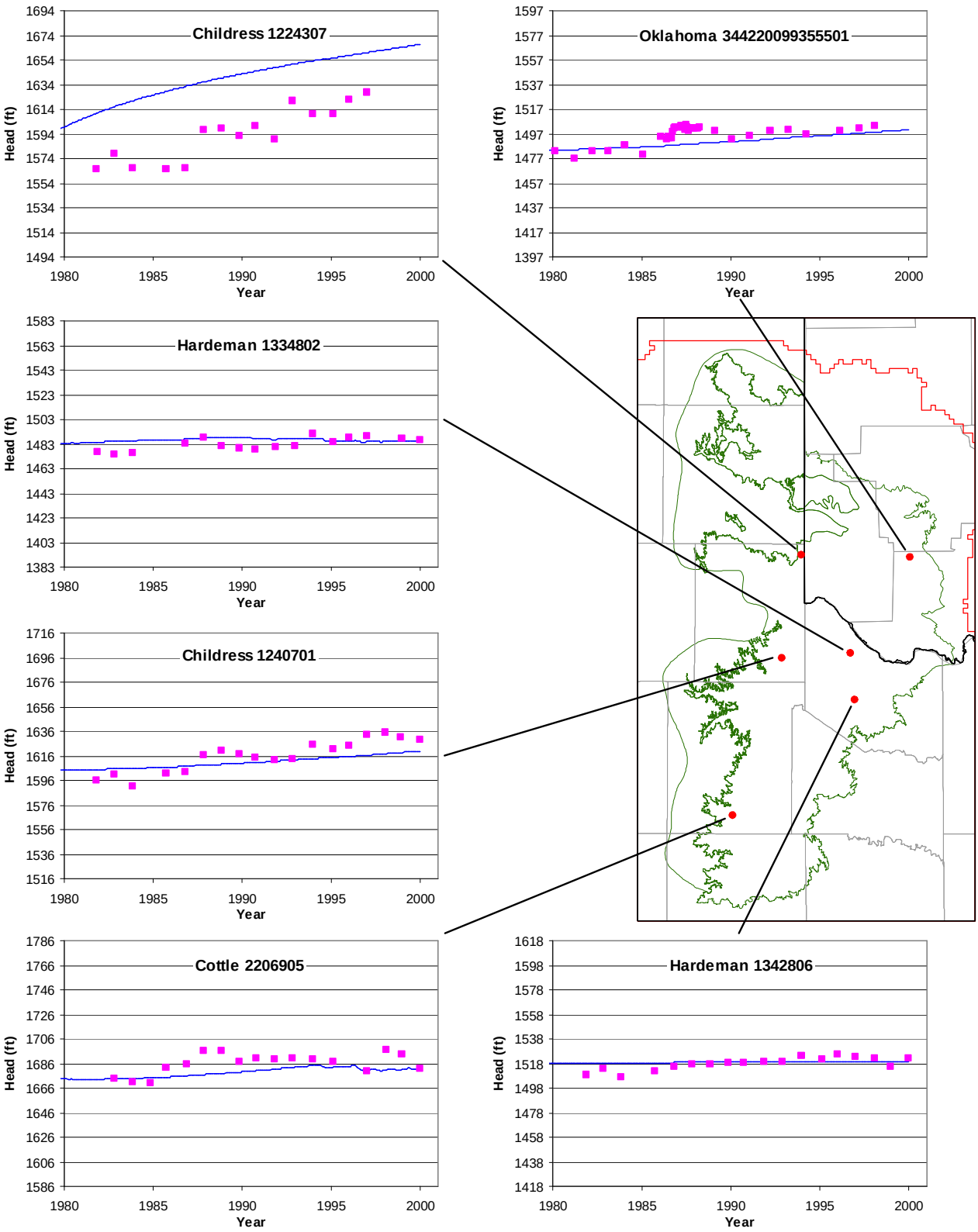

Figure 9.2.21 Selected hydrographs of simulated (lines) and measured (points) water-level elevations in the Blaine aquifer.

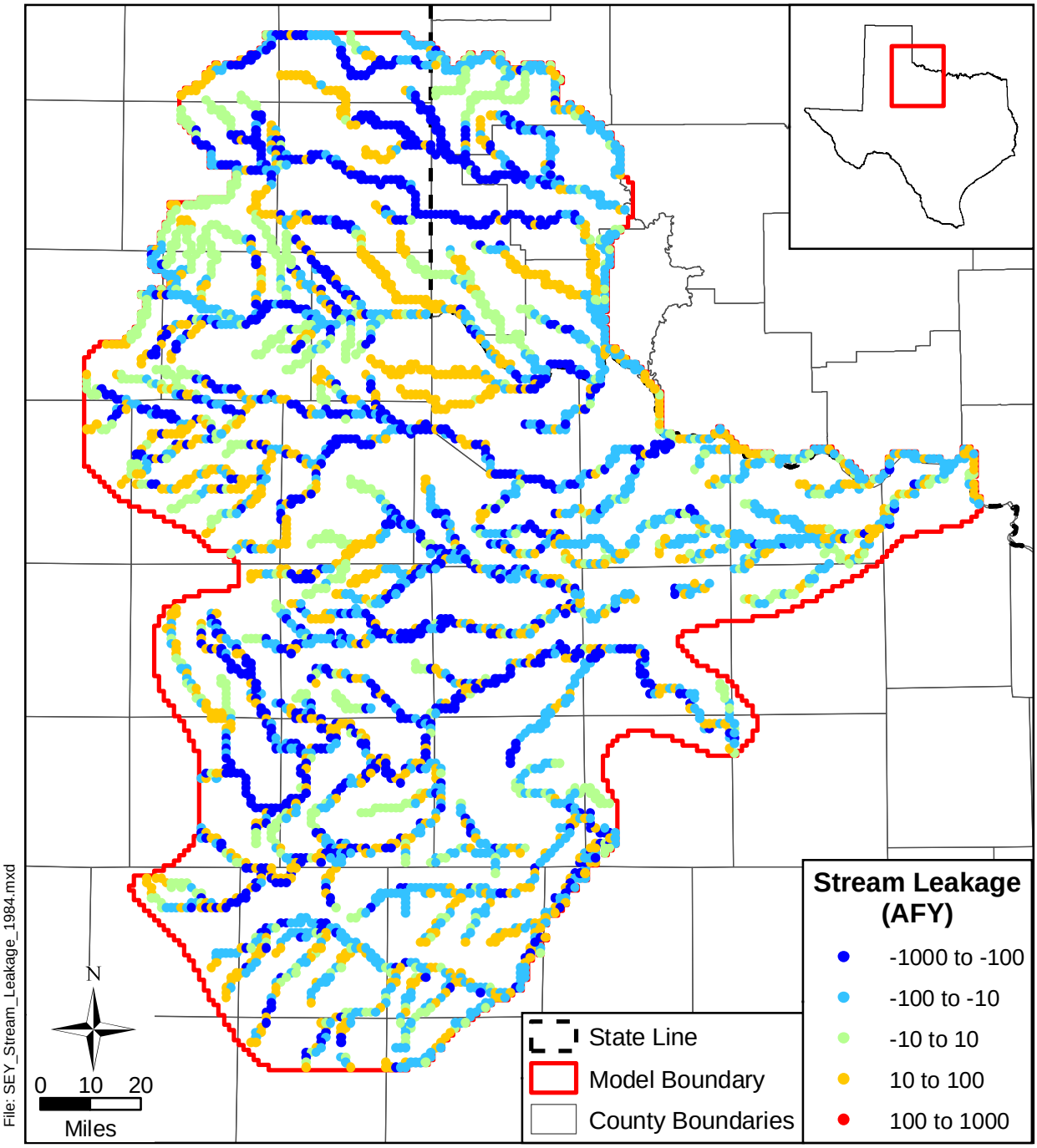

Figure 9.2.22 Simulated stream gain/loss for July 1984 (negative value indicates gaining stream cell).

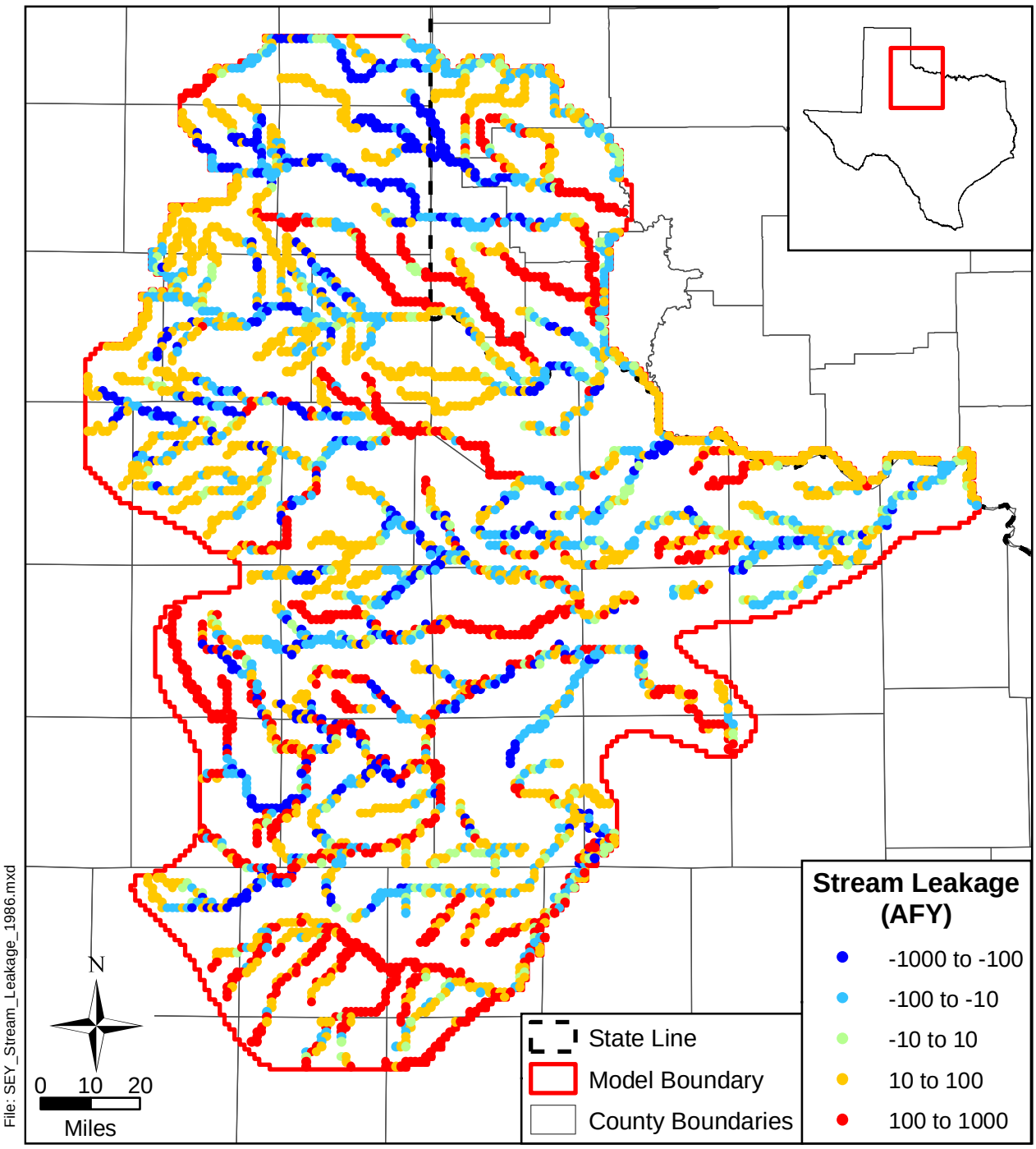

Figure 9.2.23 Simulated stream gain/loss for October 1986 (negative value indicates gaining stream cell).

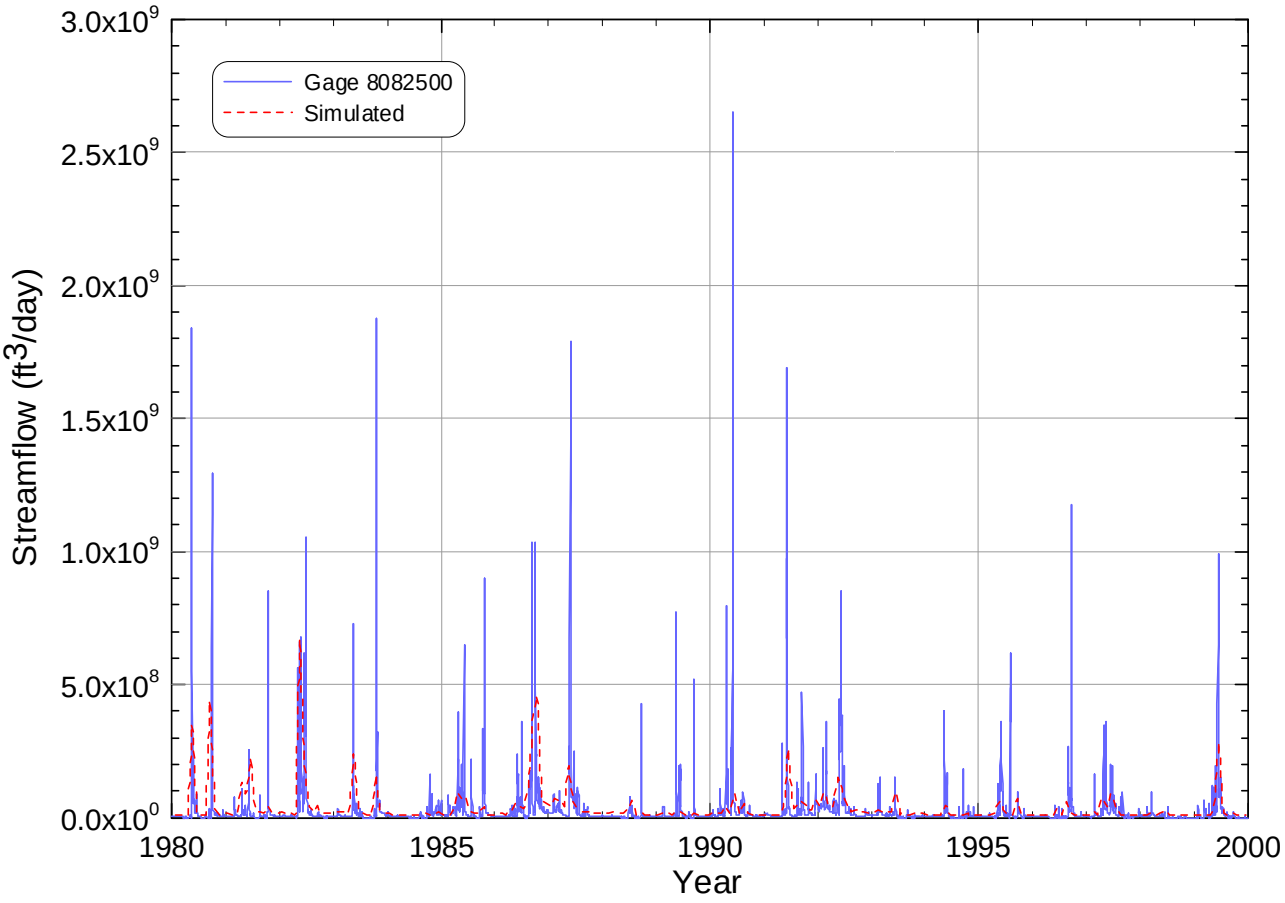

Figure 9.2.24 Simulated and measured stream flow at gaging station 8082500 on the Brazos River.

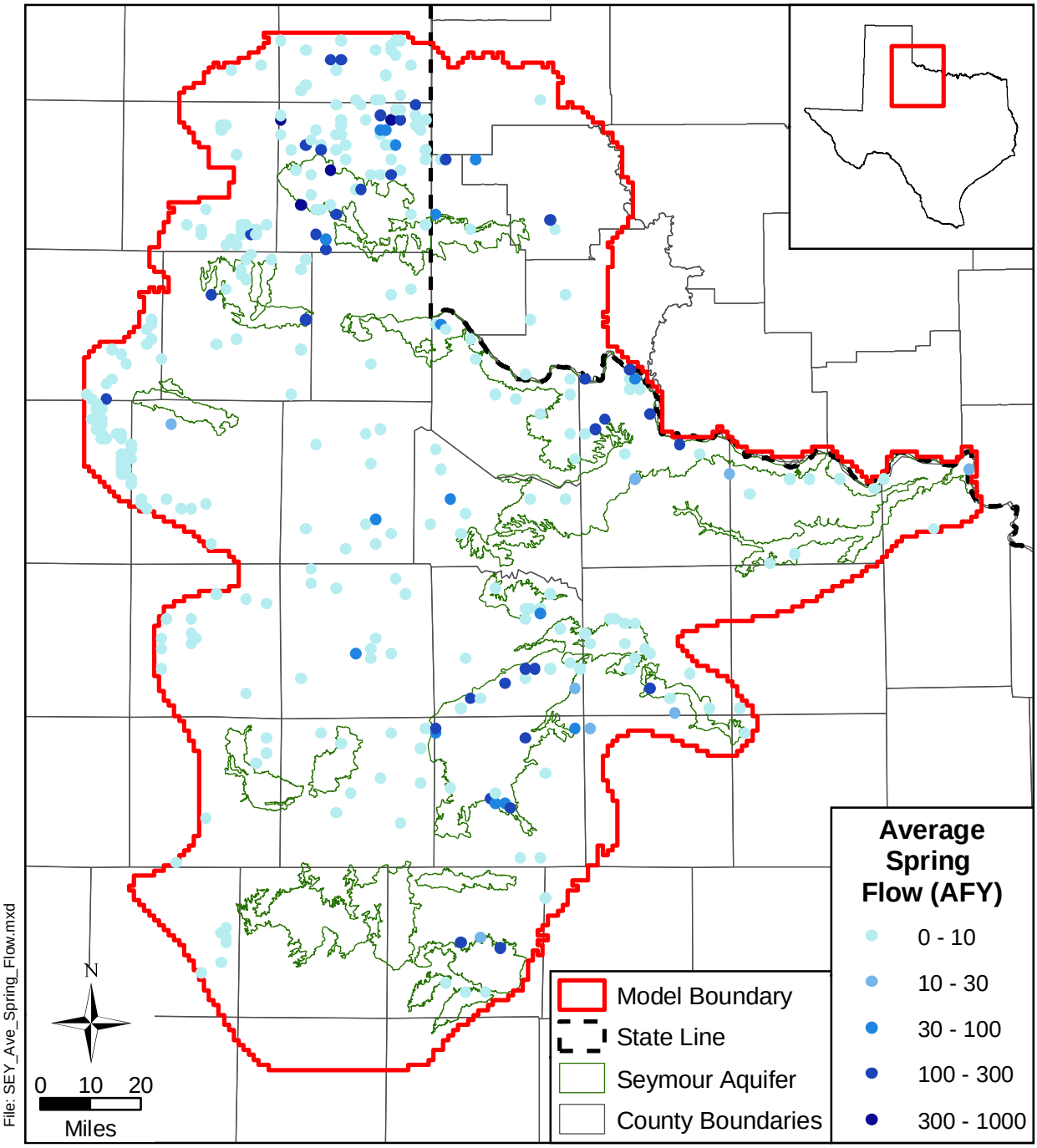

Figure 9.2.25 Average spring flow for the transient model from 1980 through 1999.

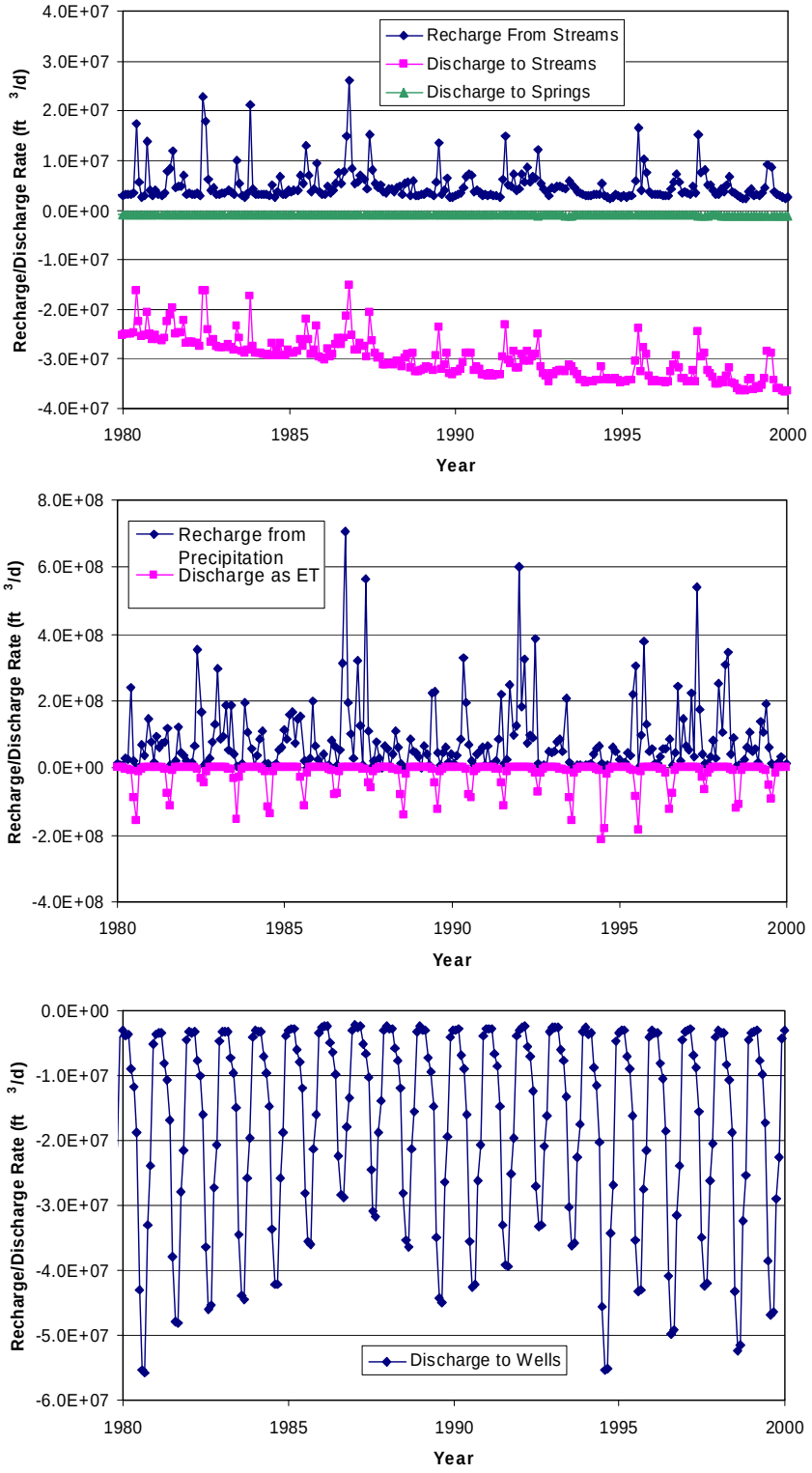

Figure 9.2.26 Time history of water budgets for (a) streams and springs, (b) recharge and ET, and (c) pumpage.

9.3 Sensitivity Analysis

Section 8.3 discussed the approach for sensitivity analyses for the steady-state model. The analyses were similar for the transient model, with the addition of several sensitivities. For the transient analysis, we completed 10 parameter sensitivities:

1. Horizontal hydraulic conductivity in layer 1,
2. Horizontal hydraulic conductivity in layer 2,
3. Vertical hydraulic conductivity in layer 1 (leakance between layers 1 and 2),
4. Recharge, model-wide,
5. Pumping, model-wide,
6. Specific yield in layer 1,
7. Specific yield in layer 2,
8. Storativity in layer 2,
9. Streambed conductance, model-wide,
10. Spring conductance, model-wide.

Equation 8.3.1 (varying linearly) for parameter variation was used for sensitivities 4, 5, 6, 7, and 8 and Equation 8.3.2 was used for the rest of the sensitivities listed above.

As with the steady-state model, the mean difference between the base simulated head and the sensitivity simulated head was calculated by applying Equation 8.3.3 at all grid blocks and also only at grid blocks where targets are present. Figure 9.3.1 shows the transient sensitivity results for layer 1 calculated for the target grid blocks and Figure 9.3.2 shows the transient sensitivity results for layer 1 calculated at all active grid blocks. The order of the two most important sensitivities – recharge and pumping, respectively – is the same between both methods, although the magnitude of the mean head differences (*MD*) differs. The difference in magnitudes is to be expected as the target cells are concentrated in areas with the greatest amounts of recharge and pumping. This indicates an adequate target coverage in layer 1. Water levels at both the targets and in all grid blocks are most sensitive to recharge. The next most sensitive parameter is pumping, which is negatively correlated with water level. This is an important result, because pumping was not varied during model calibration. Water levels are only slightly sensitive to the horizontal conductivity of layers 1 and 2, stream conductance, and

the specific yield of layer 1 and is insensitive to the specific yield of layer 2, storativity of layer 2, vertical hydraulic conductivity, and spring leakance.

Figure 9.3.3 shows the transient sensitivity results for layer 2 calculated for the target grid blocks and Figure 9.3.4 shows the transient sensitivity results for layer 2 calculated at all grid blocks. The most sensitive parameter for both the targets and all grid blocks is the horizontal hydraulic conductivity of layer 2. However, this parameter is positively correlated for the targets and negatively correlated for all grid blocks. Similarly, the specific yield of layer 2 (the second most sensitive parameter at target locations) is negatively correlated with the water levels at target locations and positively correlated with the water levels at all grid blocks. This indicates that the target locations, which are entirely located in the Blaine aquifer which, in turn, constitutes only 23 percent of layer 2 grid blocks, are not indicative of the behavior of the remainder of layer 2. Because we are most interested in the sensitivity of the Blaine aquifer water levels to changes in layer 2 parameters, this does not likely pose a problem for calibration of the Blaine aquifer. Recall also that uniform changes in Permian properties resulted in consistent behavior in the sensitivity of the Seymour water levels at target locations and all grid blocks. The third most sensitive parameter at layer 2 targets is pumping, which exhibits negative correlation. Not surprisingly, this negative correlation is less sensitive for all layer 2 grid blocks, most of which involve no pumping. The next most sensitive parameter is recharge, which occurs over all of layer 2 and is positively correlated with both target heads and heads at all grid blocks. Water levels are only slightly sensitive to stream conductance and the specific yield of layer 1 and insensitive to the horizontal conductivity of layer 1, vertical hydraulic conductivity, storativity of layer 2, and spring leakance.

Figure 9.3.5 shows the effect of varying recharge on several Seymour (layer 1) hydrographs. These figures show the same trend seen in Figure 9.3.1 where water levels increase with an increase in recharge. Some simulated hydrographs improve with an increase in recharge and some improve with a decrease in recharge. The effect of varying pumping on several Seymour hydrographs is shown in Figure 9.3.6. Similar to the trend apparent in Figure 9.3.1, an increase in pumping results in a decrease in heads. Figure 9.3.7 shows the effect of varying hydraulic conductivity in both layers 1 and 2 on simulated water levels for several Seymour hydrographs. While decreasing hydraulic conductivity improves some simulated hydrographs, the opposite effect is observed in others.

As described in Section 7.1, model convergence issues precluded the use of PEST as a calibration tool. For the same reasons, PEST was not used to calculate the Jacobian Matrix. Consequently, the original intent of calculating parameter sensitivities based on the inverse solution of the Jacobian Matrix was not possible.

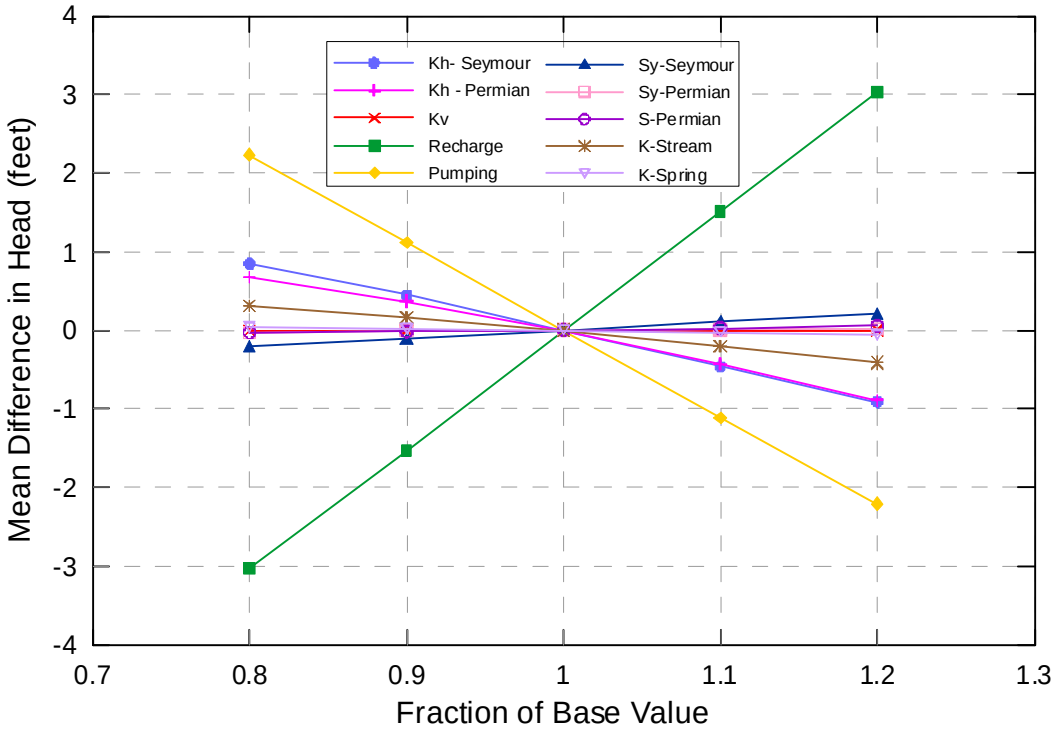

Figure 9.3.1 Transient sensitivity results for the Seymour aquifer using target locations.

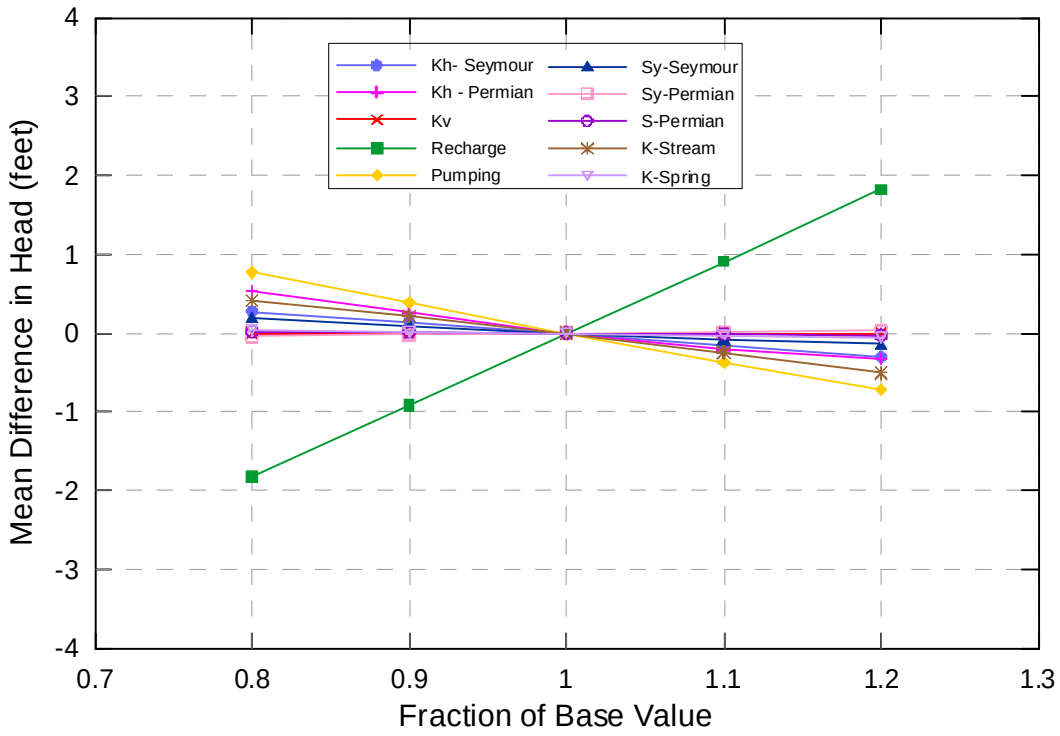

Figure 9.3.2 Transient sensitivity results for the Seymour aquifer using all active gridblocks.

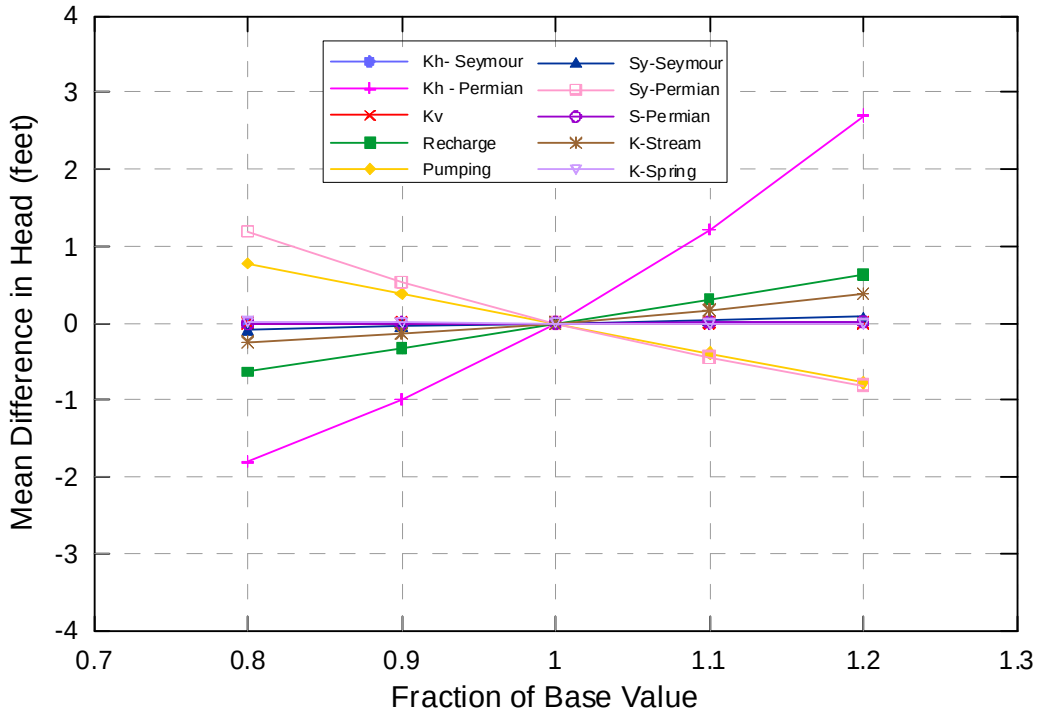

Figure 9.3.3 Transient sensitivity results for the Blaine aquifer using target locations.

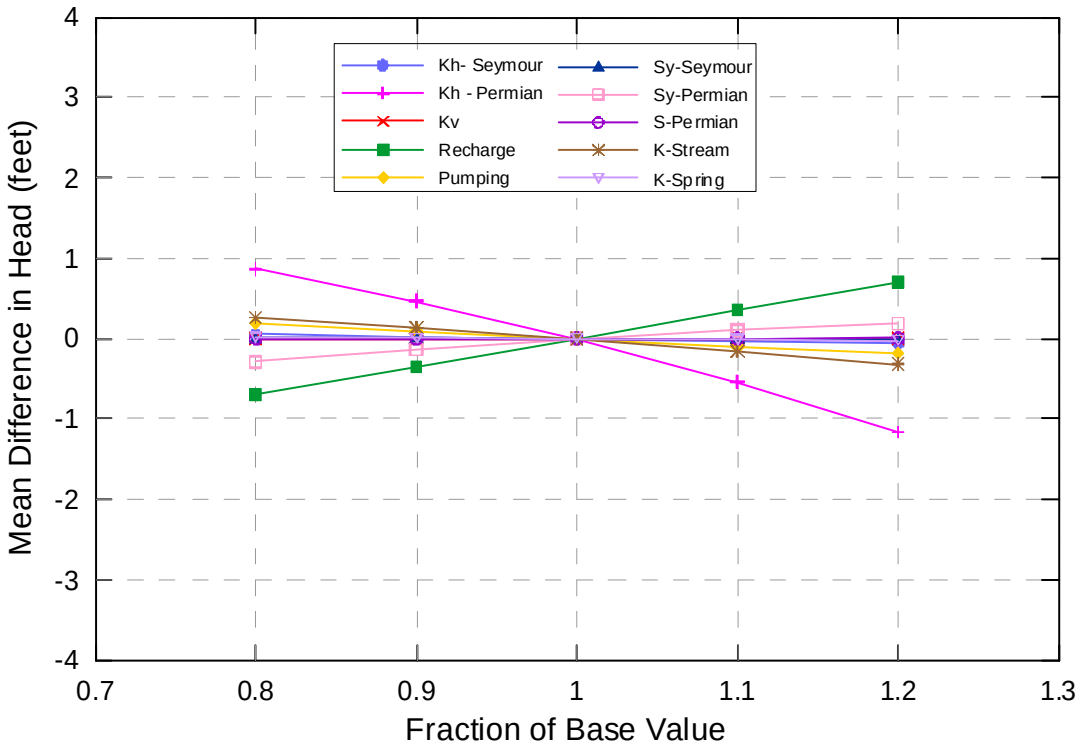

Figure 9.3.4 Transient sensitivity results for the Blaine aquifer using all active gridblocks.

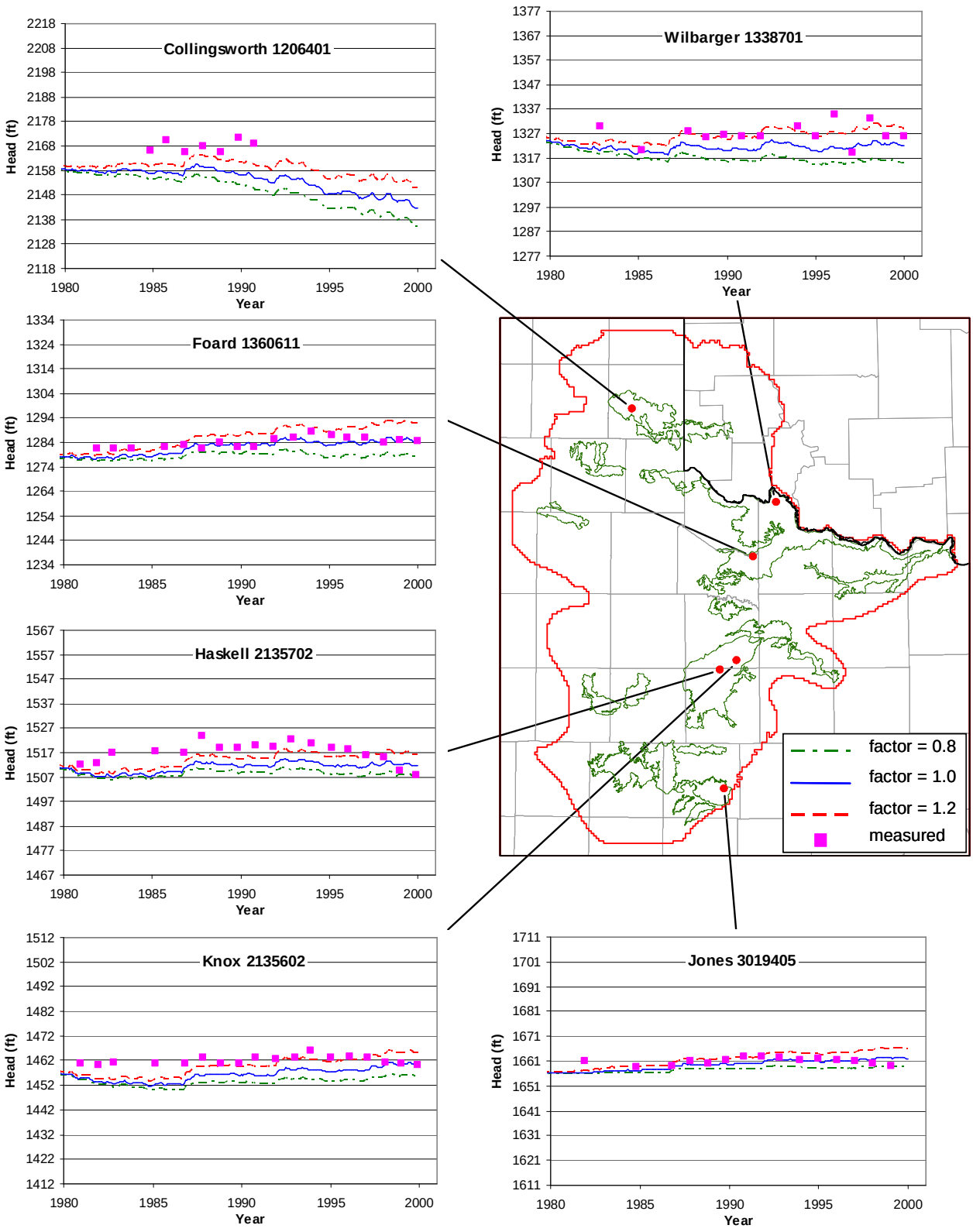

Figure 9.3.5 Transient sensitivity hydrographs for layer 1 where recharge is varied.

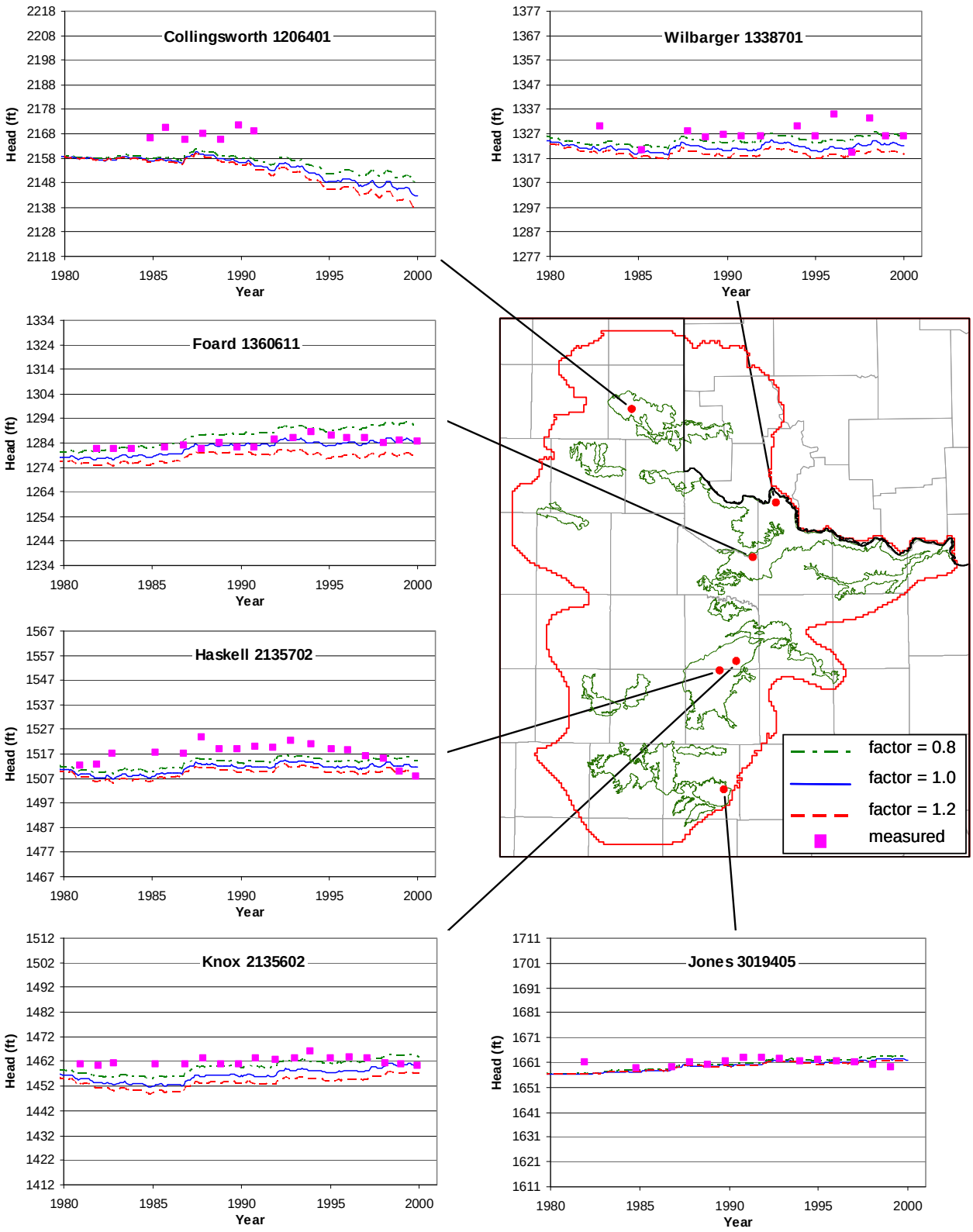

Figure 9.3.6 Transient sensitivity hydrographs for layer 1 where pumping is varied.

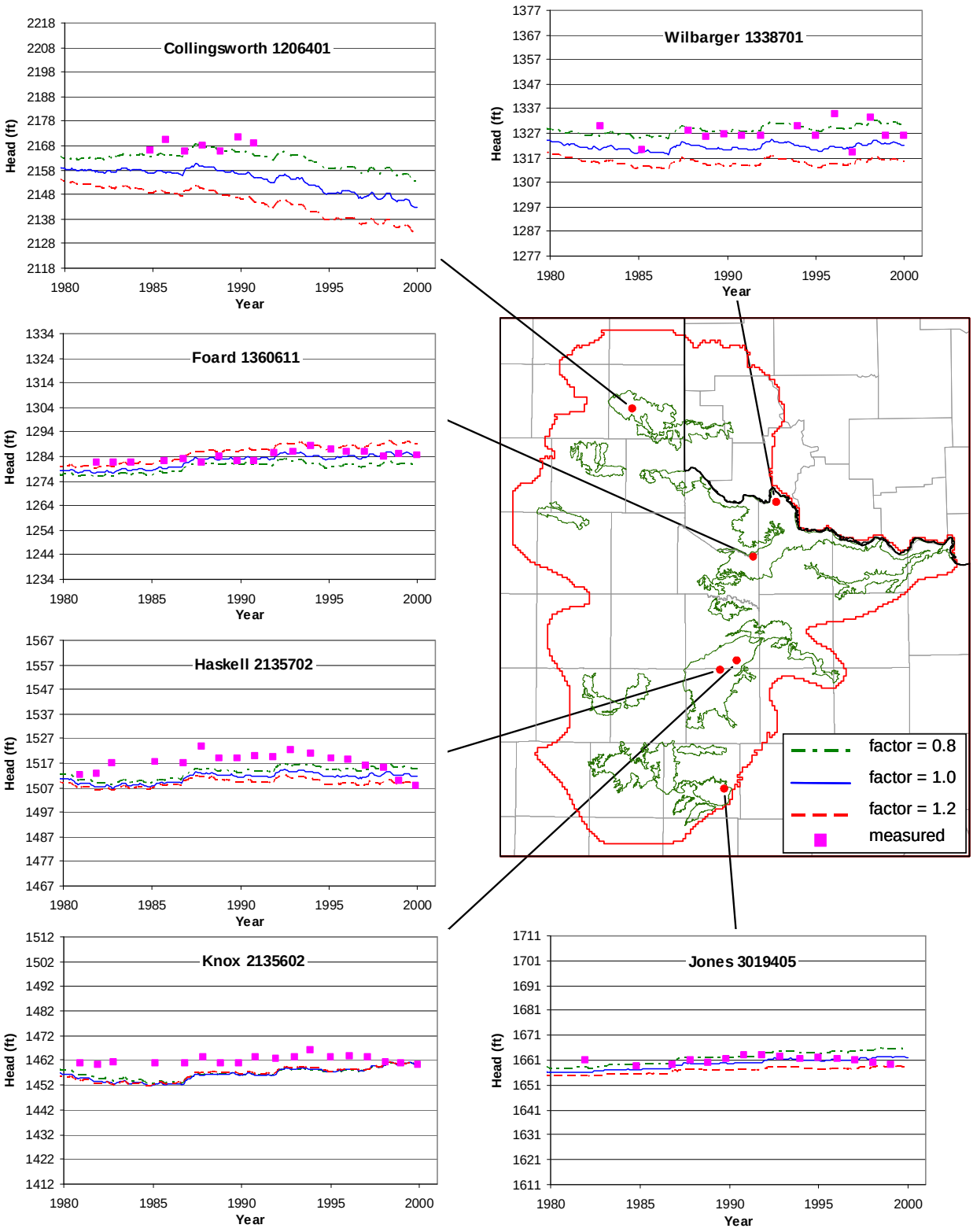

Figure 9.3.7 Transient sensitivity hydrographs for layer 1 where the horizontal hydraulic conductivities of layers 1 and 2 are varied.

This page intentionally left blank.

10.0 MODEL PREDICTIVE SIMULATIONS

The purpose of the GAM is to assess groundwater availability within the modeled Seymour aquifer region over a 50-year planning period (2000 through 2050) using RWPG water-demand projections under drought-of-record (DOR) conditions. The GAM will be used to predict changes in regional water levels (heads) and fluxes related to baseflow to major streams and rivers, spring flow, and cross-formational flow. The two most important stresses to be considered in the future predictive modeling period are the same two stresses imposed during the calibration and verification periods: recharge and pumping.

Predictive pumping demands from the RWPGs are used in the predictive mode simulations assuming that the pumping distribution for 1999 applies in the future (2000 through 2050). Predictive simulations assume average recharge conditions for the duration of the prediction ending with DOR recharge conditions. Estimates of long-term average recharge for the entire model domain do not exist. Furthermore, the complexity of determining recharge as a function of precipitation also precludes the direct use of precipitation data to calculate recharge. Therefore, the average recharge from 1960 through 1999 could not be accurately estimated. For the purposes of this report, average recharge is defined as the average recharge rate determined through calibration of the transient model which covered the period from 1975 through 1999.

Six basic predictive model runs are presented and documented: (1) average recharge through 2050, (2) average recharge ending with the DOR in 2010, (3) average recharge ending with the DOR in 2020, (4) average recharge ending with the DOR in 2030, (5) average recharge ending with the DOR in 2040, and (6) average recharge ending with the DOR in 2050.

Development of the predictive model datasets requires determination of the DOR and development of the predictive pumping datasets. Predictive pumping is discussed in Section 4.7 and the procedure for determining the predictive pumping demands is described in Appendix D. The following section discusses development of the DOR.

10.1 Drought of Record

GAM specifications require that the DOR used for model predictions be representative for the past 100 years (or longest length of available record) and be defined by severity and duration. Drought is considered a normal, recurring climatic event. It is conceptually defined by

the National Drought Mitigation Center as a protracted period of deficient precipitation resulting in extensive damage to crops with loss of yield. Operational definitions of drought are typically used to define the beginning, end, and severity of a drought over a given historical period. Operational definitions typically quantify the departure of precipitation, or some other climatic variable, from average conditions over a defined time window.

Drought indices are quantitative measures that assimilate raw data into a single value that defines how precipitation has varied from a specific norm. As discussed above, drought is a phenomenon related directly to available moisture from precipitation. Precipitation is the primary variable controlling recharge in the model region. Accordingly, precipitation data was used as the raw data for defining the DOR in the Seymour GAM region.

Within the active model area, historical precipitation data are available for over 50 stations in Texas (see Figure 2.13). All of the stations have time gaps in their data collection. Twenty eight of the gages began recording precipitation in the 1930s. The earliest monthly precipitation records in the area extend back to 1931 (20 gages).

There are various drought indices available to measure the degree that precipitation has deviated from historical norms. The typical measure is “percent of normal”, calculated by dividing the actual precipitation depth by the normal precipitation depth and multiplying by 100. This calculation could be performed over a range of time scales but is typically annualized. The normal precipitation depth is usually a long-term arithmetic mean. The available precipitation records for the individual gages within the active model were analyzed to calculate the percent of normal as an indicator of drought. Table 10.1.1 summarizes those results. This table gives the year, the number of gages having the indicated percentage of normal, and the average percentage of normal for all of the gages in the active model area combined. The latter was calculated in order to obtain an overall understanding of precipitation across the entire active model area. Only gages having a full 12-month record for the indicated year were considered in the development of Table 10.1.1. Assuming an average percentage of <70 percent of normal as an indicator of a severe drought, inspection of the table indicates severe droughts in 1952 (62 percent of normal), 1954 (67 percent of normal), 1956 (49 percent of normal), 1970 (60 percent of normal), and 1998 (65 percent of normal) based on the combined percent of normal for all of the gages.

The 1950s represents a period of historical drought in Texas including the region being modeled. Based on the combined data from all gages in the active model area, below normal precipitation occurred from 1951 to 1954, normal precipitation occurred in 1955, and the lowest amount of precipitation, based on percentage of normal, ever to occur over the active model area was recorded in 1956. In 1956, 19 of 30 gages (63 percent) recorded their lowest annual precipitation. Considering the period from 1951 through 1956, 22 of 32 gages (69 percent) recorded their lowest annual precipitation. The average precipitation, as measured in percent of normal averaged across all available gages in the active model area, is equal to 74 percent from 1951 through 1956. The same metric calculated for the peak drought year of 1956 is 49 percent of normal. The lowest annual precipitation was measured in 1970 for four of 34 gages. Considering all of the gages in the active model area, precipitation in 1970 was 60 percent of normal, which is not as low as that in 1956. In addition, 1970 was preceded and followed by several years with higher than normal precipitation indicating that the drought in 1970 was short term. Four out of 32 gages recorded lowest annual precipitation in 1998. Precipitation in 1998 was 65 percent of normal considering all gages in the active model area. Precipitation in the year prior to 1998 was higher than normal and precipitation in the year following 1998 was only slightly lower than normal indicating a short-term drought in 1998.

Figure 10.1.1 graphically shows the percentage of normal for all of the gages combined based on annual precipitation data. This figure shows that the lowest percentages of normal precipitation occurred in 1956 and 1970. The longest time periods with precipitation consistently below normal were during the 1930s, 1940s, and 1950s, with a greater deficit in precipitation in the 1950s. This is consistent with the fact that the 1950s represents a period of historical drought in Texas. Figure 10.1.2 shows the percentage of normal for all gages combined on a monthly basis between 1950 and 1960. For many months during this time period, precipitation was near zero percentage of normal. The area between the curve and 100 percent of normal for precipitation above normal is half the area for precipitation below normal, indicating twice as much below-normal precipitation as above-normal precipitation during this time period. Based solely on an analysis of drought using percentage of normal, two possible times for the DOR could be identified: June 1952 through June 1953, a 13-month period, or June 1954 through April 1955, an 11-month period.

A secondary drought index that can be used to quantify the DOR is the Standardized Precipitation Index (SPI). This index was developed to define precipitation deficits over multiple time scales (McKee et al., 1993). The SPI is calculated based upon the precipitation record for a given location. The long-term precipitation record is fit to a general probability distribution (typically the Gamma distribution). This distribution is then normally transformed and standardized so that the mean SPI for that location over the time period of interest is equal to zero. When the SPI is equal to zero, it signifies median precipitation conditions for that location based upon the time integration window specified (Edwards and McKee, 1997). Because the index is normalized, comparison of SPI values between locations (i.e., across our model domain), is simplified in that an SPI of –1 represents a similar magnitude deficit for all stations. Monthly precipitation averages are used as the raw data for the SPI calculation. A one-month SPI would represent normalized precipitation data without temporal averaging. The SPI is backward-averaged over some user-specified duration, typically between six months and three years. By lengthening this time integration window, one effectively looks at longer term precipitation trends less subject to short-term variations. Short-term deficit conditions or anomalies are of less concern for predicting groundwater conditions; for this reason, the SPI was calculated for long time periods (1-, 2-, and 3-year windows). Current SPI index maps are available online for the State of Texas for multiple time averaging periods from one month through three years at the following URL: http://www.txwin.net/Monitoring/Meteorological/Drought/spi.htm.

McKee et al. (1993) defined a classification system for defining drought conditions using the SPI. This classification is taken from Hayes (2001) and presented in the table below.

SPI Value	Precipitation Deficit Condition
2.0 and above	Extremely wet
1.5 to 1.99	Very wet
1.0 to 1.49	Moderately wet
-0.99 to 0.99	Near normal
-1.0 to –1.49	Moderately dry
-1.5 to –1.99	Severely dry
-2.0 and less	Extremely dry

McKee et al. (1993) defined a drought event as any time period over which the SPI is continuously negative and reaches a magnitude of –1.0 or less. The drought begins when the SPI first drops below zero and ends when the SPI becomes positive after reaching a low of at least -1.

Figure 10.1.3 shows the SPI for precipitation gage 413992 in Haskell County from 1950 to 1970 calculated using 1-, 2-, and 3-year averaging windows. Notice that the dry period in the 1950s occurs over a longer time period as the length of the averaging window increases. In addition, the date at which the drought begins and ends becomes later as the averaging window becomes larger, reflecting the effect of the backward averaging.

Figure 10.1.4 plots SPI curves for six representative long-term precipitation gages in the model area. A 2-year time window was used for the analysis. The gages in this figure consistently show drought conditions at some time during the 1930s, 1950s, and 1960s. A drought in the early 1970s is observed for three of the gages and in the late 1970s for three of the gages. Two of the gages show a drought in the early 1980s and one in the mid-1980s. One gage indicates a drought in the mid-1990s and another gage indicates a drought from 1994 through 2000. For most of the gages, the most severe drought occurred during the 1950s.

Records for all precipitation gages in the active model area were averaged for each month to provide input to an "overall" SPI. Figure 10.1.5 shows the SPI calculated for this average dataset for integration windows of 1, 2, and 3 years. This figure clearly shows that the longest and most severe drought for the active model area occurred in the 1950s. Thus, the SPI analysis corroborates the results of our analysis of percent of normal. The DOR is, therefore, considered to have occurred in the 1950s.

Comparison of the percent of normal analysis (Figure 10.1.2) and the SPI analysis (Figure 10.1.6) in the 1950s shows that the SPI analysis gives sustained drought conditions for a much longer time period than does the percent of normal analysis. The SPI analysis indicates that the short-term high precipitation which occurred in between longer-term low precipitation (see Figure 10.1.2) was not sufficient to end the drought. This represents a situation where wet conditions are observed on a short-term time scale but dry conditions are observed on a long-term time scale. Since groundwater responds to precipitation on a longer-term time scale, the DOR was defined using the SPI analysis with a 2-year time window. This yields a starting date of September 1951 and an ending date of February 1958 for the DOR.

Results from the SPI analysis were compared to the Palmer Drought Index. This index is based on a supply-and-demand model of soil moisture[7] and indicates prolonged and abnormal moisture deficiency or excess. Determination of soil moisture supply is relatively straightforward to calculate. Demand, on the other hand, depends on multiple factors including temperature, amount of moisture in the soil, ET, and recharge rates and is more difficult to determine. Palmer Drought Index data for the model area, which is located in Texas climate division 2, was obtained from http://lwf.ncdc.noaa.gov/oa/climate/onlineprod/ drought/main.html and is plotted in Figure 10.1.7. This figure shows that, based on this index, the longest and most severe drought in the model area occurred in the 1950s (October 1951 through February 1957) which is in general agreement with the results of the SPI analysis.

To simulate the DOR, it was necessary to estimate the effect of the lower-than-normal precipitation occurring during the DOR on the recharge over the model domain. During model calibration, recharge had to be adjusted and the spatially averaged recharge differed slightly from that of the SWAT estimates. With no means to calibrate SWAT estimates during the drought period, SWAT was not used for estimating the DOR recharge. Instead, a relationship between calibrated recharge and precipitation was generated. Figure 10.1.8 shows the calibrated average monthly recharge over the entire active model domain versus the average monthly precipitation for the 25-year period from 1975 through 1999. While a linear regression of this relationship shows a correlation coefficient of only 0.4 because precipitation is not the only factor dictating recharge, this relationship was thought to be the best available method of estimating DOR recharge. The negative intercept in the linear regression line indicates that, below a minimum average monthly precipitation rate of 1.7 in/yr, no recharge to the groundwater occurs. The recharge for each month during the DOR was calculated using this relationship and the monthly DOR precipitation.

[7] http://en.wikipedia.org/wiki/Palmer_Drought_Index

Table 10.1.1 Summary of percentage of normal analysis (1931 through 1999).

Year	Percent of Normal Precipitation																					Average Percentage for all Gages
	10	20	30	40	50	60	70	80	90	100	110	120	130	140	150	160	170	180	190	200	210	
	Number of Gages																					
1931							1	4	5	3												91
1932								1	1	2	1	2	1	2	1	1	1					133
1933						3	4	3	3													80
1934				1		4	3	2	1	1												75
1935								1	3	5	3	1	1									111
1936							1	5	4	4		1										94
1937						2	7	4		2												79
1938							1	1	9	4												96
1939						5	5	3	2													75
1940						1	3	5	3	1	1	1										92
1941															1	5	6	4	2	1	2	180
1942							1	2	2	6	6	3			1	1						109
1943					2	8	9	4	1													72
1944							1	3	4	6	8	1										101
1945					1	4	5	1	4	7	2	1	2									95
1946						2	2	4	7	4	2	3	2									95
1947							1	4	6	3	1											89
1948						3	5	3	1													73
1949									3	7	5	4	2	1								114
1950								2	2	4	2	2		1								109
1951					1	7	4	6	4	3	1											80
1952				1	8	12	6															62
1953					2	7	9	4	6	1	1											79
1954				1	3	16	7	1	2													67
1955							2	3	7	8	3	5	2	1	1							105
1956		1	7	8	5	6	2	1														49
1957										1	1	3	9	4	5	6						139
1958							3	7	7	4	5	2										96

Table 10.1.1, continued

Year	Percent of Normal Precipitation																					Average Percentage for all Gages
	10	20	30	40	50	60	70	80	90	100	110	120	130	140	150	160	170	180	190	200	210	
	Number of Gages																					
1959							1	1	4	5	11	4	3	1		1						113
1960								7	5	4	3	2	3	4	2	1						113
1961								4	8	4	4	3	2	5	2							114
1962								1	6	11	3	4	7									111
1963						9	10	5	8	1	1	1										80
1964						5	8	8	10	3	2		1									86
1965							5	8	7	11	5	3	1									97
1966							7	6	4	11	6			1								95
1967					2	3	10	3	12	2	3											84
1968									4	9	14	7	1									110
1969									4	3	10	6	7	2	1							116
1970				5	10	11	7	1														60
1971							2	3	2	2	3	5	4	3	3							111
1972							2	2	7	4	8	6	1									104
1973							1	4	3	7	5	4	1	2	1							107
1974							1		9	7	3	5	1									104
1975							1	1	5	6	4	4		1								110
1976					1	2	3	6	7	4	1	1	1									93
1977						6	5	8	3	1		1	2									85
1978								9	8	3	2	1										95
1979								7	6	5	4	3	1									102
1980					1	3	5	4	7	3	1	1	1	1								89
1981								5	8	10	7											100
1982								3	6	3	7	4	5	1								110
1983						1	1	6	4	5	5	2										101
1984					1	4	4	13	5													82
1985										9	9	5	1	1	1	1						118
1986									1		4	8	5	7	1	2		1	1			136

Table 10.1.1, continued

Year	Percent of Normal Precipitation																					Average Percentage for all Gages
	10	20	30	40	50	60	70	80	90	100	110	120	130	140	150	160	170	180	190	200	210	
	Number of Gages																					
1987								2	8	8	3	7	1									108
1988						2	3	10	6	1	2											86
1989						3	1	5	5	6	4		3									94
1990								5	4	1	3	3	4	3		1						120
1991											2	6	4	2	3	4			1			145
1992										3	4	5	2				1					125
1993							2	5	4	3	1	1										95
1994							3	8	3	4												88
1995									2		2	3	3	3	5			2				140
1996						1	4	2	6	5	3			1								94
1997								1			2	3	4	2		3						137
1998			1	2	5	11	5	4	2	2												65
1999						1	2	10	5	8	3	1										90

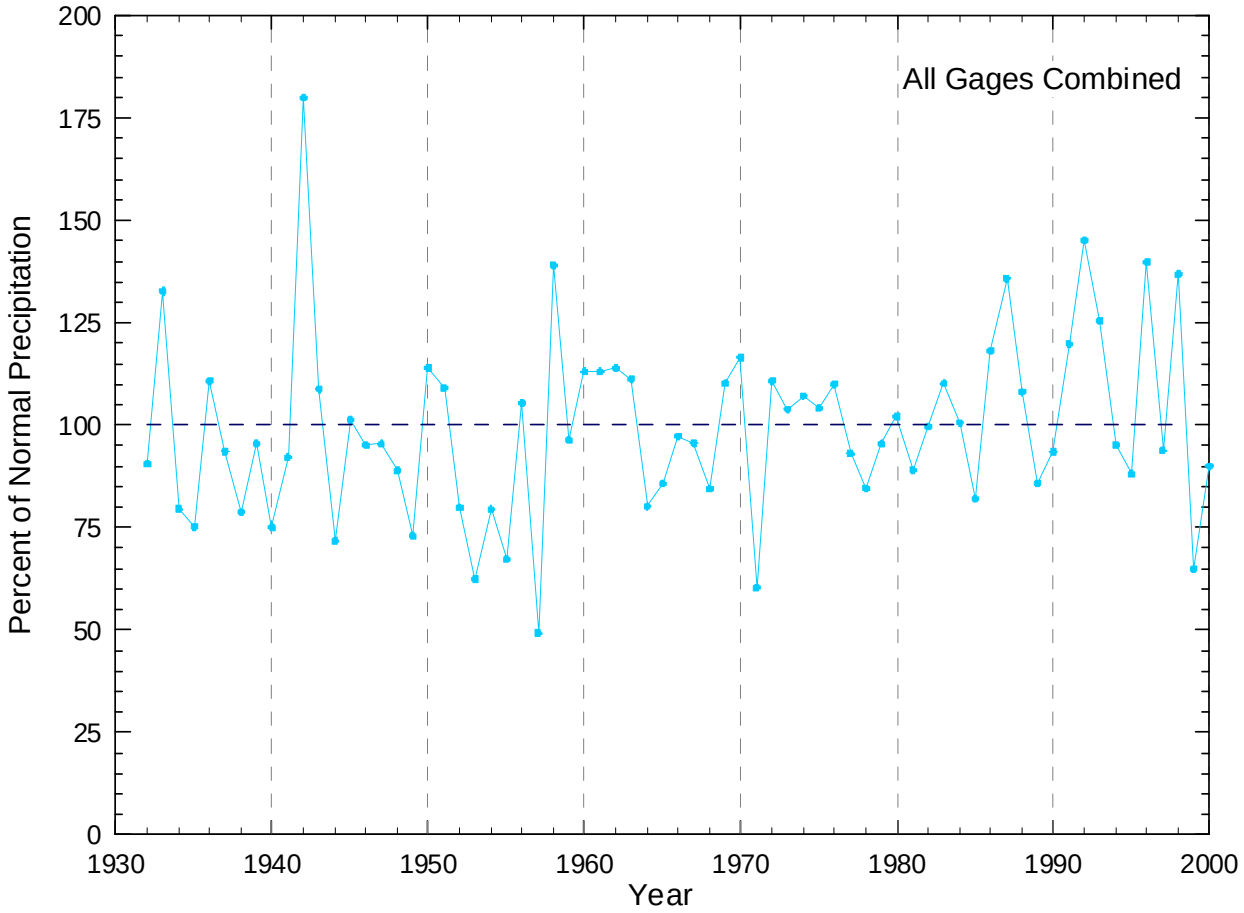

Figure 10.1.1 Percentage of normal precipitation for all gages in the model area from 1930 through 1999.

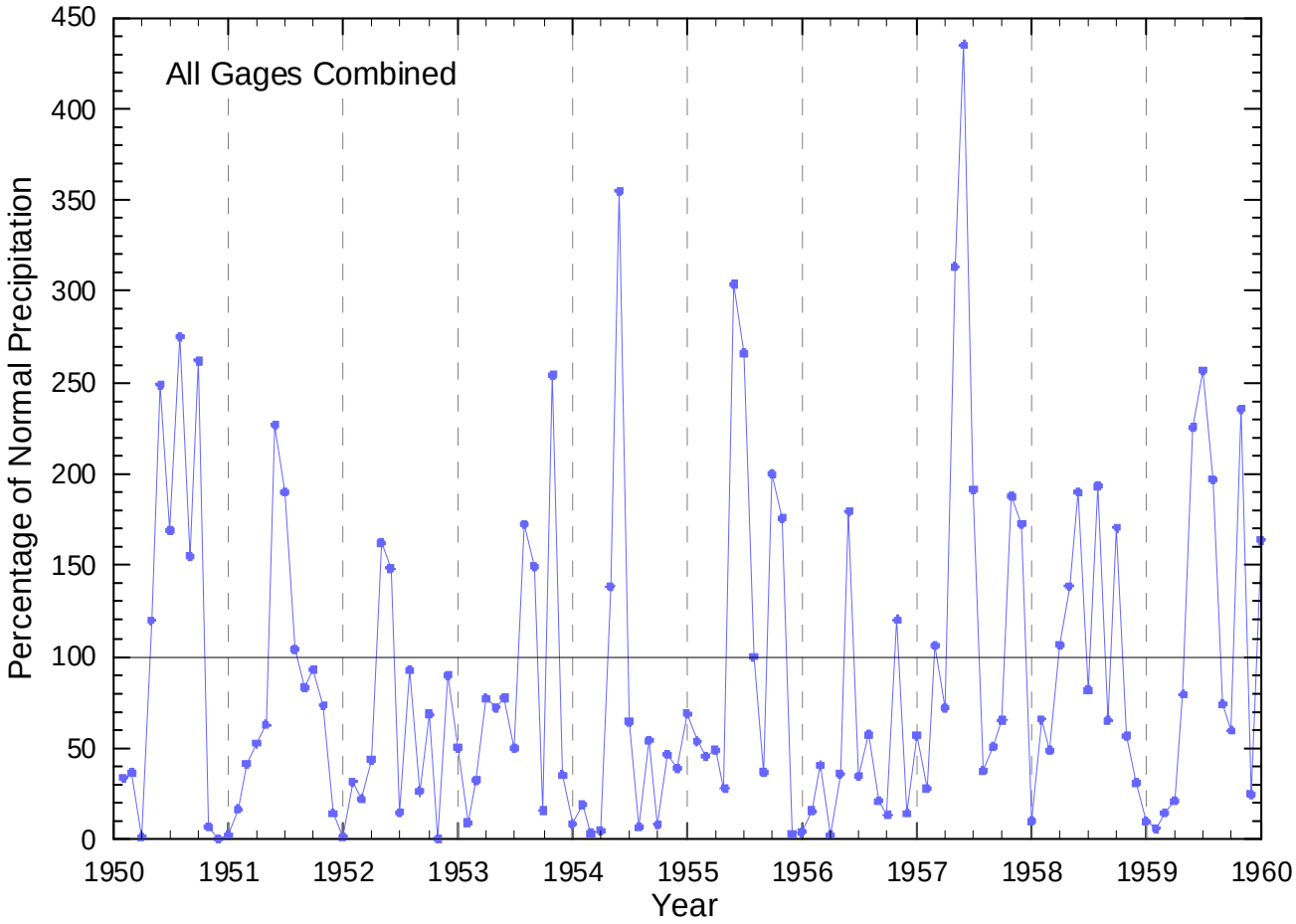

Figure 10.1.2 Percentage of normal precipitation for all gages in the model area from 1950 through 1959.

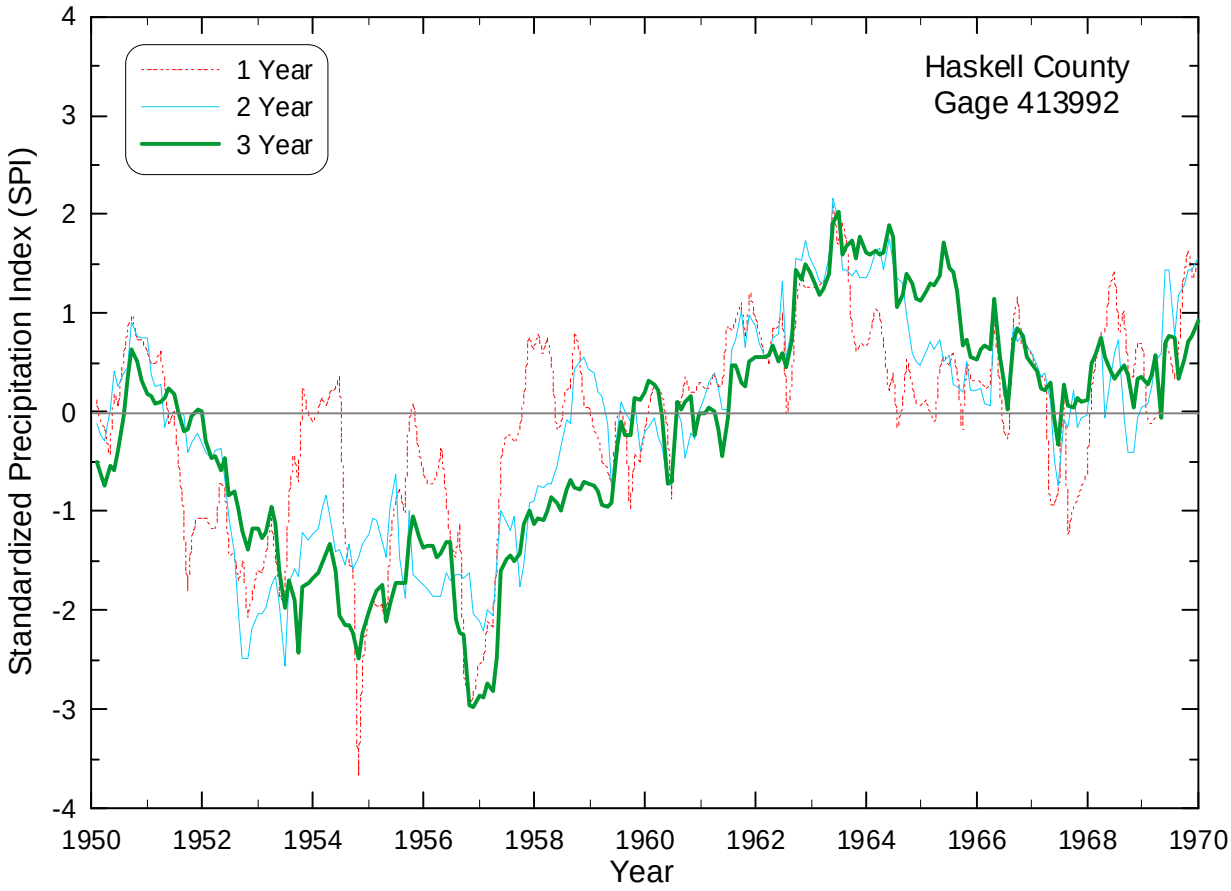

Figure 10.1.3 Standardized precipitation index (SPI) curves for the Haskell rain gage (#413992-Haskell County) for 1-year, 2-year, and 3-year time periods.

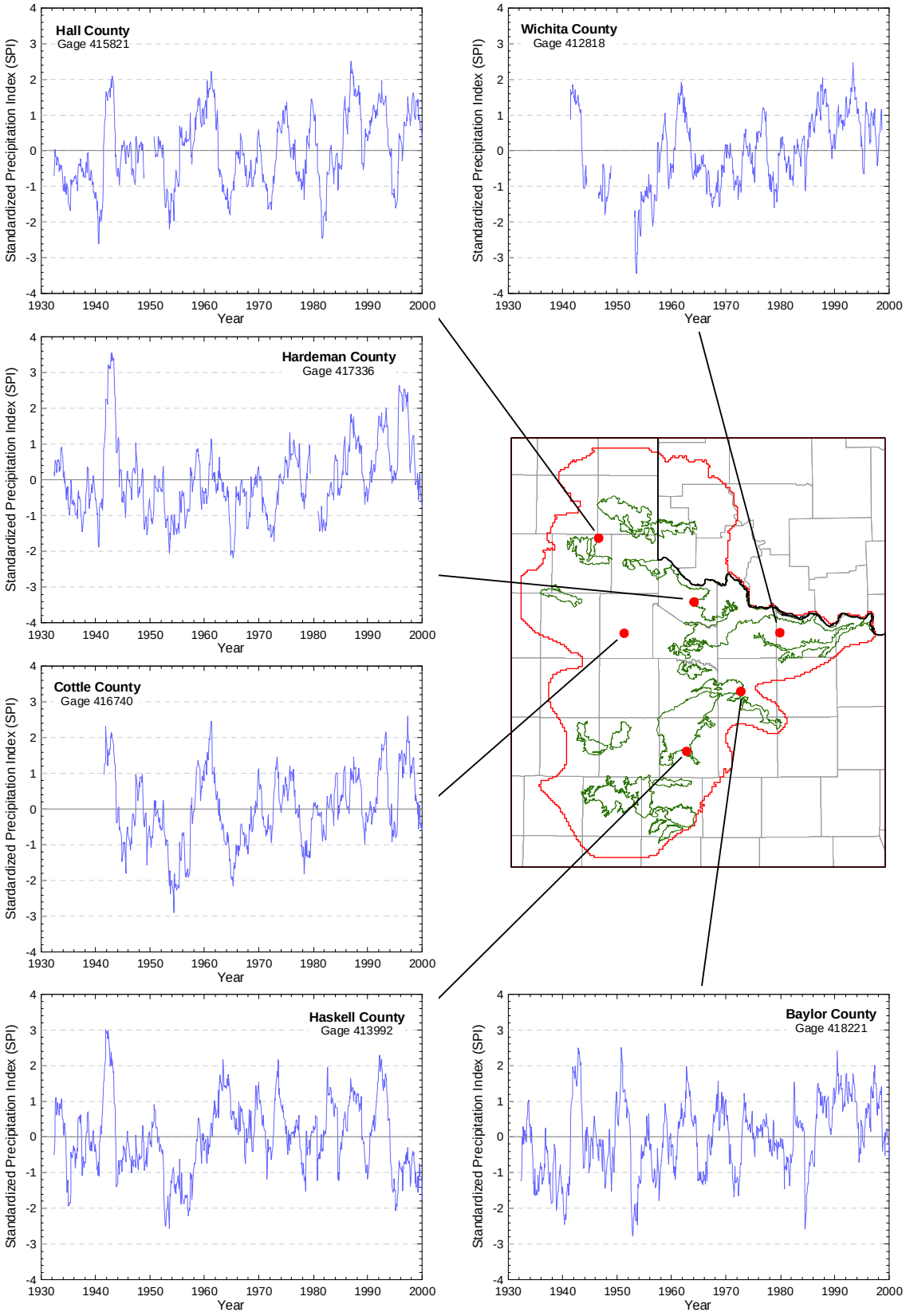

Figure 10.1.4 Standardized precipitation indices (2-year integration window) for selected precipitation gages in the model area.

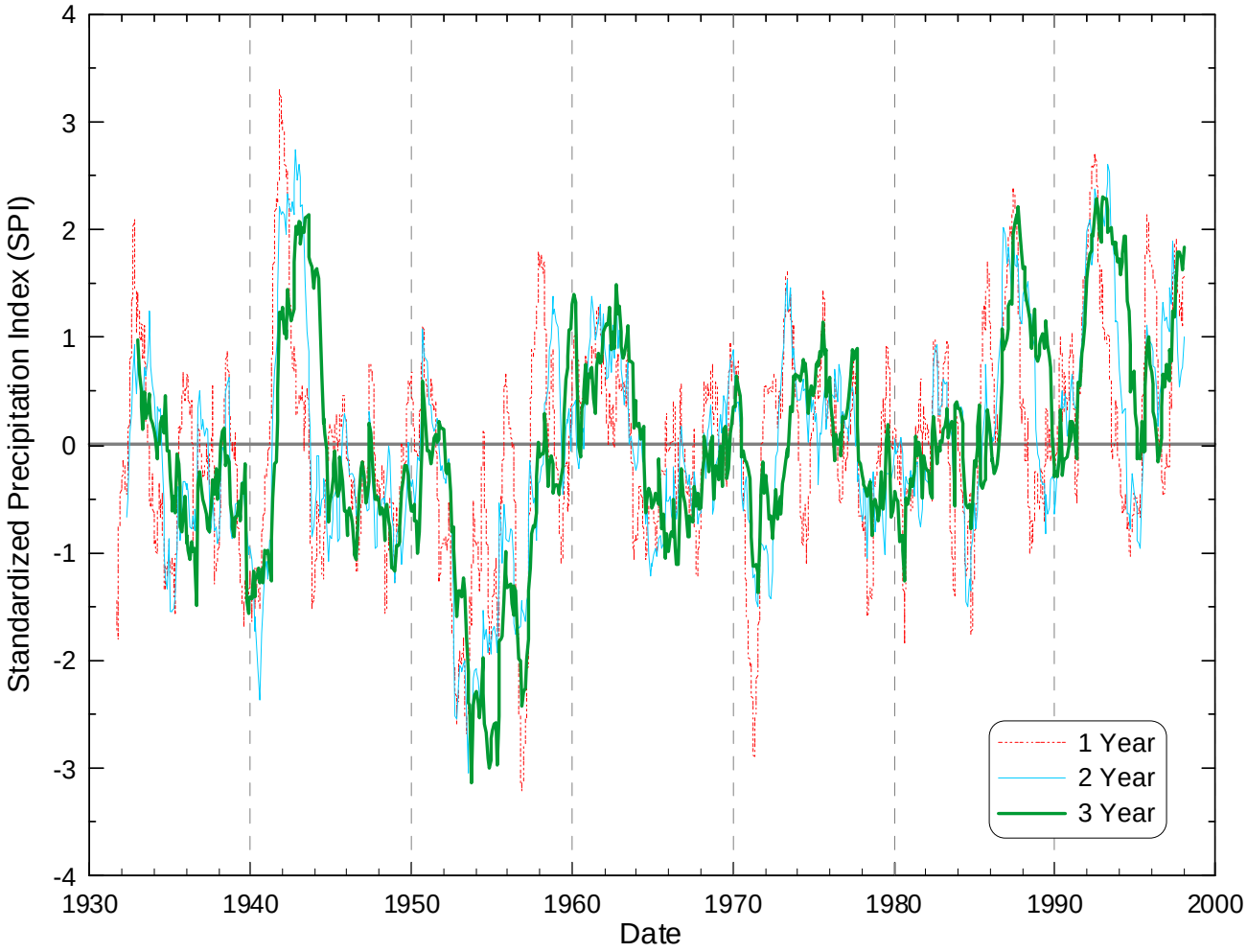

Figure 10.1.5 Standardized precipitation index (SPI) curves averaged for all gages in the model area from 1930 through 1998.

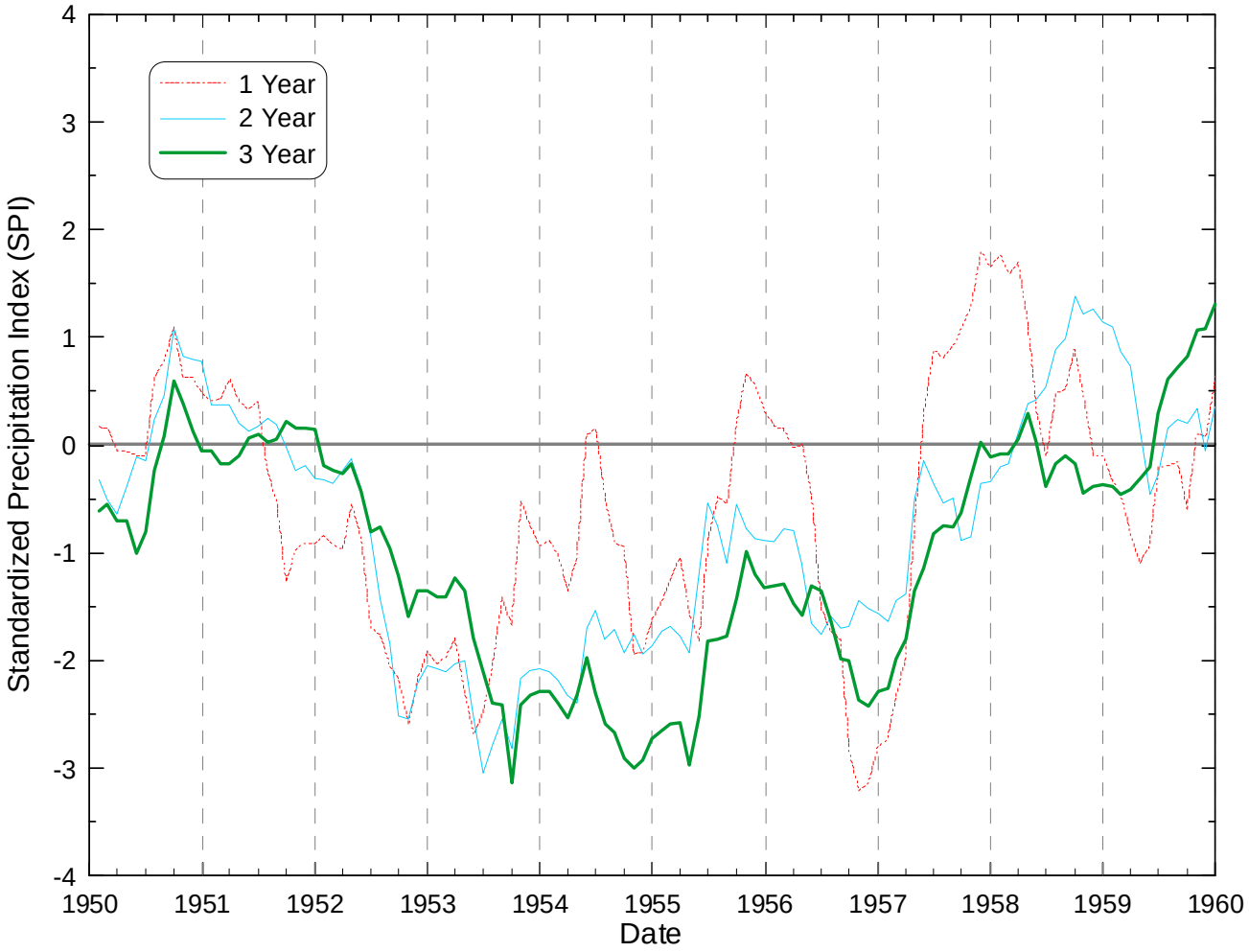

Figure 10.1.6 Standardized precipitation index (SPI) curves averaged for all gages in the model area from 1950 through 1959.

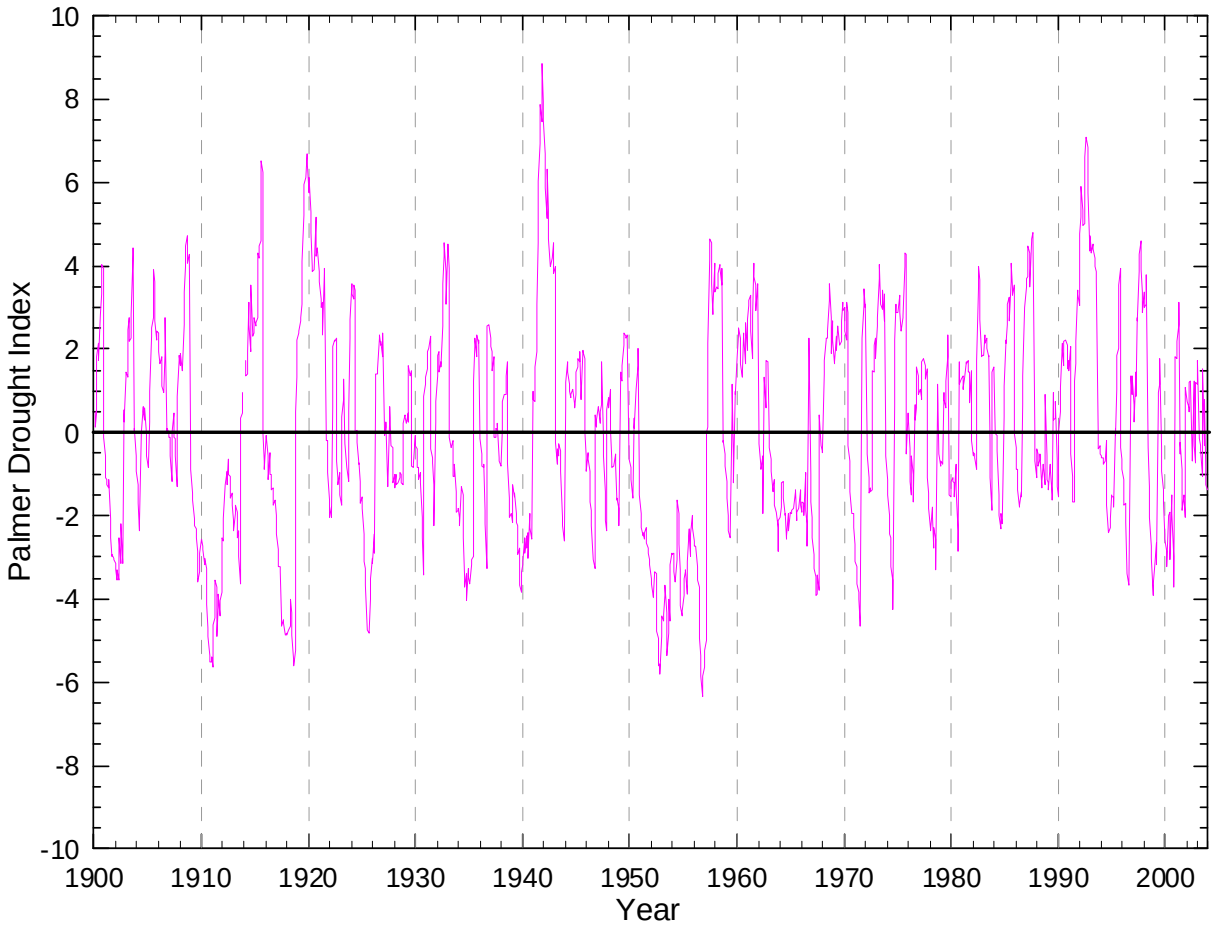

Figure 10.1.7 Palmer Drought Index for Texas Climate Division 2.

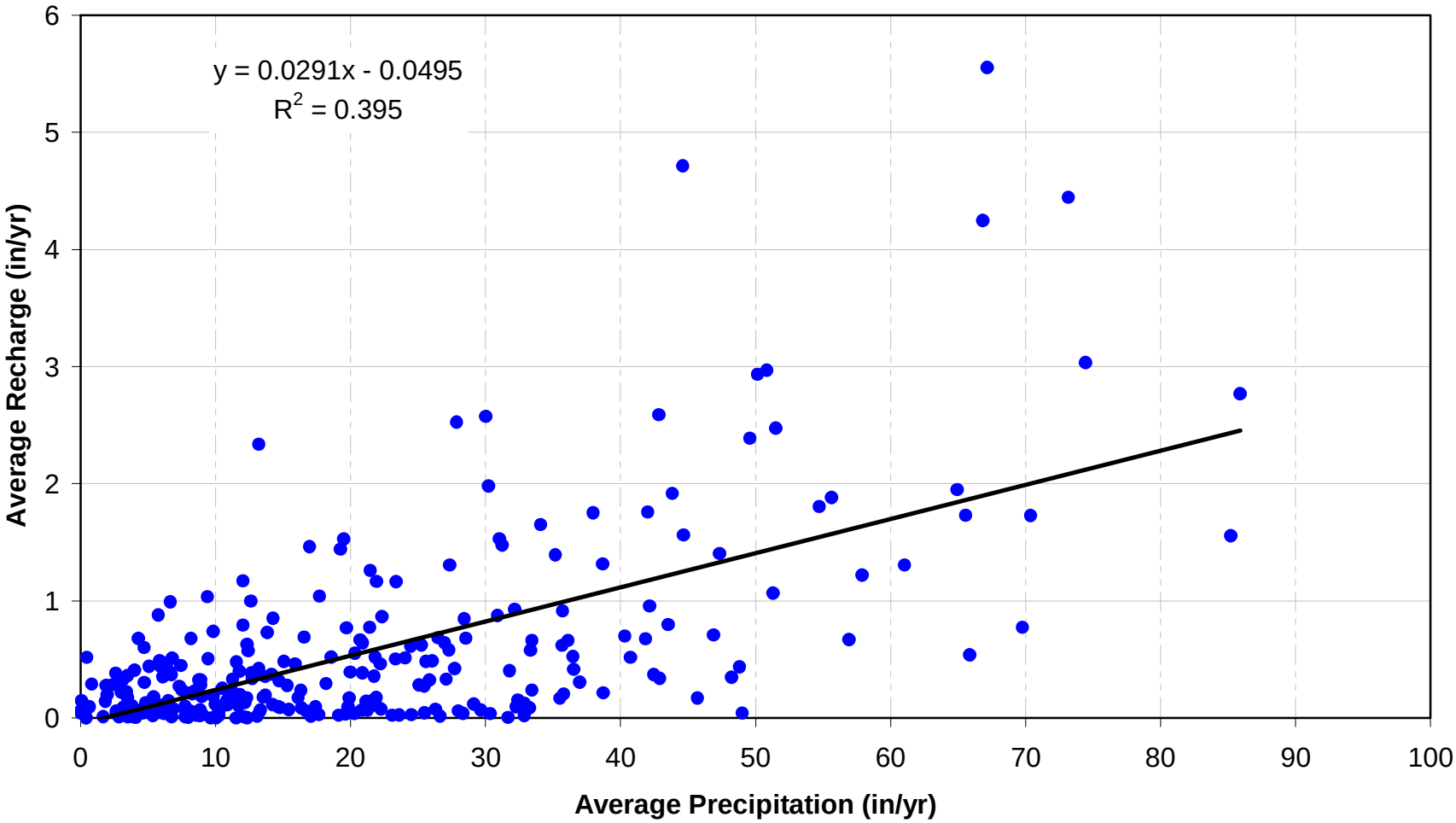

Figure 10.1.8 Calibrated average monthly recharge versus average monthly precipitation from 1975 through 1999.

10.2 Predictive Simulation Results

Water-level elevations and water-level drawdowns from the predictive simulation results are presented in this section. Specifically, this section discusses (1) the differences in water-level elevations between the five simulations that end in the DOR and terminate in 2010, 2020, 2030, 2040, and 2050 and the water-level elevations at the end of the transient simulations (December 31, 1999), and (2) the difference in results between the simulation that terminates in 2050 and has average conditions throughout and the simulation that terminates in 2050 and ends with the DOR. Note that the water-level elevations at the end of the transient simulation (December 31, 1999) are referred to as the 2000 water-level elevations in the subsequent discussion. All negative water-level differences indicate that the predictive simulation yields a lower water level than is predicted for 2000 and all positive water-level differences indicate that the predictive simulation yields a higher water level than is predicted for 2000.

The simulated water-level elevations in layer 1 at 2000 and 2010 are shown in Figure 10.2.1a and the difference in water levels between these two time periods is shown in Figure 10.2.1b. In general, water-level changes in the Seymour range between 20 and -10 feet. Over most of the aquifer, water levels decline by about 5 feet. The largest decrease in water levels (about 30 feet) is observed in Briscoe County where pumping increased from 2 AFY in the 1990s to over 4,000 AFY during the predictive time period (see Section 4.7). The largest increases in water levels are observed in northeastern Childress County and central Wilbarger County. The increase in Childress County is due to a 97 percent decrease in pumping in that county.

Figures 10.2.2a and 10.2.2b show the simulated 2000 and 2020 water-level elevations in layer 1 and the difference in water levels for these two time periods, respectively. These figures show that the declines in water levels in Briscoe County and the rises in water levels in northeastern Childress and central Wilbarger counties are larger after an additional 10 years of predictive simulation. The additional simulation time has also resulted in an increase in the size of the area of water-level rise in central Wilbarger County. With the exception of central Wilbarger County, water levels decline between zero and 20 feet in the counties with the largest pumping from the Seymour aquifer (i.e., Collingsworth, Haskell, Knox, and Wilbarger counties).

Simulated water-level elevations for 2000 and 2030 are shown in Figure 10.2.3a and the difference in water levels between these two time periods is shown in Figure 10.2.3b. Increasing the predictive simulation time to 30 years results in larger (both in size and magnitude) increases in water levels in central Wilbarger and Hardeman counties and northeastern Childress County. The difference plot shows little change in the magnitude and size of the water-level decrease in Briscoe County between the 2020-2000 difference (Figure 10.2.2b) and the 2030-2000 difference (Figure 10.2.3b). The change in water levels in pod 7 in Haskell and Knox counties is between –10 and +10 feet.

Figures 10.2.4a and 10.2.4b show the simulated 2000 and 2040 water-level elevations in layer 1 and the difference in water levels for these two time periods, respectively. All areas that show an increase in water levels for the 10-, 20-, and 30-year predictions show a larger increase in both magnitude and size for this 40-year prediction. A 10- to 20-foot decline is observed in several small areas in pods 1, 9, 10, and 11. A smaller water-level decline is observed for this simulation versus the previously discussed predictive simulations in Briscoe County due to a decrease in pumping in this county beginning in 2030.

The simulated water-level elevations for 2000 and 2050 are shown in Figure 10.2.5a. The difference in water levels for these two time periods is shown in Figure 10.2.5b. In general, the locations showing a decrease in water level of between 10 and 20 feet have become increasingly larger in pods 1, 9, 10, and 11 compared to the results of the previously discussed predictive simulations. The areas in Figure 10.2.5b showing an increase in water level are larger in both size and magnitude than for the previously discussed predictive results. In pod 7, changes in water levels since 2000 range, in general, between –10 and +10 feet. The only exceptions are a small portion of the pod in Baylor County that shows a water-level increase of between 10 and 20 feet and a small region of the pod in northeastern Knox County that shows a water-level decrease of 20 to 30 feet.

In summary, the size and magnitude of the areas showing a rise in water levels since 2000 increases as the length of the predictive simulation increases. This is most pronounced in central Wilbarger and Hardeman counties. The only location showing a decrease in water level of greater than 20 feet is in Briscoe County. This decrease is due to a substantial increase in pumpage between the historical period and the predictive period. The size of the areas of water-level decline in Collingsworth, Kent, Stonewall, and Fisher counties slightly increases as the

length of the predictive simulation increases. In pod 7, the most heavily pumped portion of the Seymour aquifer, the predictive simulations show water-level changes ranging, in general, from a 10-foot decline to a 5-foot rise.

Predictive simulations to 2050 were conducted and compared assuming two conditions. First, that average conditions are present in the aquifer over the entire time period and, second, that DOR conditions are present at the end of the simulation (i.e., during the final 76 months of the simulation). The water-level elevations at the end of these two simulations are shown in Figure 10.2.6a and the difference in water levels at the end of these two simulations is shown in Figure 10.2.6b. A negative difference indicates that the water levels for the simulation with the DOR are less than those for the simulation with average conditions throughout. In the areas of the Seymour aquifer that are most heavily pumped (i.e., pods 1, 4, and 7), the difference plot shows water levels about 4 feet lower for the simulation ending with the DOR than for the simulation with average conditions. The only exceptions to this are two small areas in pod 7 that show a difference of up to 6 feet. Differences of up to 4 feet are also seen in pod 3 and very small portions of pods 2 and 6. For pods 5, 8, 9, 10, 11, 12, 13, 14, and 15, differences in water levels for the two simulations are on the order of 1 to 2 feet. One aspect of these simulations that is misleading is that model-simulated pumping does not increase during the DOR when drier conditions may be expected to lead to greater pumping, specifically for irrigation purposes. In the simulated scenarios, the DOR only impacts climate data and subsequently, recharge. Therefore, the full effect of a DOR is likely underpredicted.

Selected hydrographs of simulated and measured water-level elevations in target wells within the Seymour aquifer for the transient calibration period and the subsequent 50-year predictive period ending in the DOR are shown in Figures 10.2.7 through 10.2.9. Predictive water levels generally either rise or decline between 2000 and November 2043 (when the DOR begins), dictated primarily by differences between predictive pumping and the historical pumping during the calibration and verification periods. The DOR, which is apparent in the decline in water levels during the final 76 months of simulation, results in relatively small water-level changes compared to those during the approximately 44 years of prediction under average recharge conditions. This implies that, water availability will be dictated more by the amount of pumping leading up to the drought than by the drought itself (under the assumed non-changing pumping conditions during the drought).

Figures 10.2.10 and 10.2.11 show the simulated 2000 and 2050 water-level elevations in layer 2 and the difference in water levels for these two time periods, respectively. Changes in water levels between the two periods range from a decline of 50 to 100 feet to a rise of 50 to 100 feet. Pumping is implemented only in the Blaine portion of layer 2 and, therefore, the largest changes are as expected in the Blaine. The changes in the Blaine aquifer are the result of differences in pumping magnitude and distribution. Changes in other areas of layer 2 range from a decline of 20 to 50 feet to a rise of 10 to 20 feet.

The water-level elevations in layer 2 for the two simulations ending in 2050, one with average conditions and the other with DOR conditions, are shown in Figure 10.2.12. The difference in water levels between these two simulations is shown in Figure 10.2.13. The most noticeable feature of this figure is that the largest differences (generally decreases in water level) occur beneath the Seymour aquifer. This is due in part to the fact that the majority of the recharge and pumping in the model occur in the Seymour aquifer. Furthermore, the confined storage in the portions of the Permian overlain by the Seymour is significantly lower than the unconfined storage in the outcrop. Therefore, even relatively small decreases in the discharge from the Seymour during the DOR will result in relatively large decreases in the Permian heads. The maximum difference, a 4- to 6-foot decline, is seen in the central portion of pod 7. Away from the Seymour aquifer, the differences in water-level elevations in layer 2 between the two simulations range from -1 to +1 feet, with the majority of the differences being between -1 and 0 feet.

Selected hydrographs of simulated and measured water-level elevations in target wells within the Blaine aquifer for the transient calibration period and the subsequent 50-year predictive period ending in the DOR are shown in Figure 10.2.14. Water levels are generally predicted to rise during this period primarily due to a decrease in predictive pumping rates from the Blaine compared to those in the calibration and verification periods. Lower recharge rates during the DOR are not as apparent in the Blaine hydrographs as they are in the Seymour hydrographs. This is because of the smaller rates of recharge in the Blaine compared to those of the Seymour.

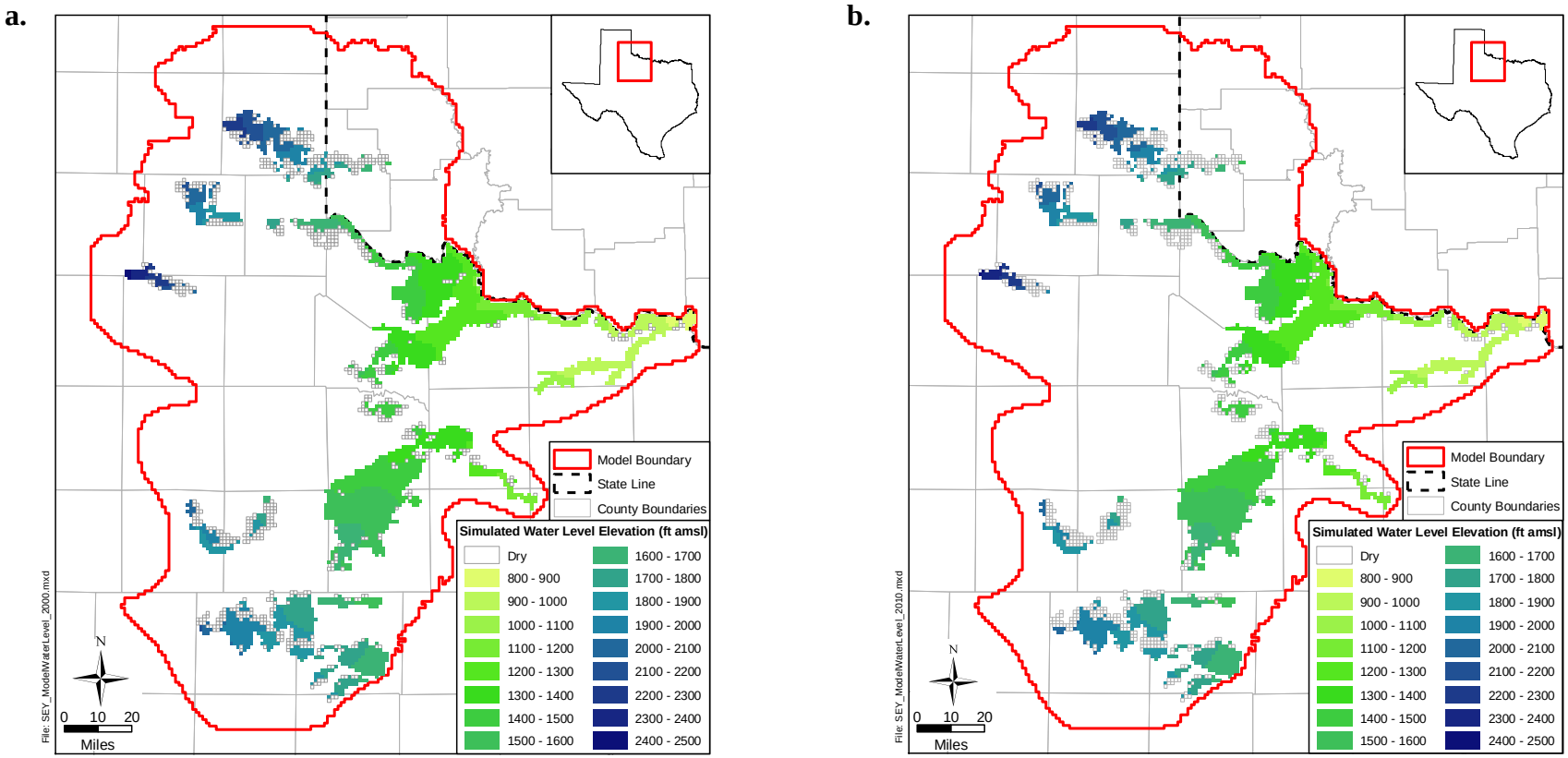

Figure 10.2.1a Simulated (a) 2000 and (b) 2010 water-level elevations for layer 1.

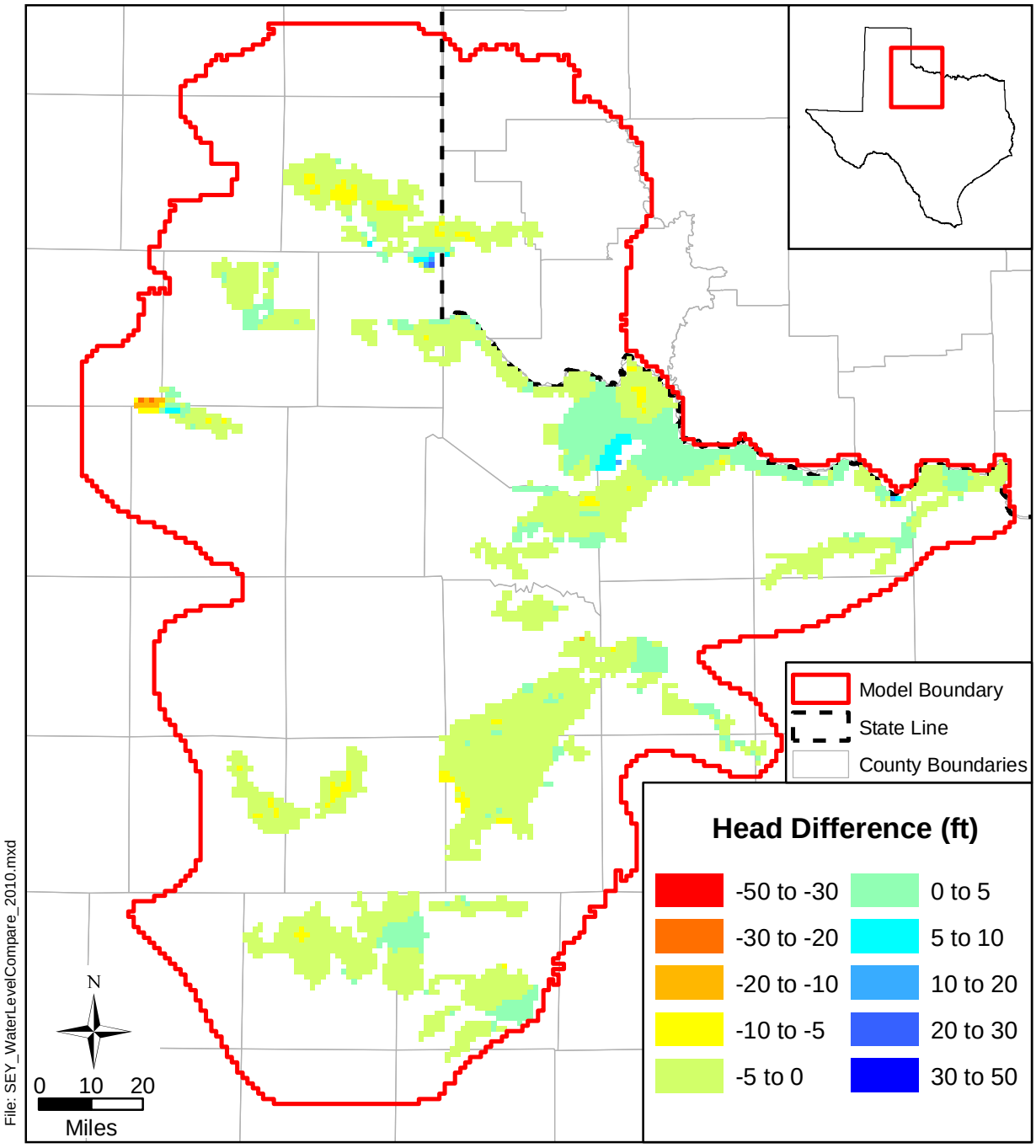

Figure 10.2.1b Difference between 2000 and 2010 simulated water-level elevations for layer 1.

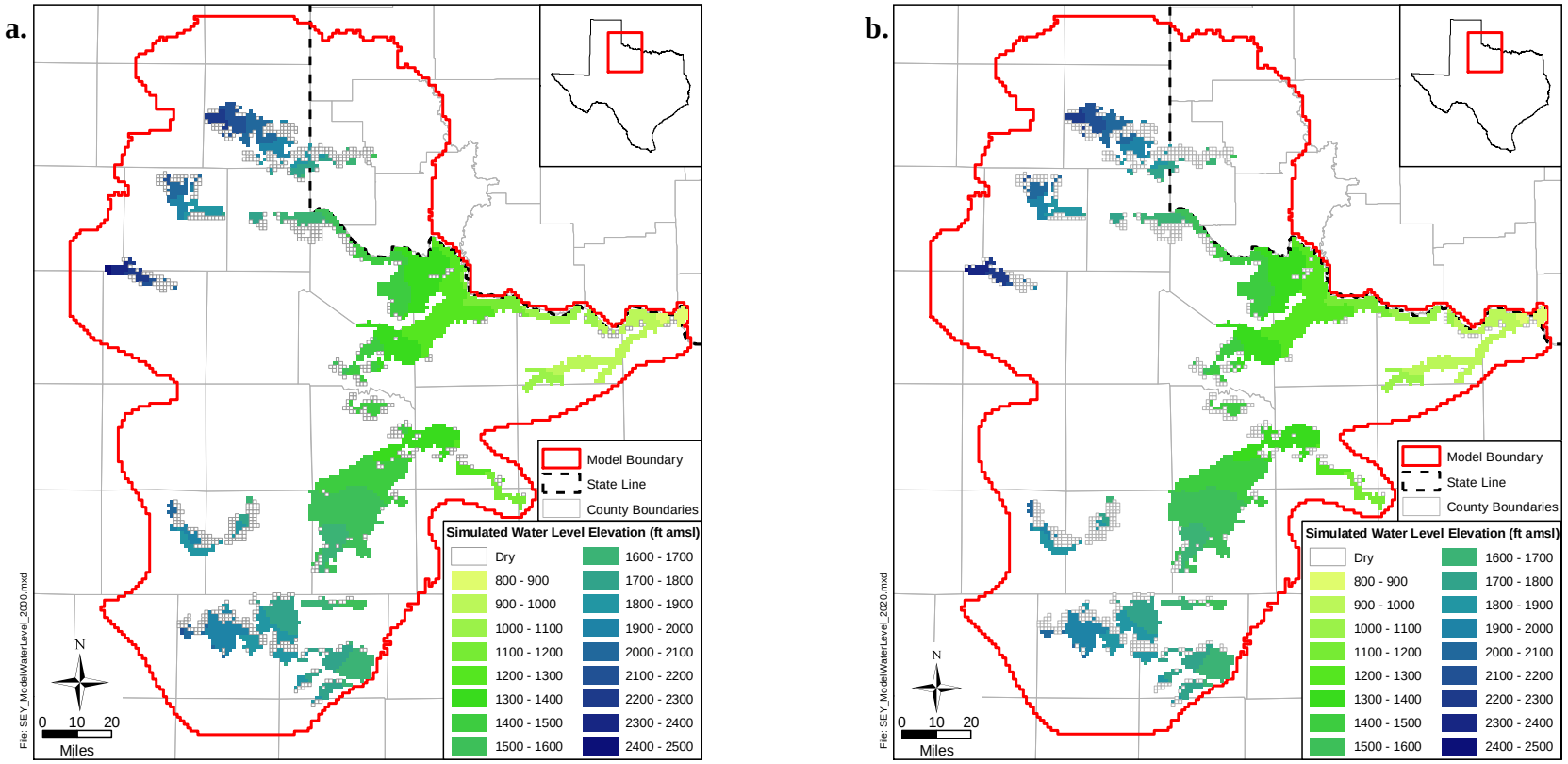

Figure 10.2.2a Simulated (a) 2000 and (b) 2020 water-level elevations for layer 1.

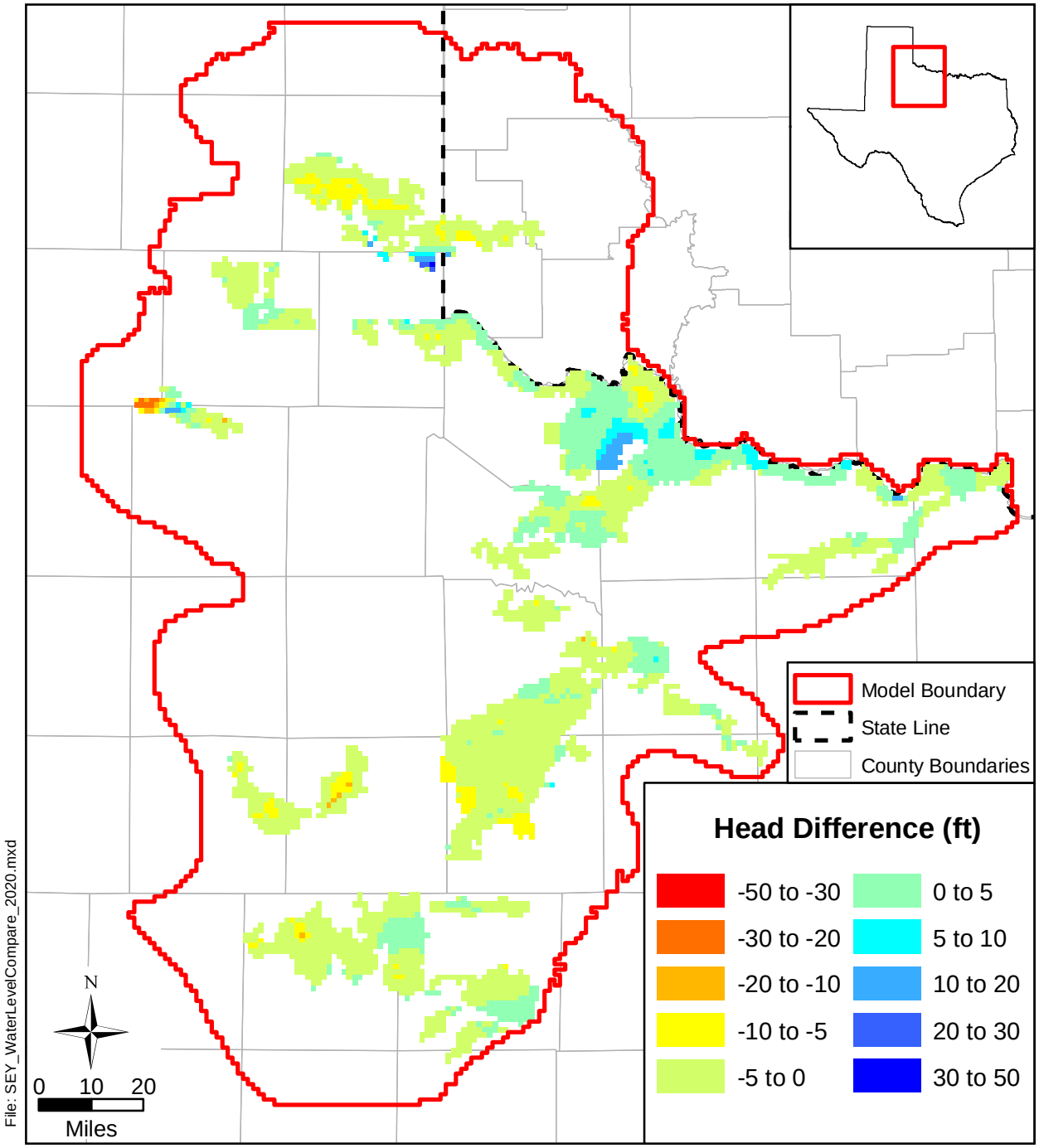

Figure 10.2.2b Difference between 2000 and 2020 simulated water-level elevations for layer 1.

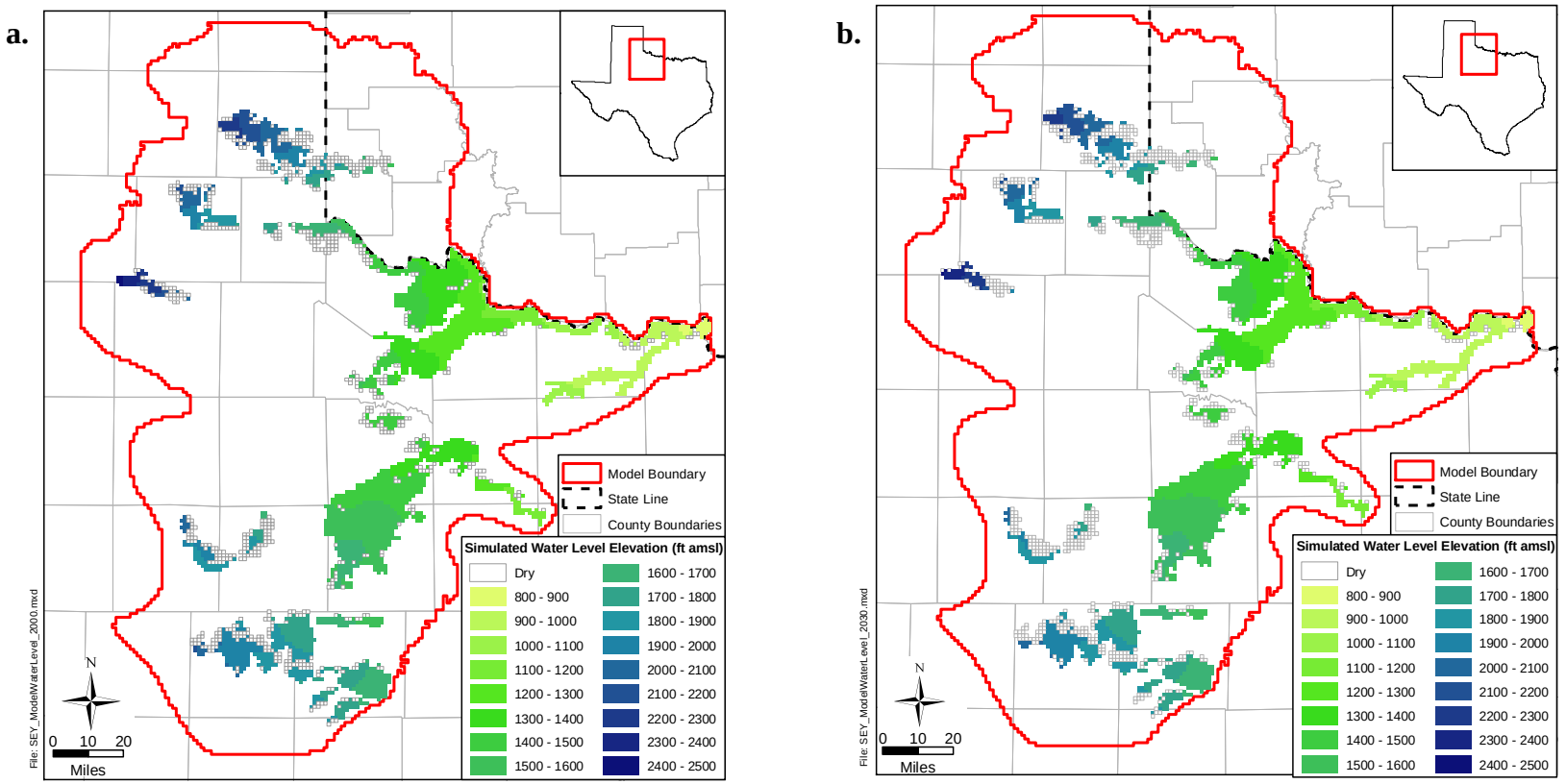

Figure 10.2.3a Simulated (a) 2000 and (b) 2030 water-level elevations for layer 1.

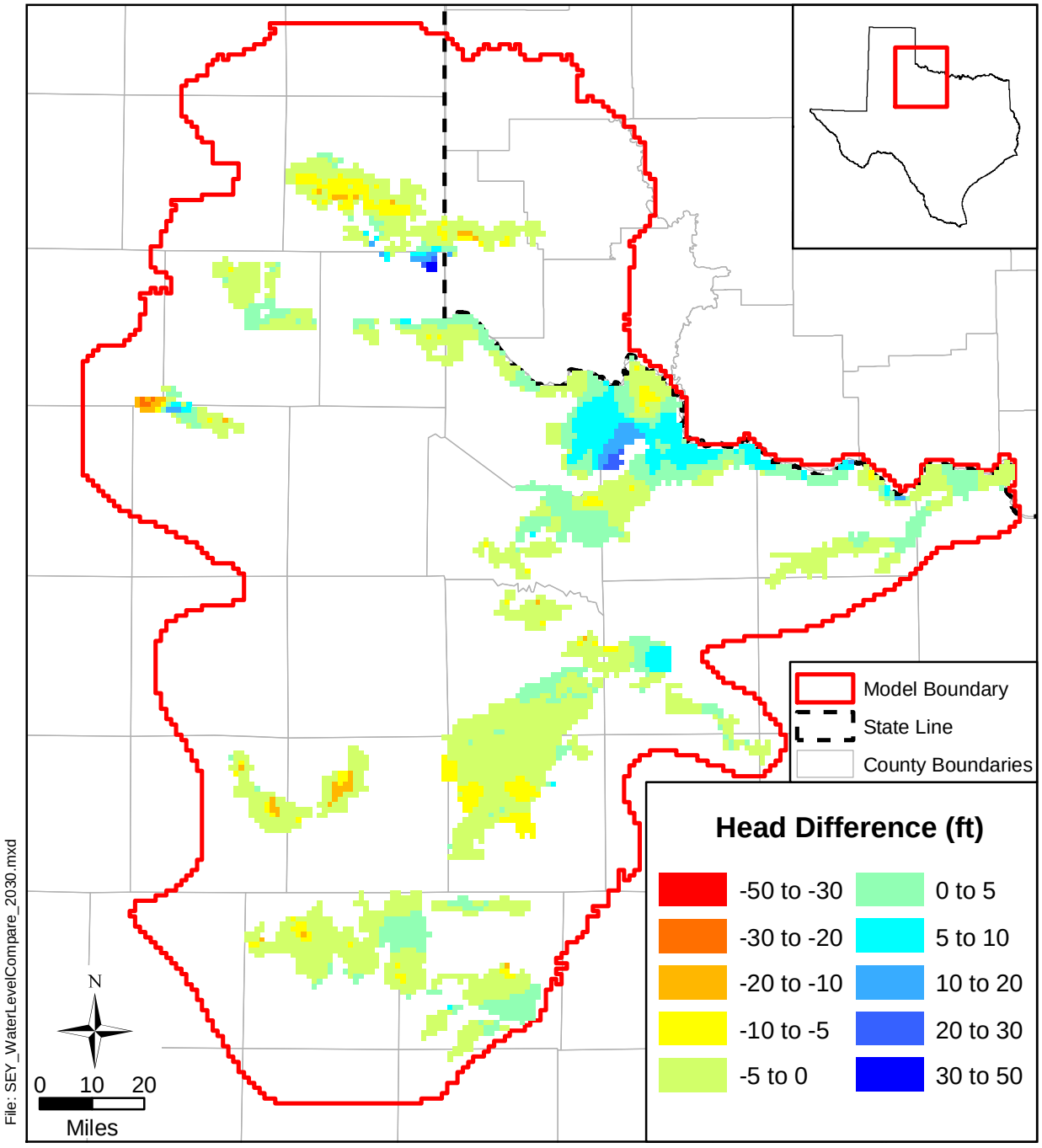

Figure 10.2.3b Difference between 2000 and 2030 simulated water-level elevations for layer 1.

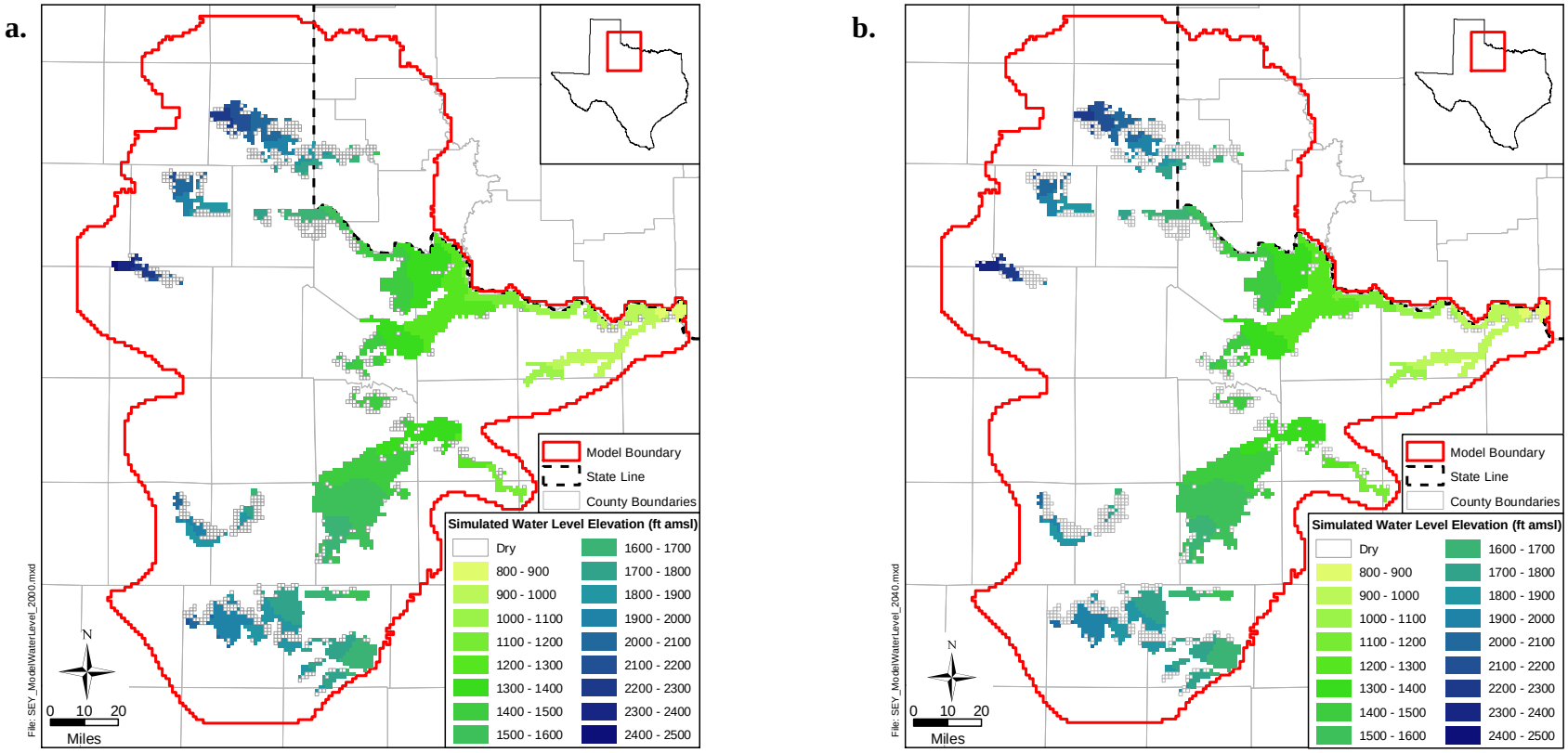

Figure 10.2.4a Simulated (a) 2000 and (b) 2040 water-level elevations for layer 1.

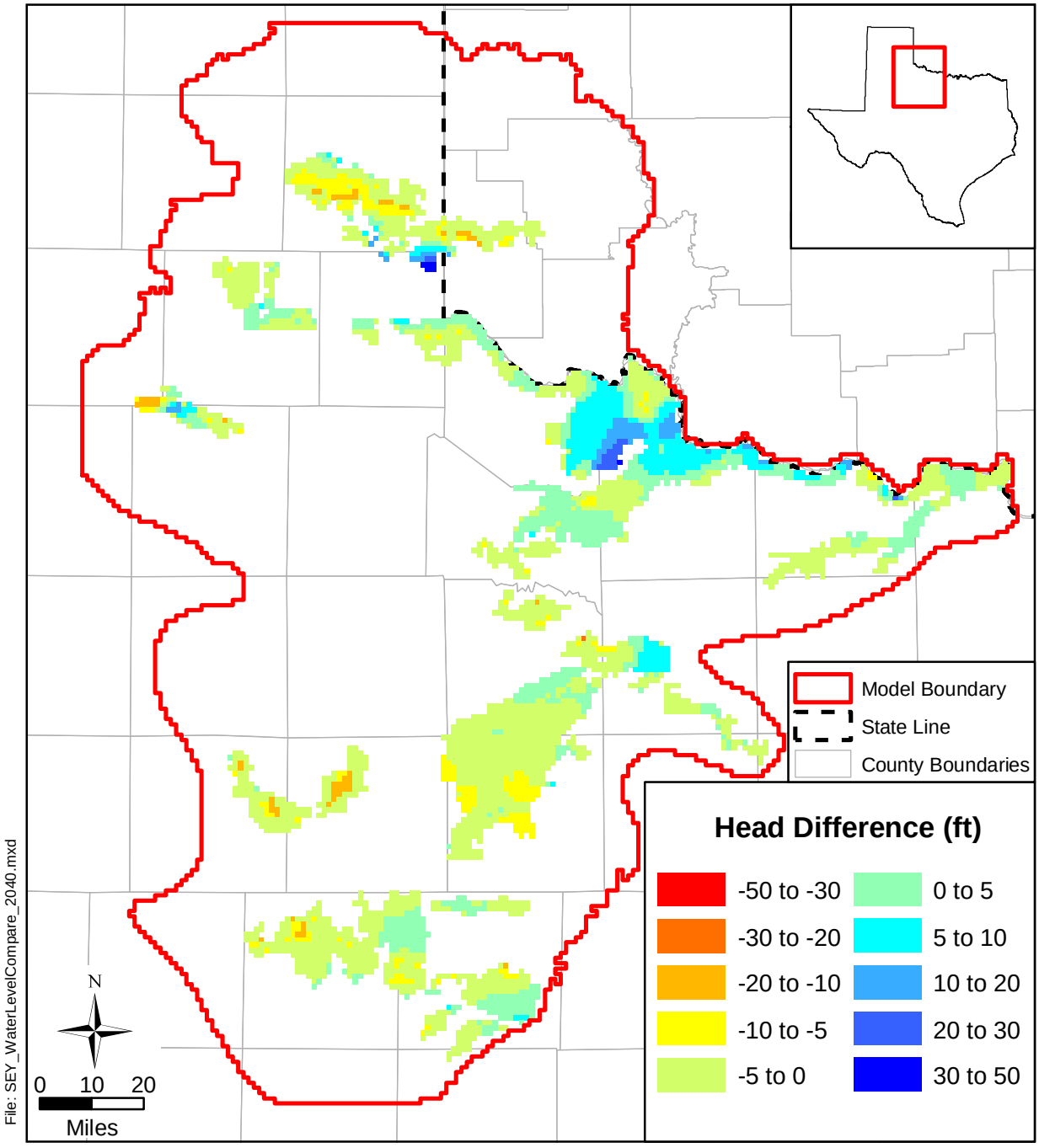

Figure 10.2.4b Difference between 2000 and 2040 simulated water-level elevations for layer 1.

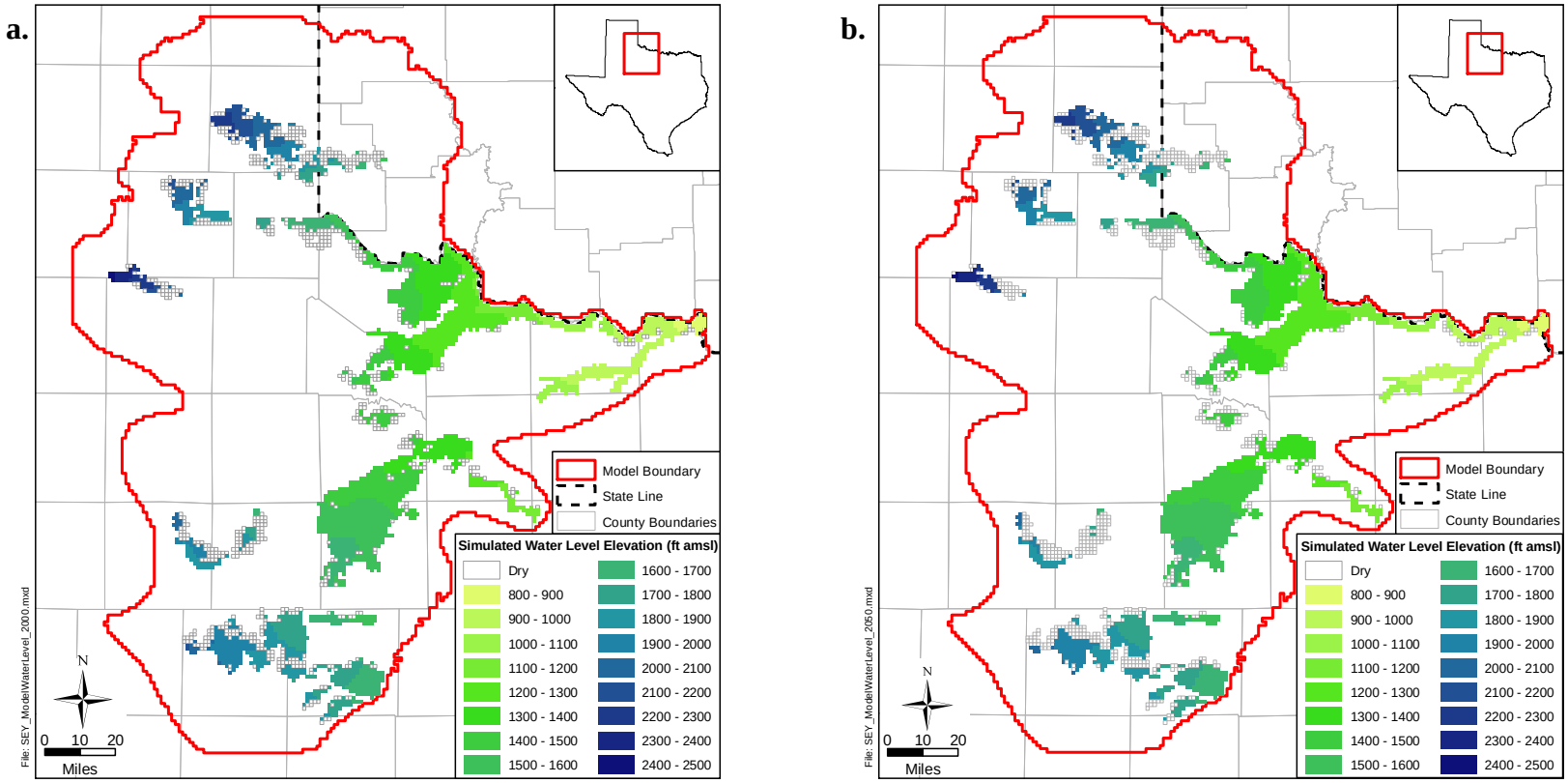

Figure 10.2.5a Simulated (a) 2000 and (b) 2050 water-level elevations for layer 1.

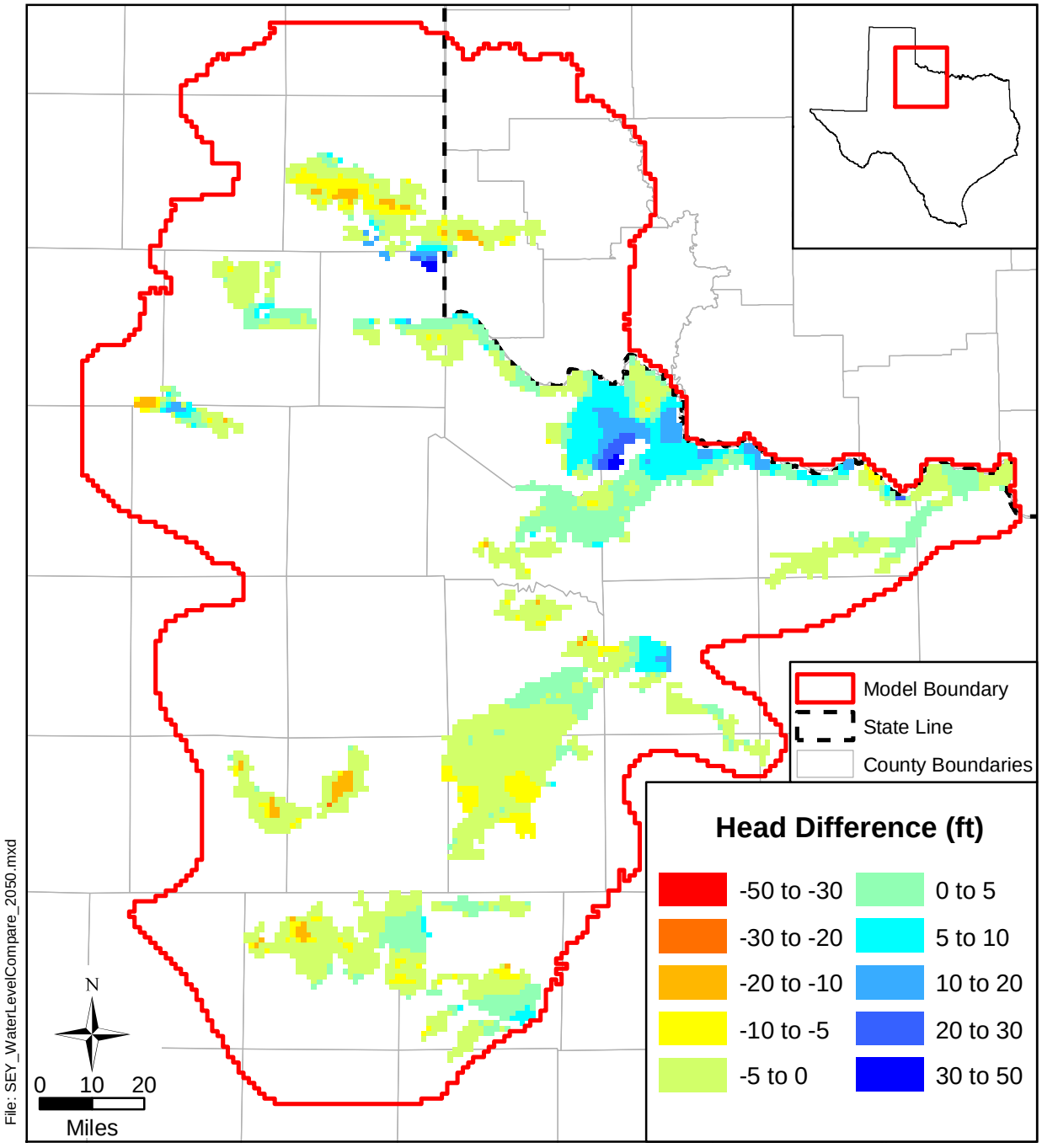

Figure 10.2.5b Difference between 2000 and 2050 simulated water-level elevations for layer 1.

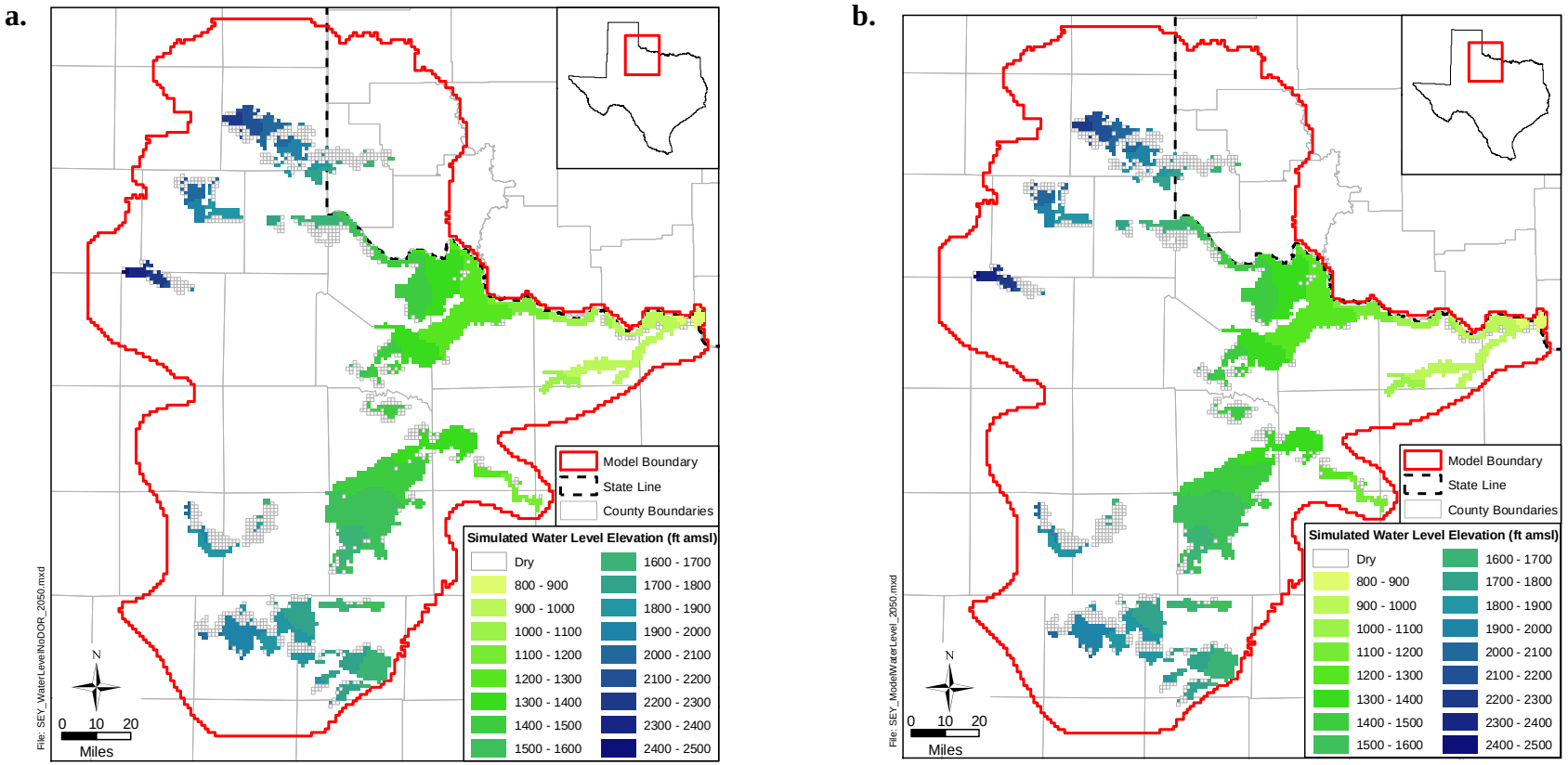

Figure 10.2.6a Simulated 2050 water-level elevations for layer 1 for (a) average conditions and (b) DOR conditions.

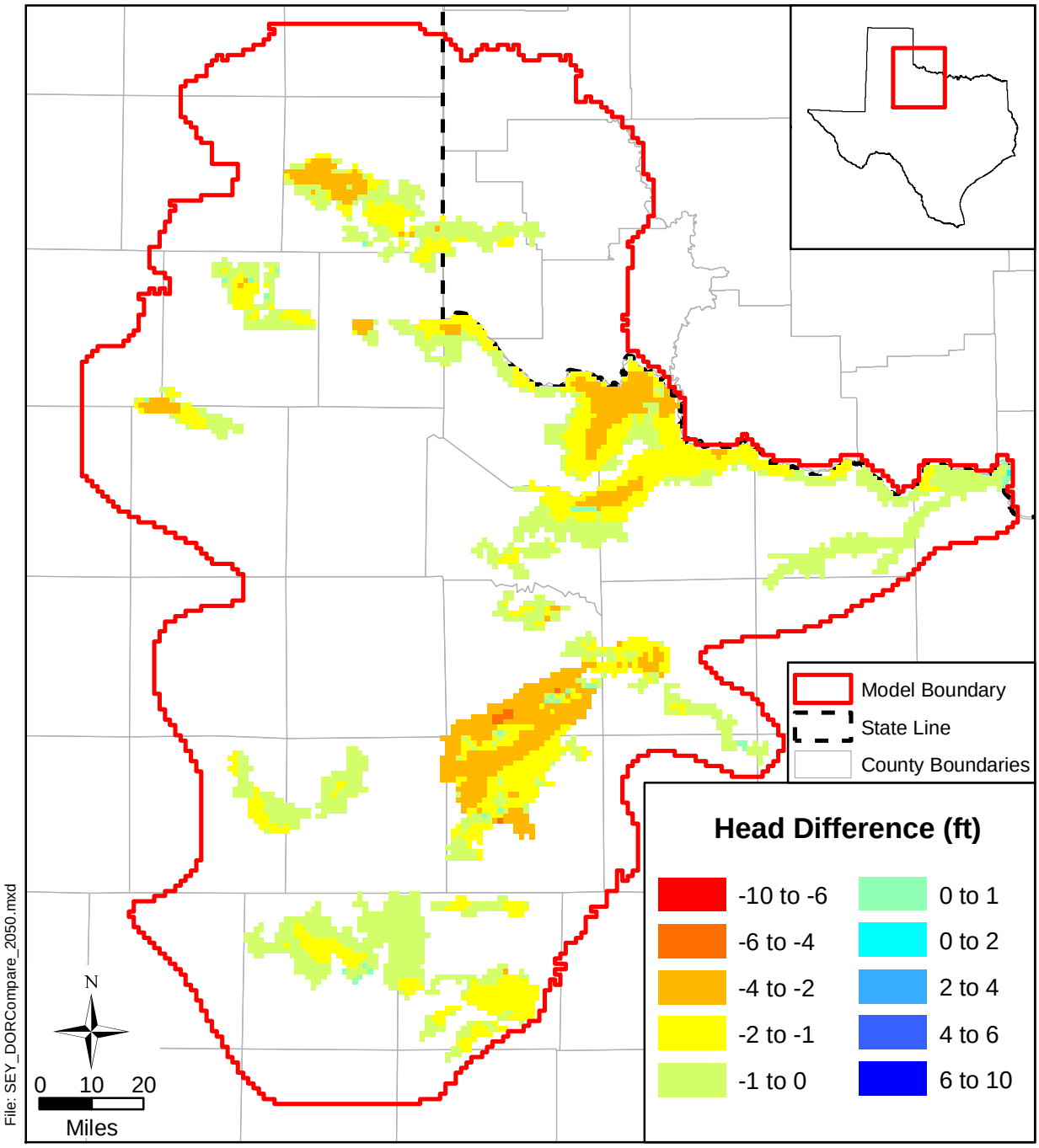

Figure 10.2.6b Difference between 2050 water-level elevations for average conditions and 2050 water-level elevations for DOR conditions for layer 1.

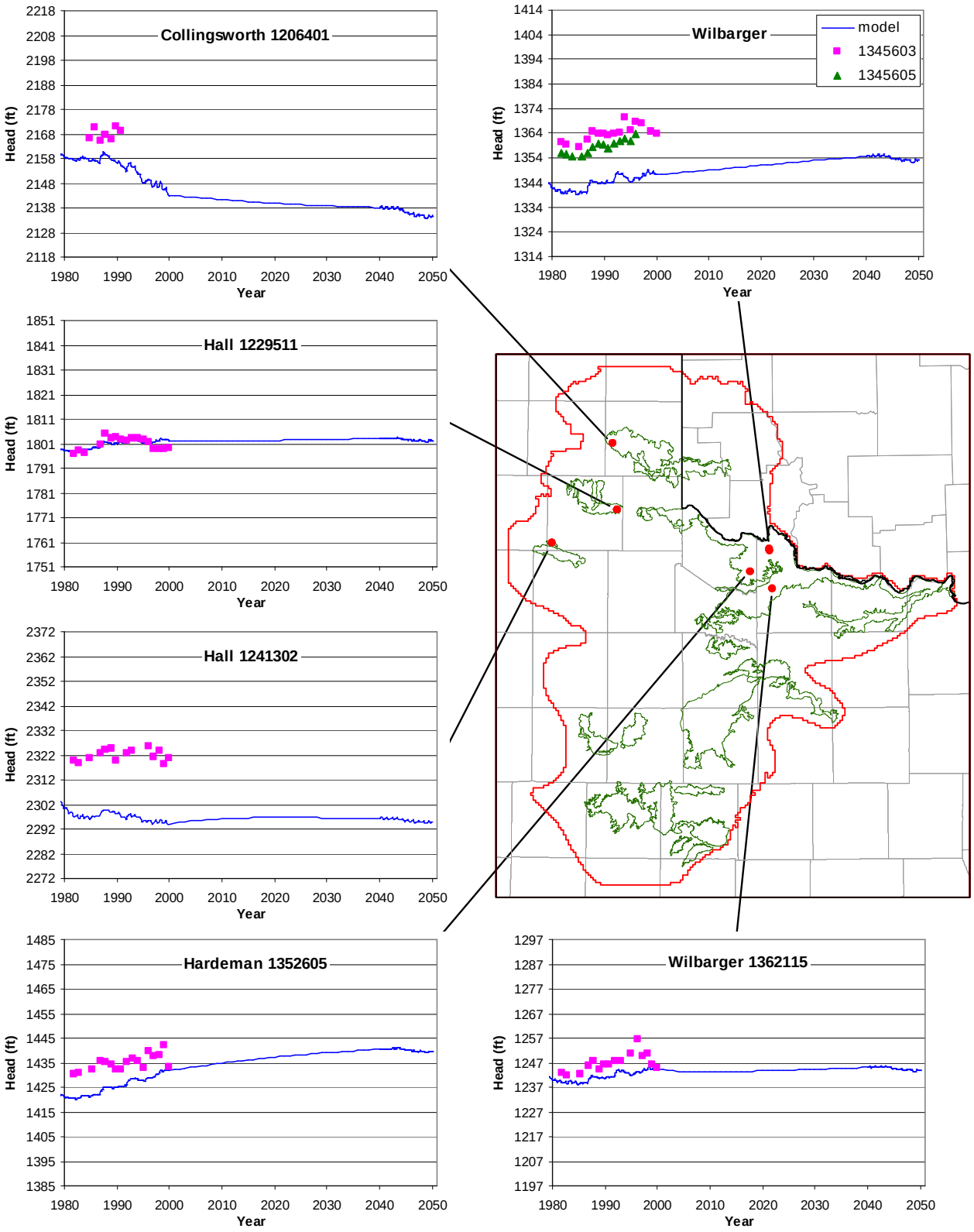

Figure 10.2.7 Selected hydrographs from predictive simulations to 2050 of simulated (lines) and measured (points) water-level elevations in Seymour pods 1, 2, 3, and 4.

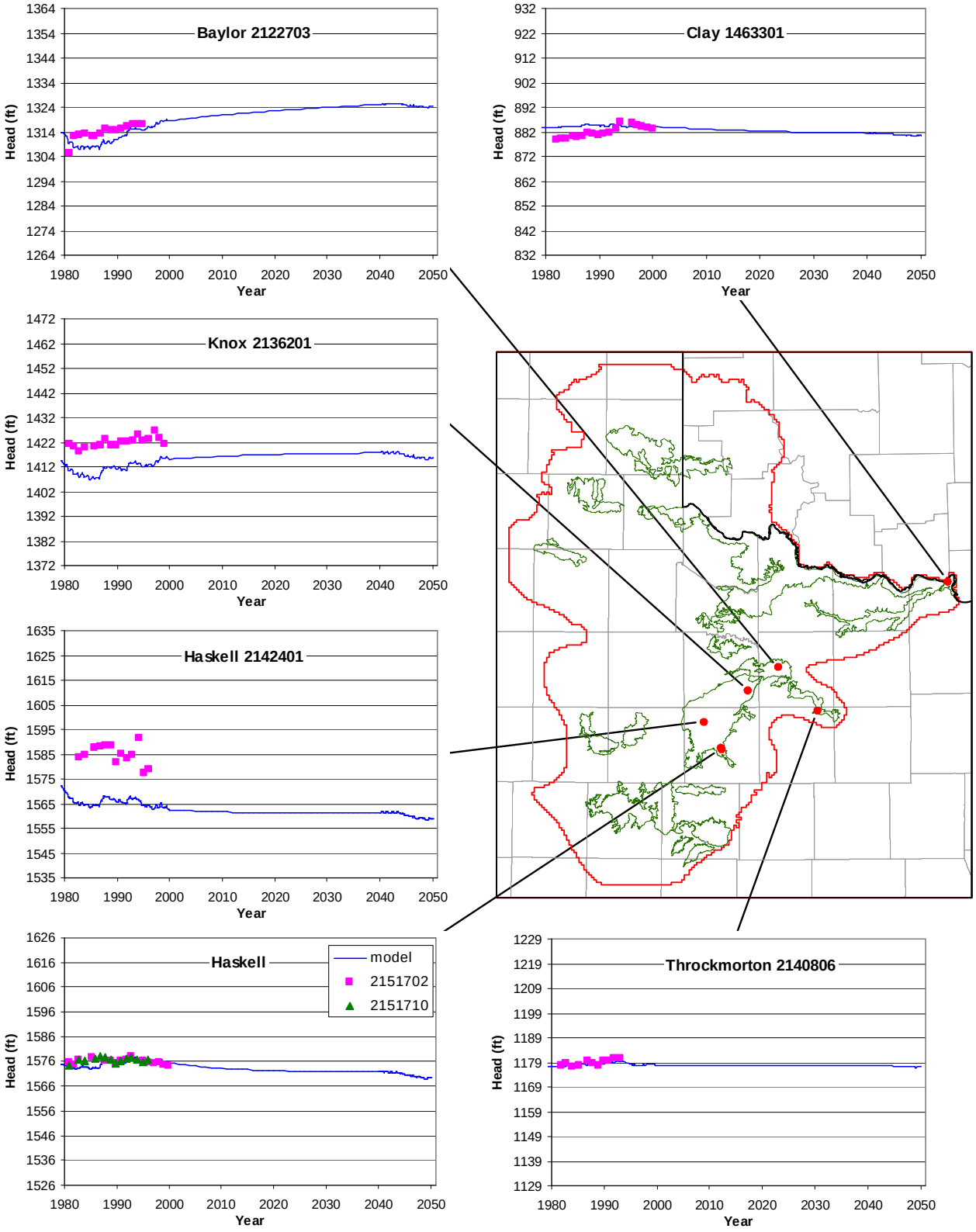

Figure 10.2.8 Selected hydrographs from predictive simulations to 2050 of simulated (lines) and measured (points) water-level elevations in Seymour pods 5, 7, and 8.

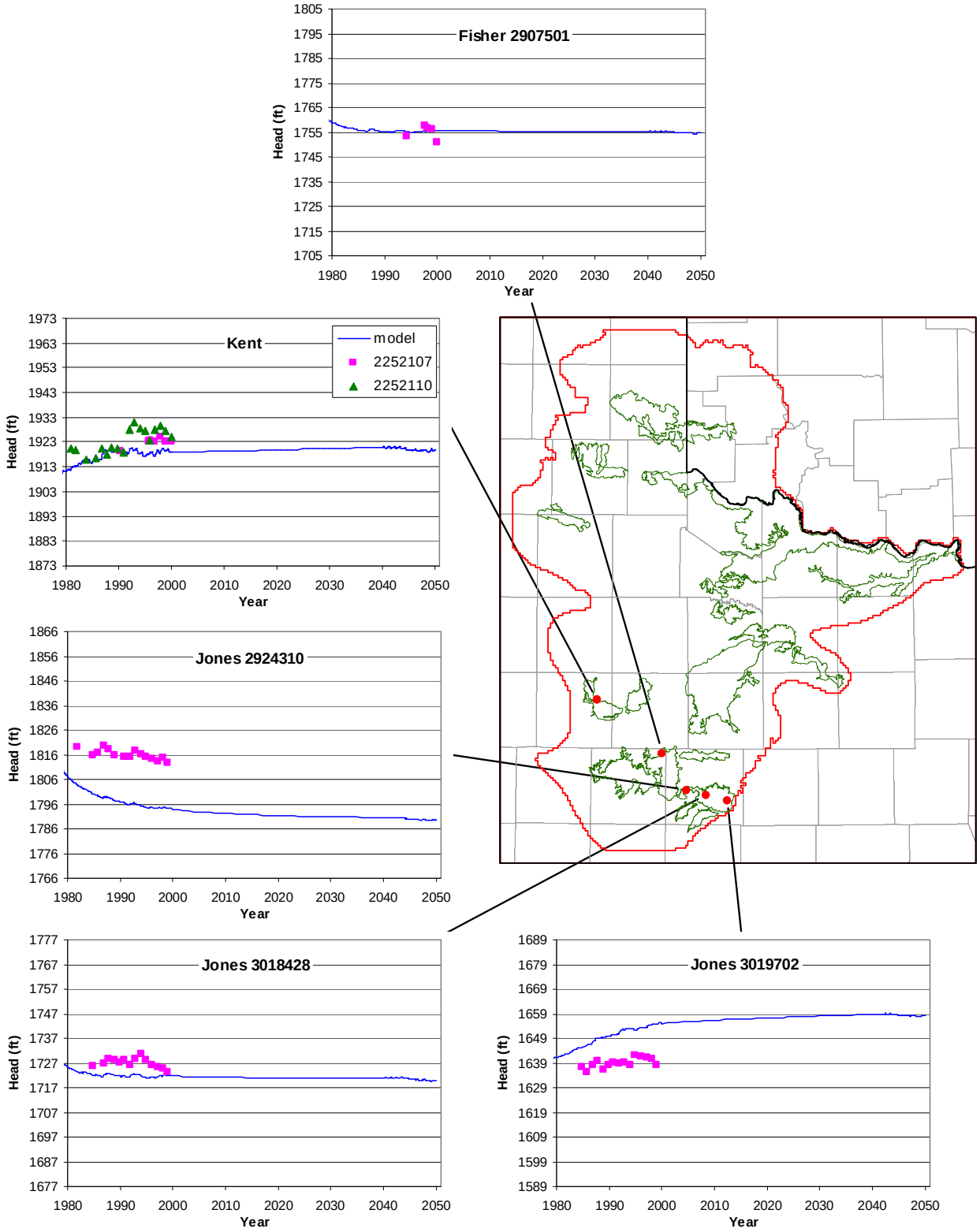

Figure 10.2.9 Selected hydrographs from predictive simulations to 2050 of simulated (lines) and measured (points) water-level elevations in Seymour pods 9, 11, and 13.

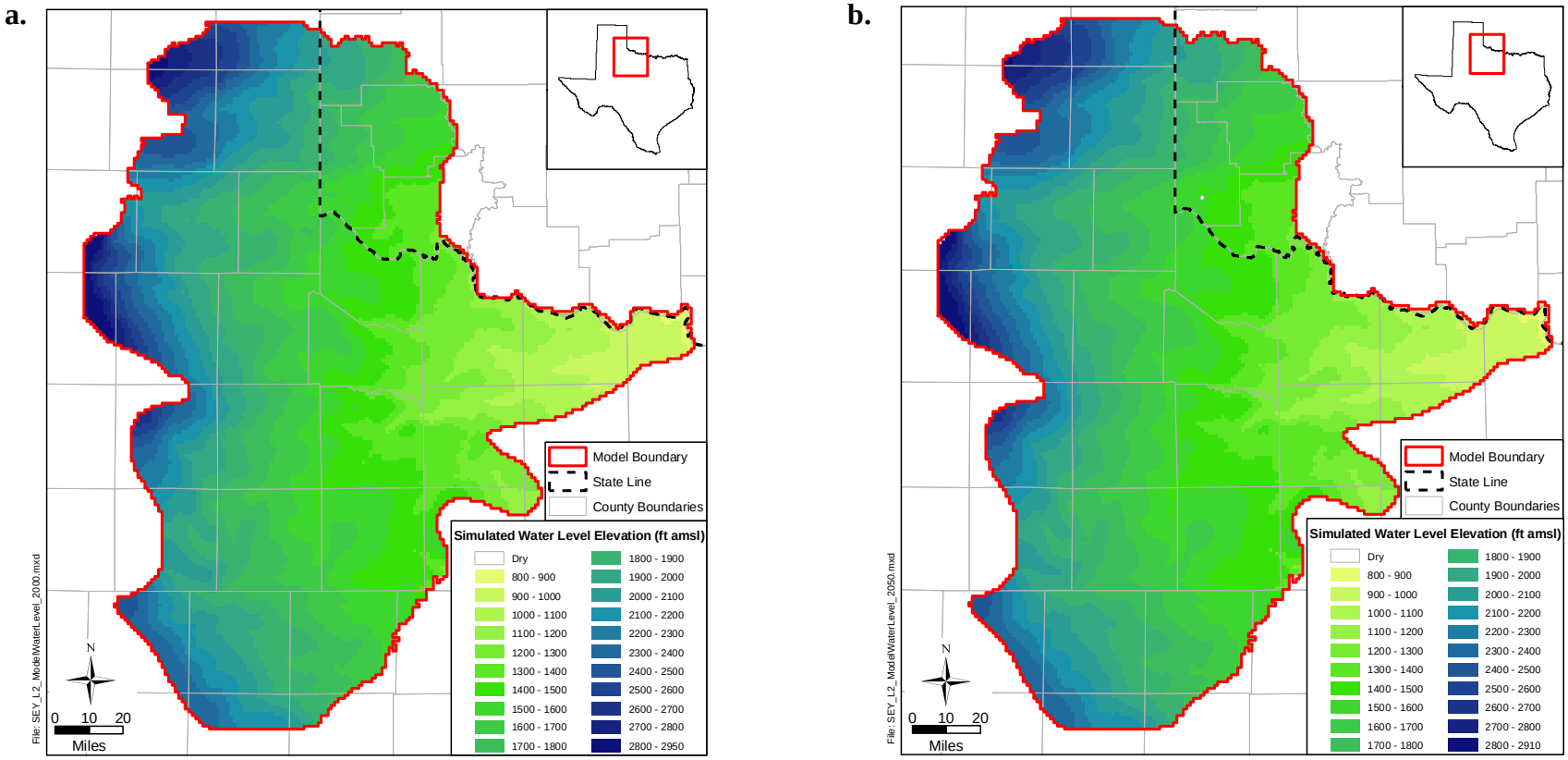

Figure 10.2.10 Simulated (a) 2000 and (b) 2050 water-level elevations for layer 2.

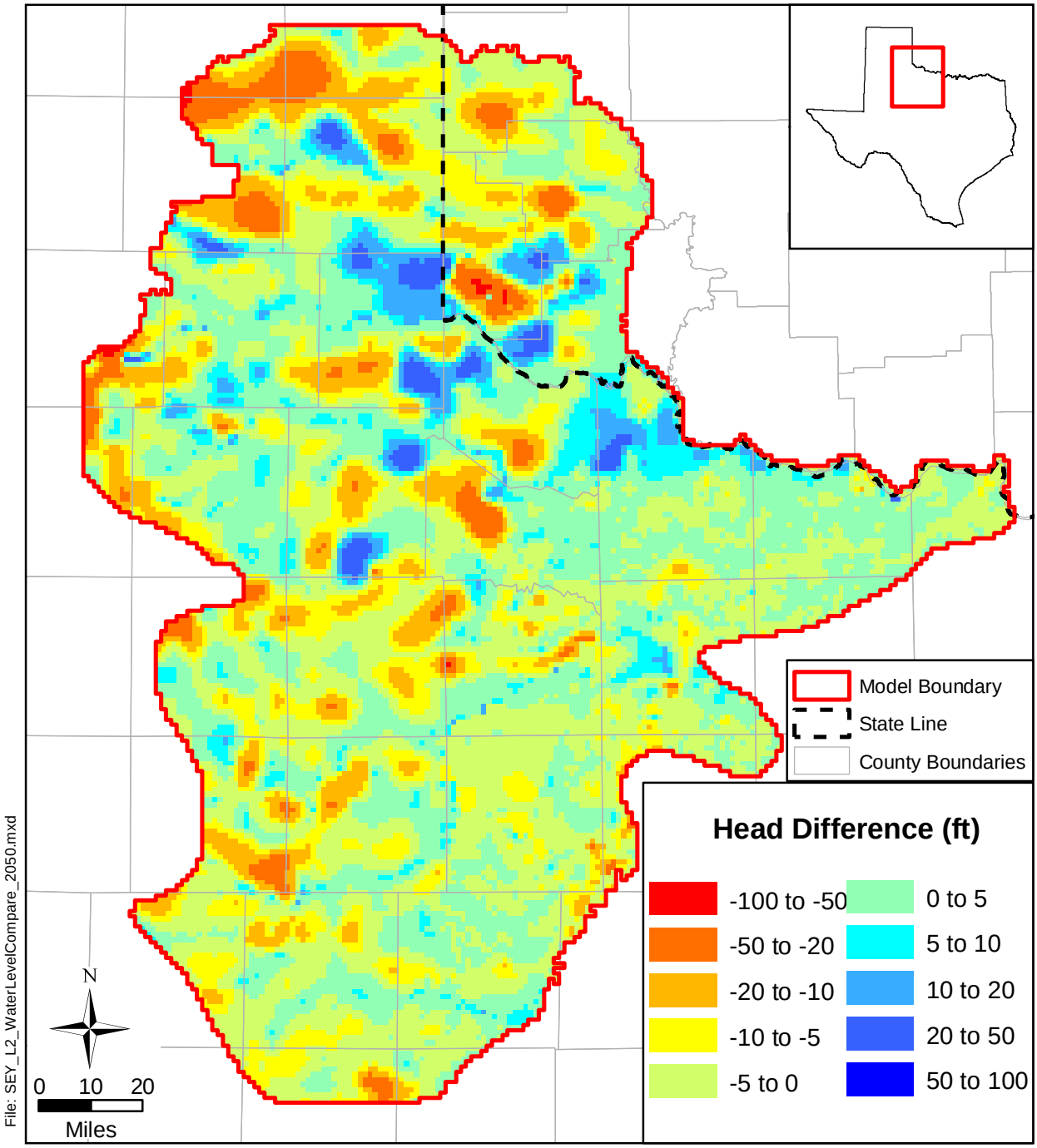

Figure 10.2.11 Difference between 2000 and 2050 water-level elevations for layer 2.

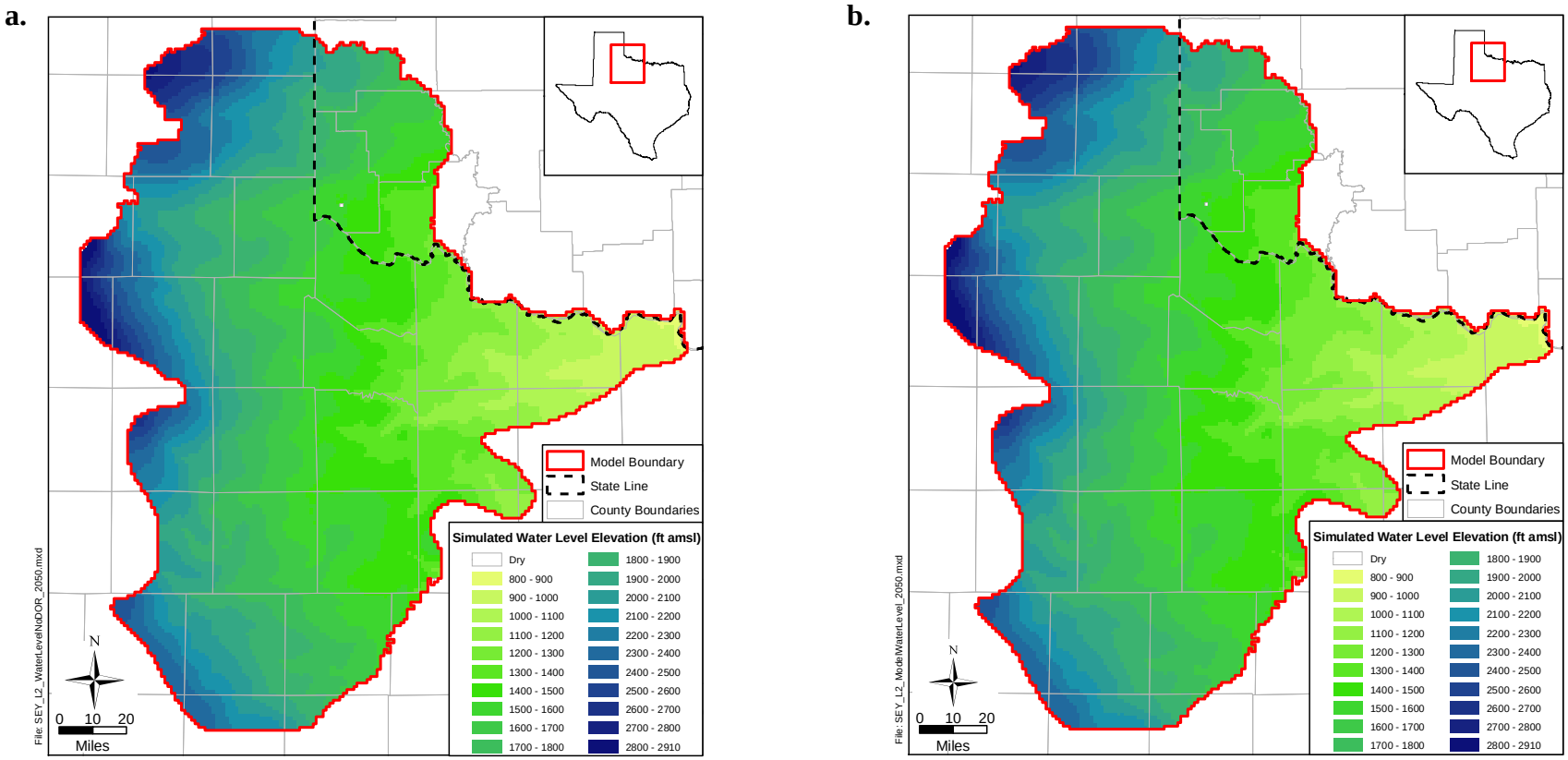

Figure 10.2.12 Simulated 2050 water-level elevations for layer 2 for (a) average conditions and (b) DOR conditions.

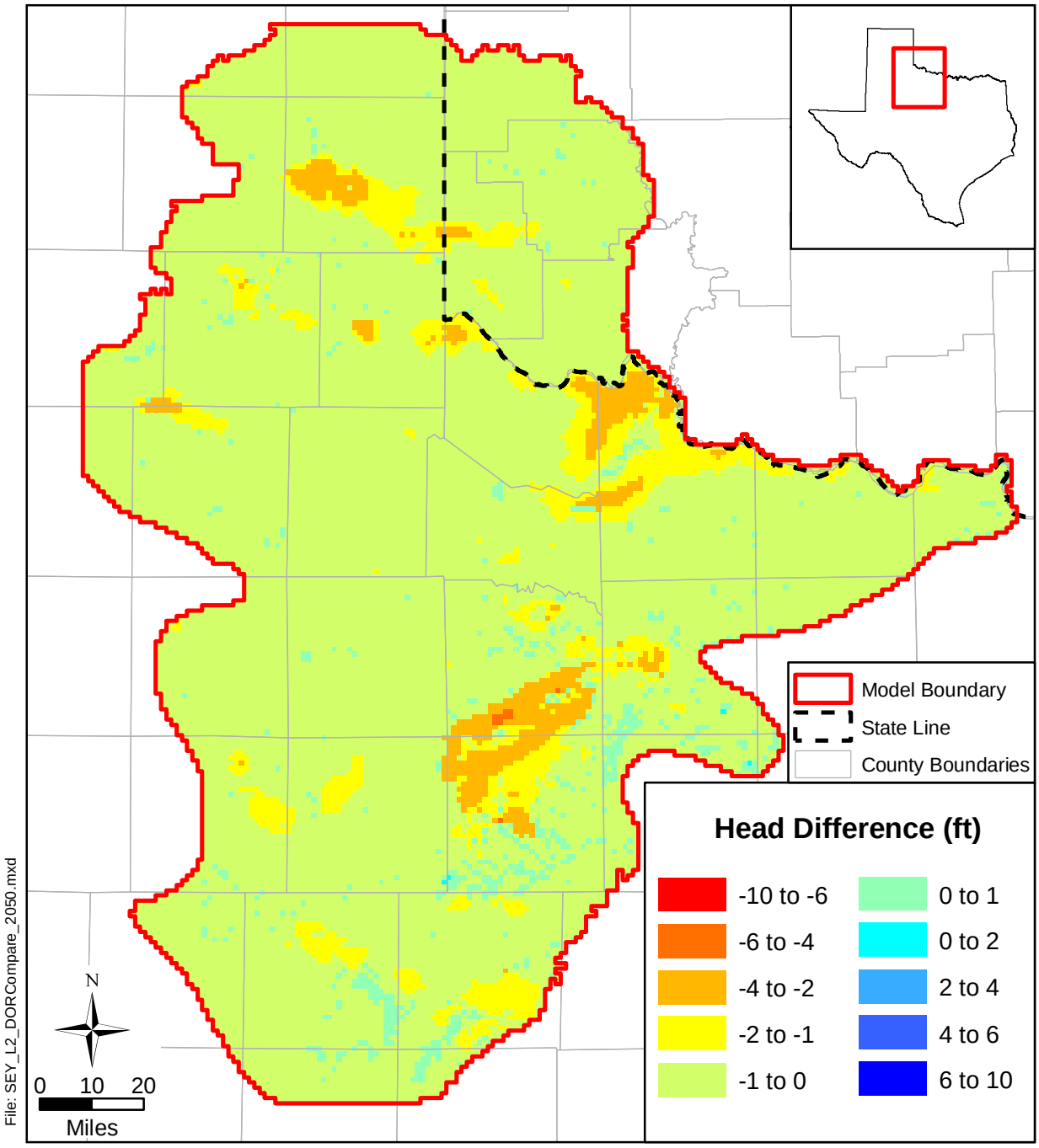

Figure 10.2.13 Difference between 2050 water-level elevations for average conditions and 2050 water-level elevations for DOR conditions for layer 2.

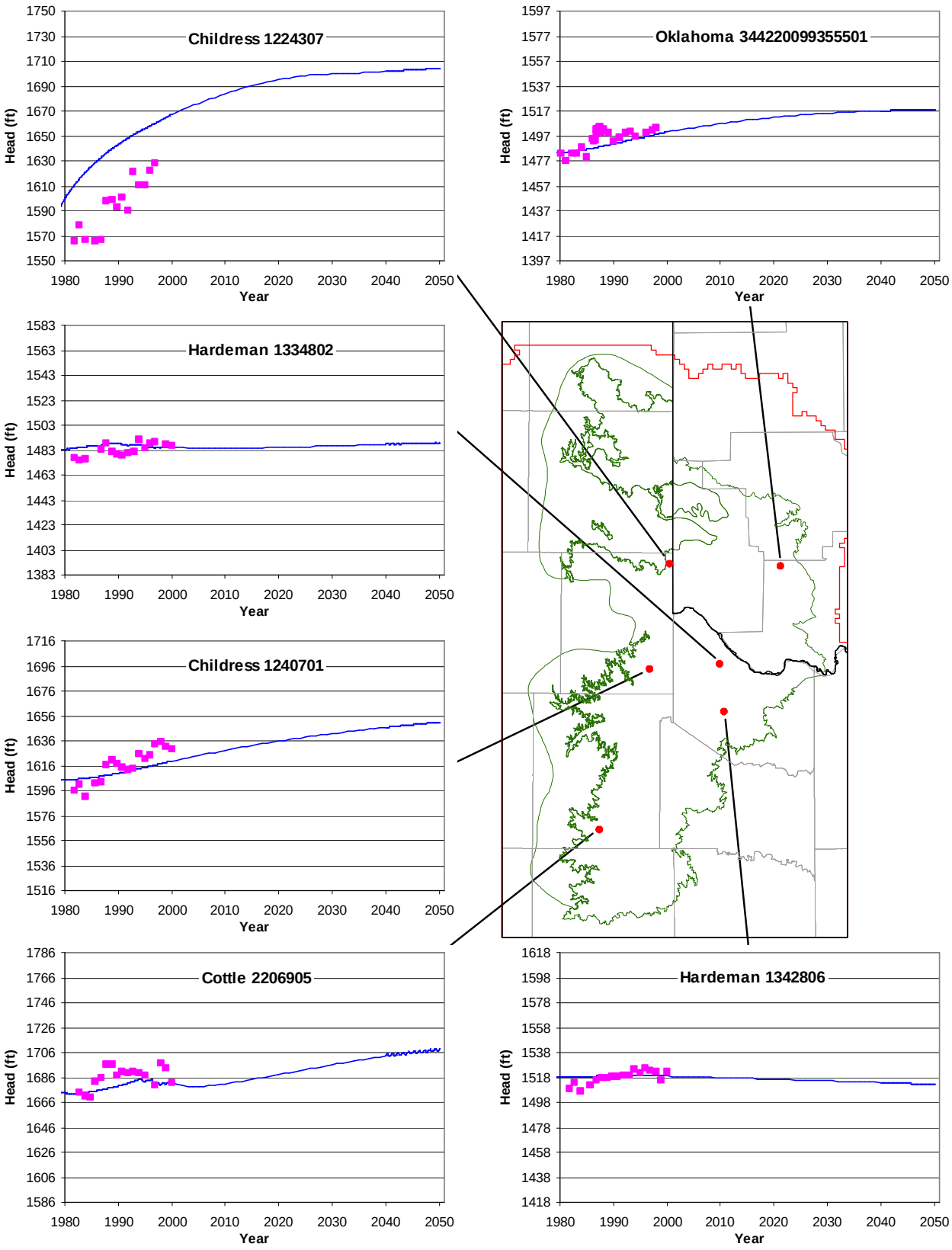

Figure 10.2.14 Selected hydrographs from predictive simulations to 2050 of simulated (lines) and measured (points) water-level elevations in the Blaine aquifer.

10.3 Predictive Simulation Water Budget

Table 10.3.1 shows the water budget for the end of transient model calibration and verification and for the final year of each of the predictive simulations. In the table, the predictive years 2010 through 2050 include the DOR except the entry labeled 2050*, which does not include the DOR. In general, the predictive simulation water budget shows similar trends and variations as those of the calibration and verification simulations. Table 10.3.1 shows an overall decrease in pumpage from 2000 to 2050 by about 15,000 AFY. This is consistent with model hydrographs which generally show an overall trend of water-level increase in the majority of the model area. In all years shown in the table, the streams are gaining more water than they are losing. Comparing the simulation to 2050 using average recharge with the simulations to 2010, 2020, 2030, 2040, and 2050 ending in the DOR shows that above average recharge occurs during the final year of the drought. While this may at first seem counterintuitive, this above average recharge is the result of the higher precipitation rates that caused the drought to end. This higher precipitation is apparent in the 1-year averaged SPI plot shown in Figure 10.1.6. The water budget over the final decade from 2040 to 2050 of the predictive runs with and without (*) the DOR is shown in Table 10.3.2. Because the DOR lasted over six years, the mass balance over the final decade better reflects the effect of the entire DOR rather than merely the final year of the DOR, when recharge increases as shown in Table 10.3.1. Table 10.3.2 shows that, overall, less recharge enters the model during DOR conditions than under average conditions. This table also shows that discharge from the model through ET decreases during the DOR. This is likely a result of lower water levels during drought conditions.

Table 10.3.1 Water budget for predictive simulations. All rates reported in AFY.

Year	Layer	Recharge	ET	Wells	Springs	Streams	Top	Bottom	Storage
1990	**1**	318,668	-14,952	-115,085	-3,605	-46,420	0	-50,385	-77,753
	2	327,394	-113,267	-32,295	-4,995	-180,682	50,385	0	-57,469
	sum	646,061	-128,218	-147,380	-8,600	-227,102	50,385	-50,385	-135,221
2000	**1**	300,690	-39,770	-110,513	-4,217	-54,171	0	-67,950	-19,925
	2	304,114	-167,882	-45,443	-5,062	-182,001	67,950	0	24,710
	sum	604,805	-207,652	-155,956	-9,279	-236,172	67,950	-67,950	4,785
2010	**1**	388,516	-37,965	-107,177	-3,923	-51,837	0	-66,261	-115,243
	2	411,571	-159,715	-43,385	-4,963	-185,788	66,261	0	-83,203
	sum	800,087	-197,681	-150,562	-8,887	-237,625	66,261	-66,261	-198,446
2020	**1**	388,744	-38,015	-105,590	-4,140	-53,367	0	-68,960	-113,502
	2	411,343	-158,750	-43,044	-5,003	-190,768	68,960	0	-79,349
	sum	800,087	-196,765	-148,634	-9,143	-244,135	68,960	-68,960	-192,851
2030	**1**	389,305	-38,151	-102,206	-4,353	-54,764	0	-72,591	-114,754
	2	410,782	-158,457	-42,725	-5,012	-194,213	72,591	0	-78,744
	sum	800,087	-196,608	-144,931	-9,365	-248,976	72,591	-72,591	-193,498
2040	**1**	388,749	-38,334	-100,189	-4,580	-56,109	0	-68,984	-112,469
	2	411,338	-158,221	-42,380	-5,006	-196,994	68,984	0	-76,888
	sum	800,087	-196,555	-142,569	-9,587	-253,103	68,984	-68,984	-189,357
2050	**1**	388,651	-38,491	-98,477	-4,805	-57,350	0	-72,808	-111,384
	2	411,436	-158,057	-42,049	-4,983	-198,959	72,808	0	-76,307
	sum	800,087	-196,548	-140,526	-9,787	-256,309	72,808	-72,808	-187,691
2050*	**1**	296,763	-40,778	-98,655	-5,350	-60,878	0	-68,704	-16,019
	2	308,022	-167,105	-42,014	-5,061	-200,850	68,704	0	30,476
	sum	604,785	-207,882	-140,669	-10,411	-261,728	68,704	-68,704	14,457

* Does not include DOR.

Table 10.3.2 Water budget for the last decade of predictive simulations to 2050 with and without the DOR. All volumes reported in acre-feet.

Year	Layer	Recharge	ET	Wells	Springs	Streams	Top	Bottom	Storage
2040 to 2050	**1**	2,494,560	-390,688	-986,613	-50,088	-588,724	0	-567,849	190,220
	2	2,612,260	-1,585,656	-421,975	-50,429	-2,001,457	567,849	0	953,163
	Sum	5,106,820	-1,976,344	-1,408,588	-100,518	-2,590,181	567,849	-567,849	1,143,384
2040 to 2050*	**1**	2,971,567	-407,103	-998,467	-52,433	-604,597	0	-668,001	-169,873
	2	3,076,282	-1,671,280	-421,608	-50,724	-1,999,486	668,001	0	308,197
	Sum	6,047,849	-2,078,383	-1,420,075	-103,158	-2,604,083	668,001	-668,001	138,324

* Does not include DOR.

11.0 LIMITATIONS OF THE MODEL

A model can be defined as a representation of reality that attempts to explain the behavior of some aspect of it, but is always less complex than the real system it represents (Domenico, 1972). As a result, limitations are intrinsic to models. Model limitations can be grouped into several categories including: (1) limitations in the data supporting a model, (2) limitations in the implementation of a model which may include assumptions inherent to the model application, and (3) limitations regarding model applicability. The limitations of this modeling study are discussed in the following paragraphs consistent with the groupings above.

11.1 Limitations of Supporting Data

Developing the supporting database for a regional model at this scale and with the large quantity of grid cells is a challenge. The primary limitations of the supporting database are:

- Limited hydraulic head targets in select Seymour pods,
- No stream/aquifer gain/loss estimates,
- Limited geologic structural data support for the Blaine aquifer, and
- Limited hydraulic property data of the underlying Permian strata.

Each of these database limitations is discussed below.

The primary type of calibration target used in most models, including this GAM, is hydraulic head. In the portions of the Seymour aquifer that have historically been studied (in Haskell, Knox, Jones, and Wilbarger counties), sufficient head targets are available for both the steady-state and transient model calibrations. However, in the remainder of the aquifer there is a lack of available head data for both steady-state and transient conditions. In some of these areas, such as Kent and Stonewall counties, data were insufficient to assess the model's ability to match aquifer conditions. Both the steady-state and transient model calibrations could be improved with more head targets in these areas.

There are no stream gain/loss estimates in the model area that can be used to calibrate stream leakages. Only a limited number of stream gages in the aquifer are amenable to estimation of losses or gains through the study region. In addition, direct comparison to stream gages is problematic because the MODFLOW stream routing package does not model runoff.

Since the Seymour aquifer is solely a water-table aquifer, it would be beneficial if publicly available surface-water models were developed for the aquifer region. These would provide better estimates of the hydrography of the area and could be coupled with MODFLOW to better constrain model calibration and predictive accuracy.

An adequate database was available from published sources for estimation of the structural surfaces of the Seymour aquifer at the scale of the model. The structure for the Blaine aquifer was well supported for the portion of the aquifer located in Oklahoma. However, a paucity of data generally exists for describing the structure of the Blaine in Texas and for the remainder of the Permian bedrock formations (model layer 2). Therefore, the structure of the Permian sediments is poorly constrained by available data. This limits accurate representation of both transmissivity and storativity in model layer 2.

The hydraulic properties of the Seymour aquifer are considered to be reasonably well known based on numerous measurements. Many of the hydraulic conductivity estimates were based on specific capacity measurements, however, which are less representative of overall aquifer transmissivity than pump tests. Although numerous measurements of the hydraulic conductivity of the Blaine aquifer are available, no spatial correlation or trends were evident in the data and a uniform value was implemented. Too few data are available for the remainder of the Permian sediments to characterize the distribution in hydraulic conductivity. This limits the ability to capture heterogeneity in the Blaine and other Permian units.

11.2 Assessment of Assumptions

There are several assumptions that are key to the model regarding construction, calibration, and prediction. These assumptions are related to the following model aspects:

- Layer 2 no-flow boundary conditions,
- Spatial variation in recharge,
- Temporal variation in recharge as derived from SWAT, and
- Groundwater maximum ET rates and extinction depth as derived by SWAT.

These are briefly discussed below along with the potential limitations of the assumption(s) used in the Seymour GAM development.

The lower boundary of model layer 2 was modeled as a no-flow boundary. The assumption of no flow is considered applicable for the base of the Blaine aquifer which is underlain by the Flowerpot Shale Formation. For the remainder of layer 2, this boundary was set at arbitrary depths because the thickness is largely arbitrary and the base of layer 2 does not represent a physical boundary. By imposing this no-flow boundary condition, it was assumed that flow directions within formations represented by layer 2 are essentially horizontal. This is considered a reasonable assumption, however, because the primary purpose of layer 2 is to provide hydraulic communication from the Seymour and Blaine aquifers to the stream boundary conditions which are largely set in the Permian. Because the thickness of layer 2 is a construct, the overall hydraulic conductance of the layer 2 formations are scaled parameters. This is not considered a serious limitation for the Seymour model, but it would be if one were trying to accurately simulate aquifer dynamics within the Permian associated with pumping.

The lateral model boundaries were also modeled as no-flow boundaries. An attempt was made to place the majority of the lateral boundaries at hydrologic divides, either river basins or topographical ridges. In other cases, the model boundaries were placed at significant distances from the Seymour and Blaine aquifers and, therefore, the areas of concentrated pumping. This is not considered a significant limitation to the model.

While average recharge estimates from SWAT were consistent with literature values for the Seymour aquifer, the spatial distribution was inconsistent with the conceptual model of the aquifer and was not used. Instead, the spatial distribution of recharge in the Seymour aquifer was assumed to be correlated to the local topography of the Seymour consistent with the research of Meyboom (1966) and Tóth (1966). Greater recharge rates were applied at topographical highs where the depth to water and subsurface infiltration gradient is presumably greater, and lower recharge rates were applied in low areas where the depth to water was smaller. The degree to which recharge and topography are related in the Seymour is unknown, and this relationship was used as a calibration parameter. This resulted in a spatial distribution of recharge that largely coincides with the spatial distribution of pumping from the Seymour aquifer because both are biased toward the thicker portions of the aquifer. The distribution is considered a reasonable estimate of actual recharge. Model recharge was not varied spatially over the Permian outcrop and this is not considered a limitation for the Seymour GAM.

Another assumption used in the transient model is that the recharge rate estimated by SWAT, when averaged spatially, is applicable for describing the temporal variations in recharge caused by variations in precipitation. The SWAT model was assumed to provide average regional estimates of recharge by using physical models and parameters representative of the area. The interflow zone in SWAT was not modeled. MODFLOW was used to reject recharge to the stream networks, which has its limitations due to the averaging of topography on a 1-mile grid-block scale. Although the spatial distribution of recharge resulting from SWAT was not used in the model, the spatial and temporal distributions of ET maximum and ET rooting depth from SWAT were used.

11.3 Limits for Model Applicability

The purpose of the GAM program is to build models to determine how regional water levels will respond to water resource development in an area smaller than a county and larger than a square mile. This is accomplished by developing regional models using a grid-block size of one square mile. These two design criteria limit the applicability of the Seymour GAM for several reasons. First, the Seymour aquifer is not regionally connected but rather consists of small isolated pods. Therefore, large-scale regional flow does not occur in the aquifer. Second, the size of the pods is small relative to the grid-block size of one square mile. Portions of all pods are less than 5 miles wide and, at their widest point, all of the pods are less than 40 miles wide. The accuracy of the model is likely representative at a scale of tens of miles. The model is probably not adequate for understanding groundwater availability at the scale of the small pods but may be useful for the larger pods. Because of the model grid scale of one square mile, the model is not capable of being used in its current state to predict aquifer responses at specific points such as a selected well at a particular municipality.

In addition, much of the Seymour is relatively thin with estimated thicknesses less than 30 feet and estimated saturated thicknesses less than 20 feet. Even relatively small errors in structure, due to averaging to 1-mile grid blocks or due to a lack of data, or relatively small errors in observed water level can significantly impact the simulated amount of water available in these cells. Representation of actual groundwater availability is most difficult in the portions of the Seymour aquifer with a thin saturated thickness. Refined models with smaller grid cells are best suited for dealing with these conditions.

Because no pre-development period could be used for the steady-state model, the steady-state period includes uncertain estimates of pumping. Any errors in these pumping estimates will impact the steady-state simulation. While observed water levels appear to be stable during the several years used as the steady-state period, even small trends in water levels would be significant in the steady-state model. These limitations in the steady-state model make comparisons of mass balance to that of the transient model difficult.

The GAM model provides a first-order approach to coupling surface water to groundwater which is adequate for the GAM model purposes. However, the model does not provide a rigorous solution to surface-water modeling.

The GAM model does not simulate transport of solutes and cannot explicitly address water quality issues. A preliminary assessment of water quality is given in this report in Section 4.8.

This page intentionally left blank.

12.0 FUTURE IMPROVEMENTS

To use models to predict future conditions requires a commitment to improve the model as new data become available or when modeling assumptions or implementation issues change. This GAM is no different. Through the modeling process, one generally learns what can be done to improve the model's performance or what data would help better constrain the model calibration. Future improvements to the model, beyond the scope of the current GAM, are discussed below.

12.1 Additional Supporting Data

Several types of data could be collected to better support future enhancement of the Seymour GAM. These include additional water-level monitoring in Seymour pods with sparse measurements, recharge studies, surface-water/groundwater studies, and addition of stream gages. Because of the character of the Seymour aquifer (e.g., small pods, thin saturated thicknesses over many areas, and a water-table aquifer intersected by many streams), all parameters related to recharge to the aquifer, flow within the aquifer, and discharge from the aquifer need to be known in order to accurately reflect processes occurring in the aquifer.

Additional water-level monitoring in Seymour pods in Hall, Motley, Childress, Wichita, Foard, Knox (pod 6 and the northern portion of pod 7), Kent, Stonewall, Fisher, and Jones (pods 11 and 12) counties would be valuable. Although pumping from these portions of the aquifer is small, it is still advantageous to monitor water levels in those areas to improve aquifer understanding and to incorporate those additional data into the model. It is also important to increase water-level monitoring in areas with future development potential even if they are not currently extensively developed. If monitoring begins prior to increased development, the GAM can be calibrated against the pre-development response to improve model predictive capability in those regions.

Recharge is the primary method by which water enters the Seymour aquifer. Since the Seymour is a shallow, water-table aquifer, long-term stability of the aquifer requires a balance between inflow through recharge and decreased discharge [capture after Bredehoeft (2002)] and outflow through pumping. Improving the understanding of recharge into the aquifer will greatly enhance future models and their ability to accurately predict future aquifer conditions based on

projected pumping estimates. Studies should be continued into the nature of recharge in the Seymour aquifer.

The Seymour is a water-table aquifer associated with multiple streams. Because streams represent a source of aquifer discharge, data on stream/aquifer interaction is critical for understanding groundwater flow within each pod of this aquifer. Knowledge of surface water/groundwater interaction requires good coverage of stream gages in the Seymour aquifer. The model's ability to represent actual aquifer conditions will be greatly enhanced with aquifer-specific data regarding surface-water/groundwater interaction. In addition, it would be beneficial if publicly available surface-water models were developed for the Seymour aquifer region. These would provide better estimates of the hydrography of the aquifer and could be coupled with MODFLOW in future model improvements.

Currently, horizontal hydraulic conductivity data are limited for the Seymour aquifer and very limited for the underlying Permian sediments. Development of the horizontal hydraulic conductivity field for the Seymour aquifer predominantly used specific capacity measurements to calculate hydraulic conductivity. Although this method serves as a useful approximation, hydraulic conductivity estimates from pump tests would be more representative of overall aquifer transmissivity. Any additional hydraulic conductivity and storativity estimates interpreted from pump tests will further help parameterize the Seymour aquifer and the Permian sediments for future improvements to this model.

Large portions of the Seymour aquifer have a thin saturated thickness. Therefore, accurate location of the aquifer base is important. Previous studies in some areas of the aquifer provided good data on the Seymour base. These areas include portions of pod 7 in Haskell and Knox counties (R.W. Harden & Associates, 1978), portions of pod 7 in Baylor County (Preston, 1978), portions of pod 4 in Wilbarger County (Price, 1979), and portions of pods 12, 13, 14, and 15 in Jones County (Price, 1978). In the remainder of the aquifer, however, coverage of data for determining the structure of the Seymour is limited. With additional data, the ability of the model to represent the geometry of the aquifer would be improved.

12.2 Future Model Implementation Improvements

A single model was used to represent the entire Seymour aquifer even though it consists of isolated pods that are not hydraulically connected. In addition, the hydraulic condition of the aquifer varies from pod to pod. Some pods are heavily pumped for irrigation purposes while others are lightly pumped. While a single model of the Seymour allows estimation of consistent boundary conditions and hydraulic properties at a regional scale, smaller refined models employing these boundary conditions and properties could overcome some of the limitations outlined in Section 11. Future modeling of this aquifer should consider each pod individually and should include a refined grid design based on the size of the pod, the hydraulic stresses within the pod, and the ultimate goal of the model. Such a refined grid would allow the representation and evaluation of the aquifer at a smaller scale and would more accurately simulate aquifer dynamics at the pod scale. With a refined grid, characterization and mapping of root depths and associated plants would improve the understanding of ET in the model. Based on the quantity of pumping in the Seymour aquifer (in descending order), pods 7, 1, and 4 are candidates for implementation of pod-scale models.

This page intentionally left blank.

13.0 CONCLUSIONS

This report documents a three-dimensional groundwater model developed for the Seymour aquifer to the GAM standards defined by the TWDB. This regional-scale model was developed using MODFLOW with the stream-routing package to simulate stream/aquifer interaction. The Seymour aquifer is modeled as one layer and the underlying Permian sediments are modeled as a second layer.

The purpose of this GAM is to provide predictions of groundwater availability though the year 2050 based on current projections of groundwater demands and including one period of DOR conditions. This GAM provides an integrated tool for the assessment of water management strategies to directly benefit state planners, RWPGs, GCDs, and UWCDs.

This GAM was developed using a modeling protocol which is standard to the groundwater model industry. This protocol includes: (1) the development of a conceptual model for groundwater flow in the aquifer, (2) model design, (3) model calibration, (4) model verification, (5) sensitivity analysis, (6) model predictions, and (7) reporting.

The model was first calibrated to steady-state conditions. The steady-state model reproduces steady-state aquifer heads well and within the uncertainty of the head estimates. The average recharge rate estimated for the entire steady-state model area was 0.6 in/yr, with an average rate of 2 in/yr applied to the Seymour aquifer. In the steady-state model, recharge accounted for approximately 94 percent of the aquifer inflow, and streams, ET, and pumping discharged approximately 48, 31, and 19 percent of the aquifer outflow, respectively. A sensitivity analysis was performed to determine which parameters had the most influence on aquifer performance and calibration. The most sensitive parameters for the steady-state model are recharge, stream conductance, and the horizontal hydraulic conductivity of layer 2.

The model was also successfully calibrated to transient aquifer conditions from 1980 through December 1989. The model satisfactorily reproduced aquifer heads during this time period. The transient-calibrated model was verified by reproducing observed aquifer conditions from 1990 through December 1999. In the transient model, recharge accounted for 94 percent of the aquifer inflow, and streams, ET, and pumping discharged approximately 35, 20 and 20 percent of the aquifer outflow, respectively. A sensitivity analysis was performed on the

transient model. The two most sensitive parameters for the transient model are recharge and pumping.

Model predictions were performed to estimate aquifer conditions for the next 50 years based upon projected pumping demands developed by the RWPGs and under DOR conditions. The model indicated that, under average conditions, water levels are predicted to rise an average of 1.6 feet in the Seymour aquifer between 2000 and 2050. In the Permian sediments, water levels are predicted to decline an average of 0.6 feet between 2000 and 2050. The simulations incorporating DOR conditions at the end of the predictive periods generally show average declines of 1.1 and 1.7 feet in the Seymour aquifer and Permian sediments, respectively, when compared to simulations of average conditions. Water-level decreases during an actual drought may be more substantial, however, because the DOR only considers climatic conditions (e.g., recharge), not the potential increase in pumping.

The model provides a basis for future refinement to address more local scale issues related to specific water resource questions. Questions regarding local drawdown to a specific well should be based upon the analytical solution to the diffusion equation or a refined numerical model. The model was built to determine how regional water levels will respond to water resource development in an area smaller than a county and larger than a square mile. In addition, the model is useful in estimating consistent boundary conditions and hydraulic properties on a regional scale that could be applied to any refined models of individual Seymour pods.

This model, like all models, has limitations and can be improved. The GAM reproduced the steady-state and transient conditions of the aquifer within the required calibration measures. More importantly, this calibrated GAM provides a documented, publicly-available tool for the assessment of future groundwater availability in the Seymour aquifer.

14.0 ACKNOWLEDGEMENTS

We greatly appreciate the interest and hospitality of the various stakeholder participants in the Seymour GAM region who offered input during the GAM development and provided rooms for the Stakeholder Advisory Forum (SAF) meetings. Interaction with these stakeholders was performed through a series of SAFs held between February 2002 and April 2004. In these meetings, stakeholders were solicited for data and were provided updates on the development of the supporting data and the model beginning in January 2003. The model described in this report has benefited from the stakeholders involvement and interest.

The INTERA team was aided significantly in their efforts by stakeholders from the Rolling Plains Groundwater Conservation District (RPGCD) and the Collingsworth County Underground Water District (CCUWD). The management for these two entities supplied up-to-date well information, reviewed and advised the project team on local issues, and supported staff with their local investigations including recharge and water-level analyses. Local knowledge from the stakeholders proved especially valuable in conceptual model development. Field review of the recharge and discharge areas was also valuable, and enabled better description of potential modeling anomalies in these areas. Special thanks to Mr. Mike McGuire and Mr. Tommy Powell (managers of the RPGCD and CCUWD, respectively). Thanks also to the staff at the city of Seymour for being gracious hosts for the SAFs.

We would also like to thank the TWDB GAM staff led originally by Robert Mace and now by Cindy Ridgeway for their support during this model development exercise. We would like specifically to thank Cindy Ridgeway for providing both technical and contract management support during the execution of this study. In addition, the GAM has benefited significantly from input and review comments from the TWDB staff during the scheduled technical review meetings.

The senior external experts, Dr. Steven Gorelick from Stanford University, Dr. Marios Sophocleous from the University of Kansas, and Dr. Graham Fogg from the University of California at Davis, shared valuable insights into various aspects of numerical modeling and provided crucial review and support during the development of the Seymour GAM. We would also like to thank various staff from INTERA for their contributions: Rainer Senger, Van Kelley, Neil Deeds, and Dennis Fryar for their input on recharge and other topics during the

project and comprehensive review during preparation of the Conceptual Model Report, Draft Report, and Final Report, and Chris Urbina for his GIS support. Finally, we would like to thank Judy Ratto of INTERA for her efforts in the editing and production of this report.

15.0 REFERENCES

Anderson, M.P., and W.W. Woessner, 1992. Applied Groundwater Modeling. Academic Press, San Diego, CA, 381 p.

Ashworth, J.B., and J. Hopkins, 1995. Aquifers of Texas. Texas Water Development Board, Report 345.

Baker, Jr., E.T., A.T. Long, Jr., R.D. Reeves, and L.A. Wood, 1963. Reconnaissance Investigation of the Ground-Water Resources of the Red River, Sulphur River, and Cypress Creek Basins, Texas. Texas Water Commission, Bulletin 6306.

Borrelli, J., C.B. Fedler, and J.M. Gregory, 1998. Mean Crop Consumptive Use and Free-Water Evaporation for Texas. Final Report to Texas Water Development Board. Grant 95-483-137. February 1998.

Bredehoeft, J.D., 2002. The Water Budget Myth Revisited: Why Hydrogeologists Model. Ground Water, 40(4), pp. 340-345.

Broadhurst, W.L., R.W. Sundstrom, and D.E. Weaver, 1951. Public Water Supplies in Western Texas. U.S. Geological Survey, Water-Supply Paper 1106.

Brown, D.M., 1996. "Reducing Modeling Uncertainty Using ASTM Ground-Water Modeling Standards," *Subsurface Fluid-Flow (Ground-Water and Vadose Zone) Modeling, ASTM STP 1288*. J.D. Ritchey and J.O. Rumbaugh, Eds. American Society for Testing and Materials.

Brune, G., 1975. Major and Historical Springs of Texas. Texas Water Development Board, Report 189.

Brune, G., 1981. Springs of Texas, Volume I. Branch-Smith, Inc.

Caran, S.C., and R.W. Baumgardner, Jr., 1990. Quaternary Geology of the Rolling Plains, *in* Morrison, R.B., ed., Quaternary Nonglacial Geology: Conterminous U.S:, The Geology of North America. Geological Society of America.

Chiang, W.H., and W. Kinzelbach, 1998. Processing MODFLOW- A Simulation System for Modeling Groundwater Flow and Pollution: Software Manual, 325 p.

Cronin, J.G., 1972. Ground Water in Dickens and Kent Counties, Texas. Texas Water Development Board, Report 158.

Deeds, N., V. Kelley, D. Fryar, T. Jones, A.J. Whallon, and K.E. Dean, 2003. Groundwater Availability Model for the Southern Carrizo-Wilcox Aquifer, prepared for the Texas Water Development Board. Available online at http://www.twdb.state.tx.us/gam/czwx_s/czwx_s.htm.

de Marsily, G., 1986. Quantitative Hydrogeology, Groundwater Hydrology for Engineers. Academic Press, Orlando, FL, 440 p.

Deutsch, C.V., and A.G. Journel, 1992. *GSLIB: Geostatistical Software Library & User's Guide*, Oxford University Press, Inc.

Doherty, J. 2002. *Manual for PEST*, 5th edition. Brisbane, Australia: Watermark Numerical Computing.

Domenico, P.A., 1972. Concepts and Models in Groundwater Hydrology. McGraw-Hill, New York.

Domenico, P.A., and F.W. Schwartz, 1998. Physical and Chemical Hydrology. John Wiley & Sons, New York, 824 p.

Duffin, G.L., and B.E. Beynon, 1992. Evaluation of Water Resources in Parts of the Rolling Prairies Region of North-Central Texas. Texas Water Development Board, Report 337.

Dutton, A.R., R.C. Reedy, and R.E. Mace, 2001. "Saturated Thickness in the Ogallala Aquifer in the Panhandle Water Planning Area- Simulation of 2000 through 2050 Withdrawal Projections". The University of Texas at Austin, Bureau of Economic Geology, Topical Report.

Edwards, D.C., and T.B. McKee, 1997. Characteristics of 20th Century Drought in the United States at Multiple Time Scales. Climatology Report Number 97-2, Colorado State University, Fort Collins, Colorado.

Fenske, J.P., S.A. Leake, and D.E. Prudic, 1996. Documentation of a Computer Program (RESI) to Simulate Leakage from Reservoirs Using the Modular Finite-Difference Ground-Water Flow Model (MODFLOW). U.S. Geological Survey, Open-File Report 96-364.

Freeze, R.A., 1969. The mechanism of natural ground-water recharge and discharge. 1. One-dimensional, vertical, unsteady, unsaturated flow above a recharging or discharging ground-water flow system. Water Resources Research, 5(1), pp. 153-171.

Freeze, R.A., 1971. Three-dimensional, transient, saturated-unsaturated flow in a groundwater basin. Water Resources Research, 7(2), pp. 347-366.

Freeze, R.A., 1975. A stochastic-conceptual analysis of one-dimensional ground-water flow in nonuniform homogeneous media. Water Resources Research, 11(5), pp. 679-694.

Freeze, R.A., and J.A. Cherry, 1979. Groundwater. Prentice-Hall, Inc., New Jersey, 604 p.

Fryar, D., R. Senger, N. Deeds, J. Pickens, T. Jones, A.J. Whallon, and K.E. Dean, 2003. Groundwater Availability Model for the Northern Carrizo-Wilcox Aquifer, prepared for the Texas Water Development Board. Available online at http://www.twdb.state.tx.us/gam/czwx_n/czwx_n.htm.

George, W.O., and C.E. Johnson, 1941. Memorandum on Ground-Water Resources in the Vicinity of Crowell, Texas. Texas State Board of Water Engineers.

Gordon, C.H., 1913. Geology and Underground Waters of the Wichita Region, North-Central Texas. U.S. Geological Survey, Water-Supply Paper 317.

Gutjahr, A.L., L.W. Gelhar, A.A. Bakr, and J.R. MacMillan, 1978. Stochastic analysis of spatial variability in subsurface flows -2, Evaluation and application. Water Resources Research, 14(5), pp. 953-959.

Harbaugh, A.W., E.R. Banta, M.C. Hill, and M.G. McDonald, 2000. MODFLOW-2000, The U.S. Geological Survey Modular Ground-Water Model-User Guide to Modularization Concepts and the Ground-Water Flow Process. U.S. Geological Survey, Open-File Report 00-92.

Harbaugh, A.W., and M.G. McDonald, 1996. User's Documentation for MODFLOW-96, An Update to the U.S. Geological Survey Modular Finite-Difference Ground-Water Flow Model. U.S. Geological Survey, Open-File Report 96-485, 56 p.

Hayes, M., 2001. Drought Indices. National Drought Mitigation Center, Available online at http://enso.unl.edu/ndmc/enigma/indices.htm.

Heitmuller, F.T., and B.D. Reece, 2003. Database of Historical Documented Springs and Spring Flow Measurements in Texas. U.S. Geological Survey, Open-File Report 03-315.

Isaaks, E.H., and R.M. Srivastava, 1989. An Introduction to Applied Geostatistics. Oxford University Press, New York.

Johnson, K.S., 1985. Structure Contour Map and Stratigraphic/Hydrologic Data on the Blaine Aquifer in the Hollis Basin of Southwestern Oklahoma. Oklahoma Geological Survey.

Johnson, K.S., 1990. Hydrogeology and Karst of the Blaine Gypsum-Dolomite Aquifer, Southwestern Oklahoma. Oklahoma Geological Survey, Special Publication 90-5.

Lanning-Rush, J. 2000. Regional Equations for Estimating Mean Annual and Mean Seasonal Runoff for Natural Basins in Texas, Base Period 1961-1990. U.S. Geological Survey, Water-Resources Investigation Report 00-4064, 27 p.

Lemon, R.G., and M.L. McFarland, 2002. Influence of Irrigation Water Quality on Peanut Production in the Texas High Plains, Final Report. Submitted to Texas Peanut Producers Board and National Peanut Board, March 2002.

Lohman, S.W., 1972. Ground-Water Hydraulics. U.S. Geological Survey, Professional Paper 708.

Mace, R.E., 2001. Estimating Transmissivity Using Specific-Capacity Data. The University of Texas, Bureau of Economic Geology, Geological Circular 01-2, 44 p. Available online at http://www.twdb.state.tx.us/gam/GAM_documents/sc_report.pdf.

Maderak, M.L., 1972. Ground-Water Resources of Hardeman County, Texas. Texas Water Development Board, Report 161.

Maderak, M.L., 1973. Ground-Water Resources of Wheeler and Eastern Gray Counties, Texas. Texas Water Development Board, Report 170.

McDonald, M.G., and A.W. Harbaugh, 1988. A Modular Three-Dimensional Finite-Difference Ground-Water Flow Model. U.S. Geological Survey, Techniques of Water-Resources Investigations, Book 6, Chapter A1.

McKee, T.B., N.J. Doesken, and J. Kleist. 1993. The relationship of drought frequency and duration to time scales. Preprints, 8th Conference on Applied Climatology, 17-22 January, Anaheim, CA, pp. 179-184.

Meyboom, P., 1966. Groundwater Studies in the Assiniboine River Drainage Basin: I. The Elevation of a Flow System in South-Central Saskatchewan. Geologic Survey of Canada, Bulletin 139.

Morris, D.E., 1967. Occurrence and Quality of Ground Water in Archer County, Texas. Texas Water Development Board, Report 52.

Nordstrom, P.L., 1991. Joint Ground-Water Quality Project with the Texas Department of Agriculture in Parts of Haskell, Knox, and Stonewall Counties. Texas Water Development Board, Report 333.

Ogilbee, W., and F.L. Osborne, Jr., 1962. Ground-Water Resources of Haskell and Knox Counties, Texas. Texas Water Development Board, Bulletin 6209.

Popkin, B.P., 1973. Ground-Water Resources of Hall and Eastern Briscoe Counties, Texas. Texas Water Development Board, Report 167.

Preston, R.D., 1978. Occurrence and Quality of Ground Water in Baylor County, Texas. Texas Department of Water Resources, Report 218.

Price, R.D., 1978. Occurrence, Quality, and Availability of Ground Water in Jones County, Texas. Texas Department of Water Resources, Report 215.

Price, R.D., 1979. Occurrence, Quality, and Quantity of Ground Water in Wilbarger County, Texas. Texas Department of Water Resources, Report 240.

Prudic, D.E., 1988. Documentation of a Computer Program to Simulate Stream-Aquifer Relations Using a Modular, Finite-Difference, Ground-Water Flow Model, U.S. Geological Survey, Open-File Report 88-729.

Runkle, D.L., and J.S. McLean, 1995. Steady-State Simulation of Ground-Water Flow in the Blaine Aquifer, Southwestern Oklahoma and Northwestern Texas. U.S. Geological Survey, Open-File Report 94-387.

Runkle, D.L., D.L. Bergman, and R.S. Fabian, 1997. Hydrogeologic Data for the Blaine Aquifer and Associated Units in Southwestern Oklahoma and Northwestern Texas. U.S. Geological Society, Open-File Report 97-50.

R.W. Harden & Associates, 1978. The Seymour Aquifer: Ground-Water Quality and Availability in Haskell and Knox Counties, Texas Volume 1 and Volume II. Texas Department of Water Resources, Report 226.

Scanlon, B.R., A. Dutton, and M. Sophocleus, 2002. Groundwater Recharge in Texas. The University of Texas at Austin, Bureau of Economic Geology, submitted to the Texas Water Development Board. Available online at http://www.twdb.state.tx.us/gam/resources/RechRept.pdf.

Scanlon. B.R., R.C. Reedy, and K.E. Keese, 2003. Examination of Groundwater Recharge in Texas Related to Aquifer Vulnerability to Contamination. Bureau of Economic Geology.

Sepulveda, N., 2003. A Statistical Estimator of the Spatial Distribution of the Water-Table Altitude. Groundwater, 41(1).

Shafer, G.H., 1957. The Use of Ground Water for Irrigation in Childress County, Texas. Texas Board of Water Engineers, Bulletin 5706.

Slade, R.M., Jr., J.T. Bentley, and D. Michaud, 2002. Results of Streamflow Gain-Loss Studies in Texas, with Emphasis on Gains From and Losses To Major and Minor Aquifers, Texas, 2000. U.S. Geological Survey, Open-File Report 02-068. Available online at http://water.usgs.gov/pubs/of/ofr02-068/.

Smith, J.T., 1970. Ground-Water Resources of Collingsworth County, Texas. Texas Water Development Board, Report 119.

Smith, J.T., 1973. Ground-Water Resources of Motley and Northeastern Floyd Counties, Texas. Texas Water Development Board, Report 165.

Sundstrom, R.W., W.L. Broadhurst, and B.C. Dwyer, 1949. Public Water Supplies in Central and North-Central Texas. U.S. Geological Survey, Water-Supply Paper 1069.

Tanji, K.K., 1990. Agricultural Salinity Assessment and Management. American Society of Civil Engineers. Manuals and Reports on Engineering Practice Number 71.

Texas Water Development Board, 1996. Survey of Irrigation in Texas 1958, 1964, 1969, 1974, 1979, 1984, 1989, and 1994. Report 347.

Texas Water Development Board, 2002. Water for Texas – 2002. Document No. GP-7-1.

Theis, C.V., R.H. Brown, and R.R. Meyer, 1963. Estimating the Transmissivity of Aquifers From the Specific Capacity of Wells. U.S. Geological Survey, Water-Supply Paper 1536-I.

Tóth, J., 1966. Mapping and interpretation of field phenomena for groundwater reconnaissance in a prairie environment, Alberta Canada. Bull. Intern. Assoc. Sci. Hydrol., 11(2), pp. 1-49.

Turner, S.F., 1936a. Foard County, Texas Records of wells, drillers' logs, and water analyses, and maps showing location of wells. State Board of Water Engineers.

Turner, S.F., 1936b. Hardeman County, Texas Records of wells, drillers' logs, water analyses, and geologic section, and maps showing location of wells. State Board of Water Engineers.

U.S. Salinity Laboratory Staff, 1954. Diagnosis and Improvement of Saline and Alkali Soils. U.S. Department of Agriculture, Agricultural Handbook 60.

Van der Leeden, F., F.L. Troise, and D.K. Todd, 1990. The Water Encyclopedia. Lewis Publishers, Boca Raton, Florida.

Warren, J.E., and H.S. Price, 1961. Flow in Heterogeneous Porous Media. Society of Petroleum Engineers Journal 1, pp. 153-169.

Wermund, E.G., 1996. River Basin Map of Texas. Bureau of Economic Geology. The University of Texas. 1 pl.

Williams, T.A., and A.K. Williamson, 1989. Estimating Water-Table Altitudes for Regional Ground-Water Flow Modeling, U.S. Gulf Coast. Groundwater, 27(3), pp. 333-340.

Willis, G.W., and D.B. Knowles, 1953. Ground-Water Resources of the Odell Sand Hills Wilbarger County, Texas. Texas Board of Water Engineers, Bulletin 5301.

Wilson, J.D., and R.L. Naff. 2004. MODFLOW-2000, the U.S. Geological Survey Modular Ground-Water Model – GMG Linear Equation Solver Package Documentation. U.S. Geological Survey, Open-File Report 2004-1261.

APPENDIX A

Brief Summary of Historical Development of the Seymour and Blaine Aquifers in Texas on a County by County Basis

This page intentionally left blank.

This appendix provides a brief summary of historical development in the Seymour and Blaine aquifers in Texas on a county by county basis. The source for the material presented here are published literature reviewed as part of the conceptual model development for the Seymour GAM. The Seymour aquifer is classified as a major aquifer in Texas and is located in north-central Texas and the Texas panhandle (see Figure 2.5 in the main body of this report). This aquifer occurs exclusively under water-table conditions and is the major source of water for all purposes in many counties. The Blaine aquifer is classified as a minor aquifer in Texas and is located predominantly in the Texas panhandle (see Figure 2.5 in the main body of this report). This aquifer occurs under both water-table and artesian conditions. Water from the Blaine aquifer is used extensively for irrigation but, due to high sulfate content, is not suitable for human consumption.

Archer County

The Blaine aquifer is not present beneath this county. The Seymour aquifer is found in only a small portion of northwestern Archer County and is not considered a source of groundwater in this county. The majority of groundwater available for use in Archer County is supplied by the portion of the Pennsylvanian-age Cisco Group found beneath the southeastern portion of the county (Morris, 1967).

Baylor County

The Blaine aquifer is not present beneath this county. Little information related to historical development of the Seymour aquifer in Baylor County was found during the literature review. Unless stated otherwise, the following discussion comes from Preston (1978). The Seymour aquifer is the major source of groundwater in this county. In the mid-1970s, approximately 80 percent of the wells in Baylor County were completed to the Seymour Formation. The portion of the Seymour aquifer that produces the greatest yields of water is located between the town of Seymour on the east, the Knox County line on the west, the Wichita River to the north, and the Brazos River to the south (i.e., the portion of pod 7 located in Baylor County; see Figure 4.1.1 in the main body of this report). The maximum thickness of the Seymour in this area is about 60 ft.

Development of the Seymour aquifer in Baylor County began in the early 1900s. In their report surveying public water supplies in central Texas, Sundstrom et al. (1949) state that, in October 1943, municipal water for the city of Seymour was obtained from four wells completed in recent stream deposits. The city of Seymour began using water from the Seymour aquifer in 1948 with the drilling of at least six wells. Additional public supply wells for the city of Seymour were drilled in 1949, 1956, 1959, 1965, and 1969. As of 1969, a total of 19 wells supplied water to the residents of the city of Seymour. Few irrigation wells were drilled in Baylor County prior to 1950. More than 100 irrigation wells were drilled during 1955, 1956, and 1957 due to the severe drought from the early 1950s to 1957. Although the development of irrigation wells continued after the drought, the rate of development was slow. Preston (1978) indicates that the amount of water available from the Seymour aquifer increased between about the 1920s and the 1960s to 1970s based on reports by 'oldtimers'.

Briscoe County

The Blaine aquifer as defined by the TWDB is not present beneath Briscoe County. A very small part of the Seymour aquifer is located beneath the southeastern tip of this county. Little information related to historical development of the Seymour aquifer in Briscoe County was found during the literature review. Popkins (1973) provides a discussion of groundwater in eastern Briscoe County but does not include any specific information regarding the alluvium making up the Seymour aquifer in this county.

Childress County

Little information related to the historical development of the Seymour and Blaine aquifers in Childress County was found during the literature review. Unless stated otherwise, the following discussion comes from Shafer (1957). The primary source of water for irrigation use is the Blaine aquifer. In 1950, about ten irrigation wells were completed in the Blaine. The number of wells completed to the Blaine and supplying water for irrigation purposes increased to about 45 in September 1953 and to about 80 in late 1955. In general, water obtained from the Blaine aquifer is use for irrigation due to its poor quality. Ten wells completed in terrace deposits of the Seymour aquifer provide water for the city of Childress. The average yield from these wells was 195 gallons per minute (gpm) in 1947 (Broadhurst et al., 1951).

Clay County

The Blaine aquifer is not present beneath Clay County. Information regarding historical development of the Seymour aquifer in this county could not be found during the literature search. Based on a survey of public water supplies in north-central Texas in the 1940s (Sundstrom et al., 1949), all water used for municipal purposes in this county was obtained from surface sources. Data found on the TWDB website give 1935 as the earliest date for a well completed to the Seymour aquifer in this county.

Collingsworth County

Little information related to historical development of the Seymour and Blaine aquifers in Collingsworth County was found during the literature review. Unless stated otherwise, the following discussion comes from Smith (1970). Aquifers of most importance for water supply in this county are the Blaine aquifer and alluvial plain, terrace, and channel deposits. Many of the wells completed to the latter are located within the outline of the Seymour aquifer. Only seven wells completed to the Seymour aquifer in this county are given on the TWDB website. Water for municipal, domestic, and stock purposes is primarily supplied by the alluvial plain, terrace, and channel deposits. Due to its poor quality, the Blaine aquifer supplies water predominantly for irrigation and industrial purposes only. In Collingsworth County, the Blaine Formation and the overlying Dog Creek Shale are often mapped as a single unit due to the difficulty in distinguishing between the two.

Use of groundwater for municipal purposes began in 1910 in Collingsworth County with the development of two wells in the alluvium by the city of Wellington. By 1948, 11 wells completed in alluvium were supplying water to the city of Wellington and two wells, also completed in alluvium, were supplying water to the city of Dodsonville (Broadhurst et al., 1951). The largest increase in groundwater pumpage for municipal purposes occurred between 1958 and 1964. Irrigation using water from the Blaine aquifer and the alluvium began on a small scale in the early 1950s. The number of irrigation wells increased to 83 in 1955 and to 151 in 1966. According to the TWDB website, the first well to tap the alluvium was completed in 1899 and the first well to tap the Blaine Formation was completed in 1896.

Cottle County

The Seymour aquifer as defined by the TWDB is present beneath Cottle County. However, this portion of the aquifer is not included as part of the Seymour GAM effort as directed by the TWDB. Very little information regarding historical development of the Blaine aquifer in Cottle County could be found during the literature search. Based on a survey of public water supplies in western Texas, Broadhurst et al. (1951) state that, in 1947, the city of Paducah obtained water from four wells located west of the city. Broadhurst et al. (1951) indicate that the source of water for these four wells was Permian age deposits. Three wells were drilled to the Blaine aquifer in Cottle County in 1949, the earliest year for completion of wells to the Blaine, according to data on the TWDB website.

Fisher County

Although a small portion of the Blaine Formation may be present beneath this county, it does not yield enough water to be classified as part of the Blaine aquifer (Ashworth and Hopkins, 1995). Information regarding historical development of the Seymour aquifer in Fisher County could not be found during the literature search. The first well completed to deposits of Quaternary age that lie within the outline of the Seymour aquifer was drilled in 1945 according to data on the TWDB website.

Foard County

Little information related to historical development of the Seymour and Blaine aquifers in Foard County was found during the literature review. The largest city in this county, Crowell, was supplied by water from a single well from 1907 to 1921 (George and Johnson, 1941). In 1921, the city began to obtain water from artificially constructed surface water impoundments (George and Johnson, 1941). George and Johnson (1941) investigated the potential for developing groundwater resources to supply water to the city of Crowell. It is likely that their investigation led to the construction of wells for use by the city because, in a survey of public water supplies, Sundstrom et al. (1949) report that the city of Crowell used six wells to supply water to its residences in 1945. The most likely source of that water was the Seymour aquifer (Sundstrom et al., 1949).

The first well drilled to the Seymour aquifer in Foard County was completed in 1920 according to data on the TWDB website. The TWDB data indicate that the first well completed to the Blaine aquifer in Foard County was drilled in 1954 (TWDB website).

Hall County

Little information related to historical development of the Seymour and Blaine aquifers in Hall County was found during the literature review. Unless stated otherwise, the following discussion comes from Popkins (1973). Wells completed to the alluvial deposits produce all of the water used for public supply in this county and most of the water used for irrigation. The Blaine aquifer underlies this county in the northeast and southeast corners. Few wells are completed to the Blaine and none are used for public supply due to poor water quality. Natural discharge from the Blaine occurs through numerous springs. A survey of public water supplies showed that the city of Estelline used two wells completed to the alluvium in 1948 (Broadhurst et al., 1951). Data on the TWDB website indicates that the first well drilled to the alluvium located within the Seymour aquifer outline was completed in 1925.

Hardeman County

Little information related to historical development of the Seymour and Blaine aquifers in Hardeman County was found during the literature review. Unless stated otherwise, the following discussion comes from Maderak (1972). The major sources of groundwater in this county are the Blaine Formation and the Quaternary-age alluvial terrace deposits. In general, water from the Blaine Formation has a high sulfate content and is not used for drinking purposes. However, Blaine water is used successfully for irrigation purposes. The hydraulic properties of the Seymour Formation and terrace deposits are similar, and these deposits are usually mapped and discussed together. Fresh water for irrigation, and municipal and domestic supply is obtained predominantly from terrace deposits. Most of the groundwater pumped in Hardeman County from either the Blaine Formation or alluvium deposits is used for irrigation. Significant use of groundwater for irrigation purposes began in Hardeman County in the early 1950s. The amount of water used for irrigation almost doubled between 1958 and 1964. In 1946, the city of Chillicothe was using four wells completed in the alluvium for its public water supply (Sundstrom et al., 1949). The earliest of those wells was dug in 1917 and the latest was drilled in

1946. The first well completed to alluvium deposits and located within the outline of the Seymour aquifer was drilled in 1912 according to data on the TWDB website. Drilling to the Blaine Formation in Hardeman County began in about 1943 (TWDB website).

Haskell County

The Blaine aquifer is not present beneath this county. Numerous reports on the Seymour aquifer in Haskell County were found during the literature review. Ogilbee and Osborne (1962) report on groundwater in Haskell and Knox counties. They focused on the occurrence, development, and chemical quality of water in the Seymour aquifer. Past, present, and potential future contamination and the current chemical quality of water in the Seymour aquifer in Haskell and Knox counties was investigated by R.W. Harden and Associates (1978). The quality of water in the Seymour aquifer in parts of Haskell, Knox, and Stonewall counties was the focus of Nordstrom (1991). He collected water samples from the Seymour in a joint effort with the Texas Department of Agriculture to evaluate the effects of pesticide use on the quality of water in the Seymour.

Unless stated otherwise, the following discussion on the Seymour aquifer in Haskell County comes from Ogilbee and Osborne (1962). The Seymour aquifer is the major (essentially only) source of water for this county. Although water from the Seymour aquifer is hard and high in nitrate concentration in some areas, it is used in the county for all purposes. Much of the water removed from the Seymour is used for irrigation purposes in the northern portion of this county. The use of Seymour water for irrigation began in 1938 and remained very low until 1950 (R.W. Harden and Associates, 1978). The number of irrigation wells completed to the Seymour aquifer increased dramatically during the drought from 1952 to 1956, and at a slower pace during the 1960s (R.W. Harden and Associates, 1978).

The historical condition of the Seymour aquifer in Haskell County is unusual in that water levels in the aquifer increased rather than decreased during the first half of the 1900s. Several long-time residents of the county indicated that the Seymour Formation was nearly dry prior to 1900. Clearing of the land for cultivation purposes resulted in increased opportunity for recharge, and an increase in precipitation resulted in the Seymour aquifer filling with water between 1900 and about 1940. A Texas Board of Water Engineers employee surveyed residents of Haskell County near the city of Rochester in 1934 and reported that:

> "the rise of ground water in this area [Haskell and Knox counties] is no myth, but a fact, that the rise has been about a foot per year with some little acceleration during the last few years, and the water has changed from hard, gip and salt water to soft, fresh water" (Ogilbee and Osborne, 1962).

Not only did the level of water rise in the Seymour Formation, but water also began to seep from the surface and water-log the land in some areas. This resulted in the development of numerous salt marshes. In some areas, previously cultivated land became nonproductive. Water level rises of up to 60 ft occurred in the Seymour Formation during this time period.

Ogilbee and Osborne (1962) summarize water-level changes in the Seymour Formation in this way:

> "Prior to cultivation of the land, water levels fluctuated in response to changes in the climatic cycle, but in general they remained near the base of the Seymour Formation. From about 1900 they rose, somewhat irregularly, as more and more land was being cultivated. During the 1930's the water levels reached their maximum altitude, causing the waterlogging of some of the low-lying lands. The water table remained at near-maximum height until about 1951 when drought and withdrawals for irrigation started a decline that continued until 1957. Rainfall, more than 4 inches above normal in 1957 and about normal in 1958, and a decrease in withdrawals caused the water table to rise slightly."

Conditions of the Seymour aquifer before and after clearing of the land for cultivation are significantly different. The Seymour was nearly dry before the land began to be cleared. As more and more land was developed for agricultural purposes, water levels within the Seymour rose with maximum water levels measured in the 1930s.

Jones County

Although a small portion of the Blaine Formation may be present beneath this county, it does not yield enough water to be classified as part of the Blaine aquifer (Ashworth and Hopkins, 1995). Little information related to historical development of the Seymour aquifer in Jones County was found during the literature review. Unless stated otherwise, the following discussion comes from Price (1978). The Seymour aquifer is the major source of groundwater

for all uses in this county. Although the Seymour Formation is present over much of the county in isolated patches, usable groundwater is obtained from only a few locations. The patch of the Seymour that yields the most significant quantities of groundwater is located southeast of the city of Anson (pod 13; see Figure 4.1.1 in the main body of this report).

The ability of the Seymour aquifer to provide water has increased or become stronger according to several long-time residents of Jones County. This increase is similar to that noted by Ogilbee and Osborne (1962) for the Seymour Formation in Haskell and Knox counties. Price (1978) attributes this increase in large part to the clearing of phreatophytes (water-consuming vegetation) in the county.

Water from the Seymour aquifer was used for irrigation on a small scale (about 31 wells) in Jones County prior to 1954. The number of Seymour irrigation wells increased to a total of 157 by the end of 1968. The largest percentage of irrigation wells (42 percent) was drilled during the 5-year period from 1961 through 1965. During this time period, precipitation in the county was, in general, above or near normal. Therefore, the time of greatest development in irrigation wells does not correspond to a period of drought. As of 1969, only limited development of groundwater from the Seymour aquifer for industrial and municipal purposes had occurred. In 1946, all cities surveyed in Jones County by Sundstrom et al. (1949) in their survey of public water supplies in Central and North-Central Texas obtained water from surface reservoirs. A total of 41 industrial wells and two municipal wells were inventoried by Price (1978) in 1968 and 1969. Most of the wells (440) completed to the Seymour aquifer in 1969 were used for domestic and livestock purposes. Based on historical water-level data, Price (1978) reports that, in general, water levels in the Seymour aquifer rose between 1953 and 1968-1969. According to data found on the TWDB website, the first well to tap the Seymour Formation was completed in 1892.

Kent County

The Blaine aquifer is not present beneath this county. Little information related to historical development of the Seymour aquifer in Kent County was found during the literature review. Unless stated otherwise, the following discussion comes from Cronin (1972). Groundwater for public supply, irrigation, and industrial use is obtained mainly from Quaternary

alluvium deposits in this county. The main source of water is the alluvium deposits located along Duck Creek.

In their survey of public water supplies in western Texas, Broadhurst et al. (1951) indicate that, in 1947, the city of Jayton, located on the eastern edge of the Seymour outline, obtained its water from two wells completed in the alluvium. One of those wells was dug in 1934 and the other drilled in 1945. Data on the TWDB website indicates that the first well to the Seymour aquifer was drilled in Kent County in 1945.

King County

The Seymour aquifer as defined by the TWDB is present beneath the north-central edge of King County. However, this portion of the aquifer is not included as part of the Seymour GAM effort as directed by the TWDB. Information regarding historical development of the Blaine aquifer in King County could not be found during the literature search. The first well completed to the Blaine Formation in this county was drilled in 1920 according to data on the TWDB website.

Knox County

The Blaine aquifer is not present beneath this county. Numerous reports on the Seymour aquifer in Knox County were found during the literature review. Ogilbee and Osborne (1962) report on groundwater in Haskell and Knox counties. They focused on the occurrence, development, and chemical quality of water in the Seymour aquifer. Past, present, and potential future contamination and the current chemical quality of water in the Seymour aquifer in Haskell and Knox counties was investigated by R.W. Harden and Associates (1978). The quality of water in the Seymour aquifer in parts of Haskell, Knox, and Stonewall counties was the focus of Nordstrom (1991). He collected water samples from the Seymour in a joint effort with the Texas Department of Agriculture to evaluate the effects of pesticide use on the quality of water in the Seymour.

Unless stated otherwise, the following discussion on the Seymour aquifer in Knox County comes from Ogilbee and Osborne (1962). The Seymour aquifer is the major (essentially only) source of water for this county. Although water from the Seymour aquifer is hard and high in nitrate concentration in some areas, it is used for all purposes in Knox County. Much of the

water removed from the Seymour is used for irrigation purposes in the southern portion of this county. The use of Seymour water for irrigation began in 1938 and remained very low until 1950 (R.W. Harden and Associates, 1978). The number of irrigation wells completed to the Seymour aquifer increased dramatically during the drought from 1952 to 1956, and at a slower pace during the 1960s (R.W. Harden and Associates, 1978).

The historical condition of the Seymour aquifer in Knox County is unusual in that water levels in the aquifer increased rather than decreased during about the first half of the 1900s. Several long-time residents of the county indicated that the Seymour Formation was nearly dry prior to 1900. Clearing of the land for cultivation purposes, which resulted in increased opportunity for recharge, and an increase in precipitation resulted in the Seymour aquifer filling with water between 1900 and about 1940.

Ogilbee and Osborne (1962) summarize water-level changes in the Seymour Formation in this way:

> "Prior to cultivation of the land, water levels fluctuated in response to changes in the climatic cycle, but in general they remained near the base of the Seymour Formation. From about 1900 they rose, somewhat irregularly, as more and more land was being cultivated. During the 1930's the water levels reached their maximum altitude, causing the waterlogging of some of the low-lying lands. The water table remained at near-maximum height until about 1951 when drought and withdrawals for irrigation started a decline that continued until 1957. Rainfall, more than 4 inches above normal in 1957 and about normal in 1958, and a decrease in withdrawals caused the water table to rise slightly."

Conditions of the Seymour aquifer before and after clearing of the land for cultivation are significantly different. The Seymour was nearly dry before the land began to be cleared. As more and more land was developed for agricultural purposes, water levels within Seymour rose, with maximum water levels measured in the 1930s.

Motley County

The Blaine aquifer is not present beneath this county. Little information related to historical development of the Seymour aquifer in Motley County was found during the literature

review. Unless stated otherwise, the following discussion comes from Smith (1973). The major aquifers in this county are the alluvium deposits and the upper deposits of the Dockum Group. Groundwater is almost the sole source of water used in Motley County. A few irrigation pumps are supplied by surface water. A factor of four increase in the use of groundwater for irrigation, municipal, and industrial purposes was observed between 1958 and 1968. The use of groundwater for irrigation purposes began in the 1950s in Motley County. The majority of groundwater used for irrigation purposes in this county is supplied by the alluvium deposits. The first two wells drilled to alluvium deposits located within the outline of the Seymour aquifer were completed in 1936 and 1950 according to data on the TWDB website.

Stonewall County

The Blaine aquifer is not present beneath this county. Information on historical development of the Seymour Aquifer in Stonewall County could not be found during the literature review. The following discussion is based on data found on the TWDB website. As of 2002, ten wells are completed to the Seymour Formation in this county; four northwest of the center of the county and six along the very eastern edge of the county near the Haskell County line. The first three wells were completed in 1942, 1950, and 1954.

Wheeler County

The Seymour aquifer as defined by the TWDB is present beneath Wheeler County. However, this portion of the aquifer is not included as part of the Seymour GAM effort as directed by the TWDB. Little information related to historical development of the Blaine aquifer in Wheeler County was found during the literature review. Unless stated otherwise, the following discussion comes from Maderak (1973). Groundwater from the Blaine aquifer in this county is not suitable for municipal or domestic uses and is used principally as a source for irrigation water. In the southeastern portion of this county, the Blaine Formation is the only source for large supplies of water. Groundwater use for irrigation purposes was insignificant in Wheeler County prior to 1955. The number of irrigation wells in the county increased by a factor of 2.6 between 1955 and 1966. The number of acre-feet pumped for irrigation purposes increased by a factor of 3.5 over this same time period. Water for irrigation is pumped from both the Blaine and Ogallala aquifers; the Blaine aquifer in the southeastern portion of the county and

the Ogallala aquifer in the western and northern portions of the county. Data on the TWDB website indicates that the first well completed to the Blaine Formation in Wheeler County was drilled in 1943.

Wichita County

The Blaine aquifer is not present beneath this county. Little information related to the historical development of the Seymour aquifer in Wichita County was found during the literature review. In their survey of public water supplies in central and north-central Texas, Broadhurst et al. (1949) state that the city of Burkburnett obtained water from 14 wells located southeast of the city in 1946. These wells were drilled between 1936 and 1943. The city of Burkburnett is located along the Red River near the center of the county. Broadhurst et al. (1949) were not sure which formation supplied water to these wells. All wells were completed to a depth of less than 50 feet. It is possible that they were completed in the Seymour aquifer along the Red River, but that cannot be verified. Both Broadhurst et al. (1949) and Gordon (1913) indicate that water for public use by the residents of Wichita Falls was obtained from a surface water supply. Data on the TWDB website indicate that the first wells completed to the Seymour aquifer in Wichita County were drilled in 1936.

Wilbarger County

The Blaine aquifer is found only below the northwestern most corner of this county. Information related to historical development of the Seymour aquifer in Wilbarger County was found in Price (1979). Unless stated otherwise, the following discussion comes from that report. The hydraulically connected Seymour aquifer and alluvium deposits of Quaternary age are a major source of groundwater in this county, which obtains most of its water from underground sources. Groundwater is used for municipal, irrigation, domestic, stock, and industrial purposes in Wichita County.

The use of Seymour water for municipal public supply began in 1890 with one well supplying water to the city of Vernon. Over the years, several different fields with wells tapping the Seymour aquifer or alluvium deposits have supplied water to the city of Vernon. Public supply wells completed to the Seymour aquifer or alluvium deposits have also been used for municipal purposes by the cities of Odell and Lockett located within Wilbarger County and the

city of Altus located in Oklahoma. Use of water from the Seymour aquifer or alluvium deposits for industrial purposes is limited.

Widespread use of groundwater for irrigation purposes began in the 1950s in Wilbarger County. The number of irrigation wells in the county increased from about 24 in 1943 to about 608 in 1971. In 1971, 88 percent of the irrigation wells produced from the Seymour aquifer and 12 percent produced from the Quaternary alluvium. Percentage wise, the period of greatest development of irrigation wells occurred from 1961 to 1970. The majority of irrigation wells tapping the Seymour aquifer are located in the Odell-Fargo area and the Lockett area and most of those tapping the Quaternary alluvium are located east of the city of Fargo.

Water levels in the Seymour and Quaternary alluvium were gradually rising before significant public-supply and irrigation development began (about 1953) according to many older residents of Wilbarger County. The areas of the county that have seen the greatest decline in water levels due to municipal and irrigation pumpage are in the vicinity of the cities of Vernon and Lockett and in the Odell-Fargo area. Data on the TWDB website indicate that the first well to tap the Seymour aquifer was completed in 1897.

This page intentionally left blank.

APPENDIX B
Compilation of Structure Data from TCEQ Well Log Records

This page intentionally left blank.

Initial review of structure data for the Seymour and Blaine aquifers in the literature and on the TWDB website revealed a paucity of data for some Seymour pods. In an effort to obtain structure data for these pods, additional data sources were evaluated. These sources included water well drilling files in the TCEQ Central Records, well data in Groundwater and Underground Water Conservation District files, Agricultural Extension Service files and communications, and local well drillers' personal communications. The most valuable source of additional information was determined to be the water well drilling files in the TCEQ Central Records. This appendix details the method used to develop a database of the well information obtained from the TCEQ records.

The TCEQ well location grid was overlain on the active model area to determine which TCEQ grids corresponded to locations in or near the Seymour aquifer (Figure B.1). For portions of the Seymour aquifer in which sufficient structure data were available from the literature and/or on the TWDB website (e.g., most of pod 7 as shown in Section 4.2 of the main body of this report), additional information from the TCEQ records was not needed and, therefore, was not collected. All available files from the TCEQ Central Records for wells located within the target areas were included in development of the database. Over 3,400 well files were identified and recorded.

For the majority of wells contained in the TCEQ records, locations are identified only at the TCEQ grid-block level, which is a 2.5-minute by 2.5-minute area. The locations of the centroids of these areas are readily available and were converted to GAM coordinates. Since individual well locations were not easily determined, all well data contained within a single grid block was averaged and assigned to the location of the centroid of the grid block. These additional point data were then combined with the literature data and data from the TWDB website to generate structure surfaces for the model layers (see Section 4.2 of the main body of this report).

Two forms of well log data were encountered during the search of the TCEQ records. Examples of the two types are shown in Figures B.2 and B.3. The portions of the forms circled in the figures indicate data collected and incorporated into the database. Example sections of the final database are shown in Figures B.4 and B.5. Table B.1 gives the data fields in the database, a description of each field, and pertinent comments about each field.

The most difficult piece of data to determine from the TCEQ records was the location of the base of the Seymour aquifer. Several different formations of Permian age underlie the Seymour aquifer. These units are, from youngest to oldest, the Quartermaster Group, the Whitehorse Group, the Blaine and San Angelo formations of the Pease River Group, the Clear Fork Group, and the Wichita Group. These units outcrop in a linear trend striking north-northeast to south-southwest across the active model area with the youngest units to the west and the oldest units to the east.

In general, determining the base of the Seymour was fairly easy for wells located in the eastern portion of the active model area where the change between the last productive sand and/or gravel was distinguishable from the underlying Permian red beds. In the western portion of the active model area, the Blaine Formation and the Whitehorse Group underlie Quaternary alluvial deposits of the Seymour aquifer. On well logs, characteristics of the Whitehorse Group and the Seymour aquifer are similar making it difficult to distinguish between the two. In some cases, it was possible to distinguish between the two units by their color; red indicated the Whitehorse Group and white indicated the Seymour aquifer. Where color could not be used, determining the base of the Seymour aquifer in the western portion of the active model area became problematic. To reduce the potential for introducing error into the structure dataset due to uncertain picks of the base of the Seymour aquifer, the deepest gravels on the well logs were assumed to be Permian in origin rather than Quaternary in this part of the model area. If this method was used to select the base of the Seymour, the data were flagged as uncertain.

A methodology within the database, referred to as Structure Assessment, was developed to handle the uncertain data. Figure B.5 shows an example of this section of the database. The first data field in this section of the database is ‘Data assessment’. This field indicates whether the data are obviously suspect. A “1” in this field signifies the data appear reasonable and a “0” signifies that the data do not appear reasonable and will not be included as part of the structure dataset. The second field is ‘Likely Surface Formation’. This field contains the name of the likely surface formation at the centroid of the TCEQ grid containing the well. If the location fell outside of the Seymour aquifer outline, the well could not be completed into or through the Seymour, and that data point was not included in the structure database. The third field is ‘Likely Aquifer Formation’. This field contains the name of the aquifer considered to be encountered by the well. Determination of the likely aquifer formation relied on knowledge of

the surface formations and dips and attitudes of the local geology by the person interpreting the well log, and knowledge of well depths and screened intervals obtained from the TCEQ records. If the data for a well appeared to be reasonable and the likely surface formation and aquifer formation were determined to be Seymour, then the depth to the base of the Seymour aquifer determined from the well log and recorded in the 'gravel/sand layer 1 base' field (see Table B.1) was entered into the 'Seymour' data field. Data in this field were kept for inclusion in the structure database. If the data appeared to be reasonable and the likely aquifer formation was determined to be the Blaine, then the depth to the base of the Blaine Formation determined from the well log and recorded in the 'gypsum top' field (see Table B.1) was entered into the 'Blaine' data field. Those data were also kept for inclusion in the structure database.

A Quality Assurance/Quality Control procedure was developed for use in generating the database from the TCEQ records. This procedure included internal peer-review of each data record at lease once and review of anomalies in the data on an individual basis. Examples of anomalies include situations where the depth to water was greater than the well depth, or where the casing was larger than the drilled diameter of the well. In instances were additional data were available to correct the anomaly, the information in the database was changed and a note to that affect was added to the record for that well. For example, the depth reported for one well was less than the depth shown on a geological log for that well. In this case, the well depth was changed to match the depth given on the log. Adding these quality controls reduced the dataset for the Seymour structure significantly (from 2,600 data point to 1,600 data points).

In the western portion of the active model area, it was difficult to distinguish definitively between the Seymour aquifer and the underlying Whitehorse Group on the well logs available in TCEQ Central Records. Although every effort was made to eliminate uncertain data, it is possible that some picks for the base of the Seymour aquifer may be incorrect. Any errors are likely to result in an estimate of Seymour thickness that is greater than the actual thickness.

Table B.1 Summary of database developed from TCEQ records.

Data Field	Description	Comments
Identification		
Well ID (Owner)	Owner's name	
TCEQ ID	ID number assigned by TCEQ	
Well Information		
Latitude	The latitude of the well	No entry denotes no well coordinates given; * denotes that a county map showing the well location is available. Sketches of well locations with respect to nearby objects such as are found on the front page of many of the older logs were not considered a reliable sources for well location.
Longitude	The longitude of the well	No entry denotes no well coordinates given; * denotes that a county map showing the well location is available. Sketches of well locations with respect to nearby objects such as are found on the front page of many of the older logs were not considered a reliable sources for the well location.
Date Drilled	Date well was completed	
Diameter (in)	Diameter of the well (not the casing) in the producing zone	Units are inches.
Depth (ft)	Depth of the well	Units are feet.
Screen (ft)	Locations of screened and/or open hole intervals in the well	Open hole intervals are denoted by "O" followed by a number indicating the base of the solid casing. Screen data were included only if specific intervals were identified; comments like "15' in bottom of well" were not considered reliable and were not included in the database.
Estimated Elevation	Approximate elevation	Available for a small number of wells and assumed to be recorded by the driller or another party.
Well Tests		
GPM	Maximum well yield (gpm) given in the records	If no drawdown or time were found in the records, the well yield was assumed to have been estimated by the driller.
Drawdown (ft)	The amount of drawdown in the well during a pumping or other test	The recorded value was entered into the database unless an obvious discrepancy was observed. For example, when drawdown is reported to be 100 feet in a well of 100 feet total depth with a static water level of 80 feet. In this case, a drawdown of 20 feet would be recorded in the database.
Time (hrs)	The elapsed time of a test for which drawdown was recorded	Units are in hours.
Specific Capacity	Calculate of well yield (gpm) divided by the drawdown for a given test	
Level		
Water Level	Depth to water	Dates for water-level measurements were recorded for the first 1,000 or so records. Without exception, this date was always within one day of when the well was drilled. In an effort to reduce repetition, recording of the date for water-level measurements was stopped and the date was assumed to be the drilled data.
Geology		
Gravel/sand layer 1 base	Depth to the base of the Seymour	
Gypsum top	Depth to the top of the Blaine Formation	Was generally marked as the first indication of gypsum on the well log.

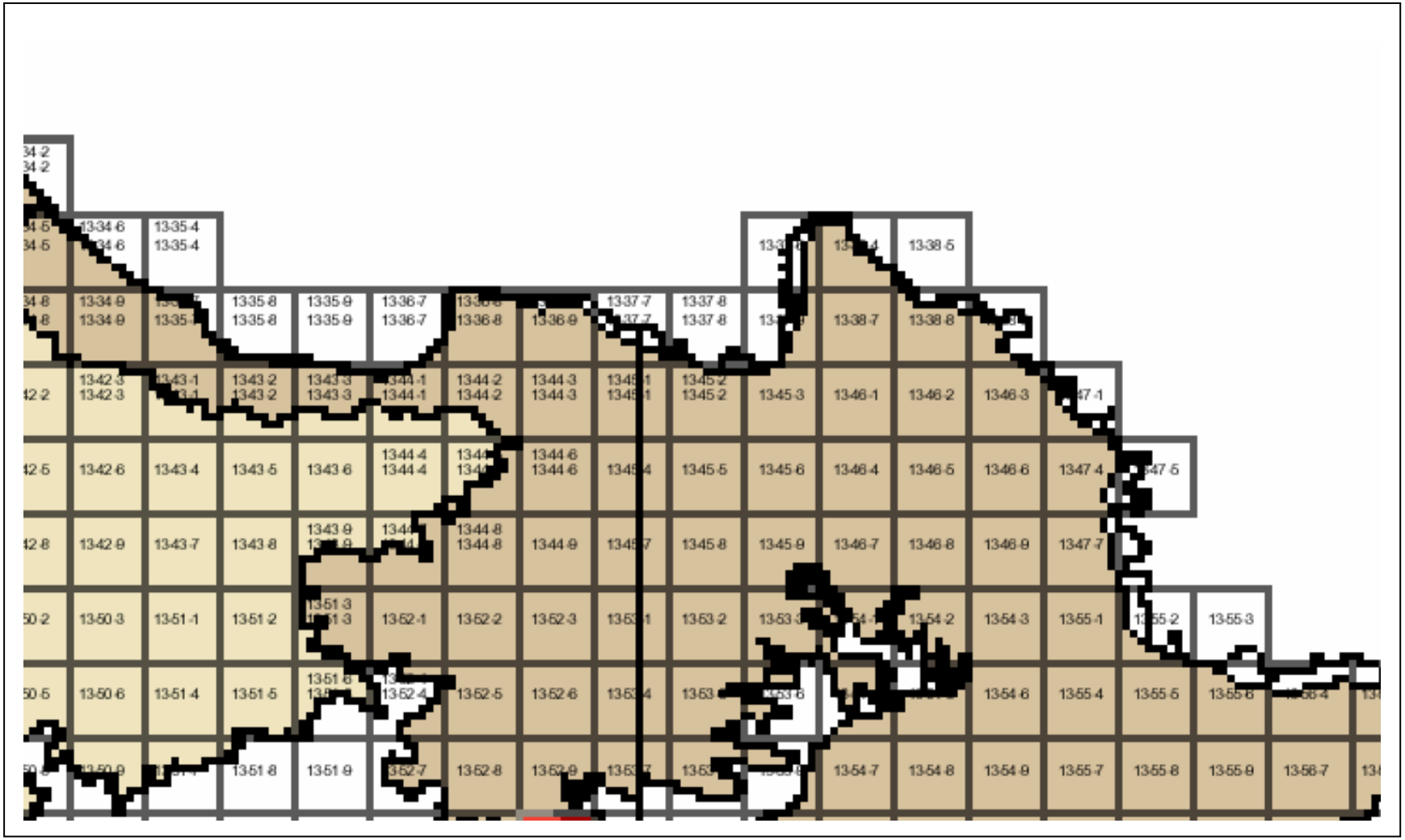

Figure B.1 Example of the TCEQ grid overlain on the Seymour aquifer in portions of Wichita and Wilbarger counties.

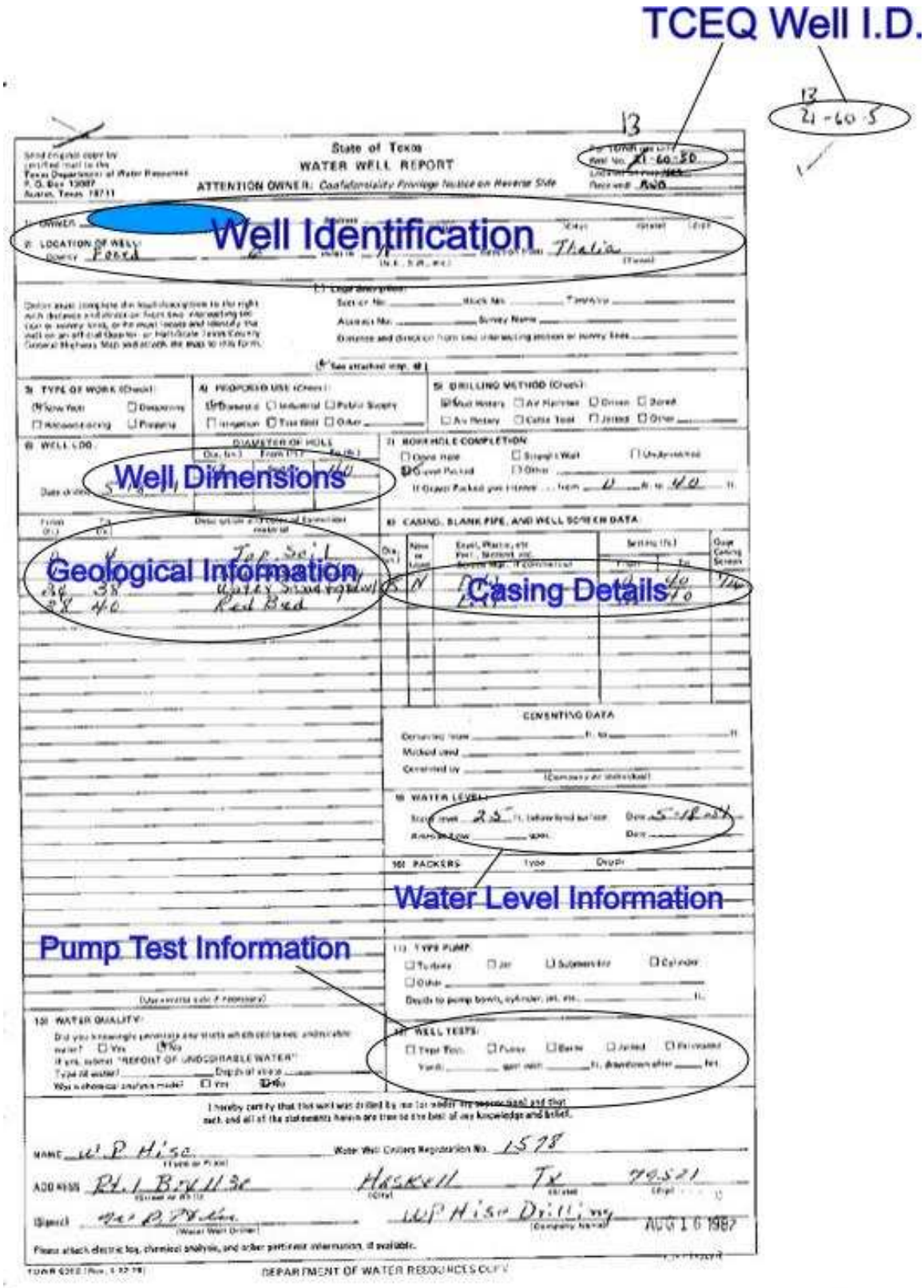

Figure B.2 Example well data sheet 1.

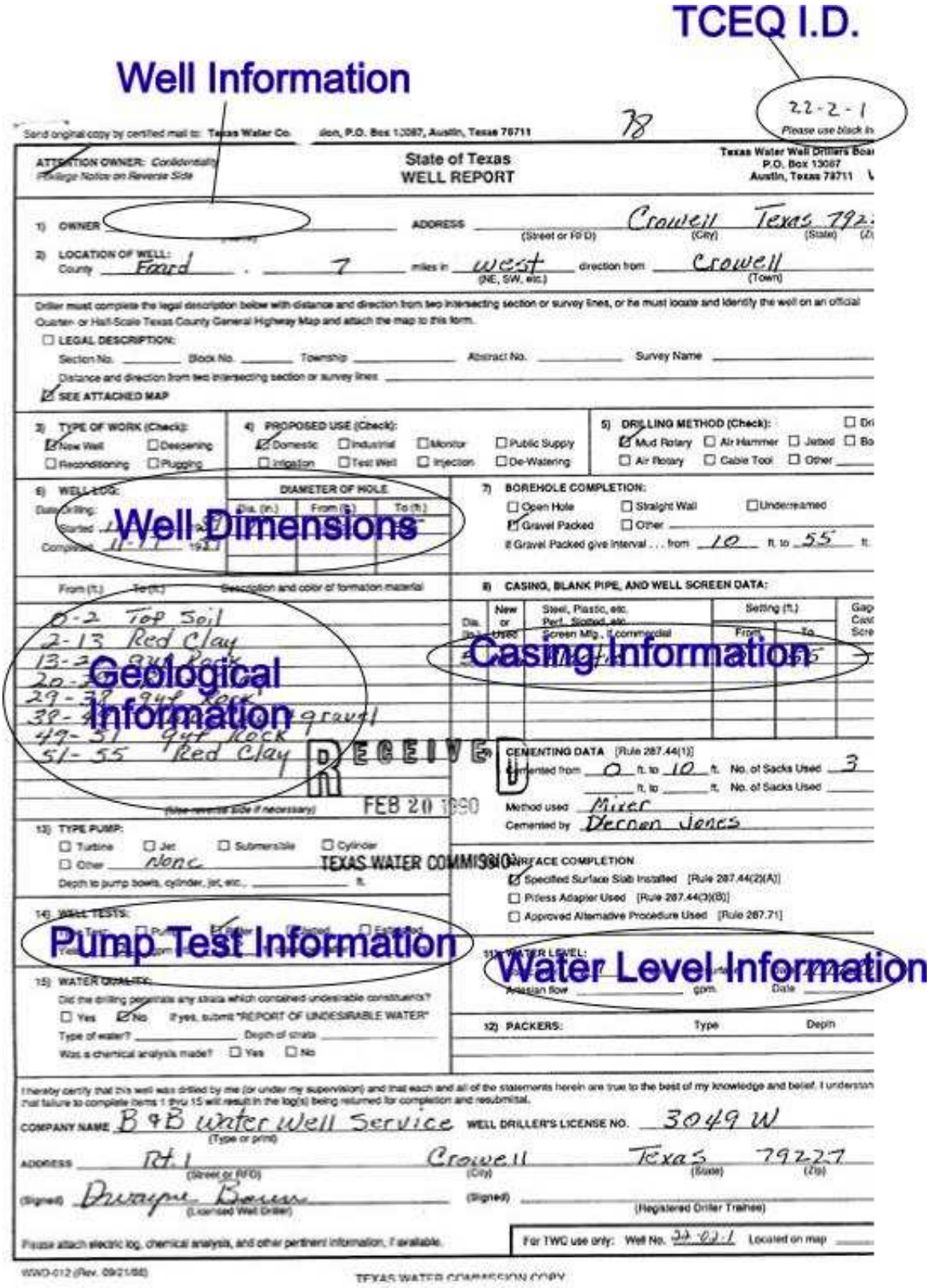

Figure B.3 Example well data sheet 2.

Identification		Well Information							Well Tests				Level	Geology	
Well ID (Owner)	TWDB ID.	Latitude	Longitude	Date Drilled	Diameter (in)	Depth (ft)	Screen (ft)	Estimated Elevation	GPM	Drawdown (ft)	Time (hrs)	Specific Capacity	Water Level	gravel / sand layer 1 base	gypsum top
H.P. Bradley	05-61-8			6/28/1983	12	40			5				31.0	26	
R.M. Standridge	12-04-3			11/5/1975	12	200	160-200							174	
W.H. Cooke	12-04-3	*		5/28/1984	9.875	70	38-58		20		0.5		18.0	60	
W.H. Cooke	12-04-3			5/28/1984	10	80	50-70		20		0.5		21.0	70	
Jim Cabbell	12-04-3			3/16/1989	26	150	70-150							150	
Jim Cabbell	12-04-3			3/28/2000	20	208	161-201		400	22	24	18	113.0	199	
Catherine Mary Ford	12-04-3	*		9/20/1991	9	100	80-100		16	0	1		86.0	97	
James Doneghy	12-04-6			10/14/1972	10	195			20	40	2	1		172	
W.R. Peggram	12-04-6			11/9/1979	12	200	180-200								
Jim Cabbell, Jr.	12-04-6			12/24/1984	8.375	175	75-110, 130-175						78.0	147	
Alfred McMurtry	12-05-1			5/23/1967	10	47	32-47		9	23	24	0	12.0		
Neil Davis	12-05-1			7/20/1968	10	135			20	10	2	2	96.0	134	
Neil Davis	12-05-1			4/3/1972	10	150			10	45		0	70.0	130	

Figure B.4 Well information database example.

Structure Assessment				
Data assessment	Likely Surface Formation	Likely Aquifer Formation	Seymour	Blaine
1	Symr	Symr	26	
1	Symr	Symr	174	
0	Symr	Symr		
0	Symr	Symr		
1	Symr	Symr	15	
1	Symr	Symr	199	
0	Symr	Symr		
1	Symr	Symr	172	
0	Symr	Symr		
1	Symr	Symr	147	
0	Symr	Symr		
1	Symr	Symr	134	
1	Symr	Symr	13	

Figure B.5 Structure assessment database example.

This page intentionally left blank.

APPENDIX C

Standard Operating Procedures (SOPs) for Processing Historical Pumpage Data TWDB Seymour GAM Project

This page intentionally left blank.

TABLE OF CONTENTS

1. Groundwater Use Source Data

1.1. Texas Water Use Data - Historical groundwater use data in Texas for the period 1980 to 2000 is derived primarily from seven tables provided by the Texas Water Development Board (TWDB) in MS Excel format, each corresponding to one of the seven major water use categories (with 3-letter abbreviation):

i. irrigation use (IRR) - "Irrigation_Master_Post1980_062602.xls"

ii. livestock use (STK) - "Livestock_Master_Post1980_072602.xls"

iii. county-other/rural domestic use (C-O) - "RuralDomestic_Master_Post1980_042902.xls"

iv. mining use (MIN) - "Mining_Master_Post1980_052402.xls"

v. manufacturing use (MFG) - "Manufacturing_Master_Post1980_052402.xls"

vi. steam electric power generation use (PWR) - "Power_Master_Post1980_052402.xls"

vii. city-municipal domestic water use (MUN) - "CityMunicipal_Master_Post1980_081402.xls"

1.1.1. Water use in the first three categories (IRR, STK, and C-O) is reported as annual summary estimates of groundwater use (in gallons and acre-feet per year) in each county-basin geospatial unit. A county-basin is the area created by the intersection of counties and river basins. For instance, because portions of Crosby County fall within the Red and Brazos River basins, there are two county-basins within Crosby County (Crosby-Red and Crosby-Brazos). No specific wells or sources of groundwater are identified for these three categories, nor are monthly sub-totals provided. Also, estimates for the years 1998, 1999, and 2000 are not provided for these three categories.

1.1.2. Water use in the other four categories (MIN, MFG, PWR, and MUN) is reported as annual and monthly self-generated groundwater use totals, in gallons, from each manufacturing, power generation, mining, or municipal water user for the years 1980 to 2000. The name, county, basin, alphanumeric code (alphanum), source aquifer, and the number of wells from which the groundwater was pumped is also provided in most cases. This data is primarily derived from the TWDB's water use surveys.

1.1.3. The use categories "City/Municipal" and "County-Other/Rural Domestic" deserve additional discussion to avoid confusion. Both are considered domestic, i.e., household water uses, and for this reason they have often been pooled together and given the 3-letter abbreviation 'MUN" or "DOM". However, because specific groundwater source location information is available from municipal and community water suppliers, but not for private rural well owners, they have been split into two use categories. To minimize confusion, the abbreviation "DOM" will not be used in this document, and the abbreviation "MUN" will refer only to City/Municipal uses. Rural domestic use will be referred to as "County-other" and abbreviated "C-O."

1.2. Accessory Data - Accessory data required to complete and spatially distribute historical groundwater pumpage data in Texas for use in the groundwater model include the following data:

1.2.1. Well information

1.2.1.1. TWDB's state well database - http://www.twdb.state.tx.us/publications/reports/GroundWaterReports/GWDatabaseReports/Database in ASCII/All Counties/weldta.txt

1.2.1.2. TWDB well followup survey - GAM_WellLocationFollowup_100101.xls

1.2.1.3. TCEQ's public water utilities database - retrieved on CD-ROM (can check for updates at http://www2.TCEQ.state.tx.us/iwud/)

1.2.1.4. USGS source information data - http://waterdata.usgs.gov/tx/nwis/inventory, and http://waterdata.usgs.gov/ok/nwis/inventory

1.2.2. irrigation monthly distribution estimates for 1980's and 1990's - IRR_GAM_MONTHLY_DISTRIBUTION.xls

1.2.3. Annual county-level summaries of Oklahoma groundwater pumpage from the Blaine aquifer by water use category for 1980, 1985, 1990, and 1995.

1.2.4. GIS data layers (as polygon shapefiles unless otherwise specified)

1.2.4.1. Texas counties (tx_tgrcnty_gam.shp)

1.2.4.2. Oklahoma counties (okcountiesgam.shp)

1.2.4.3. Texas river basins (basins_gam.shp)

1.2.4.4. 1990 census population data at block level for Texas and Oklahoma -

1.2.4.5. 2000 census population data at block level for Texas and Oklahoma -

1.2.4.6. municipal boundaries for Texas

1.2.4.7. municipal boundaries for Oklahoma

1.2.4.8. lake and reservoirs – Texas and Oklahoma

1.2.4.9. MRLC NLCD land use/land cover for north Texas (grid)

1.2.4.10. MRLC NLCD land use/land cover for Oklahoma (grid)

1.2.4.11. USGS 1:250,000 GLIS land use/land cover data for north Texas and southwestern Oklahoma

1.2.4.12. Texas irrigated farmlands 1989 survey polygons

1.2.4.13. Texas irrigated farmlands 1994 survey polygons

1.2.4.14. 30-m digital elevation models for northwest Texas (grid)

1.2.4.15. 30-m digital elevation model for southwestern Oklahoma (grid)

1.2.4.16. Seymour aquifer boundary

1.2.4.17. Blaine aquifer boundary

1.2.4.18. Model grid

1.3. Oklahoma Water Use Data – Groundwater use data were provided by the Oklahoma Water Resources Board. Oklahoma uses a permit system for groundwater withdrawals. The Oklahoma counties for which groundwater use data were initially received were Greer, Harmon, and Jackson. Later, Beckham county data were supplied.

1.3.1. Water Use Report – The spreadsheet "Parsons Report.xls" reports, for each permit number and year (1980-2000), the pumpage in acre-feet for irrigation (IRR), public supply (MUN), industrial (MFG), mining (MIN), power (PWR), commercial, "recreation fish wildlife", and "agriculture." The last three categories were minor, and were combined into the use category "C-O". The source aquifer ID was also provided for each permit number.

1.3.2. Oklahoma Spatial Data – The locations of Oklahoma water wells were provided in an Arcview shapefile "gr_wells.shp". The permit number linked with each well is listed. The metadata for this shapefiles states:

> This GIS coverage shows the locations of groundwater wells as they were approved on water rights. The well locations are described to a quarter, quarter, quarter of a section (ten-acre tract). A latitude/longitude coordinate was derived for the legal description by using a conversion program called "Okie-Loc" developed by Geo Information Systems at the University of Oklahoma. This conversion program provides the center of the ten-acre tract as the location for the well even though the well may actually be located any place within the ten acres. Most locations have not been field verified; however, in a few cases, the coordinates of the well location were determined by using a global positioning system (GPS), which would provide a more accurate point location. New well locations are approved by the Board each month on new permits and on amendments to existing permits. The coverage is updated monthly to reflect these changes.

A separate Arcview shapefile "dedlands.shp" provides the dedicated lands associated with each water use permit. This coverage was useful when the exact well associated with a given permit was not available. The metadata for this shapefiles states:

> The total amount of water that can be allocated to a groundwater right is based on the amount of land dedicated to that right. This coverage shows the dedicated lands of authorized groundwater rights as they are described in the OWRB's database. Each area of land is identified by a legal description. This description must be converted to a series of latitude/longitude points that define the area. The conversion program called "The Spatial Calculator" was developed by Geo Information Systems at the University of Oklahoma. The conversion program can convert legal descriptions by quarters and halves down to a 2.5 acre tract of land. For more information on the Spatial Calculator visit the Geo Information Systems' web page at: http://www.geo.ou.edu/. The exact size of an area that has been dedicated to a groundwater right may not be easily described by a legal description. Therefore, the polygon representing a dedicated land may not be the actual size and shape as described in the right.

2. Initial Processing

2.1. GIS Processing - Retrieve all required GIS data files, merge Texas and Oklahoma themes as required to get a single complete coverage of the project area, and convert to GAM projection according to TWDB Technical Memorandum 01-01a.

2.2. Completion of Monthly Pumpage Estimates for MUN, MFG, PWR, and MIN Uses - In the tables "Mining_Master_Post1980_052402.xls", "Power_Master_Post1980_052402.xls", "Manufacturing_Master_Post1980_052402.xls", and "CityMunicipal_Master_Post1980_081402.xls" monthly pumpage estimates are reported for the majority, but not all, of the water users. For other users, only the annual total pumpage is reported. It is necessary to estimate the monthly pumpage totals for some water users via the following procedure.

2.2.1. Complete monthly pumpage estimates for Mining using the Excel file "Mining_Master_Post1980_052402.xls"

2.2.1.1. In MS Excel using the file "Mining_Master_Post1980_052402.xls", calculate the monthly fractions of annual total water use for each record for which monthly pumpage was reported. [Note: In this procedure, 12 new columns should be added, one each for the monthly fraction for each month, e.g., fJAN, fFEB, fMAR, …fDEC.] As an example, a monthly distribution factor of 1/12, or 0.0833, would result from a uniform annual distribution with equivalent pumpage in each month.

2.2.1.2. Using a pivot table, calculate the average monthly distribution factor for each county-basin. Statistically review these average monthly fractions for outliers. Generally, monthly distribution factors fall within the range 0.035 to 0.15.

2.2.1.3. Next, for those water use records that contain an annual total water use but no monthly value, calculate estimated monthly water use values by multiplying annual total pumpage by the average monthly distribution factor in the county-basin within which it was located. If the monthly distribution factors for its county-basin contains more than two outliers, usually due to the fact that only one or two water users were located in the county-basin, use the monthly distribution factor from the nearest adjacent county-basin. (Note: For Oklahoma counties, for which no monthly values are available, use the values from the nearest Texas counties.)

2.2.1.4. Add an additional field, "Monthly Calculated" to the spreadsheet, with "N" entered in those records containing original, reported monthly pumpage values, and "Y" for those records with calculated monthly pumpage values.

2.2.2. Repeat step 2.2.1 for PWR, MFG, and MUN with the files "Power_Master_Post1980_052402.xls", "Manufacturing_Master_Post1980_052402.xls", and "CityMunicipal_Master_Post1980_081402.xls".

2.3. Create and populate a historical pumpage database in MS Access

2.3.1. Create a new blank database "Histpumpage.mdb" in MS Access

2.3.2. Import the MS Excel file "Mining_Master_Post1980_052402.xls" as an Access table **MIN_1980-2000.**

2.3.3. Import the MS Excel file "Manufacturing_Master_Post1980_052402.xls" as an Access table **MFG_1980-2000.**

2.3.4. Import the MS Excel file "Power_Master_Post1980_052402.xls" as an Access table **PWR_1980-2000.**

2.3.5. Import the MS Excel file "CityMunicipal_Master_Post1980_081402.xls" as an Access table **MUN_1980-2000.**

2.3.6. Import the table "County Codes" from the TWDB website "http://www.twdb.state.tx.us/publications/reports/GroundWaterReports/GWDatabaseReports/GWdatabaserpt.htm" that includes, for Texas Counties, the county name, county number, and county FIPS code. Add an integer field "State FIPS" and update its value with "48" in each record. Manually add records and complete values for the relevant Oklahoma Counties. Add a 1-character text field "Seymour?", and in this field place a "Y" if the county is within the Seymour model's spatial domain.

2.3.7. Create or import a new table "Basins" that includes, for all Texas River Basins, the basin name and basin number.

2.3.8. Import the table "Aquifer Codes" from the TWDB website http://www.twdb.state.tx.us/publications/reports/GroundWaterReports/GWDatabaseReports/GWdatabaserpt.htm that includes for each aquifer in Texas, the 7- or 8-character aquifer code and aquifer name. Based on information provided by the modeler and/or high-frequency matches in the state well database, identify the major aquifer ID "aquifer_id_1" associated with each aquifer code and add as an additional field.

2.4. Predicting historical pumpage for 1998-2000 – For the use categories IRR, STK, and C-O, groundwater use summaries are not reported for the years 1998 through 2000. The groundwater use for these years must be obtained by interpolation from existing data.

2.4.1. Complete pumpage estimates for IRR for 1998 to 2000 using SAS

2.4.1.1. First, import the table "Irrigation_Master_Post1980_062602.xls" into a SAS dataset.

2.4.1.2. Retrieve from the National Climate Data Center website the surface weather observations "summary of the day" climate data for all National Weather Service and cooperative weather stations within 100 miles of the project area for the period 1980 through 2000 in comma-delimited ASCII format.

2.4.1.3. Import the climate data into a SAS dataset, and calculate the weather parameters "average annual temperature" and "total annual precipitation" for the years 1980-2000 from National Weather Service cooperative weather stations. Delete those stations that have valid measurements in less than 16 of the 21 years. Also, delete data from any stations that do not have valid measurements for the years 1998, 1999, and 2000.

2.4.1.4. In Arcview, identify the weather station (with valid data for at least 16 of the 21 years) closest to each county-basin. Create a look-up table in SAS to link each county-basin with the closest weather station.

2.4.1.5. In SAS, apply linear regression in Proc REG with stepwise selection, to regress annual irrigation pumpage in each county-basin (dependent variable) vs. 1) year, 2) average annual temperature and 3) total annual precipitation from the nearest weather station for the years 1980 through 1997. Select the best valid regression equation based on the statistic Mallow's Cp, which balances the improvement in regression fit as independent variables are added to the regression with the increasing uncertainty in the resulting dependent variable estimates. Transformations (e.g., natural logarithms) of the independent variables may yield a better regression equation. There should be a regression equation for each county-basin, and water use category.

2.4.1.6. Using the regression equations and weather data for the years 1998, 1999, and 2000, in SAS, to calculate predicted pumping for these years in each county-basin. If predicted values are less than zero, a value of zero is entered. Export these predicted pumpage estimates for 1998, 1999, and 2000, import them into Excel, and append to the table containing the results for 1980-1997.

2.4.1.7. In general, this regression procedure is appropriate for pumpage changes that might be expected based on gradual annual changes (e.g., population) or year-to-year weather variability. It may not make good predictions when pumpage changes rapidly for non-weather-related factors. Review and inspect the regression-based pumpage estimates for 1998-2000 versus the TWBD-provided pumpage estimates for 1980-1997. Carefully inspect all between-year pumpage differences of more than 40%. Subjectively, if the predicted pumpage estimates do not make sense, replace the regression-based estimate with the TWDB pumpage estimate for the last year for which water use was reported (1997).

2.4.1.8. In the column "Comments", enter "weather-based regression from 1980-97 water use" or "water use from last reported year (1997)" for those years for which pumpage sums were predicted from regression or previous years, respectively.

2.4.1.9. Import this Excel table into the Access database as **IRR_1980-2000**

2.4.2. Repeat steps 2.4.1.1 - 2.4.1.8 for STK and import to the Access database as **STK_1980-2000**

2.4.3. Repeat steps 2.4.1.1 - 2.4.1.8 for C-O and import to the Access database as **C-O_1980-2000**

2.5. Correcting post-1994 County-Other Pumpage Estimates
In some counties, a major discontinuity exists between pumpage estimates provided by the TWDB for the period 1980-1994 and 1995-1997 in the category County-Other. In this case, TWDB guidance (C. Ridgeway email to Neil Deeds, July 10, 2003) suggests that pumpage estimates for 1995-2000 should be replaced with estimates calculated from the trend of 1980-1994 estimates.

2.5.1. In the spreadsheet RuralDomestic_Master_Post1980_42902.xls, calculate the relative percent difference $abs(x_2-x_1)/((x_2+x_1)/2)$ between reported pumpage estimates for 1994 and 1995 by county-basin. If the difference exceeds 33%, and the absolute difference exceeds 4 ac-ft/year, run a linear regression between the dependent variable "Pumpage(acft/yr)" and the independent variable "year" for 1980-1994. Based on the intercept and slope of this regression, predict pumpage values for 1995-2000, and replace the pumpage estimates for these years in the table with these predicted numbers. Add the comment "Estimated using linear regression from 1980-1994 estimates, due to discontinuity between pre-1995 and post-1994 estimates."

2.6. Preparing a County-Basin Shapefile and Associating Model Grid Cells with a County-Basin
Much of the reported pumpage is spatially divided into county-basin units, which consist of the area in the same county and river basin. Many counties are split between two or more river basins, thus, county-basins are equal to in size or smaller than counties.

2.6.1. To create a county-basin Arcview shapefile, in Arcview, load GIS shapefiles of counties and river basins in GAM projection. Intersect these two layers using the Geoprocessing Wizard to create a new shapefile **countybasins.shp**.

2.6.2. Associate each model grid cell with the county-basin it falls primarily within. This will be useful when we need to determine monthly distribution factors and water user group IDs (WUG IDs) for non-well-specific pumpage categories (IRR, STK, C-O). These monthly distribution factors are estimated as averages within a county-basin. **Note**: The primary county-basin is not used to spatially distribute pumpage among grid cells because it is inexact. A grid cell may be part of multiple county-basins. For spatial distribution purposes, this grid cell should be split by county-basin – then later aggregated.

2.6.2.1. Load the model grid shapefile in GAM projection. Union this shapefile with countybasins.shp using the Geoprocessing Wizard. Add a numeric field "fr_grdarea" to the attribute table, and use the field calculator function to enter its values (fr_grdarea = shape.returnarea/27878400). Here, 27878400 is the area, in square feet, of each grid cell. Export the table as a dbf file.

2.6.2.2. Import the dbf file into MS Access as a new table - **Table1**. Our goal is to identify, for each grid cell, the county-basin with which it is primarily associated.

2.6.2.3. Run a make table query, sorting the table1 records by grid_id (ascending) and fr_grd_area (descending) to create a new table, **Table2**.

2.6.2.4. Copy **Table2**, and paste only the table structure as a new table – **Grid_countybasin**.

2.6.2.5. In design view, make the field "grid_id" a primary key in the table **Grid_countybasin**.

2.6.2.6. Run an append query, to append all fields of the records from table 2 to **Grid_countybasin**. When the warning window comes up, say yes to proceed with the query. This appends only the first record for each grid_id to **Grid_countybasin**, leaving one record for each grid cell with the county basin with the largest value of "fr_grdarea". The resulting table should have one record for each grid cell in the model grid, and the county-basin name for that model grid cell.

3. Matching Pumpage to Specific Wells

Historical groundwater use from the categories MUN, MIN, MFG, and PWR is to be matched with specific wells from which it was pumped. Reported annual and monthly groundwater pumpage for these uses, derived from the annual water use surveys, is reported for each year from 1980 to 2000 for each water user. The water user is identified by a unique alphanumeric code "alphanum." The tables also list the county and river basin, as well as their water user group ID, their regional water planning group, their water use category, the major aquifer from which the groundwater was pumped, and the number of wells from which the water was pumped. These tables do not indicate the specific location off the wells, well elevation, well depth, a specific aquifer name, or other information needed for groundwater modeling. This information must be retrieved from other sources. The primary source of well information is the state well database maintained by the TWDB. Secondary sources include well data found in the TCEQ public water supply database, and the USGS site inventory. A final source is the follow-up survey provided by the TWDB in October 2001. In the absence of well information, the pumpage location may be approximated based on the facility location, if available.

3.1. Create **All_wells** table –

3.1.1. Download the state well database as a table **weldta.txt** for the entire state (under the menu "all counties combined") from the TWDB web site http://www.twdb.state.tx.us/publications/reports/GroundWaterReports/GWDatabaseReports/GWdatabaserpt.htm. Import this table into MS Access as a new table **All_Wells**. Add a field "Data Source" and enter in each record "TWDB"

3.1.2. The TCEQ water utility database includes data for some wells that are not found in the TWDB state well database. Retrieve this database from the TCEQ, and import it into the Acess database. Create an append query to link the required well data to **All_wells**, exercising care to match fields appropriately. Enter "TCEQ WUDB" in the field "Data Source" for each of these appended records.

3.1.3. The USGS site inventories for Texas http://waterdata.usgs.gov/tx/nwis/inventory and Oklahoma http://waterdata.usgs.gov/ok/nwis/inventory contain data for wells that may not be found from other sources. Run queries for site with "site type" = 'ground water' to download the well data and append it to **All_wells**. Be careful to match fields appropriately. Identify matching fields based on field descriptions in the USGS help system and the TWDB document "UM-50, Ground Water Data System Dictionary." Enter "USGS" in the field "Data Source" for these new records.

3.1.4. Append well data derived from any additional sources, such as the TWDB's followup water use survey and water quality observations or special studies by the USGS, TCEQ, or TWDB, adding an appropriate identifier to the field "Data Source."

3.1.5. Sort the database based on site/well no., and eliminate duplicate records. Also delete any oil, gas, geothermal, or observation wells, anodes, drains, or springs after a query of the attribute table on the fields "GW_type_cd" or "Site_use1_cd".

3.1.6. Enter data for any missing values for necessary fields, such as county number, county FIPS code, decimal latitude and longitude, basin, major aquifer id, etc, when they are available, using update queries with lookup tables or with formulas. Note: this can be a very labor-intensive step.

3.2. Linking MUN, MFG, PWR, and MIN water use to specific wells

3.2.1. Linking MUN water use data to the state well database – Using a make-table query to create a new table **MUN+MFG_linkedwithwellinfo**, all fields from the water use survey are merged with all fields from the state well database by joining the field "alphanum," in the table **MUN_1980-2000,** to the field

"user code econ," in the state well database table **All wells**. In many cases, several different wells may have the same "user code econ," making a one-to-many match (this is expected, since one city may own multiple wells). Check the matched wells to ensure that:

- 1) the wells are of the appropriate type (e.g., primary water use = "public supply" or "unused" for MUN use),
- 2) the well drill date precedes the water use year, and
- 3) the location and reported aquifer matches the pumpage being distributed.

Remove the wells for which this is not true. Add a field "Location Source" to the table **MUN+MFG_linkedwithwellinfo**. For the pumpage records with one or more matched well, enter the text "state well database" in this field.

3.2.2. Link MFG water use data to the state well database – Using an append query to append to the table **MUN+MFG_linkedwithwellinfo** the MFG water use, from the table MFG and matched wells based on the "user_code_econ" <=> "alphanum" join. All fields from the water use survey are merged with all fields from the state well database by joining the field "alphanum," in the table **MFG_1980-2000,** to the field "user code econ," in the table **All wells**. As in 3.2.1, remove matched wells that were drilled after the reported pumpage, wells of the wrong type, or wells with locations that do not agree with the reported pumpage. For the pumpage records with one or more matched well, enter the text "state well database" in this field "Location Source".

3.2.3. Repeat step 3.2.2 to append MIN water use with matched wells to the table **MUN+MFG_linkedwithwellinfo**, based on the table **MIN_1980-2000.**

3.2.4. Repeat step 3.2.2 to append PWR water use with matched wells to the table **MUN+MFG_linkedwithwellinfo**, based on the table **PWR_1980-2000.**

3.3. Locating unmatched pumpage 1

3.3.1. Locating unmatched MUN pumpage 1– Identify the MUN pumpage records without a matching well using a **Find Unmatched** query. Check the field "alphanum" in unmatched pumpage records of the table **MUN_1980-2000,** and "user_code_econ" in the table **All_Wells** for obvious errors that prevent automatic matching, and correct any found and repeat the steps to make the table above. Next, manually search the **All Wells** table for wells in the same county and basin, for which the user name field "owner_1" matches the field "line1" in **MUN_1980-2000**. When a match is found, add a field to the well table, and copy the "alphanum" field from the water use survey, to facilitate match-merging. Next, match this new field in the well database to "alphanum" of the water use survey, and append these matched records to the table **MUN+MFG_linkedwithwellinfo**. Enter "state well database manual match" for the field "Location Source" for these new appended records.

3.3.2. Repeat step 3.3.1 for MFG uses

3.3.3. Repeat step 3.3.1 for MIN uses

3.3.4. Repeat step 3.3.1 for PWR uses

3.4. Locating unmatched pumpage 2 – For those pumpage records not matched via the above procedures, open the TCEQ public water supply database and attempt to manually match the water user to specific wells based on the county, aquifer_id, and owner name - "A1Name." When a match is found, add a field to the well table, copy the "alphanum" field from the water use survey, perform a match-merging query, and update these new matched records to the table **MUN+MFG_linkedwithwellinfo**. Enter "TCEQ PWS database" for the field "Location Source" for these new appended records.

3.5. Locating unmatched pumpage 3 - For those pumpage records, if any, still not matched in the above procedures, manually search the TWDB follow-up survey data. When a match is found, this data must be manually copied to the table **MUN+MFG_linkedwithwellinfo** because the table format is substantially different. Enter "TWDB followup survey" for the field "Location Source" for these new appended records.

3.6. Locating unmatched pumpage 4 - For those pumpage records, if any, still not matched in the above procedures, it may be possible to identify an approximate well location via the EPA's Envirofacts facility database. In an

internet browser, go to http://www.epa.gov/enviro/html/fii/fii_query_java.html and perform a facility information query using a characteristic part of the facility name in the query field "facility site name." If a single facility of matching name is located in the same county, copy the facility latitude and longitude, in degrees, minutes, seconds into the appropriate fields of the table **MUN+MFG_linkedwithwellinfo**. Enter "facility centroid" in the field "Location Source" if Envirofacts lists that as the source of the latitude and longitude, or "facility zip code centroid" if Envirofacts lists that as the source of the latitude and longitude. Note that the median size of a zip code in Texas is approximately 5.5 square miles. Thus, pumpage located based on a zip code centroid may be very uncertain, especially in rural areas, and should be used with caution. However, in some cases an approximate location may be better than leaving the pumpage out of the model. Note: Because this step is labor-intensive, it may be acceptable to perform this procedure for only the "major" water users, as indicated by volume used.

3.7. Count wells matched - Count the number of wells matched to each pumpage record via a crosstab query on **MUN+MFG_linkedwithwellinfo**.

3.8. Apportion water use between matched wells –

3.8.1. For that water use matched to more than one well, compare the number of matched wells to the number of wells reported as used in the water use survey. If the number of matched wells exceeds the number reportedly used, inspect the well data, including the county, basin, aquifer_id, well_type, drill_date, and other fields to see if some of the wells can be excluded from consideration as the source form which the water was reportedly pumped. If so, remove that well from the table.

3.8.2. Next, we need to apportion the reported pumpage among the wells matched. Since we don't have data indicating otherwise, pumpage will be divided equally between wells. Create a new query that 1) adds a column "Num Wells Matched" indicating the number of wells matched (based on the aforementioned crosstab query) to the table **MUN+MFG_linkedwithwellinfo**, and 2) if one or more wells are matched, divides the reported pumpage in the fields "annual total in gallons" and "jan" – "dec" by the number of wells matched. Add another field "Matched wells" and enter in it the number of wells to which this pumpage was matched with and divided between.

3.8.3. Quality control check – In a query, summarize total annual water use by county-basin-year in the table **MUN+MFG_linkedwithwellinfo**. Make sure that these match the corresponding totals from the original source tables (i.e., **MUN_1980-2000**). If not, correct the situation, which may occur by double-matching some water use records to wells.

3.9. Calculate Additional Fields - In a new make-table query, create the table **Well-specific_pumpage** based on **MUN+MFG_linkedwithwellinfo,** calculate latitude and longitude as decimal degrees from degrees-minutes-seconds in new fields "lat_dd" and "long_dd." Also in the same query, calculate water use in acre-feet from gallons in new fields "Annual total in acre-ft", "JAN in acre-ft", "FEB in acre-ft",…,"DEC in acre-ft."

3.10. Append Out-of-State Data - Append the well-specific Oklahoma water use records, provided by the Oklahoma Water Resources Board or the USGS, to the table **Well-specific_pumpage**.

3.11. Summarize well-specific matching completeness – Perform queries to calculate the sum of matched water use by county-basin-year, and the total water use (matched and unmatched) by county-basin-year. Based on these queries, calculate the volumetric percent completeness of matching by county, basin, and year. Completeness should be high (e.g., >90%) to facilitate accurate accounting for water use in the model.

4. Spatial Allocation of Groundwater Pumpage to the Model Grid - The model grid is comprised of an equal-spaced grid with a size of one mile by one mile. The grid has 3 dimensions- row, column, and model layer. Each cell of the model grid is labeled with a 7-digit integer "grid_id". The first digit represents the model layer and the source aquifer, where 1 represents the modeled portions of the Seymour Aquifer, and 2 represents the Blaine Aquifer. Digits 2 through 4 represent the row number, and row 001 is the northmost row. Digits 5 through 7 represent the column, and column 001 is the westmost column. Because groundwater pumpage in the model area taps many different aquifers, in order to allocate pumpage it was useful to develop codes representing both modeled and non-modeled aquifers. Only pumpage allocated to modeled aquifers (layers 1 or 2) is modeled, but allocations to non-modeled aquifers facilitate comparing model pumpage sums to historical county-basin pumpage totals or RWPG projections. The model layer codes provided in Table 1 below were used for well-specific pumpage. For IRR, STK,

and C-O water uses, pumpage not in modeled aquifers (layers 1 or 2) was assigned to model layer "0". The model grid is represented in a MS Access table linked to an Arcview shapefile via the field "grid_id".

Table 1. Modeled and Non-Modeled Grid ID Layer Codes

Grid Layer Code	Source Aquifer/Stratum	Modeled?
0	any non-modeled aquifer (IRR, STK, C-O)	No
1	Seymour Aquifer (modeled portions)	Yes
2	Blaine Aquifer (modeled portions)	Yes
A	Alluvium	No
C	Clear Fork Group	No
D	Dockum Aquifer	No
E	Edwards/Trinity Aquifer	No
H	Hennessey Group (Oklahoma)	No
O	Ogallala Aquifer	No
P	Pennsylvanian Aquifer	No
Q	Quartermaster Group	No
S	Seymour Aquifer (non-modeled portions)	No
T	Trinity Aquifer	No
W	Wichita Group	No
X	Whitehorse /Artesia Group	No

4.1. Spatial allocation of well-specific groundwater pumpage from the categories MUN, MFG, MIN, and PWR

4.1.1. Distribute pumpage into grid cells

4.1.1.1. In MS Access, verify that all records in the table **Well-specific_pumpage** have x,y coordinates in decimal degrees.

4.1.1.2. In Access, add a new autonumbered, long integer field "Unique ID" to the table **Well-specific_pumpage**.

4.1.1.3. In Arcview, enable the Database Access extension. Add a new table **PtSrcTbl** to an ArcView project via SQL connect, including only the fields "unique_id", "well_depth", "lat_dd", and "long_dd". To perform an SQL connect, select the "SQL connect" menu item under the Project menu. Then navigate to the correct database and select the table **Well-specific_pumpage**.

4.1.1.4. Add **PtSrcTbl** as an event theme named **Wellpts** to a view based on lat/long coordinates. To do this, from the view menu, select the "add event theme" menu item, and choose long_dd for x field and lat_dd for y field in the dialog. Re-project the view to GAM projection using the View->Properties dialog box according to GAM Technical Memo 01-01 (rev A), then save it as a shapefile **Wellpts.shp**. Load **Wellpts.shp** and the model grid, also as a shapefile in GAM projection, into a new view.

4.1.1.5. Spatially join the model Grid table to the **WellPts** table. To do this make the "shape" fields of each table active, and with the **WellPts** table active, choose "join" from the table menu. This will join the 1 mile grid cell records to all of the **WellPts** records that are contained with that grid cell.

4.1.1.6. Migrate the GridId to the **WellPts** table. Do this by first adding a new 7-digit, no decimal, field to the **WellPts** table called "Grid_Id". Then, with the new field active, using the field calculator button make the new field equal to the "GridId" field from the joined table.

4.1.1.7. Delete those pumpage records outside the model domain with a "Grid_ID" of "0".

4.1.2. **Vertical Distribution**: The model includes a layer 1 representing the Seymour aquifer, and a layer 2 representing the Blaine aquifer. Pumpage from the Seymour is assigned to grid cells with a starting character of "1", while pumpage from the Blaine is assigned to grid cells with a starting character of "2". Pumping from non-modeled aquifers is assigned a starting alphabetic character representing the aquifer source (see table 1 above) if reported for well-specific uses.

4.1.3. Import the file **Wellpts.xls** to the MS Access database. Change the data type for the fields "Unique ID" and "Grid_ID" back to long integer if they were converted to double length real numbers during the import operation.

4.1.4. Run an update query to update the empty values of "Grid ID" in the table **Well-specific_pumpage** with the "Grid_ID" values from the table **Wellpts**, using an inner join on the field "Unique ID."

4.1.5. Create a new summary query **gridsum_well_specific** to summarize the pumpage for each grid_id and year from the table **Well-specific pumpage**.

4.2. Spatial allocation of irrigation groundwater pumpage – Irrigation pumpage is distributed to the irrigated farm polygons mapped in the 1989 or 1994 irrigated farmlands survey that overlie the source aquifer, weighted by the number of irrigated acres associated with each polygon. However, because the spatial locations of these farm polygons are inexact, pumpage is distributed only to the portions of the irrigated farms that are also identified as cropland based on available land use/land cover datasets. The MRLC land use classification data, based on satellite imagery from the early 1990s, is preferable to the available USGS GIRAS Anderson level II land use classification based on 1970's satellite imagery because 1) the MRLC data have a much higher resolution, and 2) the Anderson Level II classification groups cropland and pasture in a single land use class, while MRLC splits this category into four subcategories "pasture/hay", "row crops", "small grains", and "fallow". The additional resolution allows more appropriate distribution of groundwater pumpage to irrigated areas. However, a consideration should be made for land use change during the calibration period (1980-2000). Compare the area of land use category 21 (cropland and pasture) in GIRAS to the sum of land use in the MRLC NLCD categories 81 (pasture/hay), 82 (row crops), 83 (small grains), and 84 (fallow). If the areal difference is less than 1%, the land use change can be assumed to be minimal, and the MRLC considered representative of the entire period 1980-2000.

If, however, the difference in cropland/pasture between GIRAS and MRLC is greater than 1%, it is important to account for land use change during the calibration period. The irrigation pumpage for the period 1980–1989 should be distributed using the GIRAS land use dataset to the area of land use category 21 (cropland and pasture). For the period 1990-2000, the irrigation pumpage should be distributed using the MRLC NLCD dataset to the area of land use categories 81 (pasture/hay), 82 (row crops), 83 (small grains), and 84 (fallow).

Note: In the modeled area of the Seymour, cropland and pasture comprised 75.61% of the area in the GIRAS land cover dataset, and 75.40% of the area in the MRLC land cover dataset. Based on this, land use change is assumed to be minimal, and the MRLC land cover will be used for the entire period because of the advantages described above.

	USGS GIRAS	NLCD MRLC
built-up land	1.91%	1.17%
Water	0.11%	0.88%
cropland and pasture	75.61%	75.40%
orchards/vineyards/nurseries/ornamental grasses	0.05%	0.05%
rangeland/shrubland/grassland	21.00%	21.16%
Forest	0.97%	0.86%
Wetlands	0.06%	0.20%
bare rock/sand/gravel pits/quarries/transitional	0.25%	0.29%
other agricultural	0.05%	

4.2.1. Create shapefile for MRLC land use categories 61 (orchards/vineyards), 81 (pasture/hay), 82 (row crops), and 83 (small grains). - In ArcView, load MRLC grid. Select, in the new resampled grid, values 61, 81, 82 and 83, and convert to shapefile. Call it "mrlc_irrigated.shp."

4.2.2. In Arcview, using the geoprocessing wizard, clip the layers "irr_farms89.shp" and "irr_farms94.shp" to the layer "mrlc_irrigated.shp." Next, clip these same layers to the geographic extent of 1) the Seymour aquifer, saving these as new layers "seymour_irrfarms_89.shp" and "seymour_irrfarms_94.shp", and 2) the Blaine aquifer, saving these as new layers "blaine_irrfarms_89.shp" and "blaine_irrfarms_94.shp"

4.2.3. Sum the irrigated acreage within each county-basin for each of the above four new shapefiles. Next, for each irrigated farmland polygon, divide the irrigated acreage by the total irrigated acreage for the county-basin in which it lies in a new field "cb_irr_fraction."

4.2.4. Intersect each of the above 4 new shapefiles with the 1 mi. sq. model grid cells.

4.2.5. Add field "un_area_gd" and calculate the irrigated polygons' areas in sq. miles using the field calculator ("un_area_gd" = [shape].returnarea/27878400).

4.2.6. Calculate unique pumpage values for 1 mile grid cells.

4.2.6.1. Create 21 new fields (1 for each year: "pmp_80" – "pmp_00".

4.2.6.2. Using SQL Connect, query the Access table **IRR_1980-2000** for all years.

4.2.6.3. Query the records (by the year column) for each year and specific aquifer of interest (by aquifer code column) and export each query as a separate *.dbf file. "Pump_by_cb_yyyy.dbf." These tables will have a column for each use category, and can therefore also be used in livestock calculations for the same aquifer of concern.

4.2.6.4. Join the table "pump_by_cb_1980.dbf" to the attribute table "mrlc_cb_grid.shp" by countybasin. (make certain that all countybasin names are spelled the same).

4.2.6.5. Calculate "pmp_80" using the field calculator (pmp_80 = w_ar_dis89 * irrigation). Irrigation is the column of the joined table "pump_by_cb_1980" that contains the county-basin annual pumpage totals for irrigation use. Use "w_ar_dis89" for years 80-89 and use "w_ar_dis94" for years 90-00.

4.2.6.6. Repeat 4.2.6.4 – 4.2.6.5 for all years.

4.2.7. Summarize all unique pumpage totals by grid cell id.

4.2.7.1. Summarize all the "pump_un*yy*" fields by grid cell id, by using the summarize button and adding "pmp_80" (sum) through "pmp_99" (sum) in the dialog box. Name this summary file **irr_pumpbygrid_80_00**.dbf.

4.2.8. Import irrigation pumpage table back into MS Access database as a table **irrigation_total.**

4.2.8.1. In MS Access, import the attribute table for the Arcview shape file **grid_irr_*yy*.dbf** as a dbase file. This table should include one record for each possible Grid_ID, and at least the fields "Grid_ID", "year", and "pump*yy*_IRR."

4.2.9. **Vertical Distribution**: The table **Irrigation_total** now has only the grid_id of the upper model, i.e., the first digit is 1. The model includes a layer 1 representing the Seymour aquifer, and a layer 2 representing the Blaine aquifer. Pumpage from the Seymour is assigned to grid cells with a starting character of "1", while pumpage from the Blaine is assigned to grid cells with a starting character of "2". Pumping from non-modeled aquifers is assigned a value of "0"..

4.2.10. Create a new summary query **Irrigation_annual** to summarize the pumpage for each grid_id and year from the table **Irrigation_total**.

4.3. Spatial allocation of livestock groundwater pumpage – Livestock groundwater use within each county-basin is distributed evenly to all rangeland, Anderson Level II land use codes 31 (herbaceous rangeland), 32 (shrub and

brush rangeland), and 33 (mixed rangeland) of the USGS 1:250,000 GLIS land use land cover data set (http://edcwww.cr.usgs.gov/glis/hyper/guide/1_250_lulc).

4.3.1. Determine rangeland within each county-basin

4.3.1.1. In Arcview, create a rangeland-only land use shapefile by loading the USGS land use shapefiles by quadrangle, merging them as required to cover the model domain, selecting the land use codes 31, 32, and 33 in a query, then saving the theme as a new shapefile **Rangeland.shp**.

4.3.1.2. Using the Geoprocessing Wizard, intersect the Rangeland shapefile with the County-basin shapefile (make sure to use entire county basin areas, and not the "clipped to domain" version) to make a new intersection shapefile **range_countybasin.shp**.

4.3.1.3. Calculate the unique area (in square miles) of the new intersected polygons "area_un1" using the field calculator (area_un1=shape.returnarea/27878400).

4.3.1.4. Summarize the unique area by county-basin (total area of rangeland within county-basin) using the summary button.

4.3.1.5. Link the summary table back to the range_countybasin shape file and migrate it into a new field "rg_cb_tot" using the field calculator.

4.3.1.6. Determine weighted area factor "w_area1" for each polygon using the field calculator (w_area1)=(area_un1 / rg_cb_tot). W_area1 is, for each rangeland polygon, the fraction of the total rangeland area within the county-basin.

4.3.2. Intersect the rangeland/countybasin polygons with the model grid and set up for unique pumpage calculations.

4.3.2.1. Using the Geoprocessing Wizard, intersect the shapefiles range_countybasin and Model Grid to create a new shape file **rng_cb_mg.shp**.

4.3.2.2. Calculate the unique area of "intersected" polygons (area_un_grid) using the field calculator (area_un_grid=shape.returnarea/27878400). Double check that no values are greater that 1.

4.3.2.3. Determine the weighted area factor (w_area_grid) = (area_un_grid/area_un1).

4.3.3. Calculate unique pumpage "pump_un_yy" for the intersected polygons for every year (80-99).

4.3.3.1. Add the fields "pump_un80" – "pump_un99" to the **rng_cb_mg** attribute table.

4.3.3.2. Using SQL Connect, query the Access table **STK_1980-2000** for all years.

4.3.3.3. Query the records (by the year column) for each year, and specific aquifer (by aquifer code column) and export each query as a separate .dbf file. "Pump_by_cb_*yyyy*.dbf."

4.3.3.4. Join the table "pump_by_cb_1980.dbf" to the attribute table "rng_cb_mg" by countybasin. (make certain that all countybasin names are spelled the same).

4.3.3.5. Calculate "pump_un80" using the field Calculator (pump_un80 = w_area_grid * (w_area_1 * livestock)). (livestock is the column of the joined table "pump_by_cb_1980" that contains the countybasin annual pumpage totals for livestock use).

4.3.3.6. Repeat 4.3.3.4 – 4.3.3.5 for all years.

4.3.4. Summarize all unique pumpage totals by grid cell id.

4.3.4.1. Summarize all the "pump_un*yy*" fields by grid cell id, by using the summarize button and adding "pump_un_80" (sum) through "pump_un_00" (sum) in the dialog box. Name this summary file "stk_pumpbygrid_80_00.dbf".

4.3.5. Import livestock pumpage summary table back into MS Access database as a table **livestock_total**.

4.3.6. **Vertical Distribution**: The table **livestock_total** now has only the grid_id of the upper model, i.e., the

first digit is 1. The model includes a layer 1 representing the Seymour aquifer, and a layer 2 representing the Blaine aquifer. Pumpage from the Seymour is assigned to grid cells with a starting character of "1", while pumpage from the Blaine is assigned to grid cells with a starting character of "2". Pumping from non-modeled aquifers is assigned a value of "0"..

4.3.7. Create a new summary query **Livestock_annual** to summarize the pumpage for each grid_id and year from the table **Irrigation_total**.

4.4. Spatial allocation of rural domestic (C-O) groundwater pumpage.

4.4.1. Calculate the population in each 1 mile grid cell.

4.4.1.1. In Arcview, load the 1990 block-level census population shapefile. Calculate area of each census block.

4.4.1.2. Adjust block populations so that pumpage is not distributed within municipal boundaries - Load Arcview polygon shapefile of Texas and Oklahoma cities. Union this shapefile with the census block shapefile. Select census blocks that fall within city boundaries and delete those records so that rural domestic pumpage does not get distributed to cities. (Note: we're assuming that city boundaries are good surrogates for the extent of the area served by public water supply systems, whose pumpage is reported under the category "MUN"). Calculate the area of the new census blocks with cities clipped out. For blocks that were partly within cities, calculated the adjusted non-city population as the original block population multiplied by the ratio of the clipped block area to the original block area. Repeat this process for the reservoir areas.

4.4.1.3. Adjust block populations so that pumpage is not distributed within reservoir boundaries - Load Arcview polygon shapefile of Texas and Oklahoma reservoirs. Union this shapefile with the census block shapefile. Select census blocks that fall within reservoir boundaries and delete those records so that rural domestic pumpage does not get distributed to grid cells falling within reservoirs.

4.4.1.4. Calculate the area of census blocks in sq. miles in a new field "blk_area" using the Field Calculator function (blk_area=shape.returnarea / 27878400).

4.4.1.5. Load the model grid, model domain, and county-basins shapefile. Select all county-basins that are intersected by the model domain boundary. Union the selected county-basins with the model domain boundary. In the resulting shapefile, delete the polygons that are inside the model domain, leaving only areas of the county-basins that are outside of the model domain. Dissolve these polygons into one and merge with the model grid shapefile. Give this new record a grid_id of 9999999. (Adding this new area will insure that, when the county-basin total populations are calculated, the population outside of the model domain will be included).

4.4.1.6. In the Geoprocessing Wizard, intersect the census block shapefile with the model grid shapefile to create a new shape file **intrsct*90*.shp**. (Note: Because the model grid size is 1 square mile, no intersected polygon (inside the model domain) should be larger than 1 square mile. Make sure that this is the case before proceeding).

4.4.1.7. Calculate the unique area of all intersected polygons in square miles as a new field "area_un1" using the Field Calculator function (area_un1=shape.returnarea / 27878400). (so that one grid cell has an area of 1).

4.4.1.8. Add a new numeric field "pop_un1" – the unique Population of the intersected polygons. Using the Field Calculator, calculate its value as (POP_un1 = pop*90* * area_un1 / blk_area) where pop*90* is the block Population from the census file.

4.4.1.9. Sum the field "pop_un1" by grid_id using the Field Summarize function to calculate the total population within each grid cell. Join this summary table to the original grid table by grid_id and copy value into new field "pop_90".

4.4.1.10. Repeat steps 4.5.1.1 – 4.5.1.8 (no need to repeat step 4.5.1.4, just use the grid file that was

used for previous iteration).

4.4.2. Calculate the rural domestic pumpage for each 1 mile grid cell.

4.4.2.1. Intersect the county-basin shapefile with the model grid (which now has census populations for 1990 and 2000) to create a new shapefile **grid_cb_pop**.

4.4.2.2. Create new field "area_un2" and calculate unique area using field calculator ("area_un2" = [shape].returnarea/27878400)

4.4.2.3. Create two new fields "pop_un90" and "pop_un00". Calculate using the field calculator ("pop_un*yy*" = "area_un2"/ "pop_*yy*")

4.4.2.4. Using SQL Connect, query the Access table **C-O_1980-2000** for all years.

4.4.2.5. Query the records (by the year column) for each year (because Rural Domestic pumpage data is not aquifer specific, there is no need to query by aquifer) and export each query as a separate .dbf file. "Pump_by_cb_*yyyy*.dbf."

4.4.2.6. Join table "pump_by_cb_1980.dbf" to grid_cb_pop.dbf by county-basin.

4.4.2.7. Add field "pmp80." Using field calculator, calculate "pmp80" (pmp80=CO*pop_un90/cb_pop90).

4.4.2.8. Repeat steps 4.5.2.6 – 4.5.2.7 for each year. Use pop90 for years 1980-1989 and use pop00 for years 1990-2000.

4.4.2.9. As a quality control check, sum the values of "rdom_pump" for each county-basin and make sure it matches the total for the county-basin from the Access table.

4.4.2.10. Summarize pmp80 through pmp00 by grid id. Link summary back to model grid file and migrate pumpage values.

4.4.3. Import rural domestic pumpage summary table back into MS Access database as a table **rurdom_total**.

4.4.4. **Vertical Distribution**: The table **rurdom_total** now has only the grid_id of the upper model, i.e., the first digit is 1. The model includes a layer 1 representing the Seymour aquifer, and a layer 2 representing the Blaine aquifer. Pumpage from the Seymour is assigned to grid cells with a starting character of "1", while pumpage from the Blaine is assigned to grid cells with a starting character of "2". Pumping from non-modeled aquifers is assigned a value of "0"..

4.4.5. Create a new summary query **Rurdom_annual** to summarize the pumpage for each grid_id and year from the table **rurdom_total**.

5. Spatial Allocation of Oklahoma Pumpage to the Model Grid – In Oklahoma, groundwater withdrawals are subject to permitting requirements. Oklahoma annual pumpage for the years 1980 through 2000 was retrieved from the Oklahoma Water Resources Board (OWRB) in three files. The Microsoft Excel spreadsheet "Parsons_report.xls" contains reported annual water use by permit number and water use category. An Arcview point shapefile (gr_wells.shp) contains well locations (latitude and longitude) and aquifer codes associated with the permit numbers. For some water use permit numbers, specific well locations were not available. A second Arcview shapefile (dedlands.shp) provided by the OWRB contains polygons of 10-acre size for all permit numbers, derived by the OWRB from the legal description of the water use geography in the permit application. While the exact location of the well is not known, it is within the polygon. Given that the 1 square mile model grid cell size is much larger than 10 acres, use of the centroid of the polygon to identify the model grid cell of water withdrawal should result in few and minor errors.

5.1. Import the Excel file into a MS Access table **Oklahoma water use**.

5.2. In Arcview, load the shapefile **gr_wells.shp** in an Arcview view and re-project to GAM projection.

5.3. Load the shapefile **model_grid**, and run a spatial join this to **gr_wells.shp**.

5.4. In Arcview, use SQL Connect to load the table **Oklahoma water use**, then join this table to the attribute table of **gr_wells** by permit number. Create a new field "grid_id" and copy the value of the grid_id from the joined

table. Then remove the join.

5.5. Add the shapefile **dedlands.shp**, re-project to GAM projection, and spatially join **model_grid** to **dedlands.shp** based on whether the centroid of the polygon lies within the model grid cell.

5.6. Join dedlands.shp to the table **Oklahoma water use** by permit number. For those records for which "grid_id" is empty because no specific well location was identified, use the field calculator to copy the grid ID from **dedlands.shp** to the field "grid_id" in **Oklahoma water use**. Remove the joined table.

5.7. Sum the pumpage in each grid cell.

5.8. For temporal distribution of Oklahoma water use, the monthly factors of the corresponding water use categories from the bordering Texas counties will be applied to Oklahoma water use. Derivation of these monthly factors is described in the following section.

6. Temporal Distribution of Rural Domestic, Livestock, and Irrigation Groundwater Use

6.1. Temporal distribution of livestock pumpage - Because we have only annual total groundwater pumpage estimates for STK, we need to derive monthly pumpage estimates. According to TWDB GAM Technical Memo 02-02, annual total livestock pumpage may be distributed uniformly to months.

6.1.1. In the MS Access database, create a new table called **Monthly Factors** with the fields "State_code", "countyname", "basinname", "county_num", "basin_num", "data_cat", "year", and "month". The table should include a record for every county-basin within the model domain, water use category "data_cat", year (1980-2000), and month (1-12), as well as an additional annual total record (month="0") for each county-basin, year, and water use category. Add 2 new fields "mfraction" and "Monthly distribution factor source" to the new table. The former is the numeric monthly distribution factor, while the latter is a text field indicating the source of the distribution factor. For all monthly livestock water use records (data_cat=STK, month in 1-12), enter an mfactor of "0.0833" (1/12) and a monthly distribution factor source of "Tech Memo 02-02". For all annual total water use records (data_cat=STK, month =0), enter an mfactor of "1" and a monthly distribution factor source of "NA".

6.2. Temporal distribution of irrigation (IRR) pumpage - Because we have only annual total groundwater pumpage estimates for IRR, we need to derive monthly pumpage estimates.

6.2.1. Record monthly crop evapotranspiration (ET), or total water demand, for each of the Texas Crop Reporting Districts (TCRDs) that occur within the model domain, from the report "Mean Crop Consumptive Use and Free-Water Evaporation for Texas" by J. Borrelli, C.B. Fedler, and J.M. Gregory, Feb. 1, 1998 (TWDB Grant No. 95-483-137). Use these values for all years.

6.2.2. Next, determine monthly precipitation (P) for the period 1980-2000 for the locale within each of the TCRDs that occur within the model domain.

6.2.3. Determine the monthly water deficit for each month of the two periods 1980-1989 and 1990-2000 by subtracting the P values from the ET values for each TCRD. Replace negative values with zero. Sum all water deficit values by month for each of the two periods, and divide by the number of months in each period to obtain an average non-rice monthly distribution factor for each month for the two periods 1980-89 and 1990-99.

6.2.4. Enter the monthly distribution factors from step 5.2.3, above, in the table Monthly Factors for each year, county, basin, using "data_cat" = "IRR", and "Monthly Distribution Factor Source" = "ET/P Water Deficit Analysis."

6.3. Temporal distribution of rural domestic (C-O) pumpage - Because we have only annual total groundwater pumpage estimates for C-O, we need to derive monthly pumpage estimates. According to TWDB GAM Technical Memo 02-02, annual rural domestic pumpage may be distributed based on the average monthly distribution of all municipal water use within the same county-basin.

6.3.1. In a MS Access query based on the table **MUN_1980-2000**, calculate the sum of the fields "Annual total in gallons", "jan", "feb",….,"dec" for each county, basin, and year.

6.3.2. Next, calculate "mfraction," the fraction of the annual total for each month, by dividing the columns "sum of jan", "sum of feb",….,"sum of dec" by the "sum of annual total in gallons.". Transpose this

table via a query to make a table with the following fields: "countyname", "basinname", "year", "month", "mfraction", "data_cat," and "monthly distribution factor source." A value of "C-O" should be entered in the field "data_cat", and the value of "monthly distribution factor source"="this county-basin mun."

6.3.3. The values of "mfraction" are statistically reviewed for outliers. Generally, monthly distribution factors fall within the range 0.035 to 0.15. Higher or lower values can be found when there is little municipal water use in a county-basin. In this case, substitute the values of "mfraction" from an adjacent county-basin, preferably from within the same county. Update the field "monthly distribution factor source" with the name of the county-basin used as a source.

6.3.4. For Oklahoma counties, use the monthly distribution factors of the nearest Texas county-basin unless sufficient monthly municipal data is available for Oklahoma.

6.3.5. Add an annual total record for each county-basin-year, with "data_cat"="C-O", "month"="0", "mfraction"="1", and "monthly distribution factor source"="NA."

6.3.6. Using an append query, append these records to the table **Monthly Factors**.

7. Summarize Pumpage Information

7.1. Summary Queries

7.1.1. Queries for livestock - Create a new select query ***MMMYY*_STK** to calculate pumpage for the month and year of interest by multiplying the monthly factor for that month, year, and water use category, in the table **Monthly Factors**, by each entry in the imported table **Livestock_annual**. For any specified month (MMM) and year(YY), the SQL for the query **MMMYY_STK** is:

SELECT Livestock_annual.GRID_ID, Livestock_annual.DATA_CAT, Livestock_annual.Year, [MONTHLY FACTORS].MONTH, [SumPumpageAF]*[mfraction] AS PumpageAF

FROM Livestock_annual LEFT JOIN [MONTHLY FACTORS] ON (Livestock_annual.Year = [MONTHLY FACTORS].YEAR) AND (Livestock_annual.DATA_CAT = [MONTHLY FACTORS].DATA_CAT) AND (Livestock_annual.basinnum = [MONTHLY FACTORS].basinnum) AND (Livestock_annual.CountyNumber = [MONTHLY FACTORS].countynum)

WHERE (((Livestock_annual.DATA_CAT)="STK") AND ((Livestock_annual.Year)=1980) AND (([MONTHLY FACTORS].MONTH)=1))

ORDER BY [SumPumpageAF]*[mfraction];

7.1.2. Queries for irrigation – Create a new select query ***MMMYY*_IRR** to calculate pumpage for the month and year of interest by multiplying the monthly factor for that month, year, and water use category, in the table **Monthly Factors**, by each entry in the imported table **Irrigation_annual.** For any specified month (MMM) and year(YY), the SQL for the query **MMMYY_IRR** is:

SELECT Irrigation_annual.GRID_ID, Irrigation_annual.DATA_CAT, Irrigation_annual.Year, [MONTHLY FACTORS].MONTH, [SumPumpageAF]*[mfraction] AS PumpageAF

FROM Irrigation_annual LEFT JOIN [MONTHLY FACTORS] ON (Irrigation_annual.basinnum = [MONTHLY FACTORS].basinnum) AND (Irrigation_annual.CountyNumber = [MONTHLY FACTORS].countynum) AND (Irrigation_annual.Year = [MONTHLY FACTORS].YEAR) AND (Irrigation_annual.DATA_CAT = [MONTHLY FACTORS].DATA_CAT)

WHERE (((Irrigation_annual.DATA_CAT)="IRR") AND ((Irrigation_annual.Year)=1980) AND (([MONTHLY FACTORS].MONTH)=1))

ORDER BY [SumPumpageAF]*[mfraction];

7.1.3. Queries to summarize rural domestic (county-other) - Create a new select query ***MMMYY*_C-O** to calculate pumpage for the month and year of interest by multiplying the monthly factor for that month, year, and water use category, in the table **Monthly Factors**, by each entry in the imported table

Rurdom_annual. For any selected month (MMM) and year(YY), the SQL for the query **MMMYY_C-O** is:

SELECT Rurdom_annual.GRID_ID, Rurdom_annual.DATA_CAT, Rurdom_annual.Year, [MONTHLY FACTORS].MONTH, [SumPumpageAF]*[mfraction] AS PumpageAF

FROM Rurdom_annual LEFT JOIN [MONTHLY FACTORS] ON (Rurdom_annual.DATA_CAT = [MONTHLY FACTORS].DATA_CAT) AND (Rurdom_annual.Year = [MONTHLY FACTORS].YEAR) AND (Rurdom_annual.CountyNumber = [MONTHLY FACTORS].countynum) AND (Rurdom_annual.basinnum = [MONTHLY FACTORS].basinnum)

WHERE (((Rurdom_annual.DATA_CAT)="C-O") AND ((Rurdom_annual.Year)=1980) AND (([MONTHLY FACTORS].MONTH)=1))

ORDER BY [SumPumpageAF]*[mfraction];

7.1.4. Query to summarize well-specific pumpage - Create a new select query in MS Access ***MMMYY*Well-SpecificSum** to summarize the well-specific pumpage from all wells within a grid cell for the desired month or year. For any specified month and year, the SQL query for well-specific pumpage would be:

SELECT CGC_gridsum_well_specific.GRID_ID, "WS" AS DATA_CAT, CGC_gridsum_well_specific.year, CGC_gridsum_well_specific.month, CGC_gridsum_well_specific.SumPumpage_af AS PumpageAF

FROM CGC_gridsum_well_specific

WHERE (((CGC_gridsum_well_specific.year)=[Enter year]) AND ((CGC_gridsum_well_specific.month)=[Enter month]))

ORDER BY CGC_gridsum_well_specific.SumPumpage_af;

7.1.5. In order to ensure that each grid cell is included in the final summary queries, even if there is no pumpage from the cell, we must create a full grid with values of zero.

7.1.5.1. Create a new table **Zero_grid_annual** in a make-table query based on the table **grid_lkup_*area*** with one record for each grid cell and year. For instance, a model with 212 rows, 180 columns, and 6 layers, for 20 years would be create a table with 212 x 180 x 6 x 20= 4,579,200 records. In the make-table query, add a field "SumPumpageAF" with a value of zero for each record.

7.1.5.2. Create a new query ***MMMYY*_ZeroGrid** to provide zero values for each grid cell for each month. You can use any of the monthly factors, as all results will equal zero. As an example, the SQL query for January 1980 would be:

SELECT Zero_Grid_Annual.GRID_ID, Zero_Grid_Annual.DATA_CAT, Zero_Grid_Annual.Year, [MONTHLY FACTORS].MONTH, Zero_Grid_Annual.SumPumpageAF

FROM Zero_Grid_Annual LEFT JOIN [MONTHLY FACTORS] ON (Zero_Grid_Annual.basinnum = [MONTHLY FACTORS].basinnum) AND (Zero_Grid_Annual.CountyNumber = [MONTHLY FACTORS].countynum) AND (Zero_Grid_Annual.Year = [MONTHLY FACTORS].YEAR)

WHERE (((Zero_Grid_Annual.Year)=[Enter year]) AND (([MONTHLY FACTORS].MONTH)=[Enter month]) AND (([MONTHLY FACTORS].DATA_CAT)="IRR"))

ORDER BY Zero_Grid_Annual.GRID_ID;

7.1.6. In Access, create a new union query ***MMMYY*UnionofPumpage** to combine the domestic, livestock, rural domestic, and well-specific pumpage sums, as well as the zero value, for each grid cell. As an example, the SQL for any given year and month is:

SELECT * FROM [MMMYY_C-O] UNION ALL SELECT * FROM [MMMYY_IRR] UNION ALL SELECT * FROM [MMMYY_STK] UNION ALL SELECT * FROM [MMMYY_ZeroGrid] UNION ALL SELECT * FROM [MMMYYWell-specificSum];

7.1.7. Create a new select query **SumPumpageGrid_*MMMYY*** to summarize all pumpage by grid cell, grouping by grid_id, month, and year the pumpage from the above union query. As an example, the SQL for January 1980 is:

SELECT MMMYYUnionofPumpage.GRID_ID, MMMYYUnionofPumpage.Year, MMMYYUnionofPumpage.MONTH, Sum(MMMYYUnionofPumpage.PumpageAF) AS SumOfPumpageAF, Sum([PumpageAF]*[MGDfromAF]) AS PumpageMGD

FROM MMMYYUnionofPumpage LEFT JOIN UnitConversion ON MMMYYUnionofPumpage.MONTH = UnitConversion.Month

GROUP BY MMMYYUnionofPumpage.GRID_ID, MMMYYUnionofPumpage.Year, MMMYYUnionofPumpage.MONTH

ORDER BY MMMYYUnionofPumpage.GRID_ID;

7.2. Join pumpage queries to Arcview shapefile if visual display of the results for a month or year is desired.

7.2.1. In Arcview, import the MS Access query **SumPumpageGrid_*MMMYY***, and join it to the model grid cells in the Arcview shapefile based on the field "Grid_ID."

7.2.2. In Arcview, import the MS Access queries ***MMMYY*_STK, *MMMYY*_IRR, *MMMYY*_pop**, and **Well-specificpumpage.** Link these tables to the model grid cells in the Arcview shapefile based on the field "Grid_ID" and, for well-specific pumpage, "year." Selection of a grid cell in Arcview will then also select the records in each of these tables that pump from the grid cell selected.

APPENDIX D

Standard Operating Procedures (SOPs) for Processing Predictive Pumpage Data TWDB Seymour GAM Project

This page intentionally left blank.

TABLE OF CONTENTS

This page intentionally left blank.

1. Background – These procedures were developed to further implement the guidance provided by the Texas Water Development Board (TWDB) in their Technical Memorandum 02-02. The information in that technical memorandum will not be repeated here, and readers should first consult that document.

2. Groundwater Use Source Data - Predicted future groundwater use estimates for Texas are derived from the following spreadsheets provided by the Texas Water Development Board (TWDB):

   - CityMunicipal_Master_Predictive_072202.xls
   - Irrigation_Master_Predictive_072202.xls
   - Livestock_Master_Predictive_072202.xls
   - Manufacturing_Master_Predictive_072202.xls
   - Mining_Master_Predictive_072202.xls
   - Power_Master_Predictive_072202.xls
   - RuralDomestic_Master_Predictive_072202.xls
   - Predict_INDMonthlyWeighting.xls
   - Predict_MUNMonthlyWeighting.xls

These spreadsheets contain water use estimates from the 2002 state water plan for each water user group for the years 2000 through 2050. Water user groups are generally assigned for each water user category (IRR, STK, MIN, MFG, PWR, MUN, and C-O) in each county-basin. However, individual municipal water supplies within a county-basin are assigned identified as separate water user groups. The water use categories are listed below:

- IRR – irrigation
- STK – livestock
- MIN - mineral extraction
- MFG – manufacturing
- PWR – power generation
- MUN – municipal water supply, and
- C-O – county-other (rural domestic) use.

Historical groundwater use records from the categories MIN, MFG, PWR, and MUN are available for each specific water user, each assigned an alphanumeric water user code (aka "alphanum") in historical water use data tables. Specific locations and wells from which this groundwater was pumped were identified in historical pumpage records. These are known as "well-specific" water use categories. However, the particular locations of historical groundwater pumpage were generally not known for the use categories IRR, STK, and C-O. These categories are known as "non-well-specific" water use categories. Historical pumpage for these three categories was distributed spatially based on population density, land use, and other factors.

Download the above spreadsheets identified above from the TWDB web site, then import them into a new Microsoft Access database file **Predictive Pumpage**.

3. Initial Processing - Create a sub-set of data for the modeled aquifer and geographic area – The tables are queried for water use within the model domain based on the source county ID. Records for water pumpage outside the model domain were deleted. Next, records for water use from aquifers other than those of interest (based on the aquifer's major aquifer code (Seymour="04", Blaine="06", other="22", as well as the code "99".) Other records were deleted.

4. Spatially distribute well-specific pumpage –

   4.1. Identify locations of new wells – If the field "Possible_New_Wells" contained a flag "NW", it is necessary to identify the location of the new wells. The Regional Water Plan is consulted to identify the location of the new wells. In some cases a map showing the projected locations of the new wells may be available. In other cases existing well fields are referenced. Using Arcview, the grid_id(s) associated with the new well(s) should be identified and copied into a new field "grid_id". A note referencing the source of the location information is added to a new field "KD_comment".

   4.2. Matching Predictive to Historical Locations by "Alphanum" - Assume that a water user will tend to pump water in the future from the same locations from which they had pumped groundwater historically. A specific water user can best be identified in the TWDB predictive pumpage data using the field "WUG_Prime_Alpha", or if the water was purchased, the field "Seller Alpha."

4.2.1. A new field "Source_Alpha" is created and populated with the value from the field "WUG_Prime_Alpha" or, if available, the value from the field "Seller Alpha."

4.2.2. In many cases, no value of alpha_num is provided in the table for a well-specific WUG_ID, typically for MIN, MFG, and PWR. Therefore, the value(s) of "alphanum" associated with that WUG_ID in the historical pumpage table is copied to the predictive pumpage table.

4.2.3. The value of "Source_Alpha" is matched manually to the field "alphanum" in the historical pumpage datasets, and the model grid_id identified for this water user in historical pumpage distribution is manually copied to the field "Grid_ID" in the predictive pumpage table.

In many cases, more than one grid cell is associated with a given "alphanum". The predictive pumpage for each alphanum is distributed among multiple Grid ID's in an identical manner as the average for the period 1995-2000. Additional copies of predictive pumpage records are added to equal the number of grid_id's, and a field "grid_frac" is added to the predictive pumpage table, and assigned a value from 0 to 1, calculated as the average of the 1995-2000 fraction of pumpage from that grid_id for that alphanum in the historical pumpage dataset. The values of grid_frac summed to 1 for each "source_alpha."

4.3. Spatially distributing predictive well-specific pumpage for WUGs without historical pumpage - If the water use survey reports no historical pumpage for a water user group that does have predicted pumpage for 2000-2050, it may be difficult to spatially distribute the pumpage

4.3.1. First, check pre-1980 water use survey data to see if any matching water users are identified. If so, identify the wells and grid ids associated with these water users, enter the appropriate values in the fields "grid_id", "kd_comment", and "grid_frac". If not, proceed to 4.3.2 below.

4.3.2. Inspect all the wells in the state well database for water wells matching the reported water user group - e.g., same county, basin, aquifer id, water use. Split the pumpage among all matching wells, identify the grid_id for these wells, and add appropriate entries to the fields "grid_id", "kd_comment", and "grid_frac".

4.3.3. Load the MRLC and/or GIRAS land use shapefiles in Arcview - Identify grid cells within the county-basin of interest and over the aquifer of interest with land use matching that of the water user (e.g., industrial or mining). Split the pumpage among the matching grid cells, and add appropriate entries to the fields "grid_id", "kd_comment", and "grid_frac".

4.3.4. If no historical users, wells, or land use records match the water user group, it is not possible to estimate the spatial source of the pumping - Enter an appropriate comment in the field "KD_comment", a value of "9999999" in the field "grid_id", and a value of "1" in grid_frac".

4.4. Create new table summarizing annual well-specific water use –

4.4.1. Create a new table "WS_annual" for the water use category MUN containing a value of MUN pumpage for each grid_id for each year from 2000 to 2050. The pumpage for each record is calculated as the total pumpage for the year of interest multiplied by the field "grid_frac."

4.4.2. Append to the table "WS_annual" the water use for the category MFG containing a value of MFG pumpage for each grid_id for each year from 2000 to 2050. The pumpage for each record is calculated as the total pumpage for the year of interest multiplied by the field "grid_frac."

4.4.3. Append to the table "WS_annual" the water use for the category MIN containing a value of MIN pumpage for each grid_id for each year from 2000 to 2050. The pumpage for each record is calculated as the total pumpage for the year of interest multiplied by the field "grid_frac."

4.4.4. Append to the table "WS_annual" the water use for the category PWR containing a value of PWR pumpage for each grid_id for each year from 2000 to 2050. The pumpage for each record is calculated as the total pumpage for the year of interest multiplied by the field "grid_frac."

5. Spatially distribute non-well-specific pumpage – We assume that groundwater pumpage in the future is distributed within each county-basin in a similar way that it has been done in the recent past. While we do not discount the impact of changes in population and land use due to urban growth, sprawl, and other factors, we cannot reliably predict the spatial locations of these changes.

5.1. Calculate the fraction of groundwater pumpage for "C-O" use from each grid cell within a county-basin from 2000 historical data (which was based on non-city population density).

5.1.1. Run a query to summarize "C-O" groundwater pumpage in 2000 for each county-basin within the model domain.

5.1.2. For each grid_id within each county-basin, divide the "C-O" pumpage value for the year 2000 by the total "C-O" pumpage for that county-basin. Save this as a new field "Fr_pumpage" for each grid_id.

5.1.3. As a quality check, sum the values of "Fr_pumpage" for C-O by county-basin to ensure they sum to 1.

5.1.4. Create a new table or query for the water use category "C-O" containing a value of C-O pumpage for each grid_id for each year from 2000 to 2050. The pumpage for each record is calculated as the total pumpage for the year of interest multiplied by the field "Fr_pumpage" from the previous three steps.

5.2. Calculate the fraction of groundwater pumpage for "IRR" use from each grid cell within a county-basin from 2000 (which was based on NLCD land use data and the 1994 irrigated farmlands survey).

5.2.1. Run a query to summarize "IRR" groundwater pumpage in 2000 by aquifer layer (1=Seymour, 2=Blaine) for each county-basin within the model domain.

5.2.2. For each grid_id within each county-basin, divide the "IRR" pumpage value for the year 2000 by the total "IRR" pumpage for that county-basin. Save this as a new field "Fr_pumpage" for each grid_id.

5.2.3. As a quality check, sum the values of "Fr_pumpage" for IRR by county-basin to ensure they sum to 1.

5.2.4. Create a new table or query for the water use category "IRR" containing a value of IRR pumpage for each grid_id for each year from 2000 to 2050. The pumpage for each record is calculated as the total pumpage for the year of interest multiplied by the field "Fr_pumpage" from the previous three steps.

5.3. Calculate the fraction of groundwater pumpage for "STK" use from each grid cell within a county-basin from 2000 (which was based on rangeland from the NLCD land use dataset.

5.3.1. Run a query to summarize "STK" groundwater pumpage in 2000 for each county-basin within the model domain.

5.3.2. For each grid_id within each county-basin, divide the "STK" pumpage value for the year 2000 by the total "STK" pumpage for that county-basin. Save this as a new field "Fr_pumpage" for each grid_id.

5.3.3. As a quality check, sum the values of "Fr_pumpage" for STK by county-basin to ensure they sum to 1.

5.3.4. Create a new table or query for the water use category "STK" containing a value of STK pumpage for each grid_id for each year from 2000 to 2050. The pumpage for each record is calculated as the total pumpage for the year of interest multiplied by the field "Fr_pumpage" from the previous three steps.

5.4. Note: The result of this step should be three tables (or queries), one each for C-O, IRR, and STK. Each should contain, at a minimum, the fields "Grid_ID", "county_name", "basin_name", 'WUG_ID", "year", "data_cat", and "pumpage."

6. Oklahoma Pumpage – Predictions of future pumpage for portions of the model domain outside of Texas are not available from the Texas Regional Water Plans. In this case, we will assume that the pumpage will remain constant at 2000 levels for the water use categories MFG, MIN, PWR, STK, and IRR. Because population projections are available, however, we can project future water use for MUN and C-O based on the 2000 water use for each county and the ratio of projected future county population to its 2000 population.

6.1. Download from the Oklahoma Department of Commerce the actual county populations for 2000 and population projections for 2005, 2010, 2015, 2020, 2025, and 2030, the last year available, for Beckham, Greer, Harmon, and Jackson counties. Linearly interpolate values for the intervening years between 2001 and 2029 for which projections are not available. Use linear regression based on the available projections to develop population projections for 2031 through 2050.

6.2. For each year from 2000 to 2050, calculate the ratio of projected population for each year to the actual population in 2000 for each county to calculate a population ratio factor.

6.3. Multiply the historical Oklahoma pumpage value for 2000 C-O or MUN water uses by the population ratio factor to obtain a projected pumpage estimate for that year.

7. Monthly Distribution of Annual Pumpage Totals - We assume that the historical average of monthly water use distribution is a valid predictor of future monthly distribution.

   Monthly pumpage distribution factors for industrial water uses (MIN, MFG, and PWR) are supplied by the TWDB for each county in the spreadsheet "Predict_INDMonthlyWeighting.xls" Monthly distribution factors for domestic water uses (MUN and C-O) are supplied by the TWDB for each county in the spreadsheet "Predict_MUNMonthlyWeighting.xls"

   These monthly factors are imported into a new table **PredictiveMonthlyFactors.**

   For IRR water use, monthly factors must be calculated based on the recent historical distribution of monthly water use, which was based on crop water deficits. Calculate for each county-basin for the water use category "IRR" the average of mfraction for the period 1995-2000 (in the historical pumpage table "MONTHLY FACTORS"). Append these to the table **PredictiveMonthlyFactors**. There should be a monthly factor for each combination of the seven water use categories and county-basin. If no monthly factor can be calculated because there was no historical pumpage, then the monthly factor for that data_cat in the nearest other county-basin should be used.

8. Summarize Pumpage Information to Create Model Input Files - Summary queries for a given year and/or month should be performed as described in the SOP for historical pumpage data.

APPENDIX E

All Transient Hydrographs for the Seymour Aquifer

This page intentionally left blank.

This appendix contains all hydrographs of simulated and observed water-level elevations for targets in the Seymour aquifer for the transient calibration and verification periods. All hydrographs are shown on a 100-foot vertical scale for consistency. On the hydrographs, the model simulated response is shown by a line and the measured water-level elevations are shown as symbols. The hydrographs are arranged in this appendix by pod from top to bottom then left to right.

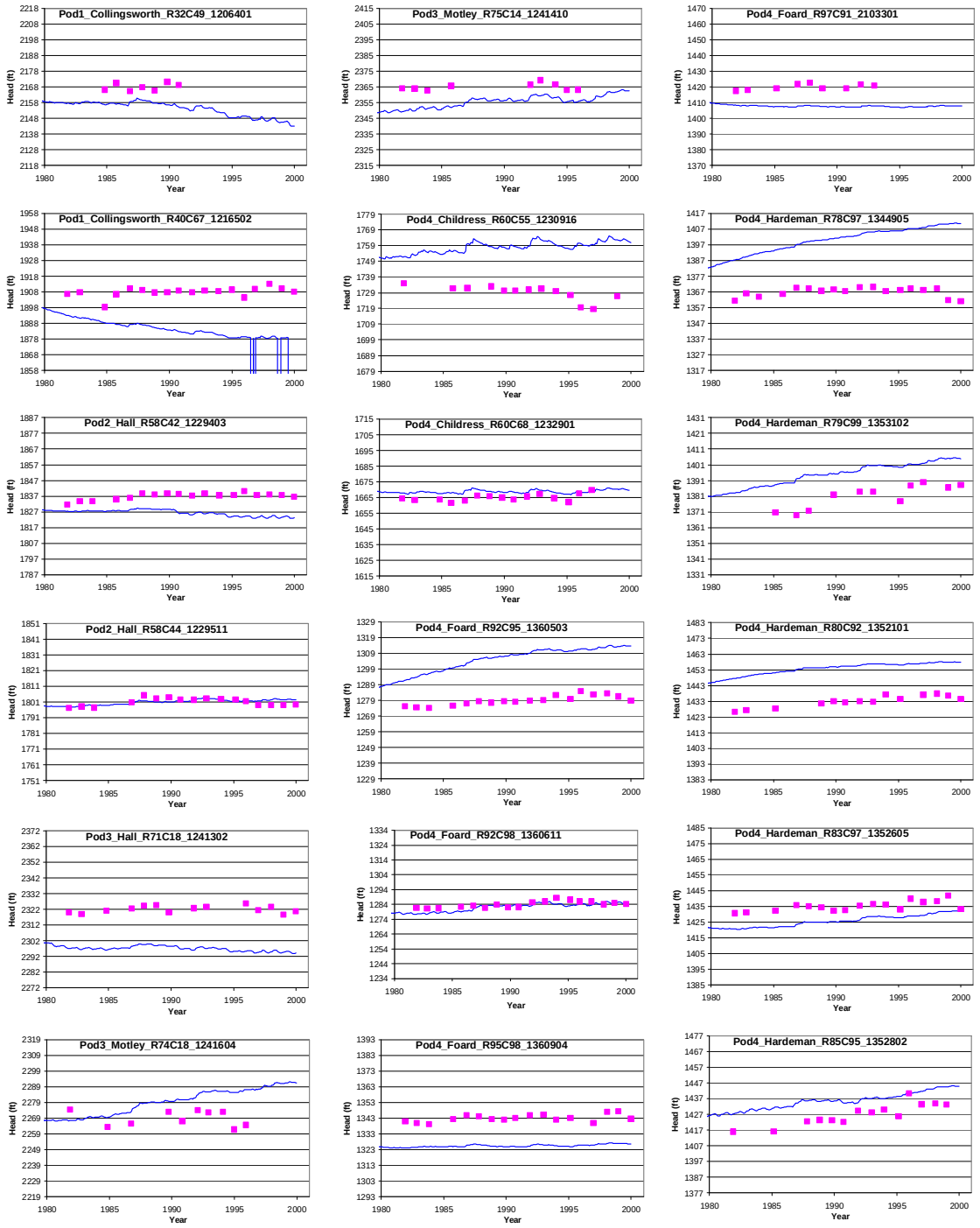

symbols – measured water-level elevations
line – model simulated response

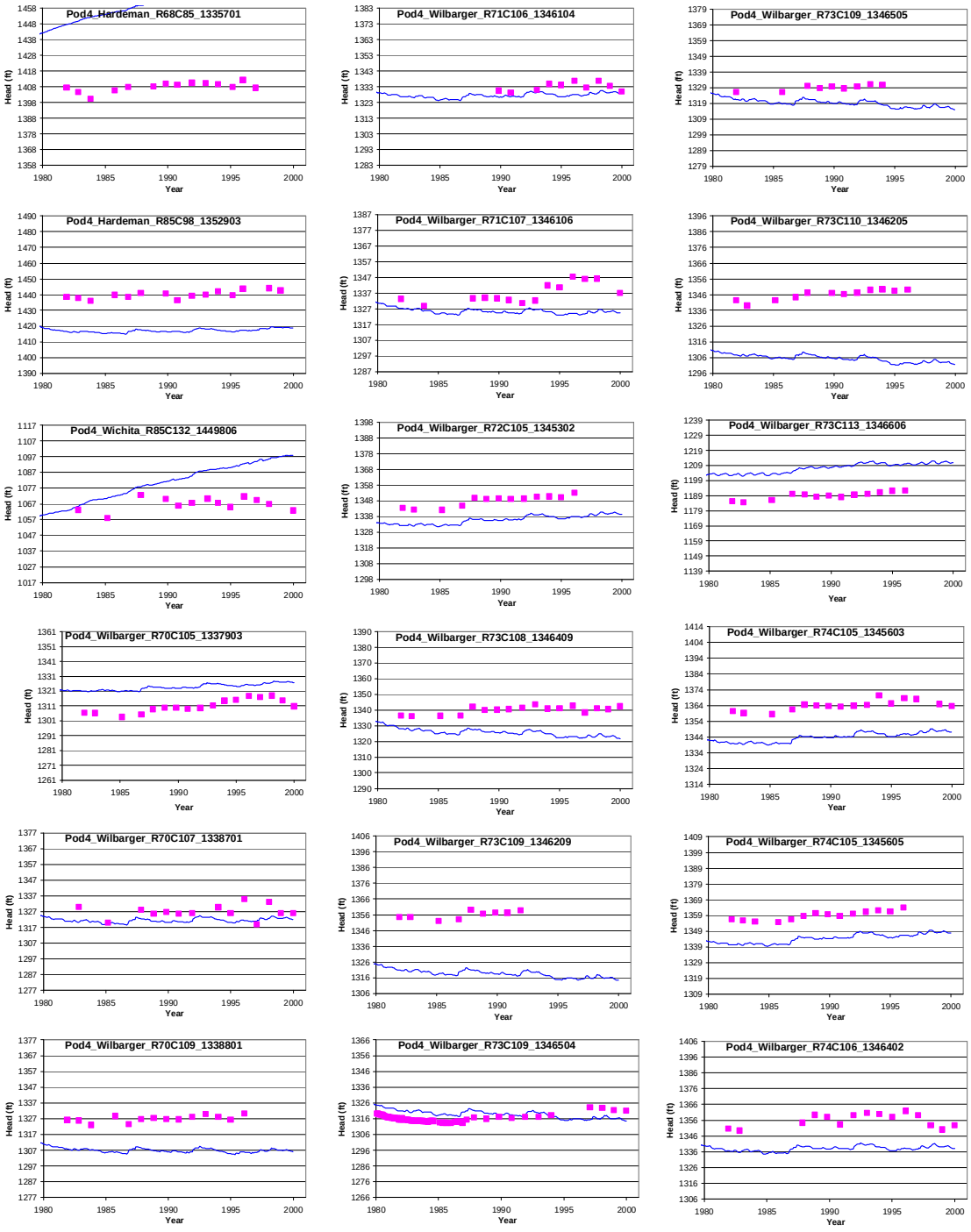

symbols – measured water-level elevations
line – model simulated response

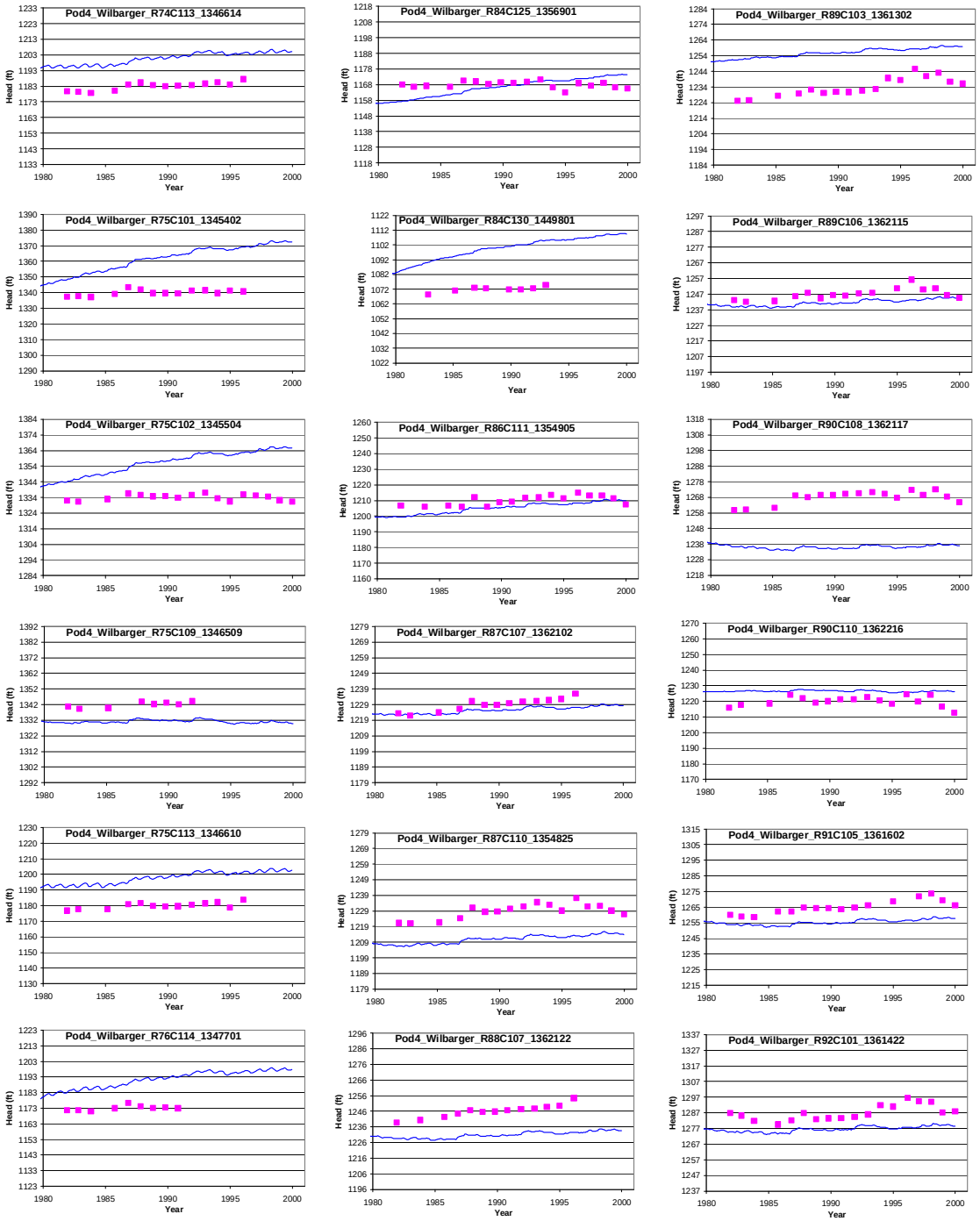

symbols – measured water-level elevations
line – model simulated response

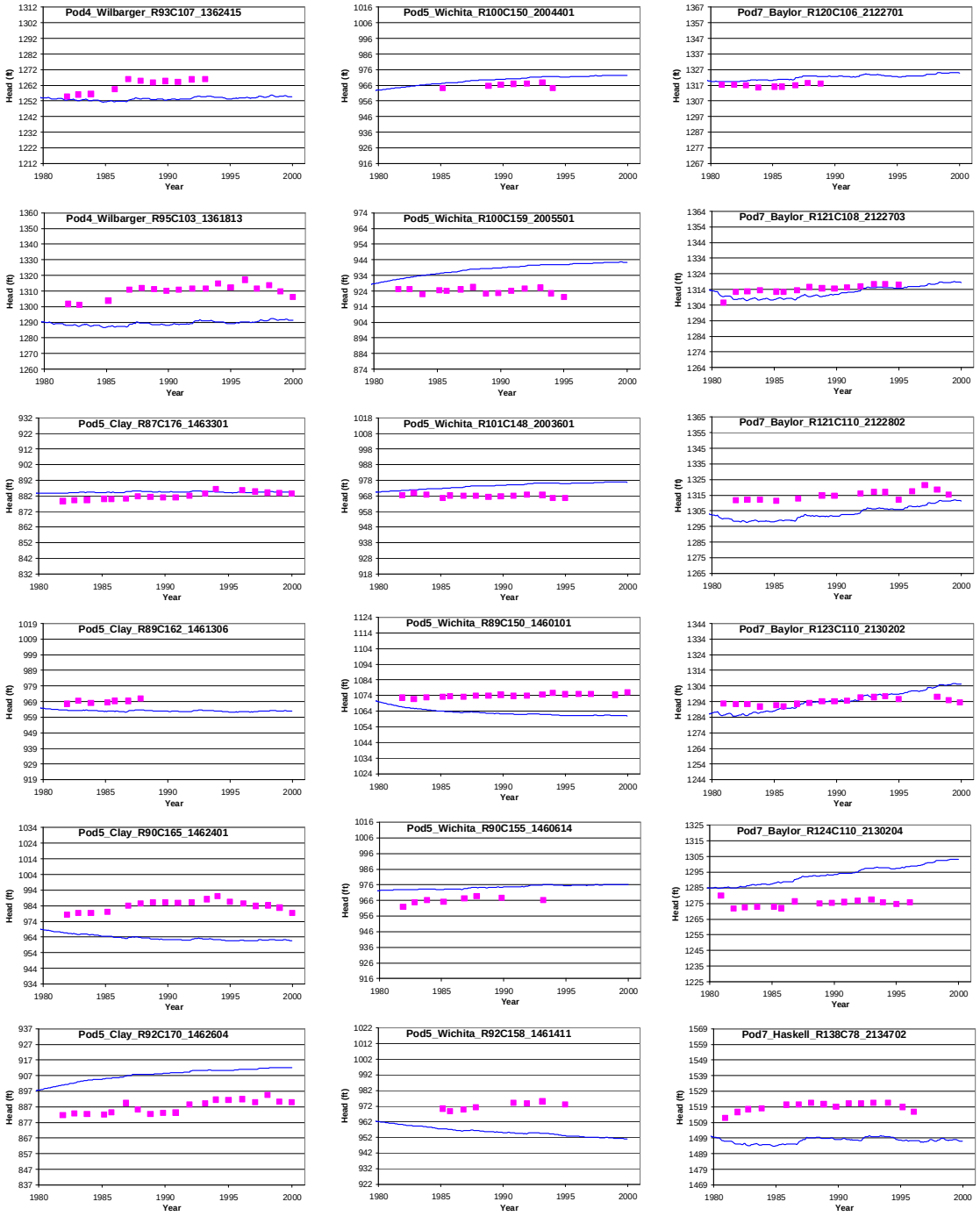

symbols – measured water-level elevations
line – model simulated response

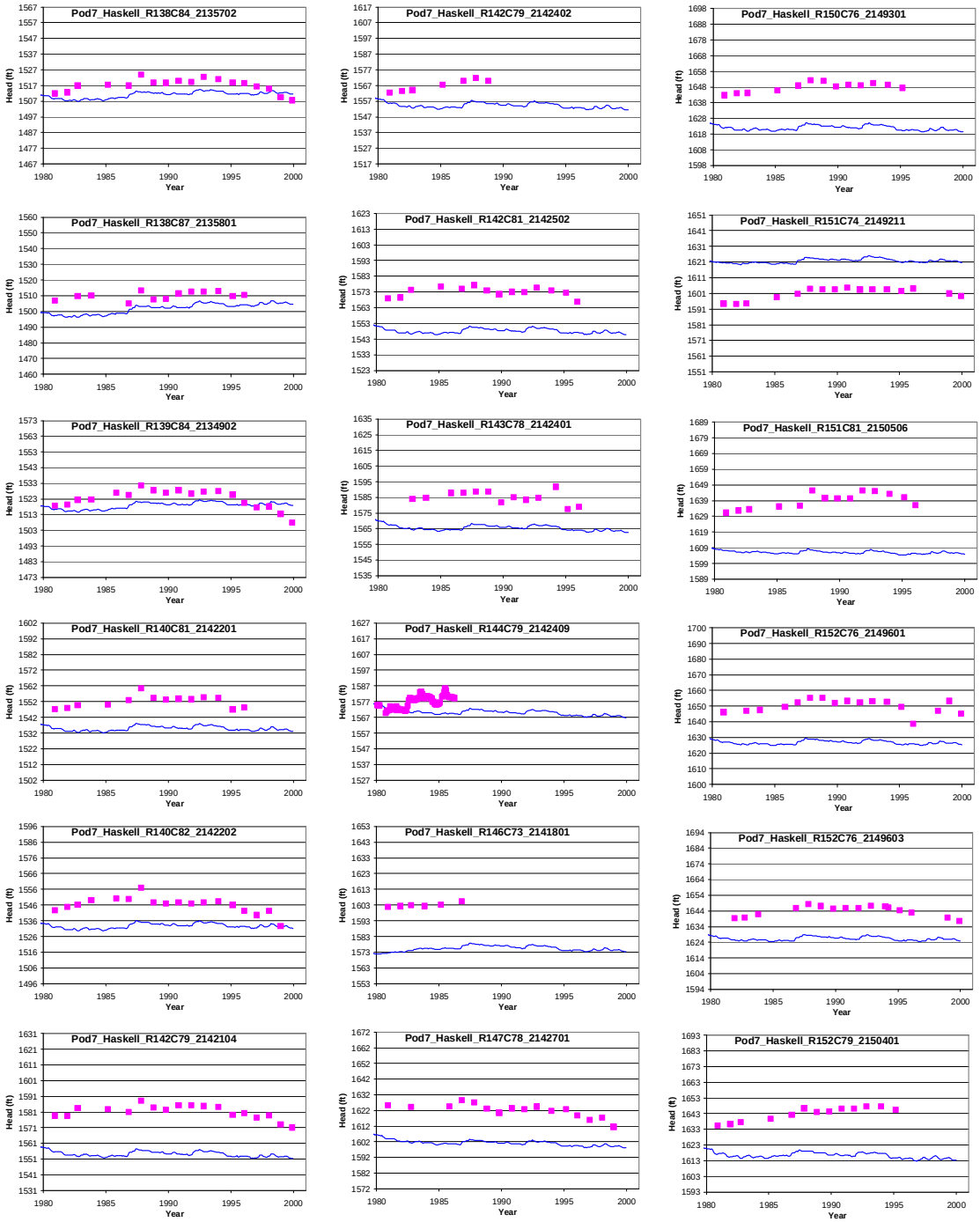

symbols – measured water-level elevations
line – model simulated response

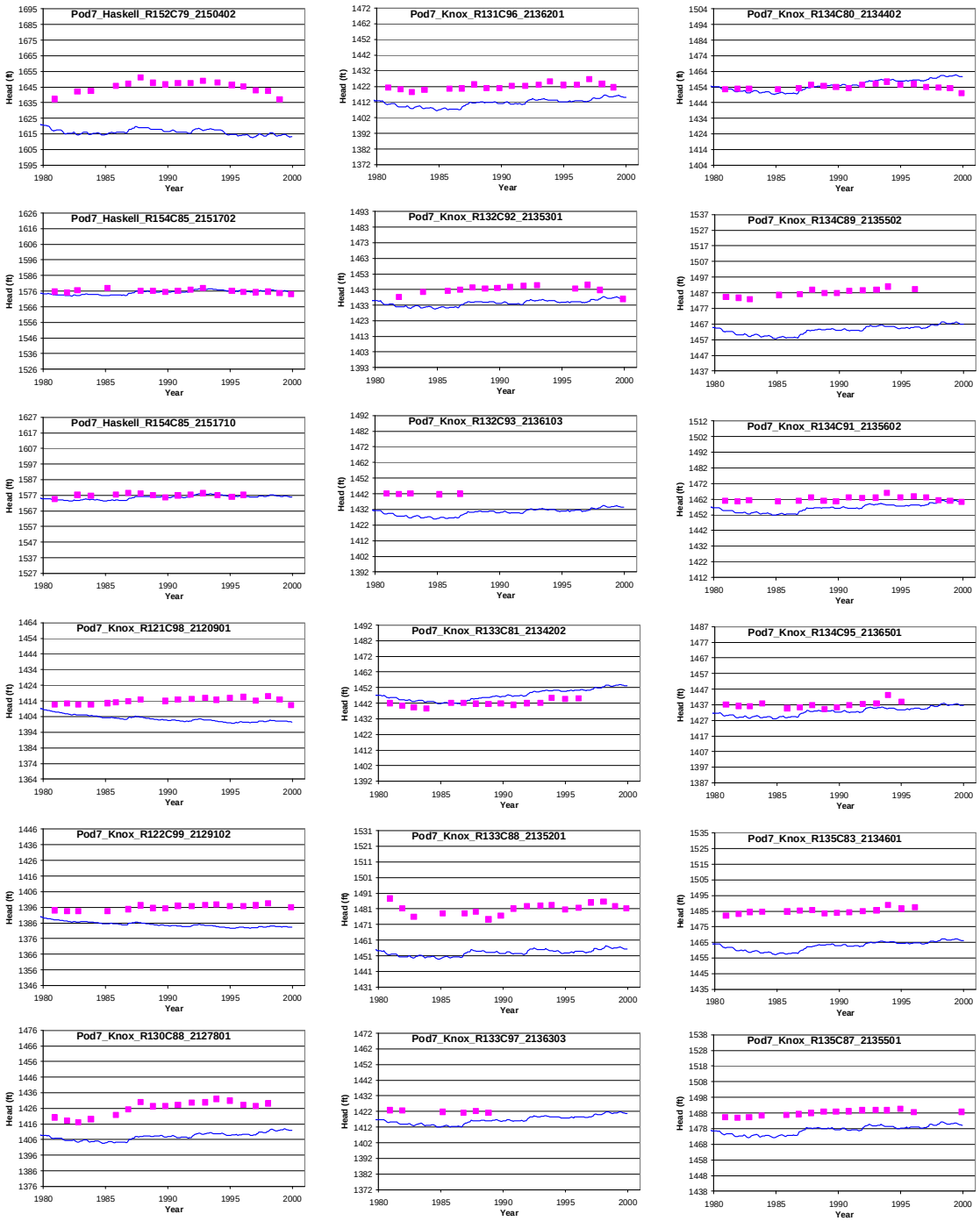

symbols – measured water-level elevations
line – model simulated response

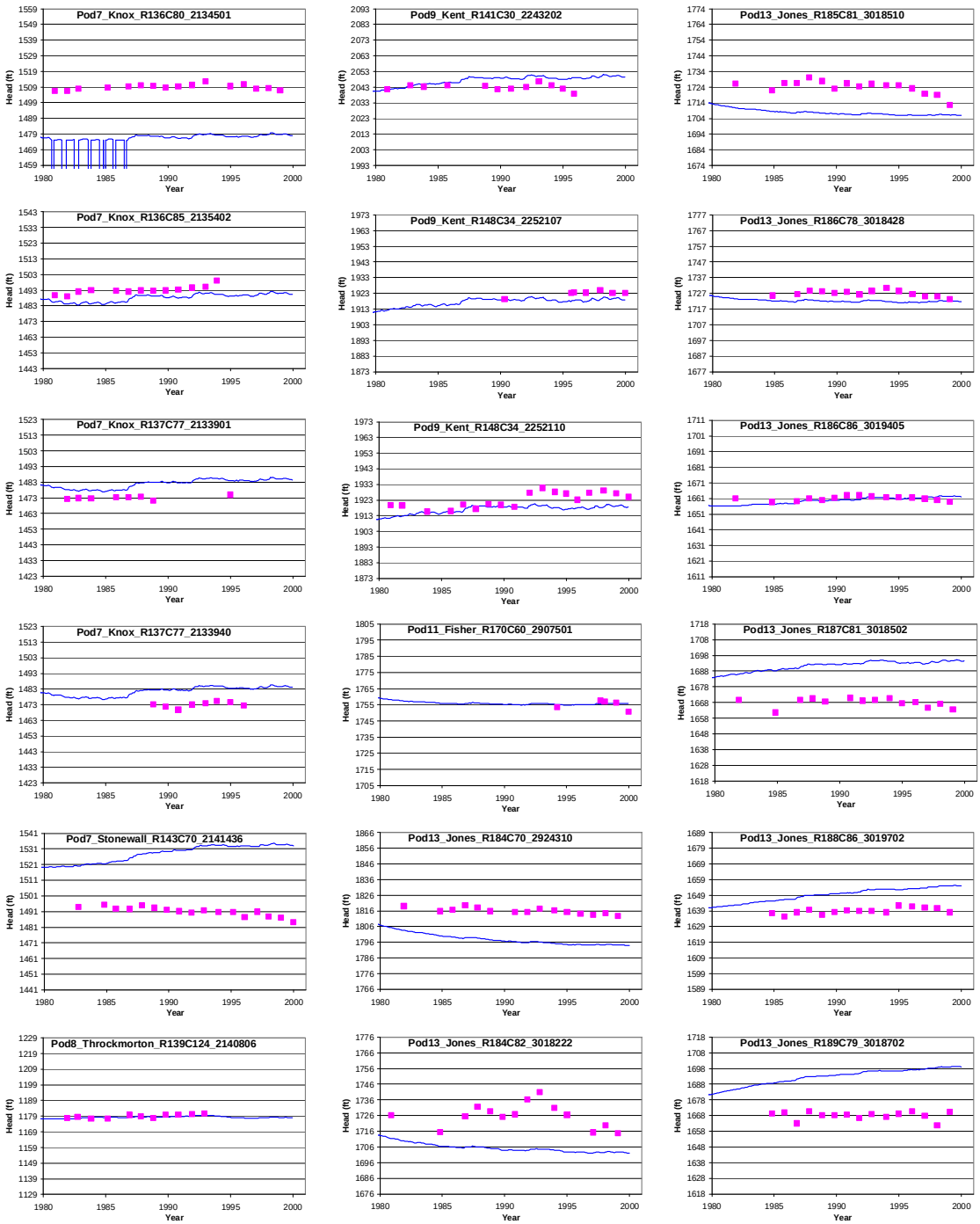

symbols – measured water-level elevations
line – model simulated response

APPENDIX F

All Transient Hydrographs for the Blaine Aquifer

This page intentionally left blank.

This appendix contains all hydrographs of simulated and observed water-level elevations for targets in the Blaine aquifer for the transient calibration and verification periods. All hydrographs are shown on a 200-foot vertical scale for consistency. On the hydrographs, the model simulated response is shown by a line and the measured water-level elevations are shown as symbols. The plots in this appendix contain pod numbers. Pod 27 identifies target wells located in the downdip portion of the Blaine aquifer and pod 28 identifies target wells located in the Blaine outcrop.

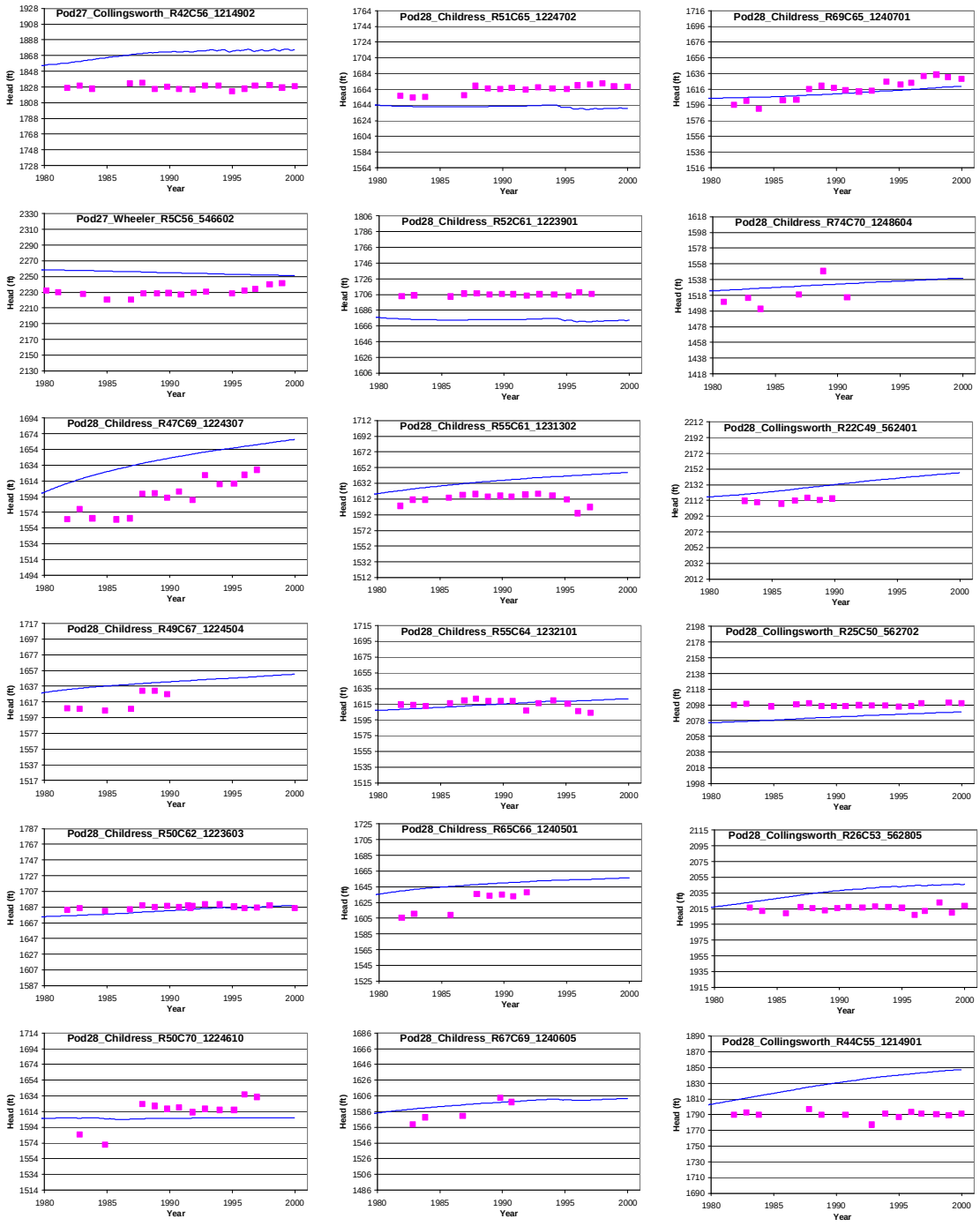

symbols – measured water-level elevations
line – model simulated response

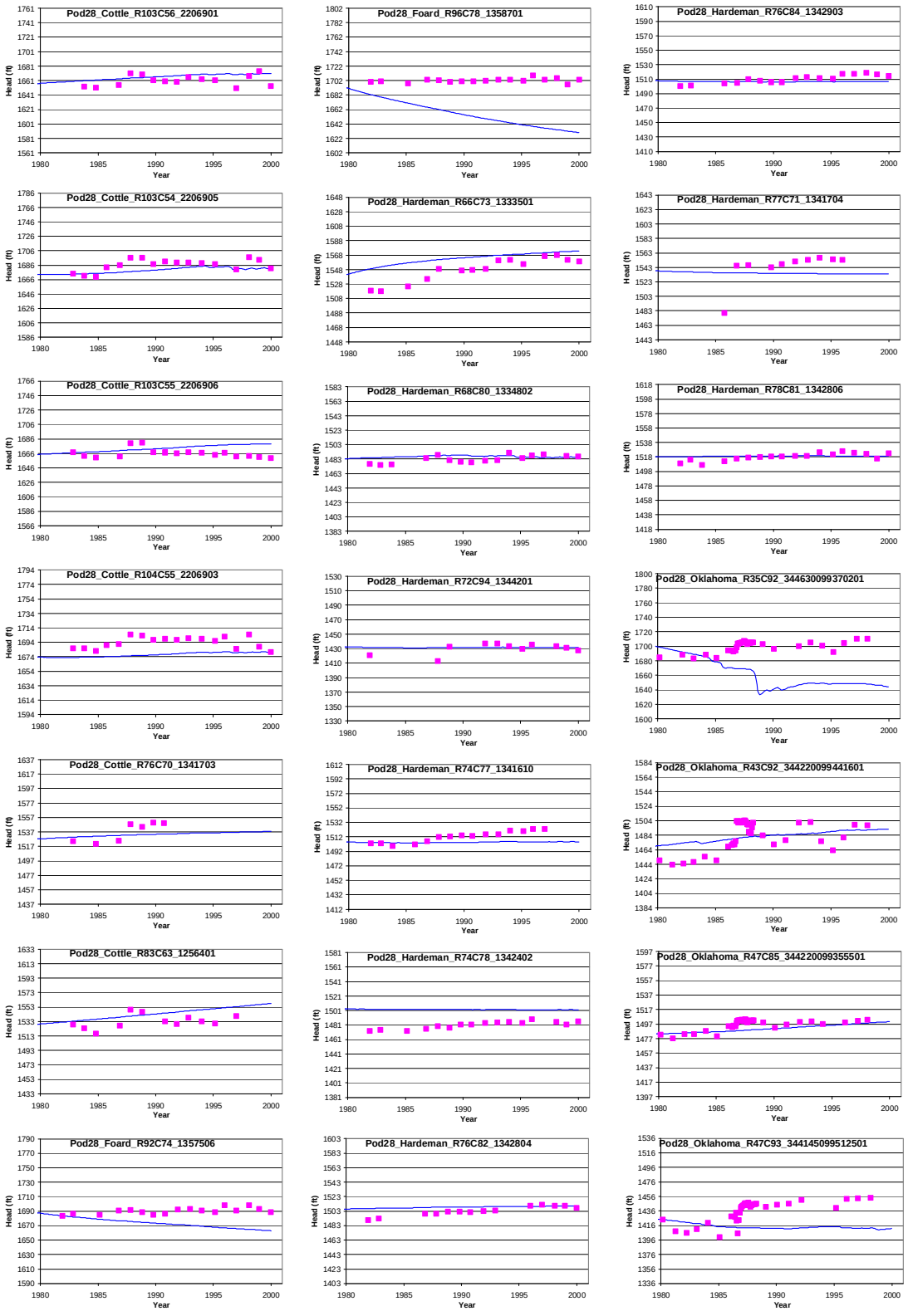

symbols – measured water-level elevations
line – model simulated response

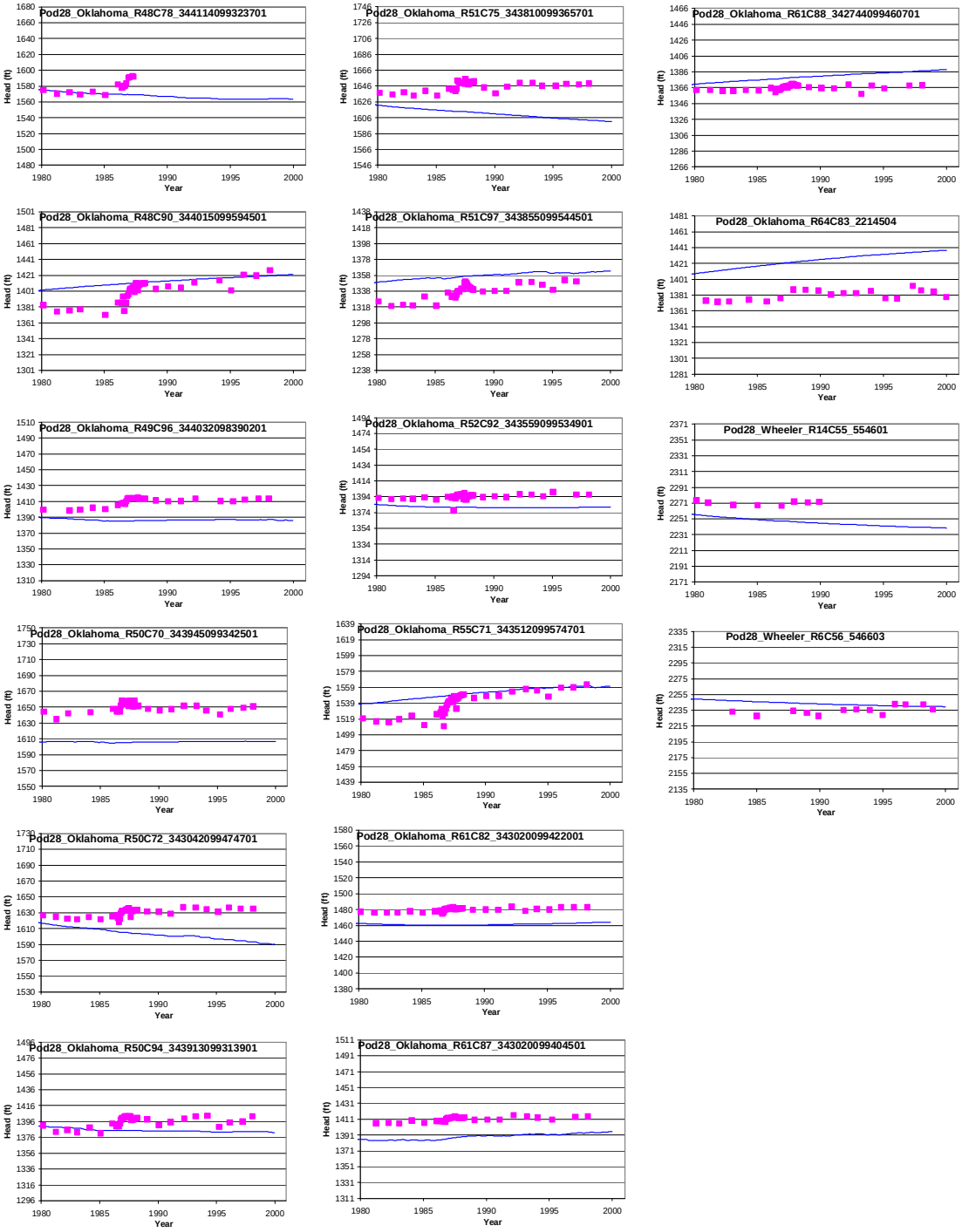

symbols – measured water-level elevations
line – model simulated response

APPENDIX G
Draft Conceptual Model Report Comments and Responses

This page intentionally left blank.

Appendix G

Responses to Texas Water Development Board Comments on the August 2003 Draft Conceptual Model Report

TEXAS WATER DELOPMENT BOARD
Review of the Draft Conceptual Model Report: Contract No. 2003-0483-0481
"Conceptual Model for the Seymour Aquifer GAM"

Note: The TWDB comments are given in regular font and responses to the comments are given in bolded italics.

Overall this report is very well written and it is mostly complete. Two topics missing from the report are a discussion in Section 4.4 on how recharge will be implemented and a discussion of evapotranspiration in Section 2.1. Also, portions of the rejected recharge discussion in Section 5 may need to be re-evaluated. In addition, there are a few other omissions and minor corrections, clarifications, and suggestions. They are detailed below.

Completed. Revisions and additional discussion have been added to address recharge implementation, evapotranspiration, and rejected recharge. The details in addressing these topics is given in response to the detailed review comments below.

CONCEPTUAL DRAFT REPORT TECHNICAL/ADMINISTRATIVE COMMENTS:

Disclaimer: We reserve the right to make additional comments after model development or as additional concerns are brought to our attention.

DRAFT REPORT- TABLE OF CONTENTS

1. No comments.

DRAFT REPORT- SECTION 1.0: INTRODUCTION

1. No comments.

DRAFT REPORT - SECTION 2.0: STUDY AREA

1. Figure 2.20/page 2-28: Please clarify if Pod 1 changes from Alluvium – Possible Lingos Formation in Texas to Seymour Formation and Alluvium in Oklahoma.

   Completed. See Figure 2.23 on page 2-32. Pod 1 changes from Alluvium – Possible Lingos Formation in Texas to Alluvium in Oklahoma.

2. Section 2.1 Physiography and Climate/pages 2-11 to 2-12: Per Exhibit B, Attachment 1, Section 3.1.1, please include a description and map of temperature and physiographic provinces (for example: http://www.lib.utexas.edu/geo/txphysio.jpg)

Completed. See the first paragraph on page 2-12 and Figure 2.9 (physiographic provinces) and the second paragraph on page 2-13 and Figure 2.12 (temperature)

3. Figure 2.10/page 2-15: Please add a more detailed legend to show variability or values of mean-annual net pan evaporation.

   Completed. See Figure 2.13 on page 2-19.

DRAFT REPORT - SECTION 3.0: PREVIOUS INVESTIGATIONS

1. No comments.

DRAFT REPORT - SECTION 4.0: HYDROGEOLOGIC SETTING

1. Section 4.1/page 4-2: Suggest incorporating a map and discussion of the stratigraphic age for the Blaine Formation of layer 2 in paragraph 3 of section 4.1

   Completed. See the second paragraph on page 4-2 and Table 4.1.1.

2. Section 4.1/page 4-2: Suggest incorporating a map and expanded discussion of hydrostratigraphy regarding Permian units of layer 2 (i.e., sedimentology and depositional history) in paragraph 4 of section 4.1.

   Completed. See the discussion beginning in the third paragraphs on page 4-2 and Table 4.1.2.

3. Section 4.2/pages 4-4 to 4-15: Suggest either more accurately referencing structure point data obtained from "Driller's logs in unnumbered early TWDB reports" or not use these data in development of structure, Table 4.2.1 and file SYMR/srcdata/geol/structure/StructurePointData.mdb.

   Completed. See Table 4.2.1 on page 4-6 and Turner (1936a; 1936b) references on page 15-7.

4. Section 4.2/pages 4-4 to 4-15: Because of the numerical approximation methods used in MODFLOW, the base of layer 2 may cause instability problems for the model. Since the base of layer 2 Permian units is arbitrary, suggest that contractor(s) consider smoothing the base of the Permian aquifer sediments with base of Blaine aquifer sediments (especially along the eastern boundary of the Blaine sediments).

   Completed. See the third paragraph on page 4-8 and Figure 4.2.9.

5. Section 4.4 Recharge/pages 4-60 to 4-61: Per Exhibit B, Attachment 1, Section 3.1.6, "Maps of recharge potential or recharge coefficients (For Example, Mace and others, 2000) shall be generated for the model area". Please update this section with a conceptual description of the SWAT approach as discussed in your RFQ and expand discussion of conceptual recharge approach in Section 4.4.

   Completed. See the discussion in Section 6.3.4 beginning in the second paragraph on page 6-9, which discusses model implementation of recharge. A reference to this discussion has been added to Section 4.4 (see the third paragraph on page 4-69).

6. Section 4.5/pages 4-64 to 4-66: Suggest discussing background information on groundwater ET in more detail. Per Section 2.1, mesquite and oak trees characterize the Rolling Plains ecological region. Suggest including a discussion of tree root extinction depths and possibly including a vegetation map of Texas (http://www.tpwd.state.tx.us/gis/veg/)

   Completed. See the discussion in Section 6.3.4 beginning in the last paragraph on page 6-9, which discusses model implementation of ET. A reference to this discussion has been added to Section 4.5 (see the first paragraph on page 4-76).

7. Figure 4.6.8/page 4-88: Suggest including estimated conductivity values (or starting ranges) on map of hydraulic conductivity zones for layer 2.

   Completed. See Figure 4.6.8 on page 4-98.

8. Section 4.7 Aquifer Discharge Through Pumping/pages 4-89 to 4-92: Please include a discussion of pumpage for the 1960s and 1970s steady state model period. Also per RFQ Attachment 1 (page 17), report shall include bar chart of yearly total historical and predicted groundwater usage. Please update this section with a bar chart showing historical and predictive pumpage for the study area.

   Completed. See the third paragraph on page 4-99 for discussion of steady-state pumpage. See Figures 4.7.38 through 4.7.60 on pages 4-147 through 4-158 for the bar charts.

DRAFT REPORT- SECTION 5.0: CONCEPTUAL MODEL OF GROUNDWATER FLOW FOR THE SEYMOUR GAM

1. Section 5.0/page 5-2 through 5-3: Portions of the rejected recharge discussion may be misconstrued, please schedule a meeting with TWDB staff to discuss alternative ways of presenting this material.

   Completed. A meeting discussing rejected recharge was held with TWDB staff. Discussion of the limited potential for capture of additional recharge under present-day conditions is given in the third paragraph on page 5-3.

DRAFT REPORT - SECTION 6.0: REFERENCES

1. No comments.

DRAFT REPORT – APPENDICES

Appendix A: Brief Summary of Historical Development of the Seymour and Blaine Aquifers on a County by County Basis

1. Introduction/page A-1: please change all references to Figure 2.3 to 2.4 in the first paragraph .

   Completed. See the first paragraph on page A-1 and figure 2.5 on page 2-8.

Appendix B: Compilation of Structure Data from TCEQ Well Log Records

1. No comments.

DRAFT REPORT EDITORIAL COMMENTS:

DRAFT REPORT- TABLE OF CONTENTS

1. Figure 2.16 please correct spelling of stratrigraphy to stratigraphy.

   Completed. See page iv.

DRAFT REPORT- SECTION 1.0: INTRODUCTION

1. No comments.

DRAFT REPORT - SECTION 2.0: STUDY AREA

1. Section 2.0/page 2-2: Please change second to last sentence from "In generally,…"to "In general,…" or "Generally,…".

   Completed. See the first paragraph on page 2-3.

2. Figure 2.4/page 2-7: Please correct spelling of "Blain, Downdip" to "Blaine, Downdip" in Minor Aquifers legend.

   Completed. See Figure 2.5 on page 2-8.

3. Figure 2.5/page 2-8: Please correct spelling "…Develpoment" to "Development" in Source caption.

   Completed. See Figure 2.6 on page 2-9.

4. Section 2.1/page 2-11: Suggest adding reference to last sentence of first paragraph of section 2.1 regarding historical change in ecosystem.

   Completed. See the second paragraph on page 2-12.

5. Figure 2.11/page 2-16: Please correct spelling "pricipitation" to "precipitation" in legend.

   Completed. See Figure 2.14 on page 2-20.

6. Section 2.2/page 2-20: Please reword first full sentence, " It is likely that the sediments originally blanketed the entire regional…" to "It is likely that the sediments originally blanketed the entire region…".

   Completed. See the first paragraph on page 2-24.

7. Section 2.2/page 2-20: Please spell out abbreviation "ft" in second paragraph.

   Completed. See page 2-24.

8. Figure 2.16/page 2-24: Please correct spelling of stratrigraphy to stratigraphy.

   Completed. See Figure 2.19 on page 2-28.

DRAFT REPORT - SECTION 3.0: PREVIOUS INVESTIGATIONS

1. Figure 3.1/page 3-3: Please correct spelling of "Blain, Downdip" to "Blaine, Downdip" in Aquifer legend.

   Completed. See Figure 3.1 on page 3-3.

DRAFT REPORT - SECTION 4.0: HYDROGEOLOGIC SETTING

1. .Section 4.6.6/page 4-78: Please reword third sentence," While horizontal hydraulic conductivity is dominated by the higher permeability sediments, vertical hydraulic conductivity will by dominated…" to ," While horizontal hydraulic conductivity is dominated by the higher permeability sediments, vertical hydraulic conductivity will be dominated…"

   Completed. See the first paragraph on page 4-89.

DRAFT REPORT- SECTION 5.0: CONCEPTUAL MODEL OF GROUNDWATER FLOW FOR THE SEYMOUR GAM

1. No comments.

DRAFT REPORT- SECTION 6.0: REFERENCES

1. No comments.

DRAFT REPORT - APPENDICES

Appendix A: Brief Summary of Historical Development of the Seymour and Blaine Aquifers on a County by County Basis

1. No comments.

Appendix B: Compilation of Structure Data from TCEQ Well Log Records

1. No comments.

CONCEPTUAL DRAFT DATA SOURCE FILES COMMENTS:

Please add listing files (*.lst) for each folder/directory to list each file contained within.

Completed.

Please make sure that the metadata files are completed with at least the minimum information required per Attachment 2 of RFP. Example - *_DEMpts_met.txt has only projection parameters and needs abstract, source, attribute details, etc.

Completed.

Please use only one metadata file per data coverage or data table. In other words there should not be any met0.txt, met1.txt, met2.txt files – only met.txt files. It is fine to have dual metadata files if they have the same information but are in different formats such as met.txt and met.htm. Example – DEM_ft_met1.doc may be integrated into DEM_ft_met2.txt within the Abstract section.

Completed. Does not apply to databases with multiple tables.

Please include geologic cross-sections used in the report within a folder under geol/.

Not applicable. Geologic cross sections were scanned from the literature.

Please make certain that correct projection parameters are being used for all GIS datasets. Example - the soils data, metadata files suggest that NAD27 was used instead of NAD83.

Completed.

PUBLIC REVIEW COMMENTS ON CONCEPTUAL DRAFT REPORT:

1. No public comments received as of October 6, 2003.

APPENDIX H
Draft Report Comments and Responses

This page intentionally left blank.

Appendix H

Responses to Texas Water Development Board Comments on the March 2004 Draft Model Report

TEXAS WATER DEVELOPMENT BOARD
Review of the Draft Report: Contract No. 2003-0483-0481
"Groundwater Availability Model for the Seymour Aquifer"

Note: The TWDB comments are given in regular font and responses to the comments are given in bolded italics.

FINAL DRAFT REPORT TECHNICAL/ADMINISTRATIVE COMMENTS:

ABSTRACT

1. No comments.

TABLE OF CONTENTS

1. No comments.

SECTION 1.0: INTRODUCTION

1. No comments.

SECTION 2.0: STUDY AREA

1. Page 2-23, paragraph 3, sentence 1 and 3: "evaporates" should be changed to "evaporites".

   Completed. See the third paragraph on page 2-24.

SECTION 3.0: PREVIOUS WORK

1. No comments.

SECTION 4.0: HYDROLOGIC SETTING

1. Elevation of top of Seymour Exhibit B (SOW) Attachment 1, Section 3.1.4, is missing.

   Completed. See Figure 4.2.4 on page 4-13..

2. Section 4.3, per Exhibit B (SOW) Attachment 1, Section 3.1.5, hydrographs will help define water-level declines and seasonal fluctuations throughout the model area. Hydrographs in figures 4.3.25 to 4.3.28 and figures 4.3.30 to 4.3.31 show long-term trends. Please include and/or discuss seasonal trends with examples, especially in the unconfined portions of the aquifers modeled.

Completed. See the discussion beginning in the third paragraph on page 4-31 and Figures 4.3.32 and 4.3.33 on pages 4-64 and 4-65.

3. Section 4.4, per Exhibit B (SOW) Attachment 1, Section 3.1.6 states important factors related to how the aquifer is recharged and effects of seasonal variations shall be examined and discussed. Please discuss if seasonal variations are observed and the effects upon the aquifers in this section of the report.

   Completed. See the discussion beginning in the first paragraph on page 4-68 and continuing through the second paragraph on page 4-69, and Figure 4.4.1.

4. INTERA SOQ page 67 states INTERA will examine additional constraints on recharge estimates based on water-level responses in shallow wells to individual recharge events, where data is available. Other helpful information for evaluating recharge, particularly recharge fluxes through the unsaturated zone, will be gathered from the USGS National Water Quality Assessment (NAWQA) program. Please clarify where in the report this is discussed and/or please update sections 4.4 with the methodology and results of this analysis.

   Completed. See the discussion in the last paragraph on page 4-67 and continuing through the third paragraph on page 4-69.

5. Section 4.5, page 4-69, per conceptual draft review comment please update this section with previous request to discuss background information on groundwater ET in more detail. Per Exhibit B (SOW) Attachment 1, Section 5.4, the "Hydrogeologic Setting' section shall discuss the information compiled and analyzed for developing the conceptual model. Later sections of the final draft report (6.3.4, and 8.1.3) discuss the use of SWAT for estimating ET. If the data used to develop figure 8.1.6 (ET extinction depth distribution) was not model calibrated, please move this figure to section 4.5 and cross-reference with later discussions. After reading the report it is understood that several of the model parameters were either calibrated in (recharge) or tied to calibration (ET). Please cross-reference in the appropriate discussion in section 4 where the reader may find the final results/figures in the subsequent chapter(s).

   Completed. The discussion of ET was moved from Section 8.1.3 to Section 6.3.4, which discusses model implementation of ET. At the end of Section 4.5, the reader is referred to Section 6.3.4 to find the ET discussion (see the first paragraph on page 4-76).

6. INTERA SOQ page 68 states INTERA will investigate the application of better methods being studied by the USGS (Lanning and Rush, 2000) for stream flow rates. The SOQ also states INTERA will check for possible stream flow data that may be available from other sources, such as the U.S. Army Corps of Engineers, and the Red River Authority of Texas as part of the Texas Clean Rivers and Red River chloride control project. Please clarify where in the report this is discussed and/or please update section 4.5 with a discussion of the methodology and results of this analysis.

   Completed. See the fifth paragraph on page 6-7 and the second paragraph on page 4-74.

7. INTERA SOQ page 66 states the more limited data on specific yield from aquifer tests will be augmented by available and inferred porosity data for the different facies. Please clarify where in the report this is discussed and/or please update section 4.6 with a discussion of the methodology and results of this analysis.

Completed. See the first paragraph on page 4-90.

8. Table 4.3.1: Please correct TWDB aquifer code for Alluvium from 110ALVM to 100ALVM.

   Completed. See Table 4.3.1 on page 4-20.

9. Figures 4.3.24 and 4.3.29: Please correct spelling of "period" in legend.

   Completed. See Figure 4.3.24 on page 4-56 and Figure 4.3.29 on page 4-61.

10. Section 4.5 (page 4-68) per Exhibit B (SOW) Attachment 1, section 5.4, please report spring flow in cubic feet per second (cfs) instead of ft3/s or f 3/s.

    Completed. See the fourth paragraph on page 4-74.

11. Please change x-axis from time steps to years 1980 to 2050 in Figure 4.7.44.

    Completed. See Figure 4.7.44 on page 4-150.

12. Provide a table or appendix that lists the data sources plotted in Figure 4.2.1.

    Completed. See the first paragraph on page 4-8.

13. Pages 4-24 and 4-25, discusses how some water levels in the Seymour were determined from a correlation of depth to water and the depth to the base of the Seymour. Are there any literature references that can be used to support this methodology? If so, please provide references.

    Completed. See the discussion beginning in the first paragraph on page 4-25. References were added.

14. Page 4-76, last sentence in paragraph 2, please clarify systematic bias and expand discussion. Logic appears slightly circular. Reported saturated thicknesses and the steady state saturated thicknesses at the same location should be equal.

    Completed. See revised discussion in the second paragraph on page 4-83.

15. Section 4.2, please reference that the methodology for the structural picks can be found in Appendix B.

    Completed. See the first paragraph on page 4-7.

16. Page 4-26, paragraph 2, sentence 2: please change "manor" to "manner".

    Completed. See the third paragraph on page 4-27.

SECTION 5.0: CONCEPTUAL MODEL OF GROUNDWATER FLOW IN THE AQUIFER

1. Page 5.1, last sentence of paragraph 2: Please change "easternmost" to "westernmost".

   Completed. See the second paragraph on page 5-1.

2. Page 5-3 paragraph 3, states cross formational flow from the Seymour occurs to underlying units. The last sentence on page 4-27 states that direction of flow between the Seymour and the underlying formations could not be determined from an evaluation of measured data. Please provide clarify and provide additional hydrogeologic analysis if needed.

   Completed. Additional clarification was added to Section 4.3.4 on page 4-29 that is consistent with the discussion in the third paragraph on page 5-3.

SECTION 6.0: MODEL DESIGN

1. Section 6.2, pages 6-2 to 6-3, states the GAM standard requires grid cells be squares with a uniform lateral dimension of 1 mile. Exhibit B (SOW) Attachment 1, Section 3.2.1, states lateral cell size shall be no greater than 1-mile by 1-mile. Please adjust sentence to reflect GAM standards.

   Completed. See the first paragraph on page 6-3.

2. Regarding page 6-10 paragraph 2: provide and explain the function used to assign recharge based on the cell thickness in layer 1. See also comment in Section 8.0. Please update as needed.

   Completed. See the discussion beginning in the third paragraph on page 6-10.

3. On page 6-16, paragraph 2, please state the anisotropy ratio assumed for the model area.

   Completed. See the second paragraph on page 6-20.

4. Page 6-9, paragraph 1, please update the link from ".edi" to ".edu".

   Completed. See the second paragraph on page 6-9.

SECTION 7.0: MODELING APPROACH

1. INTERA SOQ page 69 states the INTERA team will review the literature to define possible calibration constraints such as groundwater age dating reports and the results from the NAWQA program. Please clarify where in the report this is discussed and/or please update section 7.1 with a discussion of the results and implementation of this investigation.

   Completed. See the third paragraph on page 7-4.

2. Page 7-3, third paragraph, states the primary type of calibration target used was water levels and qualitatively stream leakages. Later in section 8.2.2 additional insight is given concerning the lack of gain/loss data and expands the 'qualitative' approach used for calibration of the Seymour GAM. Section 8.2.2 also discusses the 'qualitative' approach used for springs. Since Exhibit B (SOW) Attachment 1, section 5.4 states the 'Modeling Approach' section shall describe the approach, philosophy, and focus for calibrating the model, please introduce in more detail the 'qualitative approach' used for calibration in section 7.1 for streams and springs. In addition, the SOQ stated INTERA proposed to use PEST to aid in calibration. Please include a discussion of this method in section 7.1 of the report.

Completed. A discussion of stream and spring targets was added to Section 7.1 beginning in the fifth paragraph on page 7-3. A discussion of evaluating the use of PEST and the reasons it could not be used in the calibration was added to Section 7.1 beginning in the third paragraph on page 7-1.

3. INTERA SOQ page 71 states in addition to a standard "one-off" sensitivity analysis, the calculation of parameter sensitivities based on the inverse solution of the Jacobian Matrix will be performed. Please include a discussion of this approach in section 7.3 of the report.

   Completed. See the fourth paragraph on page 7-6.

SECTION 8.0: STEADY-STATE MODEL

1. Per Exhibit B (SOW) Attachment 1, section 5.4, the 'Steady-State Model' section shall discuss the water budget and how it compares to the conceptual model and hydrogeologic setting. Please expand section 8.2.3 with a discussion that ties in the conceptual model and hydrogeologic setting to the water budget results.

   Completed. See the fourth paragraph on page 8-17.

2. Section 8.3, please include and discuss the results of the inverse solution of the Jacobian Matrix sensitivity analysis as stated in the SOQ page 71.

   Completed. See the last paragraph on page 8-30.

3. In Section 8.1.3, page 8-3, the reader is referred to section 6.3.4 for information regarding the relationship derived between topography and spatially applied recharge. In Section 6.3.4, the reader is referred to Section 8.1.3. Neither Section provides an explanation of the actual function applied. See also Section 6.0 comments. Please update as needed.

   Completed. A description of the methodology was included in Section 6.3.4 beginning in the last paragraph on page 6-10 and a paragraph relating details pertinent to the calibration was added to Section 8.1.3 (see the fourth paragraph on page 8-4).

SECTION 9.0: TRANSIENT MODEL

1. Per Exhibit B (SOW) Attachment 1, section 5.4, the 'Transient Model' section shall discuss the water budget and how it compares to the conceptual model and hydrogeologic setting. Please expand section 9.2.3 with a discussion that ties in the conceptual model and hydrogeologic setting to the water budget results.

   Completed. See the first paragraph on page 9-21.

2. Section 9.3, please include and discuss the results of the inverse solution of the Jacobian Matrix sensitivity analysis as stated in the SOQ page 71.

   Completed. See the first paragraph on page 9-54.

SECTION 10.0: PREDICTIONS

1. Per Exhibit B (SOW) Attachment 1, section 4.0, average recharge shall be defined relative to average recharge since 1960. Section 10.0, paragraph two, states average recharge for the purposes of the report was defined from 1975 to 1999. Please provide an analysis comparing 1960 through 1999 to 1975 through 1999 average recharge.

   Completed. Discussion in paragraph 2 of page 10-1 was altered and expanded to more clearly reflect the situation.

2. Table 10.3.2, under 'Year' header please correct '2040 50 2050*' to read '2040 to 2050*'.

   Completed. See Table 10.3.2 on page 10-44.

SECTION 11.0: LIMITATIONS OF THE MODEL

1. No comments.

SECTION 12.0: FUTURE IMPROVEMENTS

1. Page 5.3 states the distribution of rooting depths throughout the Seymour aquifer is not well characterized, propose adding suggestion of characterizing and mapping of root depths and associated plants in the study area as a future improvement to enhance the understanding of ET in model.

   A sentence proposing further characterization of root depths for refined models was added to Section 12.2 (see the first paragraph on page 12-3). The sentence in Section 5 was augmented to include the difficulty of applying a single root depth to 1 mi^2 grid blocks (see the second paragraph on page 5-3).

SECTION 13.0: CONCLUSIONS

1. No comments.

SECTION 14.0: ACKNOWLEDGMENTS

1. Please update sentence in first paragraph to state "…series of SAFs held between February 2002 and April 2004" instead of "between February 2002 and March 2004".

   Completed. See the first paragraph on page 14-1.

SECTION 15.0: REFERENCES

1. Please correct spelling of “difference” in Fenske and others, 1996 citation.

   Completed. See page 15-2.

2. For the reference for Ritchey and Rumbaugh. These are the editors of this compendium of 24 papers. Please clarify which specific papers in this volume are referenced on page 7-1.

   Completed. See the second paragraph on page 7-1 and page 15-1.

APPENDIX A: BRIEF SUMMARY OF HISTORICAL DEVELOPMENT OF THE SEYMOUR AND BLAINE AQUIFERS ON A COUNTY BY COUNTY BASIS

1. No comments.

APPENDIX B: COMPILATION OF STRUCTURE DATA FROM TCEQ WELL LOG RECORDS

1. No comments.

APPENDIX C: STANDARD OPERATING PROCEDURES (SOPs) FOR PROCESSING HISTORICAL PUMPAGE DATA TWDB SEYMOUR GAM PROJECT

1. In Section 2.5, please correct the spelling of ‘discontinuity’ and ‘calculated’.

   Completed. See page C-5.

APPENDIX D: STANDARD OPERATING PROCEDURES (SOPs) FOR PROCESSING PREDICTIVE PUMPAGE DATA TWDB SEYMOUR GAM PROJECT

1. No comments.

APPENDIX E: ALL TRANSIENT HYDROGRAPHS FOR THE SEYMOUR AQUIFER

1. Please provide a comment or legend on each page of hydrographs explaining that the simulated response is a line and the measured water levels are shown by symbols. The explanation on page E-1 may not transfer if individual pages are copied in the future.

   Completed. See pages E-2 through E-8.

APPENDIX F: ALL TRANSIENT HYDROGRAPHS FOR THE BLAINE AQUIFER

1. Please provide a comment or legend on each page of hydrographs explaining that the simulated response is a line and the measured water levels are shown by symbols. The explanation on page F-1 may not transfer if individual pages are copied in the future.

   Completed. See pages F-2 through F-4.

FINAL DRAFT MODEL COMMENTS:

All files required to run the steady-state, transient (1975 – 1999), and predictive (2000 – 2050) models were included. The models ran with no problems and with several exceptions noted below results matched those presented in the draft report.

No problems were encountered using the batch file included to use PMWIN with MODFLOW 2000. However, a more detailed readme file would be more helpful especially if a user makes changes to the model using PMWIN. What files may or may not be rewritten by PMWIN for the model to still work? Step-by-step instructions would be helpful. Also, some background on the GMG solver should also be included. Was the GMG solver used with MODFLOW 96 or MODFLOW 2000?

Detail was added to the readme files. An additional README.GMG file was included detailing the use of the GMG solver. A reference to the user's manual for the GMG solver was included in Section 6.1. This manual can also be found online at http://water.usgs.gov/pubs/of/2004/1261/. The GMG solver was used with MODFLOW-2000.

In addition, the coordinate system in all of the PMWIN files needs to be referenced to real world GAM coordinates (not local model coordinates) for the map DXF files to display. In other words,

Xo = 4,554,160 (not 1,900,800)
Yo = 21,191,840 (not 2,196,480)

With x1 and y1 corrected also to allow map to be seen in real world coordinates. Please update the PMWIN files.

The PMWIN files were updated with GAM coordinates.

The following Figures and Tables need to be checked and if necessary corrected:

Figure 9.2.10, p. 9-34, Simulated December 1999 layer 2 water levels. This map does not agree with stress period 300 model for layer 2. Please verify that the correct map was plotted.

A quantitative comparison was made between the model output and the data within the shapefile shown in the figure and the two agree. The legend on Figure 9.2.10 on page 9-35, however, was changed to reflect the actual maximum water level in the data. A similar change was also made to the legend of Figure 9.2.2 on page 9-27.

Table 10.3.2, p.10-44: Please clarify if these values are cubic feet rather than acre-ft.

Completed. Table replaced with values in acre-feet (see page 10-44).

Figure 10.2.6a (a) average conditions and (b) DOR conditions, p. 10-32. Are these two switched? Should it be (a) DOR and (b) average conditions? That is what the model results suggests.

Completed. Figures switched and caption unchanged (see page 10-32)

Figure 10.2.12, p. 10-39. ditto

Completed. Figures switched and caption unchanged (see page 10-39).

Otherwise model water levels and select budgets match those reported in the draft GAM report.

TWDB staff extracted pumpage from the input model files and compared the summed results at the county level to the raw pumpage summed at the county level. For most of the Seymour modeling area the comparison between the transient historical and predictive pumpage in the model and the raw pumpage matched volumes and trends. However, please review and verify the historical pumpage assigned to the Seymour in Briscoe County (Figure 1), which appears almost twice the amount from the raw pumpage provided by TWDB. In addition for the predictive pumpage please review the model pumpage for Dickens, Kent, Motley, Stonewall, Wheeler, and Cottle counties (Figures 2-7).

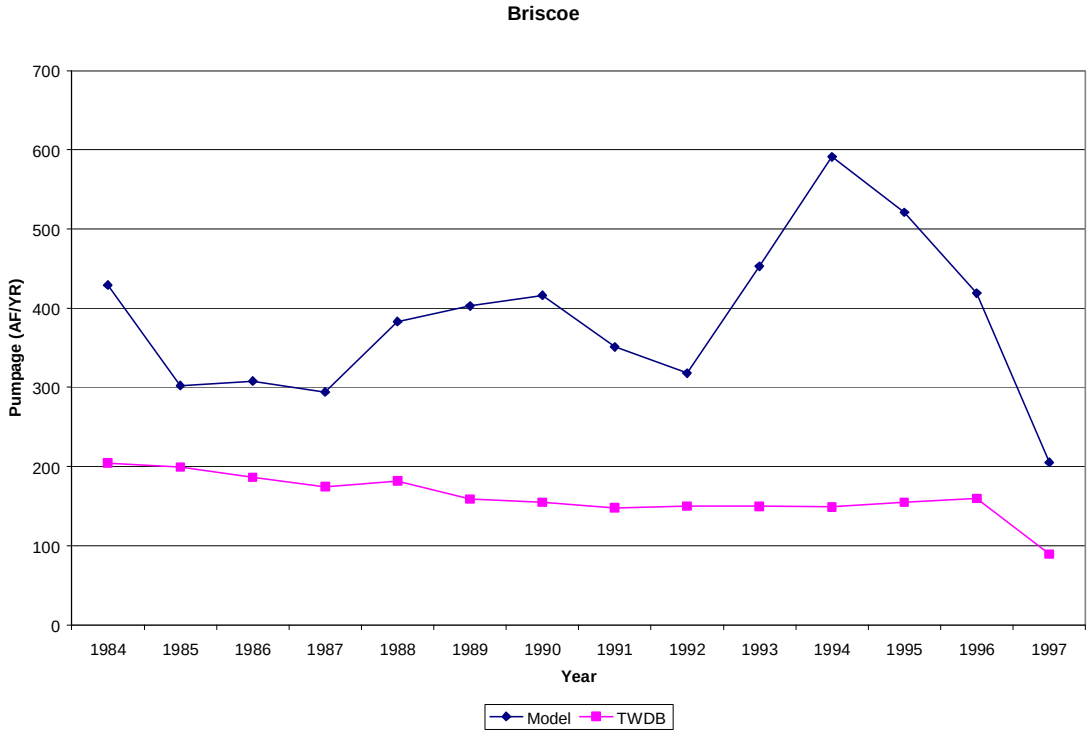

Figure 1. Comparison of total county historical groundwater pumpage for selected years 1984 to 1997 to pumpage extracted from the Seymour model for Briscoe County.

Completed. The historical and predictive pumpage assigned to the Seymour aquifer for Briscoe County has been reviewed and verified. When grid cells are overlain with county and basin boundaries, more than one county, basin, or both may be assigned to some grid cells. We have verified that pumpage was spatially assigned within the appropriate county and basin. However, all pumpage that is spatially assigned within a particular grid cell is summed and assigned to the centroid of the grid cell. When attempting to extract or analyze pumpage from the model, a certain amount of error occurs. The amount of error may be compounded if pumpage is analyzed using the model file by assigning pumpage to the county in which the centroid of the grid is located. Furthermore, Motley County, located to the south of Briscoe County, uses significantly more Seymour groundwater as compared to Briscoe County. This difference in pumping volumes exacerbates the effect of model cells

straddling county-basin lines. A discussion addressing this issue was added to the end of Section 6.3.5 (see the last paragraph on page 6-12).

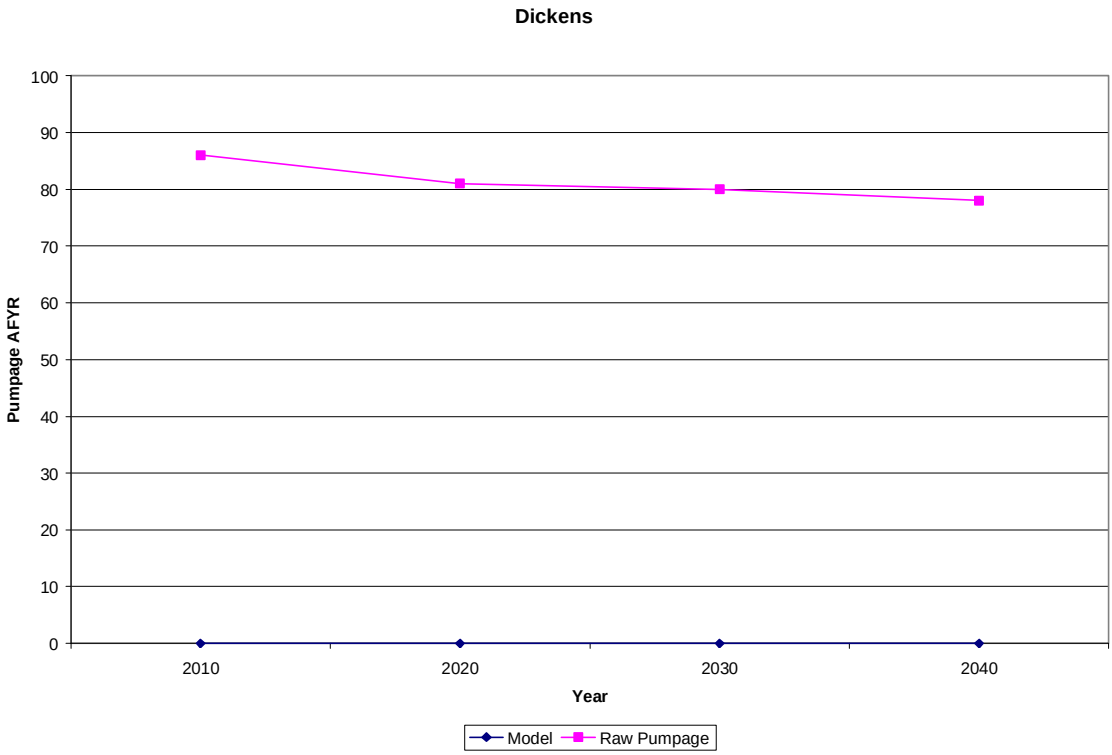

Figure 2 Comparison of predictive pumpage assigned to Seymour in Dickens County to predictive model pumpage files for Seymour aquifer.

The pods of the Seymour aquifer in Dickens County are not part of the Seymour GAM, therefore, this comment is not applicable. The pods included and not included in the model are shown in Figure 2.2.

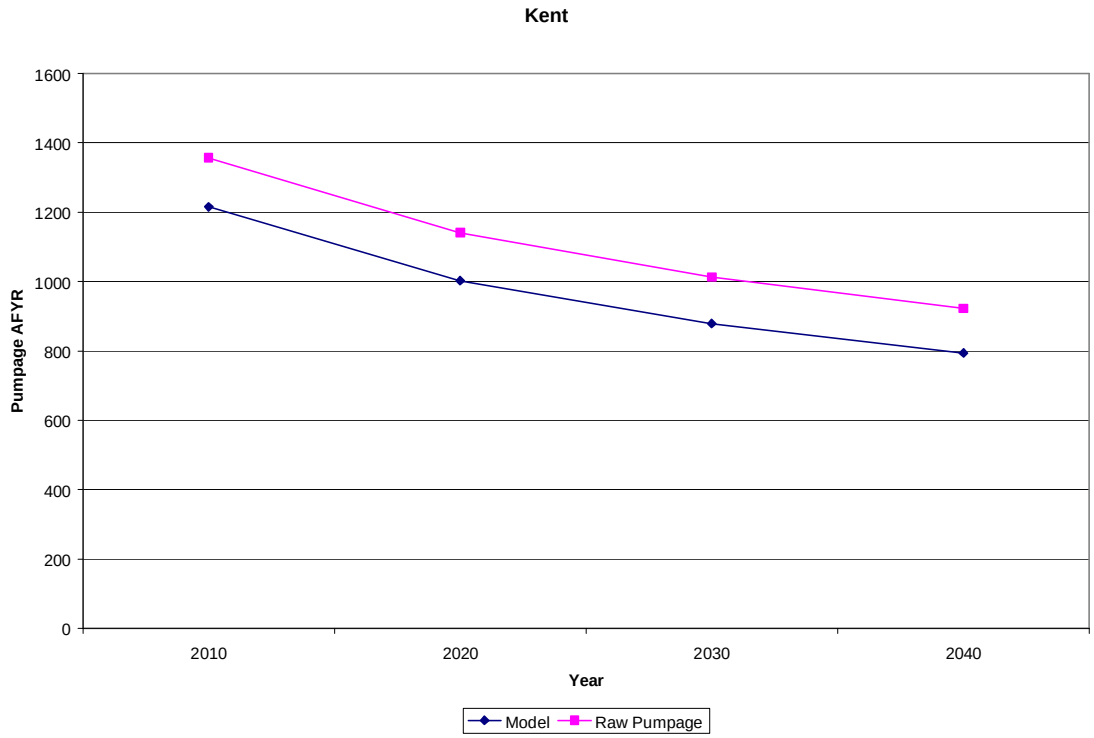

Figure 3. Comparison of predictive pumpage assigned to Seymour in Kent County to predictive model pumpage files for Seymour aquifer.

Only one pod of the Seymour aquifer in Kent County is part of the Seymour GAM. Therefore, comparing total county-wide pumpage estimates to the pumping for the Seymour aquifer included in the Seymour GAM is not applicable. The pods included and not included in the model are shown in Figure 2.2.

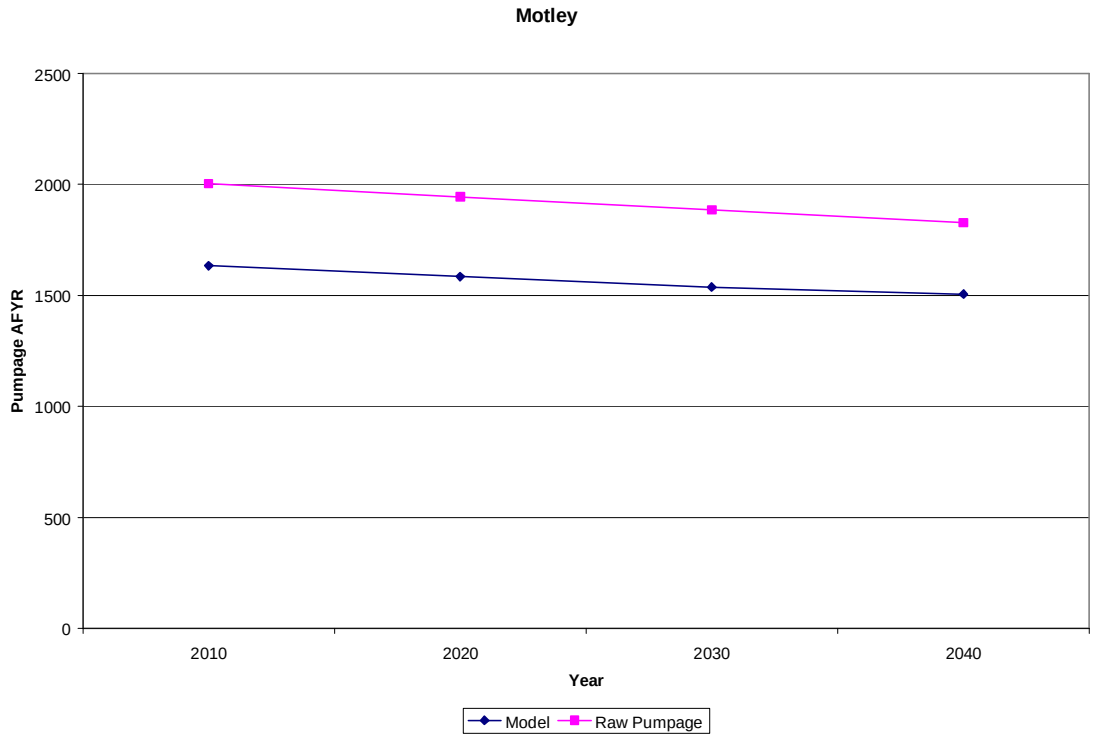

Figure 4. Comparison of predictive pumpage assigned to Seymour in Motley County to predictive model pumpage files for Seymour aquifer.

Completed. In addition to the discussion above for Briscoe County, the total raw pumpage from the TWDB for Motley County includes municipal pumpage by the City of Matador. Pumpage for this city is not included in the modeling because its source is portions of the alluvium and Quartermaster Formation not included in the Seymour GAM (see the discussions in the first paragraph on page 4-101 and the last paragraph on page 4-104).

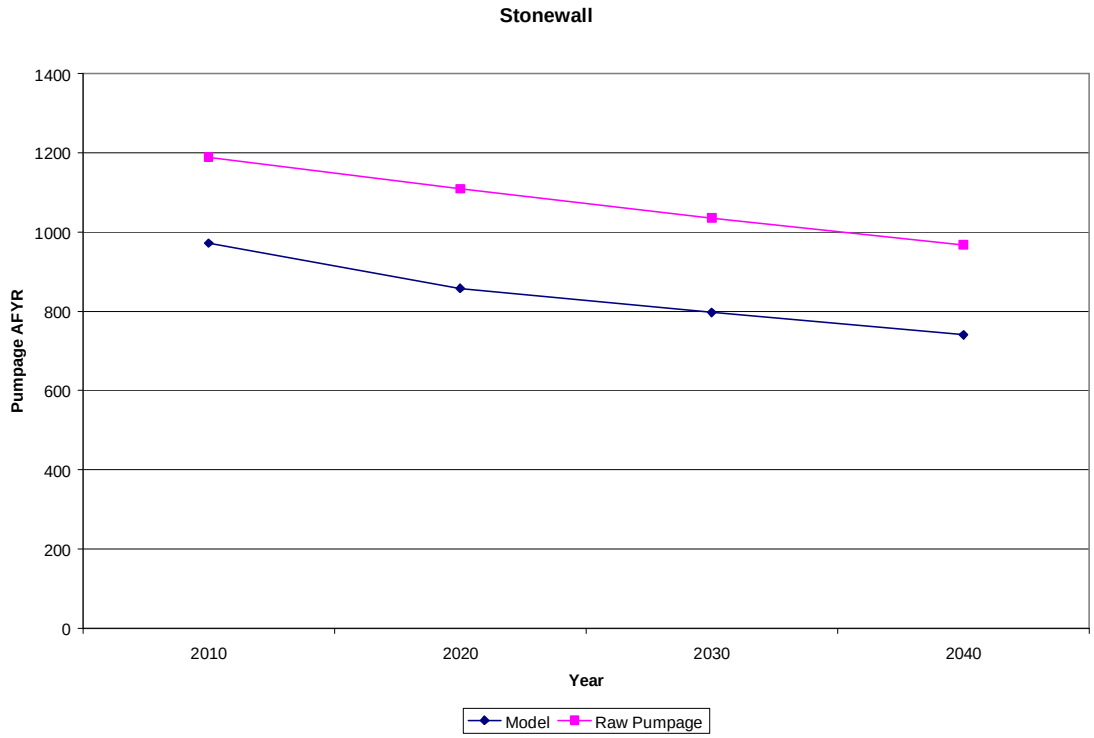

Figure 5. Comparison of predictive pumpage assigned to Seymour in Stonewall County to predictive model pumpage files for Seymour aquifer.

Completed. The reduced model pumpage, relative to the TWDB estimates, from the Seymour aquifer in Stonewall County is primarily due to municipal pumping by the City of Aspermont. Historical pumping records show that the source of water for the City of Aspermont is Seymour-aquifer wells located in neighboring Haskell County, state wells 21-49-212, 21-49-317, and 21-49-503. The predictive pumping records indicate that the Seymour aquifer in Stonewall County will be the source for future pumping by the City of Aspermont. However, the predictive pumping records do not indicate a new source or new wells being drilled in Stonewall County, nor does the regional water plan indicate a new source. Therefore, the predictive pumping for the City of Aspermont was assigned to the same wells as for historical pumping, and those wells are located in Haskell County. See the discussion in the second paragraph on page 4-105.

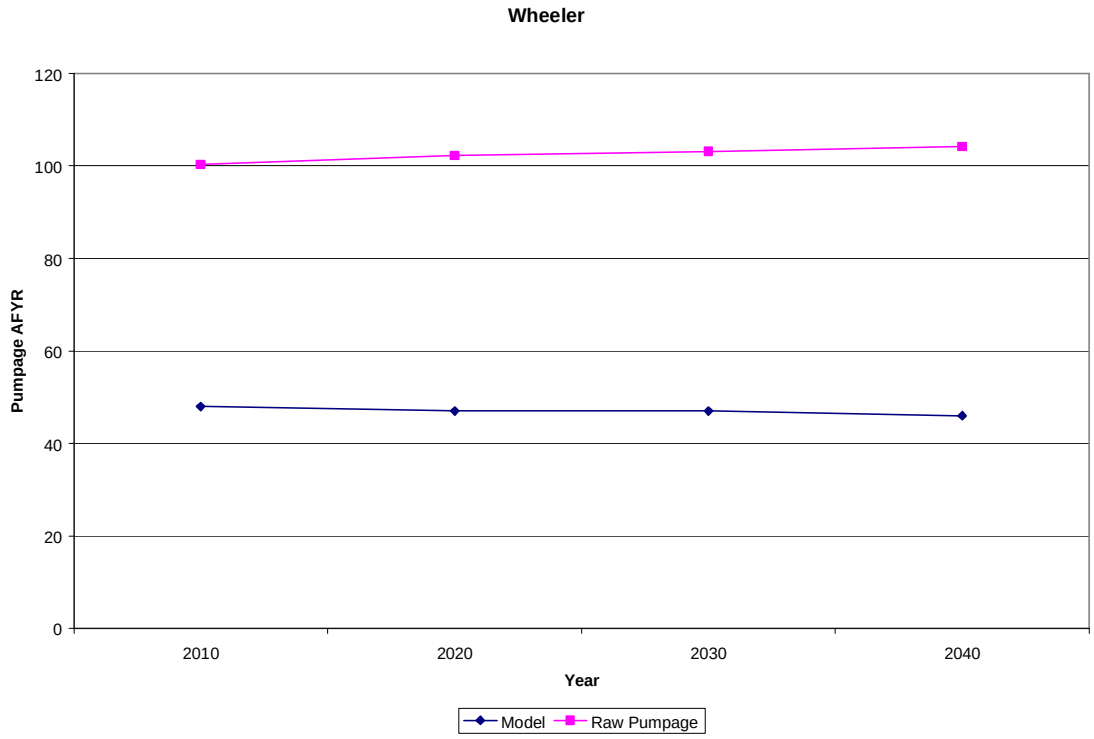

Figure 6. Comparison of predictive pumpage assigned to Seymour in Wheeler County to predictive model pumpage files for Seymour aquifer.

The pod of the Seymour aquifer in Wheeler County is not part of the Seymour GAM, therefore, this comment is not applicable. The pods included and not included in the model are shown in Figure 2.2. The only model pumping in Wheeler County is from the Blaine aquifer.

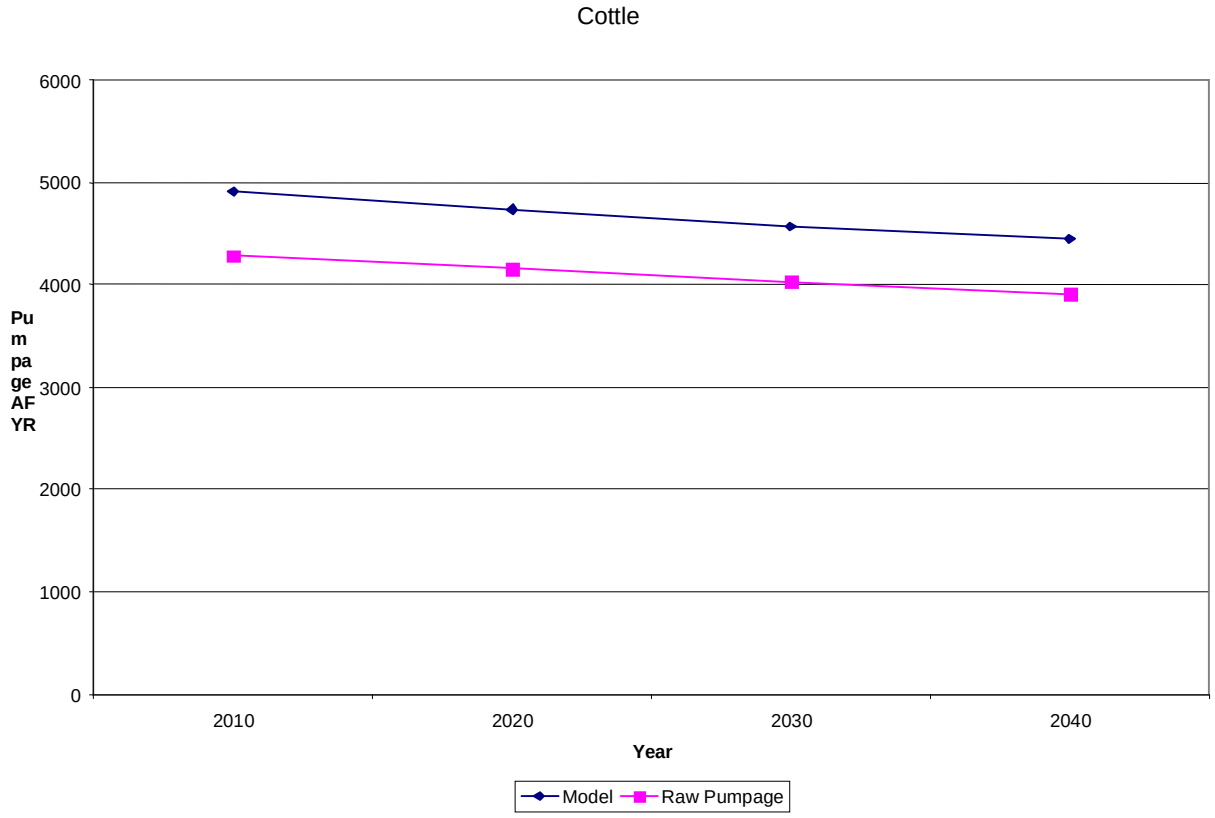

Figure 7. Comparison of predictive pumpage assigned to Seymour in Cottle County to predictive model pumpage files for Seymour aquifer.

The pods of the Seymour aquifer in Cottle County are not part of the Seymour GAM, therefore, this comment is not applicable. The pods included and not included in the model are shown in Figure 2.2. The only model pumping in Cottle County is from the Blaine aquifer.

PUBLIC REVIEW COMMENTS OF FINAL DRAFT REPORT:

Tables 4.7.3 through 4.7.11 lists water use data that includes Collingsworth County through the year 1999. Please clarify how the withdrawal rate of 25,157 AFY by all use categories in 1999 in Table 4.7.3 is less than the withdrawal rate of 25,547 AFY by irrigation alone in Table 4.7.5. Please review and update the tables, as needed.

Completed. See revised Table 4.7.5 on page 4-112.

For Collingsworth County, please discuss how the predictive pumping estimates for the years 2000 and beyond in Tables 4.7.12 and 4.7.14 can be approximately one-half that of 1999 in Tables 4.7.3 and 4.7.5 when irrigation use has not decreased, but has actually increased by one-third in the local area in the last few years? Our data shows that year 2000 irrigation demand on 23,181 acres was 32,685 acre-feet, with irrigated acreage increasing to 30,239 acres and a demand of 37,798 acre-feet by the year 2025. We estimated very little change between the years 2025 and 2050. Approximately 85% of this is Seymour Aquifer pumping, and 15% is Blaine Aquifer pumping.

Comment will be addressed by TWDB staff.

The predictive model pumpage volumes included in the Seymour GAM report were derived from data contained within the Water For Texas - 2002, State Water Plan (SWP) and the Regional Water Plans. Once a model is calibrated, the model may be used to analyze many different pumpage scenarios. According to the 2002 SWP, total demands in Collingsworth County were projected to average around 19,318 acre-feet per year for the period from 2000 to 2050. As you noted, this is lower than the 24,157 acre-feet (table 4.7.3) for pumpage extracted from the Seymour aquifer for all uses in Collingsworth County in 1999 in the model and is lower than the 2000 data mentioned above. According to the 2002 SWP the Seymour aquifer is projected to contribute approximately 73 percent of the total supplies in Collingsworth County. The supplies listed in the SWP for Collingsworth County include the Seymour aquifer, the Blaine aquifer, irrigation local supply, livestock local supply, and Other aquifer. Therefore, as noted in table 4.7.12, approximately 14,000 acre-feet per year of total pumpage was used in the predictive scenarios for the Seymour aquifer within Collingsworth County for the model runs.